

UNIVERSITY OF SOUTHAMPTON

Faculty of Natural and Environmental Sciences

Department of Chemistry

The Synthesis of A-ring Fluorinated Bile Acid Analogues

by

Joseph Michael Watts

Thesis for the degree of Doctor of Philosophy

November 2016

UNIVERSITY OF SOUTHAMPTON

ABSTRACT

FACULTY OF NATURAL AND ENVIRONMENTAL SCIENCES

Chemistry

Thesis for the degree of Doctor of Philosophy

THE SYNTHESIS OF A-RING FLUORINATED BILE ACID ANALOGUES

By Joseph Michael Watts

Bile acids are physiological detergent molecules with a function to absorb dietary lipids and hydrophobic molecules in the gastrointestinal tract. It has emerged that bile acids are also agonists for the FXR nuclear receptor and the TGR5 membrane-bound receptor, and are key in regulating metabolism *via* both genomic and non-genomic factors. It is also apparent that bile acids could play an important role in the treatment of Parkinson's disease and some cancers. A number of pharmaceutical companies have developed selective BA receptor agonists, with some progressing through clinical trials for a variety of metabolic disorders.

Fluorine is used extensively in property optimisation due to its ability to modify a plethora of physicochemical effects. By selectively introducing fluorine into the bile acid skeleton, it is possible to modify hydrogen bonding properties, and thus improvements in receptor binding are conceivable. This thesis describes the synthesis of a number of fluorinated bile acid analogues, along with a discussion of some early biological results. Two interesting cases of an intramolecular C-F•••H-O hydrogen bond within the bile acid skeleton will also be presented

Table of Contents

Table of Contents	i
List of Tables	vii
List of Figures	ix
DECLARATION OF AUTHORSHIP	xiii
Acknowledgements	xv
Abbreviations	xvii
Chapter 1: Introduction	1
1.1 Introduction to bile acids	1
1.1.1 Structure and numbering	1
1.1.2 General introduction of endogenous bile acids	1
1.1.3 Bile acid biosynthesis.....	2
1.2 Physiological role of bile acids	3
1.2.1 Absorption of dietary lipids	3
1.2.2 Historic importance of bile acids in therapeutic treatment	3
1.2.3 Agonist of the Farnesoid X receptor	4
1.2.4 Agonist of TGR5	5
1.2.5 UDCA and Parkinson’s Disease	6
1.3 Bile acid receptor agonists.....	6
1.3.1 Endogenous bile acids	6
1.3.2 Semi-synthetic agonists	7
1.3.3 Synthetic agonists	8
1.3.4 FXR binding pocket	9
1.3.5 TGR5 binding pocket.....	9
1.4 Overview of organo-fluorine chemistry.....	10
1.4.1 The C-F bond	10
1.4.2 Effect of fluorine introduction on neighbouring functional groups	11
1.4.3 Effect of fluorination on log <i>P</i> /lipophilicity	15
1.5 Project aim	18

1.5.1	Bile acid analogues	18
1.5.2	Analysis of fluorinated BAs to determine intramolecular C-F•••H-O hydrogen bond	19
Chapter 2:	Synthesis of 3-deoxy-3-fluoro analogues.....	21
2.1	Introduction.....	21
2.1.1	Retrosynthetic analysis	21
2.1.2	Fluorination chemistry	22
2.2	Synthesis of 3 β -fluoro analogues	24
2.2.1	Methyl ester formation	24
2.2.2	Fluorination	24
2.2.3	Epoxidation.....	25
2.2.4	Reduction	26
2.2.5	Product identification through ^1H and ^{19}F NMR.....	27
2.2.6	Deprotection	29
2.3	Synthesis of 3 α -fluoro analogues	30
2.3.1	Mitsunobu reaction to invert 3 α -OH	30
2.3.2	Methanolysis of 3 β -benzoate.....	31
2.3.3	Fluorination/epoxidation	31
2.3.4	Reduction and Deprotection	33
2.3.5	Product identification through ^1H and ^{19}F NMR.....	33
2.4	Synthesis of 3,3-difluoro analogue.....	34
2.4.1	Regio-selective 3 α -OH oxidation.....	34
2.4.2	MOM-protection of 7 α -OH group.....	36
2.4.3	Difluorination	37
2.4.4	Epoxidation.....	38
2.4.5	Deprotection of 3-deoxy-3,3-difluoro analogue	40
2.5	Discussion of biological results.....	41
2.5.1	Background.....	41
2.5.2	Stage 1 - Cytotoxicity screening	41
2.5.3	Stage 2 - IC ₅₀ determination	42

2.5.4	Stage 3 - Apoptosis detection	45
2.5.5	Additional stage - determination of FXR agonism in fluorinated compounds	46
2.6	Conclusion	48
Chapter 3:	Synthesis of 2- and 4-fluorinated analogues	49
3.1	2- and 4-Fluorohydrins Route 1	49
3.1.1	Retrosynthetic analysis	49
3.1.2	Fluorination chemistry	49
3.1.3	Direct fluorination of the 3-keto moiety with Selectfluor®	51
3.1.4	Silyl enol ether formation	52
3.1.5	Fluorination <i>via</i> silyl enol ether	53
3.1.6	Fluoroketone reduction	54
3.1.7	Deprotection of 2 β - and 4 β -fluorohydrins	55
3.2	2 α - and 4 α -Fluorohydrins - Route 2	56
3.2.1	Retrosynthetic analysis	56
3.2.2	Fluorination chemistry	56
3.2.3	Synthesis of 2 α -fluoro moiety <i>via</i> epimerisation of 2 β -fluoro moiety	58
3.2.4	Synthesis of 2 α -fluoro moiety <i>via</i> nucleophilic attack of a 2 β -leaving group	59
3.3	2 α - and 4 α -Fluorohydrins - Route 3	61
3.3.1	Retrosynthetic analysis	61
3.3.2	Fluorination chemistry	62
3.3.3	Large scale synthesis of Δ 2 β ,3 β - and Δ 3 β ,4 β -epoxides	64
3.3.4	Synthesis of 2 α -fluorinated BA derivatives	67
3.3.5	Synthesis of 4 α -fluorinated BA derivatives	70
3.4	Synthesis of 2,2- and 4,4-difluoro analogues	75
3.4.1	Retrosynthetic analysis	75
3.4.2	Difluorination <i>via</i> silyl enol ether	76
3.4.3	2,2-Difluoro synthesis <i>via</i> 2-keto deoxofluorination	78
3.4.4	4,4-difluoro synthesis <i>via</i> 4-keto deoxofluorination	89

3.5	Conclusion	93
Chapter 4:	Hydrogen Bonding Studies	95
4.1	Introduction to the C-F•••H-O hydrogen bond.....	95
4.1.1	Organic fluorine as a hydrogen bond acceptor.....	95
4.1.2	Case studies of C-F•••H-X interactions within rigid systems	99
4.1.3	Case studies of C-F•••H-X interactions within open chain systems.....	106
4.2	Discovery of a 7-membered C-F•••H-O H-bond.....	109
4.2.1	NMR Studies	109
4.2.2	X-ray crystallographic studies	113
4.2.3	IR studies	114
4.2.4	Theoretical calculations of C-F•••H-O bond.....	117
4.2.5	Predicted pK _{AHY} value of 3.78/4.20	119
4.2.6	Future work	120
4.3	Conclusion	121
Chapter 5:	Experimental.....	123
5.1	General Methods.....	123
5.2	General Procedures	124
5.2.1	Procedure A for 24-carboxylic acid protection as methyl ester	124
5.2.2	Procedure B for saponification of methyl ester using LiOH.....	124
5.2.3	Procedure C for protection of secondary alcohol as a MOM ether.....	124
5.2.4	Procedure D for cleavage of MOM-group using HCl.....	124
5.2.5	Procedure E for secondary alcohol oxidation using Dess-Martin Periodinane	125
5.2.6	Procedure F for methanolysis of acetate/benzoate	125
5.2.7	Procedure G for 3-keto/7-keto reduction using NaBH ₄ /CeCl ₃	125
5.3	Synthesis of 3-deoxy-3-fluoro analogues	126
5.3.1	Synthesis of 3-deoxy-3β-fluoro analogues.....	126
5.3.2	Synthesis of 3-deoxy-3α-fluoro analogues.....	130
5.3.3	Synthesis of 3-deoxy-3,3-difluoro analogues.....	135
5.4	Synthesis of 2- and 4-fluorinated analogues.....	141

5.4.1	Synthesis of 2 β - and 4 β -fluorinated analogues.....	141
5.4.2	Synthesis of 2 α - and 4 α -fluorinated analogues.....	148
5.4.3	Synthesis of 2,2-difluorinated analogues	166
5.4.4	Towards the synthesis of 4,4-difluorinated analogues	190
Bibliography		197
Appendices - Crystal structure data.....		205
A.1	X-ray structure analysis data for compound 2.22	207
A.2	X-ray structure analysis data for compound 2.30	208
A.3	X-ray structure analysis data for compound 2.1	209
A.4	X-ray structure analysis data for compound 3.13	210
A.5	X-ray structure analysis data for compound 3.15	211
A.6	X-ray structure analysis data for compound 3.76	212
A.7	X-ray structure analysis data for compound 3.78	213

List of Tables

Table 1.1 - Key features of C-X bonds. ^[45a]	10
Table 2.1 - Fluorination vs. elimination of the 3-OH in standard DAST/DCM conditions.....	32
Table 2.2 - Regio-selective 3 α -OH oxidation of 2.4.3.	36
Table 2.3 - Optimisation of MOM/BOM ether 7 α -OH protection on 2.4.4.	37
Table 2.4 - Optimisation of 3-keto difluorination on 2.37.	38
Table 2.5 - IC ₅₀ values of common cancer chemotherapies against MCF-7 and MDA-MB-231. ^[91]	44
Table 3.1 - Direct fluorination of ketone	51
Table 3.2 - Silyl enol ether formation on 2.37.	52
Table 3.3 - Attempts towards nucleophilic fluorination of 3.26.....	60
Table 3.4 - Synthesis of alkenes 2.20 and 2.21 through 3 α -OH elimination.	66
Table 3.5 - Mitsunobu reaction on 3.41.....	68
Table 3.6 - Opening of Δ 3 β ,4 β -epoxide 2.23 with HF.....	71
Table 4.1 - Selected pK _{BHX} and Δ v _{O-H} values from HBA groups by Ouvrard <i>et al.</i> ^[144]	98
Table 4.2 - Selected pK _{BHX} and K _A values from HBA groups by Dalvit <i>et al.</i> ^[145]	99
Table 4.3 - Examples of flexible fluorohydrins with measurable J _{F-OH} coupling. ^[56]	107
Table 4.4 - Comparison of key C-F•••H-O coupling constants for 3.76 and 3.78.	112
Table 4.5 - Theoretical calculations on F•••H substrates in CHCl ₃ . Obtained from published ^[51, 56] and unpublished results.	118

List of Figures

Figure 1.1 - Numbering of bile acid skeleton.....	1
Figure 1.2 - Key primary and secondary human bile acids.	2
Figure 1.3 - Hydrophobic β -face and hydrophilic α -face of cholic acid.	3
Figure 1.4 - Key constituents of colesevelam hydrochloride polymer. ^[16-17]	4
Figure 1.5 - Comparison of EC50 values of prominent bile acids. ^[19b, 24]	7
Figure 1.6 - Intercept Pharmaceutical's most promising drug candidates. ^[24, 34-35]	8
Figure 1.7 - Number of citations for the phrase "bile acid" 1970-2015. Data obtained from Web of Knowledge on 03/08/2016.	8
Figure 1.8 - A selection of synthetic FXR and TGR5 agonists. ^[43]	9
Figure 1.9 - FXR binding pocket and proposed 3 α -OH interactions. Adapted from ref. ^[34]	9
Figure 1.10 - TGR5 binding pocket and proposed 3 α -OH interactions. Adapted from ref. ^[44]	10
Figure 1.11 - Comparison of CF ₂ and CHF as isosteres of an alcohol group. ^[48]	11
Figure 1.12 - Effect of poly-fluorination on (a) acidic and (b) basic groups. ^[47]	11
Figure 1.13 - Effect of fluorination on pK _{AHY} of cyclohexanols. ^[51]	12
Figure 1.14 - Rationale behind fluorination effect on pK _{AHY} of cyclohexanols.	13
Figure 1.15 - Effect of fluorination on (a) anti-inflammatory action and (b) FXR agonism. ^[54]	14
Figure 1.16 – Effect of fluorination on conformational stability in (a) fluoroamines and (b) fluorohydrins. ^[45a, 55]	15
Figure 1.17 - Effect of fluorine introduction on lipophilicity. Adapted from ref. ^[47]	16
Figure 1.18 - Effect of fluorination on logP of fluorinated alcohol derivatives. ^[60]	17
Figure 1.19 - 3-deoxy-3-fluoro CDCA target analogues.	18
Figure 1.20 - Predicted pK _{AHY} changes in 2- and 4-fluorinated CDCA.....	19
Figure 2.1 - Synthetic plan for 3-deoxy-3-fluoro derivatives.	21

Figure 2.2 - Common deoxofluorinating reagents.	23
Figure 2.3 - Rationalisation for β -facial selectivity of epoxidation.	26
Figure 2.4 - X-ray crystal structure of $\Delta 2\beta,3\beta$ -epoxide 2.22.	26
Figure 2.5 - Expected coupling constants for geminal and vicinal ^1H - ^{19}F coupling.	27
Figure 2.6 - ^1H and ^{19}F NMR spectra of 3β -fluoro derivative.	28
Figure 2.7 - H7 coupling in 3β -fluoro derivatives 2.2.15 and 2.2.16.	29
Figure 2.8 - Desired 3α -fluoro CDCA and UDCA analogues.	30
Figure 2.9 - Key peaks in $^1\text{H}/^{19}\text{F}$ NMR spectrum of 2.3.6.	34
Figure 2.10 - Proposed mechanism for TEMPO catalysed alcohol oxidation under basic (B) conditions. [O] denotes the secondary oxidant (NaClO) which allows regeneration of the catalyst.	35
Figure 2.11 – ^1H NMR spectrum of 2.38 compound (a) before and (b) after epoxidation.	39
Figure 2.12 – ^{19}F NMR spectrum of 2.38 (a) before and (b) after epoxidation.	40
Figure 2.13 - 3-Deoxy-3-fluoro derivatives and associated DEX-numbers.	41
Figure 2.14 - Cytotoxicity screening of (a) MCF-7 and (b) MDA-MB-231 cell lines with 3-deoxy-3-fluoro analogues highlighted in red, NZP-084 is OCA and is highlighted in green. Data obtained from collaborators Prof Helen Osborne and Dr Fran Greco. ..	42
Figure 2.15 - Dose response curve for NZP-208 on cytotoxicity of (a) MCF-7; and (b) MDA-MB-231 cell lines. Data obtained from collaborators Prof Helen Osborne and Dr Fran Greco.	43
Figure 2.16 - Cell death identification of MCF-7 cell line Data obtained from collaborators Prof Helen Osborne and Dr Fran Greco.	45
Figure 2.17 - FXR reporter assay. Data obtained from collaborators Prof Helen Osborne and Dr Fran Greco.	47
Figure 3.1 - Retrosynthetic analysis of 2β - and 4β -fluoro derivatives.	49
Figure 3.2 - Common N-F based electrophilic fluorination reagents.	50

Figure 3.3 - Single crystal X-ray structures of (a) 3.13; and (b) 3.15.....	53
Figure 3.4 - Second retrosynthetic analysis of 2 α - and 4 α -fluoro derivatives.....	56
Figure 3.5 - Nucleophilic sources of fluoride.	57
Figure 3.6 - Hoffman elimination of TBAF. ^[64]	57
Figure 3.7 - Proposed enol acetate formation and subsequent hydrogenation.	59
Figure 3.8 - Second retrosynthetic analysis of 2 α - and 4 α -fluoro derivatives.....	61
Figure 3.9 - Potential transition states for 2- and 3-fluoride attack of Δ 2 β ,3 β -epoxide.	62
Figure 3.10 - Potential transition states for 3- and 4-fluoride attack of Δ 3 β ,4 β -epoxide.	62
Figure 3.11 - Acidic and basic fluoride mediated epoxide openings.	63
Figure 3.12 - Proposed route towards epoxides 2.22 and 2.23.....	64
Figure 3.13 - 3D representation of 4 α -fluorohydrins 3.76 and 3.78.	73
Figure 3.14 - Retrosynthetic analysis of 2,2-fluoro derivatives.	75
Figure 3.15 - Crude ¹⁹ F NMR spectra of TBS-OTf silyl enol ether fluorination.....	77
Figure 3.16 - ¹⁹ F NMR spectra following LDA mediated silyl enol ether formation of 3.13.	78
Figure 3.17 - Towards deoxyfluorination substrate 3.82.	79
Figure 3.18 - Key section of ¹ H NMR spectrum of 3.84.....	80
Figure 3.19 - Potential influence of 7-OR stereochemistry on 4,4-difluorination.	84
Figure 3.20 - Proposed introduction of the 4,4-difluoro moiety <i>via</i> 4-keto deoxyfluorination. .	90
Figure 4.1 - Single instance of a ≤ 2.00 Å C-F • • • H-X contact found in Howard <i>et al</i> ^[136] study.	96
Figure 4.2 - Analysis of C-H•••F interactions in neutral fragments: (a) bond distance; (b) bond angle. Adapted from ref. ^[140]	96
Figure 4.3 - Inositol derivatives synthesised by Bernet and Vasella. ^[150]	100
Figure 4.4 - Cyclophane derivative C-F•••H-O bond. Adapted from ref. ^[151]	100
Figure 4.5 - Naphthol derivative C-F•••H-O bond.....	101

Figure 4.6 - Crystal structure of 4.5. Adapted from ref. ^[153]	102
Figure 4.7 - Fluorinated carbohydrates containing a C-F•••H-O hydrogen bond.	103
Figure 4.8 - Investigations of pyranoside C-F•••H-X bonds. ^[137] All values given in Hz.....	104
Figure 4.9 - Comparison of H2-OH torsion angles in pyranosides. ^[137]	104
Figure 4.10 - Caged molecule containing exceptional C-F•••H-O bond. Adapted from ref. ^[147]	105
Figure 4.11 - F•••H interactions within rigid cyclohexanol systems.....	106
Figure 4.12 - 4 α -F•••HO-7 β -interaction within 3.76 and 3.78.	109
Figure 4.13 - Assignment of 3.78 ¹ H NMR spectrum.....	109
Figure 4.14 - Assignment of key dd as C7-OH.....	110
Figure 4.15 - C7-OH peak from ¹ H NMR spectra in CDCl ₃ and [D ₆]-DMSO.	110
Figure 4.16 - High temperature ¹ H NMR spectra of 3.78 in [D ₆]-DMSO.....	111
Figure 4.17 - ¹⁹ F NMR spectra of 3.78 at varying temperatures.....	113
Figure 4.18 - Single crystal X-ray structure of 3.78.....	114
Figure 4.19 - Single crystal X-ray structure of 3.76.....	114
Figure 4.20 - 2 α -fluoro derivatives used as IR standards.	115
Figure 4.21 - Comparison of X-H region of 3.66 and 3.78 IR spectra.	116
Figure 4.22 - Comparison of X-H region of 3.68 and 3.76 IR spectra.	117
Figure 4.23 - Correlation between calculated $V_{\alpha}(r)$ and pK_{AHY} . Adapted from ref. ^[159]	119
Figure 4.24 - Comparison of K and cK values for 1.17, 1.15 and 3.78/4.20.....	120
Figure 4.25 - Targetted 4,4-difluoro compounds 4.21 and 4.22	121

Acknowledgements

Firstly I would like to thank my supervisor Professor Bruno Linclau. His continued support, guidance and passion have been invaluable during my studies in Southampton. I am grateful for the opportunity to carry out my PhD under his supervision, and I have learnt a great deal from him. I would also like to thank my industrial supervisor Dr Alex Weymouth-Wilson for his advice, help, and excellent leadership of the growing bile acid project.

I would especially like to thank the EPSRC and Dextra Laboratories for funding the project.

I'd like to thank everyone in the Linclau group over the three years, in no particular order: Gemma, Zhong, Clement, Julian, Steph, Guillaume, Florent, Gert-Jan, Lucas, Rob, Ben, Rachel, Nick, Ramakrishna, JB, Lewis, and any others who have escaped my memory. You have all helped me along the way, and together made what can be a stressful experience into an enjoyable one. The endless listening to Taylor Swift was a particular highlight. Specific thanks go to:

- Gemma for always making me laugh, along with keeping us all safe in the lab.
- Zhong, Ben, Gert-Jan and Rachel for their detailed proofreading of my thesis.
- Clement, Julian, Steph, Guillaume, Florent, Nick and the rest of the French contingent for the joie de vivre they bring to the group.
- Zhong for keeping me company on our 5 km park runs, for all the helpful discussions in the bile acid project, and for reassuring me that everything will be "fine".
- Neil for his management of the NMR facilities and for running (and kindly explaining to me) detailed NMR experiments.
- Julie and Sarah for mass spectrometry services and Mark for X-ray structural analysis.
- Dr Jerome Graton for collaboration on the hydrogen-bonding project, and for kindly proof-reading the fourth chapter of this thesis.

Thanks go to my friends and family, especially my mum, dad and brother for their constant encouragement and support. I must thank my girlfriend Tamsin, for always being there when I need her, and for always being able to put a smile on my face, even after the toughest of days.

And finally I would like to mention my high school chemistry teacher Mr Travers. Even if you may never read this thesis, or see this acknowledgement, it is you who really inspired me to take up chemistry in the first place. I know I would not be in this position without you, so for that I'd like to say thanks.

Abbreviations

AA	Amino acid
AIM	Atoms in molecules
ASN	Asparagine
BA	Bile acid
BCCL	Breast cancer cell line
BCP	Bond critical point
BOM	Benzyloxymethyl
BSEP	Bile salt export pump
CA	Cholic acid
cAMP	Cyclic adenosine monophosphate
CDCA	Chenodeoxycholic acid
CNS	Central nervous system
COSY	Correlation spectroscopy
CSDS	Cambridge Structural Database System
DAST	Diethylaminosulfur trifluoride
DCA	Deoxycholic acid
DCM	Dichloromethane
DEAD	Diethylazodicarboxylate
DFT	Density functional theory
DIPA	Diisopropylamine
DIPEA	Diisopropylethylamine
DMAP	4-(Dimethylamino)pyridine
DMF	Dimethylformamide
DMP	Dess-Martin periodinane
DMPU	1,3-Dimethyl-2-oxohexahydropyrimidine
ESI	Electrospray Ionisation
FG	Functional group
FTIR	Fourier transform infrared spectroscopy
FXR	Farnesoid X receptor
GI	Gastrointestinal
GLP-1	Glucagon-like peptide 1
GPCR	G-protein coupled receptor
HB	Hydrogen bonding

HBA	Hydrogen-bond acceptor
HBD	Hydrogen-bond donor
HIS	Histidine
HMBC	Heteronuclear multiple-bond correlation spectroscopy
HPLC	High performance liquid chromatography
HRMS	High-resolution mass spectrometry
HSQC	Heteronuclear single-quantum correlation spectroscopy
IMHB	Intramolecular hydrogen bond(ing)
IPA	Isopropanol
IUPAC	International Union of Pure and Applied Chemistry
LCA	Lithodeoxycholic acid
LDA	Lithium diisopropylamide
LDL	Low-density lipoprotein
LRMS	Low-resolution mass spectrometry
m.p	Melting point
mCPBA	<i>meta</i> -Chloroperbenzoic acid
MF	Mitochondrial function
MOM	Methyloxymethyl
MS	Mass spectrometry
MW	Molecular weight
NASH	Non-alcoholic steatohepatitis
NBO	Natural bond orbital
NBS	<i>N</i> -Bromosuccinimide
NMP	<i>N</i> methylpyrrolidinone
NMR	Nuclear magnetic resonance
O/N	Overnight
OCA	Obeticholic acid
PBC	Primary biliary cirrhosis
PD	Parkinson's disease
PE	Petroleum ether 40/60
pTSA	<i>para</i> -Toluenesulfonic acid
R _f	Retention factor
RT	Room temperature
SAR	Structure activity relationship
SET	Single-electron transfer
SHP	Small heterodimer partner

SM	Starting material
TBAF	Tetrabutylammonium fluoride
TBAT	Tetrabutylammonium difluorotriphenylsilicate
TBS/TBDMS	<i>t</i> -butyldimethylsilyl
TEMPO	<i>N</i> -oxy-2,2,6,6-tetramethylpiperidine
TGR5	Takeda G-protein-coupled receptor 5
THF	Tetrahydrofuran
TLC	Thin layer chromatography
TMS	Trimethylsilyl
TRP	Tryptophan
TYR	Tyrosine
UDCA	Ursodeoxycholic acid
UV	Ultraviolet
VAL	Valine
vdW	van der Waals

Chapter 1: Introduction

1.1 Introduction to bile acids

1.1.1 Structure and numbering

By convention, steroids are depicted as shown below, with the A-ring on the bottom left hand side (e.g. cholestane **1.1**, **Figure 1.1**).^[1] Substitutions to the top face of the ring are denoted β and those on the bottom face as α . Bile acids are derivatives of cholestane, and have a unique *cis*-A,B ring juncture (e.g. CDCA, **1.2**), a feature which is vital for their physiological properties, but also an important consideration in chemical synthesis.^[2]

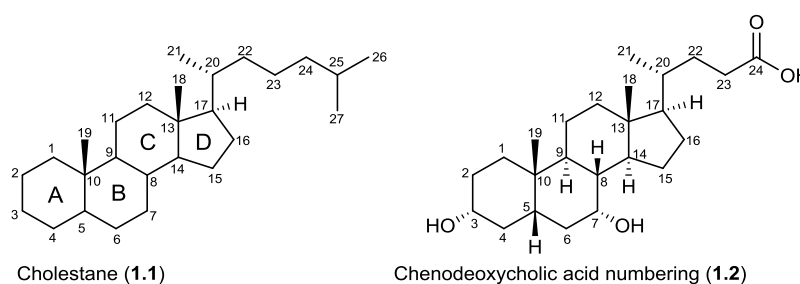


Figure 1.1 - Numbering of bile acid skeleton.

1.1.2 General introduction of endogenous bile acids

Bile acids (BAs) are a group of amphipathic steroids that form the main constituent of bile in vertebrates.^[3] The precise constitution of bile varies from species to species, but they are all products of cholesterol metabolism in the liver. In humans, cholic acid (CA) **1.3** and chenodeoxycholic acid (CDCA) **1.2** are the primary bile acids produced hepatically (**Figure 1.2**). A large proportion of BAs are conjugated to alanine and taurine at the C24 carboxylic acid to increase aqueous solubility,^{[4],[5]} before being released into the gastrointestinal (GI) tract to aid digestion (**Section 1.2.1**). In the intestine they are exposed to the gut flora, to which they are absorbed and subsequently enzymatically modified. This results in the formation of secondary bile acids deoxycholic acid (DCA) **1.4** and lithocholic acid (LCA) **1.5** through 7-deoxygenation. Ursodeoxycholic acid (UDCA) **1.6** is the 7 β -OH epimer of CDCA, and is also formed through the action of bacteria on primary BAs.

Chapter 1

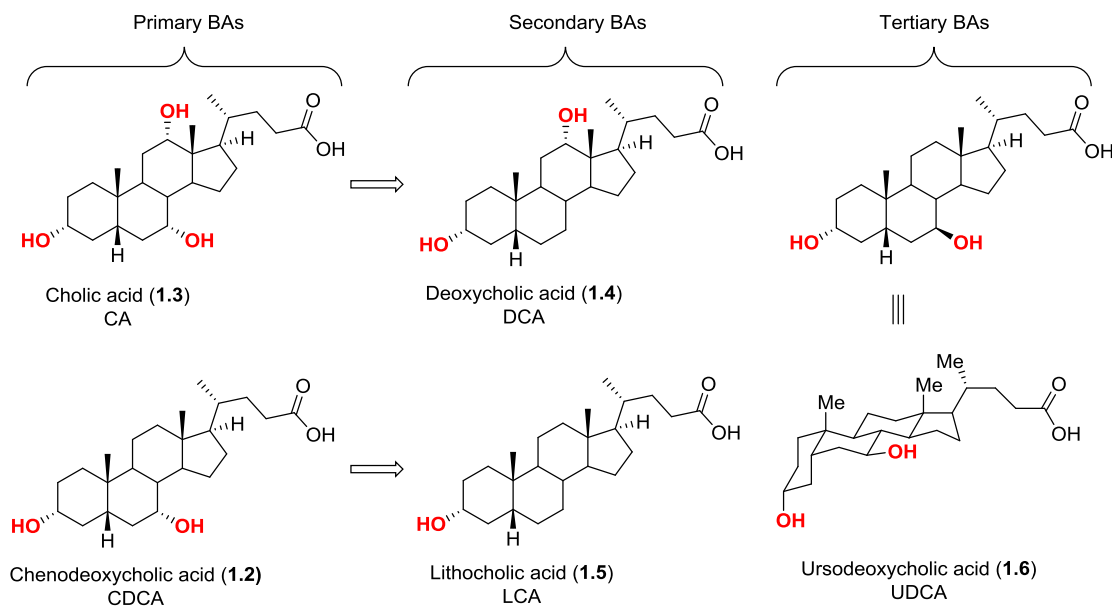
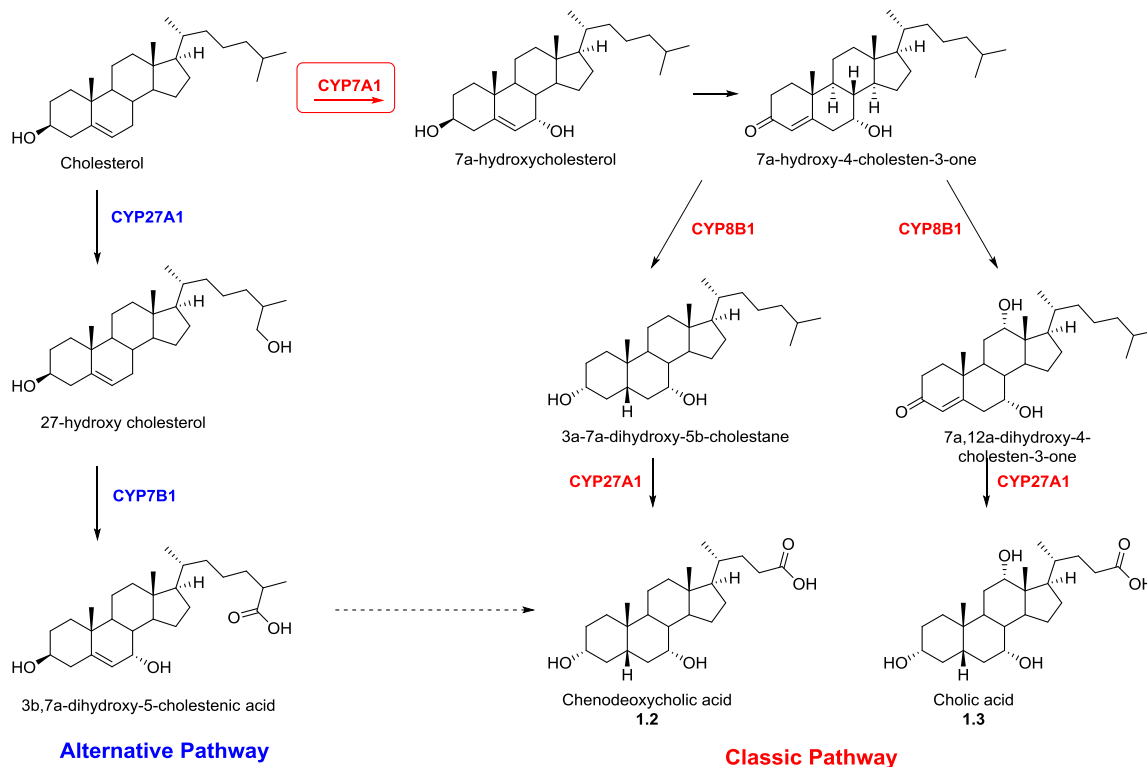


Figure 1.2 - Key primary and secondary human bile acids.

1.1.3 Bile acid biosynthesis

Two main pathways are understood to be responsible for this transformation, the classic pathway and the alternative pathway (**Scheme 1.1**).^[4b, 6] The classic (or neutral) pathway accounts for >90% of bile acid biosynthesis. It is initiated by cholesterol 7 α -hydroxylase (CYP7A1), which is also the rate limiting step. The alternative (or acidic) pathway produces <10% of the bile acid pool and is initiated by CYP27A1 which first hydroxylates cholesterol at the 27-position.



Scheme 1.1 - Bile acid biosynthesis *via* alternative (blue) and classic (red) pathways.^[4b, 6]

A high proportion (90-95%) of bile acids released for digestion are reabsorbed back into the ileum and colon, before transportation to the liver.^[4a] This recycling process is known as enterohepatic circulation, and relies on the highly regulated active transport of bile acids by intestinal epithelial cells. Although a high proportion of bile acids are involved in enterohepatic circulation, the biosynthesis of BAs is key in the homeostasis of cholesterol.^[7]

1.2 Physiological role of bile acids

1.2.1 Absorption of dietary lipids

The importance of bile acids as physiological detergents has been known for nearly fifty years.^[8] Unlike with phospholipid micelle formation where a polar 'head'-group opposes a long hydrophobic tail, the amphipathic character of bile acids arises from the two faces of the molecule (**Figure 1.3**).^[9] They aid the solubilisation, emulsification and absorption of hydrophobic molecules through the formation of mixed micelles with phospholipids.^[5]

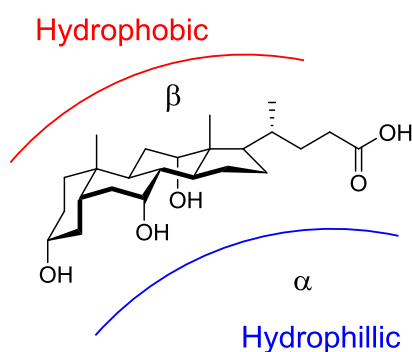


Figure 1.3 - Hydrophobic β -face and hydrophilic α -face of cholic acid.

1.2.2 Historic importance of bile acids in therapeutic treatment

1.2.2.1 Medicinal uses of UDCA

Ursodeoxycholic acid **1.6** (**Figure 1.2**) has been used for centuries in traditional Chinese medicines for the treatment of biliary stone disease.^[10] It was originally isolated from the gall bladder of bears (Ursidae), as these species are unique in producing UDCA as a primary bile acid.^[11] The structure of UDCA was first elucidated in the early 1900's, however it would take another 70-80 years before it would gain major clinical traction in the western world.^[12]

Primary biliary cirrhosis (PBC) is a chronic autoimmune disease that causes destruction of bile ducts, which progresses to liver cirrhosis and ultimately death by liver failure.^[13] UDCA is the only known treatment for PBC and has been used in this regard for a number of years. Once administered, UDCA is involved in extensive enterohepatic circulation like other endogenous BAs. Its main mechanism of action is thought to be through the displacement of hepatotoxic BAs

(DCA and LCA) from the bile acid pool.^[14] Its overall efficacy has been questioned on numerous occasions, however its regular use has been shown to lead to an overall decrease in mortality for those diagnosed with PBC.^[15]

1.2.2.2 Bile acid sequestrants

Bile acid sequestrants are a class of orally administered, non-absorbed, positively charged, polymers that bind negatively charged BAs in the GI tract, leading to their excretion.^[16] They are a class of drugs that have been tested and evaluated for 3 decades, showing a 20% reduction in LDL cholesterol accompanied by a 19% relative risk reduction of myocardial infarction (in male cases with hypercholesteromea). By preventing the reabsorption of BAs back into the gut lumen, bile acid synthesis is increased and, as BAs are synthesised from cholesterol, an overall lowering of LDL-cholesterol is seen.

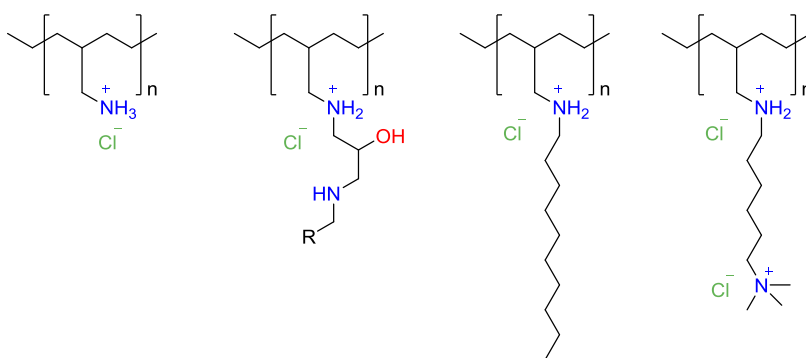


Figure 1.4 - Key constituents of colesevelam hydrochloride polymer.^[16-17]

In 2008, the second generation bile acid sequestrant colesevelam hydrochloride (**Figure 1.4**) was approved for the treatment of hyperglycaemia in type 2 diabetes.^[16-17]

1.2.3 Agonist of the Farnesoid X receptor

The Farnesoid X receptor (FXR) is a nuclear receptor first characterised by Forman *et al* in 1995.^[18] Four years later, numerous groups revealed that bile acids were found to be the endogenous ligands for this orphan receptor.^{[5],[7],[19]} When bound to BAs, FXR induces the expression of the small heterodimer partner (SHP) which in turn interferes with the transcription of CYP7A1, the rate limiting step in the neutral BA synthesis pathway - ultimately leading to a reduction in BA synthesis (**Scheme 1.1**).^[11] Activation of FXR also leads to increased bile acid secretion through the upregulation of the bile salt export pump (BSEP), induction of bile acid conjugation enzymes, and modulation of basolateral efflux, an 'overflow' system for bile acid elimination. FXR is expressed widely in tissues such as the liver and ileum which are vital in enterohepatic circulation.

In addition to the liver and GI tract, FXR has also been shown to be present in both healthy and tumorous breast tissue.^[20] Bile acids were found at high levels in breast cysts, and in the plasma of

postmenopausal women with breast cancer. These findings triggered research into the effect of FXR activation on breast cancer cell lines (BCCLs). Treatment of different BCCLs with known FXR agonists led to cell death *via* apoptosis. The mechanism of action is still poorly understood, but FXR agonism presents another possible tool to treat this life-threatening condition.^[21] There is also evidence to suggest that FXR activation may also help to enforce tumor suppression in both liver and colon cancers.^[22]

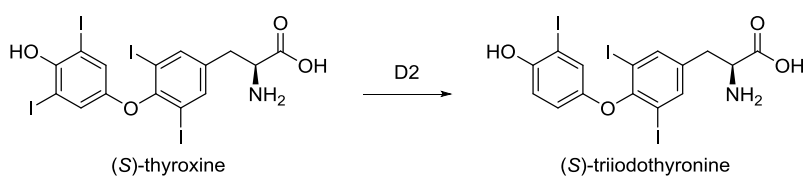
1.2.4 Agonist of TGR5

The discovery of FXR as a bile acid receptor ignited interest in the field which, in 2002, led to the discovery of a membrane bound bile acid receptor, commonly referred to as TGR5.^[23] It is a G-protein coupled receptor (GPCR) expressed in a variety of cells (e.g. gall bladder, white blood cells, brown adipose tissue, muscle, kidney, placenta and the CNS).^[11, 24] Activation of TGR5 is associated with the intracellular accumulation of cyclic adenosine monophosphate (cAMP), and the effects of this response differ depending on cell type.^[24] Some of these responses are discussed below for context.

TGR5 is expressed in several cells relevant to inflammation including monocytes and macrophages and it has recently emerged that the immunosuppressive effects of BAs is due to TGR5 activation.^{[25],[26]} A number of mechanisms are thought to contribute to TGR5's ability to modulate inflammation including the lowering of pro-inflammatory cytokines interleukin-1 α (IL-1 α), IL-1 β , IL-6 and tumour necrosis factor- α (TNF- α).^[27]

The activation of TGR5 on the surface of Kupffer cells (a population of liver macrophages) and sinusoidal endothelial cells in the liver has been shown to activate endothelial NOS (nitric oxide synthase) and induce nitric oxide (NO) release.^[26] NO is a critical signalling molecule known to act as a vasodilator, possess antiatherogenic properties, prevent platelet aggregation and monocyte-endothelial cell adhesion.^[28]

In 2006 Watanabe *et al*^[29] established that TGR5 agonism increased the energy expenditure in brown adipose tissue, an effect known to prevent obesity and insulin resistance. The intracellular accumulation of cAMP is associated with the induction of type 2 iodothyronine deiodinase (D2). Activation of D2 leads to the conversion of inactive thyroid hormone (*S*)-thyroxine (T₄, **Scheme 1.2**) into the active (*S*)-triiodothyronine (T₃), a major component in the control of cellular basal metabolism (**Scheme 1.2**).^[27]



Scheme 1.2 - Conversion of T₄ to T₃.

Recent studies have also shown the role of TGR5 activation in the release of glucagon-like peptide 1 (GLP-1), a known stimulator of insulin secretion.^[30]

1.2.5 UDCA and Parkinson's Disease

Parkinson's disease is a common, debilitating neurodegenerative disease.^[31] It currently has no known cures, and its prevalence world-wide is predicted to double by 2030. Previous attempts to develop therapies have tended to fail in clinical trials due to poorly designed *in vitro* and *in vivo* models that targeted downstream effects on toxins, rather than the root cause of the disease.

A mutation in the LRRK2 gene is the most common monogenetically inherited cause of late-onset Parkinson's disease (PD), and this mutation has been linked to poor mitochondrial function (MF).^[31] Poor MF is one of the main contributors to the pathogenesis of PD, and the recovery of this has the potential to treat the disease.^[32] Mortiboys *et al*^[33] have shown that UDCA **1.6** is able to rescue mitochondrial function in mutant LRRK2 patient tissue of those both disease manifesting and non-manifesting carriers. It therefore has great potential in future neuroprotective clinical trials.

1.3 Bile acid receptor agonists

1.3.1 Endogenous bile acids

It is evident that FXR, TGR5 and MF recovery are potential therapeutic targets, with the scope to treat diseases as diverse as diabetes, Parkinson's and some cancers.^[21, 24, 33] As endogenous BAs are natural agonists for these targets, thus they are a starting point to investigate more potent molecules.

Early screenings of the key human primary and secondary bile acids against FXR and TGR5 showed stark differences in potencies for each receptor (**Figure 1.5**).^[19b, 24] CDCA **1.2** was shown to be the strongest activator of FXR, although it binds to the receptor with a similar potency to that of LCA **1.5**. Deoxycholic acid **1.4** showed low activity against FXR, while cholic acid **1.3** was found to be inactive.

The key difference between CDCA/LCA and DCA/CA is that the former lack a 12 α -OH group. The rationale behind the dramatic difference in potencies is that the FXR pocket does not provide any

polar residues with which the 12 α -OH group can bind. This leads to repulsive interactions of DCA/CA with the receptor, and ultimately a decrease in potency.^[34] A hydrogen-bonding interaction of the 7 α -OH with the side chain oxygen of TYR366 provides a favourable energy gain for CDCA upon binding, which is the reason for its stronger interaction than LCA.

The affinities of the endogenous bile acids with TGR5 are more similar to each other, with potencies within an order of magnitude.

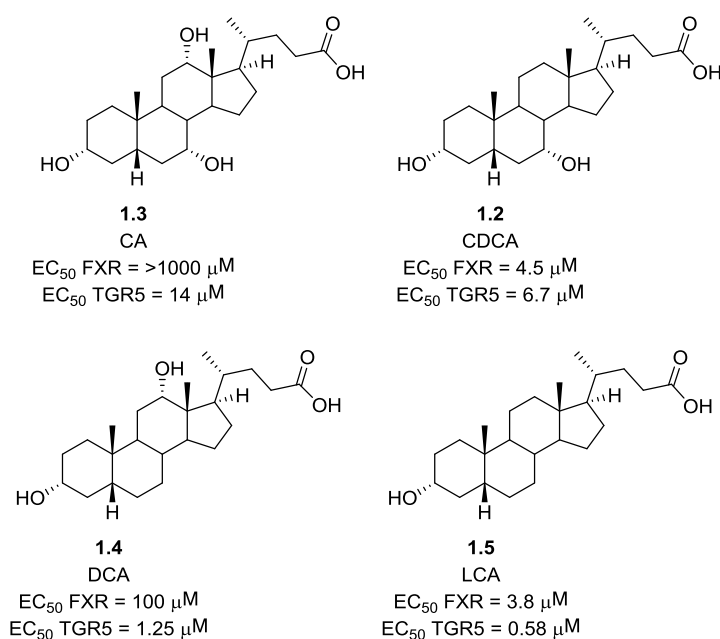


Figure 1.5 - Comparison of EC₅₀ values of prominent bile acids. ^[19b, 24]

1.3.2 Semi-synthetic agonists

Pellicciari and co-workers have consistently led the way in the development of more potent FXR and TGR5 receptor ligands.^[24, 34-35] Their discovery in 2002 that a 6 α -ethyl group increases the potency towards FXR from 4.5 μ M in CDCA **1.2** to 0.099 μ M in obeticholic acid (OCA) **1.9** was revolutionary (**Figure 1.6**). The reason for this huge increase in potency has been attributed to the 6 α -ethyl group of OCA binding with high affinity to a hydrophobic pocket within the FXR receptor.

Further functionalisation of the bile acid core led to the discovery of INT-777 (**1.10**, **Figure 1.6**)^[35b] as a potent and selective TGR5 agonist, and INT-767^[36] (**1.11**) as a potent dual FXR/TGR5 agonist.

As a result of their emerging potential as medicinal therapies, Pellicciari co-founded Intercept Pharmaceuticals as a route to further investigate BAs and guide any successful candidates through clinical trials. Obeticholic acid **1.9** has shown excellent therapeutic potential in phase 3 clinical trials for the treatment of both primary biliary cirrhosis^[37] (PBC) and non-alcoholic steatohepatitis^[38] (NASH). These diseases are in desperate need of new treatments, and the successful results of these trials has led to postulations of OCA becoming a blockbuster drug.^[39]

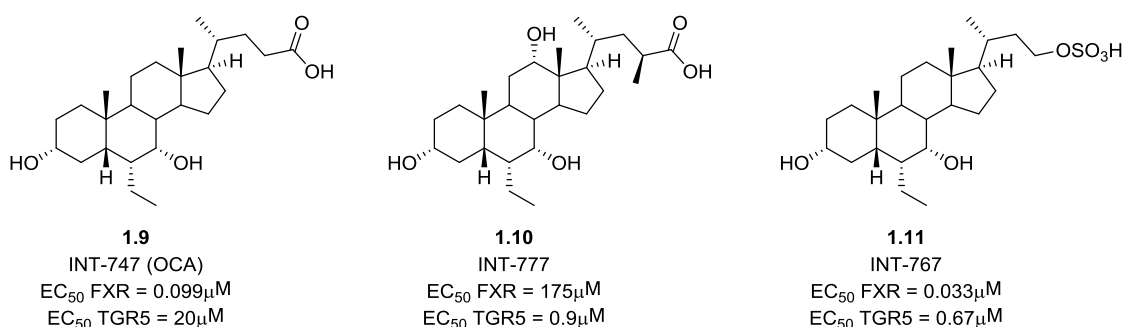


Figure 1.6 - Intercept Pharmaceutical's most promising drug candidates. [24, 34-35]

Together the findings have catapulted the field of bile acids from a niche subject, to a major therapeutic area of investigation (**Figure 1.7**).

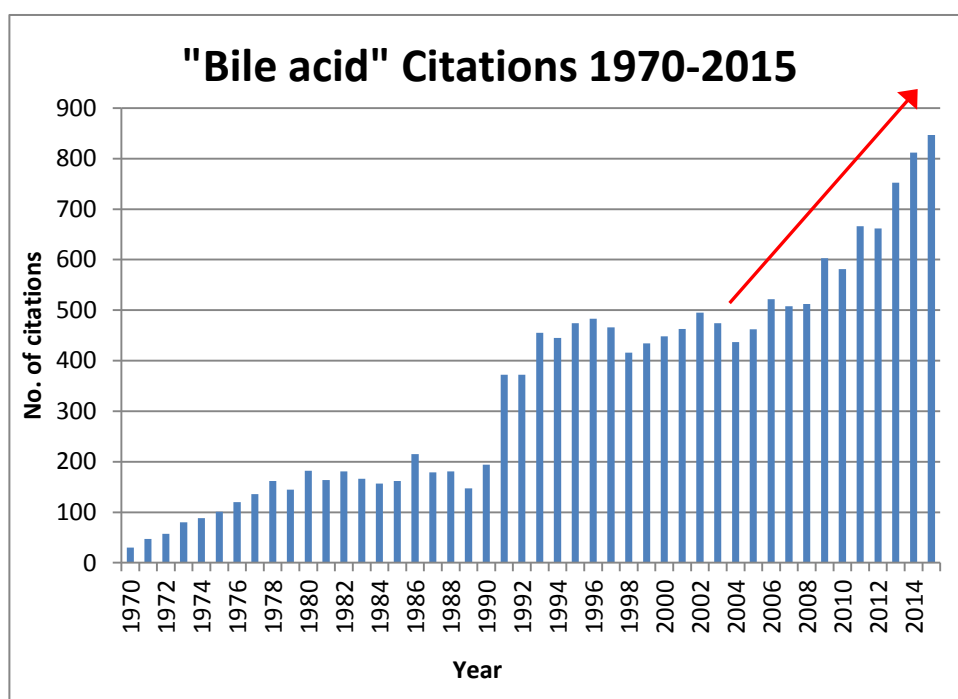


Figure 1.7 - Number of citations for the phrase "bile acid" 1970-2015. Data obtained from Web of Knowledge on 03/08/2016.

1.3.3 Synthetic agonists

There is a very high clinical potential in selective BA receptor agonists, and a number of large pharmaceutical companies (e.g. Hoffmann-La Roche,^[40] Pfizer,^[41] and Novartis^[42]) have developed completely synthetic agonists. Their structures appear to have little relation with their endogenous cousins, but a number have shown excellent potencies (**Figure 1.8**).^[43]

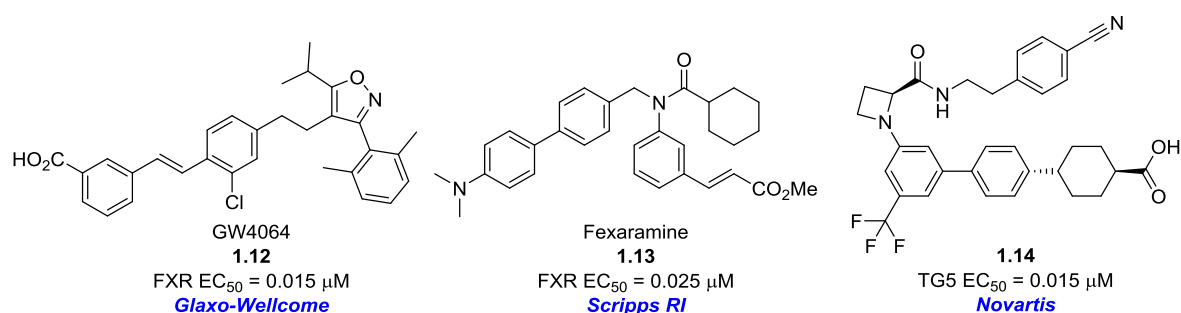


Figure 1.8 - A selection of synthetic FXR and TGR5 agonists.^[43]

1.3.4 FXR binding pocket

A crystal structure of OCA **1.9** bound to FXR was resolved in 2003 by Mi *et al.*^[34] The 3 α -OH was shown to interact with a number of polar amino acid (AA) residues in the FXR binding site including tryptophan 468, histidine 444 and tyrosine 358 (**Figure 1.9**). These residues are capable of interacting as a HBD, a HBA, and also through electrostatic dipole-dipole type interactions.

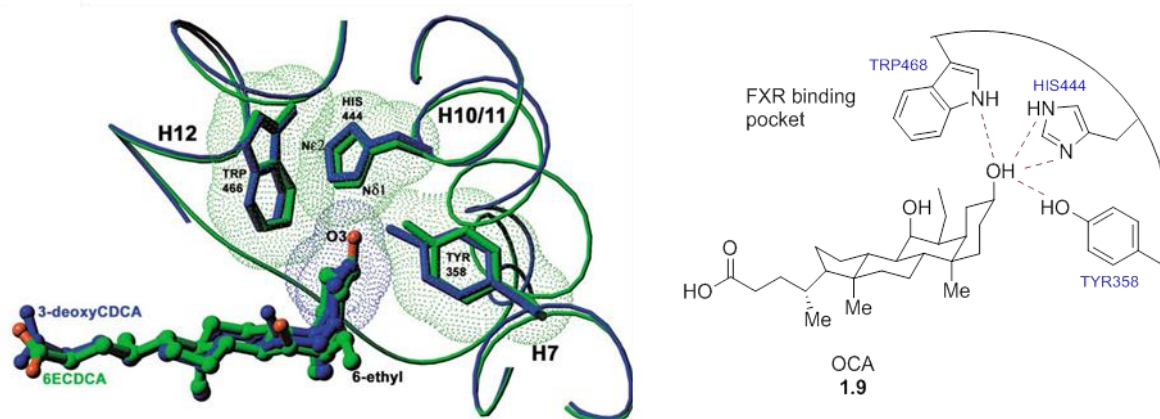


Figure 1.9 - FXR binding pocket and proposed 3 α -OH interactions. Adapted from ref.^[34]

1.3.5 TGR5 binding pocket

A high-resolution single-crystal X-ray structure of the TGR5 receptor is yet to be published, however *in silico* studies by Macchiarulo *et al.*^[44] have shed light on the potential receptor-substrate interactions (**Figure 1.10**). The two BA receptor substructures differ greatly, which is unsurprising given their diverse homologies. Similar to FXR (**Figure 1.9**), there are a number of potential interactions with polar AAs, in particular asparagine 93 and tyrosine 89.

The modulation of hydrogen bonding properties of the 3 α -OH has the potential to modify the interactions of a BA derivative with FXR and TGR5. The ultimate goal would be to discover a highly potent and selective BA receptor agonist, however any correlation between HBA/HBD capacity and receptor affinity could lead to a better understanding the FXR/TGR5 binding pockets, and the BA field in general.

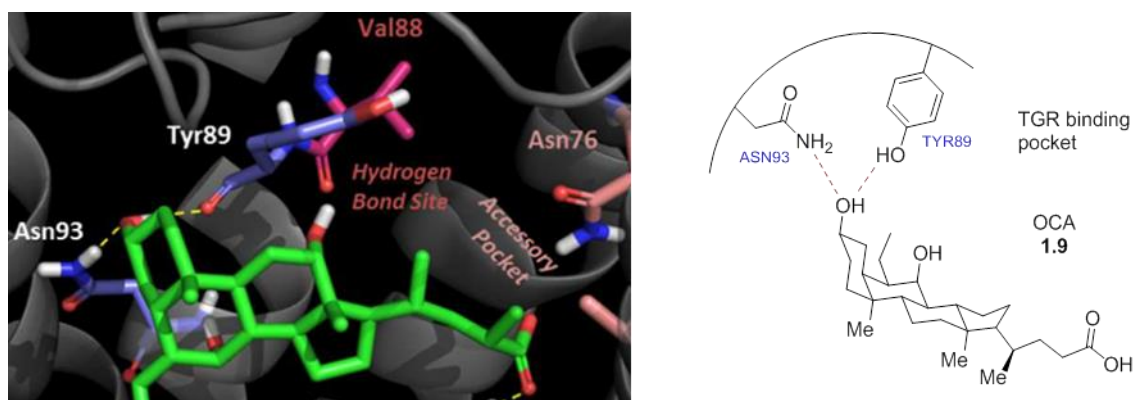


Figure 1.10 - TGR5 binding pocket and proposed 3 α -OH interactions. Adapted from ref.^[44]

1.4 Overview of organo-fluorine chemistry

1.4.1 The C-F bond

Fluorine is the most electronegative element in the periodic table, and forms very strong, short bonds to carbon.^[45] Due to the large difference in electronegativity between carbon and fluorine, the C-F bond is highly polarised. With a substantial δ^- charge residing on the fluorine and an equal δ^+ charge on the carbon, there is a large ionic component to the bond. Fluorine forms the strongest single bond to carbon (**Table 1.1**),^[45a] and the bond strength increases with higher fluorine substitution (from 453 kJ mol⁻¹ in CH₃F, to 546 kJ mol⁻¹ in CF₄) due to the ionic nature of the bond.^[46] This strong electrostatic interaction significantly lowers the lone pair donation from fluorine, and results in C-F groups being only weakly co-ordinating to hydrogen-bond donating (HBD) groups.

Table 1.1 - Key features of C-X bonds.^[45a]

C-X Bond	Bond dissociation energy / kJ mol ⁻¹	VDW radii of X / Å	Bond length / Å	Electronegativity (Pauling)
C-F	441	1.47	1.35	4.0
C-H	413	1.20	1.09	2.1
C-O	351	1.52	1.43	3.5
C-C	348	1.70	1.54	2.5
C-Cl	328	1.74	1.77	3.0
C-N	292	1.55	1.47	3.0

Considering sterics alone, the C-F bond is an excellent isostere of the C-H group.^[45a] The process of selectively replacing hydrogen with fluorine is used extensively in medicinal chemistry, often as a way to slow/prevent metabolism by hepatic enzymes (increasing biological half-life, $t_{1/2}$).^[47] The increase in electronegativity also has a profound effect on the properties of neighbouring functional groups (**Section 1.4.2**).

Despite the similar size to the C-H group, organic fluorine is more similar in terms of electrostatics to a hydroxyl group (**Table 1.1**).^[45a] The more modest change in electronegativity from C-OH to C-F leads to the formation of similar dipole-dipole interactions, but the loss of an acidic hydrogen atom precludes any HBD capacity. The exchange of a C-OH for a C-F bond is an excellent way to probe binding sites and molecular interactions due to the minimal change in sterics, and specific change in co-ordinating capacity. The CF₂ group is also an excellent isostere for a hydroxyl residue due to the similar size and dipole of CHOH (**Figure 1.11**). Gem-difluoro compounds can also be used as isosteres for carbonyl derivatives, however the change in hybridisation from sp² to sp³ can lead to other conformational changes.

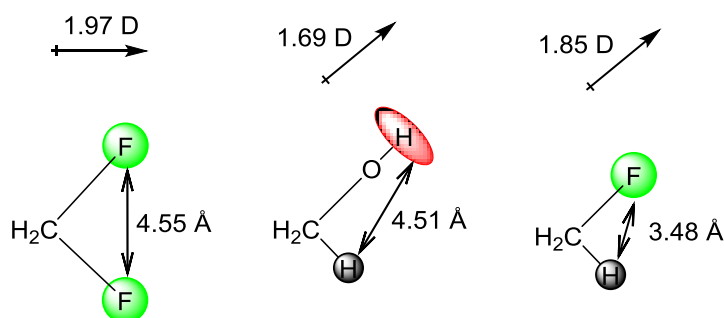


Figure 1.11 - Comparison of CF₂ and CHF as isosteres of an alcohol group.^[48]

1.4.2 Effect of fluorine introduction on neighbouring functional groups

1.4.2.1 Acidity (pK_a)/hydrogen bond donating capacity (pK_{AHY})

The extreme electronegativity of fluorine has a substantial effect on the acidity/basicity of neighbouring functional groups (FGs).^[47] A significant increase in acidity is observed in the mono-, di- and tri-fluorination of acetic acid (**Figure 1.12a**), a direct result of the strong fluorine inductive effect drawing electron density away from the carboxylic acid, stabilising a build up of the negative charge upon deprotonation.

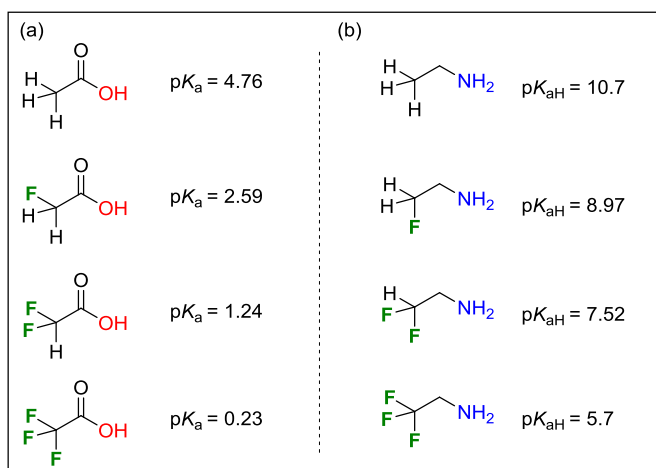


Figure 1.12 - Effect of poly-fluorination on (a) acidic and (b) basic groups.^[47]

A similar observation is seen when considering the effect of fluorination on aliphatic amine groups (**Figure 1.12b**).^[47] Increasing fluorine substitution leads to an increase in $pK_{a(H)}$ due to the inductive effect of fluorine. This technique of fluorination around amine functionalities has been used to great effect in medicinal chemistry to provide large improvements in bioavailability, *via* attenuation of basicity.^[49]

Up until recently the effect of fluorine on HBD capacity took a very simplistic approach, with assumptions that the large inductive effect meant that fluorination “*always increases hydrogen bond acidity*”.^[50] In reality the effect of fluorine introduction is more nuanced, and a recent publication by our group^[51] was able to show both significant increases and decreases in the hydrogen bond donating capacity (pK_{AHY}) of rigid cyclohexanol fluorohydrins (**Figure 1.13**).

The pK_{AHY} values of **1.15-1.24** were determined using FTIR spectroscopy (**Figure 1.13**).^[51] Introduction of a good hydrogen-bond acceptor (e.g. *N*-methylpyrrolidinone, NMP) into a dilute solution of alcohol (R-OH) leads to a decrease in the ν_{OH} stretching band, and appearance of the R-OH...NMP stretching band at a lower frequency. From the integration of these peaks at different concentrations of NMP, a value for the equilibrium constants K/K_{AHY} can be obtained. The larger the value of K (and thus pK_{AHY}), the further the equilibrium lies towards the hydrogen-bonded conformer, and the greater the hydrogen bond donating capacity of the R-OH group.

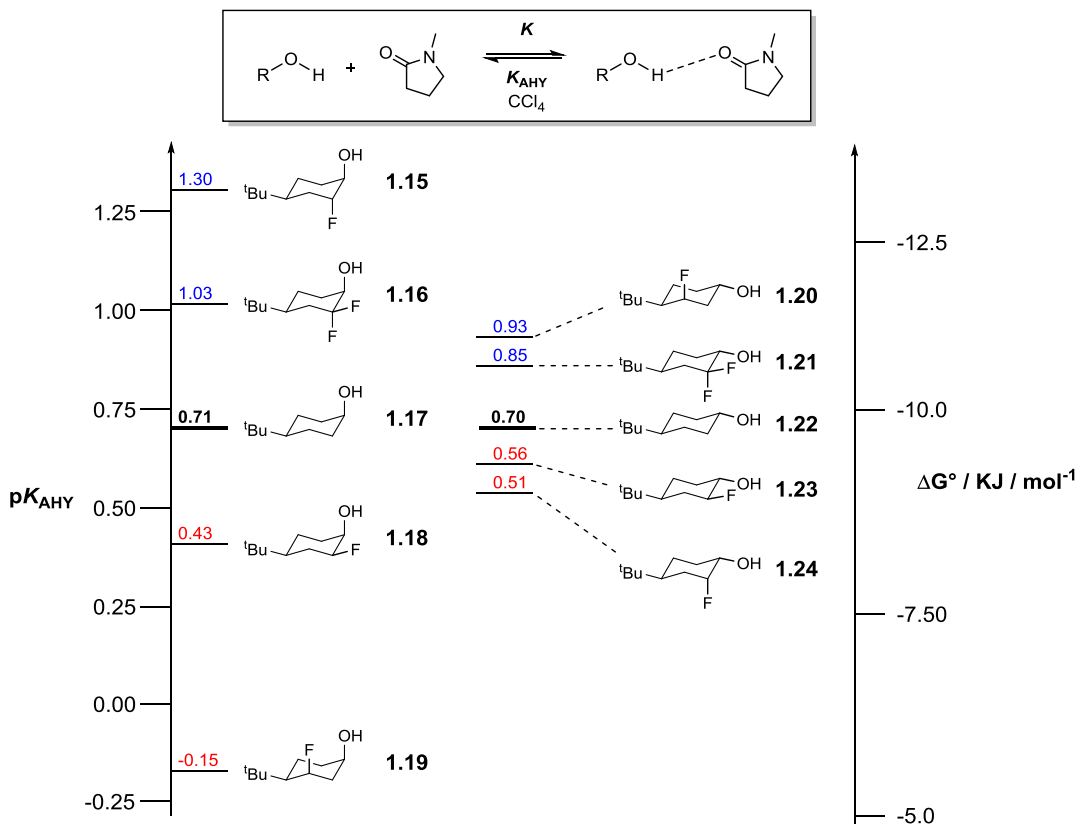


Figure 1.13 - Effect of fluorination on pK_{AHY} of cyclohexanols.^[51]

The large increase in the pK_{AHY} for fluorohydrins such as **1.15** and **1.20** (**Figure 1.13**) is concurrent with previous assumptions^[50] and can be rationalised by a simple consideration of the inductive effect of fluorine (e.g. **1.15**, **Figure 1.14**).^[51]

Large attenuations in pK_{AHY} were more unexpected however, with a near total loss of hydrogen bond donating capacity for **1.19**.^[51] This effect can be explained by the formation of a 6-membered intramolecular O-H...F-C hydrogen bonding interaction, which significantly impairs donation to other HBA groups (**Figure 1.14**). The effect was best shown through the observation of a 12.1 Hz through-space coupling between the F and H-O groups in **1.19** (in CCl_4), and indicates their close proximity in space. Atoms in molecules (AIM) calculations of **1.19** also revealed a bond critical point (BCP) between O-H...F-C, with a significant charge transfer (17 kJ mol^{-1}) between the fluorine lone pair and σ^*_{OH} .

A drop in pK_{AHY} was also observed in vicinal fluorohydrins **1.23** and **1.24**, although to a lesser extent.^[51] This effect is also explained by an intramolecular O-H...F-C interaction (**Figure 1.14**). AIM analysis indicated no BCP was present for this 5-membered ring, indicating an electrostatic rather than an H-bonding interaction is occurring.

Probably the most surprising result was that difluoro derivatives such as **1.16** and **1.21** had significantly lower pK_{AHY} values than mono-fluorinated derivative **1.15** (**Figure 1.14**), despite the larger dipole of the CF_2 vs. CHF moiety.^[51] This effect is partly rationalised by the formation of O-H...F-C interactions that lower the availability of the acidic proton, but also due to difluorohydrin **1.16** containing a C-F bond in an anti-relationship to the C-O bond.

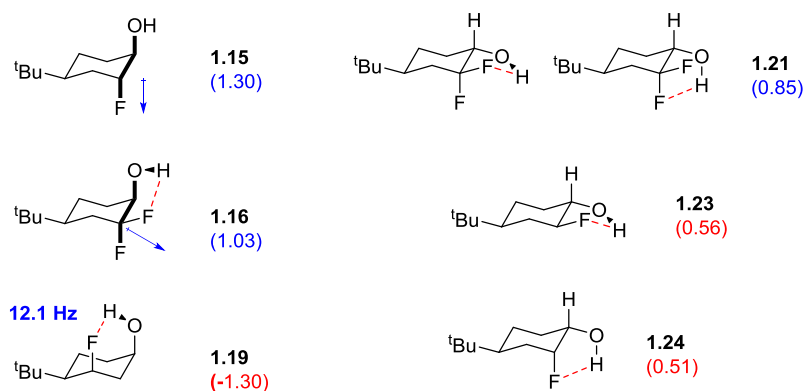


Figure 1.14 - Rationale behind fluorination effect on pK_{AHY} of cyclohexanols.

The quantitatively measured pK_{AHY} values were in excellent correlation with calculated values.^[51] The calculations were based on the Kenny molecular descriptor $[V_{\alpha}(r)]$, which is defined as the electrostatic potential of the donor atom at distance r .^[52] This will be further explored in **Section 4.2.5**.

A classic example of the use of fluorine in medicinal chemistry is 9 α -fluorohydrocortisone **1.26** (**Figure 1.15a**).^[53] The replacement of the 9 α -H in hydrocortisone **1.25** with fluorine leads to **1.26** which has a 10-fold increase in anti-inflammatory action. An explanation for this dramatic increase was not given at the time, however considering recent studies^[51] (e.g. **Figure 1.13**), it can be postulated that the pK_{AHY} modulation following fluorine introduction could lead to an increase in HBD capacity of C11-OH, leading to the increase in potency.

The effect of fluorination on potency has also been used on the CDCA **1.2** skeleton (**Figure 1.15b**).^[54] An attenuation of potency was observed in the 6 α -fluoro derivative **1.27**, while an increase is observed for the 6 β -fluoro derivative **1.28**, compared to CDCA (EC₅₀ = 4.5 μ M, **Figure 1.5**). The fluorohydrin moiety in 6 α -fluoro derivative **1.27** is analogous to that of fluorohydrin **1.18** (**Figure 1.13**) where a lower pK_{AHY} value than the control was observed. The 6 β -fluoro derivative **1.28** is analogous to that of fluorohydrin **1.15** (**Figure 1.13**) where a large increase in pK_{AHY} value vs. the control was found. The stronger HBD 7 α -OH group in **1.28** may be able to interact more strongly with a HBA amino acid residue in the FXR binding pocket, and is one possible explanation for the greater than 3-fold increase in potency over CDCA.

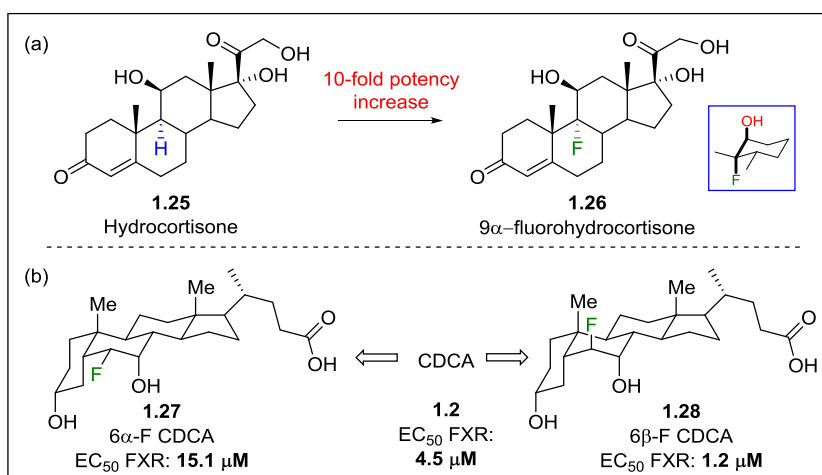


Figure 1.15 - Effect of fluorination on (a) anti-inflammatory action and (b) FXR agonism.^[54]

1.4.2.2 Conformational effects

The C-F bond may not be able to form particularly strong C-F...H-X bonds, but its large dipole allows it to influence molecular conformation quite dramatically when in the proximity of neighbouring heteroatoms. In the case of quaternary ammonium salts (e.g. **1.29** and **1.30**, **Figure 1.16a**), a favourable interaction occurs between the C-F and N-H bonds, with the two favouring alignment in solution.^[45a]

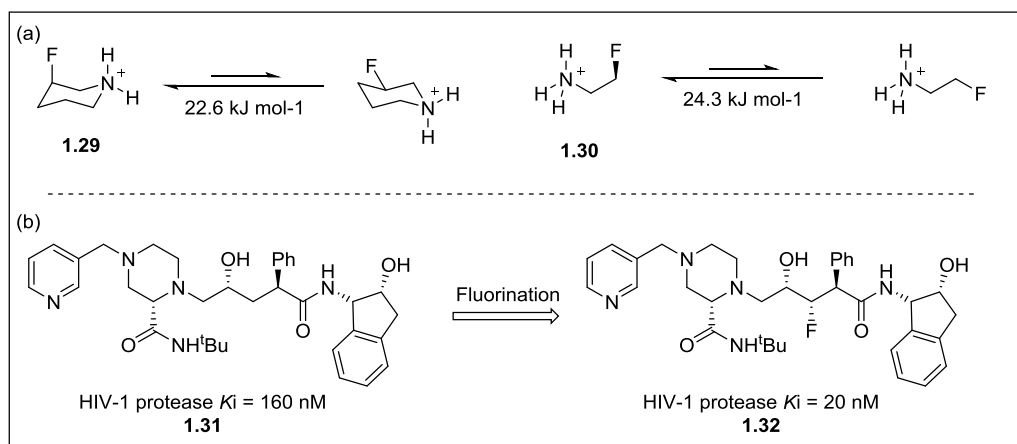


Figure 1.16 – Effect of fluorination on conformational stability in (a) fluoroamines and (b) fluorohydrins.^[45a, 55]

The influence of fluorination on the conformation of neutral alcohol groups has also been shown to have a significant effect on pharmacological properties (**Figure 1.16b**).^[55] The introduction of a vicinal-fluorine in HIV-1 protease inhibitor **1.31** led to an 8-fold potency increase in analogue **1.32**. The significant gain in potency can be explained through the stabilisation of the preferred binding conformation. A combination of dipole-dipole interactions between the C-O and C-F bonds,^[45a] along with a stabilising intramolecular O-H•••F-C interaction (**Figure 1.14**) could both lead to the stabilisation of the binding conformer.^[51, 56] These effects help to rigidify the alkyl chain, which leads to a smaller entropy loss upon binding, and thus an overall increase in affinity. Our group is also keenly interested in this area, in particular the influence of fluorination on conformer population.^[56] This will further be explored in **Chapter 4**.

1.4.3 Effect of fluorination on log*P*/lipophilicity

The affinity of a molecule or functionality for a lipophilic environment is known as lipophilicity.^[57] It is often measured as the partition coefficient between water and octanol, and its value is quoted as log*P*. Lipophilicity is the most important physicochemical property to consider in medicinal chemistry, with large contributions to molecular solubility, membrane permeability, potency, selectivity, and important impacts on metabolism and pharmacokinetics.^[58] Compounds with very high lipophilicity (>5) are often subjected to rapid metabolic turnover, poor aqueous solubility and ultimately poor uptake and absorption. The ideal value of log*D*¹ is often stated as <5, although some state that the optimum value is between 1 and 3.^[59]

¹ The distribution coefficient (log*D*) is the measure of lipophilicity for ionisable species (e.g. those containing acidic and/or basic groups) at a given pH.

The selective control of lipophilicity is key in any successful drug discovery project.^[57a, 58] Site-selective fluorination of drug candidates is one way that $\log P$ modulation can be achieved.^[47, 50, 55] On average, an increase in $\log P/D$ is observed with fluorine introduction but there are still numerous cases where a $\log P/D$ decrease is observed (**Figure 1.17**), in particular with mono-fluorinated alkyl chains. Contrastingly, site-selective fluorination of aryl derivatives generally leads to an increase in $\log P/D$.² One of the main reasons the data is skewed towards an average increase in $\log P$ is that the aryl fluoride functionality is introduced much more frequently in drug discovery programs, so there is a much larger sample size. Additionally, the $\log P/D$ of aromatic compounds was much easier to measure by the traditional UV-based determination method, which is obviously challenging for alkyl fluorides that lack a UV chromophore.

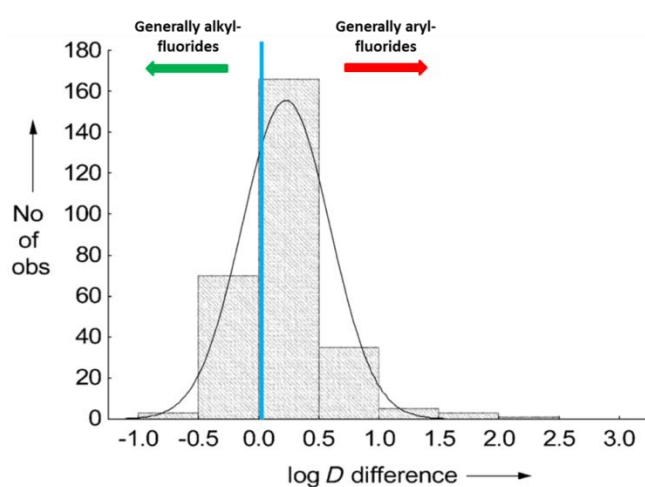


Figure 1.17 - Effect of fluorine introduction on lipophilicity. Adapted from ref.^[47]

A recent paper by our group^[60] disclosed a novel $\log P$ determination method based upon ^{19}F NMR analysis. This publication allowed for the in-depth study of fluorination/deoxyfluorination on the $\log P$ of aliphatic compounds and a number of interesting trends have emerged from these studies. Firstly, in the case of β -, γ - and δ -monofluorination (e.g. 2-fluoroethanol, **Figure 1.18a**) a significant decrease in $\log P$ was observed. In cases of trifluorination (e.g. 2-trifluoroethanol) a significant increase in $\log P$ was found compared to the unfluorinated compound. For difluorination the effect was more nuanced, and less extreme than mono- and tri-fluorination - with both slight increases and decreases of $\log P$ observed.

² As the C-F bond depolarises the aromatic ring.

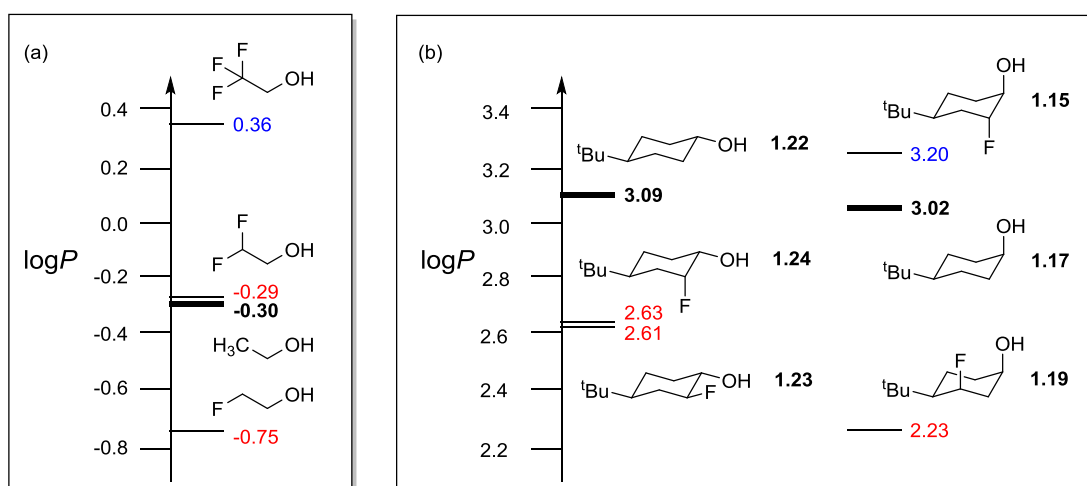


Figure 1.18 - Effect of fluorination on logP of fluorinated alcohol derivatives.^[60]

A decrease in logP was observed in the equatorial monofluoro-cyclohexanols **1.23** and **1.24**, when compared to the parent compound **1.22** (Figure 1.18b).^[60] The co-axial fluorohydrin **1.19** also showed the expected decrease in logP compared to the unfluorinated compound **1.17**. The larger decrease in logP of **1.19** vs. **1.23/1.24** is attributed to a compounding effect of the aligned C-F and C-OH dipoles, that gives the compound a very large dipole (higher polarity generally equals lower lipophilicity).³ In contrast, there was an increase in logP for vicinal trans-diaxial fluorohydrin **1.15**, this is a rare example of aliphatic monofluorination leading to an increase in lipophilicity. This result is despite a much greater acidity than the parent compound **1.17** (Figure 1.13), and was rationalised by a counteraction of the opposing C-F and C-OH dipoles, leading to an overall decrease in molecular polarity.

³ An extreme example of compounding dipoles leading to very high molecular polarities, was recently shown by O'Hagan and co-workers in an all-*cis*-hexafluorocyclohexane.[61] N. S. Keddie, A. M. Z. Slawin, T. Lebl, D. Philp, D. O'Hagan, *Nat. Chem.* **2015**, *7*, 483-488.

1.5 Project aim

1.5.1 Bile acid analogues

There is a clear scope for further research into the bile acid receptors, and the development of selective agonists is one way in which this can be achieved (**Section 1.3**). Over the years numerous publications have disclosed work towards semi-synthetic bile acid analogues,^[35-36, 54] but this research has tended to focus on modifications to either the bile acid B-ring and/or side-chain. To our knowledge, little to no research has been undertaken on developing A-ring BA analogues for the purpose of FXR/TGR5 agonism. CDCA was chosen as the substrate for FXR/TGR5 agonism, and UDCA analogues would be developed for the purposes of mitochondrial recovery in Parkinson's disease.

It is clear from **Section 1.4** that fluorine introduction is able to modify a plethora of physicochemical properties, and is thus used extensively in the pharmaceutical industry for property optimisation. This thesis will contain my work towards the synthesis of fluorinated A-ring BA derivatives, which were designed to selectively modulate substrate-receptor interactions. My efforts have been concentrated on the synthesis of two main classes of fluorinated BAs: 3-deoxy-3-fluoro analogues (**Chapter 2**) and 2- and 4-fluorinated analogues (**Chapter 3**). The rationale behind each will be briefly discussed below.

1.5.1.1 3-Deoxy-3-fluoro analogues

The selective 3-deoxy-3-fluorination of CDCA (**Figure 1.19**) has the potential to modify H-bonding properties of the 3 α -OH moiety while retaining similar sterics (i.e. **Figure 1.11**).

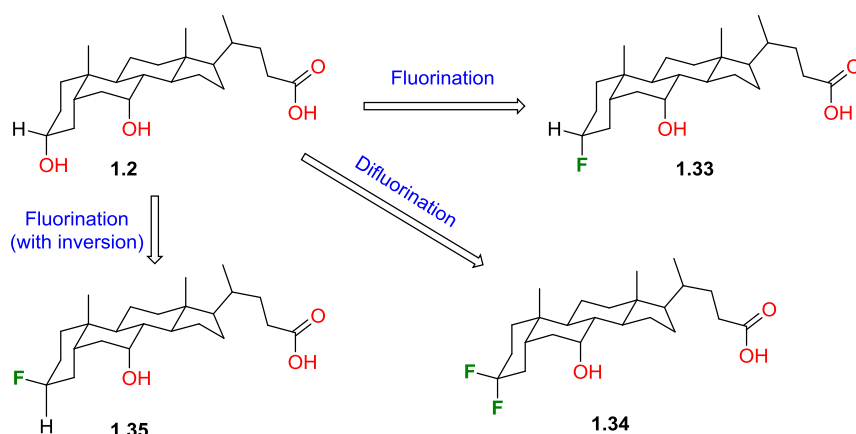


Figure 1.19 - 3-deoxy-3-fluoro CDCA target analogues.

1.5.1.2 2- and 4-Fluorinated analogues

The experimentally obtained pK_{AHY} changes from the cyclohexanol model system (**Figure 1.13**) can be applied to CDCA to predict the effect of fluorination on the acidity of the 3α -OH group (**Figure 1.20**). Hydroxyl groups coloured blue indicate a predicted increase in H-bond donating capacity, while those highlighted in red predict a decrease in H-bond donating capacity. For analogues containing a 4α -fluoro moiety (**1.38** and **1.40**) a secondary interaction with the 7α -OH is predicted and these are highlighted in green.

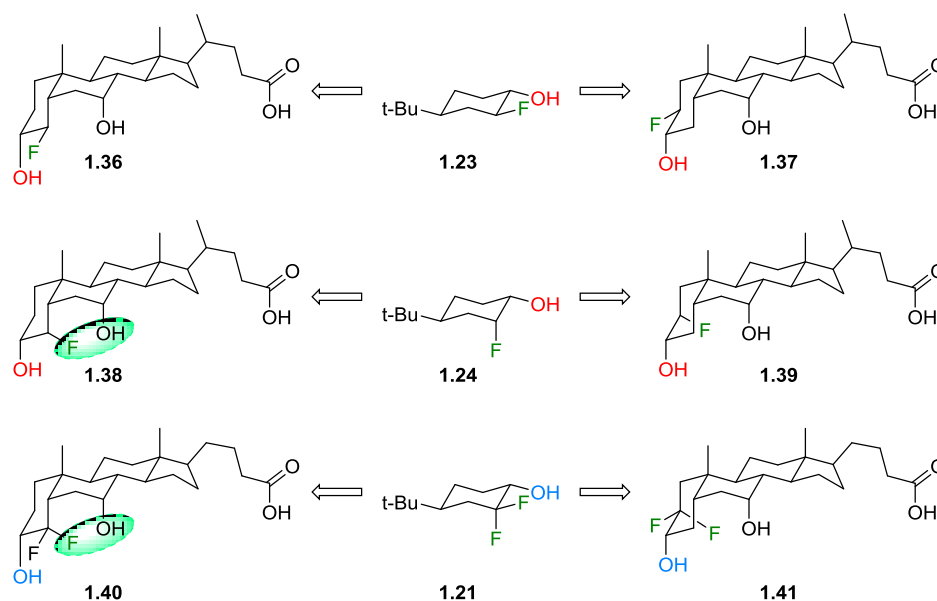


Figure 1.20 - Predicted pK_{AHY} changes in 2- and 4-fluorinated CDCA.

Where possible the UDCA (7β -OH) and iso-BA (3β -OH) analogues will also be targeted.

1.5.2 Analysis of fluorinated BAs to determine intramolecular C-F...H-O hydrogen bond

The 4α -fluorine functionalities in **1.38** and **1.40** (**Figure 1.20**) are predicted to interact with the 7α -hydroxyl moiety in the CDCA skeleton. This interaction is predicted to be similar to that of cyclohexanol **1.19** (**Figure 1.14**), but of a much greater magnitude. Close C-F...H-O interactions such as this are rare in the literature, and currently there are no published examples of a 7-membered ring (such as in **1.38** and **1.40**) involving a strong CF...H-O hydrogen bond. The study of these interactions is vital to gain better insight into the role of organic fluorine as a HBA functionality, which is key when considering the C-F bond as an isostere for the C-OH bond (**Section 1.4.1**). **Chapter 4** will discuss the experimentally and computationally derived physicochemical properties of the 4α -fluoro- 7α -hydroxy derivatives. This work will be presented in the context of other recently published molecules containing a C-F...H-O interaction.

Chapter 2: Synthesis of 3-deoxy-3-fluoro analogues

2.1 Introduction

2.1.1 Retrosynthetic analysis

A retrosynthetic analysis of the 3-deoxy-3 α -fluoro CDCA **1.33** and UDCA **2.1** analogues leads to 3-deoxy-3 α -fluoro-7-oxo bile acid **2.2** (**Figure 2.1a**), with the forward synthesis possible *via* a hydride mediated reduction. Fluoride introduction to form **2.2** can be achieved through a nucleophilic displacement and occurs with inversion of configuration. This leads to 3 β -OH-7-oxo derivative **2.3** as a required intermediate, which can be made *via* inversion of the 3 α -OH of bile acid derivative **2.6**; a starting material available from Dextra Laboratories Ltd.

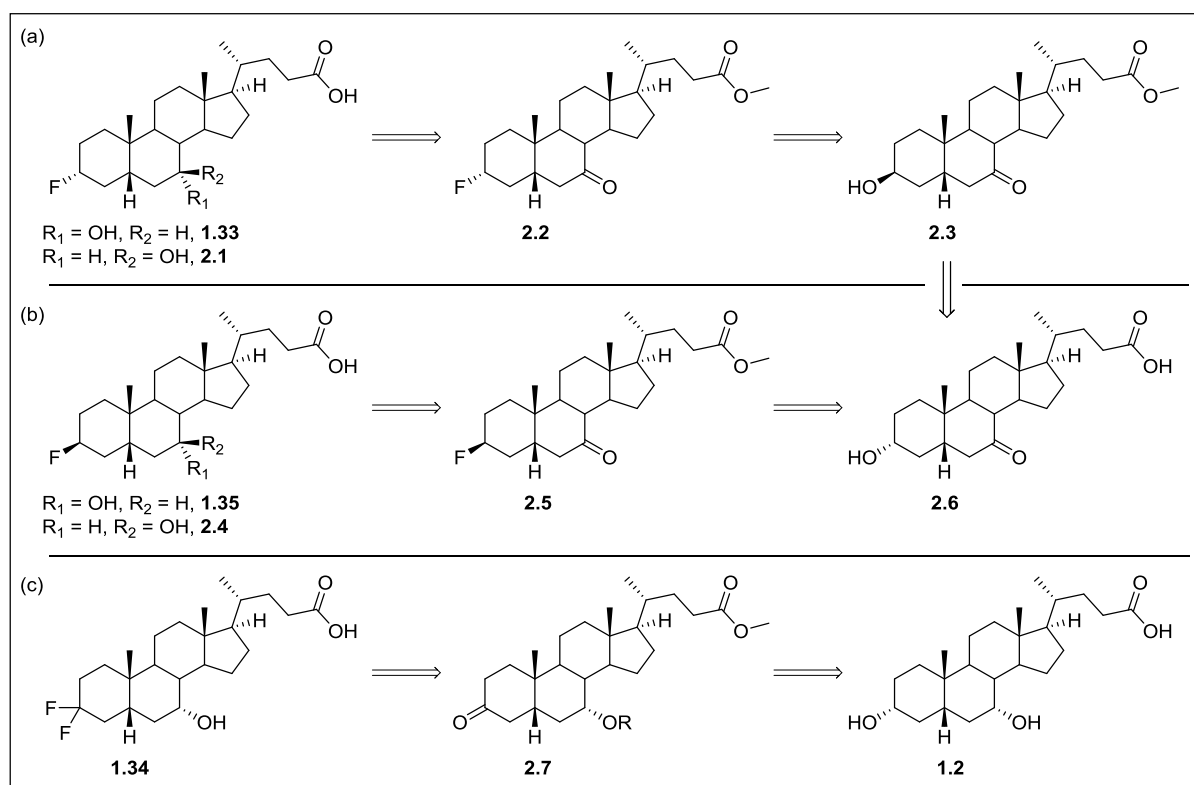


Figure 2.1 - Synthetic plan for 3-deoxy-3-fluoro derivatives.

Bile acid **2.6** is also a direct precursor of the 3-deoxy-3 β -fluoro CDCA **1.35** and UDCA **2.4** analogues, which share 3-deoxy-3 β -fluoro-7-oxo derivative **2.5** as a common intermediate (**Figure 2.1b**). This can be made from **2.6** through methyl ester formation and nucleophilic displacement by fluoride.

The 3,3-difluoro derivative **1.34** can be synthesised from 3-keto **2.7** by deoxofluorination, with the 7 α -OH group suitably protected (**Figure 2.1c**). Intermediate **2.7** can be synthesised from CDCA **1.2** *via* methyl ester protection and selective 3-OH oxidation

2.1.2 Fluorination chemistry

Despite the strong thermodynamic driving force in the formation of carbon-fluorine bonds, the high electronegativity of fluorine leads to inherent challenges in the synthesis of C-F bonds through nucleophilic displacement.^{[62],[63]} The fluoride ion forms very strong hydrogen bonds with water molecules and other HBD groups. These interactions diminish the nucleophilicity of fluoride significantly. It is possible to ensure anhydrous conditions where these interactions are excluded, however this leads to a significant increase in the basicity of fluoride, and associated side-reactions (e.g. elimination) can result.

The low cost of alkali metal fluorides (NaF, KF) make them an attractive fluoride source, but their use is limited by their high lattice energy, and thus low solubility.^{[63],[64]} Fluoride release can be increased by the use of crown ethers (e.g. KF-18-crown-6), however issues of fluoride basicity still remain. Tetrabutylammonium fluoride (TBAF) has increased solubility in organic solvents, and is available as either a solution in THF, or as a ^tBuOH complex. TBAF reagents can show enhanced nucleophilicity compared to alkali metal salts, but again the basicity can lead to side reactions.

The above reagents all require pre-activation of the alcohol as a leaving group (e.g. triflate, tosylate, mesylate). Sulfur fluoride reagents, however, can be used to perform deoxofluorination reactions in one step.^{[63],[64]} Sulfur tetrafluoride has been classically used to transform alcohols directly to alkyl fluorides, ketones to *gem*-difluorides and carboxylic acids to trifluoromethyl derivatives.^[65] In this regard it is a very useful reagent, however its toxicity and gaseous nature have deminished its general utility.

Dialkylaminosulfur trifluorides such as DAST **2.8**^[66] and Deoxo-Fluor **2.9**^[67] (**Figure 2.2**) were developed as safer, easier to handle alternatives to SF₄ for performing deoxofluorinations. They have become very popular reagents, and their synthetic utility made them the preferred reagent(s) for performing alcohol-deoxofluorinations in this thesis. Deoxofluor was developed as a reagent with higher thermal stability (>90 °C), but as DAST is more cost-effective it was preferred for lower temperature reactions.

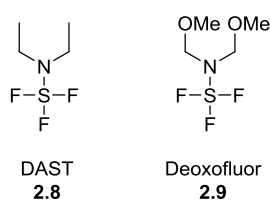
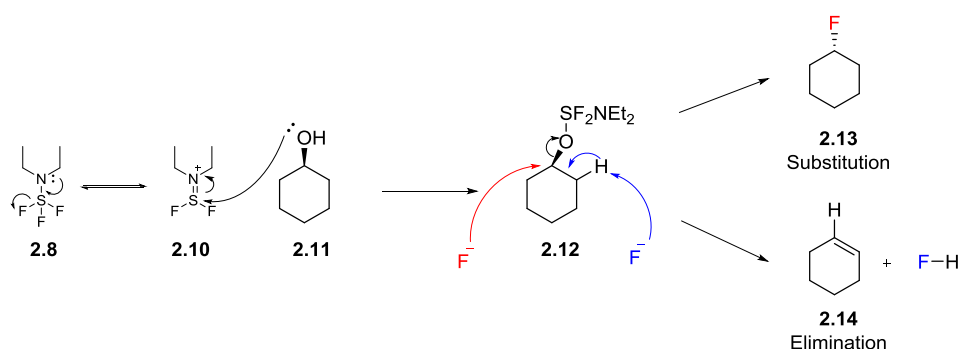


Figure 2.2 - Common deoxofluorinating reagents.

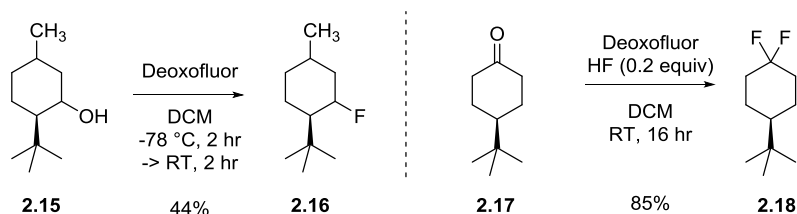
The DAST mediated deoxofluorination mechanism is shown in **Scheme 2.1**. A reversible elimination of a fluoride ion in DAST **2.8** provides an electrophilic intermediate **2.10** that is attacked by a nucleophilic alcohol group (e.g. **2.11**). The resulting $-OSF_2NEt_2$ moiety in **2.12** is an excellent leaving group that can be displaced in a nucleophilic substitution reaction by fluoride to yield **2.13** (with inversion of stereochemistry).⁴ The competing process of elimination is also prevalent given the basicity of the fluoride ion, and the excellent leaving group. Abstraction of an α -proton in **2.12** leads to alkene **2.14**, or a mixture of alkenes if the starting material is asymmetrical.



Scheme 2.1 - Competing substitution and elimination in DAST fluorination.

The reactivity of cyclic ketones towards dialkylaminosulfur trifluorides is known to be much lower than an equivalent alcohol group (**Scheme 2.2**),^[67] and thus higher temperatures and/or HF catalysis may be required to synthesise 3,3-difluorinated derivative **1.34** from ketone **2.7**. In addition to this, parallel work in the Linclau group has shown that the 7-keto moiety in BA substrates required even harsher conditions (>50 °C, neat DAST) to drive difluorination. This means that this functionality need not be protected for the synthesis of the 3-monofluorinated bile acid derivatives **2.2** and **2.5** (**Figure 2.1**).

⁴ Other members of the Linclau group have shown that S_N1 -type reactions are also possible on the BA skeleton (mainly on 7α -OH).

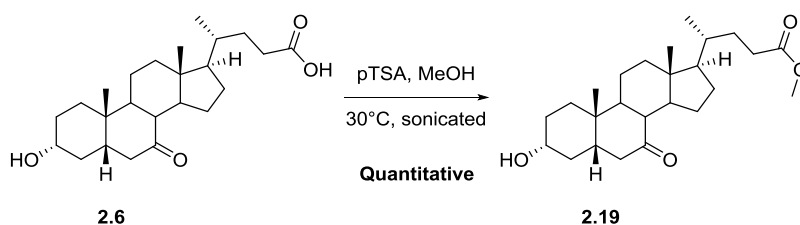


Scheme 2.2 - Comparing reactivities of alcohols and ketones towards deoxofluorination.

2.2 Synthesis of 3 β -fluoro analogues

2.2.1 Methyl ester formation

The first step required towards 3-deoxy-3 β -fluoro CDCA **1.35** and UDCA **2.4** (**Figure 2.1**) was the protection of the carboxylic acid in **2.6** (available from Dextra Laboratories Ltd) as a methyl ester **2.19** (**Scheme 2.3**).

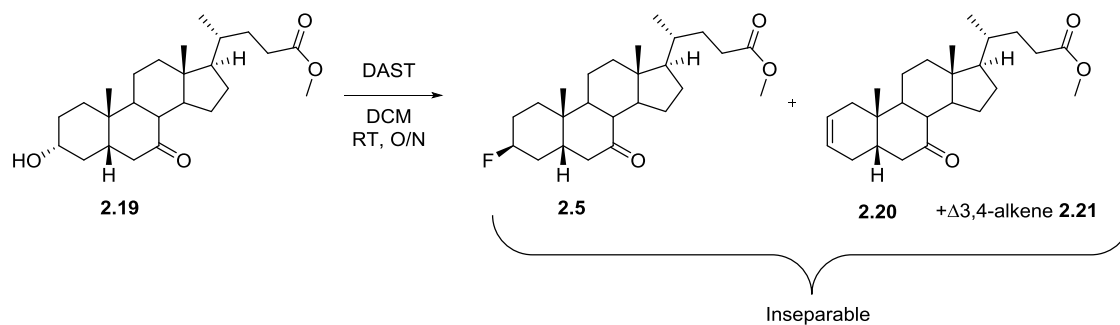


Scheme 2.3 - Formation of methyl ester of 7-keto LCA.

Many groups have published syntheses of BA derivatives, and methyl ester protection has tended to be favoured. Dolle *et al*^[68] (HCl, MeOH, reflux, 15min, 97%), Li *et al*^[69] (H₂SO₄, MeOH, RT, O/N, 95%) and Rohacova *et al*^[70] (HCl, MeOH, 2,2-dimethoxypropane, RT O/N, 94%) have all published successful methods, however previous work in the group had shown that Pelliciarri's 2012 method^[71] (pTSA, MeOH, sonication) was the most consistent. The method was applied to **2.6** (**Scheme 2.3**) and desired methyl ester **2.19** was isolated in a quantitative yield following an aqueous work up.

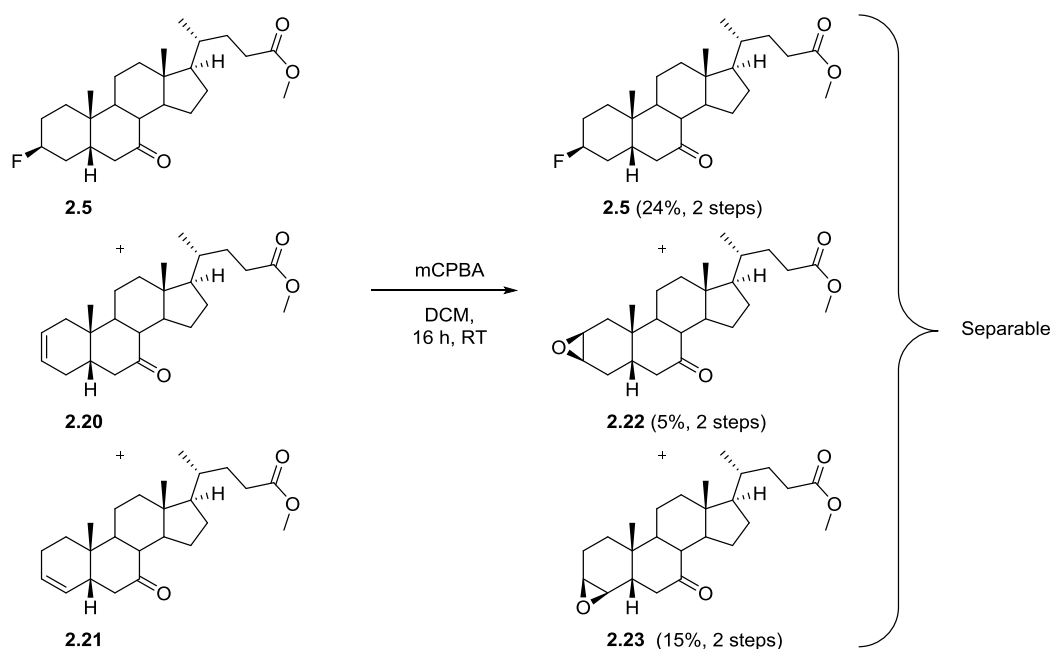
2.2.2 Fluorination

The suitably protected 3 α -hydroxy-7-oxo derivative **2.19** was now a substrate for deoxofluorination. A small scale fluorination with 1.5 equiv of DAST in DCM (**Scheme 2.4**) showed complete consumption of **2.19** after 16 h, with 50% conversion to desired 3 β -fluoro product **2.5**, along with a 30% conversion to alkenes **2.20** and **2.21**. Less than 1% difluorination of the 7-keto was observed. This reaction was subsequently scaled up (500 mg), and a similar ratio of 3 β -fluoro and mixture of alkenes was observed on analysis of the ¹H NMR spectrum. Due to their similar polarities, separation of the products through flash chromatography proved difficult.

Scheme 2.4 - Fluorination of 3 α -OH group with DAST.

2.2.3 Epoxidation

It was decided to effect an epoxidation of the alkene by-products in order to increase their polarity, and thus allow for an easier separation from the desired 3 β -fluorinated product **2.5** (Scheme 2.5).



Scheme 2.5 - Epoxidation of alkene by-products with mCPBA.

The mixture of 3 β -fluoro **2.5** and alkenes **2.20** and **2.21** was dissolved in DCM along with mCPBA (0.5 equiv overall, 1.5 equiv compared to alkene percentage) and the reaction was deemed complete after 16 h at RT (Scheme 2.5). Epoxidation increased the polarity of the by-products, and allowed for the isolation of the desired 3 β -fluoro **2.5** in a 2-step yield of 24%. The $\Delta^{2\beta,3\beta}$ -epoxide **2.22** was formed in a 5% yield (crude, 0% isolated) and $\Delta^{3\beta,4\beta}$ -epoxide **2.23** was formed in a 2-step yield of 15% (crude, 10% isolated). The low isolated yields may be due to the occurrence of Baeyer-Villiger (B-V) reactions on the 7-keto moiety. The lactone by-products of

the B-V reaction could not be isolated, but were isolated in a similar epoxidation discussed in **Section 3.4.3.1.5** (synthesis of 2,2-difluoro analogues).

The complete facial selectivity of the epoxidation step was rationalised to be towards convex β -face given that it is much less sterically hindered than the concave α -face of the bile acid (**Figure 2.3**).⁵

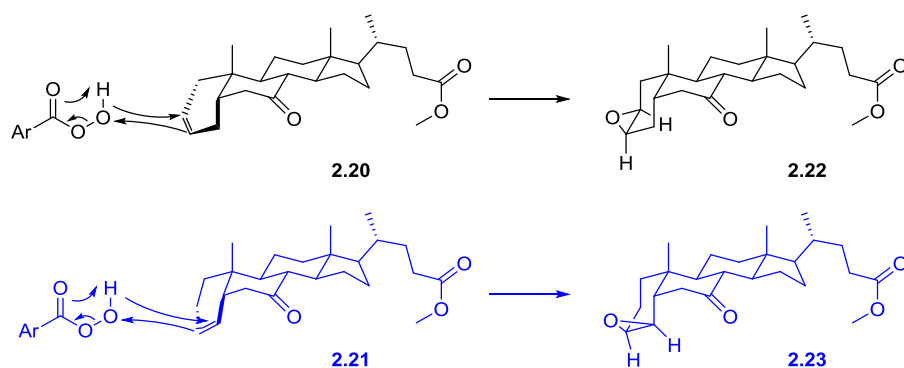


Figure 2.3 - Rationalisation for β -facial selectivity of epoxidation.

The relative stereochemistry of the $\Delta^{2\beta,3\beta}$ -epoxide was confirmed *via* single-crystal X-ray structural analysis (**Figure 2.4**). The regiochemistry of the $\Delta^{3\beta,4\beta}$ -epoxide was established via 2D NMR (in particular HMBC), and the stereochemistry was confirmed upon epoxide opening by various nucleophiles (see **Sections 3.3.5.1** - fluoride and 3.4.4.1 - acetate).

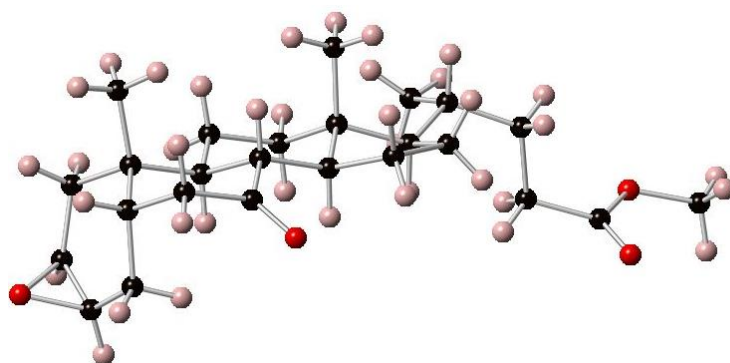


Figure 2.4 - X-ray crystal structure of $\Delta^{2\beta,3\beta}$ -epoxide 2.22.

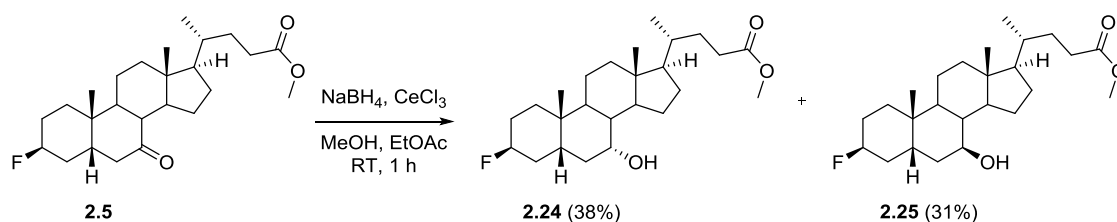
2.2.4 Reduction

As established earlier, both the iso-CDCA **1.35** and iso-UDCA **2.4** were required as final analogues (**Figure 2.1b**). Ideally the synthesis of both 7-OH epimers would be achieved in a single reduction

⁵ The facial selectivity of $\Delta^{2,3}$ - and $\Delta^{3,4}$ -silyl enol ethers towards electrophiles will be explored in **Section 3.1.5**.

step from 3 β -fluoro-7-keto **2.5** (Scheme 2.6). Festa et al^[72] had previously shown that NaBH₄ in a THF/water mixture led to the selective formation of the 7 α -OH in a quantitative yield, however such a high selectivity was undesired. Dangate et al^[73] used a Na/n-propanol system to reduce the 7-keto moiety in their BA, however this time a high selectivity towards the 7 β -OH was seen.

The reduction was first performed on **2.5** using NaBH₄/THF, but only reached 20% completion after 16 hr at room temperature and was thus too sluggish to be considered for scale up. The slow nature of the reaction can be explained by the sterically hindered nature of the 7-keto moiety, and Festa et al^[72] may have used water in their procedure to increase the reaction rate. In order to speed up the rate of reaction a Luche reduction^[74] was performed on **2.5**, using the conditions of Černý et al.^[75] The reaction was deemed complete after 1 h, and both 7 α -OH **2.24** and 7 β -OH **2.25** were isolated in good yields (Scheme 2.6). Negligible reduction of the methyl ester was observed.



Scheme 2.6 - 3 β -fluoro 7-keto reduction.

2.2.5 Product identification through ¹H and ¹⁹F NMR spectroscopy

Hydrogen and fluorine nuclei give characteristic coupling constants to a partnering atom depending on their proximity and spatial relationship.^[76] In particular, the rigidity of cyclohexane structures leads to fixed relationships between the coupling atoms, enabling further confidence of assignment. Some of the relevant experimentally derived coupling constants are shown in Figure 2.5, and these will be used as reference points throughout the remainder of this thesis.

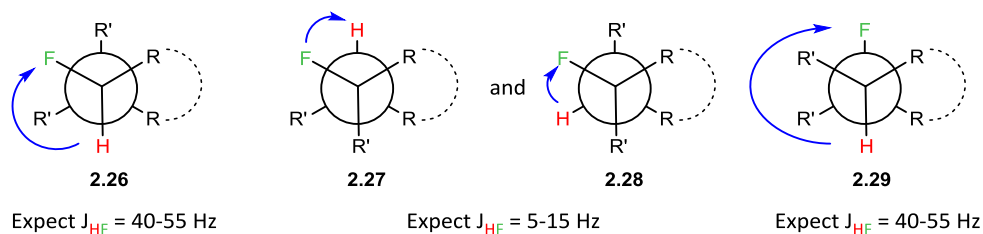


Figure 2.5 - Expected coupling constants for geminal and vicinal ¹H-¹⁹F coupling.

This information was used to confirm the stereochemistry of the 3 β -fluorine atom. Upon analysis of the ¹H NMR spectrum of **2.5** (Figure 2.6), it can be seen that there is a large coupling constant (48 Hz) between **H3** and **F**, typical of a geminal coupling (e.g. **2.26**, Figure 2.5). The proton would also be expected to couple to the *gauche* H2 and H4 protons; these couplings are unresolved in

this case, which is unsurprising given their small magnitude (0.5-2 Hz). If **H3** were axial there would also be two large axial couplings to $H_{2\alpha}$ and $H_{4\alpha}$, as this is not the case **H3** must be equatorial.

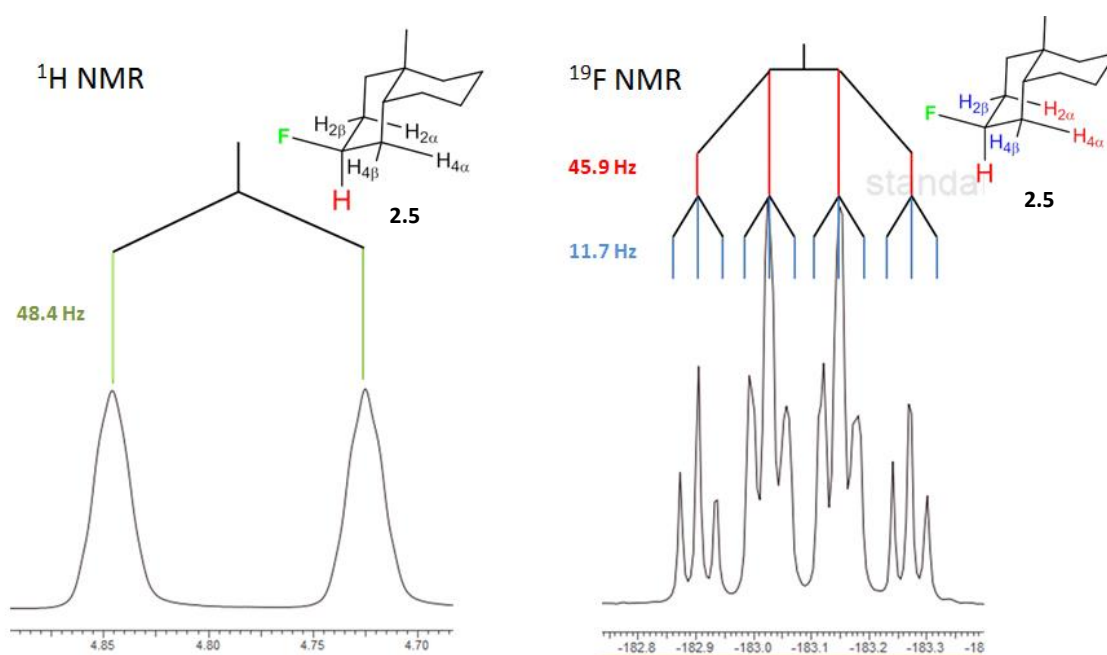


Figure 2.6 - ^1H and ^{19}F NMR spectra of 3β -fluoro derivative.

An identical approach can be taken when considering the coupling pattern of the ^{19}F NMR spectrum (Figure 2.6). As discussed above, a large geminal coupling to **H3** would be expected, but fluorine is also likely to couple to antiperiplanar protons $H_{2\alpha}$ and $H_{4\alpha}$ with a similar magnitude (e.g. 2.29, Figure 2.5), leading to a ≈ 50 Hz apparent quartet. In addition, two smaller *gauche* couplings to $H_{2\beta}$ and $H_{4\beta}$ (e.g. 2.27, Figure 2.5), would give a 5-15 Hz triplet. It can be seen in Figure 2.6 that such a quartet of triplets was present in the ^{19}F NMR spectrum, and thus the 3-fluorine must be axial.

Upon reduction of the 7-keto moiety two main products were isolated, iso-CDCA derivative **2.24** and iso-UDCA derivative **2.25** (Scheme 2.6). In the case of iso-CDCA derivative **2.24** proton **H** is in the equatorial position, and can couple to 3 equivalent *gauche* protons $H_{6\beta}$, $H_{6\alpha}$ and $H_{8\beta}$ (2-5 Hz), leading to an apparent quartet (Figure 2.7a).⁶ In the case of iso-UDCA derivative **2.25** proton **H** is in the axial position, and can couple to two antiperiplanar protons $H_{6\beta}$ and $H_{8\beta}$ (10-12 Hz) and *gauche* proton $H_{6\alpha}$ (2-5 Hz), leading to a triplet of doublets (Figure 2.7b).

⁶ The 'apparent' label is assumed in the remainder of this thesis.

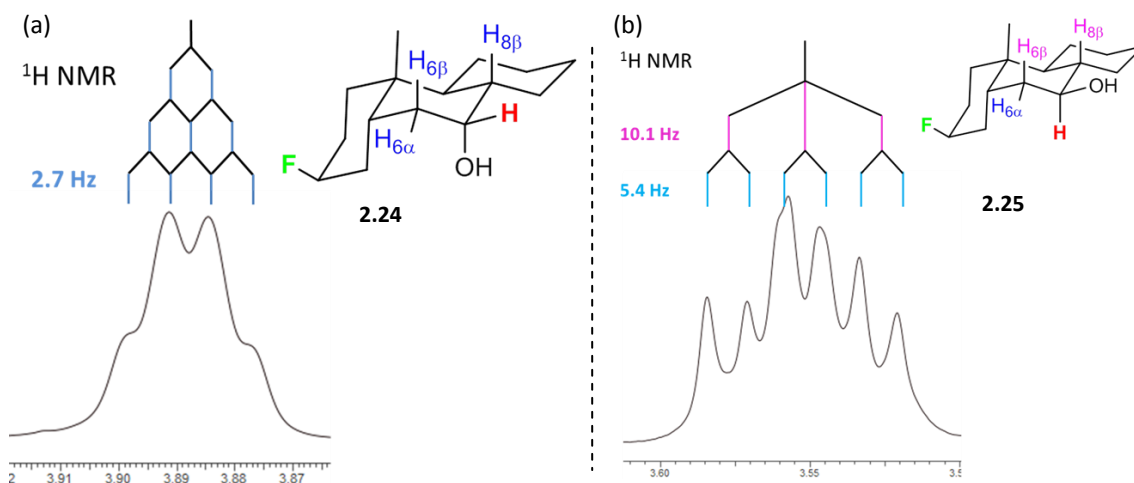
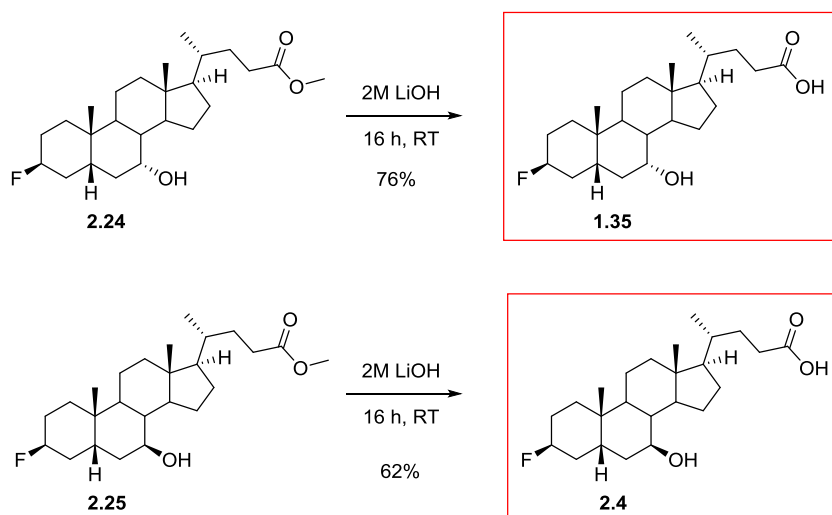


Figure 2.7 - H_7 coupling in 3β -fluoro derivatives 2.2.15 and 2.2.16.

This consideration for coupling patterns/magnitude was used to assign the stereochemistry of axial/equatorial protons in reduction/inversion reactions throughout this thesis.

2.2.6 Deprotection

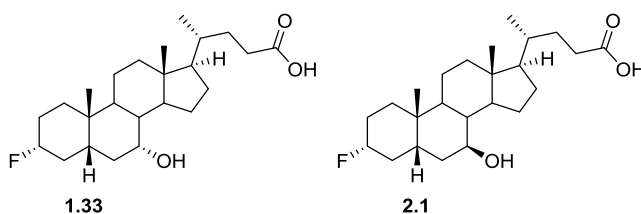
The final step towards the synthesis of the 3β -fluoro derivatives **1.35** and **2.4** (Scheme 2.7) was the saponification of the methyl ester. In the available literature, e.g. from Li *et al*^[77] and from Takashi *et al*^[78], cleavage of BA methyl ester is often described to occur under very strong basic conditions (e.g. KOH in MeOH at reflux). However for fluorinated substrates such as **2.24** and **2.25**, elimination of fluoride is a real concern under such harsh conditions. By replacing KOH with LiOH it was thought that the greater $M^+ \cdots O=C$ interaction (Li^+ is harder under HSAB rules) would increase reactivity of the ester towards nucleophilic attack, and allow for much milder conditions to be used.^[79] A small scale reaction at RT showed complete conversion to the desired carboxylic acid after 16 hr. The reaction was scaled up in the deprotection of **2.24** and **2.25** (Scheme 2.7), and following an acidic work up the two 3β -fluoro analogues **1.35** and **2.4** were isolated in good yields.

Scheme 2.7 - Deprotection of 3 β -fluoro derivatives.

2.3 Synthesis of 3 α -fluoro analogues

2.3.1 Mitsunobu reaction to invert 3 α -OH

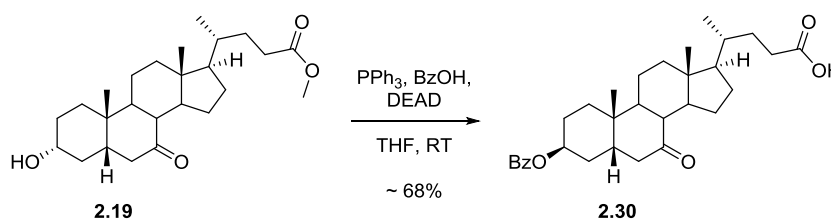
Following the synthesis of the 3 β -fluoro derivatives, attention focussed on the synthesis of the 3 α -fluoro analogues **1.33** and **2.1** (Figure 2.8). Given the success of previous DAST fluorination, this was the preferred method of fluorine introduction.

Figure 2.8 - Desired 3 α -fluoro CDCA and UDCA analogues.

The Mitsunobu reaction^{[80],[81]} is a common method to transform a primary or secondary alcohol into an ester moiety, with inversion of the stereocentre. Activation of triphenylphosphine with diethylazodicarboxylate (DEAD) leads to a highly electrophilic phosphorous centre, which is attacked by the alcohol derivative. The cationic triphenylphosphine species is an excellent leaving group (formation of O=PPh₃), and is subsequently displaced by a nucleophile (typically a carboxylic acid) in an S_N2 process to give inversion of the stereocentre.

A Mitsunobu reaction was performed on 3 α -OH derivative **2.19** using the conditions of Geoffroy *et al*^[82] (Scheme 2.8). A good conversion to the 3 β -benzoate product **2.30** was observed by ¹H NMR analysis, however the removal of by-products (O=PPh₃, DEAD derivatives) was difficult by flash chromatography. Pure product **2.30** was only isolated in a yield of 15%, with a further 53%

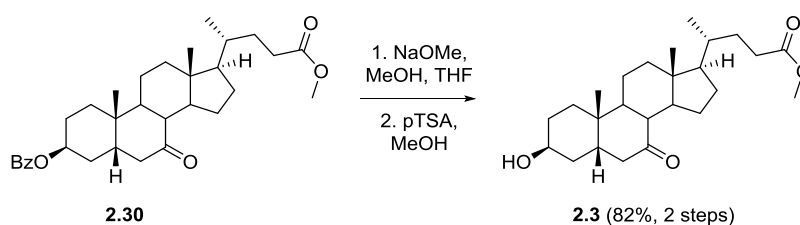
recovered in mixed fractions. The impure material was carried through to the next step without further purification.



Scheme 2.8 - Synthesis of 3 β -benzoate via Mitsunobu reaction.

2.3.2 Methanolysis of 3 β -benzoate

A basic cleavage of the 3 β -benzoate group in **2.30** was required (**Scheme 2.9**). In order to avoid transesterification or hydrolysis of the methyl ester, a methanolysis reaction was chosen.

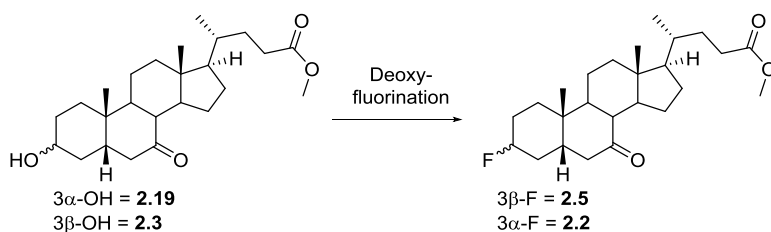


Scheme 2.9 - Synthesis of 3b-OH via Mitsunobu reaction.

Cleavage of benzoate **2.30** (**Scheme 2.9**) was performed with sodium methoxide in dry methanol. Despite attempts to ensure moisture free conditions, ~10% cleavage of the methyl ester was observed. Thus, following an aqueous work-up, the crude material was subjected to re-esterification (pTSA/MeOH, sonication). The resulting 3 β -alcohol **2.3** was then easily separable *via* flash chromatography from the impurities brought through from the previous step.

2.3.3 Fluorination/epoxidation

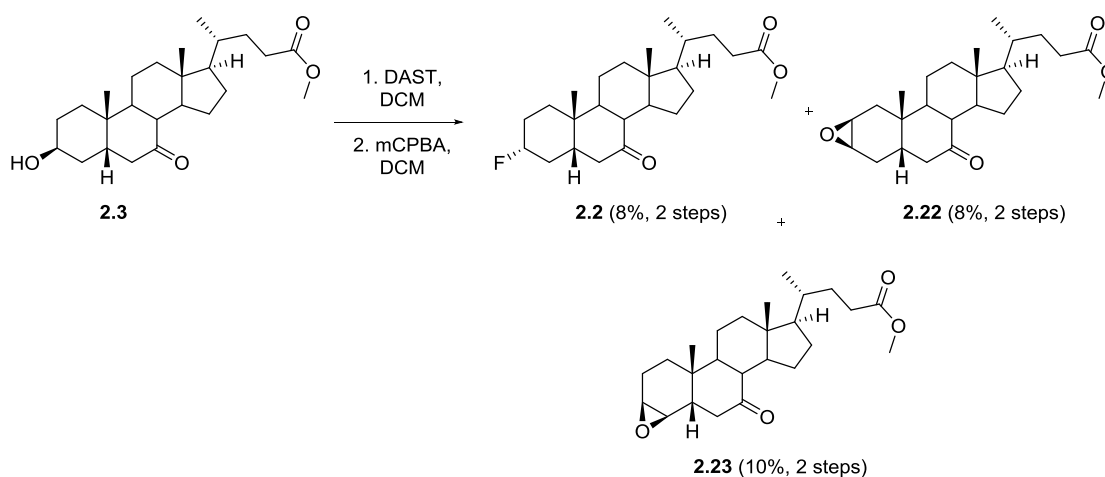
A deoxofluorination of 3 β -hydroxy-7-keto derivative **2.3** (**Figure 2.1a**) to form 3 α -fluoro-7-keto derivative **2.2** was then required. The fluorination of 3 α -hydroxy-7-keto **2.19** (**Entry 1, Table 2.1**), was discussed in **Section 2.2.2**, and this method was applied to 3 β -hydroxy-7-keto derivative **2.3** (**Entry 2**). The fluorination of the axial 3 β -OH in **2.3** led to a much higher proportion of elimination (72%) than the equatorial 3 α -OH in **2.19** (30%). The increased elimination of the axial 3 β -OH is unsurprising considering the basicity of fluoride, and the presence of trans-diaxial 2 α - and 4 α -protons that can be attacked in an E2-type elimination. The equatorial 3 α -OH in **2.19** has no antiperiplanar protons, so elimination is a much slower process in this case.

Table 2.1 - Fluorination vs. elimination of the 3-OH in standard DAST/DCM conditions.

Entry	Substrate	Reaction scale	% Elimination ^a	% Fluorination ^a
1	2.19	500 mg	30%	50%
2	2.3	400 mg	72%	20%

^a conversion judged by ¹H NMR analysis of the crude material.

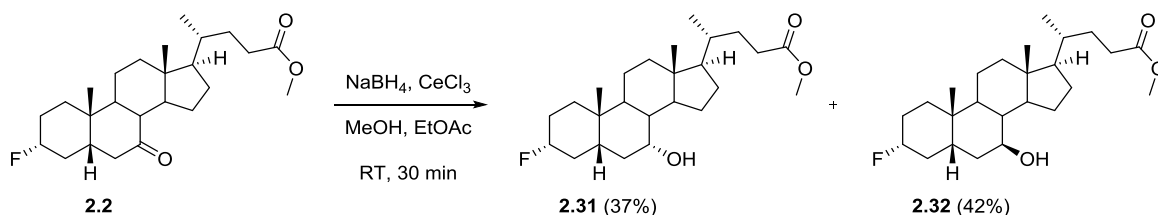
Despite the poor overall yield of the process, a sufficient amount of the 3 α -fluoro compound **2.2** was brought through, albeit contaminated with the undesired alkene(s). The inseparable mixture was once again treated with mCPBA in DCM to yield the desired 3 α -fluoro **2.2** compound; along with two epoxides **2.22** and **2.23** (Scheme 2.10).

**Scheme 2.10 - Fluorination and epoxidation of 3 β -OH derivative.**

Since this work was undertaken, a new fluorinating reagent known as PyFluor has been described.^[83] PyFluor has been shown to lead to a significantly higher proportion of substitution vs. elimination when compared to DAST and Deoxofluor. Members of our group have subsequently performed several fluorinations on the 3 β -OH-7-oxo derivative **2.3** using PyFluor, and have found significant improvements in isolated yields of the 3 α -fluoro-7-keto derivative **2.2** (50-60% isolated).

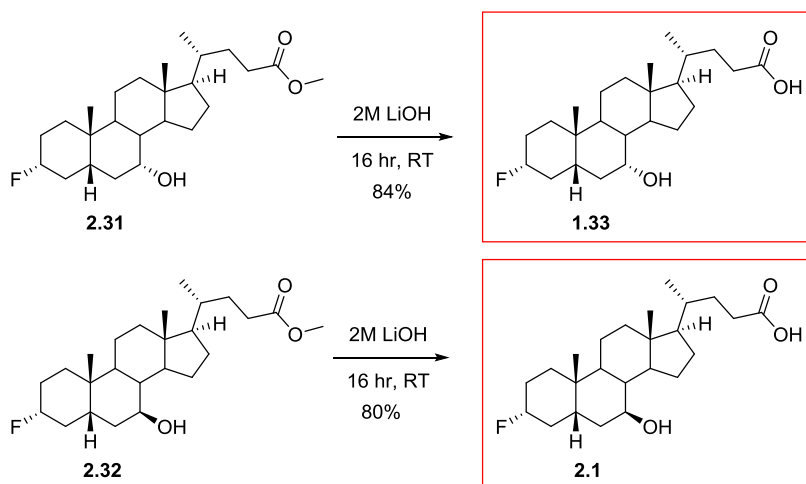
2.3.4 Reduction and Deprotection

A reduction of ketone **2.2** using Luche conditions led to the formation of 7 α -OH derivative **2.31** and 7 β -OH derivative **2.32** in good yields (**Scheme 2.11**).



Scheme 2.11 - Reduction of 7-keto moiety in 3 α -fluoro derivative **2.2.**

The methyl ester functionality was subsequently saponified in an identical fashion to before, yielding the 3 α -fluoro CDCA analogue **1.33** and 3 α -fluoro UDCA analogue **2.1** (**Scheme 2.12**), in sufficient quantities for biological testing.



Scheme 2.12 - 3-deoxy-3 α -fluoro analogues.

2.3.5 Product identification through ^1H and ^{19}F NMR

The coupling patterns of the key peaks in the ^1H and ^{19}F NMR spectra were again used to confirm the stereochemistry of the 3-fluoro derivative. Upon analysis of the ^1H NMR spectrum of **2.2** (**Figure 2.9a**), H₃ showed a large geminal coupling to fluorine (45-50 Hz), along with two medium couplings to the antiperiplanar protons H_{2 α} and H_{4 α} (10-12 Hz) and two further couplings to the vicinal *gauche* protons H_{2 β} and H_{4 β} (2-5 Hz). This coupling is only possible in the 3 α -fluoro derivative and gives excellent proof of the proposed structure. In the ^{19}F NMR spectrum (**Figure 2.9b**) one large geminal coupling to H₃ was observed (45-50 Hz), along with smaller *gauche* couplings to the vicinal protons, but these are poorly resolved. This gives further proof of the proposed structure especially when compared to the 3 β -fluoro derivative (**Figure 2.6**).

(b)

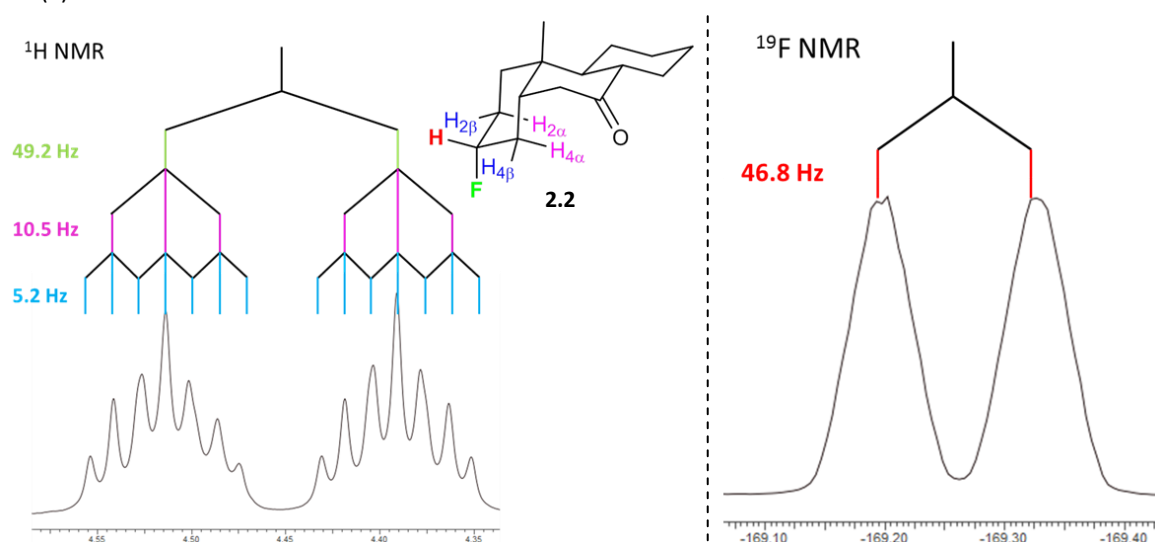
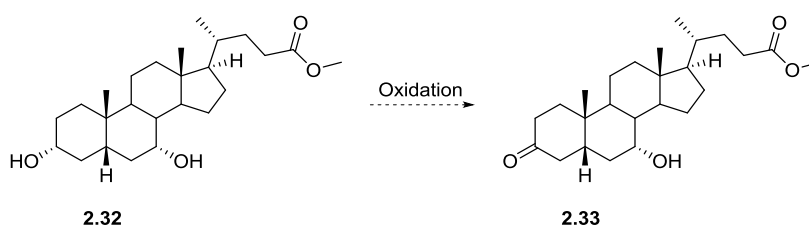


Figure 2.9 - Key peaks in $^1\text{H}/^{19}\text{F}$ NMR spectrum of 2.3.6.

2.4 Synthesis of 3,3-difluoro analogue

2.4.1 Regio-selective 3α -OH oxidation

Following carboxylic acid protection of CDCA **1.2** to yield **2.32** (analogous to **Section 2.2.1**), a selective oxidation of the 3α -OH was required to produce 3-keto derivative **2.33** (**Scheme 2.13**). DFT calculations have previously shown that the 7-OH group is more reactive towards mild oxidants compared to the 3-OH.^[73] A selective oxidation of the less hindered 3-OH therefore required the use of a sterically bulky oxidant.

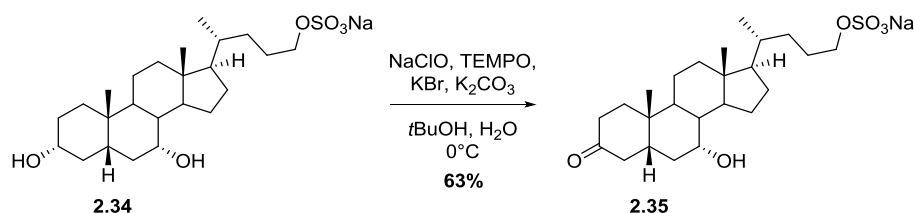


Scheme 2.13 - Proposed selective 3α -OH oxidation.

Li *et al*^[69] utilised Ag_2CO_3 on celite to great effect (98% yield), but despite the high yield of the process, other routes were initially sought due to the poor atom economy (>2.5 g of oxidant per 1 g of substrate) and relatively high cost of oxidant. Dolle *et al*^[68] reported the use of platinum oxide in an O_2 atmosphere as an equally high yielding (98%) alternative to silver carbonate, however this route was avoided due to reports in the paper of “explosion and fire” on some occasions when the reaction was performed.

In 2011 Burns *et al*^[84] published the selective oxidation of a BA 3α -OH group using *N*-oxy-2,2,6,6-tetramethylpiperidine (TEMPO, **Figure 2.10**) and sodium hypochlorite, albeit on a slightly different

substrate (**2.34**, **Scheme 2.14**). This oxidation, was found to have a reasonable yield (>60%) which, coupled with the availability of the reagents, is why this method became the primary route of investigation.



Scheme 2.14 - Burns *et al* method for 3-OH oxidation.

TEMPO is a mild oxidant that can be employed in both catalytic and stoichiometric amounts to oxidise alcohols into the corresponding carbonyl.^[85] Much work has been done to elucidate the oxidation mechanism, with a widely accepted version depicted in **Figure 2.10**. The relative rates of TEMPO reactions have been shown to vary greatly depending on the steric interference from neighbouring groups, explaining the observed selectivity towards 3-OH vs. 7-OH oxidation (**Scheme 2.14**).

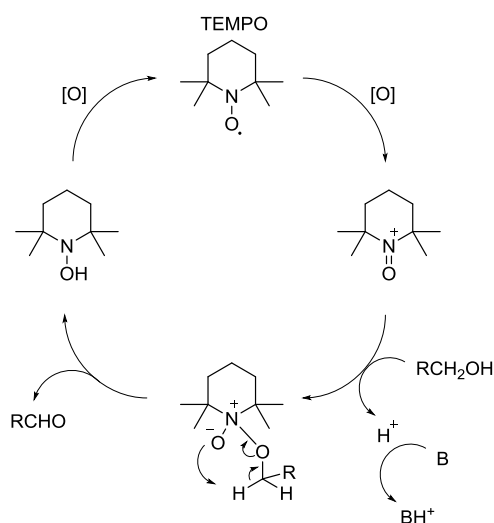
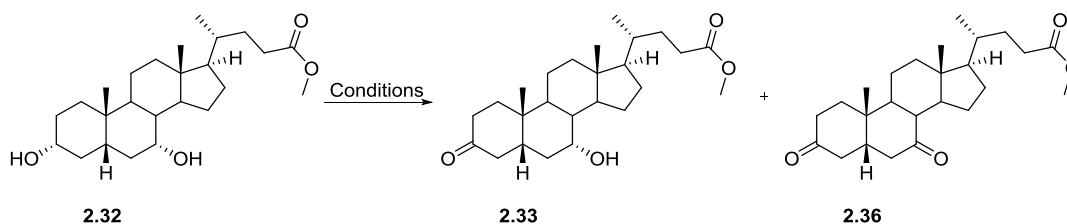


Figure 2.10 - Proposed mechanism for TEMPO catalysed alcohol oxidation under basic (B) conditions. [O] denotes the secondary oxidant (NaClO) which allows regeneration of the catalyst.

The optimisation of the regioselective 3 α -OH oxidation is shown in **Table 2.2**. Despite following the previously described method,^[84] an initial experiment (**Entry 1**) only gave the desired 3-keto compound **2.33** in low yield, with 3,7-diketo derivative **2.36** the most significant isolated compound. This result is of little surprise considering the high excess of oxidant (8 equiv). It was thus decided to reduce the amount of oxidant, along with varying the rate of addition, choice of solvent and overall reaction time. A reaction with significantly less oxidant (**Entry 2**) increased the yield of desired 3-keto **2.33** although di-keto by-product **2.36** was still formed. Slowing the rate of

addition (**Entry 3**) did not lead to an increase in yield the yield of **2.33**. Reactions in isopropanol and methanol (**Entries 4** and **5** respectively) failed. Some success was found with acetonitrile as solvent (**Entries 7** and **8**), although the yield of **2.33** was lower than when *t*-butanol was used (**Entry 6**). Ultimately, the highest yield for this reaction (**Entry 9**) was found by slightly increasing the reaction time and equivalents of oxidant. Pleasingly, the 66% yield was higher than that found by Burns *et al.*^[84]

Table 2.2 - Regio-selective 3 α -OH oxidation of 2.4.3.



Entry	Reagents	Addition time / h	Solvent system	Reaction scale	Yield (isolated)
1	5% NaClO (8 equiv)	2	<i>t</i> BuOH/H ₂ O	1.0 g	2.33 (3%), 2.36 (25%)
2	11%* NaClO (1.5 equiv)	2	<i>t</i> BuOH/H ₂ O	100 mg	2.33 (major), 2.36 (minor)
3	11%* NaClO (1.5 equiv)	4	<i>t</i> BuOH/H ₂ O	100 mg	2.33 (major), 2.36 (minor)
4	11%* NaClO (1.5 equiv)	2	IPA/H ₂ O	100 mg	No reaction
5	11%* NaClO (1.5 equiv)	2	MeOH/H ₂ O	100 mg	No reaction
6	11%* NaClO (1.5 equiv)	2	<i>t</i> BuOH/H ₂ O	3.9 g	2.33 (52%), 2.36 (trace)
7	11%* NaClO (1.5 equiv)	2	MeCN/H ₂ O	100 mg	2.33 (major), 2.36 (minor)
8	11%* NaClO (1.5 equiv)	2	MeCN/H ₂ O	10.0 g	2.33 (45%), 2.36 (trace)
9	11%* NaClO (3.0 equiv)	6	<i>t</i> BuOH/H ₂ O	10.0 g	2.33 (66%), 2.36 (trace)

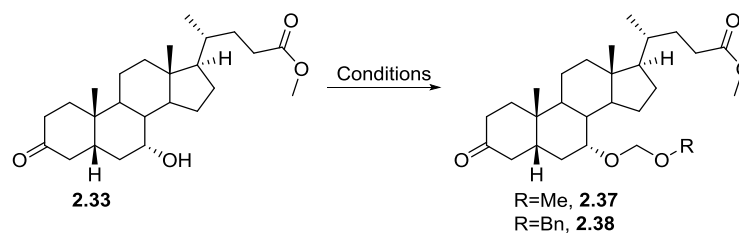
All reactions carried out with TEMPO (1.1eq), with KBr and K₂CO₃ (both excess). * \approx 11%.

2.4.2 MOM-protection of 7 α -OH group

In order to allow for the subsequent 3-keto fluorination, the 7 α -OH group required protection (**Table 2.3**). Following the route of Li *et al.*^[69] MOM ether functionalisation was considered.

Utilisation of their method (dimethoxy methane, P_2O_5) was unsuccessful, with an inseparable mixture of >5 compounds forming over the course of the 1.5 h reaction (**Entry 1**). Oishi *et al*^[86] had reported the similar 7 α -BOM ether synthesis, and their procedure was repeated successfully, with a good conversion to **2.38** (**Entry 2**). Their procedure was modified for the synthesis of 7 α -MOM ether **2.37**, which proved effective (**Entries 3 and 4**). Diisopropylethylamine (DIPEA) is used as a non-nucleophilic, weak base to neutralise the HCl produced in the reaction.

Table 2.3 - Optimisation of MOM/BOM ether 7 α -OH protection on 2.4.4.



Entry	Conditions	Reaction scale	Yield
1	DMM, P_2O_5	100mg	Unsuccessful
2	BOMCl, DIPEA	100mg	Successful* (2.38)
3	MOMCl, DIPEA	100mg	69% (2.37)
4	MOMCl, DIPEA	1.2g	93% (2.37)

*unpurified

2.4.3 Difluorination

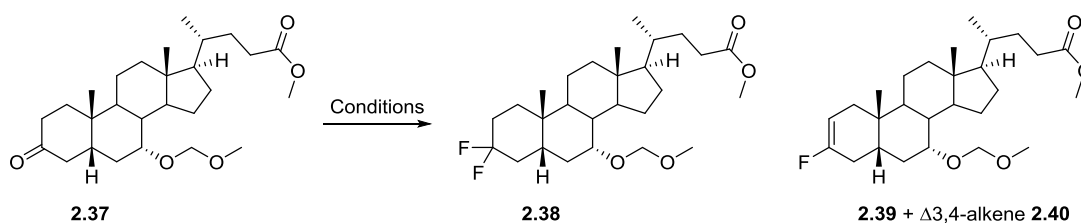
Following 7 α -OH protection, a difluorination of the 3-keto could be effected (**Table 2.4**). As mentioned in **Section 2.2.2**, deoxofluorinating reagents such as DAST and Deoxofluor can readily fluorinate alcohol and carbonyl groups.^[66-67] The initial reaction (**Entry 1**) showed some conversion to product (TLC analysis), although after 2 days at >40 °C no further reaction was seen. Analysis of the ^{19}F NMR spectrum showed the emergence of a peak characteristic of a CF_2 group, indicating that the desired compound **2.38** had indeed formed; however only a low level of conversion was obtained.⁷

In order to find a more effective set of conditions, a screen of small scale reactions was performed (**Entries 2-5**). The HF catalysed fluorination in DCM (**Entry 3**) proved the most successful, with the greatest conversion of SM to product observed. A smaller amount of starting material **2.37** was seen in the higher temperature reactions (**Entries 4 and 5**), but the formation of a significant

⁷ The relative conversion of C=O to CF_2 group was judged using ^{13}C NMR spectroscopy with the loss of a carbonyl shift at δ 212 ppm and the emergence of the characteristic CF_2 doublet of doublets at δ 125 ppm.

number of by-products made these reactions less preferable. The most successful reaction (**Entry 3**) was scaled up (**Entry 6**) to allow for enough fluorinated material to be brought forward towards the final compound. The competing process of elimination again proved an issue in this fluorination, with the fluoroalkene by-products **2.39** and **2.40** inseparable from the desired 3,3-difluoro **2.38** by flash chromatography and HPLC. The ratio of 3,3-difluoro **2.38** to fluoroalkenes **2.39/2.40** was roughly 4:1.

Table 2.4 - Optimisation of 3-keto difluorination on 2.37.

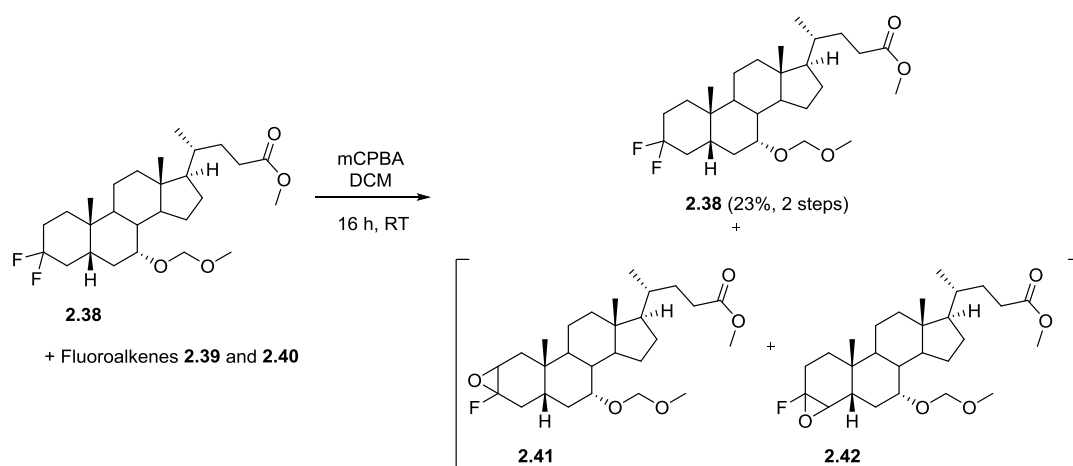


Entry	Reagents ^a	Solvent	Temp / °C	Reaction scale	Conversion ^b
1	DAST	DCM	45 (2 d)	400 mg	Little conversion, few by-products
2	DAST	DCM	45 (16 h)	30 mg	Little con., few by-products
3	DAST, HF.pyr (0.05 eq)	DCM	45 (16 h)	30 mg	Greater con., few by-products
4	DAST	Toluene	110 ^c (16 h)	30 mg	High levels of by-products
5	DAST, HF.pyr (0.05 eq)	Toluene	110 ^c (16 h)	30 mg	High levels of by-products
6	DAST, HF.pyr (0.05 eq)	DCM	45 (16 h)	500 mg	375 mg of di-fluoro/fluoroalkene

^a All reactions using 3 equivalents of DAST; ^b As measured by TLC and/or ¹³C/¹⁹F NMR. ^c The use of such harsh conditions would be repeated with Deoxofluor in the future.

2.4.4 Epoxidation

The fluoroalkenes **2.39** and **2.40** were removed by epoxidation (**Scheme 2.15**). Epoxidation was trialled using *m*-chloroperbenzoic acid (*m*CPBA) in DCM and, following overnight stirring, led to complete consumption of the undesired fluoroalkenes (**Scheme 2.15**). Standard flash chromatography led to the successful isolation of the desired 3,3-difluoro compound **2.38** in a yield of 23% over two steps. Unfortunately, the fluorinated epoxides **2.41** and **2.42** could not be isolated.



Scheme 2.15 - Removal of fluoroalkenes through epoxidation.

Upon epoxidation the characteristic fluoroalkene peak at ~5 ppm in the ^1H NMR spectra disappears, along with the impurities around the diastereotopic $-\text{O}-\text{CH}_2-\text{O}-$ MOM protons (**Figure 2.11**).



Figure 2.11 – ^1H NMR spectrum of 2.38 compound (a) before and (b) after epoxidation.

A similar observation was found upon analysis of the ^{19}F NMR spectrum (**Figure 2.12**). The fluoroalkene peak at -107 ppm is very prominent in the inseparable mixture; upon epoxidation/separation the disappearance of this peak in the ^{19}F NMR spectrum shows the effective removal of the by-product.

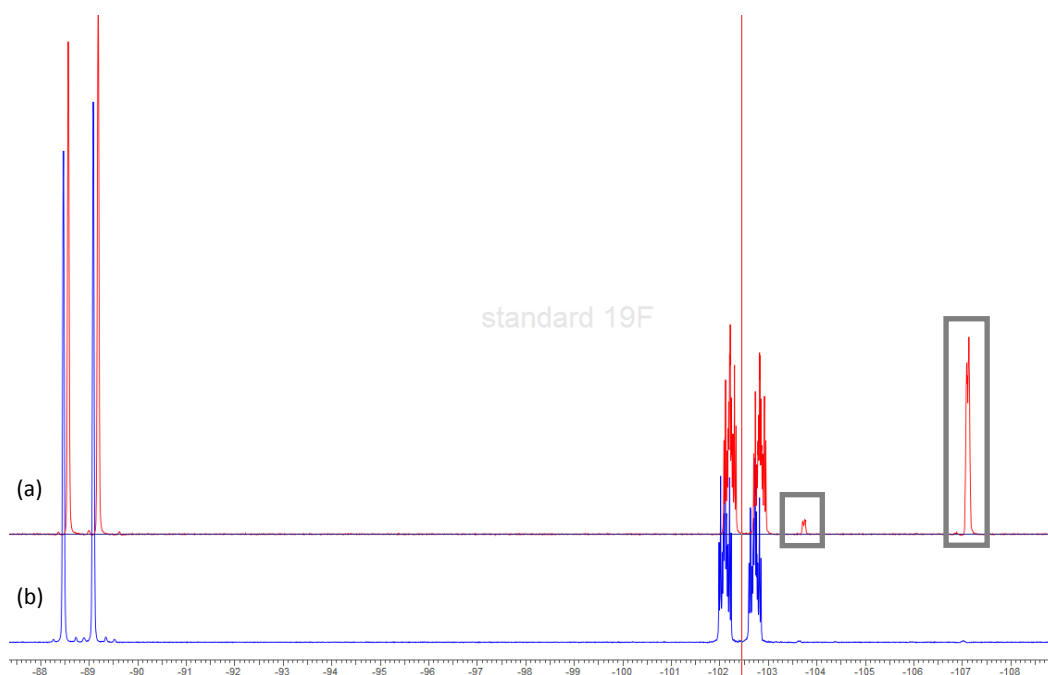
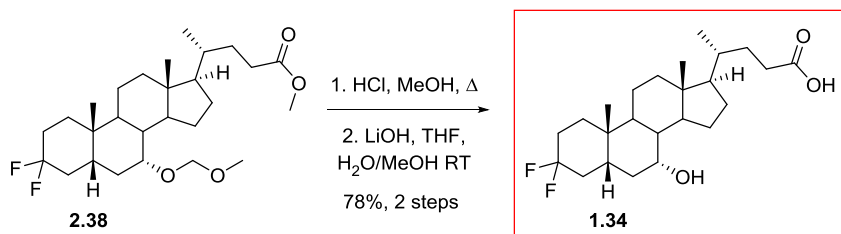


Figure 2.12 – ^{19}F NMR spectrum of **2.38** (a) before and (b) after epoxidation.

2.4.5 Deprotection of 3-deoxy-3,3-difluoro analogue

A simultaneous deprotection of the $7\alpha\text{-OH}$ and carboxylic groups was required in order to furnish the 3,3-difluoro analogue. Li *et al*.^[77] performed their -MOM deprotection using dilute HCl at $75\text{ }^\circ\text{C}$, followed with saponification of the methyl ester. These conditions were applied to difluoro derivative **2.38** (Scheme 2.16), and yielded the final deprotected analogue **1.34** in a good yield.



Scheme 2.16 - Deprotection of 3,3-difluoro derivative.

2.5 Discussion of biological results

2.5.1 Background

All fluorinated BA derivatives, including some discussed in **Chapter 3**, were sent to our collaborators Prof Helen Osborne and Dr Fran Greco (University of Reading). These molecules were screened against two breast cancer cell lines (BCC), MCF-7^[87] (oestrogen/progesterone receptor positive) and MDA-MB-231^[88] (estrogen/progesterone receptor negative). MCF-7 was chosen to mimic oestrogen responsive cancer (easier to treat), while MDA-MB-231 (triple negative) which is not responsive to the monoclonal antibody Heceptin,^[89] presented a clinically challenging form of the disease.

2.5.2 Stage 1 - Cytotoxicity screening

Each analogue (**Figure 2.13**) was subjected to an MTT assay^[90] with 72 hr incubation at 10 μ M concentration, for both the MCF-7 (**Figure 2.14a**) and MDA-MB-231 (**Figure 2.14b**) cell lines.⁸

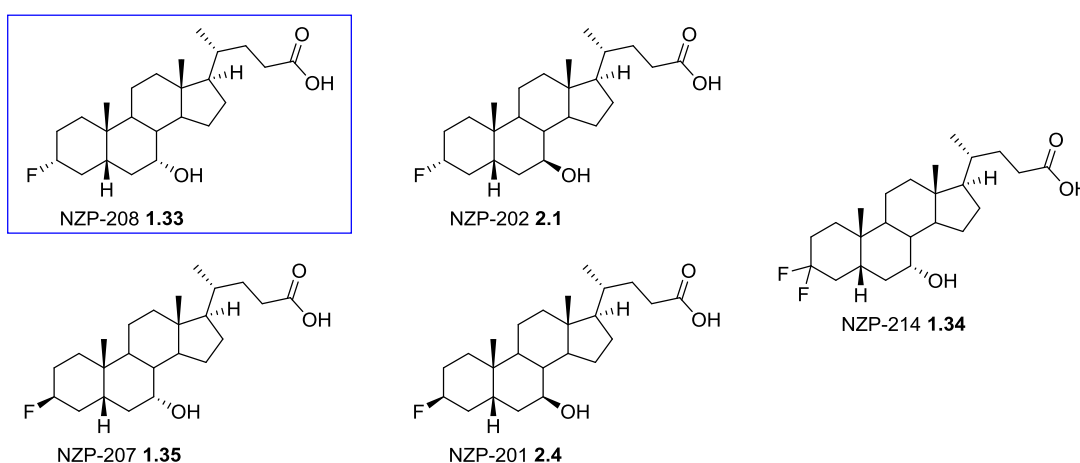


Figure 2.13 - 3-Deoxy-3-fluoro derivatives and associated DEX-numbers.

⁸ The MTT assay is a colorimetric assay to measure cell proliferation/survival. The assay detects only living cells, and can be used to measure the cytotoxicity of a given compound.

Conditions of study quoted from the Biological Evaluation Report: “Anti-proliferative assay: The anti-proliferative activities of the compounds were assessed using the MTT assay at 72 h of treatment. For this, MCF-7 cells were seeded at a density of 4×10^4 cells/mL and MDA-MB-231 cells were seeded at a density of 2×10^4 cells/mL into 96 well plates and incubated for 24 h to allow attachment. After 24 h, the cells were treated with these synthesised derivatives at single doses (10 μ M) and at a range of concentrations (0 to 250 μ M (stage 2)) for 67 h. After 67 h, the MTT assay¹ was carried out by the addition of 20 μ L of MTT (5mg/mL) solution in PBS into each well and the cells were incubated for 5 h. The purple crystals formed were dissolved in 100 μ L of DMSO and the plates were read at 570 nm using a SPECTRA max UV spectrometer (Bio-Rad). The data represented are the mean of the three individual experiments. The cell viability of the control is considered to be 100%.” Prof Helen Osborne and Dr Fran Greco, 13th June 2016.

Out of these compounds, only NZP-208 (3-deoxy-3 α -fluoro-CDCA, **1.33**, **Figure 2.14**) showed <50% cell viability compared to the control, showing high activity against both cell lines. These high levels of cytotoxicity are in direct contrast to the four remaining 3-deoxy-3-fluoro derivatives (NZP-201, 202, 207 and 214, **Figure 2.14**), despite their structural similarities. It is currently unclear why this should be the case, and we await further biological studies before solid conclusions are drawn. None of the other A-ring fluorinated bile acids synthesised in this report showed a cell viability of <50%.

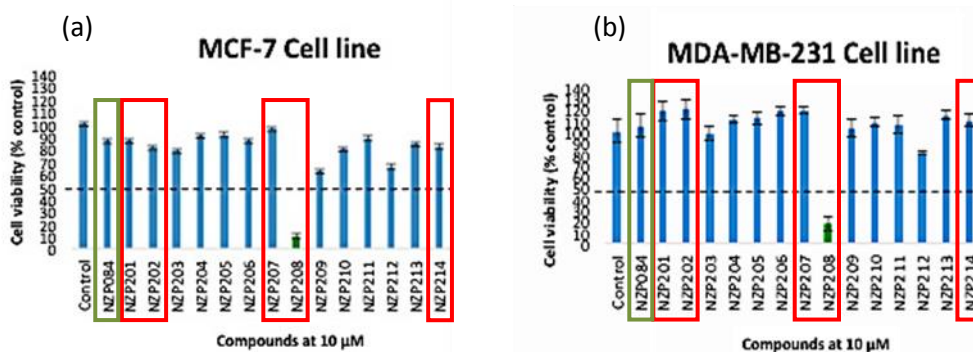


Figure 2.14 - Cytotoxicity screening of (a) MCF-7 and (b) MDA-MB-231 cell lines with 3-deoxy-3-fluoro analogues highlighted in red, NZP-084 is OCA and is highlighted in green.

Data obtained from collaborators Prof Helen Osborne and Dr Fran Greco.

2.5.3 Stage 2 - IC₅₀ determination

Following this successful early result, it was vital to probe this cytotoxic effect further. Any compound that showed a cell viability of <50% in the initial screening (**Figure 2.14**), was investigated further at different concentrations.⁹ Smooth dose-response curves were found for both the MCF-7 and MDA-MB-231 cell lines (**Figure 2.15a** and **b** respectively), allowing calculation of an accurate IC₅₀ value. An IC₅₀ value is a measure of how much of a given molecule is required to inhibit a particular biological process. The value is calculated from a dose response curve plotted against cell viability and the IC₅₀ is the concentration at which cell viability is 50%.

⁹ Conditions of study quoted from the Biological Evaluation Report: "The MTT assay with 72 h incubation was conducted as outlined above (stage 1 section), at a range of concentrations (25 µM -0.05 µM). Each experiment was carried out in triplicate." Prof Helen Osborne and Dr Fran Greco, 13th June 2016.

(a) MCF-7 cell line

(b) MDA-MB-231 cell line

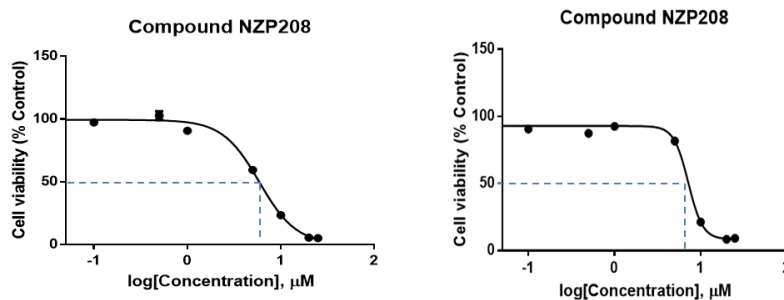


Figure 2.15 - Dose response curve for NZP-208 on cytotoxicity of (a) MCF-7; and (b) MDA-MB-231 cell lines. Data obtained from collaborators Prof Helen Osborne and Dr Fran Greco.

The IC₅₀ values for NZP-208 were calculated to be 6.44 μM for the MCF-7 cell line and 7.16 μM for MDA-MB-231. Uhr *et al*^[91] have recently published a paper with extensive screening of common chemotherapeutic agents against 42 breast cancer cell lines. The MCF-7 and MDA-MB-231 were two such cell lines, and **Table 2.5** contains the IC₅₀ values obtained from Additional file 1 (40064_2015_1406_MOESM1_ESM.xls) in the supporting information. It is interesting to note that despite some agents (notably the taxols, doxorubicin, bortezomib and tipifarnib) showing nanomolar potencies, most of the compounds tested were active in the same micromolar range as NZP-208. This does not necessarily indicate that NZP-208 will be a clinically effective chemotherapy, but it is certainly an exciting place to start further research.

Table 2.5 - IC₅₀ values of common cancer chemotherapies against MCF-7 and MDA-MB-231.^[91]

Drug	Cell Line	
	MCF-7 IC ₅₀ / M	MDA-MB-231 IC ₅₀ / M
Tamoxifen	5.69 x 10 ⁻⁶	9.79 x 10 ⁻⁶
Tipifarnib (Zarnestra®)	2.86 x10 ⁻⁸	3.25 x 10 ⁻⁷
Gefitinib (Iressa®)	1.00 x10 ⁻⁵	1.0 x 10 ⁻⁵
Doxorubicin	8.94 x 10 ⁻⁹	3.28 x 10 ⁻⁷
Methotrexate	1.39 x 10 ⁻⁸	2.10 x 10 ⁻⁹
5-Fluorouracil	2.21 x 10 ⁻⁶	2.58 x 10 ⁻⁶
Vorinostat (Zolinza®)	7.83 x 10 ⁻⁷	1.32 x 10 ⁻⁶
Erlotinib (Tarceva®)	1.00 x 10 ⁻⁵	1.00 x 10 ⁻⁵
Vandetanib (Zactima®)	1.00 x 10 ⁻⁵	4.80 x 10 ⁻⁶
Quisinostat (JNJ-26481585)	5.75 x 10 ⁻⁹	1.61 x 10 ⁻⁸
Serdemetan (JNJ-26854165)	1.69 x 10 ⁻⁶	4.74 x 10 ⁻⁷
Bortezomib (Velcade®)	8.35 x 10 ⁻⁹	4.43 x 10 ⁻⁹
Sirolimus	5.82 x 10 ⁻⁸	4.75 x 10 ⁻⁹
17-AAG	9.34 x 10 ⁻⁸	6.83 x 10 ⁻⁷
Nutlin-3	2.01 x 10 ⁻⁶	1.00 x 10 ⁻⁵
Sorafenib (Nexavar®)	5.10 x 10 ⁻⁶	4.27 x 10 ⁻⁶
Lapatinib (Tykerb®)	4.00 x 10 ⁻⁶	6.57 x 10 ⁻⁸
Panobinostat (Faridak®)	1.20 x 10 ⁻⁸	1.55 x 10 ⁻⁸
Decitabine (Dacogen®)	4.72 x 10 ⁻⁷	6.57 x 10 ⁻⁸
JNJ-208	1.00 x 10 ⁻⁵	1.00 x 10 ⁻⁵
Belinostat (Beleodaq®)	4.19 x 10 ⁻⁷	4.10 x 10 ⁻⁷
Sunitinib (Sutent®)	4.47 x 10 ⁻⁶	2.52 x 10 ⁻⁶
Docetaxel	1.12 x 10 ⁻⁹	5.35 x 10 ⁻¹⁰
Azacitidine (Vidaza®)	3.73 x 10 ⁻⁶	1.00 x 10 ⁻⁵
Cisplatin	1.00 x 10 ⁻⁵	3.25 x 10 ⁻⁷
Dasatinib (Sprycel®)	1.00 x 10 ⁻⁵	6.76 x 10 ⁻⁸
ARQ197	2.60 x 10 ⁻⁷	3.28 x 10 ⁻⁷
MI-219	8.15 x 10 ⁻⁷	1.00 x 10 ⁻⁵
Brivanib	1.00 x 10 ⁻⁵	6.48 x 10 ⁻⁶
JNJ-707	5.99 x 10 ⁻⁶	3.85 x 10 ⁻⁶
JNJ-493	1.00 x 10 ⁻⁵	3.65 x 10 ⁻⁶
Paclitaxel	1.79 x 10 ⁻⁹	1.49 x 10 ⁻⁹
Mitoxantrone	1.48 x 10 ⁻⁸	2.65 x 10 ⁻⁹
Veliparib	1.71 x 10 ⁻⁴	6.42 x 10 ⁻⁶

2.5.4 Stage 3 - Apoptosis detection

A final stage of screening was required to determine whether the effective substrates were causing cell death via apoptosis or necrosis. Apoptosis and necrosis are considered as dichotomous mechanisms of cell death; the former is a very regulated form of cellular disassembly, while the latter is an accidental or uncontrolled cell death.^[92] The controlled apoptosis mechanism leaves behind recyclable cellular content and generally avoids the release of inflammatory fragments, with little local disruption. If a cell has died via apoptosis it must have occurred *via* a discreet signalling process, that ultimately may be untwined to lead to a mechanism of action. The uncontrolled nature of necrosis however often leads to cell rupture and the release of inflammatory agents, leading to greater disruption of local cells. If a cell is found to have died *via* necrosis, it is often very difficult to understand how death has occurred, so determination of a mechanism of action is more difficult.

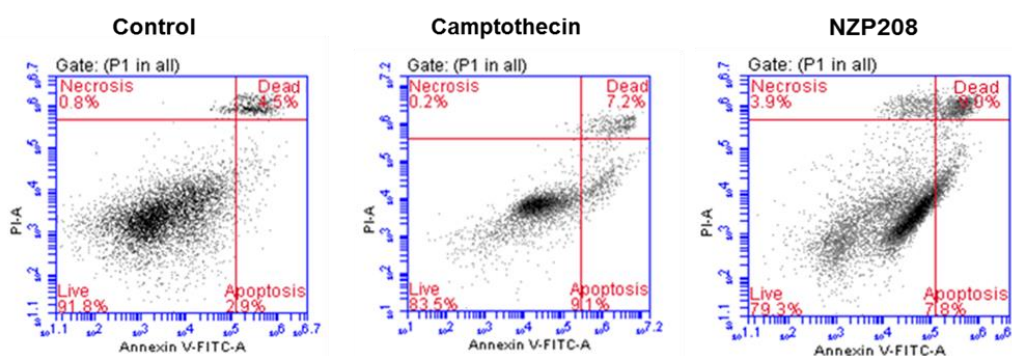


Figure 2.16 - Cell death identification of MCF-7 cell line¹⁰ Data obtained from collaborators Prof Helen Osborne and Dr Fran Greco.

¹⁰ Conditions of study quoted from the Biological Evaluation Report: "Apoptosis in MCF-7 and MDA-MB-231 cells was assayed by annexin V and propidium iodide (PI) co-staining using an Annexin-V-FITC staining kit (BD, Pharmingen™, UK) according to the manufacturer's instruction. 1×10^6 MCF-7 and MDA-MB-231 cells were plated into a 6 well plate (3.4×10^5 cells/mL, 3 mL/well). After 24 h incubation, the cells were treated without and with test compounds (at their IC50 concentration) for 24 h. The cells were harvested using Accutase™ Cell Detachment Solution (1 mL/well) for 5 min at 37 °C. Accutase was inactivated by addition of complete medium (2 mL). The cells were collected by centrifugation at 100 x g and the pellet was washed twice with cold PBS and then resuspended in 1 mL of annexin-binding buffer. 100 µL of the cell suspension was transferred to a 1.5 mL eppendorf tube and 5 µL of FITC-conjugated annexin V and 5 µL of PI was added and incubated in the dark for 15 min at room temperature. After 15 min incubation, 400 µL of annexin binding buffer was added to the cells and the fluorescence was measured using BD accuri™ instrument flow cytometry. The instrument was set for FL 1 (annexin V-FITC) vs FL3 (PI) bivariate analysis. Data from 10,000 cells/sample was collected and dot plots of FL1 vs FL3 were generated. The quadrants were set based on the population of healthy, unstained cells in untreated samples compared to cells treated with a known apoptotic inducer camptothecin (5 µM) for 24 h. BD CSampler™ software was used to calculate the percentage of the cells in the respective quadrants. The experiment was performed in triplicate" Prof Helen Osborne and Dr Fran Greco, 13th June 2016.

Camptothecin is an anticancer drug known to lead to cell death via apoptosis, and was used as a positive control in these experiments (**centre, Figure 2.16**).^[93] As can be seen in these experiments it does show a high percentage of cell death *via* apoptosis in the MCF-7 cell line, especially when compared to the negative control (**left, Figure 2.16**). A slightly lower percentage of apoptosis was seen for NZP-208 compared to camptothecin (**right, Figure 2.16**), but this was still shown to be a statistically significant induction. A statistically significant induction of cell death *via* apoptosis was also seen for NZP-208 in the MDA-MB-231 cell line.

2.5.5 Additional stage - determination of FXR agonism in fluorinated compounds

As outlined in **Section 1.2.3** the rationale behind screening bile acids against breast cancer cells lines was due to the literature precedence for FXR regulated apoptosis in these cells.^{[20],[21]} As part of their studies Swales *et al*^[20] and Alasmael *et al*^[21] concluded that FXR agonism either by GW4064 **1.12 (Figure 1.8)** or CDCA **1.2** led to breast cancer cell death *via* apoptosis, however this is in direct contradiction with our results.

FXR reporter cells (FXR-responsive promoter gene functionally linked to luciferase) were treated with a sample of the chosen analogue and incubated for 24 h, before the luminescence of the sample was tested. This was repeated in a dose dependent manner (**Figure 2.17**).

In order to show luminescence the FXR promoter gene must be activated, and due to the low concentrations used only highly potent derivatives would show activity. It was clear that only GW4064 **1.12 (Figure 1.8)** and NZP-084 (OCA, **1.9, Figure 1.6**) showed substantial activity. No significant FXR agonism was seen in NZP-208 despite being dosed in a higher concentration (10 μ M) than its IC₅₀ value against MCF-7 and MDA-MB-231. That is not to say that NZP-208, nor any of the other fluorinated bile acids are inactive against FXR, just that it is unlikely to be eliciting this cytotoxic effect *via* FXR agonism. It is interesting to note that at the 10 μ M cytotoxicity stage (**Figure 2.14**) NZP-084 showed negligible influence on cell viability, even in great excess of its known EC₅₀ value for FXR (**Figure 1.6**); if FXR agonism was the reason for the cytotoxic effects of bile acids OCA should have shown a much greater activity. We suspect that another mechanism/receptor is responsible for the cytotoxicity of NZP-208, however detailed mechanistic studies are still required.

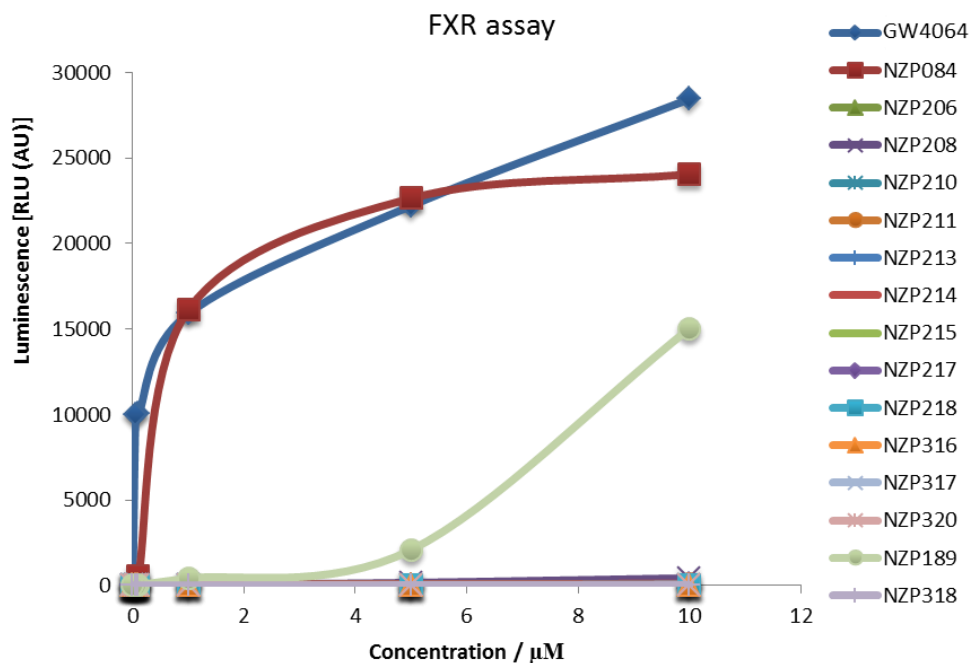


Figure 2.17 - FXR reporter assay.¹¹ Data obtained from collaborators Prof Helen Osborne and Dr Fran Greco.

¹¹ Conditions of study quoted from the Biological Evaluation Report: "FXR reporter cells consisting of an FXR-responsive promoter gene functionally linked to the luciferase gene were defrosted and seeded into a 96-well plate and these cells were immediately dosed with the test compounds at different concentrations (10-0.05 μM) according to the manufacturer's protocol. After 24 h incubation in the presence of the test compound or solvent (DMSO), the cell viability of these treated/untreated reporter cells was measured to eliminate false negative results using the fluorescence-based live cell multiplex (LCM) assay. The fluorescence from the live cells was measured using the plate reader with the filter combination of [485nmEx | 535nmEm]. Following this, the induction of luciferase activity, which is the measure of the agonist activity, was quantified by using a luminometer (TECAN) according to the manufacturer's protocol." Prof Helen Osborne and Dr Fran Greco, 13th June 2016.

2.6 Conclusion

Five 3-deoxy-3-fluoro derivatives were synthesised in sufficient quantities for biological evaluation, using DAST as the fluorinating reagent. Overall, fluorination was achieved in moderate yields, with poor yields for the fluorination of axial hydroxyl groups. Significant formation of alkene by-products hampered purification, however epoxidation led to an increase in polarity allowing for the separation of these impurities. Luche reduction conditions were successfully employed to reduce the 7-keto moiety to the corresponding 7 α -OH and 7 β -OH, allowing for the isolation of both CDCA and UDCA derivatives.

Biological screening has shown that 3-deoxy-3 α -fluoro CDCA is able to exert a cytotoxic effect on two commonly used breast cancer cell lines, and calculation of the IC₅₀ value from dose response curves has shown potencies similar to currently marketed drugs. The compound was shown to exert its effect *via* apoptosis, although activation of FXR is not believed to lead to the downstream cytotoxic effects.

Chapter 3: Synthesis of 2- and 4-fluorinated analogues

3.1 2- and 4-Fluorohydrins Route 1

3.1.1 Retrosynthetic analysis

A retrosynthetic analysis of 2 α - **1.39** and 2 β -fluoro CDCA **1.37** leads back to 2 α - and 2 β -fluoro ketones **3.1** and **3.2** respectively (**Figure 2.1**), with the forward synthesis achieved through a borohydride mediated 3-keto reduction and global deprotection. The 2 α - and 2 β -fluoro moieties can be introduced through an electrophilic fluorination of ketone **3.5**, with the 7 α -OH and carboxylic acid functionalities suitably protected (the derivative of **3.5** where R = MOM was synthesised in **Section 2.4.1**). Electrophilic fluorination of ketone **3.5** is also likely to form the corresponding 4 α - and 4 β -fluoro ketones **3.3** and **3.4**, which can then be used to make 4 α -fluoro **1.38** and 4 β -fluoro **1.36** CDCA analogues.

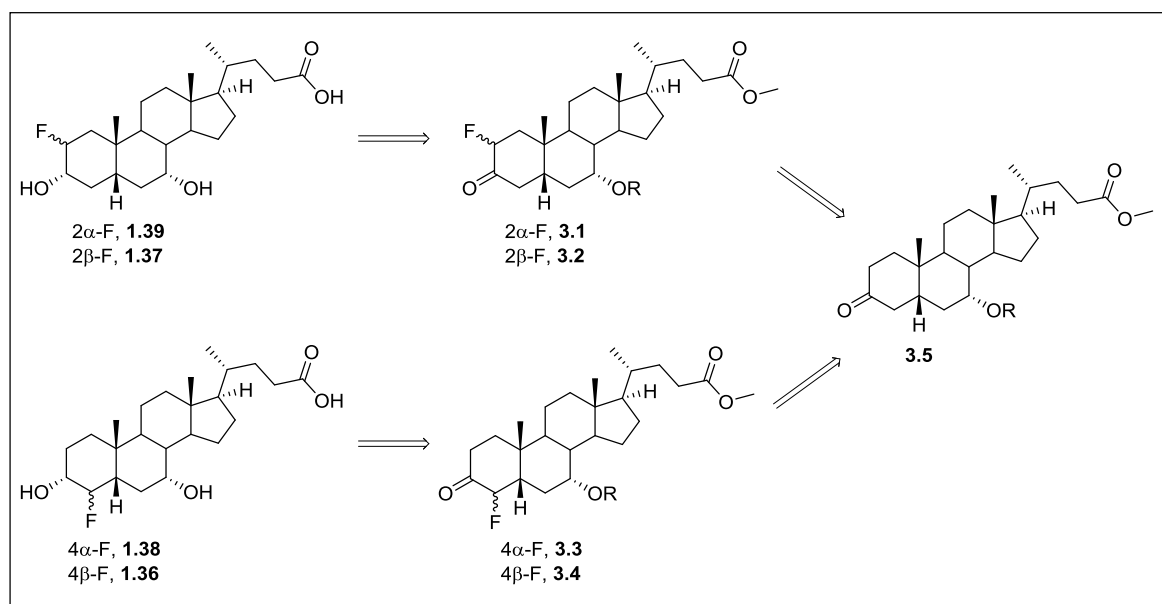


Figure 3.1 - Retrosynthetic analysis of 2 β - and 4 β -fluoro derivatives.

3.1.2 Fluorination chemistry

Electrophilic sources of fluorine ("F⁺") are a useful tool to introduce fluorine into organic molecules. Fluorine is the most electronegative element, and thus activation to form "F⁺" requires bonding to a similarly electronegative group.^{[62],[94]} The simplest, and most reactive form of electrophilic fluorine is F₂ gas, however obvious safety concerns and issues with selectivity preclude its use in a non-specialist laboratory. Taming of the high oxidation potential of fluorine through the development of O-F based reagents (e.g. fluoroxy perfluoroalkanes, acyl hypofluorites, fluoroxy sulfates), Cl-F reagents (e.g. perchloryl fluoride) and XeF₂ was initially

successful, but their widescale use and commercial production has generally been discontinued due to safety concerns, handling difficulties, and poor functional group tolerance. These reagents have largely been superseded by N-F based compounds including *N*-fluorobis(phenyl)sulfonimide (NFSI, **3.6**, **Figure 3.2**), *N*-fluoropyridinium salts (e.g. **3.7** and **3.8**) and 1-Chloromethyl-4-fluoro-1,4-diazoniabicyclo[2.2.2]octane bis(tetrafluoroborate) (Selectfluor[®], **3.9**).

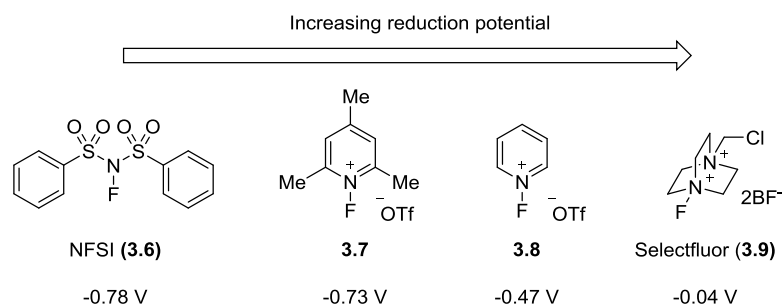
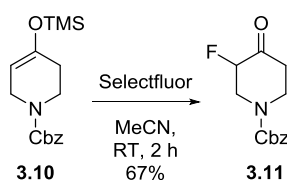


Figure 3.2 - Common N-F based electrophilic fluorination reagents.

The availability of bench stable, crystalline solids such as these has been crucial in developing conditions for selective electrophilic fluorinations.^{[62],[94]} In general, two classes of *N*-fluoro electrophilic reagents are used, neutral N-F reagents (e.g. **3.6**) and positively charged ammonium N-F reagents (**3.7-3.9**, **Figure 3.2**). The relative reactivity of “F⁺” reagents correlates with the electron withdrawing potential of the bounded *N*-group, with cationic species (**3.7** and **3.8**) much more reactive than neutral species (**3.6**), and dicationic species (e.g. **3.9**) of even greater reactivity.

The higher electronegativity of fluorine vs. nitrogen, means that a partial negative charge (δ^-) still resides on the fluorine atom, however nucleophilic attack into the low-lying $\sigma^*_{\text{N-F}}$ bond occurs at fluorine, as the equivalent orbital is sterically inaccessible on the nitrogen atom. This $S_{\text{N}}2$ displacement mechanism is generally accepted, however single-electron transfer (SET) based processes have also been proposed.^{[62],[94]}

Nucleophilic enol/enolate derivatives are common substrates for electrophilic fluorination reactions.^{[62],[94],[95]} In our group, direct fluorinations using H⁺/Selectfluor[®] have been shown to be successful, as have DMF/Selectfluor[®] systems (similar to Stavner *et al*^[96]), and both are potential methods to fluorinate 3-keto derivative **3.5** (**Figure 3.1**). Fujimoto *et al*^[97] have published a fluorination of silyl enol ether **3.10** (**Scheme 3.1**), forming the corresponding fluoroketone **3.11** in a yield of 67%, and such a 2-step method will also be explored.

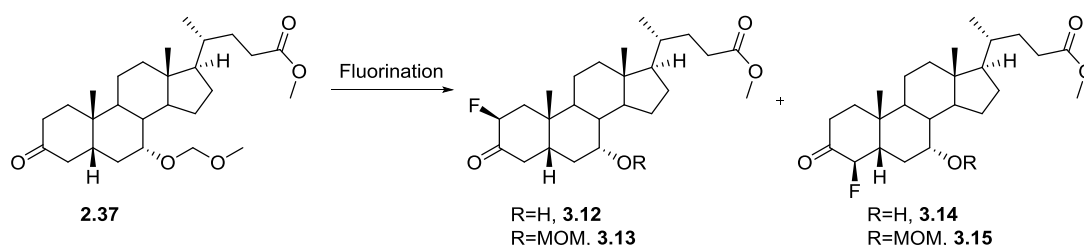


Scheme 3.1 - Fujimoto et al fluorination of silyl enol ether using Selectfluor®

3.1.3 Direct fluorination of the 3-keto moiety with Selectfluor®

The 7 α -MOM protected ketone **2.37** was made previously (Section 2.4.1) so was utilised in the preparation of the desired 2-fluoro and 4-fluoro ketones (Figure 3.1). The synthesis of these was first attempted *via* direct fluorination with Selectfluor® (Table 3.1).

Table 3.1 - Direct fluorination of ketone



Entry	Reagents (equiv)	Time / h	Temperature / °C	Scale	Result
1	Selectfluor® (1.1), AcOH (0.1), MeCN	18	80	100 mg	Cleavage of MOM-group. 3.12 : 3.14 ≈1:10
2	Selectfluor® (3), DMF	16 1	RT - 100 °C	100 mg	Partial ceavage of MOM-group (~25%). 2β-fluoro: 4β-fluoro ≈1:6

An initial reaction using acetic acid/Selectfluor® in acetonitrile was performed (Entry 1, Table 3.1). A significant amount starting material remained after 2 h at 80 °C, so the reaction mixture was stirred for a further 16 h until complete consumption of **2.37**. To our surprise, analysis of the ¹H and ¹⁹F NMR spectra of the crude material showed complete selectivity towards β -fluorination.¹² Unfortunately, complete cleavage of the MOM protecting group under the acidic conditions was also observed. A higher proportion of 4 β -fluorinated product **3.14** vs. 2 β -fluoro **3.12** (≈10:1) was also found. The structures of 2 β -fluoroketone and 4 β -fluoroketone were confirmed following

¹² This β -selectivity towards electrophilic reagents was also observed in Section 2.2.3.

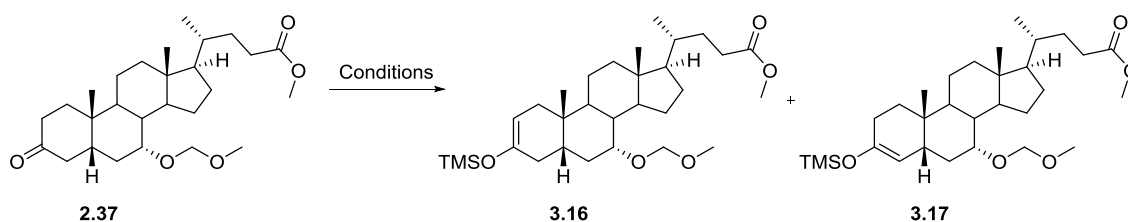
analysis of the ^1H and ^{19}F NMR spectra (H_2 of **3.12/3.13** is a ddd, $J=49.4, 13.5, 5.6$ Hz, H_4 of **3.14/3.15** is a dd, $J=46.8, 11.7$ Hz).

A reaction using Selectfluor[®] in DMF was then attempted (**Entry 2, Table 3.1**). It was first stirred at RT (16 h) although no progress was observed. The reaction was then warmed to 100 °C (1 h) to drive the reaction towards completion. Partial cleavage of the MOM-group was found again, although to a lesser extent than under acid catalysis. A slightly higher proportion of the 2 β -fluorinated products **3.12/3.13** was observed upon analysis of the ^1H and ^{19}F NMR spectra, however 4 β -fluorination to yield **3.14/3.15** still dominated.

3.1.4 Silyl enol ether formation

In order to avoid cleavage of the 7 α -MOM group in **2.37**, and to investigate whether a higher proportion of the 2 β -fluoro derivative **3.13** can be obtained, a fluorination *via* silyl enol ethers **3.16** and **3.17** was investigated (**Table 3.2**).

Table 3.2 - Silyl enol ether formation on 2.37.



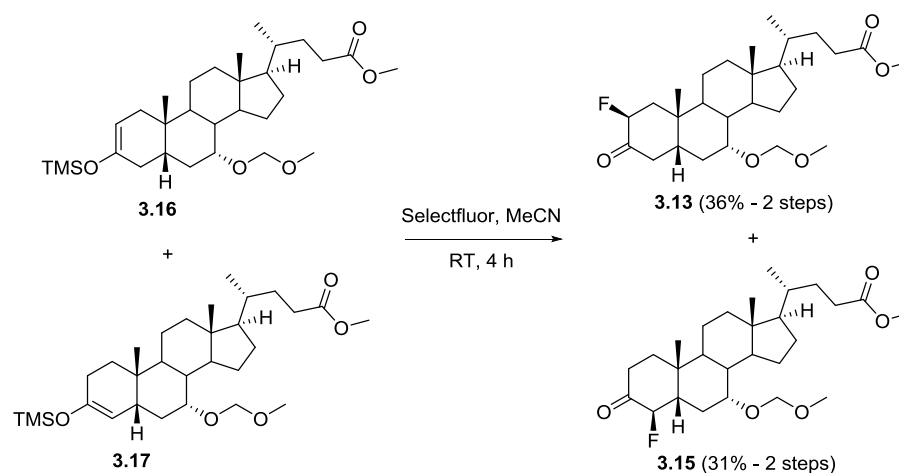
Entry	Reagents (eq)	Time / h	Temperature / °C	Scale	Reaction Outcome
1	TMSCl (1.5), Et ₃ N (3)	18	80	100 mg	No reaction
2	TMSCl (2), Et ₃ N (2), NaI (2)	1.5	70	100 mg	No reaction
3	TMS-OTf (1.1), Et ₃ N (2)	2	0-RT	100 mg	3.16 : 3.17 ($\approx 1:1$ ratio)
4	TMS-OTf (1.1), Et ₃ N (2)	2	0-RT	1.0 g	3.16 : 3.17 ($\approx 1:1$ ratio)

Allevi *et al*^[98] had published the selective synthesis of a BA $\Delta 2,3$ -silyl enol ether using trimethylsilyl chloride and triethylamine. Karimi *et al*^[99] had also performed a similar reaction (with addition of sodium iodide) on another cis-decalin system which yielded the desired $\Delta 2,3$ -silyl enol ether in quantitative yield. These reaction conditions were applied to **2.37** in attempts to synthesise silyl enol ether(s), but they both proved unsuccessful (**Entries 1 and 2, Table 3.2**).

Barlow *et al*^[100] used trimethylsilyl trifluoromethanesulfonate (TMS-OTf) as a more reactive alternative to TMSCl in their synthesis of silyl enol ethers. These conditions were applied to ketone **2.37** (Entries **3** and **4**, Table **3.2**), and led to the formation of the Δ 2,3- **3.16** and Δ 3,4- **3.17** silyl enol ethers in a roughly 1:1 ratio. Separation of the silyl enol ether mixture was not attempted due to their inherent instability, with the crude mixture of isomers used directly in the next step. No silyl enol ether formation on the C24 methyl ester was observed through ¹H NMR analysis.

3.1.5 Fluorination *via* silyl enol ether

A fluorination of the silyl enol ethers **3.16/3.17** (Scheme **3.2**) was performed using the conditions of Fujimoto *et al*^[97] (Scheme **3.1**). Complete selectivity towards β -fluorination was seen again, with the resulting 2 β - **3.13** and 4 β -fluoroketones **3.15** formed in high yields. The two fluoroketones were readily separable *via* flash chromatography.



Scheme 3.2 - Fluorination of silyl enol ethers **3.16 and **3.17**.**

The structures of 2 β -fluoroketone **3.13** and 4 β -fluoroketone **3.15** (Scheme **3.2**) were confirmed by ¹H and ¹⁹F NMR analysis, and subsequently *via* single crystal X-ray structural analysis (Figure **3.3**).

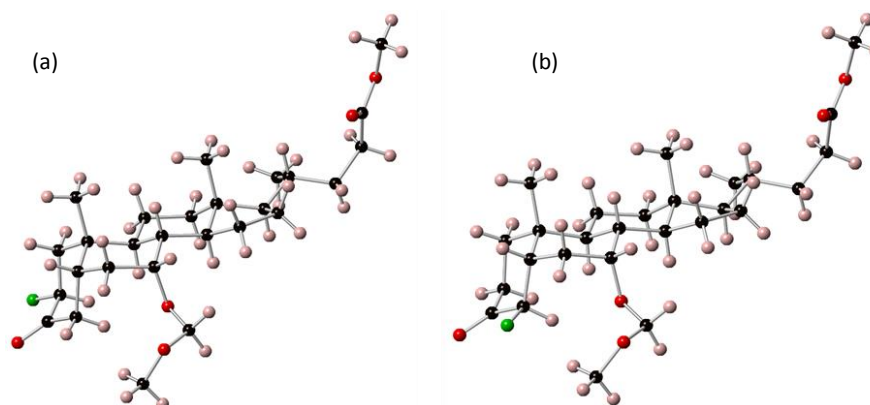
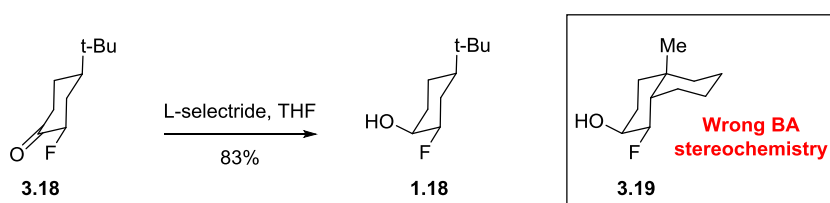


Figure 3.3 - Single crystal X-ray structures of (a) **3.13; and (b) **3.15**.**

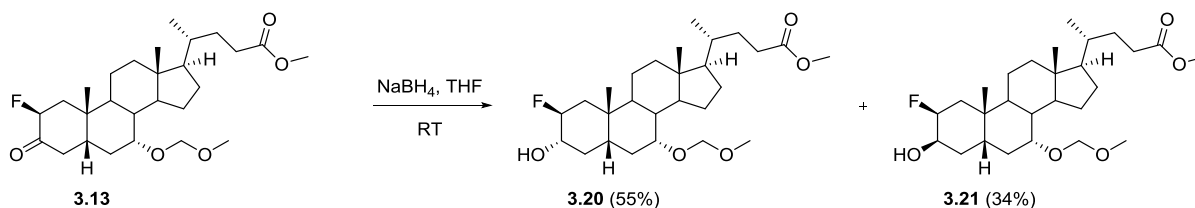
3.1.6 Fluoroketone reduction

A reduction of the 2 β -fluoro-3-oxo derivative **3.13** was required (Figure 3.1), and selectivity towards the equatorial (3 α -OH) was desired. Our group^[51] have previously published the selective reduction of fluorinated cyclohexanones using L-selectride (Scheme 3.3). The bulky reducing agent attacked at the equatorial face of fluoroketone **3.18** to give axial alcohol **1.18**. These reduction conditions would lead to the undesired 3 β -hydroxy derivative (e.g. **3.19**) if they were applied to the 2 β - **3.13** or 4 β -fluorinated **3.15** BA derivatives. A less selective reduction was therefore sought.



Scheme 3.3 - Selective reduction of equatorial fluoroketones

Hence, a reduction of **3.13** was performed using sodium borohydride in tetrahydrofuran (Scheme 3.4).

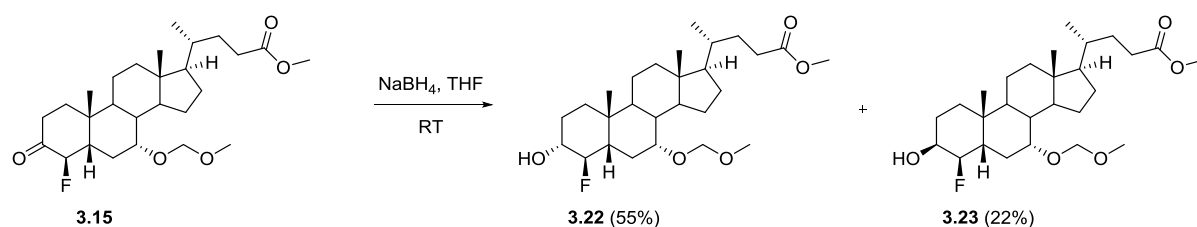


Scheme 3.4 - Reduction of **3.13**.

The reaction proved successful, with the 3 α -hydroxy **3.20** and 3 β -hydroxy **3.21** fluorohydrins isolated in a \approx 3:2 ratio. The CDCA **3.20** and iso-CDCA **3.21** derivatives were separable *via* flash chromatography, and their structures were confirmed by analysis of the *J*-coupling in the ¹H NMR spectra.¹³

The reduction procedure was then performed on 4-fluoroketone **3.15** (Scheme 3.5) to yield 3 α -hydroxy-4 β -fluoro **3.22** and 3 β -hydroxy-4 β -fluoro **3.23** in a \approx 2.5:1 ratio, which were readily separable *via* flash chromatography.

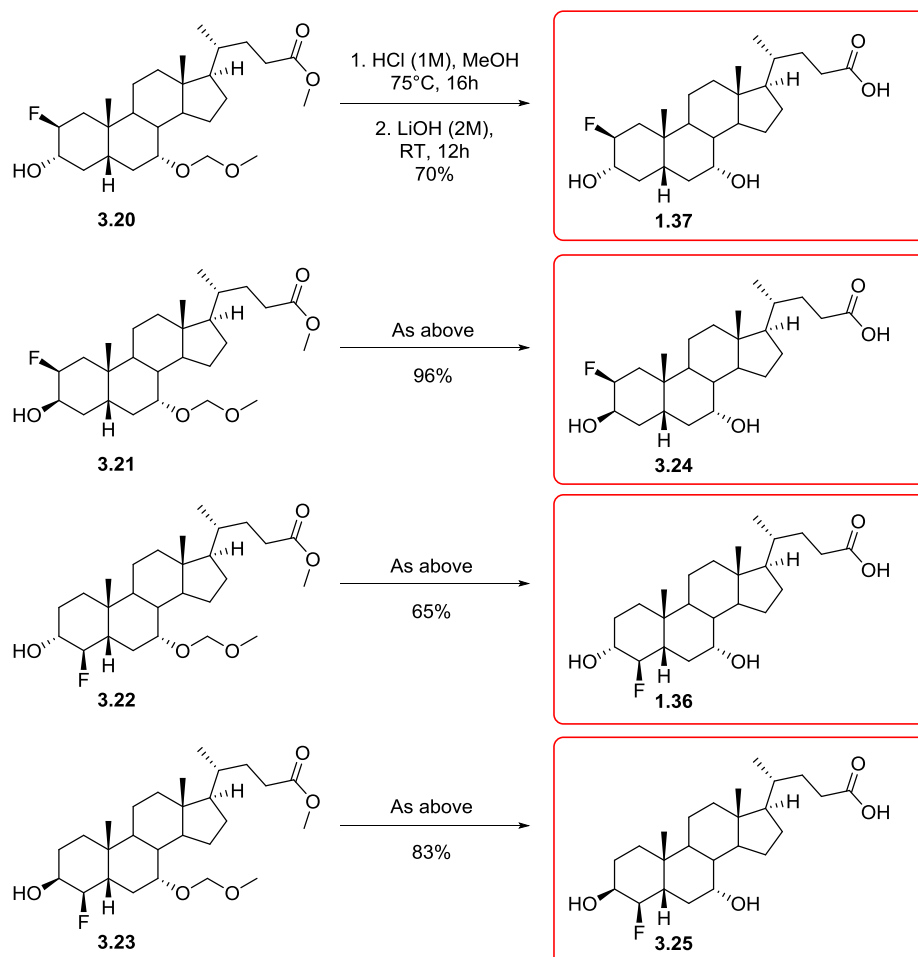
¹³ H₂ of **3.20** is a dddd, *J*=52.3, 12.0, 8.6, 4.4 Hz, 1H, while H₂ of **3.21** is a dddd, *J*=47.7, 12.1, 4.4, 2.8 Hz, 1H. The key difference between the two spectra is the coupling to H₃ (highlighted in red). Where H₃ is axial (**3.20**) a large antiperiplanar coupling is observed (8.6 Hz), Where H₃ is equatorial (**3.21**) a much smaller *gauche* coupling is observed (2.8 Hz).



Scheme 3.5 - Reduction of 3.15.

3.1.7 Deprotection of 2 β - and 4 β -fluorohydrins

A deprotection of both the 7 α -OH and carboxylic acid groups was required to yield the desired 2 β -fluoro (**1.37**, **3.24**) and 4 β -fluoro (**1.36**, **3.25**) analogues (Scheme 3.6). The method of Li *et al*^[77] discussed in Section 2.2.6 was applied successfully to all four 2 β - and 4 β -fluorohydrin derivatives (**3.20-3.23**) with good isolated yields. No elimination products (e.g. epoxides) were observed *via* TLC or NMR analysis.

Scheme 3.6 - Deprotection of 2 β - and 4 β -fluorohydrin analogues.

3.2 2 α - and 4 α -Fluorohydrins - Route 2

3.2.1 Retrosynthetic analysis

Given the complete selectivity of electrophilic fluorination towards the 2 β - and 4 β -fluorinated products, an alternative strategy towards 2 α - and 4 α -fluorination was required. Two retrosynthetic analyses of 2 α -fluoro CDCA **1.39** were initially considered (**Figure 3.4a**).

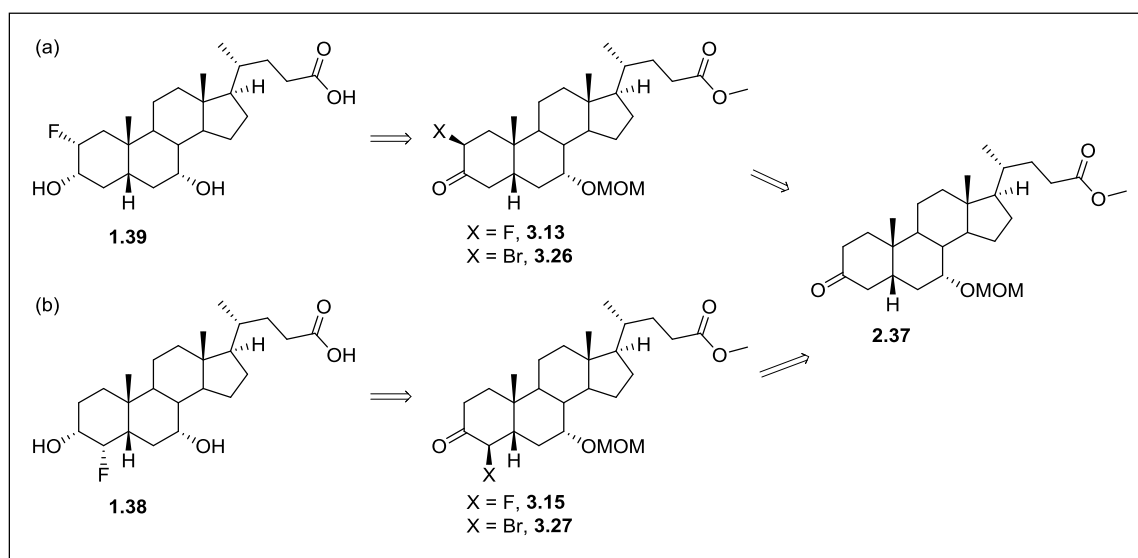


Figure 3.4 - Second retrosynthetic analysis of 2 α - and 4 α -fluoro derivatives.

The first and simplest of these retrosynthetic analyses proceeds *via* an epimerisation of 2 β -fluoro-3-keto derivative **3.13** (**Figure 3.4a**). This can be achieved via simple basic or acidic catalysis, but its success depends on the equilibrium lying towards the axial 2 α -fluorinated product. The synthesis of 2 β -fluoro derivative **3.13** from **2.37** was discussed in **Section 3.1.5**. A second retrosynthetic analysis leads back to an intermediate containing a 2 β -leaving group (e.g. bromide, **3.26**), such as that synthesised by Carreira and co-workers.^[101] A simple S_N2 displacement of the leaving group in **3.26** with a suitable source of fluoride can be envisioned, to yield the 2 α -fluorinated product. Deprotection of the 7 α -OH and carboxylic acid groups can then lead to **1.39**.

A comparable retrosynthesis of the 4 α -fluoro analogue **1.38** can also be performed (**Figure 3.4b**).

3.2.2 Fluorination chemistry

A nucleophilic displacement of the 2 β -bromide in **3.26** with fluoride appears trivial (**Figure 3.4**), however the high basicity of fluoride is a real concern (**Section 2.1.2**). In order to negate these issues it was vital to pursue a number of different fluorinating reagents with varying reactivities. Four sources of fluoride with a wide breadth of reactivities are; silver (I) fluoride,

tetrabutylammonium fluoride **3.28** (TBAF, **Figure 3.5**), caesium fluoride and tetrabutylammonium difluorotriphenylsilicate **3.29** (TBAT).

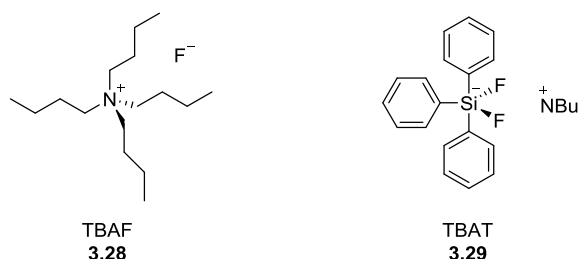


Figure 3.5 - Nucleophilic sources of fluoride.

Silver (I) fluoride is often used in the formation of alkyl fluorides from alkyl halides.^[102] Reactions are possible under mild conditions, on relatively hindered substrates (e.g. bromoadamantanes),^[103] and it is available as an anhydrous solid. It is light sensitive however, and relatively expensive.

TBAF **3.28** is a source of fluoride frequently used in the mild deprotection of silyl protecting groups and other desilylation reactions.^[104] It is also a useful fluorinating reagent, with a good solubility in organic solvents and high cost-effectiveness.^[105] The complete drying of tetraalkylammonium species such as TBAF is difficult however, with the high basicity of fluoride leading to Hoffman elimination under anhydrous conditions (**Figure 3.6**).^[64] Residual water can lead to alcohol formation **3.33**, rather than the desired alkyl fluoride **3.31** (see **Scheme 3.7**).^[106]

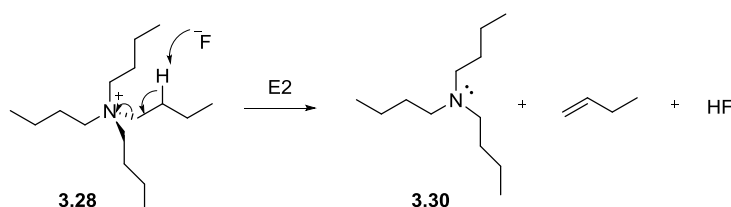
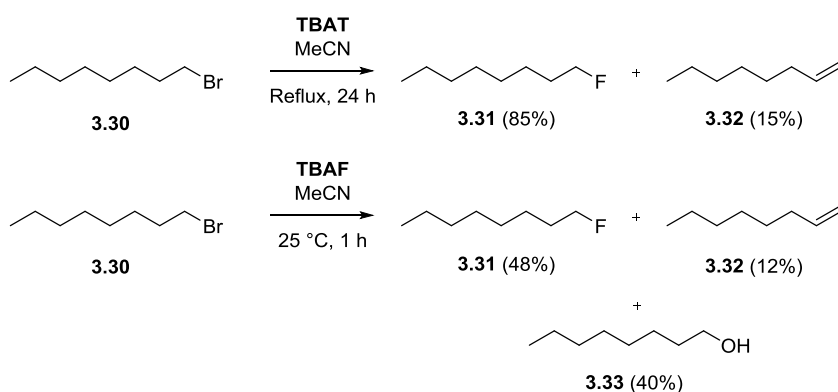


Figure 3.6 - Hoffman elimination of TBAF.^[64]

Like other alkali metal fluorides CsF is very cost effective. It also has the lowest ionic strength of the alkali fluorides, meaning caesium fluoride has both a higher nucleophilicity and greater solubility in organic solvents. Strong hydrogen bonding and high basicity still prevail however.

Tetrabutylammonium difluorotriphenylsilicate **3.29** (**Figure 3.5**) was developed by Pilcher et al^[106] as an anhydrous source of fluoride. The silicate complex slightly lowers the nucleophilicity of the fluoride ion, but a significant attenuation of basicity, relative to other F⁻ sources (e.g. TBAF - **Scheme 3.7**),^[106] makes it an excellent source of nucleophilic fluoride. It is very costly however, and of low atom economy.

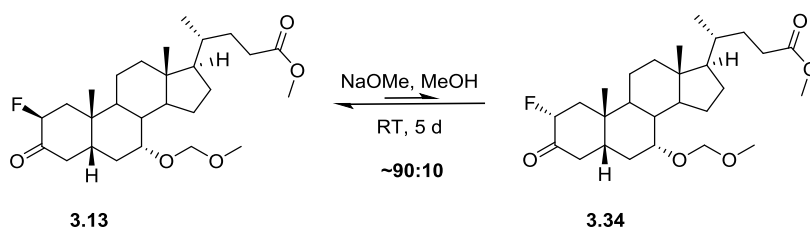


Scheme 3.7 - Comparing reactivities of TBAT vs. TBAF.

3.2.3 Synthesis of 2 α -fluoro moiety *via* epimerisation of 2 β -fluoro moiety

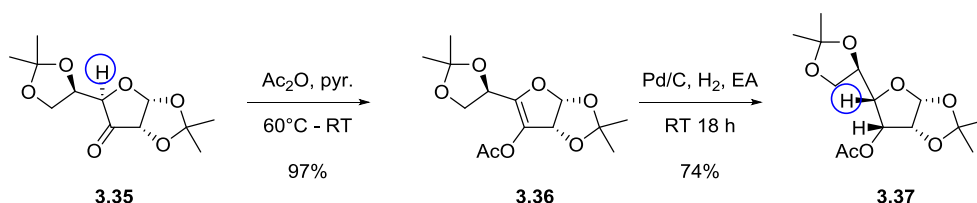
3.2.3.1 Basic epimerisation of 3.1.16

A base-catalysed epimerisation was performed on the 2 β -fluoro ketone **3.13** (Scheme 3.8), with 0.1 eq of NaOMe for 5 days at RT. Unfortunately, the equilibrium lay towards the 2 β -fluoro **3.13** (90%), rather than the 2 α -fluoro **3.34** (10%). The low equilibria ratio, and poor separation of **3.13** from **3.34** made this an unviable route towards 2 α -fluorinated derivatives.

Scheme 3.8 - Equilibration of 2 β -fluoroketone epimers.

3.2.3.2 Epimerisation of 3.1.16 through enol acetate formation

Isomerisation of an α -ketonic stereogenic (e.g. **3.35**, Scheme 3.9) centre can also be achieved through enol acetate formation, *via* an sp^2 hybridised centre (e.g. **3.36**), to yield the isomerised product (**3.37**) after hydrogenation.^[107]

Scheme 3.9 - Raju et al^[107a] use of enol acetates to invert an α -ketonic stereocentre.

A key consideration for selectivity is that hydrogenation will occur at the least hindered face of the enol acetate. In the case of 2 β -fluoro derivative **3.13**, provided enol acetate formation was selective towards the $\Delta_{2,3}$ -isomer **3.38**, hydrogenation is then likely to occur to the less-hindered

β -face, yielding the desired 2α -fluoro and 3α -hydroxy stereochemistry in derivative **3.39** (Figure 3.7).

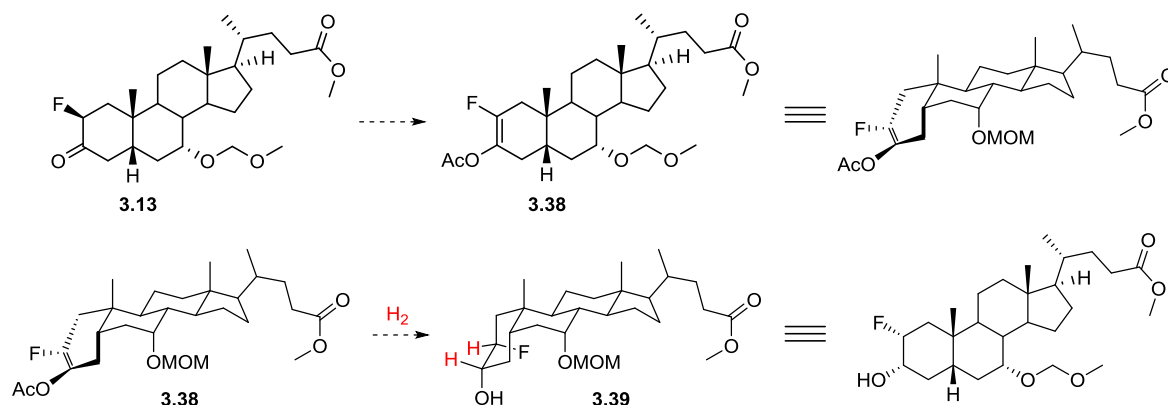


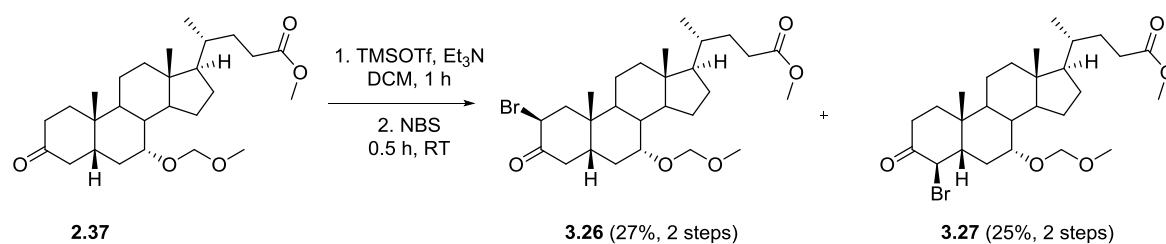
Figure 3.7 - Proposed enol acetate formation and subsequent hydrogenation.

The acetic anhydride/pyridine method that was shown to be effective by Raju *et al.*^[107a] (Scheme 3.9) was first performed on 2β -fluoro ketone **3.13**, however no reaction was observed *via* TLC or through ^1H NMR analysis. An alternative method^[107c] using isopropenyl acetate with catalytic H_2SO_4 yielded a complex mixture of products which could not be purified. A number of other enol acetate syntheses have been published in the literature: replacing pyridine with perchloric acid or DMAP to catalyse the reaction,^[107d, 108] replacing Ac_2O with acetyl chloride,^[107f] and the use of pTSA^[107c, 107g] instead of H_2SO_4 . However, due to time constraints this route was not pursued.

3.2.4 Synthesis of 2α -fluoro moiety *via* nucleophilic attack of a 2β -leaving group

The synthesis of 2α - and 4α -fluorinated derivatives (Figure 3.4) *via* nucleophilic substitution was subsequently explored. The α -bromination of a 3-keto BA derivative has been achieved before, with Br_2/AcOH tending to be the favoured conditions.^[101, 109] The ease of reaction is a benefit of using such conditions, however overall these were unpreferred due to issues of overbromination,^[101] and poor-selectivity towards the 2β -brominated product.^[109]

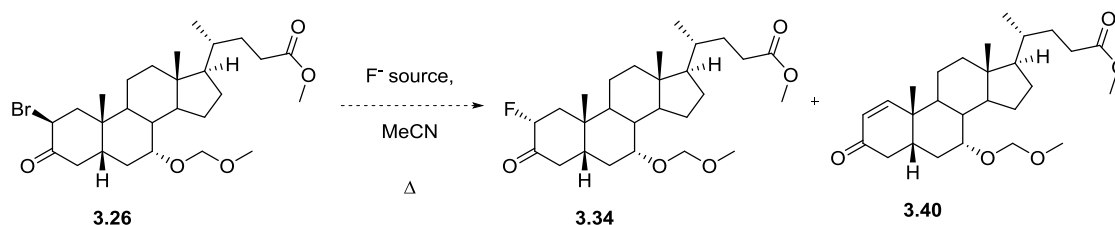
The desired 1:1 regioselectivity of ketone α -halogenation had been achieved in Section 3.1 *via* silyl enol ether derivatives **3.16** and **3.17** (Table 3.2), and due to the synthesis of a pre-formed enolate, no overhalogenation was possible. These conditions were applied to ketone **2.37** (Scheme 3.10), with Selectfluor[®] replaced by *N*-bromosuccinimide as a source of Br^+ .



Scheme 3.10 - α -Bromination of 3-keto CDCA derivative 2.37.

The resulting 2 β -bromo **3.26** (Scheme 3.10) and 4 β -bromo **3.27** compounds were formed in a reasonable yield, and in a roughly 1:1 ratio. The 4 β -bromo compound **3.27** decomposed from a thick colourless gum into a brown amorphous solid within hours of synthesis, despite storing in the freezer under darkness, making it less synthetically useful. The 2 β -bromo compound **3.26** was more stable however, and was subjected to a series of nucleophilic sources of fluoride (Table 3.3).

Table 3.3 - Attempts towards nucleophilic fluorination of 3.26.



Entry	F ⁻ Source	Solvent	25 °C	60 °C	90 °C
1	Ag(I)F	MeCN	No reaction	Formation of unknown ¹	N/A
2	TBAF	MeCN	Elimination to form 3.40 ²	N/A	N/A
3	CsF	MeCN	No reaction	Partial elimination to 3.40 (\approx 20%)	Elimination to 3.40 ²
4	TBAT	MeCN	No reaction	Partial elimination to 3.40 (\approx 50%)	Elimination to 3.40 ²

¹ Product could not be identified *via* standard analytical methods (e.g. NMR, mass spec, IR); ² due to small scale of reactions no isolated yield was obtained.

Reactions were all performed under darkness in acetonitrile; initially starting at room temperature, and warming if reactions were slow. After stirring overnight, the TBAF reaction (Entry 1, Table 3.3) had led to elimination to form the Δ 1,2-enone **3.40** (as shown by ¹H NMR analysis: H₁ (6.8 ppm, d, *J*=10.3 Hz), H₂ (5.9 ppm, d, *J*=10.1 Hz) similar to literature values).^[109] Starting material remained in reactions with the other F⁻ sources (Entries 2-4). The remaining reactions were warmed to 60°C overnight. The AgF reaction (Entry 2) led to the complete conversion to an unknown, which was neither the desired 2 α -fluoro **3.34**, the 2 β -bromo starting

material **3.26**, ketone **2.37** nor enone **3.40**. At 60 °C the CsF and TBAT reactions (**Entries 3 and 4**) both led to partial elimination to enone **3.40**. Heating to 90°C for a further 24 hr led to complete elimination in both the CsF and TBAT reactions. No fluorination was observed in any sample through the analysis of the ^{19}F NMR spectra.

3.3 2 α - and 4 α -Fluorohydrins - Route 3

3.3.1 Retrosynthetic analysis

The failure of previous routes (**Sections 3.1 and 3.2**), meant an alternative method was required to synthesise the 2 α -fluoro **1.39** and 4 α -fluoro **1.38** CDCA analogues (**Figure 3.8**). The $\Delta^{2\beta,3\beta}$ -epoxide **2.22** and $\Delta^{3\beta,4\beta}$ -epoxide **2.23** synthesised in **Section 2.2.3** (which were separable *via* flash chromatography) had inspired us to pursue a route *via* nucleophilic epoxide opening.

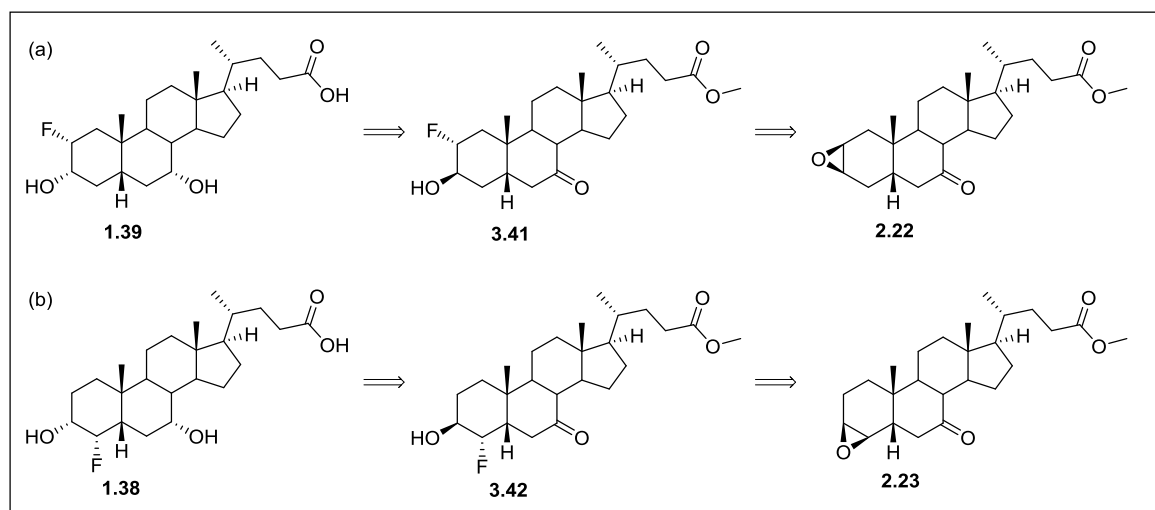


Figure 3.8 - Second retrosynthetic analysis of 2 α - and 4 α -fluoro derivatives.

Hence, a retrosynthetic analysis of 2 α -fluoro CDCA **1.39** to the $\Delta^{2\beta,3\beta}$ -epoxide **2.22** leads *via* 2 α -fluoro-3 β -hydroxy analogue **3.41** (**Figure 3.8a**). Considering the half-chair structure of epoxide **2.22** (**Figure 3.9**), nucleophilic epoxide opening is predicted to occur at the desired 2 α -position *via* the more favourable chair transition state **3.43**. Opening of epoxide **2.22** with a suitable source of fluoride would therefore lead to fluorohydrin **3.41**, and through 3-hydroxy isomerisation and 7-keto reduction, 2 α -fluoro CDCA **1.39** would be accessible.

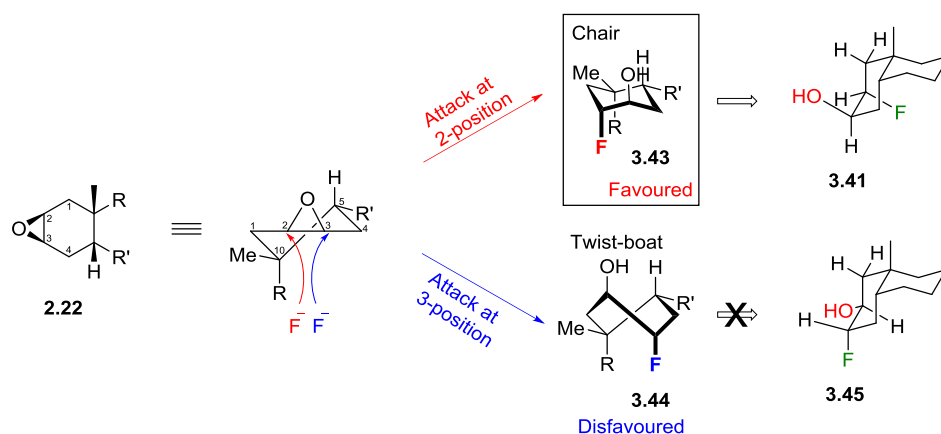


Figure 3.9 - Potential transition states for 2- and 3-fluoride attack of $\Delta^{2\beta,3\beta}$ -epoxide.

A similar retrosynthesis of 4 α -fluoro CDCA 3.42 can be considered (Figure 3.8b). Epoxide opening of the $\Delta^{3\beta,4\beta}$ -epoxide 2.23 is predicted to occur at the desired 4 α -position *via* the more stable chair transition state 3.48, leading to fluorohydrin 3.42 (Figure 3.10). Selectivity towards 4 α -nucleophilic attack of a $\Delta^{3\beta,4\beta}$ -epoxide BA derivative was also observed by Tavares da Silva *et al.*^[110] Isomerisation of the 3 β -hydroxyl to the desired 3 α -OH, along with 7-keto reduction and methyl ester hydrolysis could then lead to 4 α -fluoro CDCA 1.38.

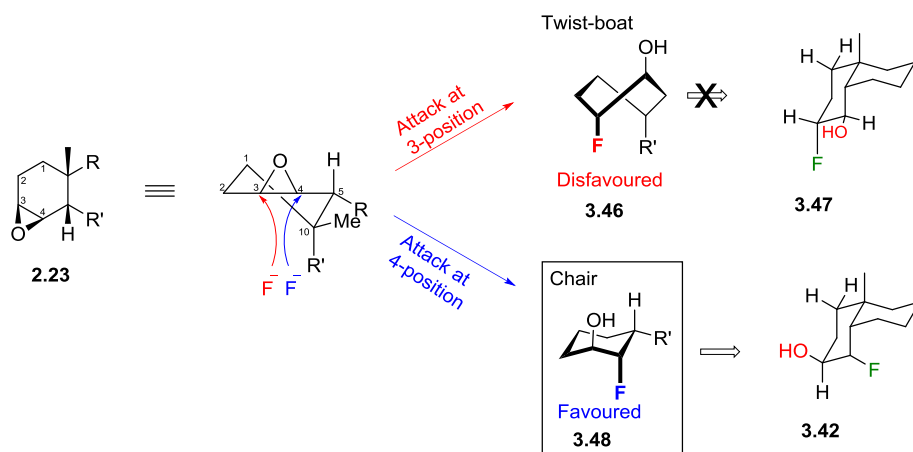


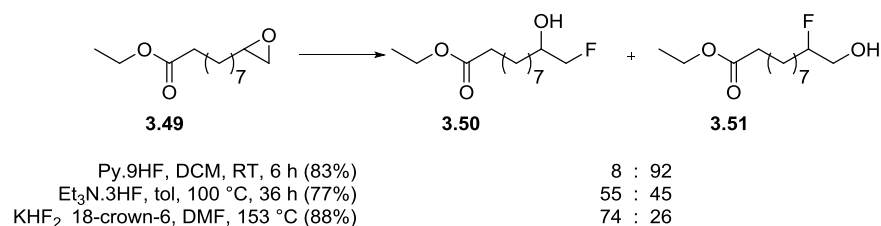
Figure 3.10 - Potential transition states for 3- and 4-fluoride attack of $\Delta^{3\beta,4\beta}$ -epoxide.

3.3.2 Fluorination chemistry

Acidic sources of fluoride are able to open epoxides with high regio- and stereo-selectivity.^{[111],[112]} A number of hydrogen fluoride reagents exist, each with varying physical properties and reactivities.^{[111],[112],[113],[114],[115]} A feature of all HF reagents is their inherent toxicity, and a consideration of this is vital for all such reactions. The most widely used source of HF is probably anhydrous hydrogen fluoride, although its low boiling point (19.5 °C) and highly corrosive nature hinder its use in small scale synthesis.^{[111],[116]} Aqueous HF (hydrofluoric acid) is easier to handle, however the hydration of the fluoride ion significantly impairs the nucleophilicity of F⁻. Due to the

significant limitations of these reagents, a number of important HF-organic base reagents (e.g. HF.pyridine - Olah's reagent^[117], 3HF.Et₃N^[118], HF.DMPU^[119]) have been developed.

Pyridinium poly(hydrogen fluoride) generally contains ≈70% HF and ≈30% pyridine by weight, which equates to a 9:1 molar ratio.^{[112],[114]} HF.pyridine is a stable liquid at room temperature, although it is still a highly acidic (second after anhydrous HF), fuming reagent that is capable of etching borosilicate glass.^{[116],[120]} The high acidity of Olah's reagent leads to a much higher reactivity towards epoxides compared with other HF-based reagents (**Scheme 3.11**).^[121] The acidic nature also leads to a pronounced selectivity towards secondary fluorination **3.51** over primary fluorination **3.50** (92:8) in the case of primary epoxides (e.g. **3.49**).



Scheme 3.11 - Comparing reactivities of HF sources.^[121]

This selectivity is rationalised by an acidic reaction pathway (**Figure 3.11**). Protonation of the epoxide leads to cationic intermediate **3.52**, leading to carbocation formation on the more electron rich secondary carbon, and attack of the fluoride to yield **3.51**. In the case of cyclic epoxides such as **2.22** and **2.23** (**Figure 3.8**) the difference in carbocation stability on C2 and C3 is thought to be negligible, and product selectivity is likely to result from the most stable transition state (**Figure 3.9** and **Figure 3.10**).

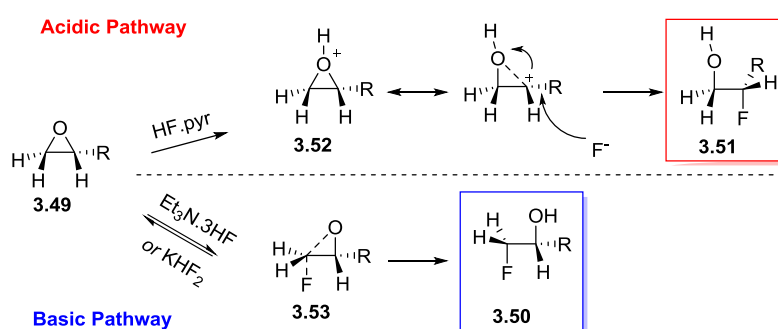


Figure 3.11 - Acidic and basic fluoride mediated epoxide openings.

Triethylamine trihydrogen fluoride (Et₃N.3HF, TREAT HF) is another readily available source of HF, with the key advantage of not corroding borosilicate glass,^[113, 116] a direct result of the lower acidity of TREAT HF vs. HF.pyridine. The higher basicity of triethylamine compared to pyridine, and fewer equivalents of acid (Et₃N.3HF vs. pyridine.9HF), are the reason for this significant change in reactivity.^[122] The higher basicity of TREAT HF also makes the fluoride ion more nucleophilic

which, coupled with the lower acidity, can lead to a significant difference in reaction selectivity (**Scheme 3.11**) and mechanistic pathway (**Figure 3.11**).^[120-121] In the case of primary epoxides (**Scheme 3.11**), treatment with Et₃N.3HF leads to the formation of a greater proportion of primary fluorination **3.50** compared to the competing secondary fluorination **3.51** (55:45). This result can be explained by significantly lower acidic activation of the epoxide **3.49** (**Figure 3.11**) resulting in lower secondary fluorination *via* the more stable carbocation. Instead, the higher nucleophilicity of fluoride in TREAT HF leads to a dominance of the basic reaction pathway. This direct epoxide attack favours primary fluorination at the least hindered oxirane carbon, leading to **3.50**. With this lower epoxide activation, more forcing reaction conditions are required (**Scheme 3.11**).

Potassium hydrogen difluoride (KHF₂) and tetrabutylammonium bihydrogen trifluoride (^tBu₄NH₂F₃) are examples of solid sources of HF.^[115, 120, 123] Caution must still be taken when handling them, but they are considerably safer than TREAT HF and HF.pyridine. They are more similar to Et₃N.3HF in terms of reactivity, with high selectivity towards primary fluorination **3.50** compared to the competing secondary fluorination **3.51** (74:26, **Scheme 3.11**). They are much less reactive towards epoxides than HF-amine complexes however, and even more forcing conditions are required.

3.3.3 Large scale synthesis of Δ2β,3β- and Δ3β,4β-epoxides

In order to pursue this route, an efficient synthesis of epoxides **2.22** and **2.23** had to be accomplished (**Figure 3.12**). Epoxidation of the alkene mixture had been achieved in **Section 2.2.3**, and this method could be repeated on a large scale. A new method towards alkenes **2.20** and **2.21** was required however, as their synthesis as by-products of deoxofluorination (**Scheme 2.4**) was not suitable on a large scale.

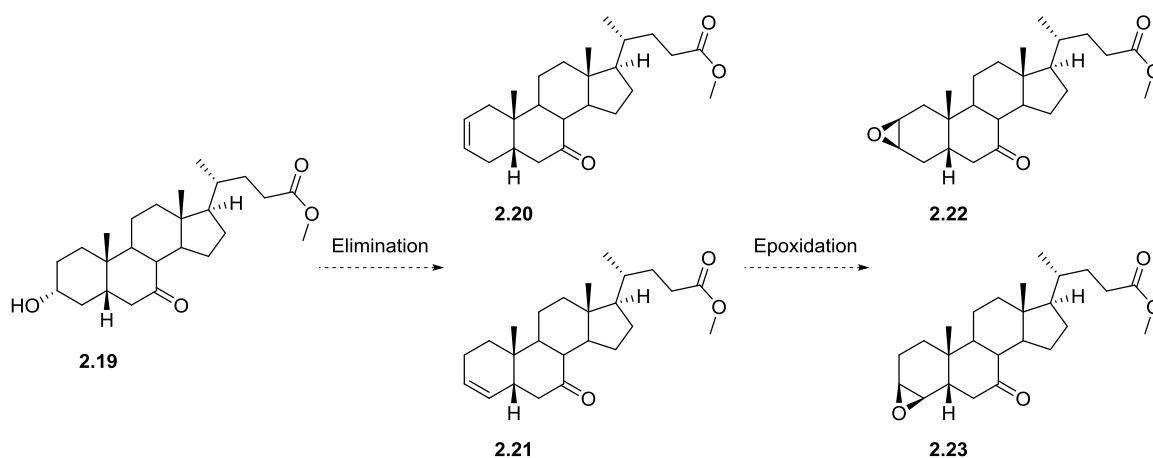
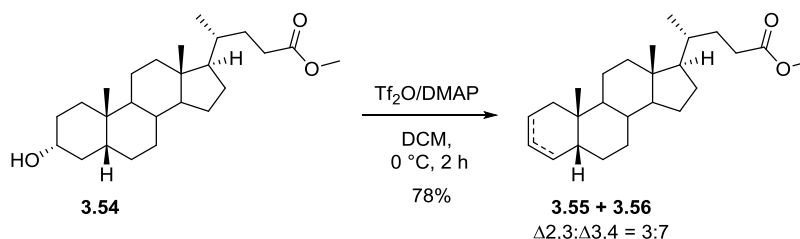


Figure 3.12 - Proposed route towards epoxides 2.22 and 2.23.

3.3.3.1 Alkene synthesis using Tf₂O/organic base

Kumar *et al*^[124] have reported a one-pot method for the elimination of secondary alcohol groups on a variety of steroid skeletons. The method uses triflic anhydride to generate an excellent leaving group from the hydroxyl residue, which can then be eliminated with a suitable base to yield the corresponding alkene(s) in good yield. In their procedure Kumar *et al*^[124] reported a mixture of Δ 2,3- **3.55** and Δ 3,4-alkenes **3.56** when the reaction was performed on LCA methyl ester **3.54** (Scheme 3.12).



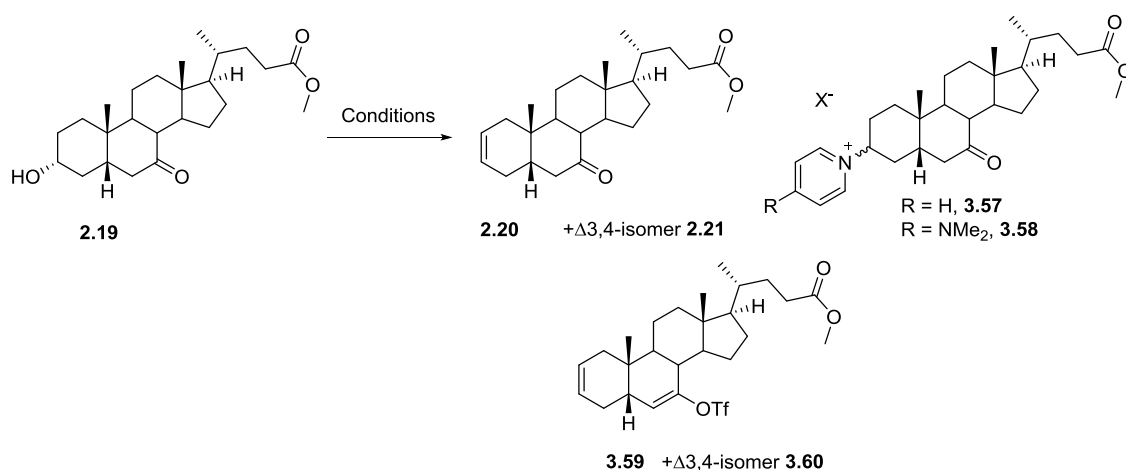
Scheme 3.12 - Kumar *et al* method for steroidal 2° alcohol elimination.^[124]

These conditions were applied to **2.19** in order to synthesise the desired alkenes **2.20** and **2.21** (Figure 3.12). A number of organic bases (pyridine, Et₃N, lutidine, DMAP) were investigated for the elimination of the 3 α -OH group of **2.19** (Table 3.4). An initial reaction using pyridine as the base (Entry 1, Table 3.4) led to the formation of desired mixture of alkenes **2.20/2.21**, in a 1:1 ratio with the pyridinium substitution products **3.57** as a mixture of 3 α - and 3 β -epimers. The base was changed to lutidine (2,6-dimethylpyridine, Entry 2) as a more sterically hindered alternative to pyridine in order to lower nucleophilic substitution. The reaction did lead to only negligible formation of the undesired pyridinium salt, however the desired alkene mixture was formed in a low yield (13%). A significant amount of the remaining material was the enol triflate products **3.59/3.60** (33%), which made this base unsuitable. A subsequent reaction with triethylamine as the base (Entry 3) led to even greater formation of enol triflates **3.59/3.60**, and none of the desired 7-keto alkene mixture **2.20/2.21** could be identified. Two small scale reactions using DMAP as the base (Entries 4 and 5) proved very successful with significant formation of the desired alkenes **2.20/2.21**, and only minor substitution to yield **3.58**. The reaction was scaled up (Entry 6), however much higher substitution to the pyridium salt **3.58** was observed, despite the procedure remaining the same.

All previous reactions (Entries 1-6, Table 3.4) had been allowed to warm to RT, as little to no progress was observed at the 0 °C reaction temperature reported in the literature.^[124] The lower overall yields obtained, and discrepancy between reactions of different scale (Entries 4-6) was thought to be a result of the rate of substitution occurring faster than the desired elimination at higher temperatures.^[124] It was therefore decided to slow the rate of warming, and follow

reaction progress at intermediate temperatures (**Entry 7**). The reaction was initially held at 0-5 °C but no reaction occurred. Warming slightly to 10 °C led to a successful reaction after 2 h. Following an aqueous work up the desired alkenes **2.20/2.21** were formed in a good yield. Attempts to separate the alkenes by flash chromatography were unsuccessful, and the $\Delta^{2,3}$ - and $\Delta^{3,4}$ -isomers were carried through as a mixture.

Table 3.4 - Synthesis of alkenes 2.20 and 2.21 through 3 α -OH elimination.

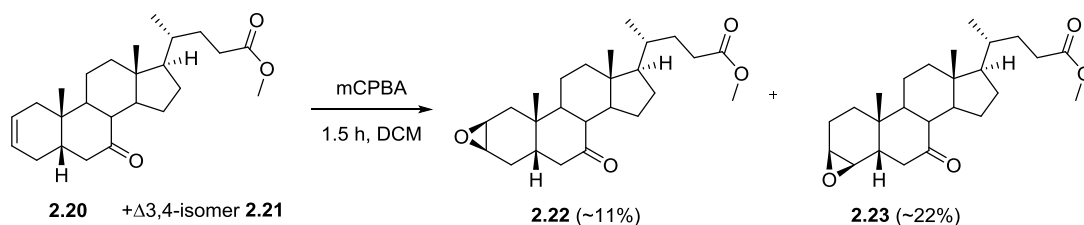


Entry	Conditions	Base	Scale	Product(s)
1	Tf ₂ O (1.1 equiv), base (3 eq), DCM, 0 °C - RT	Pyridine	100 mg	2.20/2.21 : 3.57 \approx 1:1*
2	Tf ₂ O (1.5 equiv), base (3 eq), DCM, 0 °C - RT	Lutidine	500 mg	2.20/2.21 (13%), 3.59/3.60 (33%)
3	Tf ₂ O (1.5 equiv), base (3 eq), DCM, 0 °C - RT	Et ₃ N	100 mg	3.59/3.60 (73%)
4	Tf ₂ O (1.05 eq), base (3 eq), DCM, 0 °C - RT	DMAP	200 mg	2.20/2.21 (major)*, 3.58 (minor)*
5	Tf ₂ O (1.05 equiv), base (3 eq), DCM, 0 °C - RT	DMAP	1.0 g	2.20/2.21 (31%), 3.58 (minor)*
6	Tf ₂ O (1.05 equiv), base (3 eq), DCM, 0 °C - RT	DMAP	5.5 g	2.20/2.21 (16%), 3.58 (35%)
7	Tf ₂ O (1.05 equiv), base (3 eq), DCM, 0 - 10 °C	DMAP	60 g	2.20/2.21 (66%), 3.58 (minor)*

*Not isolated, observed through ¹H NMR analysis of the crude material.

3.3.3.2 Δ 2,3- and Δ 3,4-alkene epoxidation

The epoxidation of alkenes **2.20** and **2.21** was performed in an identical fashion to that shown in **Scheme 2.5**, but the epoxides **2.22** and **2.23** were only formed in a relatively poor isolated yield (33% total, **Scheme 3.13**). Separation of epoxides **2.22** and **2.23** was more difficult on a larger scale and this contributed towards the low isolated yields. Baeyer-Villiger side reactions may also have occurred, but these by-products could not be isolated.

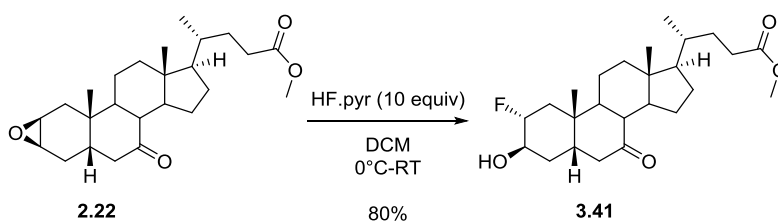


Scheme 3.13 - Epoxidation of alkenes 2.20 and 2.21.

3.3.4 Synthesis of 2 α -fluorinated BA derivatives

3.3.4.1 Opening of Δ 2 β ,3 β -epoxide with HF.pyridine

The nucleophilic opening of Δ 2 β ,3 β -epoxide **2.22** was first attempted with HF.pyridine due to its higher acidity compared to other HF reagents, allowing the reactions to be performed at lower temperatures (see **Scheme 3.11**). The reaction was performed using 10 equiv. of HF.pyridine and, following purification, the expected 2 α -fluoro derivative **3.41** was isolated in a good yield (**Scheme 3.14**).



Scheme 3.14 - Opening Δ 2 β ,3 β -epoxide 2.22 with HF.pyridine.

The regio- and stereochemistry of fluorination was confirmed through analysis of the coupling patterns/magnitudes in the ^1H and ^{19}F NMR spectra.

3.3.4.2 Isomerisation of 3 β -hydroxy group

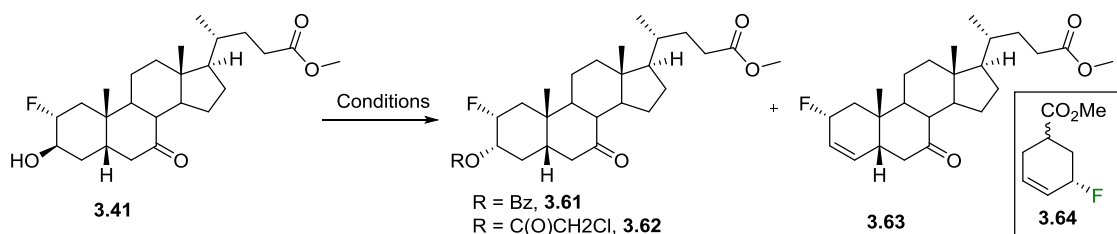
Fluorination of epoxide **2.22** had installed the fluorine at the desired 2 α -position **3.41** (**Scheme 3.14**) but had resulted in the undesired 3 β -OH stereochemistry. An isomerisation of the 3 β -hydroxy moiety was required.

3.3.4.2.1 Mitsunobu Reaction on 3.2.3

The Mitsunobu reaction^[80] was used in **Section 2.3.1** in order to invert the stereochemistry of the 3 α -OH derivative **2.19** to the 3 β -OH derivative **2.30** (**Scheme 2.8**). On this occasion an inversion from 3 β -OH derivative **3.3.1** to 3 α -OH derivative **3.2.24** was required (**Table 3.5**).

The conditions shown in **Scheme 2.8** were applied to 3 β -OH derivative **3.41** (**Entry 1, Table 3.5**) however this led to a poor conversion to the desired 3 α -OBz derivative **3.61**. It was thought that this poor conversion may be a result of the hindered nature of the cis-decalin ring preventing attack of the α -face. Saiah *et al*^[125] have previously shown that chloroacetic acid can be successfully used to invert sterically hindered alcohols, where bulkier acids (e.g. benzoic) have proved unsuccessful. However, with chloroacetic acid as the nucleophile, no conversion to **3.62** was seen by either ¹H or ¹⁹F NMR analysis (**Entry 2**). A subsequent reaction using BzOH (**Entry 3**) with increased equivalents of PPh₃, DEAD and carboxylic acid gave a much greater conversion (\approx 75%) to the desired 2 α -fluoro-3 α -benzoate **3.61**, along with an unknown by-product proposed to be **3.63**. The allyl fluoride could form through the elimination of the 3 β -OBz leaving group, rather than the desired nucleophilic substitution. It is proposed following analysis by mass spectrometry, and through comparison of key chemical shifts upon NMR analysis,¹⁴ with an allyl fluoride (**3.64**) synthesised by Lee *et al*.^[126]

Table 3.5 - Mitsunobu reaction on 3.41.



Entry	Conditions	Acid (eq)	Scale	Yield
1	PPh ₃ , DEAD (1.5 eq each), THF	Benzoic (1.5)	10 mg	\approx 10% 3.61 ; 90% 3.41 .* No elimination observed.
2	PPh ₃ , DEAD (1.5 eq each), THF	Chloro-acetic (1.5)	10 mg	No reaction.
3	PPh ₃ , DEAD (2.5 eq each), THF	Benzoic (2.5)	1.05 g	\approx 75% 3.61 ; 15% 3.41 ; 10% 3.63 .*

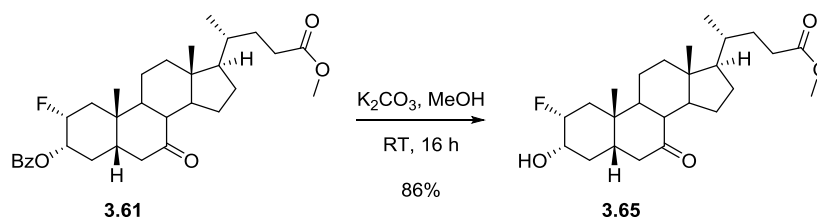
* As judged by ¹H and ¹⁹F NMR analysis of the crude material.

¹⁴ CHF in **3.63** δ = 5.94-5.66 ppm (m); CHF in **3.64** δ = 5.67-5.60 ppm (m). ¹⁴ CHF in **3.63** δ = -167.6 ppm (tt, J =45.1, 15.6 Hz); CHF in **3.64** δ = -162.1 (m, *trans*-isomer), -172.4 (m, *cis*-isomer).

The reagents/by-products (e.g. $O=PPh_3$) were found to have similar polarities to the desired product **3.61**. This led to difficulties in purification (also found in **Section 2.3.1**), preventing isolation of pure product. An accurate yield could not be determined, but the cleanest fractions ($\approx 30\%$ overall) were brought forward.

3.3.4.2.2 Benzoate methanolysis of **3.61**

A methanolysis of benzoate **3.61** was performed in dry methanol with catalytic potassium carbonate (**Scheme 3.15**),^[127] yielding alcohol **3.65** in a yield of 86%.¹⁵

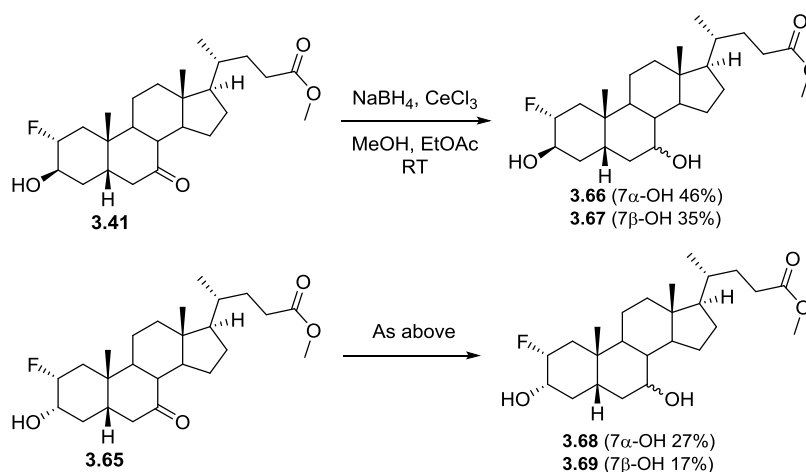


Scheme 3.15 - Benzoate methanolysis of **3.61.**

3.3.4.3 Synthesis of 2 α -fluoro analogues

3.3.4.3.1 Reduction of 7-keto moiety of **3.41** and **3.65**

Luche reduction conditions were applied to derivatives **3.41** and **3.65** (**Scheme 3.16**). The 7-keto moiety was successfully reduced in each case, with the 7 α -OH and 7 β -OH derivatives separable *via* flash chromatography on both occasions. 2 α -fluoro derivatives **3.66-3.69** were isolated in good to medium yields.



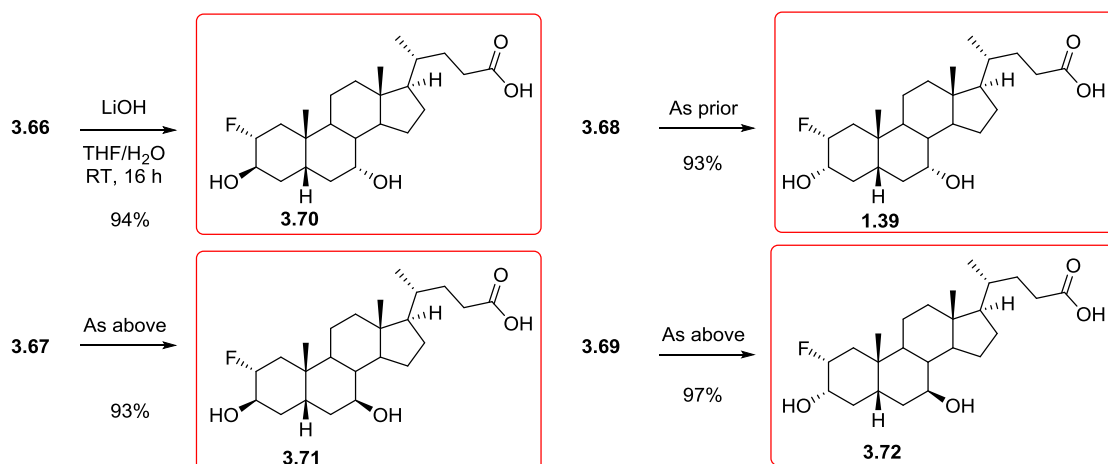
Scheme 3.16 – Reduction of **3.41 and **3.65**.**

¹⁵ Yield judged by ^1H NMR analysis.

3.3.4.3.2 Hydrolysis of methyl ester in 2 α -fluorinated derivatives

A methyl ester hydrolysis was performed on 2 α -fluorinated derivatives **3.66-3.69** (Scheme 3.17).

The reactions proceeded with excellent yields, and no elimination products were observed.



Scheme 3.17 - Deprotection of 2 α -fluoro analogues.

3.3.5 Synthesis of 4 α -fluorinated BA derivatives

3.3.5.1 Opening of Δ 3 β ,4 β -epoxide with HF

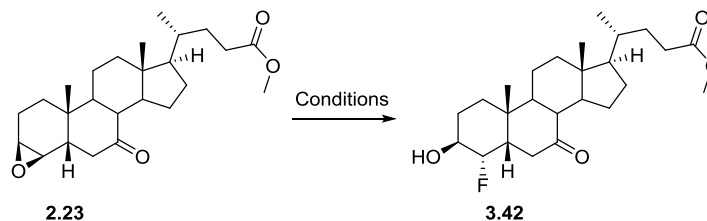
The fluorination conditions used successfully on the Δ 2 β ,3 β -epoxide **2.22** (Scheme 3.14) were applied to the Δ 3 β ,4 β -isomer **2.23**, however no reaction was observed (Entry 1, Table 3.6). The reaction was warmed to RT and stirred for 24 h with a further 10 equiv of HF.pyridine, however only starting material was recovered. A set of small scale reactions using alternative conditions, with other HF-based reagents (see Section 3.3.2), were performed in order to synthesise the desired fluorohydrin **3.42** (Table 3.6).

The amount of HF.pyridine was first increased in order to provide more forcing reaction conditions (Entries 2 and 3, Table 3.6). Both reactions led to a far superior conversion to the desired fluorohydrin, along with an impurity thought to be a fluoroalkene. Due to the serious hazards associated with HF.pyridine, which would be heightened in larger scale reactions, other synthetic routes were explored (Entries 4-6).

Reactions with KHF_2 and $\text{NEt}_3 \cdot 3\text{HF}$ as sources of HF led solely to recovered starting material (Entries 4 and 5 respectively, Table 3.6).^[128] A further reaction using $\text{NBu}_4\text{H}_2\text{F}_3$ (Entry 6, conditions of Barbier *et al*^[129]) as the source of HF led to the formation of >6 products, none thought to be the desired fluorohydrin **3.42**. Identification of these by-products was not attempted due to the small reaction scale and difficult separation. This left only the HF.pyridine mediated fluorination as a possible route towards fluorohydrin **3.42**. Subsequent scale up reactions were performed

with a minimal amount of DCM to solubilise the reactants, leading to an increase in the effective concentration of HF (**Entries 7 and 8**). This allowed a reduction in the amount of HF used (≈ 30 equiv, **Entry 8**), and ultimately a safer reaction procedure and easier quenching/purification.¹⁶

Table 3.6 - Opening of $\Delta 3\beta,4\beta$ -epoxide 2.23 with HF.



Entry	F ⁻ Source (equiv)	Solvent/temp	Time	Scale	Yield
1	70% HF.pyr (≈ 20)	DCM / 25 °C	3 d	20 mg	No reaction
2	70% HF.pyr (≈ 1000)	DCM / 25 °C	2 h	10 mg	3.42 : fluoroalkene ^a $\approx 60:40^b$
3	70% HF.pyr (≈ 500)	DCM / 25 °C	2 h	10 mg	3.42 : fluoroalkene ^a $\approx 60:40^b$
4	KHF ₂ (2.5)	HO(CH ₂) ₂ OH / 160 °C	3 d	10 mg	No progress
5	NEt ₃ .3HF (≈ 10)	DCM / 25 °C	3 d	10 mg	No progress
6	NBu ₄ H ₂ F ₃ (3)	1,2-DCE / 90 °C	3 d	10 mg	>6 compounds formed, no 3.42 .
7	70% HF.pyr (≈ 375)	DCM / 0 °C	2 h	75 mg	3.42 : fluoroalkene ^a $\approx 60:40.^b$
8	70% HF.pyr (≈ 30)	DCM / 25 °C	2 h	1.3 g	3.42 : fluoroalkene ^a $\approx 60:40$, 28% isolated yield.

^a Peak at -119 ppm (d, $J=15.6$ Hz) in ¹⁹F NMR spectrum characteristic of a fluoroalkene, unfortunately the complete structure could not be elucidated; ^b Unpurified, value obtained through ¹H and ¹⁹F NMR spectral analysis of the crude material.

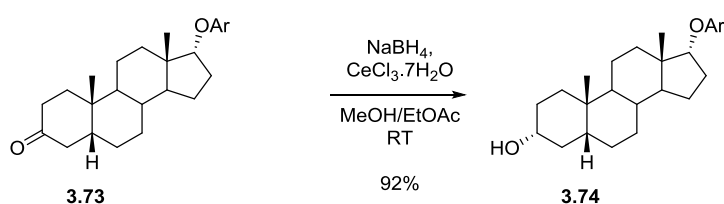
Co-axial 4-fluorohydrin **3.42** (**Table 3.6**) was selectively formed in the reaction, with no 3-fluorination observed (**see Figure 3.10**). The regio- and stereochemistry of fluorine was confirmed

¹⁶ Minor etching of the glass was observed following concentrated HF.pyridine reactions, however this was not deemed sufficient to compromise the strength of the reaction vessel.

through analysis of the ^1H and ^{19}F NMR spectra, and also through single crystal X-ray structural analysis which will be discussed in **Chapter 4 (Figure 4.18 and Figure 4.19)**.

3.3.5.2 Isomerisation of the 3β -hydroxy group in **3.42** through oxidation/reduction

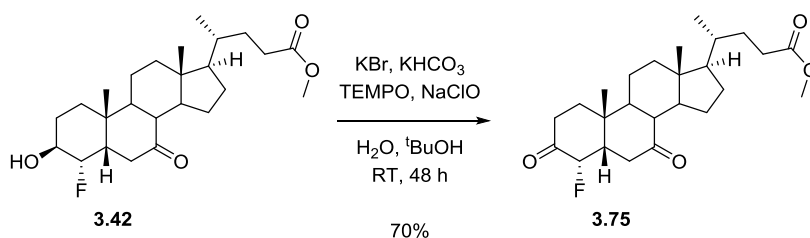
An isomerisation of the 3β -OH functionality was again required. The purification problems associated with 2α -fluoro derivative **3.41** following Mitsunobu reaction (see **Section 3.3.4.2**), led to the use of an alternative 3-hydroxy isomerisation method being sought. Černý *et al.*^[75] have shown that excellent selectivity towards the 3α -OH can be achieved by reduction of the 3-keto moiety in BA derivative **3.73** under Luche conditions (**Scheme 3.18**).^[74] This method could be used to isomerise the 3β -OH in **3.42** to the desired 3α -stereochemistry, *via* the 3-keto intermediate.



Scheme 3.18 - Černý *et al.* reduction of 3-keto bile acid derivative using Luche conditions.^[75]

3.3.5.2.1 Oxidation of **3.42**

A TEMPO based oxidation of the 3β -OH group was achieved in **Section 2.4.1**. These conditions were applied to 3β -OH **3.42**, and the diketo compound **3.75** was isolated in a yield of 70% (**Scheme 3.19**).



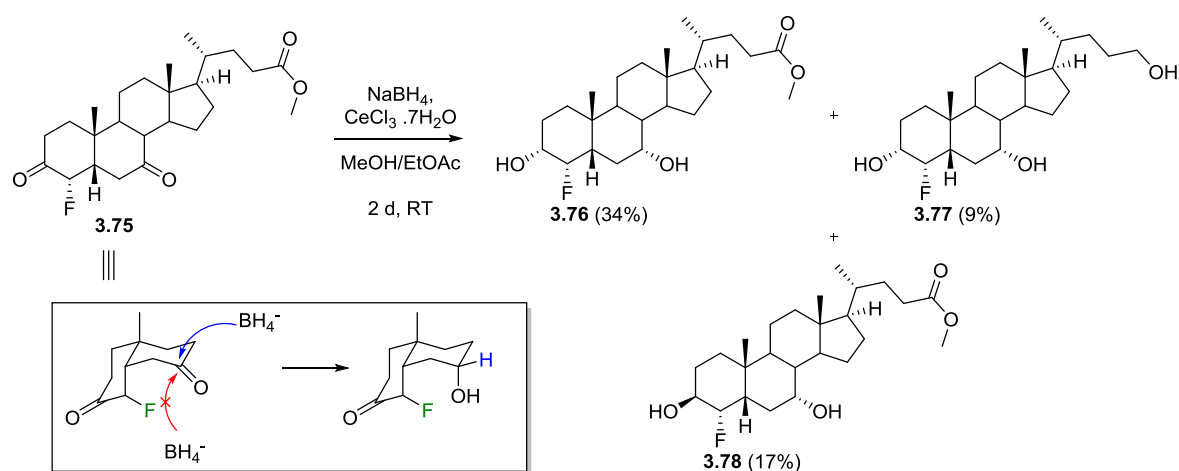
Scheme 3.19 - Oxidation of **3.42** 3β -OH group.

3.3.5.2.2 Reduction of **3.75**

The reduction of diketo **3.75** was achieved using the conditions of Černý *et al.*^[75] The reduction proved slower than previously (**Scheme 2.6** and **Scheme 3.16**), which is thought to be due to the presence of the 4α -fluoro moiety hindering 7-keto reduction through stereoelectronic effects, but was achieved (**Scheme 3.20**) with a large excess of sodium borohydride (10 equiv), and a longer reaction time (2 days).

Following chromatography, the desired 4α -fluoro-CDCA derivative **3.76** (**Scheme 3.20**) was isolated in a yield of 35%, along with 4α -fluoro-CDCA cholanol derivative **3.77** (9%) which was

formed by CeCl_3 activated methyl ester reduction. The other major isolated product was the 3β -OH derivative **3.78** (17%). This selectivity towards 7α -OH formation is thought to result from steric hindrance from the 4α -fluoro moiety, preventing α -facial attack of the 7-keto group.



Scheme 3.20 - Luche reduction of 4α -fluoro-3,7-diketo intermediate.

The relative stereochemistry of the reduction products was confirmed through analysis of the ^1H and ^{19}F NMR spectra (see **Section 2.2.5** for example). Detailed analysis of these molecules also indicated the presence of a strong $\text{C-F} \cdots \text{H-O}$ hydrogen bond between the 4α -fluoro and 7α -OH moieties (**Figure 3.13**). These interactions will be discussed in **Chapter 4**.

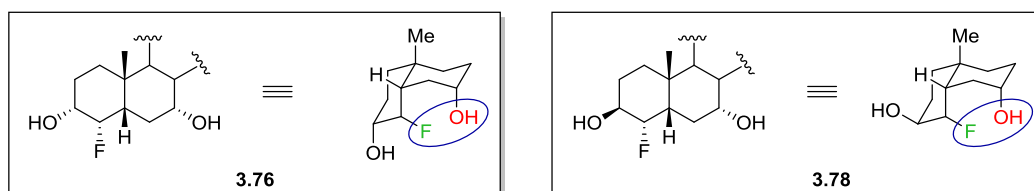
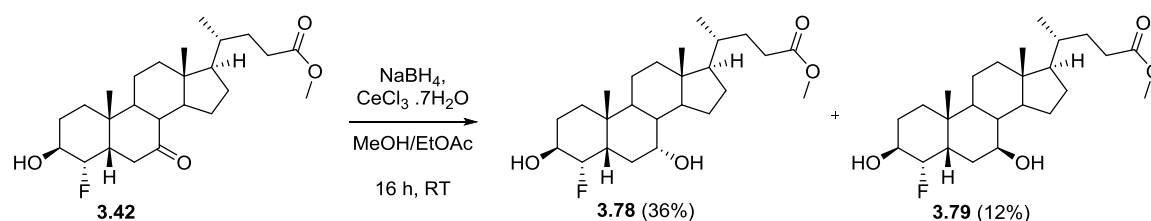


Figure 3.13 - 3D representation of 4α -fluorohydrins **3.76 and **3.78**.**

3.3.5.3 Synthesis of 4α -fluoro analogues

3.3.5.3.1 Reduction of **3.42**

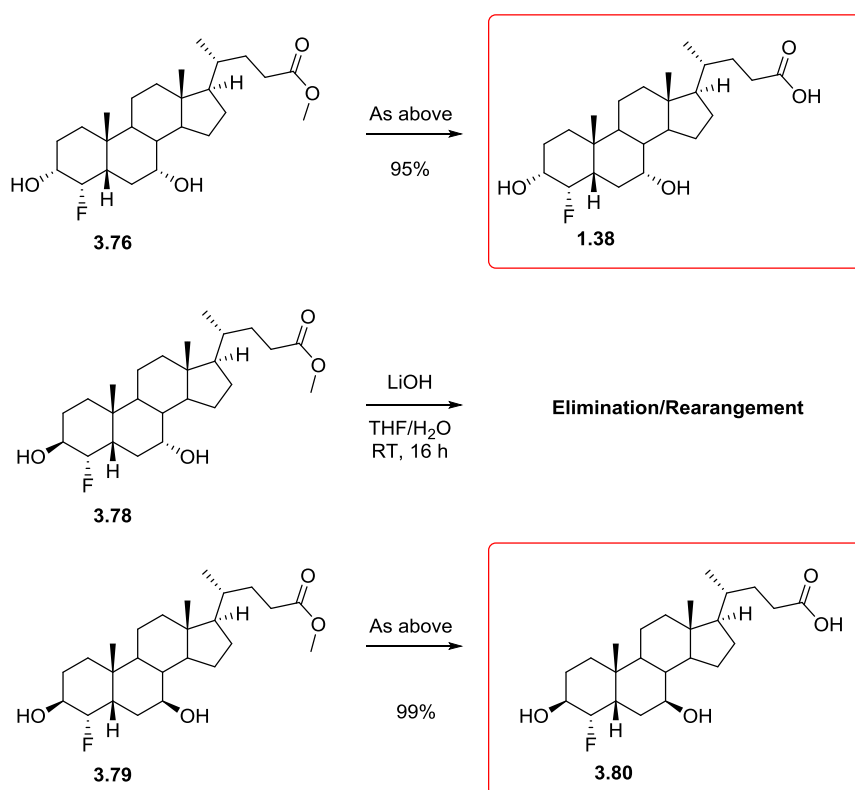
Luche reduction conditions were applied to 4α -fluoro derivative **3.42** (**Scheme 3.21**), but surprisingly both the iso-CDCA **3.78** and iso-UDCA **3.79** derivatives were formed on this occasion. Each were successfully isolated following flash chromatography. Similar to the reduction of **3.75** (**Scheme 3.20**), forcing reduction conditions were required to reach completion of the reaction.



Scheme 3.21 - Reduction of 3.42.

3.3.5.3.2 Hydrolysis of methyl ester in 4 α -fluorinated derivatives

A methyl ester hydrolysis was performed on 4 α -fluorinated derivatives **3.76**, **3.78** and **3.79** (Scheme 3.22). The reactions of derivatives **3.76** and **3.79** showed excellent conversion to final analogues **1.38** and **3.80** respectively. The hydrolysis of **3.78** was less successful however, and basic hydrolysis led to the formation of a number of by-products. Unfortunately these by-products were of similar polarity to the desired analogue, so isolation was not possible. The reason for this poor yield is thought to be due to the increased acidity of the 3 β -OH in **3.78**,¹⁷ this makes alcohol deprotonation much more favourable, leading to a greater potential for Δ 3 β ,4 β -epoxide formation (and potential side reactions of this by-product).

Scheme 3.22 - Deprotection of 4 α -fluorinated derivatives.

¹⁷ Discussed in Section 4.2.5.

3.4 Synthesis of 2,2- and 4,4-difluoro analogues

3.4.1 Retrosynthetic analysis

Two retrosynthetic analyses of 2,2-difluoro CDCA **1.41** were initially considered (**Figure 3.14**). Similar retrosynthetic analyses can be performed on 4,4-difluoro CDCA, but this has not been included for concision.

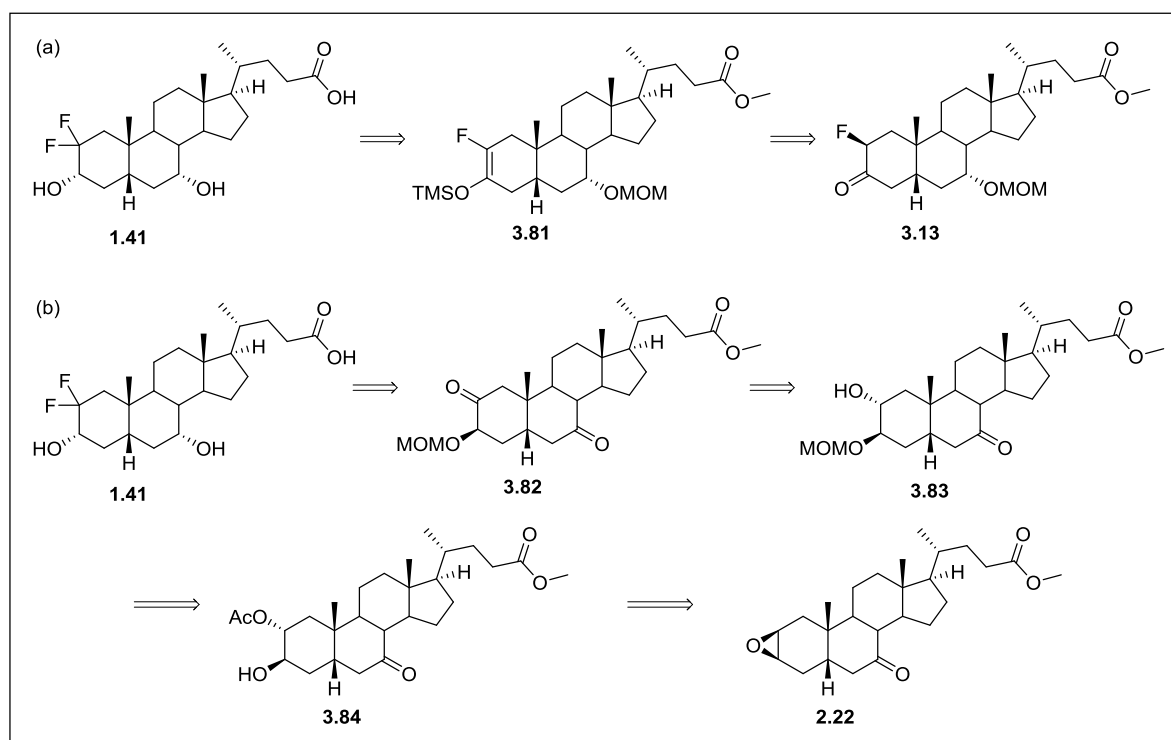


Figure 3.14 - Retrosynthetic analysis of 2,2-fluoro derivatives.

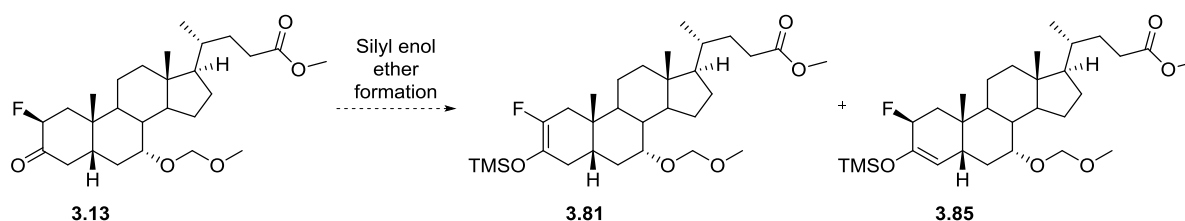
The first retrosynthetic analysis of 2,2-difluoro analogue **1.41** (**Figure 3.14a**) leads back to the previously synthesised 2 β -fluoroketone **3.13** (**Section 3.1.5**). The forward synthesis could be achieved with the formation of the corresponding $\Delta^{2,3}$ -silyl enol ether **3.81**, followed by an electrophilic fluorination using Selectfluor[®] (see **Section 3.1.2** for background), to provide the 2,2-difluoro functionality. Reduction of the 3-keto, and deprotection of the 7 α -OH and carboxylic acid groups would yield the final compound **1.41**. This route relies on the regioselective formation of the $\Delta^{2,3}$ -silyl enol ether **3.81**, and problems may arise if the reaction is unselective, or if the undesired regioisomer is preferentially formed.

A second retrosynthetic analysis of **1.41** gives 2-keto **3.82** as a potential intermediate (**Figure 3.14b**). The deoxofluorination of **3.82** is expected to be selective towards the less-hindered 2-keto functionality, as the 7-keto moiety has been previously shown (by other members of the Linclau group) to only react under very forcing conditions (neat DAST, >50 °C).^[67] Intermediate **3.82** could

be accessed from epoxide **2.22** through nucleophilic opening with an acetate group which, as previously explained, is predicted to occur at the 2 α -position (**Figure 3.9**). This would then be followed by 3 β -OH protection and 2 α -OH deprotection to form **3.83**, then oxidation of the 2 α -OH group to form **3.82**.

3.4.2 Difluorination *via* silyl enol ether

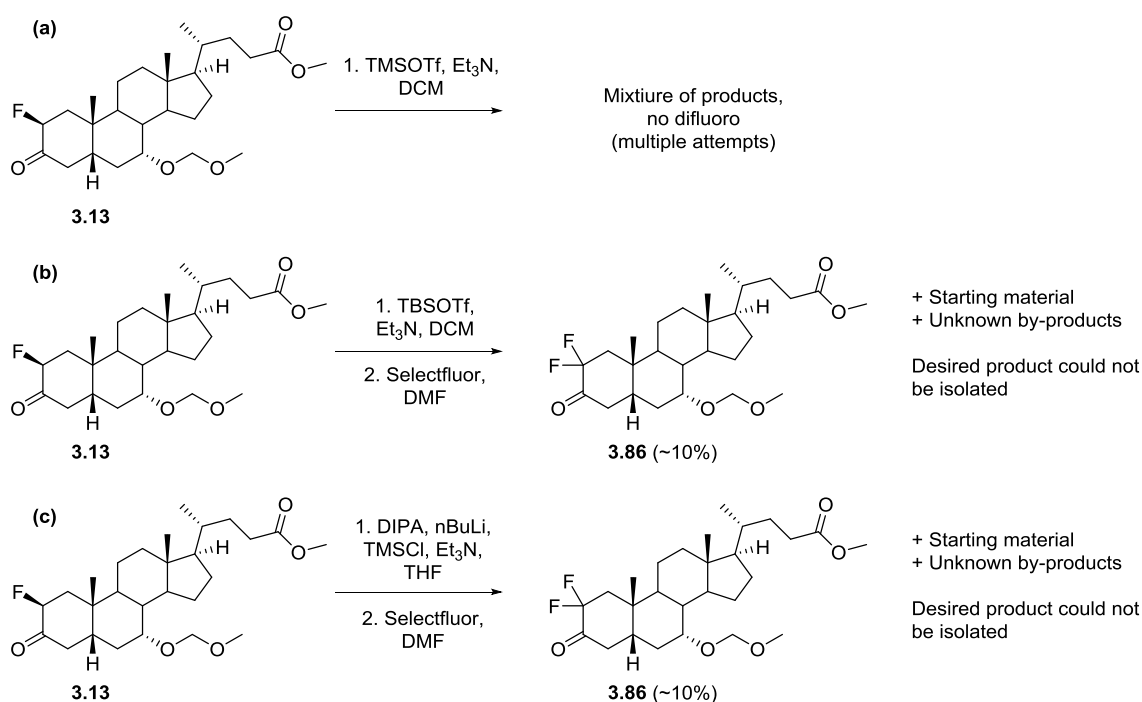
The successful fluorination of silyl enol ethers with Selectfluor[®] was described in **Section 3.1** with 2 β -fluoro **3.13** and 4 β -fluoro **3.15** derivatives synthesised in good yields (**Scheme 3.2**). The formation of difluoro moieties through the formation of fluorosilyl enol ethers has been shown on other substrates,^[51, 130] so could be applied to 2 β -fluoroketone **3.13** (**Scheme 3.23**).



Scheme 3.23 - Silyl enol ethers formation on 3.13.

A number of silyl enol ether formations were attempted in order to synthesise the desired 2,2-difluoro derivative **3.86** (**Scheme 3.24**). Characterisation of the silyl enol ethers **3.81** and **3.85** by analysis of the ¹H and ¹⁹F NMR spectra proved difficult. Accurate mass spectrometry was also not feasible due to product degradation. Hence, silyl enol ethers **3.81** and **3.85**, along with any residual SM **3.13** and potential by-products, were subjected to fluorination with Selectfluor[®] without intermediate purification.

The conditions used successfully in the formation of silyl enol ethers **3.16** and **3.17** (**Table 3.2**) were applied to 2 β -fluoro derivative **3.13** (**Scheme 3.24a**). TLC analysis following treatment with TMSOTf/Et₃N appeared to show complete conversion to a spot characteristic of silyl enol ethers (low polarity, UV active, highly active in KMnO₄ dip), however analysis of the crude ¹H and ¹⁹F NMR spectra was inconclusive. The crude material was treated with Selectfluor[®], however no formation of the difluoro moiety was observed following ¹⁹F NMR analysis, with mono-2 β -fluorinated derivatives (including SM) the main products observed. Significant degradation of the MOM group was also observed following analysis of the ¹H NMR spectrum. This may be a result of the highly Lewis acidic TMS-OTf reacting more rapidly with the acid-labile -MOM group in **3.13**, than with the fluoroketone moiety. This reaction was repeated on numerous occasions using different batches of TMS-OTf, unfortunately these proved unsuccessful.



Scheme 3.24 - Attempts towards 2,2-difluoro through electrophilic fluorination.

To prevent side-reactions on the -MOM ether protecting group of **3.13**, the silylating reagent was changed to the more sterically bulky *t*-butyldimethylsilyl (TBS) triflate (**Scheme 3.24b**). The formation of the silyl enol ether was performed with TBS-OTf in an analogous fashion to TMS-OTf (**Table 3.2**), however the reaction was significantly slower (5 h for TBS-OTf vs. 1 h for TMS-OTf). The reaction mixture was concentrated *in vacuo* and dissolved directly in DMF before the addition of Selectfluor®. Following an aqueous work up, ¹⁹F NMR analysis showed the formation of the desired difluoro moiety (-105 - -100 ppm) along with monofluoroderivatives (-195 ppm), and a number of fluorinated impurities (**Figure 3.15**). Separation of these by-products proved difficult *via* flash chromatography due to their similar polarities. Overall the desired compound **3.86** had only been formed in a ~10% yield. Attempts to repeat and optimise this reaction failed, with inconsistent yields found. A significantly lower level of -MOM ether degradation was observed.

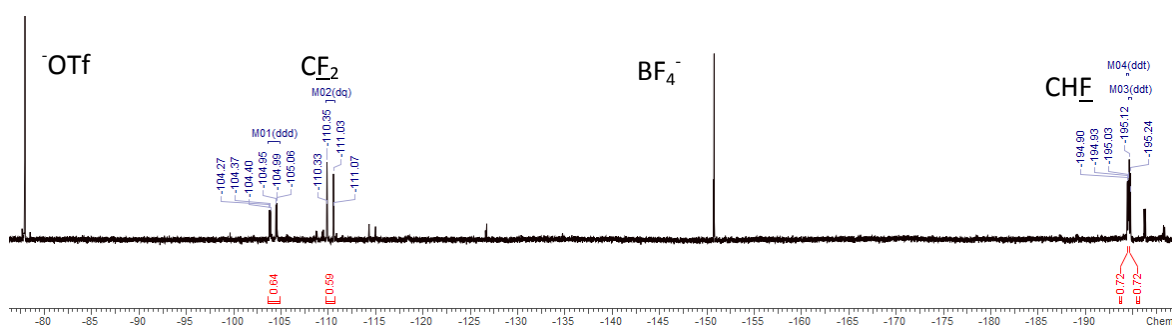


Figure 3.15 - Crude ¹⁹F NMR spectra of TBS-OTf silyl enol ether fluorination.

An LDA-mediated silyl enol ether formation was also attempted (**Scheme 3.24c**). The reaction is performed under basic conditions, in which acetals such as the -MOM ether functionality in **3.13**

are more stable. The lithium diisopropylamide species was generated *in situ* from n-BuLi and diisopropylamine at $-78\text{ }^{\circ}\text{C}$, before the addition of TMS-Cl and 2 β -fluoroketone **3.13**. Following an aqueous work up the formation of the desired silyl enol ethers **3.81** and **3.85** was indicated by analysis of the ^{19}F NMR spectrum (Figure 3.16). The material was directly subjected to fluorination (DMF, Selectfluor[®]) at RT. The reaction profile was very similar to that produced *via* the TBS-OTf mediated fluorination (Figure 3.15), as was the yield of the desired 2,2-difluoro derivative **3.13**. Unfortunately **3.13** could not be isolated cleanly from the other fluorinated products, and this route towards 2,2-difluoro CDCA **1.41** (Figure 3.14a) was abandoned.

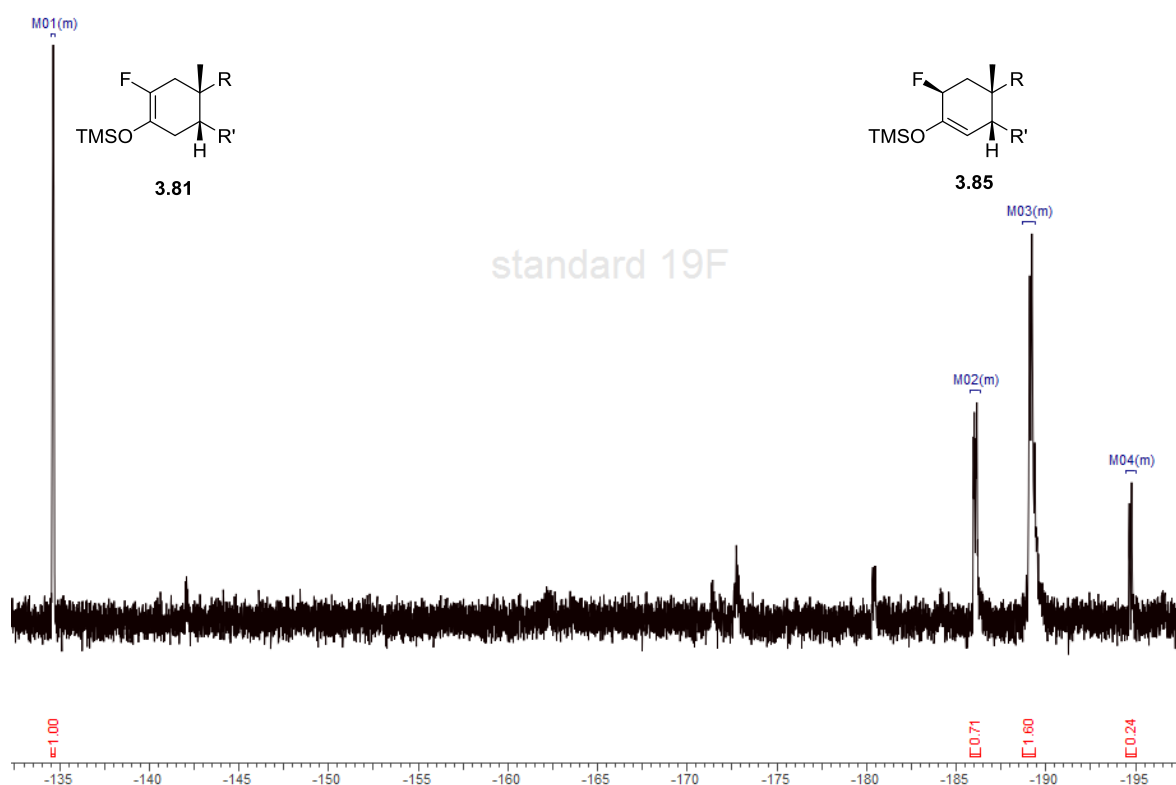


Figure 3.16 - ^{19}F NMR spectra following LDA mediated silyl enol ether formation of **3.13**.

Fluorinations of the 4 β -fluoroketone **3.15** were also attempted, however these were deemed to be equally unfeasible routes towards the desired 4,4-difluoro analogues.

3.4.3 2,2-Difluoro synthesis *via* 2-keto deoxofluorination

The key issue found in the route towards 2,2-difluoro CDCA **1.41** *via* electrophilic fluorination was poor selectivity. The lack of selectivity led to the formation of numerous fluorinated species, which led to low overall yields and difficult separation. A route avoiding electrophilic fluorination was proposed (Figure 3.14b). This pathway used DAST as a deoxofluorination reagent, which was previously shown to give good selectivities in difluorination reactions (e.g. Section 2.4).

3.4.3.1 Via 7-Keto derivative 3.82

Epoxide **2.22** has been used previously to install the 2 α -fluoro substituent through selective opening with fluoride (**Scheme 3.14**), a rationale that was extended to epoxide opening with acetate (**Figure 3.14**). Following a series of manipulations deoxofluorination substrate **3.82** can be generated (**Figure 3.17**).

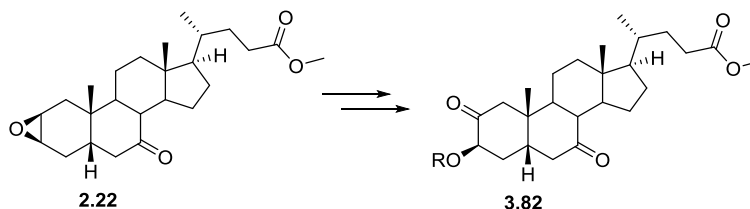
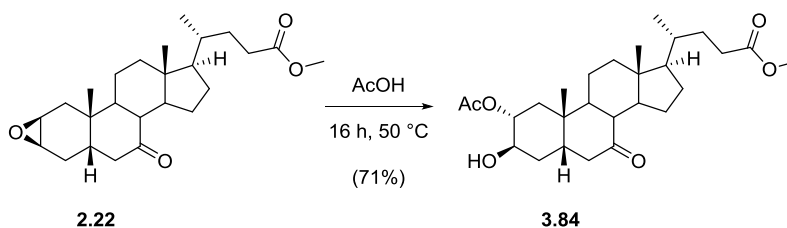


Figure 3.17 - Towards deoxofluorination substrate 3.82.

3.4.3.1.1 Opening of epoxide 3.22 with acetic acid

Acetate epoxide opening of **2.22** was predicted to occur *via* the more stable chair transition state (**Figure 3.9**) to yield the desired 3 β -hydroxy derivative **3.84**. Epoxide **2.22** was treated with acetic acid and warmed to 50 °C for 16 h. Following flash chromatography, 2 α -acetate **3.84** was isolated in a good yield (**Scheme 3.25**).



Scheme 3.25 - Opening of epoxide 2.22 with acetic acid.

The relative regio- and stereo-chemistry of the product was confirmed through analysis of the ^1H NMR spectrum (**Figure 3.18**). Both the H₂ and H₃ peaks for compound **3.84** appeared as quartets (2-5 Hz) in the ^1H NMR spectrum, this is indicative of coupling to 3 *gauche* protons. H_{2 β} can couple to H_{3 α} along with H_{1 α} and H_{1 β} , all of which have a *gauche* spatial relationship. In **3.84** H_{3 α} also has a *gauche* spatial relationship to H_{2 β} along with H_{4 α} and H_{4 β} . If epoxide opening had occurred at the 3-position, then **3.87** would be the resulting product. In this case both the H_{2 α} and H_{3 β} peaks would be expected to have two large couplings to antiperiplanar protons in the ^1H NMR (10-12 Hz), along with a smaller *gauche* coupling (2-5 Hz). It is clear from **Figure 3.18** that 2 α -attack of the acetate must have occurred.

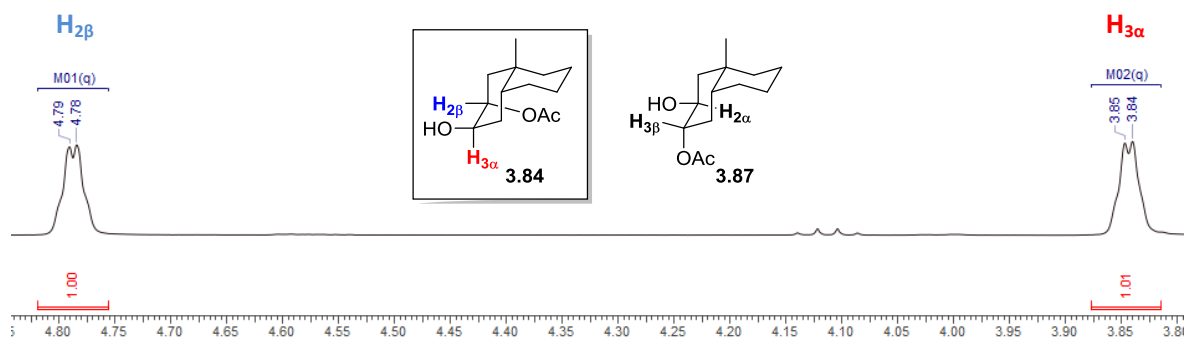
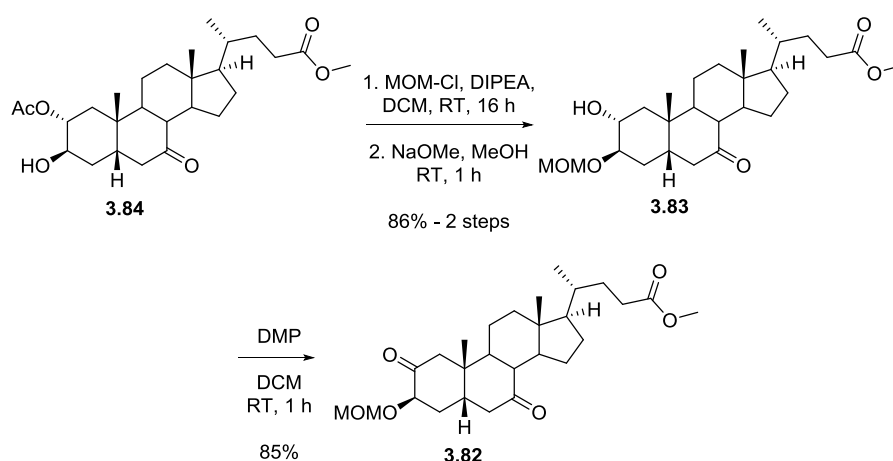


Figure 3.18 - Key section of ^1H NMR spectrum of **3.84**.

3.4.3.1.2 Synthesis of deoxofluorination substrate **3.82**

Protection of the 3β -hydroxy moiety was required to allow for selective oxidation of the 2β -OH to (**Figure 3.14**). Acetate groups are cleaved under basic conditions (e.g. hydroxide, methoxide) so it was important to choose a protecting group that was stable to these conditions. It was also vital that 3β -OH protecting group was able to withstand treatment with DAST, which was the proposed deoxofluorinating reagent. Alcohol protection as a methoxymethyl ether (-MOM) was achieved in **Section 2.4.2**. As an acetal this functionality is stable to basic conditions, and was also able to withstand 3-keto fluorination with DAST, even with additional HF.pyridine (see **Table 2.4**). The conditions of the previous MOM protection were repeated on 3β -OH derivative **3.84**, and the desired 3β -MOM protected product was synthesised in a quantitative yield (**Scheme 3.26**). This transformation was followed by cleavage of the 2α -acetate with sodium methoxide which led to the desired 2α -OH **3.83** in a good isolated yield.



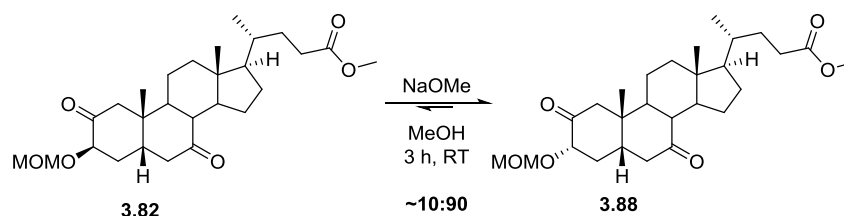
Scheme 3.26 - Synthesis of deoxofluorination substrate **3.82**.

An oxidation of the 2α -OH functionality in **3.83** was subsequently required. Previous BA alcohol oxidations had been performed successfully using a NaClO/TEMPO system (e.g. **Scheme 3.19**). TEMPO is able to react rapidly with these unhindered 2° alcohols, however it reacts slowly with 2° alcohols next to tertiary centres (e.g. 7α -OH of **2.32**, **Table 2.2**). The 2α -OH of **3.83** was therefore

predicted to react slowly with a TEMPO based oxidation, so an alternative oxidant was required. One suitable alternative to the NaClO/TEMPO oxidation system is Dess-Martin periodinane (DMP).^[131] Alcohol **3.83** was treated with DMP, and complete conversion to the 2-keto intermediate was achieved in 1 hour (**Scheme 3.26**). Following an aqueous work up, the desired product **3.82** was isolated in a good yield.

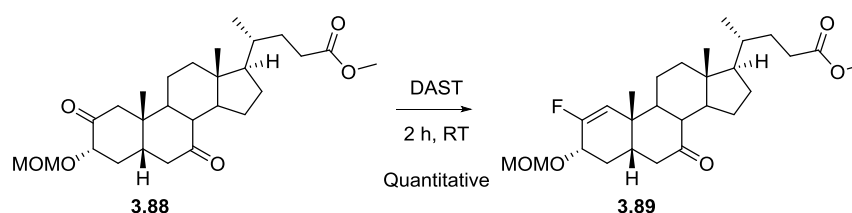
3.4.3.1.3 Epimerisation of 3 β -MOM group and subsequent fluorination

Given the 3-MOM group was in the undesired β -position, an epimerisation was attempted (**Scheme 3.27**). The reaction was performed with sodium methoxide in methanol, and led to a >90% conversion to the 3 α -MOM stereochemistry **3.88**, with <10% of the undesired 3 β -MOM derivative **3.82** (based on ¹H NMR analysis). A similar ratio of the axial:equatorial products was observed in the epimerisation of **3.13** (**Scheme 3.8**), unfortunately the two isomers were not readily separable (as judged by TLC analysis).



Scheme 3.27 - 3 β -MOM epimerisation of 3.82.

A deoxofluorination of the **3.88** 2-keto moiety was then required (**Scheme 3.28**). Diethylaminosulfur trifluoride (DAST) had been used successfully in the fluorination of cyclic ketones (**Table 2.4**), a method that was directly applicable to the fluorination of **3.88**. The reaction was performed in neat DAST, but to our surprise complete conversion to the fluoroalkene **3.89** was found (**Scheme 3.28**).¹⁸ Nevertheless, no fluorination of the C7-ketone was observed.

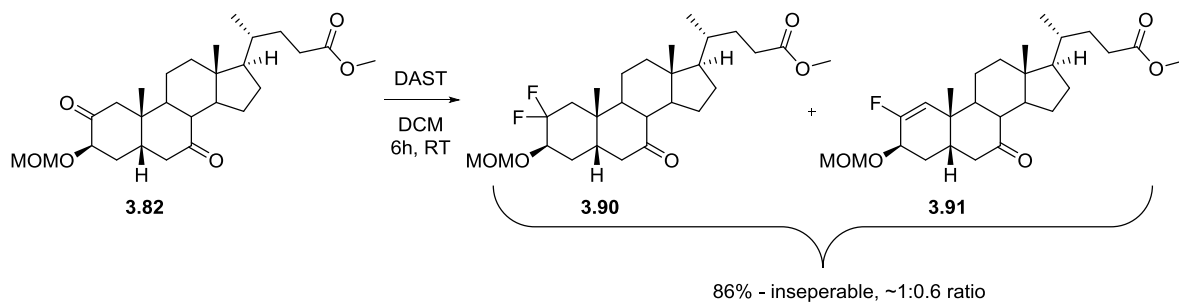


Scheme 3.28 - Deoxofluorination of 3.88.

¹⁸ Key peak upon ¹H NMR analysis was H1 δ = 5.29 (d, J = 17.9 Hz, 1H), confirming Δ 1,2-alkene regiochemistry of **3.89**.

3.4.3.1.4 DAST Deoxofluorination of 3.82

Given this unsuccessful result, deoxofluorination of the 3 β -MOM derivative **3.82** was attempted (**Scheme 3.29**). Ketone **3.82** was dissolved in DCM, then treated with DAST (11 equiv) at room temperature. The reaction was deemed complete after 6 hours, and purified to yield 2,2-difluoro **3.90** and 2-fluoro alkene **3.91** in a ratio of 1:0.6. Negligible fluorination of the 7-keto was observed. Unfortunately **3.90** and **3.91** had very similar polarities, and were not separable *via* flash chromatography.

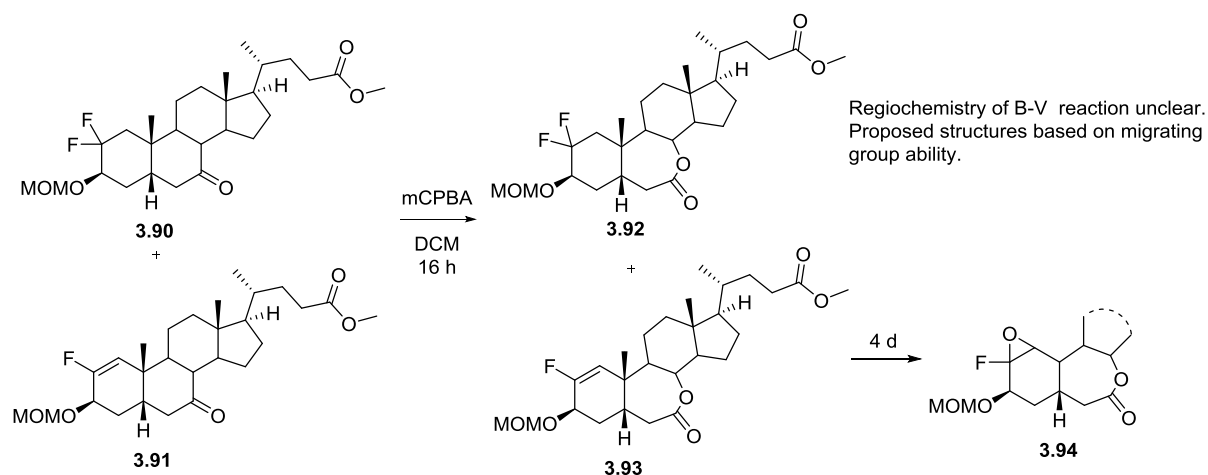


Scheme 3.29 - DAST Deoxofluorination of 3.82.

3.4.3.1.5 Attempted epoxidation of 3.90/3.91 mixture with mCPBA

The challenging separation of fluoroalkenes from a difluorinated derivative was also found in **Section 2.4**. On that occasion effecting an epoxidation of the undesired fluoroalkenes sufficiently increased its polarity to allow for chromatographic separation (see **Figure 2.11** and **Figure 2.12**). The side reactions associated with Baeyer-Villiger-type processes is the obvious concern, however this did not take place with previous epoxidations on substrates containing a 7-keto moiety (**Scheme 2.5** and **Scheme 2.10**).

The epoxidation conditions were thus applied to the inseparable mixture of **3.90** and **3.91** (**Scheme 3.30**). Unfortunately on this occasion the Baeyer-Villiger process was faster than the competing epoxidation, leading to lactones **3.92** and **3.93**. The epoxidation of the fluoro-alkene **3.93** to **3.94** was eventually forced by extended reaction times and a greater excess of oxidant. Due to the small scale of reaction, no isolated yields were obtained.

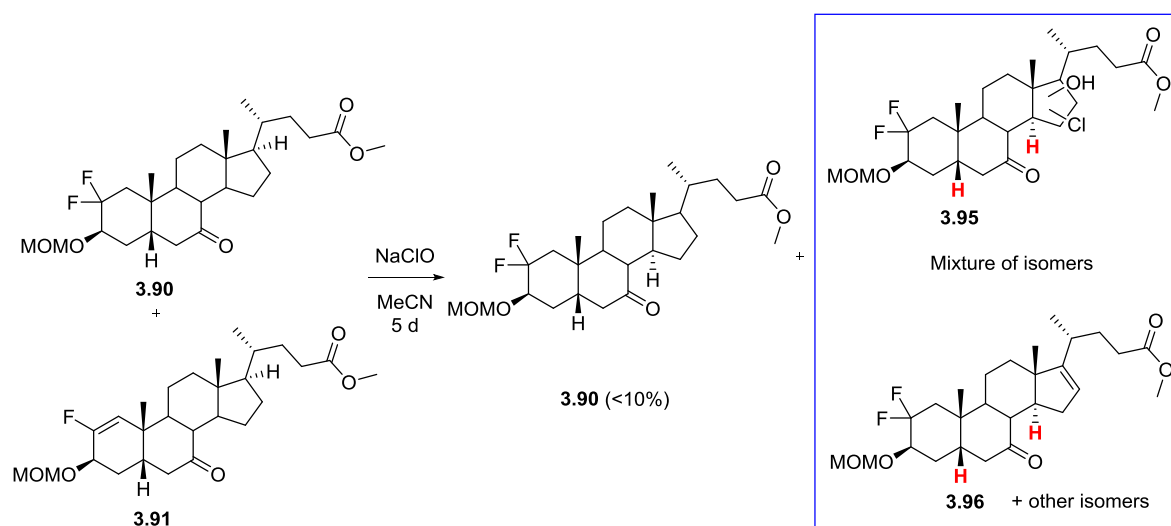


Scheme 3.30 - Epoxidation of 2-fluoroalkene 3.91 with mCPBA.

3.4.3.1.6 Epoxidation of 3.90/3.91 mixture with NaClO

The reason for the significantly slower epoxidation of fluoro alkene **3.91** is thought to be due to the electron withdrawing effects of the fluorine, which makes the alkene less nucleophilic, and slows the reaction rate with the electrophilic mCPBA. One way around the side reaction is to use an alternative epoxidising reagent, e.g. NaClO which can not lead to Baeyer-Villiger-type reactions. Coe *et al*^[132] have shown that NaClO solutions can be used to epoxidase electron poor fluoro-alkenes. These conditions were applied to the inseperable mixture of **3.90** and **3.91** (**Scheme 3.31**). Reaction progress was very slow, with no change in the profile of the ¹⁹F NMR spectrum after 16 h. The reaction mixture was stirred for an extended amount of time and further oxidant added (10 equiv), however after 5 days no consumption of the fluoroalkene was observed.

The reaction was stopped, and following an aqueous work up, ¹H NMR analysis showed significant degradation of 2,2-difluoro **3.90**. Purification was attempted *via* flash chromatography, however **3.90** could not be separated from the by-products of the reaction (**Scheme 3.31**). The full structures of these by-products could not be identified, however they are thought to be products such as **3.95** and **3.96** that could have formed through oxidation of the most electron rich C-H bonds (i.e tertiary centres). The structures are proposed through mass spectrometry analysis of the purified reaction, and are comparable to previous C-H oxidations of the steroid skeleton.^[71, 133] Other likely oxidation sites are highlighted in red.



Scheme 3.31 - Bleach oxidation of 3.90/3.91 leading to remote C-H oxidation.

3.4.3.2 An alternative 7-OH protecting group strategy

The protecting group strategy of this reaction needed to be re-thought as the 7-keto functionality was clearly inappropriate. The protection as a MOM group was proposed as it had been shown to withstand the conditions of DAST deoxofluorination (**Scheme 3.29**). It also became clear that a 7 β -configuration (i.e. **3.98**, rather than 7 α -MOM **3.97**), would be advantageous for the synthesis of the 4,4-difluoro derivative (**Figure 3.19**). With 7 β -MOM protection (**3.98**) the 4-keto would be much less sterically hindered for the fluorination step, compared to 7 α -MOM protection.

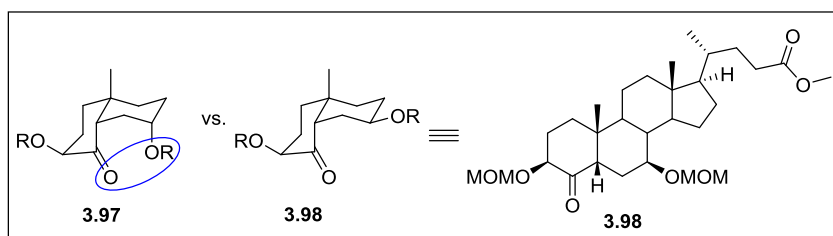


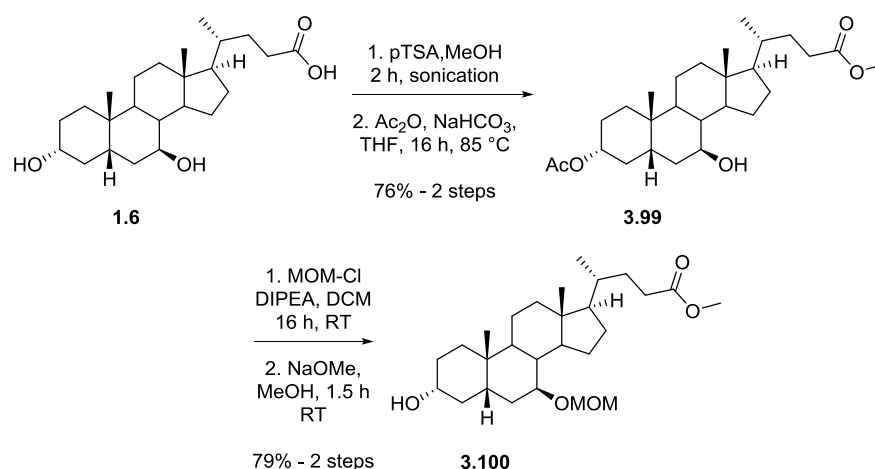
Figure 3.19 - Potential influence of 7-OR stereochemistry on 4,4-difluorination.

The synthesis of **3.98** is based on the UDCA (**1.6**) skeleton, and the transformations involved in **Section 3.4.3.1** would be repeated.

3.4.3.2.1 Synthesis of 3 α -OH,7 β -MOM protected derivative 3.100

A methyl esterification of UDCA **1.6** (donated by Dextra Laboratories Ltd.) was performed using the standard method,^[71] and the methyl ester was isolated in a quantitative yield (**Scheme 3.32**). A selective protection of the 3 α -OH was subsequently required. Pellicciari *et al*^[71] have described conditions to successfully perform this transformation on the CDCA skeleton, and were able to obtain very high yields (93%). The conditions were applied to the UDCA intermediate, and the

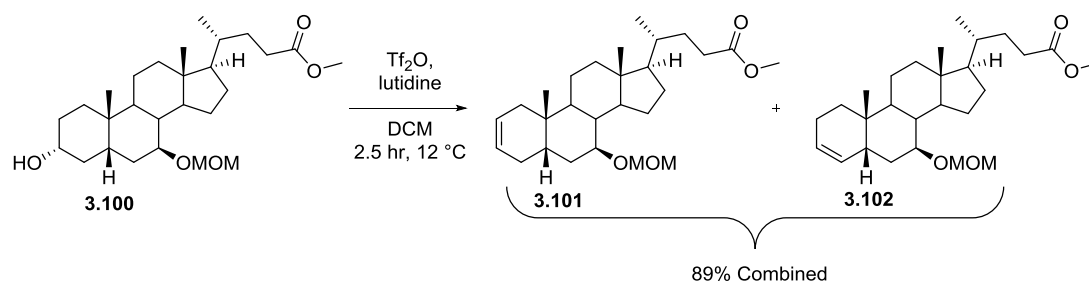
3 α -acetylated product **3.99** was isolated in a good yield. Subsequent protection of the 7 β -OH as the methoxymethyl ether, and methanolysis of the 3 α -acetate yielded derivative **3.100** in a two-step yield of 79%.



Scheme 3.32 - Synthesis of UDCA protected derivative 3.4.26

3.4.3.2.2 Synthesis of 2-keto derivative 3.106

An elimination of the 3 α -OH was performed using the Tf₂O mediated method described in **Section 3.3.3.1**. The 7-MOM protection allowed for the use of lutidine as the organic base,¹⁹ and the alkenes **3.101** and **3.102** were isolated as a mixture in a yield of 89% (**Scheme 3.33**). Minimal amounts of substitution products were observed.

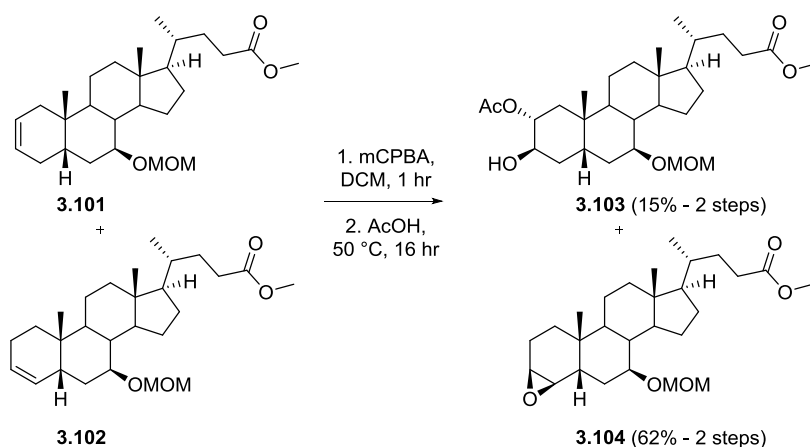


Scheme 3.33 - Tf₂O/lutidine mediated 3-OH elimination of 3.100.

The alkene mixture was subjected directly to epoxidation with mCPBA (**Scheme 3.34**), with good conversion observed through ¹H NMR analysis. The mixture of epoxides was not separable *via* flash chromatography, however the higher reactivity of the Δ 2 β ,3 β -epoxide towards nucleophiles (e.g. fluoride, **Table 3.6**) was exploited. The mixture of Δ 2 β ,3 β - and Δ 3 β ,4 β -epoxides was treated with acetic acid and warmed to 50 °C overnight. Complete conversion of the Δ 2 β ,3 β -epoxide to 2 α -acetate **3.103** was observed, while the Δ 3 β ,4 β -epoxide **3.104** remained untouched (**Scheme**

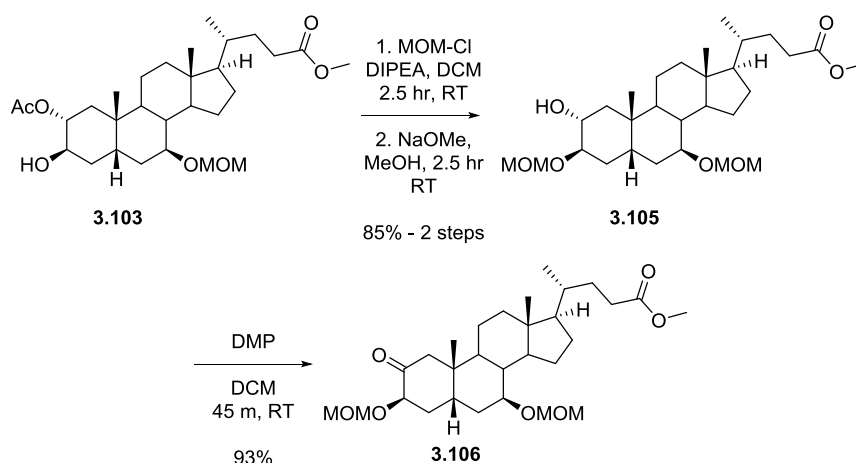
¹⁹ Lutidine/Tf₂O led to 7-enol triflate formation with the 7-keto functionality.

3.34). The two products had sufficiently different polarities to allow for chromatographic separation. The reactions of $\Delta^{3\beta,4\beta}$ -epoxide **3.104** will be discussed in **Section 3.4.4.2**.



Scheme 3.34 - Synthesis of 3.103 and 3.104.

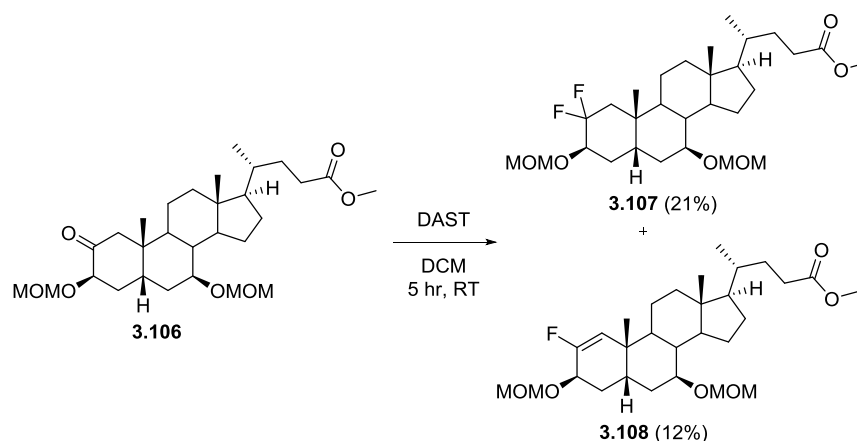
Protection of the 3β-OH of **3.103** as the MOM-ether, followed by methanolysis of the 2α-acetate yielded compound **3.105** in good yield (**Scheme 3.35**). Oxidation of the 2α-hydroxy derivative with DMP led to the formation of 2-keto derivative **3.106**.



Scheme 3.35 - Synthesis of 3.106.

3.4.3.2.3 Deoxofluorination of 3.106

The 2-keto derivative **3.106** was then subjected to deoxofluorination using DAST (**Scheme 3.36**). The conversion to the difluorinated **3.107** and the 2-fluoro alkene **3.108**, as indicated by ^{19}F NMR analysis of the crude reaction mixture, was shown to have occurred in a similar ratio to that of the 7-keto derivative (**Scheme 3.29**). Pleasingly, on this occasion the two products were readily separable by flash chromatography.

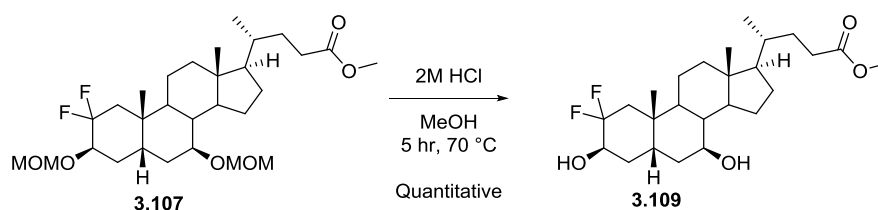


Scheme 3.36 - Deoxofluorination of 3.106.

Despite not being included in the original synthesis plan (**Figure 1.19** and **Figure 1.20**), the 2-fluoroalkene functionality was deemed an interesting substrate for biological testing purposes, and its synthesis was also furthered.

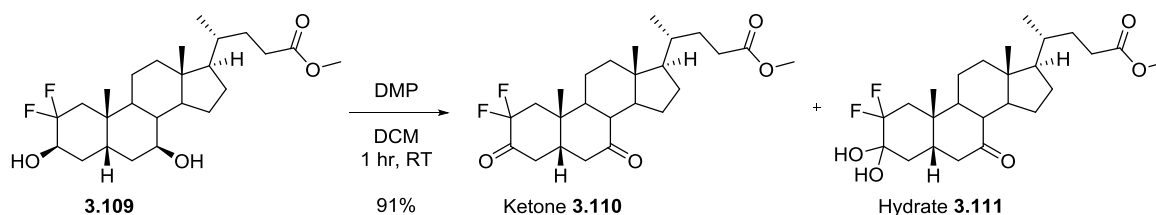
3.4.3.2.4 Deprotection and hydroxyl isomerisation of the 2,2-difluoro derivatives

Following a standard HCl mediated -MOM ether deprotection of **3.107**, 3 β ,7 β -diol **3.109** was isolated in a quantitative yield.



Scheme 3.37 - Double MOM deprotection of 3.107.

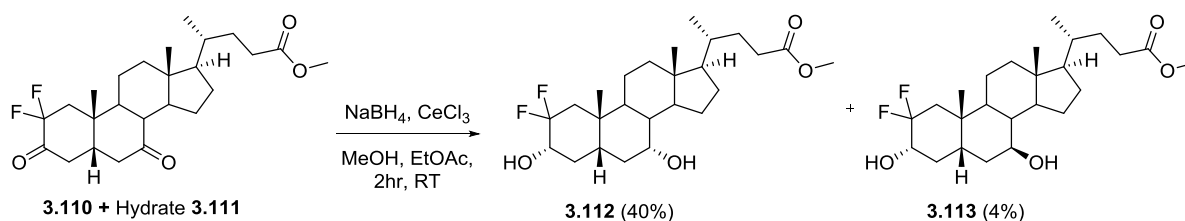
The preferred method of 3 β -OH isomerisation was *via* oxidation and selective reduction to the 3 α -OH species (**Scheme 3.18**). The 3 β ,7 β -diol **3.109** was then successfully oxidised with DMP to yield desired diketo derivative **3.110**, along with the hydrate **3.111**. Hydration of difluoro ketones is favoured due to the strongly electron withdrawing effect of the CF₂ group, resulting in enhanced carbonyl electrophilicity.^[134]



Scheme 3.38 - DMP oxidation of 3 β ,7 β -diol 3.109.

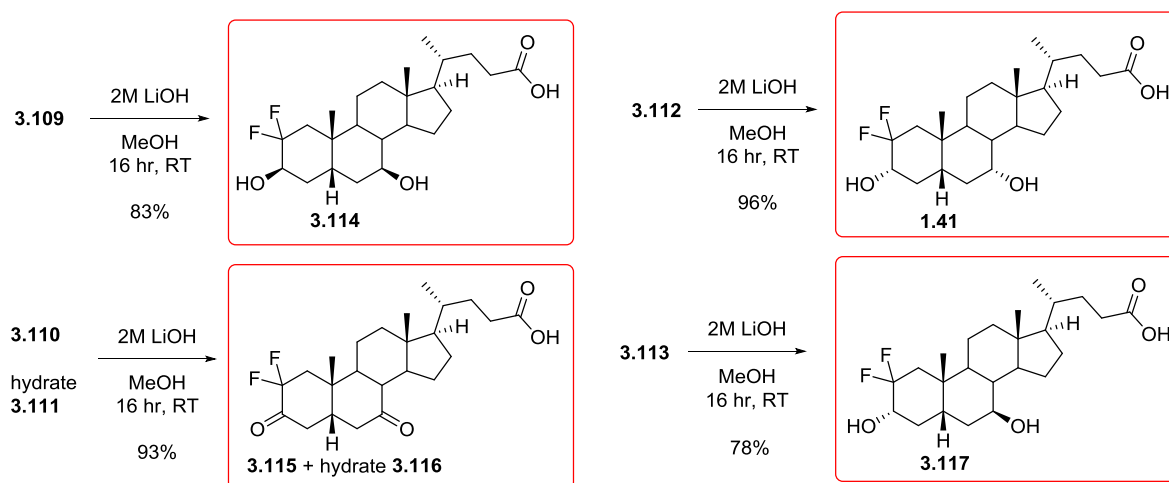
Chapter 3

Reduction of the mixture of **3.110** and **3.111** was achieved under Luche conditions^[75] to yield 2,2-difluoro CDCA derivative **3.112** and 2,2-difluoro UDCA derivative **3.113** (**Scheme 3.39**).



Scheme 3.39 - Diketo reduction of 3.110/3.111.

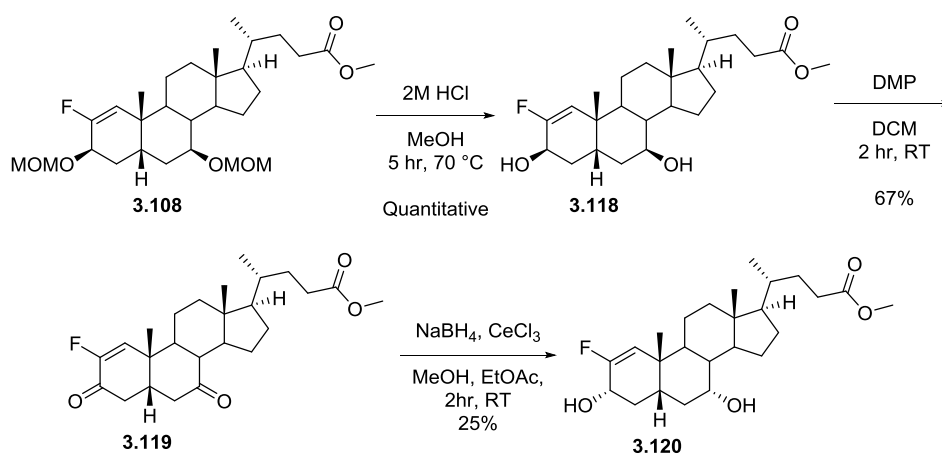
Finally, the methyl esters **3.109-3.113** were cleaved using standard LiOH mediated ester hydrolysis conditions (**Scheme 3.40**), leading to BA analogues **1.41** and **3.114-3.117**.



Scheme 3.40 - Deprotection of 2,2-difluorinated derivatives.

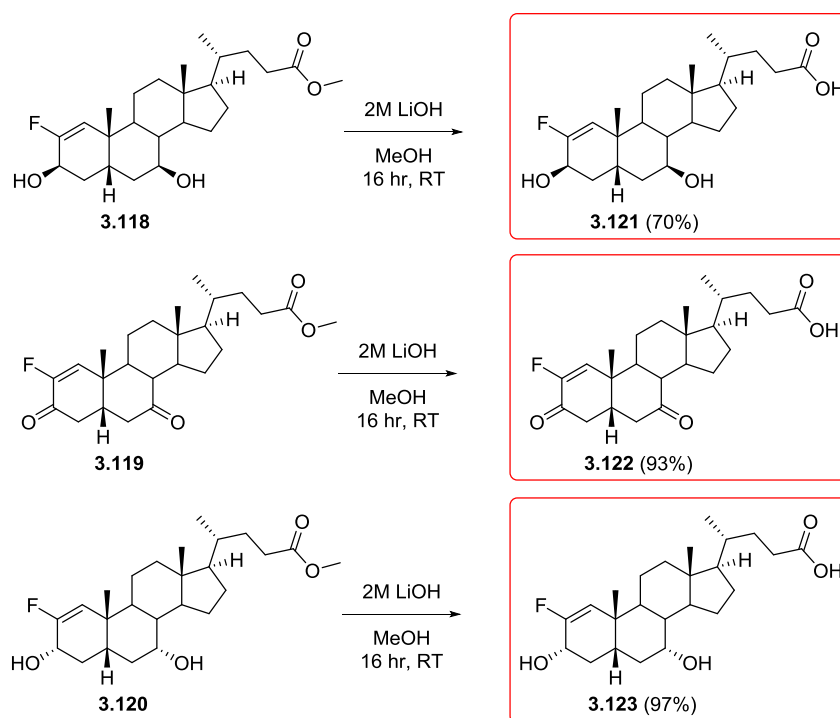
3.4.3.2.5 Hydroxyl isomerisation and deprotection of 2-fluoroalkene derivatives

Fluoroalkene **3.108** was subjected to double MOM-cleavage under acidic conditions, to yield 3 β ,7 β -diol **3.118** in a quantitative yield (**Scheme 3.41**). Oxidation of **3.118** with DMP led to the formation of 3,7-diketone **3.119**. A borohydride mediated reduction of **3.119** led to the formation of 3 α ,7 α -dihydroxy derivative **3.120**. Unfortunately none of the 3 α ,7 β -hydroxy isomer could be isolated. The reason for the low overall yield is thought to be due to over reduction of the methyl ester, however these 24-hydroxy by-products could not be isolated.



Scheme 3.41 - Hydroxyl isomerisation of 2-fluoroalkene derivatives.

The 2-fluoroalkene derivatives **3.118-3.120** were subjected to ester saponification (**Scheme 3.42**), leading to analogues **3.121-3.123** in good to excellent yields.



Scheme 3.42 - Deprotection of 2-fluoro alkene derivatives.

3.4.4 4,4-difluoro synthesis *via* 4-keto deoxofluorination

The synthesis of 4,4-difluoro derivative **3.125** was first attempted *via* fluorination of the corresponding 4-keto derivative **3.124**, which is accessible from epoxide **2.23** (**Figure 3.20**) using reactions discussed previously.

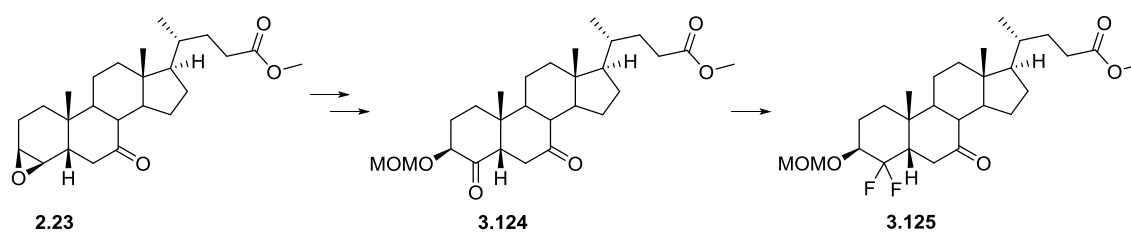


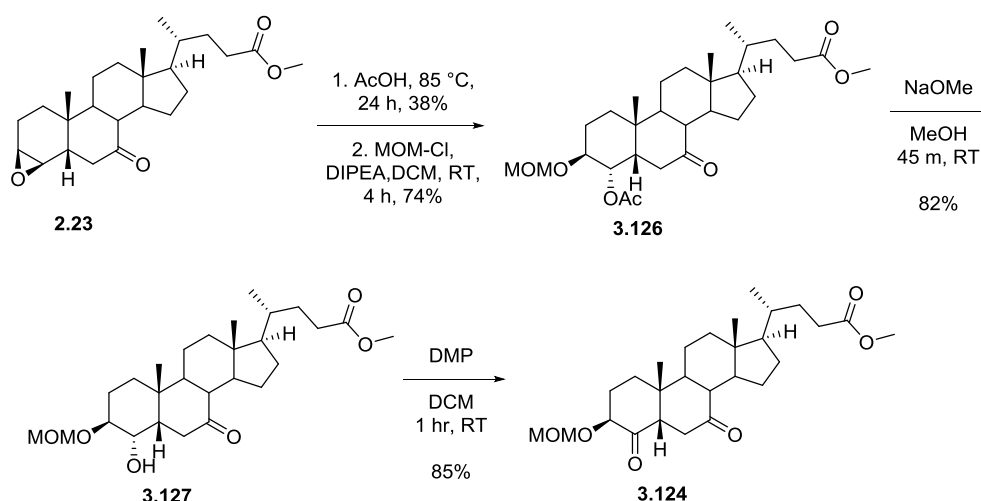
Figure 3.20 - Proposed introduction of the 4,4-difluoro moiety *via* 4-keto deoxyfluorination.

3.4.4.1 Towards 4,4-difluorination of 4,7-diketo derivative

3.4.4.1.1 Synthesis of 4,7-diketo derivative **3.124**

Epoxide **2.23** was first reacted with acetic acid in order to introduce the acetate moiety with predicted 4 α -stereochemistry (**Scheme 3.43**). The reaction was first warmed to 50 °C, however a significant amount of SM **2.23** still remained after 60 h (75-80%). The reaction was subsequently heated to 80-85 °C for 24 h, at which point complete consumption of the SM was observed. Following chromatographic purification, a significantly lower yield of the 4 α -acetate derivative **3.126** was obtained (38%) compared to the equivalent 2 α -acetate **3.84** (71% - **Scheme 3.25**). The harsher conditions required to open the Δ 3 β ,4 β -epoxide were thought to lead to a number of side reactions (also seen in **Table 3.6** with fluoride openings). Unfortunately due to their similar polarities the by-products could not be isolated/identified.

The 3 β -hydroxy-4 α -acetate product was treated with MOM-Cl/DIPEA leading to intermediate **3.126** (**Scheme 3.43**). Methanolysis of **3.126** led to the formation of 4 α -hydroxy derivative **3.127**, before an oxidation with DMP led to the desired 4,7-diketo derivative **3.124**.

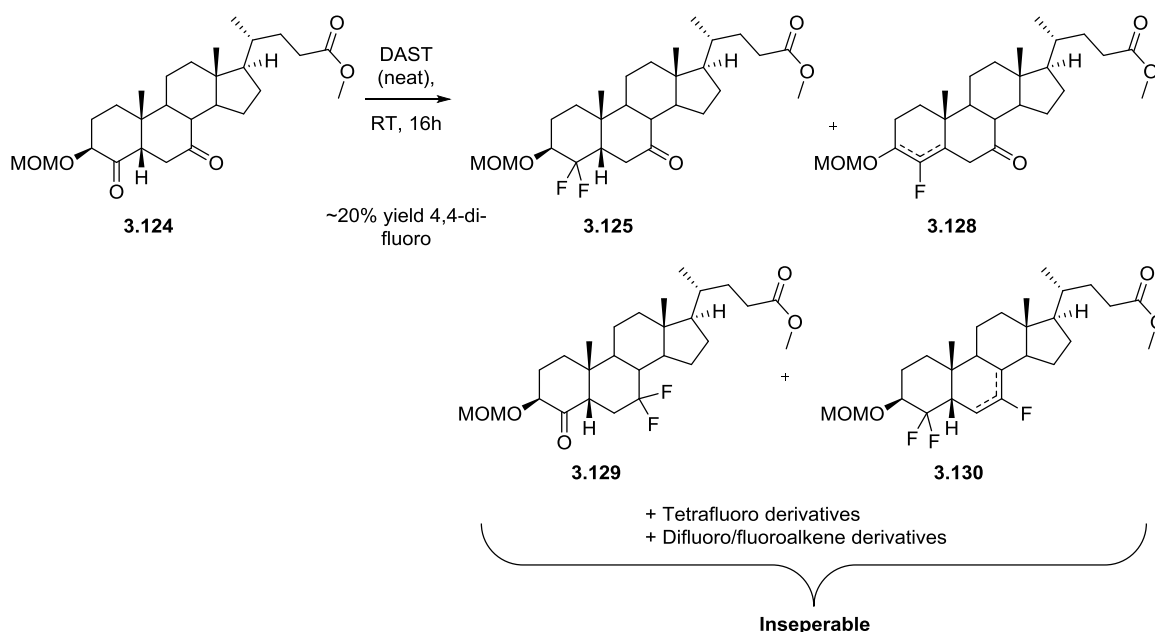


Scheme 3.43 - Synthesis of 4,7-diketo derivative **3.124**.

3.4.4.1.2 Deoxofluorination of 4,7-diketo derivative **3.124**

Deoxyfluorination substrate **3.124** was treated with neat DAST, and progress monitored *via* TLC. Reaction progress was significantly slower than with 2,7-diketone **3.82** (Scheme 3.29), and was not deemed complete until ≈ 16 h at room temperature. This extended reaction time did lead to the formation of the formation of the desired 4,4-difluoro derivative **3.125** along with the 4-fluoro alkene **3.128**. However significant difluorination of the 7-keto moiety was also observed, leading to **3.129**, along with fluoroalkene formation with **3.130**. Unfortunately these products were not separable by flash chromatography, and their structures are proposed following analysis of the ^{19}F NMR spectra of the most pure fractions.

The 4-keto moiety in **3.124** is more hindered (two neighbouring 3° centres) compared to the 2-keto derivative (one neighbouring 3° centre), this rationalises the slower deoxofluorination reaction of **3.124** vs. **3.82**. The lower reactivity of the 4-keto moiety towards DAST leads to a reactivity comparable to that of the 7-keto, with deoxofluorination reactions occurring at both sites (Scheme 3.44).

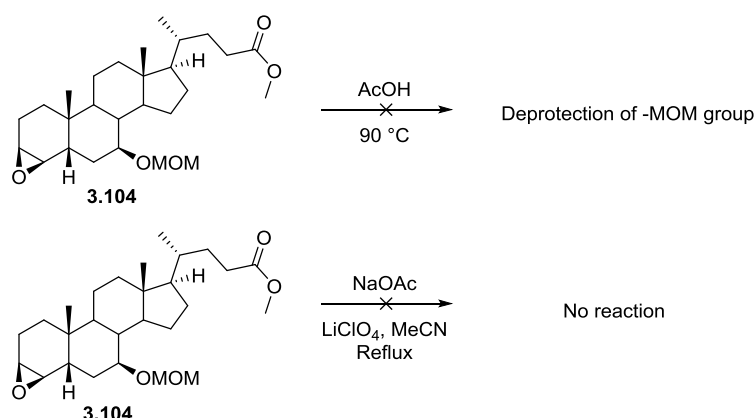


Scheme 3.44 - 4-keto deoxofluorination reaction on **3.124**.

3.4.4.2 Towards 4,4-difluorination of 4-keto,7 β -MOM derivative

The lack of selectivity seen in the deoxofluorination of **3.124** (Scheme 3.44) indicated that the 7-keto functionality was not suitable, and an alternative protecting group strategy was required. The synthesis of 7 β -MOM protected derivative **3.104** was shown in Scheme 3.34, and it was deemed a potential substrate for 4,4-difluorination. Unfortunately the low reactivity of **3.104** towards nucleophilic attack, which had allowed for its isolation in pure form (Scheme 3.34), also

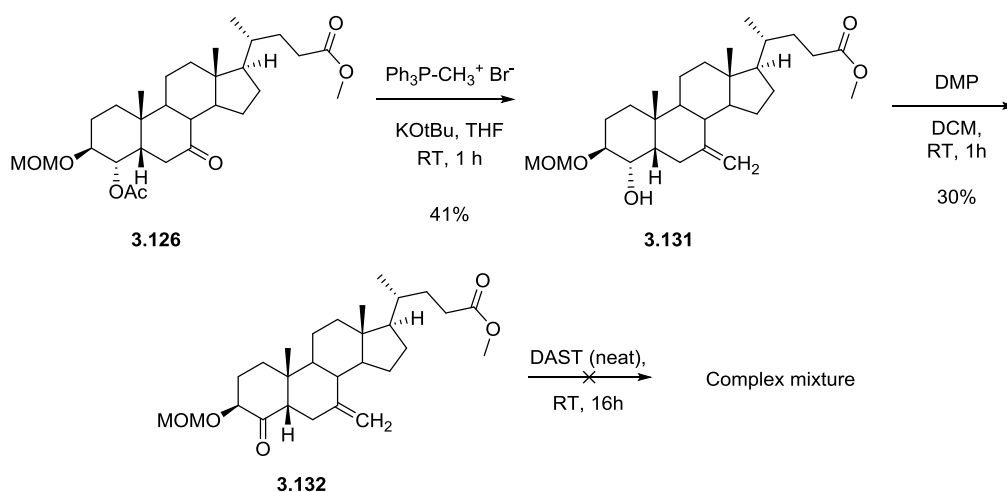
prevented opening under forcing acidic and basic conditions (**Scheme 3.45**). An alternative method towards 4-keto was required.



Scheme 3.45 - Attempts to open $\Delta 3\beta,4\beta$ -epoxide 3.104 with acetate.

3.4.4.3 Towards 4,4-difluorination of 4-keto, 7-methylene derivative

Protection of the 7-ketone as a methylene was considered (**Scheme 3.46**). The synthesis of intermediate **3.126** was shown in **Scheme 3.43**, and this was subjected to a Wittig olefination to install the 7-methylene group leading to compound **3.131**, with concomitant cleavage of the 4 α -acetate group. Subsequent oxidation of the 4 α -hydroxy gave compound **3.132**, as a substrate for deoxofluorination. Unfortunately the treatment of 4-keto derivative **3.132** with DAST did not lead to the desired formation of the 4,4-difluorinated derivative, instead a complex mixture of products was formed. The individual products could not be separated, but significant degradation of the 7-methylene group was observed through analysis of the ¹H NMR spectrum.



Scheme 3.46 - Attempted 4,4-difluorination of 4-keto, 7-methylene derivative.

Work towards 4,4-difluorinated bile acid derivatives is being continued by other members of the Linclau group.

3.5 Conclusion

A total of nineteen 2- and 4-fluorinated bile acid derivatives were synthesised, including each of the desired 2 β -/4 β -, 2 α -/4 α - and 2,2-difluorinated species with high purity and in sufficient quantities for biological testing. The exact site of fluorination of each analogue was confirmed by analysis of the ^1H and ^{19}F NMR spectra.

The 2 β - and 4 β -fluorinated species were synthesised through an electrophilic fluorination of the Δ 2,3- and Δ 3,4-silyl enol ethers using Selectfluor[®]. Complete selectivity towards fluorination on the β -face was observed, due to the intrinsic nature of the *cis*-A,B ring-juncture. The final analogues were yielded following a borohydride mediated 7-keto reduction and global deprotection.

The 2 α - and 4 α -fluorinated derivatives were made *via* the Δ 2 β ,3 β - and Δ 3 β ,4 β -epoxides. Epoxide opening with HF.pyridine installed the desired 2 α - and 4 α -fluorine substituents with high selectivity, a result predicted through analysis of the proposed transition states. Isomerisation of 3 β -hydroxy moiety was achieved with either a Mitsunobu reaction (2 α -fluoro) or an oxidation/selective reduction (4 α -fluoro) to yield the desired 3 α -OH stereochemistry. Borohydride mediated 7-keto reduction and methyl ester deprotection yielded the final analogues.

The 2,2-difluorinated analogues were synthesised through deoxofluorination of the 2-keto species, which was made through the Δ 2 β ,3 β -epoxy-7 β -MOM protected derivative *via* selective opening with acetate. Difluorination was achieved in a good yield and the mixture of 2,2-difluoro- and 2-fluoroalkenes was separable by flash chromatography. Oxidation/selective reduction of the 3 β ,7 β -diol lead to the desired CDCA and UDCA derivatives, and methyl ester deprotection led to the final analogues. Unfortunately the corresponding 4,4-difluoro analogues could not be isolated due to the lower reactivity of the 4-ketone towards deoxofluorination.

Biological testing of the 2-/4-fluorinated, and 3-deoxy-3-fluoro analogues against the BA receptors (FXR, TGR5) is underway. From the compounds discussed in this thesis a number of interesting 'hits' have emerged, but we await further data (e.g. accurate EC₅₀ values) before drawing any solid conclusions.

Chapter 4: Hydrogen Bonding Studies

4.1 Introduction to the C-F•••H-O hydrogen bond

Hydrogen bonding interactions are widespread in biological systems,^[135] and they form a vital part of numerous biological processes (e.g. enzyme-substrate complexes).^[136] The C–F bond is often used as an isostere for C–OH in property optimisation, as the two functionalities have similar sterics and dipole magnitude (**Section 1.4.1**). It is clear however that C–F and C–OH groups are not identical in terms of hydrogen bonding properties, and a detailed understanding of how organic fluorine acts as a HBA acceptor is vital if it is to be used effectively in property optimisation.^[137]

The IUPAC definition of the hydrogen bond reads: “*The hydrogen bond is an attractive interaction between a hydrogen atom from a molecule or a molecular fragment X–H in which X is more electronegative than H, and an atom or a group of atoms in the same or a different molecule, in which there is evidence of bond formation*”.^[138] Hence, it may be assumed that the high electronegativity of fluorine (**Table 1.1**, see **Section 1.4.1**) would make it an excellent hydrogen bond acceptor. Inorganic fluoride (F⁻) is known to be an excellent hydrogen bond acceptor, however the ability of organic fluorine (i.e. C–F) to interact as an effective hydrogen bond acceptor has been debated widely over the years.^[45a, 46, 50, 135, 139]

The specific geometry of a C–X•••H–Y interaction is required to be 110–180°, with a linear relationship generally strongest.^[138]

One significant consideration is the charge transfer from the lone pair of the HBA atom **X** into the vacant $\sigma^*_{\text{H-Y}}$ on the HBD group (where X and Y are electronegative atoms, e.g. N, O, F).^[45a, 138] Fluorine is often considered a poor co-ordinator as the electron lone pairs are held very strongly by the nucleus, resulting in low polarisability. However, there remains no general agreement about the exact capacity of organic fluorine to act as a HBA, as discussed below.

4.1.1 Organic fluorine as a hydrogen bond acceptor

4.1.1.1 X-ray data mining

A classical way in which C–F•••H–O interactions have been investigated is through comprehensive “mining” of crystallographic databases.^[135-136, 139-140] An early example of such an investigation was by Howard *et al*.^[136] who set out to find “*How Good is Fluorine as a Hydrogen Bond Acceptor?*” in 1996. Their study focussed on finding short F•••H contacts in the Cambridge Structural Database

System (CSDS). Only short interactions (≤ 2.35 Å) were considered as this would present a similar distance to an O•••H binding interaction with a biological receptor. From their study emerged 548 structures, with a total of 1163 unique organic fluorine environments. Of these only 166 possessed a short C-F•••H-X contact (≤ 2.35 Å), and most of these were dismissed as X = C and were not deemed to be truly hydrogen bonding. Interactions with acidic -OH and -NH groups were rare (12 and 28 instances respectively). Only one compound (**4.1**, **Figure 4.1**) was found to contain a C-F•••H-O contact of ≤ 2.00 Å, and this interaction was only likely to be so strong due to enforcement by a secondary O-H•••O=C interaction. The authors deemed that short C-F•••H-X contacts were very rare.

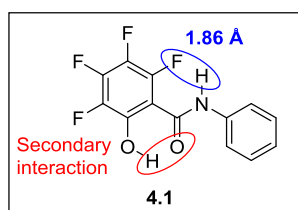


Figure 4.1 - Single instance of a ≤ 2.00 Å C-F•••H-X contact found in Howard *et al.*^[136] study.

A more recent study by D’Oria *et al.*^[140] found a similar proportion of short C-H•••F contacts, after they “*exhaustively reinvestigated*” the field. Interactions of < 2.35 Å were again uncommon, and even fewer very short bonds (< 2.00 Å) were found (**Figure 4.2a**). The study also showed very few linear C-H•••F interactions (indicative of stronger H-bonding interactions), with most $\approx 120^\circ$ in magnitude (**Figure 4.2b**).^[138]

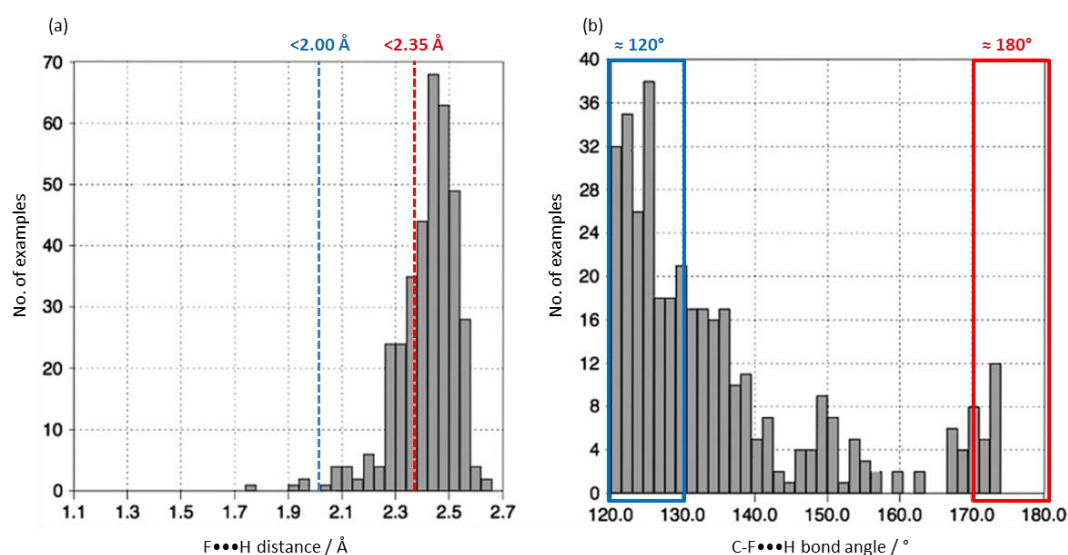


Figure 4.2 - Analysis of C-H•••F interactions in neutral fragments: (a) bond distance; (b) bond angle. Adapted from ref.^[140]

Overall, they classified neutral and charged C-H•••F interactions into weak (> -17 kJ mol⁻¹), moderate ($-17.1 - -58$ kJ mol⁻¹) or strong hydrogen bonds ($-58.1 - -209.2$ kJ mol⁻¹).^[140] The authors

found through X-ray data “mining” and computer simulations of the methane-fluoromethane complex, that C-H•••F interactions only formed weak hydrogen bonds

This conclusion was in line with those made in the seminal work by Dunitz^[46, 141] that “*organic fluorine hardly ever makes hydrogen bonds.*”

4.1.1.2 Solution phase experiments

Solution phase methods to probe HBA ability were pioneered by Taft^[142] and Arnett^[143] in the 1960s and, more recently, these methods have been adapted by Ouvrard *et al*^[144] and Dalvit *et al*^[145] for the study of C-F•••H-X interactions, including quantification of the bond strength.

4.1.1.2.1 IR studies

In 1999 Ouvrard *et al*^[144] published their work comparing the basicity (or hydrogen bond acceptor ability, pK_{BHX})²⁰ of alkyl halides with other HBA groups (e.g. O, N, P, S). The relative HBA ability of a donor atom was obtained by calculating the formation constant (K_f) of the hydrogen bonded (HB) complex (**Equation 1** - where $\log_{10}K_f = pK_{\text{BHX}}$). This was measured using a 1:1 mixture of HBA molecule (B = base) and 4-fluorophenol as the reference HBD molecule, with concentration values obtained through integration of the O–H IR bands for the free 4-fluorophenol and the HB complex (which appear at different wavenumbers).

Equation 1 - Concentration derived formation constant (K_f) of a hydrogen bond.

$$K_f / \text{dm}^3 \text{mol}^{-1} = [\text{HB complex}] / [\text{B}] \times [\text{4-fluorophenol}]$$

Ouvrard *et al*^[144] observed that organic fluorine (in the form of monofluoroalkanes) is able to act as a HBA functionality, with relative donor ability (pK_{BHX}) increasing with the +I effect of the R-group (**Table 4.1**). They were considered weak HBA though, with pK_{BHX} values only reaching that of SEt_2 and SeEt_2 for the stronger fluorine HBAs, much lower than oxygen and nitrogen groups.

A correlation between hydrogen bond strength and $\Delta\nu_{\text{O-H}}$ was also observed (**Table 4.1**).^[144] As a hydrogen bond (C-X•••H-Y) is formed by donation of a lone pair on the X atom into the vacant $\sigma^*_{\text{H-Y}}$ orbital, an overall weakening of the H-Y bond generally results. Bond strength is a key factor in IR stretching frequency (ν), and many studies have found that a lower stretching frequency for

²⁰ Denoted as pK_{HB} in original paper.

H-Y is observed upon hydrogen bonding.^[146] This so-called ‘red-shift’ is another way to quantify hydrogen bond strength by using IR spectrometry, through comparing the magnitude of $\Delta\nu$.^[147]

Table 4.1 - Selected pK_{BHX} and $\Delta\nu_{\text{O-H}}$ values from HBA groups by Ouvrard *et al.*^[144]

Compound	pK_{BHX}	$\Delta\nu(\text{OH}) / \text{cm}^{-1}$
1-Fluoroadamantane	0.26	70
Fluorocyclohexane	0.09	59
1-Fluorooctane	0.02	44
1,3-Difluoropropane	-0.27	32
EtNH ₂	2.17	351
Et ₂ O	1.01	150
Et ₂ S	0.22	146
Et ₂ Se	0.14	145

Interactions of the type C-F•••H-X, can be more complicated however with both decreases (‘red-shifts’) and increases (‘blue-shifts’) in IR stretching frequency possible,^[147] even with good HBD groups (e.g. X = O, N). ‘Red-shifts’ generally arise through the aforementioned weakening of the H-X bond through hyperconjugation.^[148] Contrastingly, ‘blue shifts’ indicate a strengthening of the H-X bond, and are ascribed to polarisation and/or rehybridisation effects. The latter type are often referred to as ‘improper H-bonds’.

4.1.1.2.2 NMR studies

To further quantify the role of fluorine as a hydrogen-bond acceptor in the solution phase, Dalvit *et al.*^[145] used the method of Taft^[142] to investigate the C-F•••H-X interaction using ¹⁹F NMR spectroscopy. Upon hydrogen bond formation the ¹⁹F signal of the 4-fluorophenol (HBD molecule) is shifted upfield, and it was observed that the larger the change in chemical shift ($\Delta\delta$), the stronger the H-bonding interaction. A value of the formation constant K_f (**Equation 1**)²¹ can be obtained through titration of acetophenone into a 1:1 mixture of a given HBA and 4-fluorophenol, and observing the $\Delta\delta$. This study showed that organofluorine is able to act as a HBA, but it was again concluded that this interaction was weak, with 1-fluoroheptane and (fluoromethyl)benzene giving a K_f value ≈ 25 times less than acetophenone (**Table 4.2**). Interestingly, the HBA capability of (difluoromethyl)benzene was significantly lower than the monofluorinated derivatives ($K_f \approx 56$ times less than acetophenone), and (trifluoromethyl)benzene was too poor a HBA to produce a K_f

²¹ Referred to as K_a in Dalvit’s publication.

value. Values of pK_{BHX} were also calculated using this method, and were of similar magnitude to those of Ouvrard *et al* (Table 4.1).^[144] Dalvit *et al* used a lower temperature in their experiment (-2 °C vs. 25 °C for Ouvrard), and hence slightly stronger complexation (and higher pK_{BHX} values) were observed.

Computational calculations of fluoroethane-methanol complexes again showed HBA ability was in the order: $\text{CH}_2\text{F} > \text{CHF}_2 > \text{CF}_3$.

Table 4.2 - Selected pK_{BHX} and K_{A} values from HBA groups by Dalvit *et al*.^[145]

Compound	pK_{BHX}	K_{A}
Acetophenone	1.56	36.0
1-fluoroheptane	0.16	1.45
(Fluoromethyl)benzene	0.13	1.36
(Difluoromethyl)benzene	-0.19	0.64

4.1.1.3 C-F...H-X interactions in the solid vs. liquid phase

In the solution phase organic fluorine (especially monofluorinated species) has been shown to act as a hydrogen bond acceptor, albeit weakly.^[144-145] Contrastingly, if only the crystallographic data is considered,^[46, 136, 140] it may be concluded that organic fluorine rarely acts as a hydrogen bond acceptor.

One potential reason why the C-F...H-X bond is observed so infrequently in X-ray structures, is that crystal packing is dictated by a number of factors including; H-bonding, van der Waals (vdW) forces and molecular shape, all of which play a role in the formation of the the minimum energy packing system.^[149] Competing interactions by stronger HBA and HBD atoms (e.g. O, N) tend to dominate weaker hydrogen bonds to fluorine, with C-F...H-X interactions only arising in situations where the relevant atoms happen to be in the right location. In apolar media (e.g. CDCl_3 solution), the greater substrate separation can limit such competing interactions, allowing weak C-F...H-X interactions to influence inter- and intra-molecular bonding, and be experimentally observable (Sections 4.1.1.2.1 and 4.1.1.2.2).^[150]

4.1.2 Case studies of C-F...H-X interactions within rigid systems

As established, the weak nature of the C-F...H-X hydrogen bond means that it can often be outcompeted by stronger HBA (e.g. N and O moieties), and as a result strong C-F...H-X hydrogen bonding interactions are rare in the literature. Examples identified are typically intramolecular,

within highly rigid structures, where the fluorine and hydrogen atoms are forced close to one another. A few key case studies of such interactions will be presented below for context.

4.1.2.1 Fluorinated inositol derivative 4.11A

In a seminal contribution, Bernet and Vasella^[150] proposed a weak intramolecular C-F•••H-O hydrogen bond within inositol derivative **4.3** through the observation of a 8.8 Hz coupling between the fluorine atom and C4-OH (**Figure 4.3**). The coupling magnitude of C4-OH with H4 (8.3 Hz) is indicative of a fixed $\approx 150^\circ$ H-O-C-H bond angle, as opposed to the unfluorinated derivative **4.2** which showed a $^3J_{\text{H4-OH}} = 4.3$ Hz indicative of free rotation about the C4-OH bond. This interaction was only observed in apolar solvents (e.g. CDCl_3), and the interaction is broken in the more polar $[\text{D}_6]$ -DMSO. The authors did not mention analysis of the ^{19}F NMR spectrum of **4.3**.^[150]

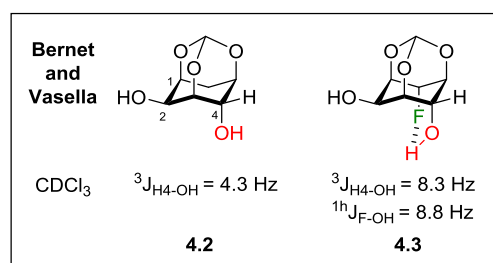


Figure 4.3 - Inositol derivatives synthesised by Bernet and Vasella.^[150]

4.1.2.2 Cyclophane skeleton

In 2004 Takemura *et al*.^[151] published the cyclophane skeleton **4.4**, designed to investigate the probability of a C-F•••H-O interaction between the remote functional groups (**Figure 4.4**).

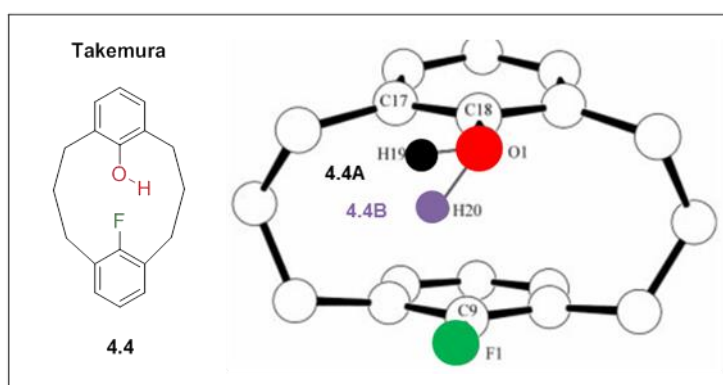


Figure 4.4 - Cyclophane derivative C-F•••H-O bond. Adapted from ref.^[151]

A crystal structure of cyclophane **4.4** showed the presence of two main structures: 80% non-H-bonding **4.4A**, and 20% H-bonding **4.4B** (**Figure 4.4**).^[151] The two phenyl rings form a strong π -stacking interaction in the crystal, with the aromatic rings in parallel orientation. The donor

proton in **4.4A** lies parallel to the phenyl ring (1.7° off), with an C-F•••H-O bond distance of 2.90 Å. Contrastingly, the -OH residue in **4.4B** is twisted 'down' towards the fluorine atom (51.3° away from ring). The F•••H bond distance is just 2.11 Å, which is well below the VDW radii (2.67 Å) of the two atoms, and very short compared to other literature values (see **Figure 4.2a**). The O-H-F bond angle of 131.6° is similar to the majority of C-F•••H-O interactions however (**Figure 4.2b**). Interestingly, a significant lengthening of the O-H bond was observed between the **4.4A** and **4.4B** crystal conformations (0.82 Å vs. 0.99 Å). This indicates electron donation in **4.4B** from F lone pair into the $\sigma^*_{\text{H-O}}$, leading to lengthening of the O-H bond.

Analysis of the ^1H NMR spectrum of **4.4** showed the C-F•••H-O interaction through the observation of a $^1\text{H}_{\text{OH-F}}$ coupling (6.0 Hz), in an apolar solvent ($[\text{D}_{14}]$ -methylcyclohexane). This coupling disappeared in a better HBA solvent ($[\text{D}_6]$ -DMSO).^[151]

The ^{19}F NMR spectra of this compound appeared as a broad singlet in both the proton coupled and de-coupled spectra. This is in direct contrast to an analogue that lacked the phenolic functionality (which showed the expected coupling/decoupling patterns). This was not commented on by the authors (see **Section 4.2.1**).

This interesting case indicates that even when crystal packing forces lead to a structure that allows for intramolecular hydrogen bonding (**4.4B**, **Figure 4.4**), there is still competition with other interactions (e.g. conjugation of oxygen lone pairs into aromatic ring - **4.4A**).

4.1.2.3 Naphthol derivatives

Calculations by Rozas *et al*^[152] had predicted the presence of a strong intramolecular C-F•••H-O interaction in the *cis*-conformer of 8-fluoro-naphthol (**4.5-cis**). This conformer benefited from a stabilisation energy of 16.4 kJmol⁻¹ over **4.5-trans** (**Figure 4.5**) at the B3LYP/6-31G** level of theory. Takemura *et al*^[153] followed up their cyclophane studies with the synthesis of **4.5**, in order to investigate this interaction experimentally. 5-Fluoro-naphthol derivative **4.6** was synthesised as a reference compound.

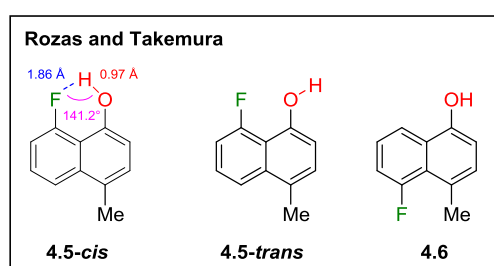


Figure 4.5 - Naphthol derivative C-F•••H-O bond.^[152-153]

A single crystal X-ray structure of **4.5** was obtained, however this did not show the predicted intramolecular C-F•••H-O interaction.^[153] Instead, a tetrameric #-shaped substructure involving the **4.5-trans** conformer was observed (**Figure 4.6a**). A donor proton was shown to be shared between the oxygen and fluorine acceptors (**Figure 4.6a**), and this interaction was intermolecular rather than the predicted intramolecular one (**Figure 4.5**). A F•••H bond distance of 2.41 Å was observed in this intermolecular interaction, along with an F-H-O bond angle of 138°. An O•••H bond distance of 2.03 Å and an O-H-O bond angle of 151° were also observed, indicating this was the dominant interaction.

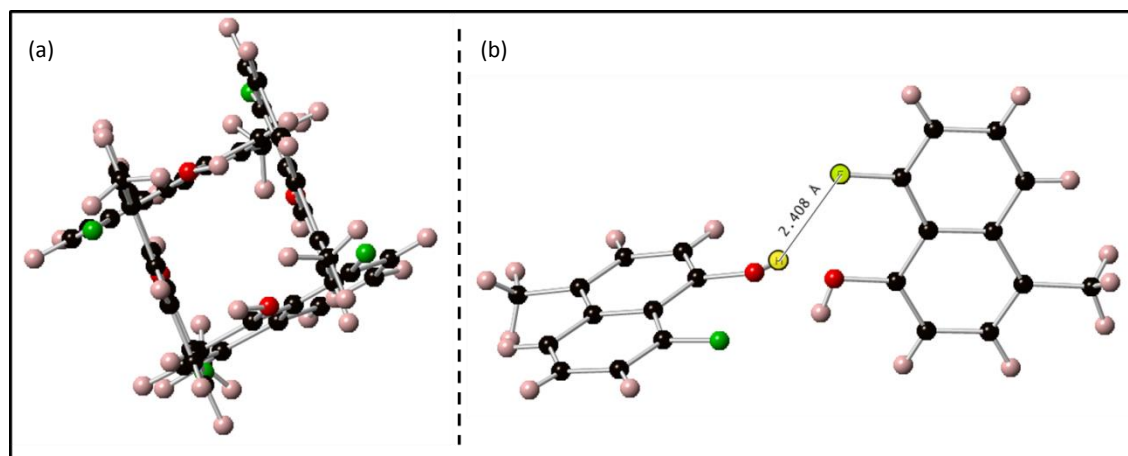


Figure 4.6 - Crystal structure of 4.5. Adapted from ref.^[153]

In solution phase studies it was shown that the tetrameric **4.5-trans** structure dissociated in favour of **4.5-cis** (**Figure 4.5**). The intramolecular C-F•••H-O interaction was observed in **4.5-cis** by a large ^1H $J_{\text{H-F}}$ coupling (28.4 Hz), while the -OH in **4.6** appeared as a singlet (both in CDCl_3). This coupling decreased to 4.4 Hz in $[\text{D}_8]$ -THF, and 2.6 Hz in $[\text{D}_6]$ -DMSO, indicating the intramolecular C-F•••H-O interaction could be disrupted with by stronger HBAs in solution.^[153] This is a good example of how C-F•••H-O interactions may differ between solution phase and solid phase observations (see **Section 4.1.1.3**).

4.1.2.4 Fluorinated carbohydrates

A number of fluorinated carbohydrates have shown intramolecular F•••H interactions.^[137, 154] The rigid sugar skeleton can provide a 1,3-diaxial relationship between the fluorine and hydroxyl residues; an environment that leads to a close C-F-H-O relationship, and the potential for an intramolecular F•••H bond (e.g. the fluorinated inositol derivative **4.3**, **Figure 4.3**). The skeleton can also provide competing H-bonding interactions (e.g. C3-OH, Q5), which can help probe the strength of the interaction, and ring protons that can be used to gauge torsion angles based on $^3J_{\text{H-OH}}$ magnitudes.

Two of the earliest examples of such substrates are **4.7**^[154b] and **4.8**^[154a] (**Figure 4.7a**), published by Takagi and co-workers in the 1990s. Originally developed as antibiotics, carbohydrates **4.7** and **4.8** were observed to have a $^1\text{H}J_{\text{OH-F}}$ coupling (7.5 Hz and ≈ 10 Hz, respectively), but the C-F•••H-O hydrogen bond was not identified at the time. Large $^3J_{\text{H-OH}}$ couplings were observed for both **4.7** and **4.8**, indicating an antiperiplanar H-C-O-H orientation.

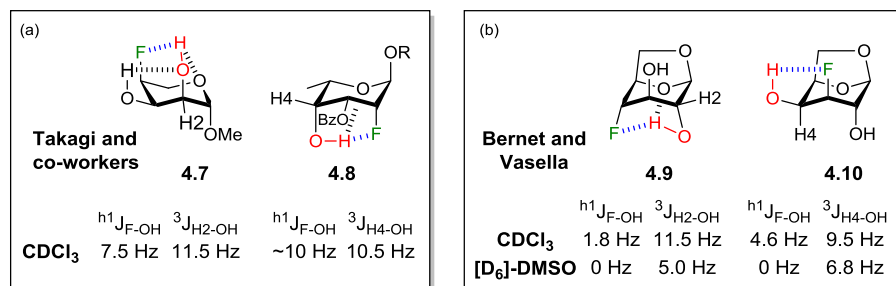
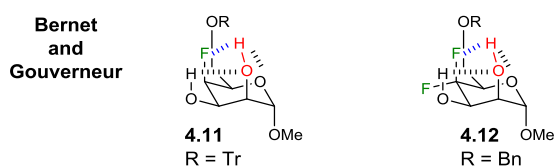


Figure 4.7 - Fluorinated carbohydrates containing a C-F•••H-O hydrogen bond.^[150, 154]

Bernet and Vasella^[154c] published their synthesis of a series of fluorinated levoglucosan derivatives (e.g. **4.9** and **4.10**, **Figure 4.7b**) in 2007. A small $^1\text{H}J_{\text{OH-F}}$ coupling was observed in **4.9** (CDCl_3) indicating that the fluorine atom is acting as a hydrogen bond acceptor. In $[\text{D}_6]\text{-DMSO}$ no C-F•••H-O is observed, indicating C2-OH is now engaged in intermolecular H-bonding to the solvent. A $^3J_{\text{H2-OH}}$ coupling of 11.5 Hz (in CDCl_3) corresponds to a H-C-O-H torsion angle of $\approx 180^\circ$, indicating that the C2-OH is orientated towards the fluorine and O5 hydrogen bond acceptors. This coupling decreases to 5.0 Hz in $[\text{D}_6]\text{-DMSO}$, indicative of a freely rotation C-OH bond. A similar C-F•••H-O interaction was observed in **4.10**, although the larger $^3J_{\text{H4-OH}}$ in $[\text{D}_6]\text{-DMSO}$ for **4.10** (6.4 vs. 5.0 Hz) indicates that the C-F•••H-O was only partially replaced by H-bonding to the solvent. Analysis by IR spectrometry was not considered a useful tool for analysing the C-F•••H-O bond by the authors.^[154c]

Gouverneur and co-workers^[137] also investigated pyranoside C-F•••H-O interactions, focussing on the comparison of CHF vs. CF_2 as donors in a C-F•••H-O bond. A wide range of substrates were characterised, however only the trends of **4.11** and **4.12** are included for concision (**Figure 4.8**). A $^1\text{H}J_{\text{F-OH}}$ coupling of 9.1 Hz was observed for **4.11** in apolar solvents (CDCl_3 and $[\text{D}_8]\text{-toluene}$) indicating the presence of a C-F•••H-O hydrogen bond. This is corroborated by a secondary $^3J_{\text{H2-OH}}$ coupling (12.1 Hz) which confirms an antiperiplanar relationship with H2-OH (**Figure 4.9**). The -OH group is therefore fixed in space, pointing towards the fluorine atom, although interactions with O5 and C3-OH are also thought to contribute to this rigidity. As expected, the magnitude of the coupling decreases in a solvent of greater HBA ability ($[\text{D}_8]\text{-THF}$), and confirms partial C2-OH bonding to the solvent. The $^1\text{H}J_{\text{F-OH}}$ is greatly reduced in $[\text{D}_6]\text{-DMSO}$, and the $^3J_{\text{H2-OH}}$ coupling of ~ 5 Hz is characteristic of free C-OH rotation.



Solvent	$^1\text{H}_{\text{F-OH}}$	$^3\text{J}_{\text{H2-OH}}$	$^1\text{H}_{\text{F-OH}}$	$^3\text{J}_{\text{H2-OH}}$
[D ₈]-tol	9.1	12.1	1.5	9.2
CDCl ₃	9.1	12.1	1.5	9.7
[D ₈]-THF	5.6	9.3	0	6.2
[D ₆]-DMSO	1.0	4.8	0	4.7

Figure 4.8 - Investigations of pyranoside C-F•••H-X bonds.^[137] All values given in Hz.²²

The CF₂ moiety in **4.12** shows a marked decrease in coupling magnitude (compared to **4.11**) in apolar systems ([D₈]-toluene and CDCl₃, **Figure 4.8**), with a complete loss of $^1\text{H}_{\text{F-OH}}$ in polar solvents ([D₈]-THF and [D₆]-DMSO).^[137] The lower $^1\text{H}_{\text{F-OH}}$ coupling is due to a weaker C-F•••H-O bond, which is a result of the equatorial fluorine atom withdrawing electron density from, and impairing the HBA ability of, the axial fluorine atom. The CF₂ moiety was considered a worse HBA than CHF, which was the same conclusion subsequently made by Dalvit *et al*^[145] (**Section 4.1.1.2.2**). The ring oxygen (O5) is able to outcompete the fluorine donor in CF₂ derivative **4.12** (**Figure 4.9**), resulting in a shallower H2-C2-O-H torsion angle (~150°), and the lower $^3\text{J}_{\text{H2-OH}}$ value.

Theoretical calculations supported the experimental results.

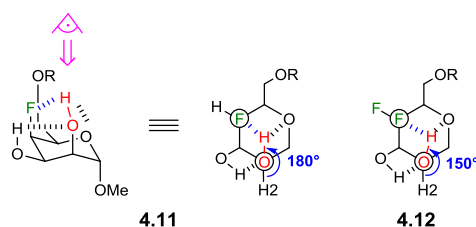


Figure 4.9 - Comparison of H2-OH torsion angles in pyranosides.^[137]

4.1.2.5 Tricyclic cage system

In 2014 Strubel *et al*^[147] published their synthesis and characterisation of cage-structure **4.13**, which contained a very large $^1\text{H}_{\text{F-OH}}$ coupling of 68 Hz (**Figure 4.10**). A single crystal X-ray structure helped to confirm the presence of a strong C-F•••H-O interaction, with a very short C-F•••H-O

²² Negligible impact was observed for changes in C6-OH protecting group (e.g. -Piv, -Tr, -Bn), nor any significant change when the C3-OH protecting group was altered (e.g. -Ac, -Tf).

contact of 1.58 Å (**Figure 4.10**).^[147] Along with this, a nearly linear O-H-F relationship was observed (171°), which is indicative of a strong hydrogen-bond according to the IUPAC definition.^[138]

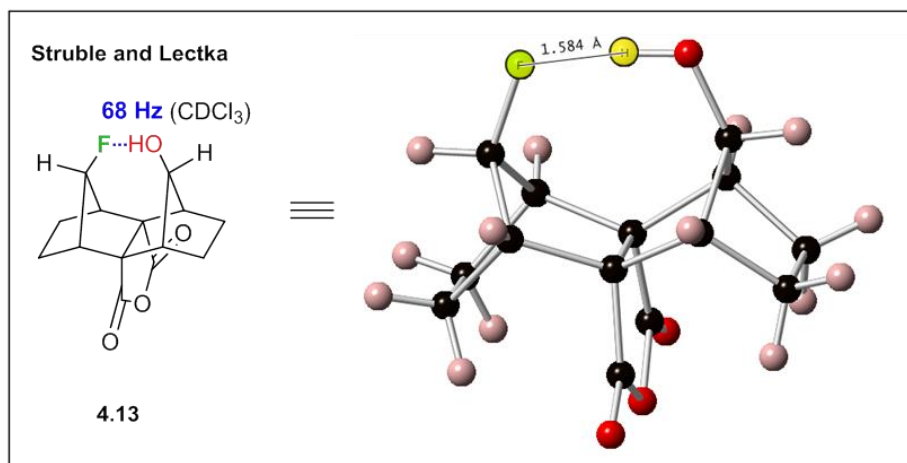


Figure 4.10 - Caged molecule containing exceptional C-F...H-O bond. Adapted from ref.^[147]

Theoretical calculations that probe the nature of the C-F...H-O bond are vital in the understanding of these interactions, and two methods used extensively are the NBO^[155] (natural bond orbital) and AIM (atoms in molecules) analysis methods.^[51, 56] These computational methods can indicate hydrogen bond formation through electron density (ρ) calculations. High electron density between two atoms indicates a charge transfer is occurring, and thus a bond has formed. A bond critical point (BCP) value can be obtained, and value of this can indicate to what degree H-bond interaction is occurring.^[156] An appreciable BCP was observed in **4.13** ($\rho = 0.052$ e), indicative of a relatively strong hydrogen bonding interaction.^[157]

4.1.2.6 Fluorinated cyclohexanols

Fluorinated cyclohexanol **1.19** (**Figure 4.11**) published by our group,^[51] displayed a $J_{\text{F-OH}}$ coupling of 12.1 Hz indicating the presence of a C-F...H-O bond.²³ This interaction was linked to a large decrease in hydrogen bond donating capacity of fluorohydrin **1.19** when compared to the unfluorinated equivalent. Fluorohydrins **1.23** and **1.24** also showed a decrease in HBD capacity of the -OH group, but significantly smaller $^1\text{H}_{\text{F-OH}}$ coupling values were observed in these compounds (unpublished results - credit Gia Huy Bui).

²³ First discussed in **Section 1.4.2.1**.

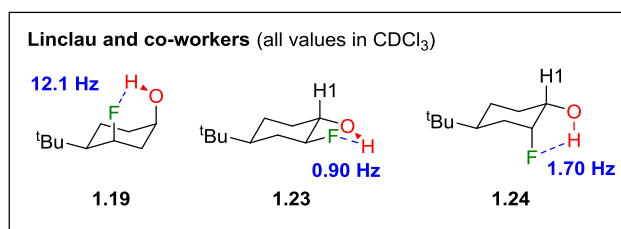


Figure 4.11 - F•••H interactions within rigid cyclohexanol systems.^[51]

NBO^[155] and AIM^[51, 56] analysis methods were used to investigate the C-F•••H-O interaction within fluorohydrin **1.19** (Figure 4.11).^[51] The calculations revealed a significant charge transfer between the fluorine lone pair(s) into the σ^*_{OH} bond of the acceptor of (17.1 kJ mol⁻¹), around the region of a weak hydrogen bond.^[140] A bond critical point between the F and H atoms ($\rho = 0.019$ e) was also observed, a value typical of hydrogen-bond interactions.^[157] No BCP was calculated between the C-F•••H-O of cyclohexanols **1.23** and **1.24**, and only a weak charge transfer into the σ^*_{OH} (3 and 4.1 kJ mol⁻¹ respectively), indicating such interactions are not typical hydrogen bonds.

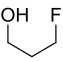
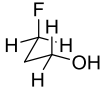
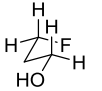
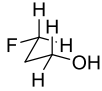
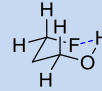
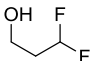
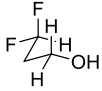
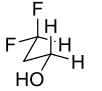
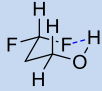
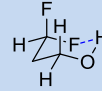
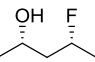
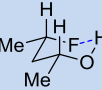
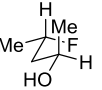
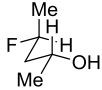
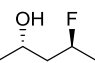
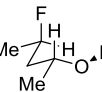
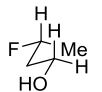
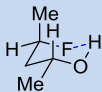
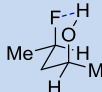
4.1.3 Case studies of C-F•••H-X interactions within open chain systems

Up until very recently it was still unclear whether such C-F•••H-O IMHBs were the result of true bonding interactions or were forced consequences of molecular structure.^[56] It had been calculated that a C-F•••H-O hydrogen bonded conformation of flexible fluorohydrins such as 3-fluoropropan-1-ol **4.14** (Table 4.3) should be occurring, however as these were present at such a low population at ambient temperature, no $^1\text{H}_{\text{F-OH}}$ could be detected.^[158] No intramolecular C-F•••H-O bond could be detected in either 2-fluoro-ethanol, or 4-fluoro-butan-1-ol by $^1\text{H}/^{19}\text{F}$ NMR analysis in the study either. Entropy penalties and solvation effects were attributed for the lack of $^1\text{H}_{\text{F-OH}}$ coupling by the authors, and they indicated that rigidification (e.g. introduction of a cyclic backbone) may be required to establish a C-F•••H-O interaction in these systems.

A recent publication by our group^[56] was able to show that strengthening the backbone was not required to observe a $^1\text{H}_{\text{F-OH}}$ coupling in δ -fluorohydrins. Using rigorously dried CDCl₃, the group showed that 3-fluoropropan-1-ol (**4.14**) exhibited a measurable $^1\text{H}_{\text{F-OH}}$ coupling constant of 1.4 Hz at ambient temperature (Table 4.3). This observation formed part of a larger study based on the δ -fluorohydrin backbone (e.g. **4.14-4.16**). The experimentally obtained $^1\text{H}_{\text{F-OH}}$ values were combined with a thorough computational analysis to understand the major conformers present at ambient (25 °C) and cold (-50 °C) temperatures. NBO^[155] and AIM^[51, 56] analysis methods were used to investigate the IMHB C-F•••H-O interaction within **4.14**. The strength of the bonding interaction was calculated to be 20.4 kJ mol⁻¹, which is in the region of a moderate hydrogen bond (see Section 4.1.1.1). A short C-F•••H-O contact (2.07 Å) was also calculated in the IMHB conformer (8%/10%, 25 °C/-50 °C).

Despite a similar IMHB conformer population (total = 9%/7%), 3,3-difluoropropan-1-ol **4.15** was observed to have a significantly lower $^1\text{H}J_{\text{F-OH}}$ coupling constant than monofluoro derivative **4.14** (1.4 vs. 0.4 Hz at ambient temperature).^[56] Calculations of the C-F•••H-O bond within **4.15** show that it is much longer (2.18 Å/ 2.20 Å) and weaker (16.6 / 16.1 kJ mol⁻¹) than **4.14** however, due to the lower co-ordinating potential of the CF₂ group (vs. CHF). This aligns well with the work of Gouverneur^[137] and Vulpetti.^[145]

Table 4.3 - Examples of flexible fluorohydrins with measurable $J_{\text{F-OH}}$ coupling.^[56]

2D structure	Major conformations in CHCl ₃ ^{a,b}				$^1\text{H}J_{\text{F-OH}} / \text{Hz}^a$
 4.14	 54%/62%	 15%/12%	 13%/10%	 8%/10%	1.4 / 1.7
 4.15	 59%/75%	 18%/11%	 5%/4%	 4%/3%	0.4 / 0
 syn-4.16	 39%/59%	 28%/20%	 21%/15%	-	6.6 / 9.9
 anti-4.16	 68%/82%	 10%/5%	 6%/5%	 3%/2%	1.9 / 1.8

^a at 25 °C/-50 °C; ^b calculated at MP2/6-311++G(2d,p)//MPWB1K/6-31+G(d,p) level of theory.

Interestingly, there was a significant difference in $^1\text{H}J_{\text{F-OH}}$ coupling magnitude between the 4-fluoropentane-2-ol diastereoisomers (**syn-4.16** and **anti-4.16**), despite having very similar calculated C-F•••H-O contacts (2.00 Å and 2.01 Å, respectively), and calculated hydrogen bond energies (24.4 and 23.7 kJ mol⁻¹, respectively). In **syn-4.16** the most stable conformer at both 25 °C (39% of total) and -50 °C (59% of total) is the IMHB conformation, which is due to the methyl substituents of the pentanol chain favouring a pseudo-equatorial orientation, which re-enforce the C-F•••H-O interaction. In **anti-4.16**, the most stable conformer (68%/82%) again places the methyl substituents in the favoured pseudo-equatorial orientation, however no IMHB is possible in this conformation. Both IMHB conformers of **anti-4.16** require a methyl substituent to occupy a pseudo-axial orientation which is disfavoured, and leads to a lower population of the C-F•••H-O conformation (total = 9%/7%). As the $^1\text{H}J_{\text{F-OH}}$ coupling magnitude is an average across

Chapter 4

all species, those with higher populations of IMHB conformation(s) will contain a higher percentage of the C-F•••H-O bonding, and thus a higher $^1J_{\text{F-OH}}$ coupling is observed.

4.2 Discovery of a 7-membered C-F...H-O H-bond

The synthesis of the two 4 α -fluoro derivatives **3.76** and **3.78** (Figure 4.12) was described in Section 3.3.5 as intermediates in the synthesis of BA receptor agonists. The effect of fluorine on the 3-OH group could be predicted by considering previous pK_{AHY} studies,^[51] but the effect on the proximal 7 α -OH was to be established. The close proximity of the fluorine and hydroxyl residues meant that a strong C-F...H-O bond was likely.

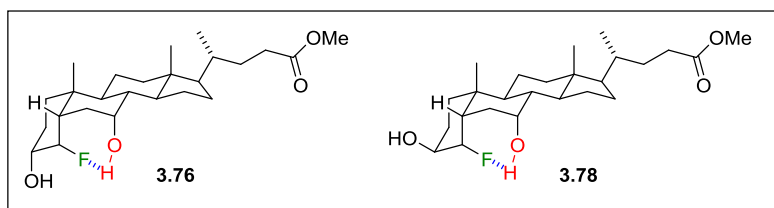


Figure 4.12 - 4 α -F...HO-7 β -interaction within **3.76** and **3.78**.

4.2.1 NMR Studies

4.2.1.1 ^1H NMR Analysis

The C7-OH proton appeared as a doublet of doublets ($J = 35.0, 11.2$ Hz) in the NMR spectrum of **3.78** in CDCl_3 (Figure 4.15), with a chemical shift of 3 ppm. This was somewhat unusual as -OH chemical shifts for BAs tend to be obscured by the ≈ 2.0 -1.0 ppm multiplet in apolar solvents.

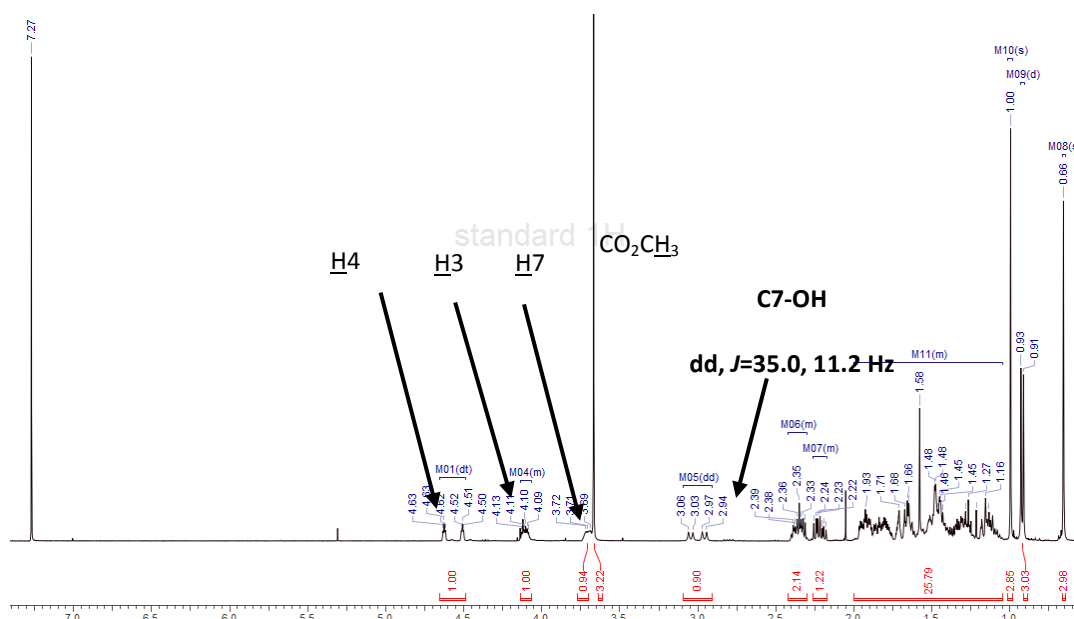


Figure 4.13 - Assignment of **3.78** ^1H NMR spectrum.

The assignment of C7-OH was confirmed through D₂O-exchange and 2D COSY experiments (**Figure 4.14**). The 35.0 Hz $^1\text{H}_{\text{F-OH}}$ assignment was confirmed through a fluorine decoupled ^1H NMR experiment. This is, to our knowledge, the second largest intramolecular C-F•••H-O coupling interaction observed, only exceeded by that of the tricyclic compound **4.13** synthesised by Struble *et al*^[147] (67 Hz - **Figure 4.10**).

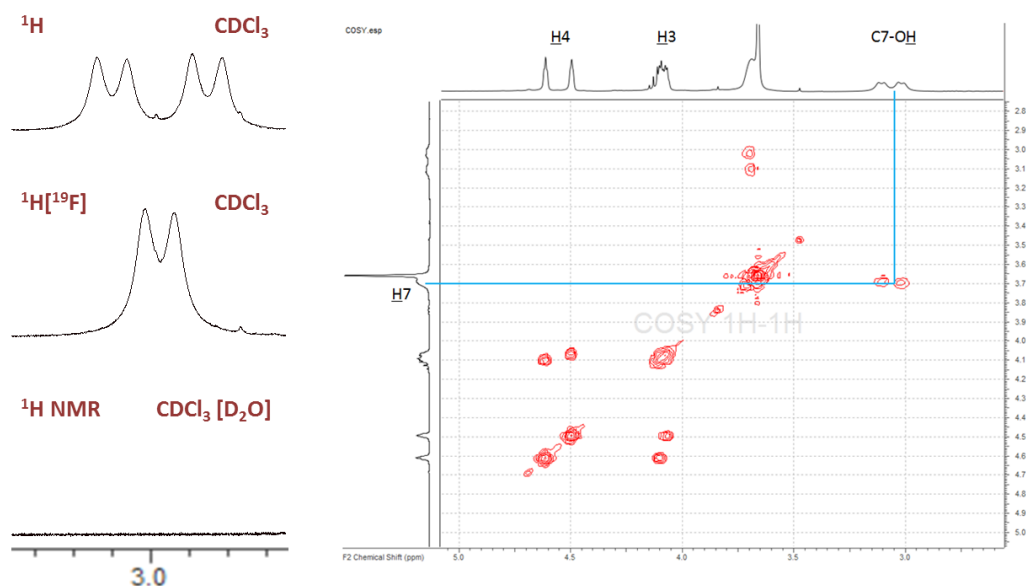


Figure 4.14 - Assignment of key dd as C7-OH.

The magnitude of the secondary doublet ($^3J_{\text{OH-H}} = 11.2$ Hz) is indicative of an antiperiplanar orientation of C7-OH and H7, clearly showing the position of C7-OH relative to the 4 α -fluoro atom (**Figure 4.15**).

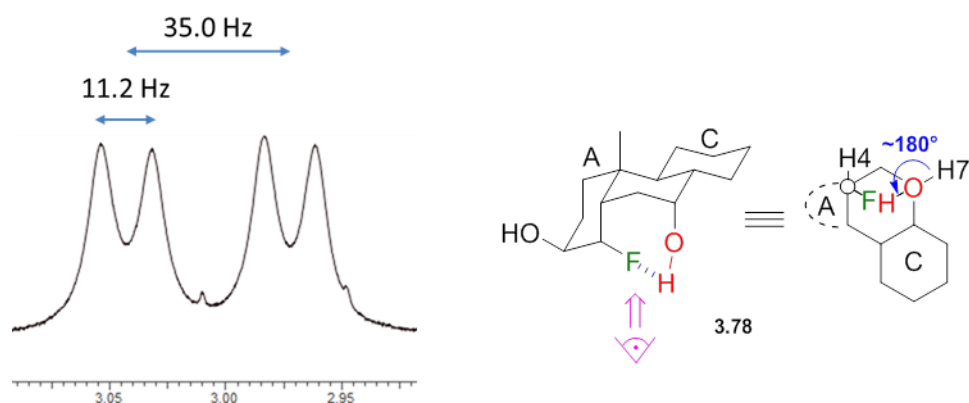


Figure 4.15 - C7-OH peak from ^1H NMR spectra in CDCl_3 and $[\text{D}_6]\text{-DMSO}$.

A similar intramolecular C-F•••H-O coupling was observed for the 3 α -OH derivative **3.76**, however this was of even greater magnitude (39.4 Hz) compared to the 3 β -OH derivative **3.78** (**Table 4.4**). This larger coupling indicates a stronger C-F•••H-O interaction, which can be rationalised by considering the 3 β -functionality which is in an antiperiplanar orientation to the C-F bond. In the case of **3.78**, the electronegative -OH group will reduce the electron density on the

fluorine atom, making the fluorine a poorer donor. In the case of **3.76**, a 3β -H atom is present, and $\sigma_{\text{C-H}} \rightarrow \sigma_{\text{C-F}}^*$ hyperconjugation can occur.^[45a] This makes the fluorine atom more electron rich in **3.76**, and therefore greater donation from the fluorine lone pair into the $\sigma_{\text{O-H}}^*$ can occur.

The C-F•••H-O interaction was further investigated through NMR experiments in solvents of greater HBA-capacity than CDCl_3 . Unfortunately in $[\text{D}_6]$ -DMSO at room temperature, the C7-OH peak²⁴ of **3.78** overlapped with other proton environments in the ^1H NMR spectra, with only half of the peak discernible (**Figure 4.16**).²⁵ The visible portion indicated a $J_{\text{OH-H7}}$ of 6.7 Hz, although the $^1\text{H}J_{\text{OH-F}}$ value could not be elucidated. Pleasingly, analysis of a high temperature (80 °C) ^1H NMR spectrum of **3.78** showed a significant downfield shift of the C7-OH peak ($\Delta\delta \approx -0.25$ ppm), and separation from the overlapping signals. A $J_{\text{OH-F}}$ value of 17.9 Hz was observed, along with a secondary 6.7 Hz coupling assigned as the $J_{\text{OH-H7}}$ coupling. NMR experiments at different temperatures can lead to variations in coupling constants (as seen in the loss of the C3-OH doublet at 80 °C), however due to the preservation of the 6.7 Hz coupling, and correlation between $J_{\text{OH-F}}$ and $J_{\text{OH-H7}}$ magnitudes (**Table 4.4**) we have good confidence in the stated value. It was also interesting to observe that at 100 °C neither 3β -OH, nor 7α -OH could be easily identified, with peaks merging to form a broad singlet ($\delta = 3.05$ ppm). In all other systems the C7-OH peak was visible at ambient temperature.

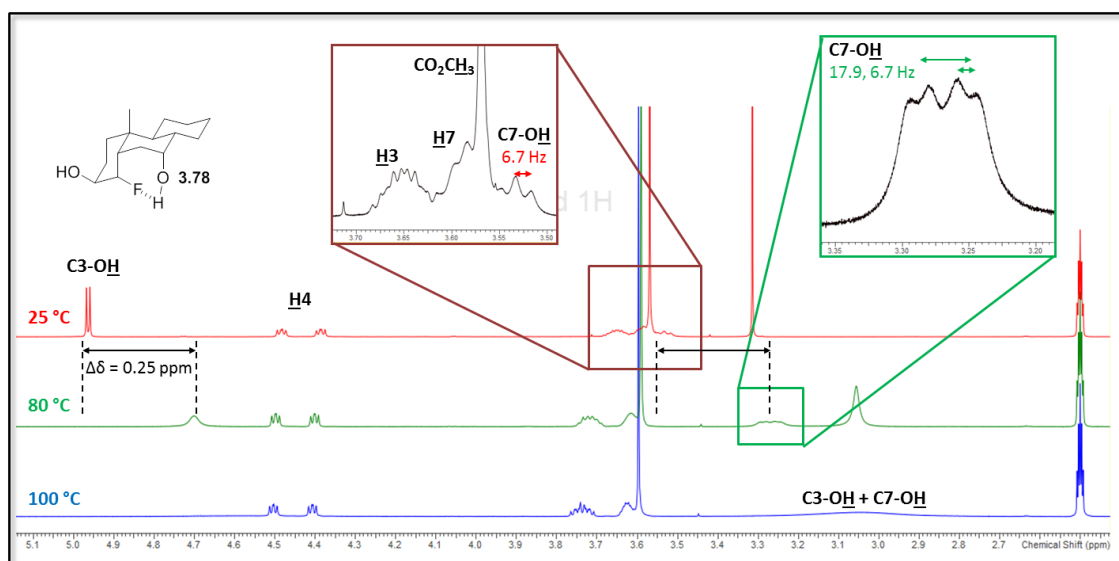


Figure 4.16 - High temperature ^1H NMR spectra of **3.78 in $[\text{D}_6]$ -DMSO.**

²⁴ Assigned through 2D NMR (COSY, HSQC, HMBC) and deuterium exchange experiments.

²⁵ Clearly, if the methyl ester functionality were not present then the peak visibility of the C7-OH peak would improve. However as shown in **Section 3.3.5.3.2**, the basic deprotection of **3.78** was not possible. Acidic BA deprotections had been trialed on other BA substrates, but were unsuccessful.

As the polarity of the solvent increases a gradual decrease in both the $^1\text{H}J_{\text{OH-F}}$ and $^3J_{\text{OH-H7}}$ was observed (**Table 4.4**).²⁶ This effect is caused by the higher HBA ability of the solvent partially out-competing the intramolecular C-F•••H-O hydrogen bond. The better the HBA, the higher the proportion of C7-OH bonded to solvent, and thus the average value of the $^1\text{H}J_{\text{OH-F}}$ coupling magnitude decreases. The effect is mirrored in the $J_{\text{OH-H7}}$ values which show poorer H7-C7-O-H alignment as H-bonding to the solvent increases. It was pleasing to note that the coupling is still retained even in $[\text{D}_6]$ -DMSO, unlike the majority of C-F•••H-O interactions discussed in **Section 4.1.2** (e.g. **4.3**, **4.4**, **4.9**, **4.10**, **4.12**). This indicates that the intramolecular bond within **3.76** and **3.78** is stronger than such examples. The smaller $\Delta J_{\text{OH-F}}$ between CDCl_3 and $[\text{D}_6]$ -Acetone/ CD_3CN for **3.76** compared to **3.78**, aligns well with the explanation of relative C-F•••H-O bond strength between the two isomers.

Table 4.4 - Comparison of key C-F•••H-O coupling constants for 3.76 and 3.78.

Solvent	3.76		3.78	
	$^1\text{H}J_{\text{OH-F}} / \text{Hz}$	$^3J_{\text{OH-H7}} / \text{Hz}$	$^1\text{H}J_{\text{OH-F}} / \text{Hz}$	$^3J_{\text{OH-H7}} / \text{Hz}$
CDCl_3	39.4	11.8	35.0	11.2
$[\text{D}_6]$ -Acetone	38.9 ^a	11.6 ^a	31.8	10.6
CD_3CN	38.2 ^a	11.4 ^a	30.4	10.4
$[\text{D}_6]$ -DMSO	35.3 ^a	10.3 ^a	17.9 ^b	6.7 ^b

^a Values measured on $\underline{\text{C}}24\text{-OH}$ **2.2.31** rather than, $\underline{\text{C}}24\text{O}_2\text{Me}$ **2.2.29** due to lack of material. The 24-functionality was shown to have no effect on the intramolecular F•••H in CDCl_3 and computational calculations; ^b. The value given is from a spectrum taken at 80 °C where there was no signal overlap.

4.2.1.2 ^{19}F NMR Observations

Analysis of the ^{19}F NMR spectrum of **3.76** showed the expected coupling constants (tt, $J = 52.5$, 36.0), arising from coupling to the vicinal proton $\underline{\text{H}}4$, two antiperiplanar protons $\underline{\text{H}}3$ and $\underline{\text{H}}5$, and a $^1\text{H}J_{\text{F-OH}}$ coupling to $\underline{\text{C}}7\text{-OH}$.

The ^{19}F NMR spectra of **3.78** were slightly unusual however, with only a broad singlet observed in all experiments (**Figure 4.17**). This was the case for both apolar (CDCl_3) and polar solvents ($[\text{D}_6]$ -DMSO) at room temperature, and in proton coupled and decoupled spectra. A low temperature experiment (-50 °C, CDCl_3) showed a slight narrowing of the peak, but no clear resolution was

²⁶ All performed at a concentration of ≈ 10 mg/mL, which this was able to show a general trend in solvent polarity effect on $^1\text{H}J_{\text{OH-F}}$. Additional experiments at different concentrations/temperatures may be required to fully quantify this effect.

observed. High temperature studies (80 °C and 100 °C, [D₆]-DMSO) did not lead to greater resolution either. To our knowledge this is not a common feature of fluorine NMR spectra, but we do not currently have a definitive explanation for the reasons behind this effect.

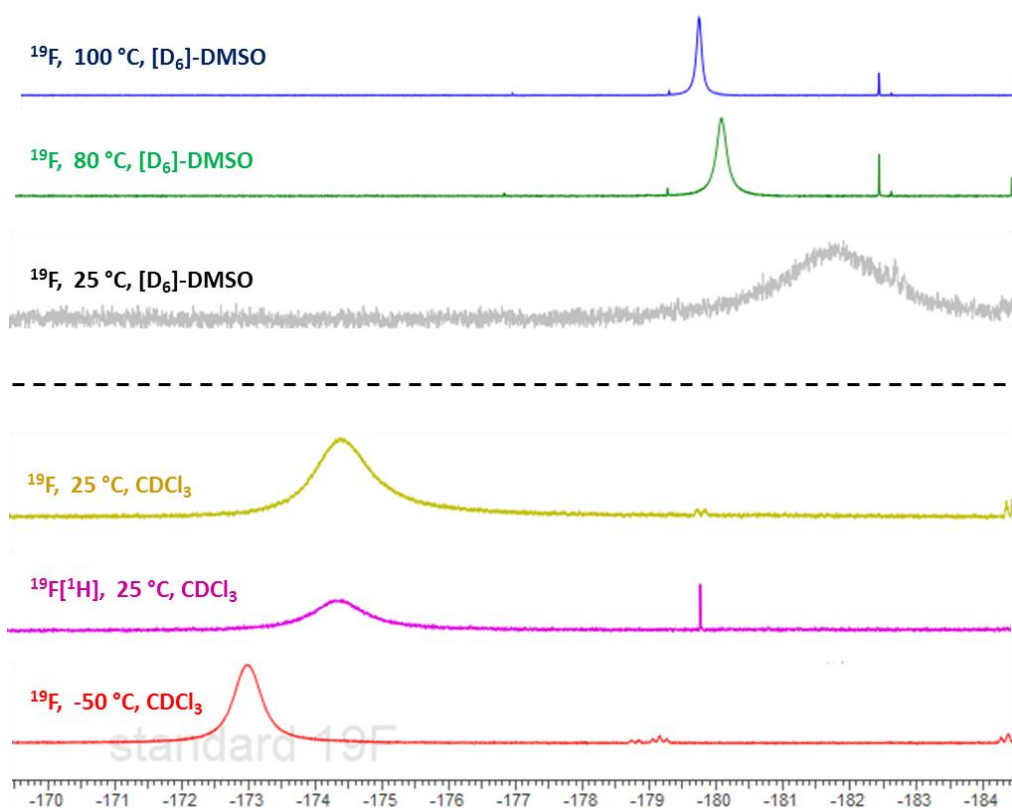


Figure 4.17 - ¹⁹F NMR spectra of **3.78** at varying temperatures.

A broad singlet in the ¹⁹F NMR spectrum was also found by Takemura *et al.*^[151] in their synthesis of **4.4** (**Figure 4.4**), however no comment on this unusual phenomenon was made in the paper, and no additional evidence could be found in the supporting information for comparison.

4.2.2 X-ray crystallographic studies

Single crystal X-ray structures of both **3.76** and **3.78** were obtained. Analysis of the X-ray structure of **3.78** (**Figure 4.18**) showed a very short intramolecular C-F•••H-O contact (1.90 Å). This value is much smaller than the combined vdW radii of the two atoms (2.67 Å),^[158] and much less than the value of 2.35 Å stipulated by Howard *et al.*^[136] to be required for an effective C-F•••H-O bond. The bond distance is larger than that obtained by Struble *et al.*^[147] (1.58 Å) for their cage-like structure containing a C-F•••H-O bond, however it is much shorter than the cyclophane C-F•••H-O bond (2.11 Å) published by Takemura *et al.*^[151] In fact, at just 1.90 Å, the intramolecular C-F•••H-O bond within **3.78** is amongst the shortest ever found in the literature (**Figure 4.2a**) for a neutral C-F fragment.^[140] Interestingly, the C-F•••H-O interaction is preferential to the C3-Q of a neighbouring molecule in the unit cell. The LH7-C7-O-H bond angle was found to be 164°,

corroborating with the ^1H NMR data in the occurrence of a linear interaction (**Table 4.4**). It is also interesting to observe that the $\text{C}_4\text{--C}_5$ and $\text{C}_7\text{--O}_\text{H}$ bonds (blue dotted lines) are not in the expected parallel alignment, and are instead forced apart by the $\text{C-F}\cdots\text{H-O}$ interaction.

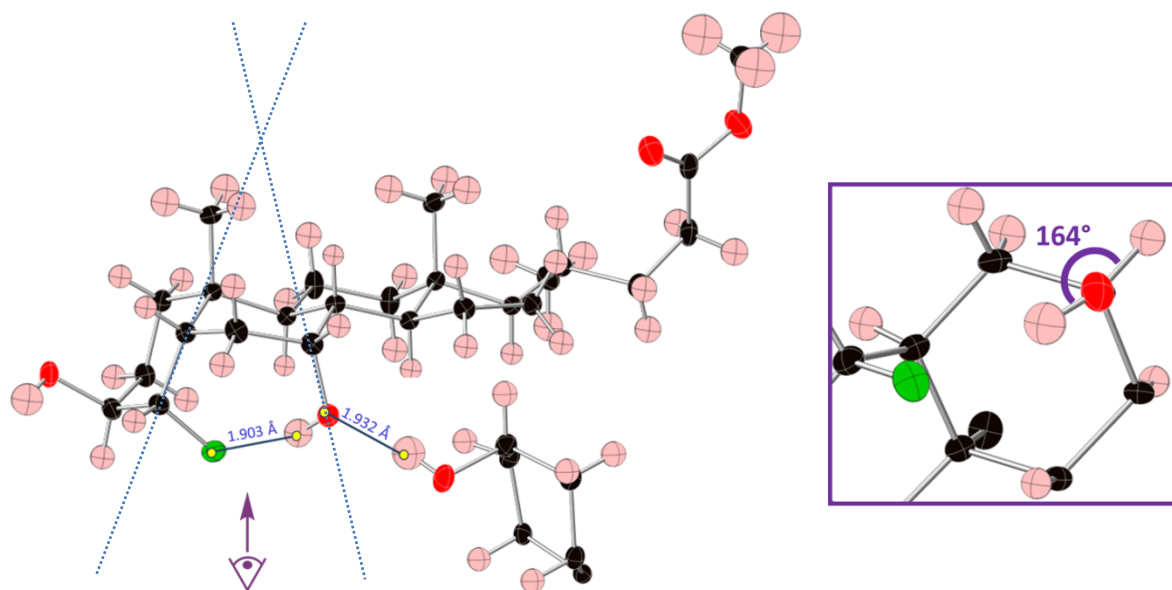


Figure 4.18 - Single crystal X-ray structure of 3.78.

A slightly longer $\text{F}\cdots\text{H-O}$ contact (1.93 Å) was observed in the crystal structure of **3.76** (**Figure 4.19**), which is somewhat surprising given that a larger $\text{F}\cdots\text{H}$ coupling was observed for this molecule. This result again highlights the difference between solid and solution state measurement of the $\text{C-F}\cdots\text{H}$ interaction (see Sections 4.1.1.3 and 4.1.2.3). The bond angle LF-O-H was shown to be 152.0° in **3.76**, which compares to value of 162.7° in **3.78**. The LF-O-H bond angles are lower than observed by Struble *et al.*^[147] for their cage-like structure **4.13** (171°).

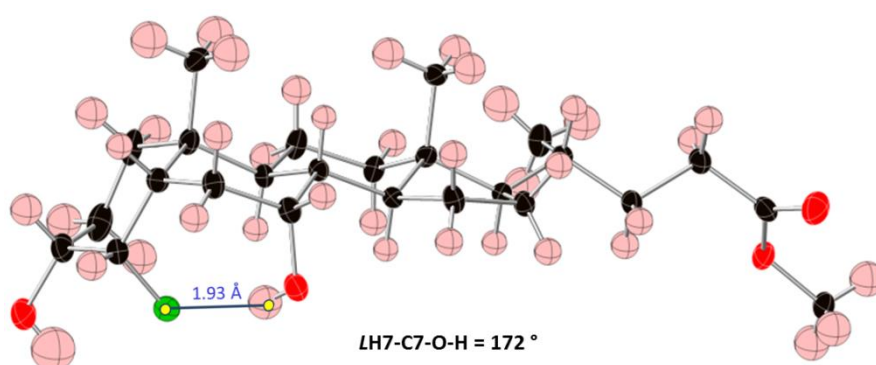


Figure 4.19 - Single crystal X-ray structure of 3.76.

4.2.3 IR studies

IR studies were then used to probe the nature of the $\text{C-F}\cdots\text{H-O}$ bond. The corresponding 2α -fluoro derivatives **3.68** and **3.66** were used as standards for **3.76** and **3.78** respectively (**Figure**

4.20), as they are structurally similar at the 3-OH, but they do not exhibit an intramolecular C-F...H-O hydrogen bond with the 7 α -OH.

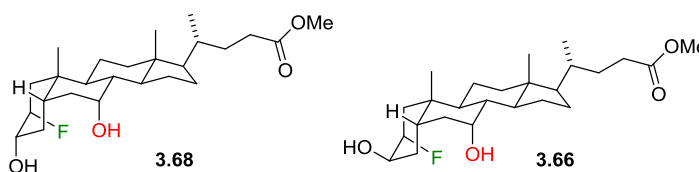


Figure 4.20 - 2 α -fluoro derivatives used as IR standards.

The infrared spectra of all compounds were collected as thin films, and only the key X-H region is shown for clarity (**Figure 4.21** and **Figure 4.22**). The IR spectrum of 2 α -fluoro derivative **3.66** (**Figure 4.21a**) showed only one overlapping peak for both the C3-OH and C7-OH ($\approx 3446\text{ cm}^{-1}$). The broadness of the peak is typical for acidic groups such as O-H and N-H. Differing degrees of H-bonding with neighbouring molecules will result in different levels of donation into the $\sigma^*_{\text{X-H}}$, differing strengths of the X-H bond, leading to a wide range of IR peaks, and thus a broad $\nu_{\text{O-H}}$ band. This indicates that in **3.66**, both the C3-OH and C7-OH are freely co-ordinating.

The C3-OH and C7-OH bands in the IR spectrum of **3.78** do not overlap however (**Figure 4.21b**). A broad band typical of an O-H bond was observed (3390 cm^{-1}) at a similar wavenumber to the O-H band of **3.66** (**Figure 4.21a**), and this was assigned as the C3O-H bond. A second, much narrower, O-H band is also present (3568 cm^{-1}), indicating a different H-bonding environment. This band was assigned as the C7O-H bond, and the significant narrowing indicates that the C7-OH is involved in a much lower degree of free H-bonding. This is unsurprising given previous experiments probing the intramolecular C-F...H-O hydrogen bond, which indicated it was still preserved in the solid state (e.g. **Figure 4.18**). Free hydroxyl groups tend to have a stretching band in excess of 3600 cm^{-1} ,^[51] indicating that the C7O-H of **3.78** bond is somewhat red-shifted compared to a hypothetical free C7O-H. Interestingly, fluorinated cyclohexanol **1.19** (**Figure 4.11**), which too had an observable C-F...H-O hydrogen bond, displayed a $\nu_{\text{O-H}} = 3619\text{ cm}^{-1}$. This indicates that the IMHB is stronger within **3.78** than **1.19**, as greater donation from the fluorine lone pair into the $\sigma^*_{\text{O-H}}$ is occurring. Additional solution phase studies are required to fully quantify this interaction.

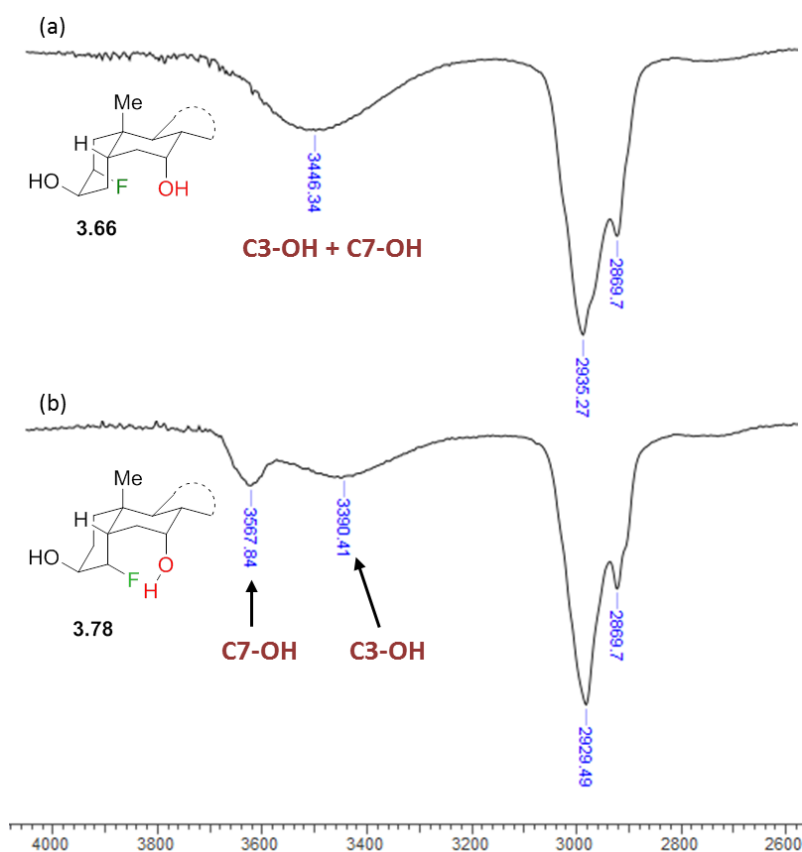


Figure 4.21 - Comparison of X-H region of 3.66 and 3.78 IR spectra.

The IR spectrum of 2 α -fluoro CDCA derivative **3.68** (Figure 4.22a) was very similar to that of **3.66**, with the C3O-H and C7O-H bonds producing a broad band (3417 cm⁻¹) typical of freely co-ordinating X-H bonds. The IR spectrum of 4 α -fluoro CDCA derivative **3.76** (Figure 4.22b) was similar to that of **3.78** with a broad C3O-H band (3415 cm⁻¹) and a narrow C7O-H band (3587 cm⁻¹). Again, the narrowness of the band suggests that the C7-OH group is not freely co-ordinating due to the formation of an intramolecular C-F...H-O hydrogen bond.

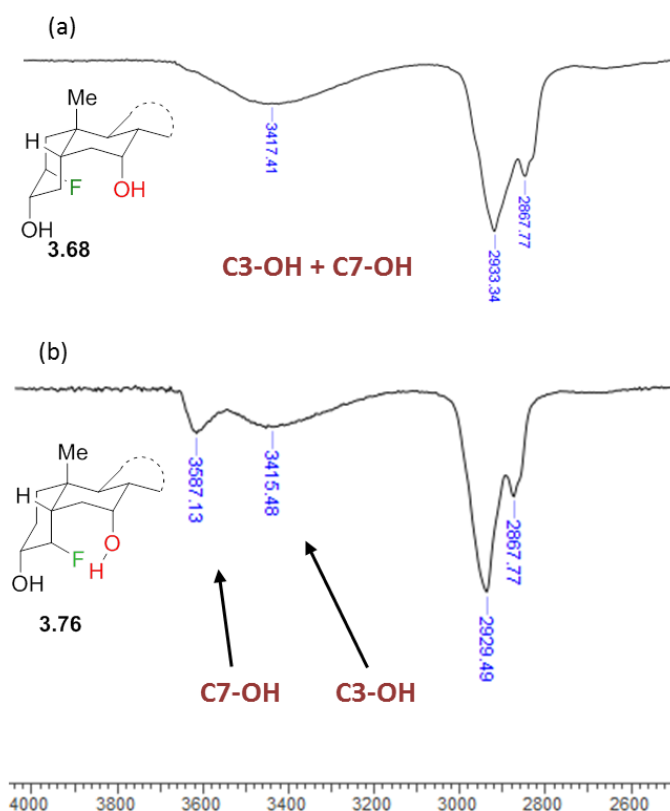


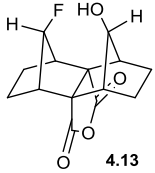
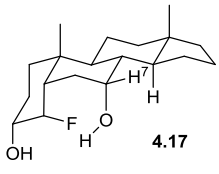
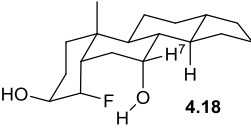
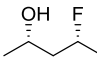
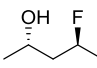
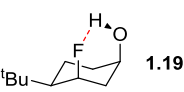
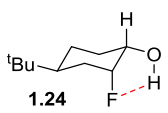
Figure 4.22 - Comparison of X-H region of **3.68** and **3.76** IR spectra.

4.2.4 Theoretical calculations of C-F•••H-O bond

Experimental evidence gathered through NMR (Section 4.2.1), X-ray (Section 4.2.2) and IR (Section 4.2.3) based methods have together shown the presence of a strong intramolecular C-F•••H-O interaction within **3.76** and **3.78**. Computational studies were conducted by our collaborators at the Université de Nantes (Dr. J. Graton and Prof. Dr. J.-Y. Le Questrel) to further characterise this interaction.

The values for the 4 α -fluoro derivatives **3.76** and **3.78** synthesised in this report are shown alongside other C-F•••H containing molecules for comparison (Table 4.5). To ease demand on computational resources, only the rigid steroid structure was included for calculations (4.17 and 4.18). However, the lack of the C17 side chain was shown to have a negligible impact on the values obtained. NBO^[155] and AIM^[51, 56] analysis confirmed a charge transfer from the fluorine lone pair into the $\sigma^*_{\text{O-H}}$ orbital for both **4.17** and **4.18**, along with the presence of a bond critical point (BCP) between the fluorine and hydrogen atoms (Table 4.5), which together confirm a C-F•••H-O hydrogen bond is present.

Table 4.5 - Theoretical calculations on F•••H substrates in CHCl₃. Obtained from published^[51, 56] and unpublished results.

F•••H Substrate	Population %	$d_{\text{OH}\cdots\text{F}} / \text{\AA}$	$\rho_{\text{bcp}}^{[a]}$	$E_{\text{HB}}^{[b]}$	$E_{n \rightarrow \sigma^*}^{(2)[c]}$	$J_{\text{OH-F}} / \text{Hz}$
 4.13	-	1.58	0.052	-	-	68
 4.17	99.2	1.93	0.0317	41.0	48.2	39.5
 4.18	99.9	1.90	0.0311	40.1	47.8	35.0
 <i>syn</i> -4.16	39%	2.00 ^[d]	0.0206	24.4	25.1	6.6
 <i>anti</i> -4.16	6%	2.01 ^[d]	0.0203	23.7	24.7	1.9
 1.19	99.7	2.03 ^[d]	0.0192	-	17.1	12.1
 1.24	97.5	2.29 ^[d]	0	-	4.1	1.7

[a] electron density at the bond critical points from AIM analysis, in e bohr⁻³; [b] HB energy at the MP2/6-31+G(d,p) level, in kJ mol⁻¹; [c] Interaction energies from the n_{F} fluorine lone pair to the σ_{OH}^* antibonding orbital at the MPWB1K/6-31+G(d,p) level, in kJ mol⁻¹; [d] calculated value.

Calculations revealed that there was nearly total population of the C-F•••H-O conformation (**Table 4.5**), which is in agreement with the data obtained experimentally (in particular X-ray analysis - **Section 4.2.2**). The electron density value, ρ , of >0.03 e bohr⁻³ at the BCP indicates a stronger C-F•••H-O bond is present compared to previously calculated interactions (e.g. **Entries 3-6**), and is within the region expected for a reasonably strong H-bond.^[157] For comparison, these

ρ values at the BCP are higher than the H-bonding interactions within water [(H₂O)₂ - 0.0198 e bohr⁻³] and hydrogen fluoride [(HF)₂ - 0.0262 e bohr⁻³], but weaker than that of the tricyclic compound **4.13**. The energy of the F•••H hydrogen-bond was calculated for **4.17** and **4.19**, and both can be classed as moderate H-bonds (Section 4.1.1.1).^[140]

4.2.5 Predicted pK_{AHY} value of 3.78/4.20

The Kenny molecular descriptor $V_{\alpha}(r)$ is defined as: “the electrostatic potential (V) at a distance (r) from the donor hydrogen on an axis defined by the nuclei of the hydrogen atom and the atom to which it is bonded”.^[52] Studies have shown excellent correlation between the calculated value of $V_{\alpha}(r)$ and measured values for hydrogen-bond donating capacity (pK_{AHY}) - Figure 4.23.^[159]

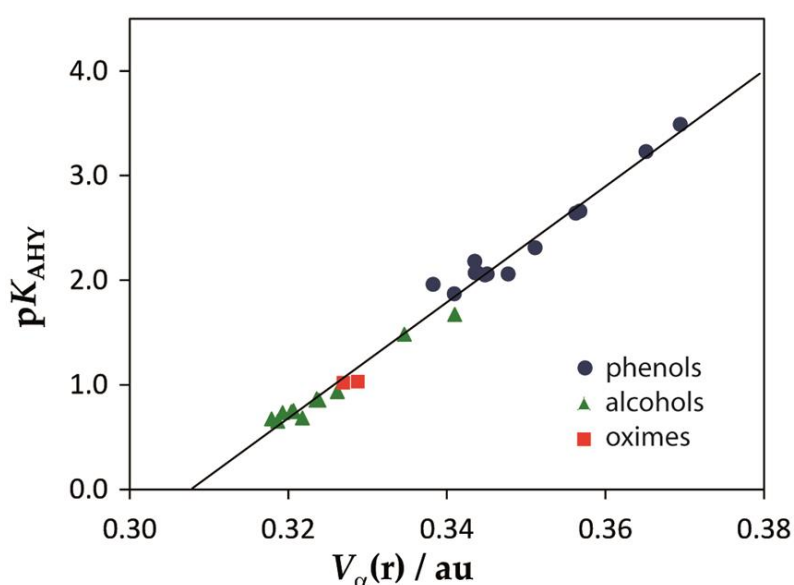


Figure 4.23 - Correlation between calculated $V_{\alpha}(r)$ and pK_{AHY}. Adapted from ref.^[159]

While the 7 α -OH functionality of **3.76/3.78** is thought to be a very poor H-bond donor due to the intramolecular C-F•••H-O hydrogen bond (see Figure 4.21 and Figure 4.22), the 3-OH, in particular the 3 β -OH of **3.78/4.20**, was expected to possess good HBD capacity. In Section 1.4.2.1, the pK_{AHY} of a variety of rigid cyclohexanols was discussed, with the trans-diaxial derivative **1.15** shown to be a particularly good H-bond donor, compared to the unfluorinated reference **1.17** (Figure 4.24).^[51]

The same trans diaxial motif of **1.15** is also present in **3.78/4.20** (Figure 4.24), and thus the 3 β -OH would also be expected to have a high hydrogen-bond donating capacity. Theoretical calculations of the hydrogen bond donating capacity of **4.20** not only revealed that it was a good hydrogen bond donating group (calculated pK_{AHY} 1.67), but that that the equilibrium lies more than 2.5

times towards the hydrogen bonded conformer ($cK = 46.8$)²⁷ than cyclohexane **1.15** ($K = 19.9$), and nearly 10 times that of unfluorinated derivative **1.17** ($K = 5.1$).

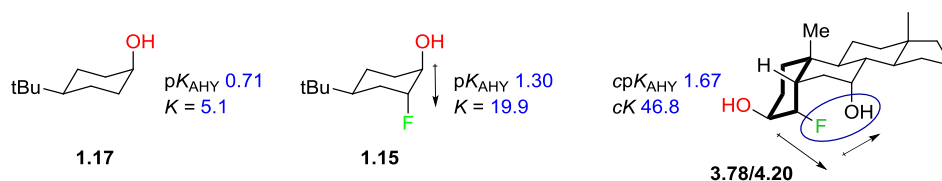


Figure 4.24 - Comparison of K and cK values for **1.17, **1.15** and **3.78/4.20**.**

The large increase in hydrogen bond donating capacity between **1.15** and **4.20** is thought to be caused by the strong C-F•••H-O interaction. The significant donation from the fluorine lone pair into the $\sigma^*_{\text{O-H}}$ (Table 4.5) increases the electron withdrawing potential of the C-F bond. In the case of the 3β -OH group of **4.20**, this leads greater stabilisation of the negative-charge build-up upon H-bonding, making the FG much more acidic than **1.15**. However, no experimental pK_{AHY} values have yet been obtained due to the requirement for much larger quantities of material for the IR based studies,²⁸ than could be synthesised. However, due to the excellent correlation between pK_{AHY} and electrostatic potential (Figure 4.23),^[52] we have good confidence in the calculated values.

4.2.6 Future work

The large scale synthesis of **3.76** and **3.78** were challenging due low reaction yields, a result of the forcing conditions required to introduce the 4α -fluoro- 7α -hydroxy motif (Section 3.3.5). Member(s) of the Linclau group are continuing this research, in particular the synthesis of **3.78** (and side-chain modified analogues) in order to obtain an accurate experimental pK_{AHY} value.

We are also interested in the synthesis of 4,4-difluoro- 7α -hydroxy derivative **4.21** and **4.22** (Figure 4.25) in order to gain a more complete understanding of the C-F•••H-O interaction. Early calculations have revealed this interaction to be weaker than the monofluorinated derivatives, in line with the results published by Gouverneur^[137] and Vulpetti.^[145] Issues with regioselectivity hampered the synthesis of these key compounds (Section 3.4.4), however this work is also being furthered by current member(s) of the Linclau group.

²⁷ cK = calculated equilibrium constant. cpK_{AHY} = calculated hydrogen bond donating capacity.

²⁸ As repeated studies are required, at different concentrations of the *N*-methylpyrrolidinone HBA.

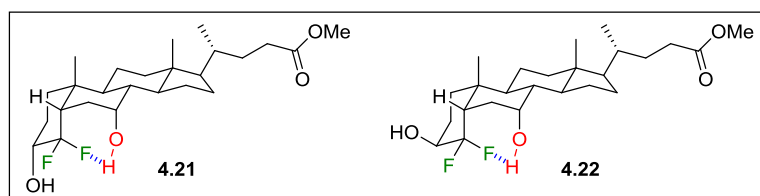


Figure 4.25 - Targetted 4,4-difluoro compounds 4.21 and 4.22

4.3 Conclusion

A 7-membered intramolecular C-F...H-O hydrogen bond within two BA derivatives was investigated through NMR spectroscopy, IR spectrometry, single crystal X-ray analysis, and computational studies, all indicating that a strong interaction was present.

NMR analysis showed a large $^1\text{H}J_{\text{F-OH}}$ coupling constant between the 4 α -fluoro moiety and the 7 α -OH, indicating their close spatial relationship. The coupling magnitude was larger for the 3 β -H derivative compared to the 3 β -OH derivative, and this was rationalised by considering hyperconjugation effects. The size of the coupling decreased as the polarity (and thus HBA ability) of the solvent increased, although the C-F...H-O hydrogen bond of both derivatives was still retained in [D₆]-DMSO.

The presence of a short C-F...H-O contact was also observed in the single crystal X-ray structure of both the 3 α -OH and 3 β -OH derivatives (~1.90 Å). Such a short C-F...H-O interaction is very rare in the literature, and indicates the presence of a hydrogen bond. Similar C7O-H bond lengths were observed in both the 4 α -fluorinated species, with a slightly shorter contact in 3 β -OH derivative **3.78**.

Infrared spectrometry showed the presence of two key O-H bands for each of the IMHB compounds. A broad band typical of freely co-ordinating O-H functional groups was assigned as the C3O-H for both compounds. A narrower band at a higher frequency was assigned as the C7O-H, which indicated that this functionality is involved in an intramolecular C-F...H-O hydrogen bonding interaction strong enough to be preserved in the solid state.

Computational analysis performed by our collaborators at the Université de Nantes, revealed that a C-F...H-O hydrogen bond existed within the two 4 α -fluorinated compounds.

Chapter 5: Experimental

5.1 General Methods

Chemical reagents were obtained from commercial sources and used without further purification, unless stated otherwise. Anhydrous solvents were distilled immediately prior to use, with the exception of anhydrous DMF which was purchased in sealed containers from commercial sources. THF was distilled from Na/benzophenone immediately prior to use. DCM and Et₃N were dried over CaH₂. All glassware was flame-dried under vacuum and cooled under N₂ prior to use. Water or air sensitive reactions were performed under inert atmosphere, using dry solvents.

Reactions were monitored by TLC (Merck Keiselgel 60 F254, aluminium sheet). Detection was carried out using one of the following dyeing reagents. Anisaldehyde-reagent: A solution of 5.1 mL p-anisaldehyde, 2.1 mL AcOH and 6.9 mL H₂SO₄ in 186 mL EtOH gives a reagent that will show varied coloured spots after development with a heat gun. KMnO₄-reagent: A solution of 3 g KMnO₄, 20 g K₂CO₃ and 5 mL NaOH (aq., 5%) in 300 mL H₂O gives a reagent that will show yellow spots after development with a heat gun.

Column chromatography was performed on silica gel (60 Å, particle size 35-70 µm). All reported solvent mixtures are volume measures. Preparative HPLC was carried out using a Biorad Bio-Sil D 90-10 column (250×22 mm at 15mL min⁻¹).

¹H, ¹⁹F, ¹³C NMR spectra were recorded at room temperature on a BRUKER AV300/400/500 spectrometer. ¹H and ¹³C chemical shifts (δ) are quoted in ppm relative to residual solvent peaks as appropriate. ¹⁹F spectra were externally referenced to CFC1₃. The coupling constants (*J*) are given in Hertz (Hz). The proton NMR signals were designated as follows: s (singlet), d (doublet), t (triplet), q (quartet), quin (quintet), sxt (sextet), spt (septet), m (multiplet), or a combination of the above.

IR spectra were recorded as neat films on a Nicolet 380 FT-IR. Absorption peaks are given in cm⁻¹ and the intensities were designated as follows: w (weak), m (medium), s (strong), br (broad). Optical rotations were recorded on an OPTICAL ACTIVITY POLAAR 2001 polarimeter at 589 nm. Melting points were recorded on a Reichert melting point apparatus, equipped with a Reichert microscope. Low resolution ES mass spectra were recorded on a WATERS ZMD single quadrupole system. High resolution mass spectra were recorded on the Bruker Apex III FT-ICR-MS.

5.2 General Procedures

5.2.1 Procedure A for 24-carboxylic acid protection as methyl ester

The method of Pellicari was used.^[71] CDCA **1.2** (25.0 g, 64 mmol, 1 equiv) was dissolved in HPLC grade MeOH (500 mL) before adding *p*-toluene sulfonic acid (1.21 g, 6.4 mmol, 0.1 equiv) and sonicating at 30 °C for 2 h. Once deemed complete by TLC analysis the solvent was removed *in vacuo*, before dissolving the residue in EtOAc (400 mL), washing the organics with sat. NaHCO₃ (2 × 150 mL), water (250 mL) and brine (250 mL). The organic phase was then dried (Na₂SO₄) and concentrated to yield methyl 3 α ,7 α -dihydroxy-5 β -cholanoate **2.32** as a white/pale yellow solid (26.0 g, quantitative).

5.2.2 Procedure B for saponification of methyl ester using LiOH

To a solution of methyl 3 β -fluoro-7 α -hydroxy-5 β -cholanoate **2.24** (43 mg, 0.11 mmol, 1 equiv) in MeOH (3 mL) was added 2M LiOH (0.55 mL, 1.1 mmol, 10 equiv) and the solution allowed to stir overnight at RT. Solvent removed *in vacuo* and the crude residue acidified with 2M HCl, before extracting with EtOAc (2 × 10 mL). Combined organics washed with water (10 mL) and brine (10 mL), dried (Na₂SO₄) and concentrated to yield 3 β -fluoro-7 α -hydroxy-5 β -cholanolic acid **1.35** (33 mg, 0.08 mmol, 76%) as a thick colourless gum.

5.2.3 Procedure C for protection of secondary alcohol as a MOM ether

To a solution of methyl 7 α -hydroxy-3-oxo-5 β -cholanoate **2.33** (3.0 g, 7.41 mmol, 1 equiv) in dry DCM (50 mL) was added DIPEA (3.83 mL, 22.2 mmol, 3 equiv) and MOM-Cl (2.82 mL, 37.1 mmol, 5 equiv) at 0 °C. The reaction mixture was warmed to room temperature before allowing to stir overnight. Once complete, the reaction mixture was quenched with water (25 mL) and methanol (25 mL) before separating the layers and extracting the aqueous with EtOAc (4×75 mL) and washing the combined organics with brine (2×150 mL). The organic phase was then dried (Na₂SO₄) and concentrated *in vacuo* to yield 3.8 g of crude material which was purified by flash chromatography (PE/EtOAc : 75:25) yielding a white solid methyl 7 α -methoxymethoxyl-3-oxo-5 β -cholanoate **2.37** (3.10 g, 6.9 mmol, 93%).

5.2.4 Procedure D for cleavage of MOM-group using HCl

Methyl 2,2-difluoro-3 β ,7 β -dimethoxymethoxyl-5 β -cholanoate **3.107** (1.5 g, 1.76 mmol, 1 equiv) was dissolved in MeOH (50 mL) and 2M HCl (10 mL), then the mixture was warmed to 70 °C for 5

hr. Reaction mixture was cooled, and concentrated *in vacuo*, azeotroping to complete dryness (MeOH×3, CHCl₃×1) to yield methyl 2,2-difluoro-3β,7β-dihydroxy-5β-cholanoate **3.109** as a white foamy solid (1.3 g, quantitative yield).

5.2.5 Procedure E for secondary alcohol oxidation using Dess-Martin Periodinane

Methyl 2α-acetoxy-3β-methoxymethoxyl-7-oxo-5β-cholanoate **5.3** (3.1 g, 6.12 mmol, 1 equiv) was dissolved in dry MeOH (30 mL) before the addition of 25% NaOMe in MeOH (20 mL) and the RM stirred at RT. Deemed complete after 1 hr, reaction acidified to pH 4-5 with 2M HCl (≈15 mL) and diluted with H₂O (15 mL). Aqueous extracted with DCM (2×75 mL), combined organics washed with NaHCO₃ (100 mL), dried (Na₂SO₄) and concentrated to yield methyl 2α-hydroxy-3β-methoxymethoxyl-7-oxo-5β-cholanoate **3.83** as a gummy solid (2.45 g, 5.27 mmol, 86%). Used without further purification.

5.2.6 Procedure F for methanolysis of acetate/benzoate

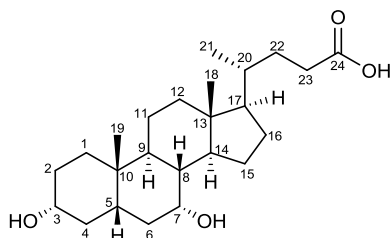
Methyl 2α-acetoxy-3β-methoxymethoxyl-7-oxo-5β-cholanoate **5.3** (3.1 g, 6.12 mmol, 1 equiv) was dissolved in dry MeOH (30 mL) before the addition of 25% NaOMe in MeOH (20 mL) and the RM stirred at RT. Deemed complete after 1 hr, reaction acidified to pH 4-5 with 2M HCl (≈15 mL) and diluted with H₂O (15 mL). Aqueous extracted with DCM (2×75 mL), combined organics washed with NaHCO₃ (100 mL), dried (Na₂SO₄) and concentrated to yield methyl 2α-hydroxy-3β-methoxymethoxyl-7-oxo-5β-cholanoate **3.83** as a gummy solid (2.45 g, 5.27 mmol, 86%). Used without further purification.

5.2.7 Procedure G for 3-keto/7-keto reduction using NaBH₄/CeCl₃

Using the conditions of Černý.^[75] To a solution of methyl 3β-fluoro-7-oxo-5β-cholanoate **2.5** (110mg, 0.27 mmol, 1 equiv) and CeCl₃ (80 mg, 0.33 mmol, 1.2 equiv) in MeOH (5 mL) and EtOAc (2 mL) was added NaBH₄ (11 mg, 0.30 mmol, 1.1 equiv) over the course of 5 min. The solution was stirred for 30 min, at which point further NaBH₄ (10 mg, 1 equiv) was added and stirred for a further 30 min to drive the reaction towards completion. Reaction quenched with ice cold 2M HCl (15 mL) and the aqueous washed with EtOAc (2 × 15 mL). The combined organic were washed with sat NaHCO₃ (15 mL) and water (15 mL), dried (Na₂SO₄) and concentrated to yield 90 mg of a thick colourless oil. Purified by flash chromatography (PE/EtOAc : 90:10→75:25) to yield methyl 3β-fluoro-7α-hydroxy-5β-cholanoate **2.24** (43 mg, 0.11 mmol, 39%) and methyl 3β-fluoro-7β-hydroxy-5β-cholanoate **2.25** (34 mg, 0.08 mmol, 31%), both as gummy solids.

5.3 Synthesis of 3-deoxy-3-fluoro analogues

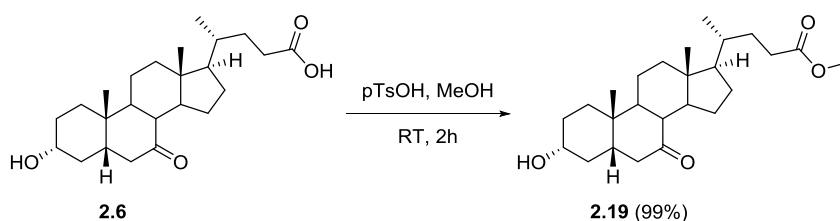
The synthesis and characterisation of the following compounds is presented in the order of reactions discussed in **Chapter 2**. The steroid numbering system is presented again for convenience.



Chenodeoxycholic acid numbering (1.2)

5.3.1 Synthesis of 3-deoxy-3 β -fluoro analogues

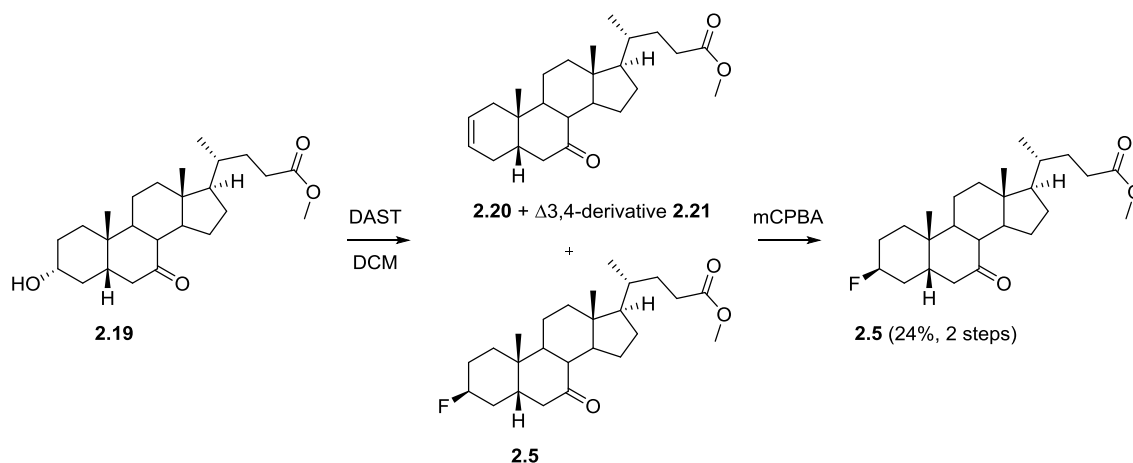
Methyl 3 α ,7 α -dihydroxy-5 β -cholanoate (2.19)



Following general procedure A, carboxylic acid **2.6** (7.8 g, 20 mmol, 1 equiv) was protected and purified to yield **2.19** as a white/pale yellow solid (8.0 g, 19 mmol, 99%).

2.19: Formula: C₂₅H₄₀O₄; **MW** 404.6; **m.p.** 102 - 104 °C (lit. 107 - 108°C); **R_f** (PE/ EtOAc : 50/50) : 0.25; **I.R** 3402 (br. w), 2935 (m), 2870 (m), 1736 (s), 1709 (s), 1435 (m), 1169 (m), 733 (m) cm⁻¹; **¹H NMR** (300MHz, CDCl₃): δ 3.67 (s, 3H, CO₂CH₃), 3.61 (tt, *J*=10.5, 5.3 Hz, 1H, H₃), 2.86 (dd, *J*=12.3, 6.0 Hz, 1H, H_{6 β}), 2.43-2.31 (m, 2H), 2.27-2.14 (m, 2H), 2.09-1.23 (m, 20H), 1.20 (s, 3H, H₁₉), 1.17-1.06 (m, 3H), 0.92 (d, *J*=6.6 Hz, 3H, H₂₁), 0.66 (s, 3H, H₁₈) ppm; **¹³C NMR** (100 MHz, CDCl₃): δ 212.0 (C₇), 174.6 (C₂₄), 70.8 (C₃), 54.7, 51.5 (CO₂CH₃), 49.5, 48.9, 46.1, 45.4 (C₆), 42.7, 42.6, 38.9 (CH₂), 37.4 (CH₂), 35.2, 35.1, 34.1 (CH₂), 31.0 (CH₂), 31.0 (CH₂), 29.8 (CH₂), 28.2 (CH₂), 24.8 (CH₂), 23.0 (C₁₉), 21.6 (CH₂), 18.3 (C₂₁), 12.0 (C₁₈) ppm; **MS (ESI+)** *m/z* : 404.9 [M+H]⁺, 809.5 [2M+H]⁺.

Data consistent with literature^[160]

Methyl 3 β -fluoro-7-oxo-5 β -cholanoate (2.5)

Fluorination: To a solution of alcohol **2.19** (500 mg, 1.24 mmol, 1 equiv) in DCM (25 mL) was added DAST (250 μ L, 1.85 mmol, 1.5 equiv) and the reaction was allowed to stir for 16 h at RT. Incomplete after O/N stirring so further DAST added (100 μ L) to drive reaction to completion, and stirred for 24 hr. Reaction was diluted with DCM (5 mL) before quenching with sat. aq. NaHCO₃ (10 mL) and separating the layers. Aqueous washed with further DCM (5 mL) before the combined organics were washed with water (10 mL) and brine (10 mL), dried (Na₂SO₄) and concentrated to yield 480 mg of a yellow thick oil. Crude NMR indicated a 50% conversion to the desired β -fluoro compound, along with 30% undesired alkene. The mixture was inseparable *via* standard flash chromatography, used without further purification in epoxidation reaction.

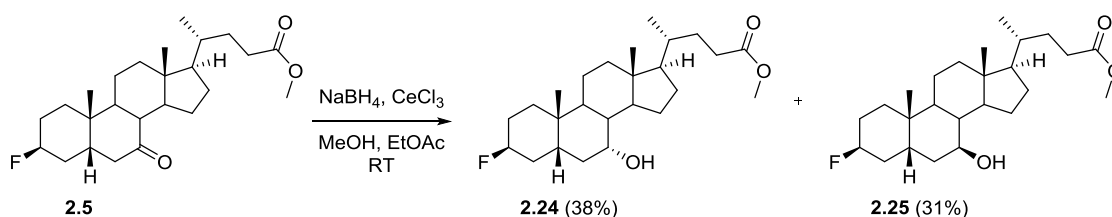
¹H NMR (400MHz, CDCl₃): δ 5.64 - 5.25 (m, 0.8H, C=CH, alkene by-product), 4.72 (d, $J=48.4$ Hz, 1H, CHF), 3.59 - 3.56 (m, 3H, CO₂CH₃), 2.89 - 2.70 (m, 1H, H_{6 β}), 2.49 - 2.44 (m, 0.3H), 2.41 - 1.21 (m, 23H), 1.17 (s, 2H, H₁₉), 1.15 (s, 1H, H₁₉), 0.86 - 0.82 (m, 3H, H₂₁), 0.59 (s, 3H, H₁₈) ppm; **Selected ¹³C NMR** (100 MHz, CDCl₃): δ 212.0 (C₇), 211.9 (C₇), 174.3 (C₂₄), 174.3 (C₂₄), 129.3 (C=C, alkene by-product), 127.2 (C=C), 125.2 (C=C), 124.0 (C=C), 88.6 (d, $J=167.3$ Hz, C-F), 75.2 (C-OH, starting material) ppm; **¹⁹F NMR** (376MHz, CDCl₃): δ -183.05 (qt, $J=46.0, 12.0$ Hz) ppm; **[¹H]¹⁹F NMR** (376MHz, CDCl₃): δ -183.05 (s) ppm.

Epoxidation: To a solution of 3 β -fluoro and alkene mixture (480 mg, \approx 1.2 mmol, 1 equiv) in DCM was added *m*CPBA acid (100 mg, 0.6 mmol, \approx 0.5 equiv) and allowed to stir O/N at RT. Consumption of undesired alkene incomplete after overnight reaction so further *m*CPBA (60 mg, 0.3 mmol) was added and the progress monitored *via* TLC. Reaction deemed complete and quenched with sat. aq. NaHCO₃ (15 mL), the layers were separated and aqueous washed with further DCM (20 mL). Combined organics were washed with water (20 mL) and brine (20 mL), dried (Na₂SO₄) and concentrated to yield 400 mg of a thick colourless oil. Crude purified *via* flash chromatography (PE/EtOAc : 93:7 \rightarrow 85:15) to yield the desired 3 β -fluoro compound **2.5** as a

gummy solid (120 mg, 0.30 mmol, 24%). Δ 2,3- and Δ 3,4-epoxides (**2.22** and **2.23**) were also formed, but not cleanly isolated - their characterisation will be discussed in **Section 5.4.2**.

2.5: Formula: $C_{25}H_{39}FO_3$; **MW** 406.6; **m.p.** N/A; **R_f** (PE/acetone : 70:30) 0.76; **I.R** 2939 (m), 2870 (w), 1740 (s), 1709 (s), 1435 (w), 1207 (w), 1165 (w), 1018 (w); **¹H NMR** (400MHz): δ 4.79 (d, $J=48.4$ Hz, 1H, H₃), 3.64 (s, 3H, CO₂CH₃), 2.88 (dd, $J=12.6, 6.1$ Hz, 1H, H_{6\beta}), 2.41 (t, $J=11.2$ Hz, 1H, H_{8\beta}), 2.33 (ddd, $J=15.5, 11.0, 5.0$ Hz, 1H, H₂₃), 2.25-1.27 (m, 22H), 1.22 (s, 3H, H₁₉), 1.16 - 1.02 (m, 2H), 0.90 (d, $J=6.4$ Hz, 3H, H₂₁), 0.64 (s, 3H, H₁₈) ppm; **¹³C NMR** (100 MHz, $CDCl_3$): δ 212.2 (C₇), 174.5 (C₂₄), 88.8 (d, $J=167.3$ Hz, C₃), 54.7, 51.4 (CO₂CH₃), 49.5 (C₈), 48.8, 44.8 (C₆), 42.6, 42.3, 41.5, 38.9 (CH₂), 35.3, 35.1, 32.4 (d, $J=22.0$ Hz, C₄), 31.0 (C₂₃), 30.9 (CH₂), 29.1 (CH₂), 28.2 (CH₂), 25.5 (d, $J=21.3$ Hz, C₂), 24.7 (CH₂), 23.3 (C₁₉), 21.9 (CH₂), 18.3 (C₂₁), 12.0 (C₁₈) ppm; **¹⁹F NMR** ($CDCl_3$, 376MHz): δ -183.10 (qt, $J=45.9, 11.7$ Hz) ppm; **[¹H]¹⁹F NMR** ($CDCl_3$, 376MHz): δ -183.10 (s) ppm; **MS (ESI+)** m/z : 407.2 [M+H]⁺, 426.6 [M+Na]⁺; **HRMS** (HPLC-ESI) : [M+H]⁺ Calcd: 407.2956; Found: 407.2956.

Methyl 3 β -fluoro-7 α -hydroxy-5 β -cholanoate (2.24) and methyl 3 β -fluoro-7 β -hydroxy-5 β -cholanoate (2.25)



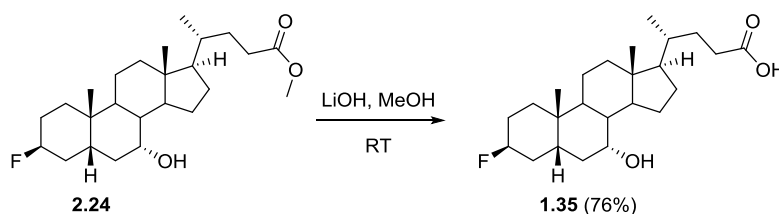
To a solution of ketone **2.5** (110 mg, 0.27 mmol, 1 equiv) and $CeCl_3$ (80 mg, 0.33 mmol, 1.2 equiv) in MeOH (5 mL) and EtOAc (2 mL) was added $NaBH_4$ (11 mg, 0.30 mmol, 1.1 equiv) over the course of 5 min. The solution was stirred for 30 min, at which point further $NaBH_4$ (10 mg, 1 equiv) was added and stirred for a further 30 min to drive the reaction towards completion. Reaction quenched with ice cold 2M HCl (15 mL) and the aqueous washed with EtOAc (2 \times 15 mL). The combined organics were washed with sat $NaHCO_3$ (15 mL) and water (15 mL), dried (Na_2SO_4) and concentrated to yield 90 mg of a thick colourless oil. Purified by flash chromatography (PE/EtOAc : 90:10 \rightarrow 75:25) to yield 7 α -OH **2.24** (43 mg, 0.11 mmol, 39%) and 7 β -OH **2.25** (34 mg, 0.08 mmol, 31%), both as gummy solids. (**General procedure G**).

7 α -OH 2.24: Formula: $C_{25}H_{41}FO_3$; **MW** 408.6; **m.p.** N/A; **R_f** (PE/EtOAc : 70/30) : 0.56; **I.R** 3444 (br. w), 2931 (s), 2866 (m), 1740 (s), 1446 (m), 1169 (m), 1022 (m); **¹H NMR** (400MHz, $CDCl_3$): δ 4.82 (d, $J=49.3$ Hz, 1H, H₃), 3.87 (q, $J=2.1$ Hz, 1H, H₇), 3.66 (s, 3H, CO₂CH₃), 2.46 (dddd, $J=49.0, 15.0, 13.0, 2.0$ Hz, 1H, H_{4\alpha}), 2.34 (ddd, $J=15.5, 11.0, 5.0$ Hz, 1H, H₂₃), 2.22 (ddd, $J=15.6, 9.4, 6.5$ Hz, 1H, H_{23'}), 2.05-1.07 (m, 28H), 0.95 (s, 3H, H₁₉), 0.92 (d, $J=6.5$ Hz, 3H, H₂₁), 0.67 (s, 3H, H₁₈) ppm; **¹³C NMR** (100 MHz, $CDCl_3$): δ 174.7 (C₂₄), 90.0 (d, $J=166.5$ Hz, C₃), 68.7 (C₇), 55.8, 51.5 (CO₂CH₃), 50.4, 42.7,

39.6 ($\underline{\text{C}}\text{H}_2$), 39.3, 36.3, 35.3, 35.3, 34.6 (d, $J=19.8$ Hz, $\underline{\text{C}}4$), 33.8 ($\underline{\text{C}}\text{H}_2$), 32.1, 31.0 ($\underline{\text{C}}23$), 30.9 ($\underline{\text{C}}\text{H}_2$), 30.0 ($\underline{\text{C}}\text{H}_2$), 28.1 ($\underline{\text{C}}\text{H}_2$), 25.9 (d, $J=21.3$ Hz, $\underline{\text{C}}2$), 23.7 ($\underline{\text{C}}\text{H}_2$), 23.0 ($\underline{\text{C}}19$), 20.9 ($\underline{\text{C}}\text{H}_2$), 18.2 ($\underline{\text{C}}21$), 11.7 ($\underline{\text{C}}18$) ppm; ^{19}F NMR (376MHz, CDCl_3): δ -184.90 - -185.42 (m) ppm; $[^1\text{H}]^{19}\text{F}$ NMR (376MHz, CDCl_3): δ -185.18 (s) ppm; **MS (ESI+)** m/z : 371.2 $[\text{M}+\text{H}, -\text{H}_2\text{O}, -\text{HF}]^+$, 391.2 $[\text{M}+\text{H}, -\text{H}_2\text{O}]^+$; **HRMS** (HPLC-ESI) : $[\text{M}+\text{Na}]^+$ Calcd: 431.2932; Found: 431.2934.

7 β -OH 2.25: Formula: $\text{C}_{25}\text{H}_{41}\text{FO}_3$; **MW** 408.6; **m.p.** N/A; **R_f** (PE/EtOAc : 70/30) : 0.44; **I.R** 3749 (br. w), 2931 (s), 2866 (m), 1740 (s), 1446 (m), 1377 (m), 1169 (m), 1022 (m); ^1H NMR (400MHz, CDCl_3): δ 4.83 (d, $J=49.6$ Hz, 1H, $\underline{\text{H}}3$), 3.66 (s, 3H, CO_2CH_3), 3.54 (td, $J=10.0, 5.3$ Hz, 1H, $\underline{\text{H}}7$), 2.35 (ddd, $J=15.5, 11.0, 5.0$ Hz, 1H, $\underline{\text{H}}23$), 2.22 (ddd, $J=15.5, 9.6, 6.4$ Hz, 1H, $\underline{\text{H}}23'$), 2.03 - 1.01 (m, 30H), 0.99 (s, 3H, $\underline{\text{H}}19$), 0.93 (d, $J=6.4$ Hz, 3H, $\underline{\text{H}}21$), 0.69 (s, 3H, $\underline{\text{H}}18$) ppm; ^{13}C NMR (100 MHz, CDCl_3): δ 174.7 ($\underline{\text{C}}24$), 89.5 (d, $J=167.3$ Hz, $\underline{\text{C}}3$), 71.3 ($\underline{\text{C}}7$), 55.8, 54.9, 51.5 (CO_2CH_3), 43.7, 43.5, 40.1 ($\underline{\text{C}}\text{H}_2$), 38.6, 37.5, 36.1 ($\underline{\text{C}}\text{H}_2$), 35.2, 34.3, 32.5 (d, $J=22.0$ Hz, $\underline{\text{C}}4$), 31.0 ($\underline{\text{C}}23$), 31.0 ($\underline{\text{C}}\text{H}_2$), 29.8 ($\underline{\text{C}}\text{H}_2$), 28.6 ($\underline{\text{C}}\text{H}_2$), 26.8 ($\underline{\text{C}}\text{H}_2$), 25.8 (d, $J=21.3$ Hz, $\underline{\text{C}}2$), 23.7 ($\underline{\text{C}}19$), 21.5 ($\underline{\text{C}}\text{H}_2$), 18.4 ($\underline{\text{C}}21$), 12.1 ($\underline{\text{C}}18$) ppm; ^{19}F NMR (CDCl_3 , 376MHz): δ -183.17 - -184.06 (m) ppm; $[^1\text{H}]^{19}\text{F}$ NMR (376MHz, CDCl_3): δ -183.63 (s) ppm; **MS (ESI+)** m/z : 371.2 $[\text{M}+\text{H}, -\text{H}_2\text{O}, -\text{HF}]^+$, 391.2 $[\text{M}+\text{H}, -\text{H}_2\text{O}]^+$; **HRMS** (HPLC-ESI) : $[\text{M}+\text{Na}]^+$ Calcd: 431.2932; Found: 431.2947.

3 β -fluoro-7 α -hydroxy-5 β -cholanic acid (**1.35**)

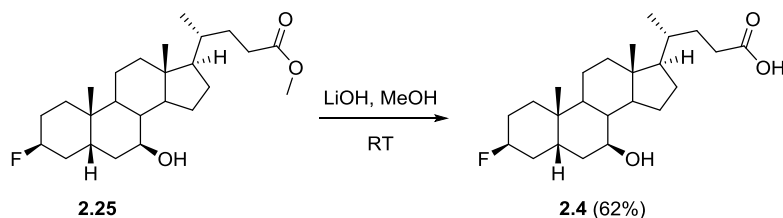


To a solution of methyl ester **2.24** (43 mg, 0.11 mmol, 1 equiv) in MeOH (3 mL) was added 2M LiOH (0.55 mL, 1.1 mmol, 10 equiv) and the solution allowed to stir overnight at RT. Solvent removed *in vacuo* and the crude residue acidified with 2M HCl, before extracting with EA (2 \times 10 mL). Combined organics washed with water (10 mL) and brine (10 mL), dried (Na_2SO_4) and concentrated to yield **1.35** (33 mg, 0.08 mmol, 76%) as a thick colourless gum. (**General procedure B**)

1.35: Formula: $\text{C}_{24}\text{H}_{39}\text{FO}_3$; **MW** : 394.6; $[\alpha]_D^{25}$ +6.6 (c 0.5, CHCl_3 , 21 $^\circ\text{C}$); **m.p.** N/A; **R_f** (Petrol ether/EtOAc : 75/25) : 0.18; **I.R** 2931 (s), 2870 (m), 1709 (s), 1446 (w), 1265 (w), 1022 (w); ^1H NMR (400MHz, CDCl_3): δ 4.83 (d, $J=49.1$ Hz, 1H, $\underline{\text{H}}3$), 3.89 (q, $J=2.7$ Hz, 1H, $\underline{\text{H}}7$), 2.57-2.34 (m, 2H, $\text{H}4\alpha + \underline{\text{H}}23$), 2.26 (ddd, $J=15.5, 9.7, 6.4$ Hz, 1H, $\underline{\text{H}}23'$), 2.06 - 1.04 (m, 27H), 0.96 (s, 3H, $\underline{\text{H}}19$), 0.94 (d, $J=6.6$ Hz, 3H, $\underline{\text{H}}21$), 0.68 (s, 3H, $\underline{\text{H}}18$) ppm; ^{13}C NMR (100 MHz, CDCl_3): δ 180.1 ($\underline{\text{C}}24$), 90.0 (d, $J=166.5$ Hz, $\underline{\text{C}}3$), 68.8 ($\underline{\text{C}}7$), 55.8, 50.4, 42.7, 39.6 ($\underline{\text{C}}\text{H}_2$), 39.3, 36.3, 35.3, 35.3, 34.6 (d, $J=20.5$ Hz, $\underline{\text{C}}4$), 33.8 ($\underline{\text{C}}\text{H}_2$),

32.1, 31.0 ($\underline{\text{C}}_{23}$), 30.7 ($\underline{\text{C}}_{\text{H}_2}$), 30.0 ($\underline{\text{C}}_{\text{H}_2}$), 28.1 ($\underline{\text{C}}_{\text{H}_2}$), 25.9 (d, $J=20.5$ Hz, $\underline{\text{C}}_2$), 23.7 ($\underline{\text{C}}_{\text{H}_2}$), 23.0 ($\underline{\text{C}}_{19}$), 20.9 ($\underline{\text{C}}_{\text{H}_2}$), 18.2 ($\underline{\text{C}}_{21}$), 11.8 ($\underline{\text{C}}_{18}$) ppm; ^{19}F NMR (376MHz, CDCl_3): δ -184.88 - -185.55 (m) ppm; $[^1\text{H}]^{19}\text{F}$ NMR (376MHz, CDCl_3): δ -185.21 (s) ppm; **MS (ESI+)** m/z : 357.2 $[\text{M}+\text{H}, -\text{H}_2\text{O}, -\text{HF}]^+$, 377.2 $[\text{M}+\text{H}, -\text{H}_2\text{O}]^+$; **HRMS (HPLC-ESI)** : $[\text{M}+\text{Na}]^+$ Calcd: 417.2775; Found: 417.2784.

3 β -fluoro-7 β -hydroxy-5 β -cholanic acid (**2.4**)

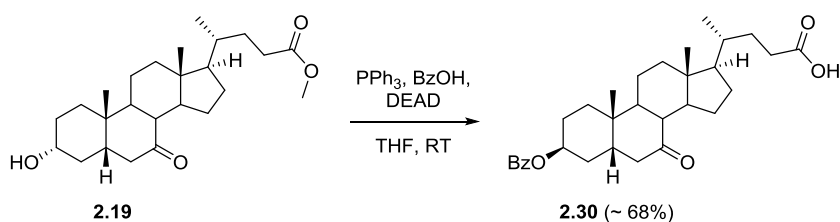


Using general procedure B, **2.25** was saponified to yield **2.4** (22 mg, 0.06 mmol, 62%) as a white solid.

2.4: Formula: $\text{C}_{24}\text{H}_{39}\text{FO}_3$; **MW** 394.6; $[\alpha]_{\text{D}} +39.3$ (c 0.5, CHCl_3 , 21 °C); **m.p.** 153–155 °C; **R_f** (PE/EtOAc : 75/25) : 0.16; **I.R** 2928 9 (s), 2866 (m), 1709 (s), 1446 (m), 1261 (m), 1018 (m); ^1H NMR (400MHz, CDCl_3): δ 4.84 (d, $J=49.1$ Hz, 1H, $\underline{\text{C}}_3$), 3.55 (td, $J=10.1, 5.4$ Hz, 1H, $\underline{\text{H}}_7$), 2.40 (ddd, $J=15.5, 11.0, 5.0$ Hz, 1H, $\underline{\text{H}}_{23}$), 2.26 (ddd, $J=15.5, 9.4, 6.6$ Hz, 1H, $\underline{\text{H}}_{23'}$), 1.97 - 1.03 (m, 25H), 1.00 (s, 3H, $\underline{\text{H}}_{19}$), 0.94 (d, $J=6.4$ Hz, 3H, $\underline{\text{H}}_{21}$), 0.69 (s, 3H, $\underline{\text{H}}_{18}$) ppm; ^{13}C NMR (100 MHz, CDCl_3): δ 179.8 ($\underline{\text{C}}_{24}$), 89.5 (d, $J=167.3$ Hz, $\underline{\text{C}}_3$), 71.4 ($\underline{\text{C}}_7$), 55.8, 54.9, 43.8, 43.5, 40.1 ($\underline{\text{C}}_{\text{H}_2}$), 38.6, 37.5, 36.1 ($\underline{\text{C}}_{\text{H}_2}$), 35.2, 34.3, 32.5 (d, $J=21.3$ Hz, $\underline{\text{C}}_4$), 31.0 ($\underline{\text{C}}_{23}$), 30.8 ($\underline{\text{C}}_{\text{H}_2}$), 29.8, ($\underline{\text{C}}_{\text{H}_2}$) 28.6 ($\underline{\text{C}}_{\text{H}_2}$), 26.8 ($\underline{\text{C}}_{\text{H}_2}$), 25.9 (d, $J=21.3$ Hz, $\underline{\text{C}}_2$), 23.7 ($\underline{\text{C}}_{19}$), 21.5 ($\underline{\text{C}}_{\text{H}_2}$), 18.3 ($\underline{\text{C}}_{21}$), 12.1 ($\underline{\text{C}}_{18}$) ppm; ^{19}F NMR (376MHz, CDCl_3): δ -183.15 - -184.15 (m) ppm.; $[^1\text{H}]^{19}\text{F}$ NMR (376MHz, CDCl_3) δ -183.62 (s) ppm; **MS (ESI+)** m/z : 357.2 $[\text{M}+\text{H}, -\text{H}_2\text{O}, -\text{HF}]^+$, 377.2 $[\text{M}+\text{H}, -\text{H}_2\text{O}]^+$; **HRMS (HPLC-ESI)** : $[\text{M}+\text{Na}]^+$ Calcd: 417.2775; Found: 417.2782.

5.3.2 Synthesis of 3-deoxy-3 α -fluoro analogues

Methyl 3 β -benzoyloxy-7-oxo-5 β -cholanoate (**2.30**)

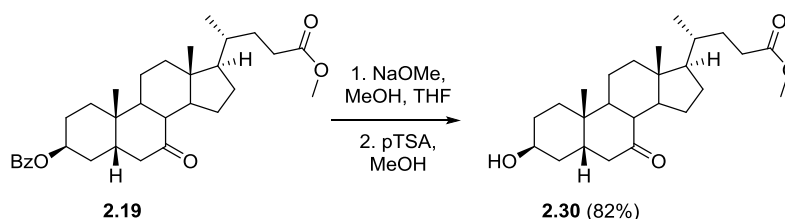


To a solution of alcohol **2.19** (1.41 g, 3.48 mmol, 1 equiv), PPh_3 (1.37 g, 5.23 mmol, 1.5 equiv) and benzoic acid (640 mg, 5.23 mmol, 1.5 equiv) in dry THF (20 mL), was added DEAD (0.96 mL, 5.23 mmol, 1.5 equiv) over the course of 5 min. The resulting yellow solution was allowed to stir

overnight at RT, at which point TLC analysis showed complete consumption of SM along with the formation of ~4 new spots. Solvent was removed *in vacuo*, before subjecting directly to flash chromatography (PE/Et₂O : 90:10→ PE/EtOAc 90:10) yielding the pure benzoate **2.30** as a white solid (285 mg – used for analysis) along with 80% pure benzoate (1.15g – used without further purification in subsequent step, ~68% overall yield).

2.30: Formula: C₃₂H₄₄O₅; **MW** 508.7; **m.p.** 136-138°C; **R_f** (PE/EtOAc : 85/15) : 0.46; **I.R** 2943 (m), 2870 (w), 1709 (s), 1450 (w), 1277 (s), 1111 (m), 910 (s), 729 (s), 714 (s); **¹H NMR** (400MHz, CDCl₃): δ 8.01 (dd, *J*=7.6, 1.5 Hz, Ar-H *ortho*), 7.54 (tt, *J*=7.3, 1.5 Hz, Ar-H *para*), 7.42 (t, *J*=7.6 Hz, 2H, Ar-H *meta*), 5.26 (br. s, 1H, H₃), 3.64 (s, 3H, CO₂CH₃), 2.90 (dd, *J*=12.5, 6.1 Hz, 1H, H_{6β}), 2.42 (t, *J*=11.2 Hz, 1H, H_{8β}), 2.38 - 2.12 (m, 4H), 2.03 - 1.29 (m, 17H), 1.27 (s, 3H, H₁₉), 0.91 (d, *J*=6.4 Hz, 3H, H₂₁), 0.65 (s, 3H, H₁₈) ppm; **¹³C NMR** (100 MHz, CDCl₃): δ 212.0 (C₃), 174.5 (C₂₄), 165.5 (PhC₂O), 132.7, (Ar-C *para*), 130.7 (Ar-C *ipso*), 129.3 (2xAr-C *ortho*), 128.2 (2xAr-C *meta*), 70.1 (C₃), 54.7, 51.3, 49.4 (C₈), 48.8, 44.9 (C₆), 42.5, 42.3, 42.2, 38.8 (CH₂), 35.4, 35.1, 31.7 (CH₂), 30.9 (CH₂), 30.9 (CH₂), 30.0 (CH₂), 28.1 (CH₂), 24.7 (CH₂), 24.6 (CH₂), 23.6 (C₁₉), 21.9 (CH₂), 18.3 (C₂₁), 11.9 (C₁₈) ppm; **MS (ESI+)** *m/z* : 509.3 [M+H]⁺, 526.3 [M+NH₄]⁺, 531.3 [M+Na]⁺; **HRMS** (HPLC-ESI) : [M+NH₄]⁺ Calcd: 526.3257; Found: 526.3527.

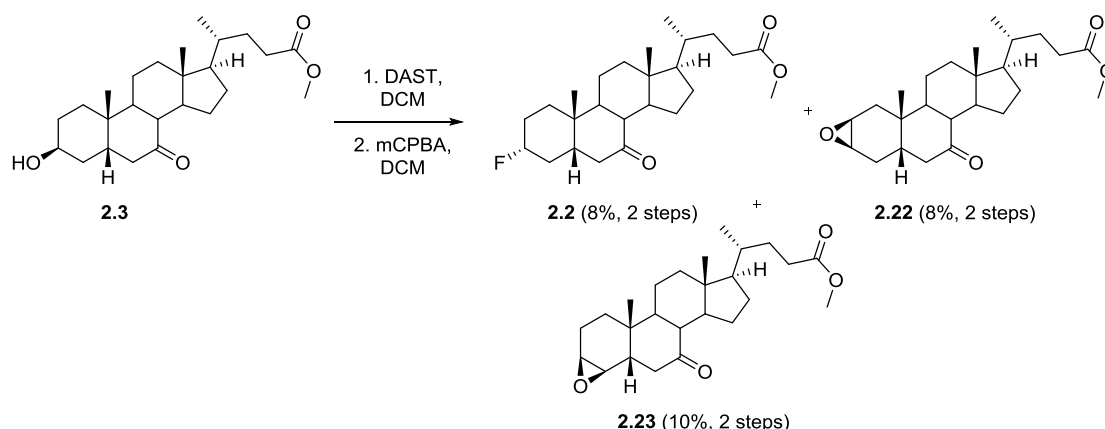
Methyl 7-oxisolithocholate (2.30)



Using general procedure F, benzoate **2.19** (1.15 g, 2.26 mmol, 1 equiv) was methanolysed. Procedure A was then used to reform the methyl ester. Purified *via* flash chromatography (PE/EtOAc : 70:30→60:40) to yield **2.30** as a white solid (750 mg, 1.85 mmol, 82%).

2.30: Formula: C₂₅H₄₀O₄; **MW** 404.6; **m.p** 109–110 °C **R_f** (PE/EtOAc : 65/35) : 0.22; **I.R** 3375 (br. w), 3425 (br. w), 2935 (m), 2874 (w), 1732 (m), 1705 (m), 910 (m), 729 (s); **¹H NMR** (400MHz, CDCl₃): δ 4.04 (quin, *J*=2.2 Hz, 1H, H₃), 3.64 (s, 3H, CO₂CH₃), 2.87 (dd, *J*=12.5, 6.0 Hz, 1H, H_{6β}), 2.39 (t, *J*=11.2 Hz, 1H, H₈), 2.35 - 2.08 (m, 4H), 2.05 - 1.23 (m, 20H), 1.21 (s, 3H, H₁₉), 1.17-0.92 (m, 3H), 0.90 (d, *J*=6.4 Hz, 3H, H₂₁), 0.64 (s, 3H, H₁₈) ppm; **¹³C NMR** (100 MHz, CDCl₃): δ 212.8 (C₇), 174.6 (C₂₄), 66.4 (C₃), 54.7, 51.4 (CO₂CH₃), 49.5 (C₈), 48.8, 45.1 (C₆), 42.6, 42.3, 41.2, 38.9 (CH₂), 35.6, 35.1, 34.5 (CH₂), 31.0 (CH₂), 30.9 (CH₂), 28.9 (CH₂), 28.2 (CH₂), 27.4 (CH₂), 24.7 (CH₂), 23.5 (C₁₉), 21.9 (CH₂), 18.3 (C₂₁), 12.0 (C₁₈) ppm; **MS (ESI+)** *m/z* : 405.2 [M+H]⁺, 427.3 [M+Na]⁺; **HRMS** (HPLC-ESI) : [M+H]⁺ Calcd: 405.2999; Found: 405.2997.

Methyl 3 α -fluoro-7-oxo-5 β -cholanoate (2.2) + methyl 3 β ,4 β -epoxy-7-oxo-5 β -cholanoate (2.22) + methyl 2 β ,3 β -epoxy-7-oxo-5 β -cholanoate (2.23)



Fluorination: To a solution of alcohol **2.3** (360 mg, 0.89 mmol, 1 equiv) in dry DCM (10 mL) was added DAST (300 μ L, 2.22 mmol, 2.5 equiv) and the solution allowed to stir overnight at RT. Complete consumption of SM at this point and reaction quenched with sat NaHCO₃ (10 mL), layers separated and aqueous washed with further DCM (10 mL). Combined organics washed with water (10 mL) and brine (10 mL), dried (Na₂SO₄) and concentrated to yield 380 mg of a thick yellow oil. Crude ¹H NMR indicated ~20% conversion to desired 3 α -fluoro compound, alkene by-product representing the majority of the crude material. Alkene and 3 α -fluoro compound inseparable *via* chromatography – combined with another batch for epoxidation/separation.

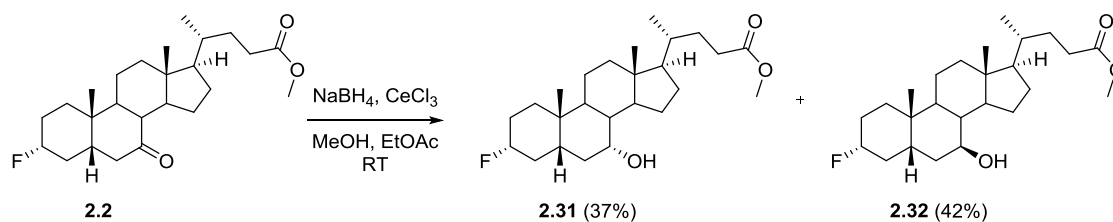
Epoxidation: To a solution of 3 α -fluoro compound and alkene by-products (~400 mg, 1.0 mmol, 1 equiv) in dry DCM (1 mL) was added mCPBA (360 mg, 1.4 mmol, 1.4 equiv) and allowed to stir for 24 hr at RT. Oxidant quenched with sat. Na₂S₂O₃ (30 mL) and allowed to stir for 10 min. The layers were separated and aqueous washed with further DCM (15 mL), combined organics washed with sat. NaHCO₃ (15 mL), water (15 mL) and brine (15 mL), dried (Na₂SO₄) and concentrated to yield 430 mg of a pale yellow gum. Crude was purified *via* flash chromatography (PE/EtOAc : 88:12) to yield 3 α -fluoro **2.2** (66 mg, 0.16 mmol, 8% - gummy solid) and epoxides **2.22** (62 mg, 0.15 mmol, 8% - white solid) and **2.23** (80 mg, 0.20 mmol, 10% - gummy solid).

2.2: Formula: C₂₅H₃₉FO₃; **MW** 406.6; **m.p.** N/A; **R_f** (PE/EtOAc : 75/25) : 0.65; **I.R** 2943 (s), 2874 (m), 1736 (s), 1709 (s), 1435 (w), 1373 (w), 1169 (w), 991 (w); **¹H NMR** (400MHz, CDCl₃): δ 4.45 (dtt, $J=49.2, 10.5, 5.2$ Hz, 1H, H3), 3.65 (s, 3H, CO₂CH₃), 2.84 (ddd, $J=12.5, 5.5, 1.2$ Hz, 1H, H6 β), 2.38 (t, $J=11.6$ Hz, 1H, H8), 2.34 (ddd, $J=15.5, 11.0, 5.0$ Hz, 1H, H23), 2.13-2.27 (m, 2H, H23 + unknown), 2.07 - 1.67 (m, 9H), 1.55 - 1.22 (m, 9H), 1.19 (s, 3H, H19), 1.16 - 1.06 (m, 3H), 0.91 (d, $J=6.4$ Hz, 3H, H21), 0.64 (s, 3H, H18) ppm; **¹³C NMR** (100 MHz, CDCl₃): δ 211.3 (C7), 174.6 (C24), 92.0 (d, $J=173.1$ Hz, C3), 54.7, 51.4 (CO₂CH₃), 49.4, 48.8, 45.4 (d, $J=11.0$ Hz, C5), 45.1 (CH₂), 42.6, 42.6, 38.8 (CH₂), 35.1, 35.1 (d, $J=1.5$ Hz, C10), 34.2 (d, $J=18.3$ Hz, C4), 33.2 (d, $J=11.0$ Hz, C1), 31.0 (C23), 30.9 (CH₂),

28.2 ($\underline{\text{C}}_2$), 27.1 (d, $J=18.3$ Hz, $\underline{\text{C}}_2$), 24.7 ($\underline{\text{C}}_2$), 22.8 (d, $J=2.9$ Hz, $\underline{\text{C}}_{19}$), 21.7 ($\underline{\text{C}}_2$), 18.3 ($\underline{\text{C}}_{21}$), 12.0 ($\underline{\text{C}}_{18}$) ppm; ^{19}F NMR (CDCl_3 , 376MHz): δ -169.27 (d, $J=46.8$ Hz) ppm; $[^1\text{H}]^{19}\text{F}$ NMR (376MHz, CDCl_3): δ -169.27 (s) ppm; **MS (ESI+)** m/z : 407.2 $[\text{M}+\text{H}]^+$, 429.2 $[\text{N}+\text{Na}]^+$; **HRMS (HPLC-ESI)** : $[\text{M}+\text{H}]^+$ Calcd: 407.2956; Found: 407.2962.

For characterisation of **2.22** and **2.23** see **Section 5.4.2**.

Methyl 3 α -fluoro-7 α -hydroxy-5 β -cholanoate (2.31) and methyl 3 α -fluoro-7 β -hydroxy-5 β -cholanoate (2.32)



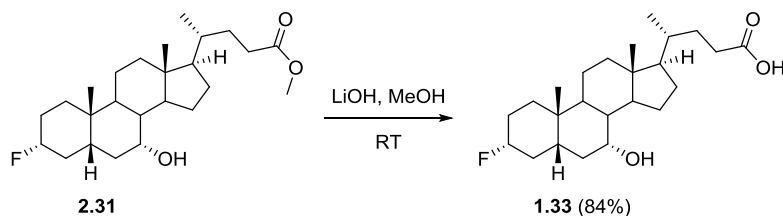
Using general procedure G, ketone **2.2** (60mg, 0.15 mmol, 1 equiv) was reduced and then purified by flash chromatography (PE/EtOAc : 85:15) to yield 7 α -OH **2.31** (23 mg, 0.06 mmol, 37%) and 7 β -OH **2.32** (30 mg, 0.06 mmol, 42%), both as gummy solids.

7 α -OH 2.31: **Formula:** $\text{C}_{25}\text{H}_{41}\text{FO}_3$; **MW** 408.6; **m.p.** N/A; **R_f** (PE/EtOAc : 85/15) : 0.27; **I.R** 3444 (br. w), 3545 (br. w), 2939 (s), 2870 (m), 1740 (s), 1443 (w), 1369 (w), 1169 (w), 976 (w); ^1H NMR (400MHz, CDCl_3): δ 4.36 (dtt, $J=49.2, 10.5, 5.2$ Hz, 1H, $\underline{\text{H}}_3$), 3.87 (q, $J=1.8$ Hz, 1H, $\underline{\text{C}}_7$), 3.67 (s, 3H, CO_2CH_3), 2.48-2.31 (m, 2H, $\underline{\text{C}}_4\alpha + \underline{\text{C}}_{23}$), 2.23 (ddd, $J=15.5, 9.5, 6.5$ Hz, 1H, $\underline{\text{C}}_{23}'$), 2.10 - 1.05 (m, 27H), 0.93 (d, $J=6.4$ Hz, 3H, $\underline{\text{H}}_{21}$), 0.91 (s, 3H, $\underline{\text{H}}_{19}$), 0.67 (s, 3H, $\underline{\text{H}}_{18}$) ppm; ^{13}C NMR (100 MHz, CDCl_3): δ 174.7 ($\underline{\text{C}}_{24}$), 93.4 (d, $J=170.9$ Hz, $\underline{\text{C}}_3$), 68.3 ($\underline{\text{C}}_7$), 55.7, 51.5, 50.4, 42.7, 40.9 (d, $J=11.0$ Hz), 39.5 ($\underline{\text{C}}_2$), 39.4, 36.4 (d, $J=17.6$ Hz, $\underline{\text{C}}_4$), 35.3, 35.1, 34.4 ($\underline{\text{C}}_2$), 34.4 (d, $J=5.5$ Hz, $\underline{\text{C}}_2$), 32.8, 31.0 ($\underline{\text{C}}_2$), 31.0 ($\underline{\text{C}}_2$), 28.1 ($\underline{\text{C}}_2$), 27.8 (d, $J=17.6$ Hz, $\underline{\text{C}}_2$), 23.7 ($\underline{\text{C}}_2$), 22.6 (d, $J=2.9$ Hz, $\underline{\text{C}}_{19}$), 20.6 ($\underline{\text{C}}_2$), 18.2 ($\underline{\text{C}}_{21}$), 11.8 ($\underline{\text{C}}_{18}$) ppm; ^{19}F NMR (CDCl_3 , 376MHz): δ -167.43 (d, $J=50.3$ Hz) ppm; $[^1\text{H}]^{19}\text{F}$ NMR (376MHz, CDCl_3): δ -167.43 (s) ppm; **MS (ESI+)** m/z : 371.2 $[\text{M}+\text{H}, -\text{H}_2\text{O}, -\text{HF}]^+$, 391.2 $[\text{M}+\text{H}, -\text{H}_2\text{O}]^+$; **HRMS (HPLC-ESI)** : $[\text{M}+\text{Na}]^+$ Calcd: 431.2932; Found: 431.2938.

7 β -OH 2.32: **Formula:** $\text{C}_{25}\text{H}_{41}\text{FO}_3$; **MW** 408.6; **m.p.** N/A; **R_f** (PE/EtOAc : 85/15) : 0.13; **I.R** 3749 (br. w), 2940 (s), 2866 (m), 1740 (s), 1450 (m), 1366 (m), 1169 (w); ^1H NMR (400MHz, CDCl_3): δ 4.46 (dtt, $J=49.5, 10.7, 5.1$ Hz, 1H, $\underline{\text{H}}_3$), 3.67 (s, 3H, CO_2CH_3), 3.60 (ddd, $J=11.1, 8.5, 5.4$ Hz, 1H, $\underline{\text{H}}_7$), 2.36 (ddd, $J=15.5, 11.0, 5.0$ Hz, 1H, $\underline{\text{H}}_{23}$), 2.23 (ddd, $J=15.5, 9.5, 6.5$ Hz, 1H, $\underline{\text{H}}_{23}'$), 2.09 - 0.98 (m, 30H), 0.95 (s, 3H, $\underline{\text{H}}_{19}$), 0.93 (d, $J=6.5$ Hz, 3H, $\underline{\text{H}}_{21}$), 0.68 (s, 3H, $\underline{\text{H}}_{18}$) ppm; ^{13}C NMR (100 MHz, CDCl_3): δ 174.7 ($\underline{\text{C}}_{24}$), 92.9 (d, $J=172.4$ Hz, $\underline{\text{C}}_3$), 71.2 ($\underline{\text{C}}_7$), 55.6, 54.8, 51.5, 43.7, 43.7, 41.9 (d, $J=10.3$ Hz, $\underline{\text{C}}_5$), 40.0 ($\underline{\text{C}}_2$), 39.1, 36.6 ($\underline{\text{C}}_2$), 35.2, 34.2 (d, $J=17.6$ Hz, $\underline{\text{C}}_4$), 34.1, 34.0 (d, $J=11.0$ Hz, $\underline{\text{C}}_1$), 31.0 ($\underline{\text{C}}_2$), 31.0

(CH₂), 28.6 (CH₂), 27.6 (d, *J*=18.3 Hz, C₂), 26.8 (CH₂), 23.2 (d, *J*=2.9 Hz, C₁₉), 21.2 (CH₂), 18.4 (C₂₁), 12.1 (C₁₈) ppm; ¹⁹F NMR (CDCl₃, 376MHz): δ -167.82 (d, *J*=50.3 Hz) ppm; [¹H]¹⁹F NMR (376MHz, CDCl₃): δ -167.82 (s) ppm; **MS (ESI+)** *m/z* : 371.2 [M+H, -H₂O, -HF]⁺, 391.2 [M+H, -H₂O]⁺; **HRMS** (HPLC-ESI) : [M+NH₄]⁺ Calcd: 426.3378; Found: 426.3374.

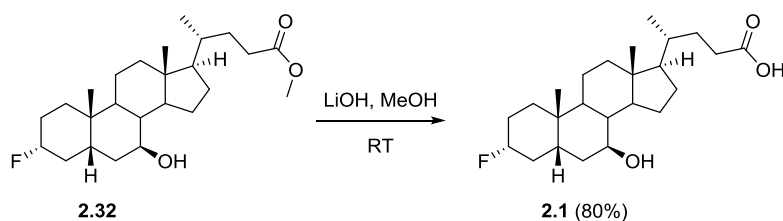
3α-fluoro-7α-hydroxy-5β-cholanic acid (**1.33**)



Using general procedure B, methyl ester **2.31** (23 mg, 0.06 mmol, 1 equiv) was saponified to yield **1.33** (20 mg, 0.05 mmol, 84%) as a thick colourless gum.

1.33: Formula: C₂₄H₃₉FO₃; **MW** 394.6; [**α**]_D +4.6 (c 0.5, CHCl₃, 21 °C); **m.p.** N/A; **R_f** (Petrol ether/EA : 70/30) : 0.15; **I.R** 2935 (s), 2870 (m), 1709 (s), 1261 (w), 1076 (w), 972 (w); ¹H NMR (400MHz, CDCl₃): δ 4.37 (dtt, *J*=49.2, 10.5, 5.2 Hz, 1H, H₃), 3.88 (q, *J*=2.7 Hz, 1H, H₇), 2.51-2.35 (m, 2H, H_{4α} + H₂₃), 2.26 (ddd, *J*=15.5, 9.6, 6.4 Hz, 1H, H_{23'}), 2.07 - 1.05 (m, 26H), 0.95 (d, *J*=6.5 Hz, 3H, H₂₁), 0.91 (s, 3H, H₁₉), 0.67 (s, 3H, H₁₈) ppm; ¹³C NMR (100 MHz, CDCl₃): δ 180.0 (C₂₄), 93.4 (d, *J*=171.7 Hz, C₃), 68.4 (C₇), 55.8, 50.4, 42.7, 40.9 (d, *J*=11.0 Hz, C₅), 39.5 (CH₂), 39.4, 36.4 (d, *J*=17.6 Hz, C₄), 35.3, 35.1 (d, *J*=1.5 Hz, C₁₀), 34.5 (CH₂), 34.4 (CH₂), 32.8, 31.0 (C₂₃), 30.8 (CH₂), 28.1 (CH₂), 27.9 (d, *J*=17.6 Hz, C₂), 23.7 (CH₂), 22.6 (d, *J*=2.9 Hz, C₁₉), 20.6 (CH₂), 18.2 (C₂₁), 11.8 (C₁₈) ppm; ¹⁹F NMR (376MHz, CDCl₃): δ -167.40 (d, *J*=50.3 Hz) ppm; [¹H]¹⁹F NMR (376MHz, CDCl₃): δ -167.41 (s) ppm; **MS (ESI+)** *m/z* : 357.2 [M+H, -H₂O, -HF]⁺; **HRMS** (HPLC-ESI) : [M+NH₄]⁺ Calcd: 412.3221; Found: 412.3222.

3α-fluoro-7β-hydroxy-5β-cholanic acid (**2.1**)



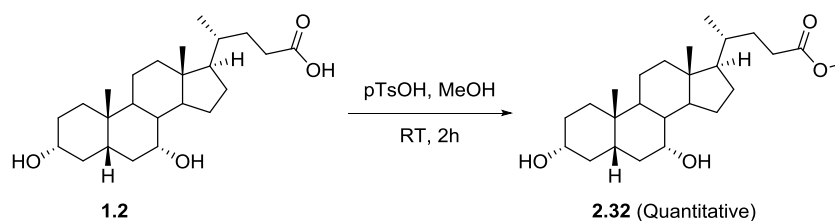
Using general procedure B, methyl ester **2.32** (30 mg, 0.07 mmol, 1 equiv) was saponified to yield **2.1** (22 mg, 0.06 mmol, 80%) as a white solid.

2.1: Formula: C₂₄H₃₉FO₃; **MW** 394.6; [**α**]_D +11.0 (c 0.5, CHCl₃, 21 °C); **m.p.** 162–163 °C; **R_f** (PE/EtOAc : 70/30) : 0.22; **I.R** 2928 (s), 2854 (m), 1736 (s), 1716 (s), 1454 (w), 1365 (m), 1230 (m),

1215 (m), 1018 (m); $^1\text{H NMR}$ (400MHz, CDCl_3): δ 4.47 (dtt, $J=49.2, 10.5, 5.2$, Hz, 1H, H_3), 3.67 - 3.56 (m, 1H, H_7), 2.41 (ddd, $J=15.5, 11.0, 5.0$ Hz, 1H, H_{23}), 2.27 (ddd, $J=15.5, 9.5, 6.5$ Hz, 1H, H_{23}'), 2.07 - 0.98 (m, 34H), 0.97 - 0.93 (m, 6H, $\text{H}_{19} + \text{H}_{21}$), 0.69 (s, 3H, H_{18}) ppm; $^{13}\text{C NMR}$ (100 MHz, CDCl_3): δ 179.5 (C_{24}), 92.9 (d, $J=171.7$ Hz, C_3), 71.3 (C_7), 55.6, 54.9, 43.8, 43.7, 41.9 (d, $J=10.3$ Hz, C_5), 40.0 (CH_2), 39.2, 36.6 (CH_2), 35.2, 34.2 (d, $J=17.6$ Hz, C_4), 34.1, 34.0 (d, $J=9.8$ Hz, C_1), 30.9 (CH_2), 30.8 (C_{23}), 28.6 (CH_2), 27.6 (d, $J=18.3$ Hz, C_2), 26.8 (CH_2), 23.2 (d, $J=2.9$ Hz, C_{19}), 21.2 (CH_2), 18.3 (C_{21}), 12.1 (C_{18}) ppm; $^{19}\text{F NMR}$ (376MHz, CDCl_3): δ -167.82 (d, $J=50.3$ Hz) ppm; $[\text{H}]^{19}\text{F NMR}$ (376MHz, CDCl_3): δ -167.82 (s) ppm; **MS (ESI+)** m/z : 357.2 $[\text{M}+\text{H}, -\text{H}_2\text{O}, -\text{HF}]^+$; **HRMS** (HPLC-ESI) : $[\text{M}+\text{NH}_4]^+$ Calcd: 412.3221; Found: 412.3216.

5.3.3 Synthesis of 3-deoxy-3,3-difluoro analogues

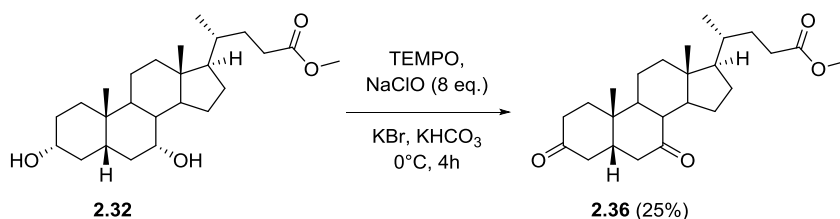
Methyl 3 α ,7 α -dihydroxy-5 β -cholanoate (2.32)



The method of Pellicari was used^[71] CDCA **1.2** (25.0 g, 64 mmol, 1 equiv) was dissolved in HPLC grade MeOH (500 mL) before adding *p*-toluene sulfonic acid (1.21 g, 6.4 mmol, 0.1 equiv) and sonicating at 30 °C for 2 h. Once deemed complete by TLC analysis the solvent was removed *in vacuo*, before dissolving the residue in EtOAc (400 mL), washing the organics with sat. NaHCO_3 (2 \times 150 mL), water (250 mL) and brine (250 mL). The organic phase was then dried (Na_2SO_4) and concentrated to yield **2.32** as a white/pale yellow solid (26.0 g, quantitative). (**General procedure A**).

2.32: Formula: $\text{C}_{25}\text{H}_{42}\text{O}_4$; **MW** 406.6; **m.p.** 64 – 68 °C (lit. 66-68 °C); **R_f** (pet ether/EA : 60:40) 0.09; $^1\text{H NMR}$ (400MHz, CDCl_3): δ 3.84 (q, $J=2.4$ Hz, 1H, H_7), 3.66 (s, 3H, CO_2CH_3), 3.44 (tt, $J=10.9, 4.5$ Hz, 1H, H_3), 2.34 (ddd, $J=15.5, 11.0, 5.0$ Hz, 1H, H_{23}), 2.28-2.15 (m, 2H, $\text{H}_{23}' + \text{unknown}$), 2.12-0.97 (m, 26H), 0.93 (d, $J=6.2$ Hz, 3H, H_{21}), 0.90 (s, 3H, H_{19}), 0.65 (s, 3H, H_{18}) ppm; $^{13}\text{C NMR}$ (100 MHz, CDCl_3): δ 174.7 (C_{24}), 71.9 (C_3), 68.4 (C_7), 55.8, 51.4 (CO_2CH_3), 50.4, 42.6, 41.5, 39.8 (CH_2), 39.6 (CH_2), 39.4, 35.3 (CH_2 , only visible in DEPT135), 35.3, 35.0, 34.6 (CH_2), 32.8, 31.0 (C_{22} or C_{23}), 31.0 (C_{22} or C_{23}), 30.6 (CH_2), 28.1 (CH_2), 23.6 (CH_2), 22.7 (C_{19}), 20.6 (CH_2), 18.2 (C_{21}), 11.7 (C_{18}) ppm; **MS (ESI+)** m/z : 429.1 $[\text{M}+\text{Na}]^+$.

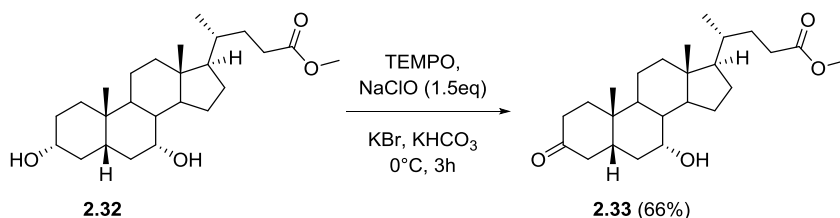
Data consistent with literature.^[68-69]

Methyl 3,7-dioxo-5 β -cholanoate (2.36)

The method of Burns was used.^[84] To a solution of **2.32** (1.0 g, 2.46 mmol, 1 equiv) in water (1.5 mL) and *t*-butanol (5 mL), was added KBr (0.59 g, 4.92 mmol, 2 equiv), K₂CO₃ (2.46 g, 24.6 mmol, 10 equiv) and *N*-oxy-2,2,6,6-tetramethylpiperidine (0.42 g, 2.71 mmol, 1.1 equiv). The solution was cooled to 0 °C, before the addition of NaClO solution (5%, 29 mL, 19.7 mmol, 8 equiv) portion wise over the course of 4 h. The reaction was quenched with slow addition of a solution of Na₂S₂O₃ (5.0 g, 20.1 mmol) dissolved in water (40 mL) before extracting the aqueous with EtOAc (4×75 mL). The combined organic phases were washed with water (100 mL) and brine (100 mL), before drying (Na₂SO₄) and the solvent removed *in vacuo* to yield a crude material (1.05 g). The crude was separated through flash chromatography (PE/EtOAc : 75:25) to yield **2.36** as a white solid (0.24 g, 0.61 mmol, 25%).

2.36: Formula: C₂₅H₃₈O₄; **MW** 402.6; **m.p.** 156 - 158°C (lit. 154 - 155 °C); **R_f** (PE/EtOAc : 75:25) 0.45; **¹H NMR** (400MHz, CDCl₃): δ 3.64 (s, 3H, CO₂CH₃), 2.86 (dd, *J*=12.8, 5.4 Hz, 1H, H_{6 β}), 2.48 (t, *J*=11.4 Hz, 1H, H_{4 α}), 2.40 -1.34 (m, 20H), 1.29 (s, 3H, H₁₉), 1.26 - 0.94 (m, 4H), 0.91 (d, *J*=6.4 Hz, 3H, H₂₁), 0.67 (s, 3H, H₁₈) ppm; **¹³C NMR** (100 MHz, CDCl₃): δ 211.1 (C=O), 210.2 (C=O), 174.6 (C₂₄), 54.8, 51.5, 49.6, 48.9, 47.8, 45.0 (CH₂), 42.9 (CH₂), 42.8, 42.7, 38.9 (CH₂), 36.8 (CH₂), 35.4, 35.4 (CH₂), 35.2, 31.0 (CH₂), 31.0 (CH₂), 28.2 (CH₂), 24.8 (CH₂), 22.4 (C₁₉), 22.1 (CH₂), 18.4 (C₂₁), 12.1 (C₁₈) ppm.

Data consistent with literature^[161]

Methyl 7 α -hydroxy-3-oxo-5 β -cholanoate (2.33)

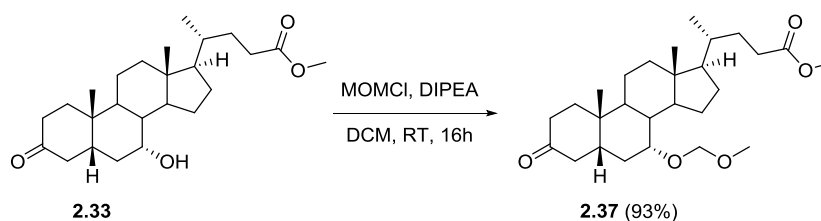
To a solution of **2.32** (10.0 g, 24.6 mmol, 1 equiv) in water (25 mL) and *t*-butanol (100 mL) was added KBr (5.9 g, 49.0 mmol, 2 equiv), KHCO₃ (24.6 g, 246 mmol, 10 equiv) and TEMPO (5.0 g, 32.0 mmol, 1.3 equiv). The solution was cooled to 0 °C before adding ≈11% NaClO solution (54.2 mL,

73.2 mmol, 3.0 equiv) portion wise over the course of 6 h. The reaction was quenched with slow addition of sodium thiosulfate solution (300 mL, 1.2 M, 350 mmol). The aqueous was extracted with EtOAc (2×300 mL), which were combined and washed with brine (300 mL) and water (300 mL) before drying (Na_2SO_4) and removing the solvent *in vacuo*. The resulting bright red thick oily crude (15 g) was purified using flash chromatography (PE/EtOAc : 80:20→65:35) to yield a white solid **2.33** (6.5 g, 16.0 mmol, 66%).

2.33: Formula: $\text{C}_{25}\text{H}_{40}\text{O}_4$; **MW** 404.6; **m.p.** 126 - 128°C (lit 128 - 129 °C); **R_f** (PE/EtOAc : 70:30) 0.24; **¹H NMR** (400MHz, CDCl_3): δ 3.93 (br s., 1H, H7), 3.67 (s, 3H, CO_2CH_3), 3.40 (t, $J=14.4$ Hz, 1H, H4 $_{\alpha}$), 2.46 - 1.10 (m, 30H), 1.01 (s, 3H, H19), 0.95 (d, $J=6.6$ Hz, 3H, H21), 0.71 (s, 3H, H18) ppm; **¹³C NMR** (100 MHz, CDCl_3): δ 213.1 (C3), 174.7 (C24), 68.4 (C7), 55.8, 51.5 (CO_2CH_3), 50.3, 45.6 (CH2), 43.2, 42.7, 39.5 (CH2), 39.4, 37.0 (CH2), 36.8 (CH2), 35.3, 35.3, 33.9 (CH2), 33.3, 31.0 (CH2), 30.9 (CH2), 28.1 (CH2), 23.7 (CH2), 21.9 (C19), 21.0 (CH2), 18.3 (C21), 11.8 (C18) ppm; **MS (ESI+)** m/z : 422.1 $[\text{M}+\text{NH}_4]^+$, 427.1 $[\text{M}+\text{Na}]^+$.

Data consistent with literature^[68-69]

Methyl 7 α -methoxymethoxyl-3-oxo-5 β -cholanoate (1.4.7)



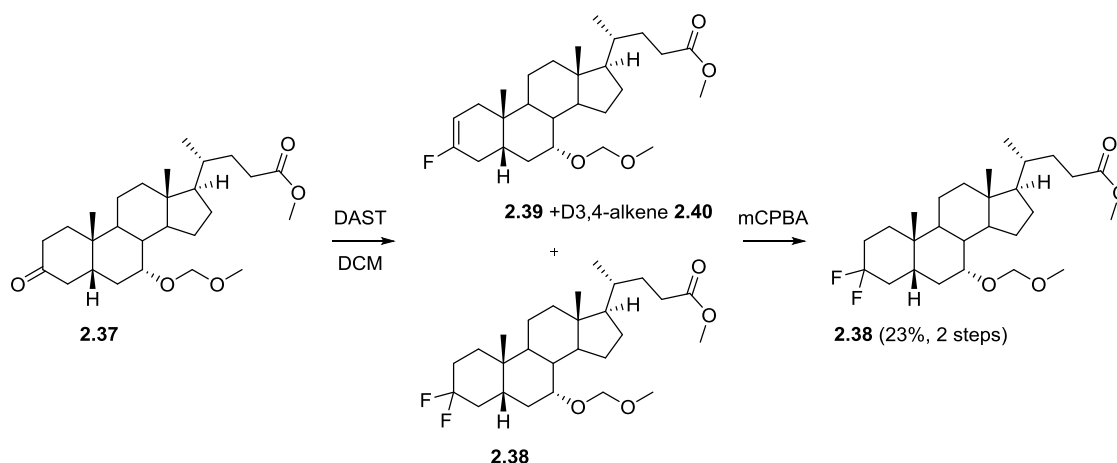
To a solution of **2.33** (3.0 g, 7.41 mmol, 1 equiv) in dry DCM (50 mL) was added DIPEA (3.83 mL, 22.2 mmol, 3 equiv) and MOM-Cl (2.82 mL, 37.1 mmol, 5 equiv) at 0 °C. The reaction mixture was warmed to room temperature before allowing to stir overnight. Once complete, the reaction mixture was quenched with water (25 mL) and methanol (25 mL) before separating the layers and extracting the aqueous with EtOAc (4×75 mL) and washing the combined organics with brine (2×150 mL). The organic phase was then dried (Na_2SO_4) and concentrated *in vacuo* to yield 3.8 g of crude material which was purified by flash chromatography (PE/EtOAc : 75:25) yielding a white solid **2.37** (3.10 g, 6.9 mmol, 93%). (**General procedure C**).

2.37: Formula: $\text{C}_{27}\text{H}_{44}\text{O}_5$; **MW** 448.6; **m.p.** 106 - 108°C (lit. 101 °C); **R_f** (PE/EtOAc : 80:20) 0.27; **¹H NMR** (400MHz, CDCl_3): δ 4.68 (d, $J=6.8$ Hz, 1H, O-CHH-O), 4.55 (d, $J=6.8$ Hz, 1H, O-CHH-O), 3.72 - 3.62 (m, 4H, CO_2CH_3 with H7), 3.43 - 3.28 (m, 4H, OCH_3 with H4 $_{\alpha}$), 2.49 - 1.05 (m, 27H), 1.03 (s, 3H, H19), 0.94 (d, $J=6.4$ Hz, 3H, H21), 0.69 (s, 3H, H18) ppm; **¹³C NMR** (100 MHz, CDCl_3): δ 213.2 (C3), 174.7 (C24), 96.0 (O-CH2-O), 75.0 (C7), 56.3, 55.7, 51.5, 49.8, 45.2 (CH2), 43.2, 42.6, 39.4, 39.3 (CH2), 36.9 (CH2), 36.8 (CH2), 35.4, 35.2, 33.7, 31.0 (CH2), 31.0 (CH2), 30.4 (CH2), 28.1 (CH2), 23.7

($\underline{\text{C}}_2$), 21.9 ($\underline{\text{C}}_{19}$), 21.0 ($\underline{\text{C}}_2$), 18.3 ($\underline{\text{C}}_{21}$), 11.8 ($\underline{\text{C}}_{18}$) ppm; **MS (ESI+)** m/z : 449.3 [$\text{M}+\text{H}$] $^+$, 471.1 [$\text{M}+\text{Na}$] $^+$.

Data consistent with literature^[69]

Methyl 3,3-difluoro-7 α -methoxymethoxy-5 β -cholanoate (**2.38**)



Fluorination: To a solution of ketone **2.37** (500 mg, 1.11 mmol, 1 equiv) in dry DCM (15 mL) at 0 °C was added DAST (450 μL , 3.34 mmol, 3 equiv) and HF.pyridine (70% HF, 2 drops, c.a. 0.05 equiv). The reaction was warmed to reflux and deemed complete after O/N heating. The RM was diluted with DCM (10 mL) and quenched with SLOW addition of saturated NaHCO_3 solution (10 mL). The layers were separated, aqueous washed with further DCM (30 mL), before the combined organics were washed with water (50 mL) and brine (50 mL), dried (Na_2SO_4) and concentrated to yield 520 mg of a bright yellow-orange thick oil. The crude was purified by flash chromatography (PE/EtOAc : 90:10 \rightarrow 70:30) to yield a pale solid (375 mg) containing ~70% of desired di-fluoro compound **2.38** along with ~30% of fluoroalkene(s) **2.39/2.40** (elimination products). Further purification attempted by flash chromatography (PE/EtOAc : 90:10) although this was unsuccessful in removing fluoroalkene impurities.

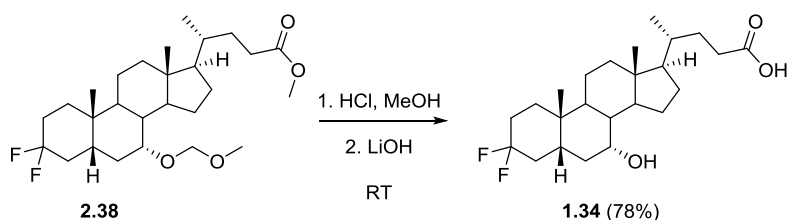
$^1\text{H NMR}$ (400MHz, CDCl_3): δ 4.96 (d, $J=17.7$ Hz, 0.3H, $\underline{\text{H}}\text{C}=\underline{\text{C}}\text{F}$), 4.70 (d, $J=7.0$ Hz, 0.3H, $\text{O}-\underline{\text{C}}\text{H}\underline{\text{H}}-\text{O}$), 4.68 (d, $J=7.0$ Hz, 0.7H, $\text{O}-\underline{\text{C}}\text{H}\underline{\text{H}}-\text{O}$), 4.55 (d, $J=7.0$ Hz, 0.7H, $\text{O}-\underline{\text{C}}\text{H}\underline{\text{H}}-\text{O}$), 4.50 (d, $J=7.0$ Hz, 0.3H, $\text{O}-\underline{\text{C}}\text{H}\underline{\text{H}}-\text{O}$), 3.67 - 3.65 (m, 3H, $\text{CO}_2\underline{\text{C}}\underline{\text{H}}_3$), 3.63 - 3.59 (m, 1H), 3.38 (s, 3H, $\text{O}\underline{\text{C}}\underline{\text{H}}_3$), 2.70 (dtd, $J=37.2, 13.7, 4.9$ Hz, 1H, $\underline{\text{H}}_{4\alpha}$), 2.42 - 2.29 (m, 1H), 2.28 - 2.11 (m, 2H), 2.10 - 0.99 (m, 25H), 0.98 - 0.95 (m, 3H, $\underline{\text{H}}_{19}$), 0.92 (d, $J=6.5$ Hz, 3H, $\underline{\text{H}}_{21}$), 0.65 (s, 3H, $\underline{\text{H}}_{18}$) ppm; $^{13}\text{C NMR}$ (100 MHz, CDCl_3): δ 174.7 ($\underline{\text{C}}_{24}$), 174.6 ($\underline{\text{C}}_{24}$), 156.6 (d, $J=252.4$ Hz, $\text{C}=\underline{\text{C}}-\text{F}$), 124.2 (dd, $J=241.4, 239.2$ Hz, $\underline{\text{C}}\text{F}_2$), 108.1 (d, $J=13.9$ Hz, $\underline{\text{C}}=\text{C}-\text{F}$) 96.0 ($\text{O}-\underline{\text{C}}\text{H}_2-\text{O}$), 95.2 ($\text{O}-\underline{\text{C}}\text{H}_2-\text{O}$), 75.0 ($\underline{\text{C}}_7$), 73.5 ($\underline{\text{C}}_7$), 56.3, 56.2, 56.2, 55.7, 55.6, 51.4, 49.8, 42.5, 42.5, 39.9, 39.5, 39.4, 36.8 (dd, $J=24.2, 21.3$ Hz, $\underline{\text{C}}\text{H}_2\underline{\text{C}}\text{F}_2$), 35.4, 35.4, 35.4, 35.4, 34.9, 34.2, 33.9, 32.9, 32.6, 32.4, 31.0, 30.7, 30.1, 29.3 (dd, $J=25.7, 22.0$ Hz, $\underline{\text{C}}\text{H}_2\underline{\text{C}}\text{F}_2$), 28.1, 23.7, 23.6, 22.5, 22.2 (d, $J=2.9$ Hz, $\underline{\text{C}}_{19}$), 21.5 (d, $J=2.9$ Hz, $\underline{\text{C}}_{19}$), 21.0, 20.8, 18.3 ($\underline{\text{C}}_{21}$), 11.7 ($\underline{\text{C}}_{18}$), 11.7 ($\underline{\text{C}}_{18}$) ppm;

^{19}F NMR (CDCl_3 , 376MHz): δ -88.98 (d, $J=232.3$ Hz, 0.7F, $\underline{\text{F}}_{3\alpha}$), -102.62 (dddt, $J=230.6$, 36.4, 32.9, 12.1 Hz, 0.7F, $\underline{\text{F}}_{3\beta}$), -107.44 - -106.98 (m, 0.3F, $\text{HC}=\underline{\text{C}}_{\underline{\text{F}}}$) ppm; [^1H] ^{19}F NMR (CDCl_3 , 376MHz): δ -88.98 (d, $J=230.6$ Hz, 0.7F, $\underline{\text{F}}_{3\alpha}$), -102.62 (d, $J=230.6$ Hz, 0.7F, $\underline{\text{F}}_{3\beta}$), -107.22 (s, 0.3F, $\text{HC}=\underline{\text{C}}_{\underline{\text{F}}}$) ppm.

Epoxidation: To a solution of difluoro **2.38** and fluoroalkenes **2.39/2.40** (combined 300 mg, \sim 0.70 mmol, 1 equiv) in DCM (20 mL) was added *m*CPBA (46 mg, 0.27 mmol, 0.4 equiv). The solution was stirred overnight at RT at which point crude ^{19}F NMR showed complete consumption of the undesired fluoroalkene. Reaction quenched with sat. NaHCO_3 (15 mL), layers separated and organics washed with further NaHCO_3 (10 mL), water (10 mL) and brine (10 mL), dried (Na_2SO_4) and concentrated to yield 260 mg of a pale yellow solid. Crude combined with a previous batch and purified *via* flash chromatography (PE/EtOAc : 94:6 \rightarrow 90:10) to yield clean difluorinated bile acid **2.38** as a white solid (120 mg, 0.25 mmol, 23% two steps).

2.38: Formula: $\text{C}_{27}\text{H}_{44}\text{F}_2\text{O}_4$; **MW** 470.64; **m.p.** 110 - 112 $^\circ\text{C}$; **R_f** (PE/EtOAc : 80/20) : 0.64; **I.R** 2935 (m), 2874 (w), 1734 (s), 1369 (m), 1149 (m), 1095 (s), 1034 (s); ^1H NMR (400MHz, CDCl_3): δ 4.68 (d, $J=6.8$ Hz, 1H, O- $\underline{\text{C}}\text{H}\underline{\text{H}}$ -O), 4.55 (d, $J=7.0$ Hz, 1H, O- $\underline{\text{C}}\text{H}\underline{\text{H}}$ -O), 3.66 (s, 3H, $\text{CO}_2\underline{\text{C}}\text{H}_3$), 3.62 (d, $J=2.4$ Hz, 1H, $\underline{\text{H}}_7$), 3.38 (s, 3H, $\text{O}\underline{\text{C}}\text{H}_3$), 2.70 (dtd, $J=37.2$, 13.7, 4.9 Hz, 1H, $\underline{\text{H}}_4\alpha$), 2.35 (ddd, $J=15.5$, 10.6, 5.3 Hz, 1H, $\underline{\text{H}}_{23}$), 2.22 (ddd, $J=15.6$, 9.4, 6.5 Hz, 1H, $\underline{\text{H}}_{23}'$), 1.97 (dt, $J=12.3$, 3.1 Hz, 1H), 1.93 - 0.99 (m, 24H), 0.96 (s, 3H, $\underline{\text{H}}_{19}$), 0.92 (d, $J=6.5$ Hz, 3H, $\underline{\text{H}}_{21}$), 0.65 (s, 3H, $\underline{\text{H}}_{18}$) ppm; ^{13}C NMR (100 MHz CDCl_3): δ 174.6 ($\underline{\text{C}}_{24}$), 124.2 (dd, $J=241.4$, 239.2 Hz, $\underline{\text{C}}_3$), 95.9 (O- $\underline{\text{C}}\text{H}_2$ -O), 74.9 ($\underline{\text{C}}_7$), 56.3 ($\text{O}\underline{\text{C}}\text{H}_3$), 55.6, 51.4 ($\text{CO}_2\underline{\text{C}}\text{H}_3$), 49.8, 42.5, 39.4 (d, $J=9.5$ Hz), 39.3, 39.2 ($\underline{\text{C}}\text{H}_2$), 36.8 (dd, $J=24.2$, 21.3 Hz, $\underline{\text{C}}_4$), 35.3, 34.9 (d, $J=1.5$ Hz, $\underline{\text{C}}_{10}$), 32.9 (d, $J=9.5$ Hz, $\underline{\text{C}}\text{H}_2$), 32.4, 31.0 ($\underline{\text{C}}\text{H}_2$), 31.0 ($\underline{\text{C}}\text{H}_2$), 30.0 ($\underline{\text{C}}\text{H}_2$), 29.2 (dd, $J=24.9$, 22.0 Hz, $\underline{\text{C}}_2$), 28.1 ($\underline{\text{C}}\text{H}_2$), 23.6, ($\underline{\text{C}}\text{H}_2$) 22.2 (d, $J=2.9$ Hz, $\underline{\text{C}}_{19}$), 20.8 ($\underline{\text{C}}\text{H}_2$), 18.3 ($\underline{\text{C}}_{21}$), 11.7 ($\underline{\text{C}}_{18}$) ppm; ^{19}F NMR (376MHz, CDCl_3): δ -88.88 (d, $J=230.6$ Hz, $\underline{\text{F}}_{3\alpha}$), -102.52 (dddt, $J=230.6$, 36.4, 32.9, 12.1 Hz, 1F, $\underline{\text{F}}_{3\beta}$) ppm; [^1H] ^{19}F NMR (376MHz, CDCl_3): δ -88.99 (d, $J=232.4$ Hz, 1F, $\underline{\text{F}}_{3\alpha}$), -102.62 (d, $J=232.4$ Hz, 1F, $\underline{\text{F}}_{3\beta}$) ppm; **MS (ESI+)** *m/z* : 488.2 [$\text{M}+\text{NH}_4$] $^+$, 493.2 [$\text{M}+\text{Na}$] $^+$; **HRMS (HPLC-ESI)** : [$\text{M}+\text{Na}$] $^+$ Calcd: 493.3095; Found: 493.3100.

3,3-difluoro-7 α -hydroxy-5 β -cholanolic acid (**1.34**)



Using general procedure D, followed by procedure B, 3,3-difluoro analogue **2.38** (110 mg, 0.23 mmol, 1 equiv) in MeOH (5 mL) was deprotected to yield **1.34** (74 mg, 0.18 mmol, 78%) of a colourless gummy solid.

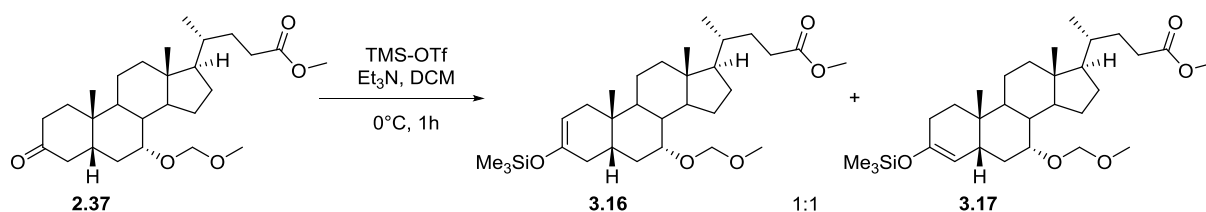
1.34: Formula: $C_{24}H_{38}F_2O_3$; **MW** 412.6; $[\alpha]_D^{25}$ +36.8 (c 0.5, $CHCl_3$, 21 °C); **m.p.** N/A; **R_f** (Petrol ether/EA : 75/25) : 0.14; **I.R** 2935 (m), 2874 (w), 1709 (s), 1369 (w), 1265 (w), 1095 (s), 923 (m), 737 (m); **¹H NMR** (400MHz, $CDCl_3$): δ 3.88 (q, $J=2.6$ Hz, 1H, H7), 2.72 (dtd, $J=37.2, 13.7, 4.9$ Hz, 1H, H4 α), 2.39 (ddd, $J=15.5, 11.0, 5.0$ Hz, 1H, H23), 2.25 (ddd, $J=15.8, 9.6, 6.4$ Hz, 1H, H23'), 2.02 - 1.03 (m, 26H), 0.95 (s, 3H, H19), 0.94 (d, $J=6.6$ Hz, 3H, H21), 0.67 (s, 3H, H18) ppm; **¹³C NMR** (100 MHz $CDCl_3$): δ 180.2 (C24), 124.1 (dd, $J=241.7, 238.8$ Hz, C3), 68.4 (C7), 55.8, 50.3, 42.7, 39.5 (CH₂), 39.3, 39.2, 37.2 (dd, $J=20.9, 23.8$ Hz, C4), 35.3, 35.0, 33.4 (CH₂), 32.9 (d, $J=9.5$ Hz, C1), 32.1, 31.0 (C23), 30.7 (CH₂), 29.3 (dd, $J=22.0, 24.9$ Hz, C2), 28.1 (CH₂), 23.6 (CH₂), 22.2 (d, $J=2.9$ Hz, C19), 20.8 (CH₂), 18.2 (C21), 11.7 (C18) ppm; **¹⁹F NMR** ($CDCl_3$, 376MHz): δ -89.06 (d, $J=232.3$ Hz, F3 α), -102.61 (dddt, $J=230.6, 36.4, 32.9, 12.1$ Hz, F3 β) ppm; **[¹H]¹⁹F NMR** (376MHz, $CDCl_3$): δ -89.06 (d, $J=232.3$ Hz, F3 α), -102.61 (d, $J=232.4$ Hz, F3 β) ppm; **MS (ESI+)** m/z : 355.2 [M+H, -H₂O, -HF]⁺, 375.2 [M+H, -H₂O]⁺; **HRMS** (HPLC-ESI) : [M+NH₄]⁺ Calcd: 430.3127; Found: 430.3133.

5.4 Synthesis of 2- and 4-fluorinated analogues

The synthesis and characterisation of the following compounds is presented in the order of reactions discussed in **Chapter 3**.

5.4.1 Synthesis of 2 β - and 4 β -fluorinated analogues

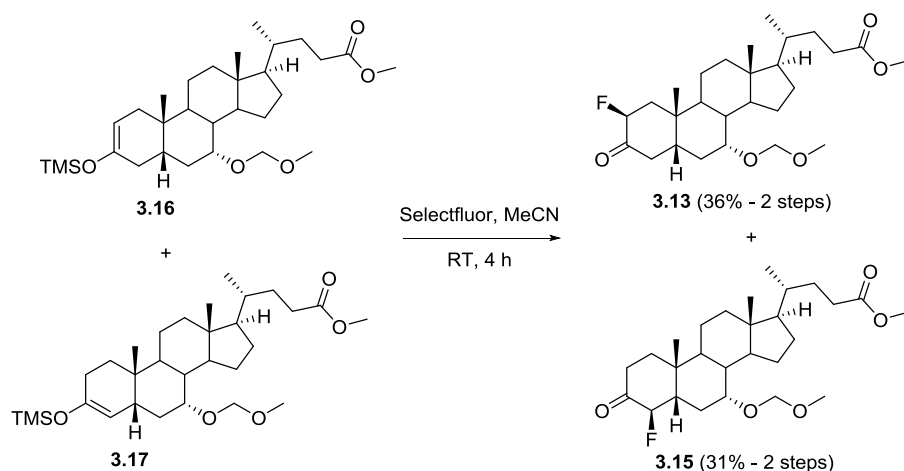
Methyl 7 α -methoxymethoxyl-3-trimethylsilyloxy-5 β -chol-2-eneoate (3.16) and methyl 7 α -methoxymethoxyl-3-trimethylsilyloxy-5 β -chol-3-eneoate (3.17)



Following method of Barlow *et al.*^[100] To a solution of **2.37** (1.0 g, 2.23 mmol, 1 equiv) in dry DCM (20 mL) at 0°C was added Et₃N (0.62 mL, 4.46 mmol, 2 equiv) and trimethylsilyl triflate (0.44 mL, 2.45 mmol, 1.1 equiv). The reaction mixture was allowed to stir for 1 hr before diluting with further DCM (150 mL) and quenching with sat. NaHCO₃ (100 mL). The layers were separated and the aqueous was extracted with further DCM (3×100 mL), which were combined and washed with brine (150 mL), dried (Na₂SO₄) and concentrated to yield a colourless oil (1.2 g) which contained **3.16** and **3.17** in a roughly 1:1 ratio. This crude material was used in subsequent steps without further purification.

3.16/3.17: Formula: C₃₀H₅₂O₅Si; **MW** 520.8; **m.p.** N/A; **R_f** (Petrol ether/EtAOAc : 85/15) : 0.65; **¹H NMR** (400MHz, CDCl₃): δ 4.80-4.44 (m, 3H, O-CH₂-O + C=CH), 3.67 (s, 3H, CO₂CH₃), 3.66-3.56 (m, 1H, H₇), 3.40 (s, 1.5H, OCH₃), 3.36 (s, 1.5H, OCH₃), 2.51-1.08 (m, 31H), 0.99-0.95 (m, 3H, H₁₉), 0.93 (d, *J*=6.2 Hz, 3H, H₂₁), 0.66 (br. s., 1.5H, H₁₈), 0.65 (br. s., 1.5H, H₁₈), 0.21-0.15 (m, 9H, Si(CH₃)₃) ppm.

Methyl 2β-fluoro-7α-methoxymethoxyl-3oxo-5β-cholanoate (3.13) and methyl 4β-fluoro-7α-methoxymethoxyl-3oxo-5β-cholanoate (3.15)



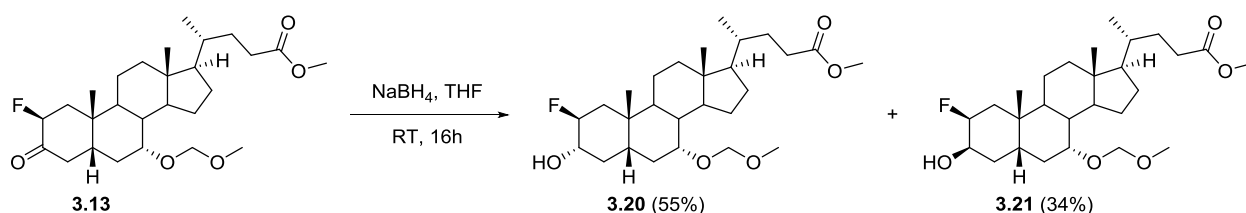
Following method of Fujimoto *et al.*^[97] To a solution of **3.16** and **3.17** (1.10 g, 2.2 mmol, 1 equiv) in dry acetonitrile was added Selectfluor® (1.20 g, 3.3 mmol, 1.5 equiv), allowing the reaction mixture to stir at room temperature for 4 h. The solvent was removed *in vacuo* before diluting with EtOAc (100 mL) and water (100 mL). The layers were separated before extracting the aqueous with further EtOAc (2×100 mL). The combined organics were then washed with brine (150 mL), dried (Na₂SO₄) and concentrated to yield 1.05 g of a pale yellow solid crude. The crude material was purified using flash chromatography (PE/EtOAc : 80:20) to yield white solid **3.13** (377 mg, 0.81 mmol, 36% over two steps) and white solid **3.15** (321 mg, 0.69 mmol, 31% over two steps).

3.13: Formula: C₂₇H₄₃FO₅; **MW** 466.6; **m.p.** 150 - 152°C; **R_f** (pet ether/EA : 80:20) 0.19; **I.R.** 2935 (m), 2871 (w), 1736 (s), 1439 (w), 1147 (m), 1035 (s) cm⁻¹; **¹H NMR** (400MHz, CDCl₃): δ 5.05 (ddd, *J*=49.4, 13.5, 5.6 Hz, 1H, H₂), 4.67 (d, *J*=6.8 Hz, 1H, O-CHH-O), 4.54 (d, *J*=6.8 Hz, 1H, O-CHH-O), 3.67 (s, 4H, CO₂CH₃ + H₇), 3.48 (t, *J*=13.9 Hz, 1H, H_{4α}), 3.37 (s, 3H, OCH₃), 2.52 (dt, *J*=12.7, 6.1 Hz, H_{1α}), 2.42 - 1.12 (m, 27H), 1.08 (s, 3H, H₁₉), 0.95 (d, *J*=6.6 Hz, 3H, H₂₁), 0.69 (s, 3H, H₁₈) ppm; **¹³C NMR** (100 MHz, CDCl₃): δ 206.0 (d, *J*=13.2 Hz, C₃), 174.7 (CO₂C₃), 96.2 (O-C₂-O), 89.5 (d, *J*=189.3 Hz, C₂), 74.9 (C₇), 56.4 (OC₃), 55.6, 51.5 (CO₂C₃), 49.6, 44.3, 43.9 (C₄), 43.4 (d, *J*=15.4 Hz, C₁), 42.5, 39.4, 39.1 (C_H₂), 37.9 (d, *J*=10.3 Hz, C₁₀), 35.4, 34.3, 31.0 (C_H₂), 30.9 (C_H₂), 30.0 (C_H₂), 28.1 (C_H₂), 23.7 (C_H₂), 21.9 (C₁₉), 21.1 (C_H₂), 18.3 (C₂₁), 11.8 (C₁₈) ppm; **¹⁹F NMR** (CDCl₃, 376MHz): δ -195.19 ppm (ddt, *J*=49.2, 9.6, 6.2 Hz); **[¹H]¹⁹F NMR** (CDCl₃, 376MHz): δ -195.21 ppm (s); **MS (ESI+)** *m/z* : 484.2 [M+NH₄]⁺, 489.1 [M+Na]⁺; **HRMS** (HPLC-ESI) : [M+Na]⁺ Calcd. 489.2987; Found. 489.2994.

3.15: Formula: C₂₇H₄₃FO₅; **MW** 466.6; **m.p.** 139 - 141°C; **R_f** (pet ether/EA : 80:20) 0.31; **I.R.** 2942 (m), 2871 (w), 1737 (s), 1436 (w), 1147 (m), 1066 (m), 1031 (s) cm⁻¹; **¹H NMR** (400MHz, CDCl₃): δ

5.78 (dd, $J=46.8, 11.7$ Hz, 1H, H4), 4.77 (d, $J=6.8$ Hz, 1H, O-CHH-O), 4.59 (d, $J=6.8$ Hz, 1H, O-CHH-O), 3.78 (q, $J=2.7$ Hz, 1H, H7), 3.67 (s, 3H, CO₂CH₃), 3.40 (s, 3H, OCH₃), 2.52 (td, $J=14.4, 4.9$ Hz, 1H), 2.42 - 1.11 (m, 24H), 1.07 (s, 3H, H19), 0.94 (d, $J=6.4$ Hz, 3H, H21), 0.70 (s, 3H, H18) ppm; ¹³C NMR (100 MHz, CDCl₃): δ 206.1 (d, $J=13.2$ Hz, 1C, C3), 174.7 (CO₂CH₃), 95.5 (O-CH₂-O), 93.7 (d, $J=187.8$ Hz, C4), 74.0 (C7), 56.4, 55.7, 51.5 (CO₂CH₃), 50.5 (d, $J=16.1$ Hz, C5), 49.7, 42.5, 39.2, 39.1 (CH₂), 37.6 (d, 7.3 Hz), 36.9 (CH₂), 35.4 (CH₂), 35.4, 34.9, 31.0 (CH₂), 31.0 (CH₂), 28.1 (CH₂), 25.3 (d, $J=1.5$ Hz, CH₂), 23.7, (CH₂) 21.9 (C19), 21.1 (CH₂), 18.3 (C21), 11.8 (C18) ppm; ¹⁹F NMR (CDCl₃, 376MHz): δ -200.67 ppm (ddd, $J=46.8, 12.1, 6.9$ Hz); [¹H]¹⁹F NMR (CDCl₃, 376MHz): δ -200.67 ppm (s); MS (ESI+) : m/z 484.2 (M+NH₄)⁺, 489.1 (M+Na)⁺; HRMS (HPLC-ESI) : [M+Na]⁺ Calcd. 489.2987; Found. 489.2979.

Methyl 2β-fluoro-3α-hydroxy-7α-methoxymethoxyl-5β-cholanoate (3.20) and methyl 2β-fluoro-3β-hydroxy-7α-methoxymethoxyl-5β-cholanoate (3.21)



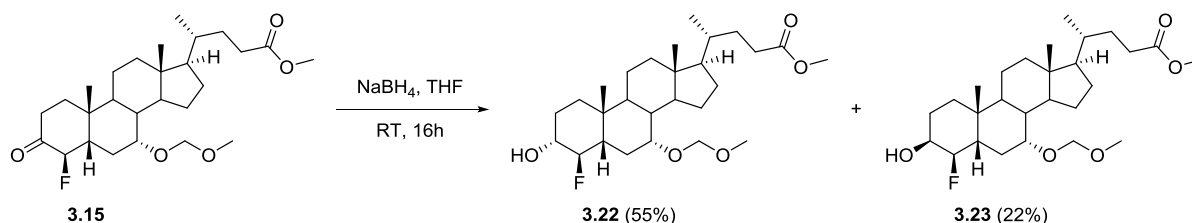
To a solution of **3.13** (260 mg, 0.56 mmol, 1 equiv) in anhydrous tetrahydrofuran (20 mL) was added sodium borohydride (64 mg, 1.70 mmol, 3 equiv) and the reaction mixture allowed to stir overnight at room temperature. Once deemed complete by TLC analysis the reaction was diluted with EtOAc (150 mL) and quenched with water (100 mL), separating the layers before extracting the aqueous with further EtOAc (2×100 mL). The combined organics were then washed with water (150 mL) and brine (150 mL) before drying (Na₂SO₄) and concentrating *in vacuo* to yield 306 mg of a pale crude oil. The crude was purified by flash chromatography (PE/EtOAc: 65:35) to yield **3.20** as a white solid (144 mg, 0.307 mmol, 55%) and **3.21** as a colourless gum (88 mg, 0.19 mmol, 34%).

3.20: Formula: C₂₇H₄₃FO₅; **MW** 468.7; **m.p.** 92 - 94°C; **R_f** (PE/EtOAc: 70:30) 0.23; **I.R.** 3440 (br. w), 2934 (m), 2870 (w), 1736 (m), 1145 (m), 1033 (s), 729 (s) cm⁻¹; ¹H NMR (400MHz, CDCl₃): δ 4.68 (d, $J=6.8$ Hz, 1H, O-CHH-O), 4.54 (d, $J=7.1$ Hz, 1H, O-CHH-O), 4.40 (dddd, $J=52.3, 12.0, 8.6, 4.4$ Hz, 1H, H2), 3.66 (s, 3H, CO₂CH₃), 3.62 - 3.47 (m, 2H, H3 with H7), 3.37 (s, 3H, OCH₃), 2.48 - 1.01 (m, 27H), 0.99 (s, 3H, H19), 0.92 (d, $J=6.4$ Hz, 3H, H21), 0.64 (s, 3H, H18) ppm; ¹³C NMR (100 MHz, CDCl₃): δ 174.7 (C24), 95.6 (O-CH₂-O), 93.8 (d, $J=170.9$ Hz, C2), 74.5 (d, $J=17.6$ Hz, C3), 74.3 (C7), 56.2 (OCH₃),

55.6, 51.4 (CO₂CH₃), 49.6, 42.4, 41.0 (d, *J*=1.5 Hz), 40.4 (d, *J*=15.3 Hz, C₁), 39.3, 39.2 (CH₂), 38.1 (d, *J*=11.0 Hz, C₁₀), 35.5 (d, *J*=8.1 Hz, CH₂), 35.3, 34.3, 31.0 (CH₂), 31.0 (CH₂), 29.8 (CH₂), 28.1 (CH₂), 23.6 (CH₂), 22.7 (C₁₉), 20.9 (CH₂), 18.3 (C₂₁), 11.7 (C₁₈) ppm; ¹⁹F NMR (CDCl₃, 376MHz): δ -187.47 (ddq, *J*=52.3, 12.7, 7.1 Hz) ppm; [¹H]¹⁹F NMR (CDCl₃, 376MHz): δ -187.49 (s) ppm; MS (ESI+) *m/z* : 486.1 [M+NH₄]⁺, 491.2 [M+Na]⁺; HRMS (HPLC-ESI) : (M+NH₄)⁺ Calcd. 486.3589; Found. 486.3588.

3.21: Formula: C₂₇H₄₃FO₅; **MW** 468.7; **m.p.** N/A; **R_f** (PE/EtOAc : 70:30) 0.32; **I.R.** 3459 (br. w), 2932 (m), 2873 (w), 1737 (m), 1439 (w), 1146 (m), 1034 (s), 732 (m) cm⁻¹; ¹H NMR (400MHz, CDCl₃): δ 4.72-4.51 (m, 3H, H₂ + O-CH₂-O), 4.20 - 4.09 (m, 1H, H₃), 3.66 (s, 3H, CO₂CH₃), 3.59 (d, *J*=2.4 Hz, 1H, H₇), 3.38 (s, 3H, OCH₃), 2.45 (ddd, *J*=15.2, 12.4, 2.2 Hz, 1H, H_{4α}), 2.35 (ddd, *J*=15.0, 10.3, 5.1 Hz, 1H, H₂₃), 2.22 (ddd, *J*=15.6, 9.5, 6.5 Hz, 1H, H_{23'}), 2.06-1.05 (m, 25H), 1.02 (s, 3H, H₁₉), 0.93 (d, *J*=6.6 Hz, 3H, H₂₁), 0.65 (s, 3H, H₁₈) ppm; ¹³C NMR (100 MHz, CDCl₃): δ 174.7 (CO₂CH₃), 95.8 (O-CH₂-O), 90.6 (d, *J*=171.7 Hz, C₂), 74.8 (C₇), 68.0 (d, *J*=17.6 Hz, C₃), 56.2 (OCH₃), 55.6, 51.4 (CO₂CH₃), 49.8, 42.5, 39.4, 39.3 (CH₂), 37.7 (d, *J*=11.7 Hz, C₁₀), 35.4, 34.9, 34.6 (d, *J*=16.1 Hz, C₁), 33.7 (d, *J*=6.6 Hz, C₄), 33.6, 31.0 (C₂₃), 31.0 (CH₂), 29.3 (d, *J*=1.5 Hz, CH₂), 28.1 (CH₂), 23.7 (CH₂), 23.0 (C₁₉), 21.1 (CH₂), 18.3 (C₂₁), 11.7 (C₁₈) ppm; ¹⁹F NMR (CDCl₃, 376MHz): δ -187.31 (dquin, *J*=47.2, 7.5 Hz) ppm; [¹H]¹⁹F NMR (376MHz, CDCl₃): δ -187.33 (s) ppm; MS (ESI+) *m/z* : 486.0 [M+NH₄]⁺, 491.1 [M+Na]⁺; HRMS (HPLC-ESI) : (M+Na)⁺ Calcd. 491.3143; Found. 491.3148.

Methyl 4β-fluoro-3α-hydroxy-7α-methoxymethoxyl-5β-cholanoate (3.22) and methyl 4β-fluoro-3β-hydroxy-7α-methoxymethoxyl-5β-cholanoate (3.23)

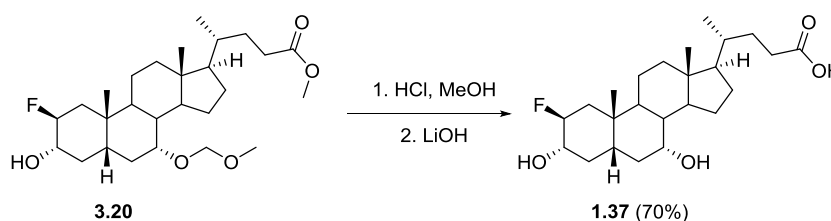


To a solution of **3.15** (287 mg, 0.62 mmol, 1 equiv) in anhydrous THF (25 mL) was added NaBH₄ (73 mg, 1.93 mmol, 3 equiv) and the reaction mixture allowed to stir overnight at RT. Once deemed complete by TLC analysis the reaction was diluted with DCM (100 mL) and quenched with water (100 mL), separating the layers before extracting the aqueous with further DCM (2×100 mL). The combined organics were then washed with brine (2×150 mL) before drying (Na₂SO₄) and concentrating to yield 300 mg of a colourless oil. The crude was purified by flash chromatography (PE/EtOAc : 80:20) to yield the separated epimers **3.22** (160 mg, 0.34 mmol, 55 %) and **3.23** (64 mg, 0.14 mmol, 22%), both as white solids.

3.22: Formula: C₂₇H₄₃FO₅; **MW** 468.7; **m.p.** 82 - 84°C; **R_f** (PE/EtOAc : 75:25) 0.28; **I.R.** 3436 (br. w), 2935 (m), 2871 (w), 1737 (m), 1450 (w), 1147 (m), 1090 (m), 1031 (s) cm⁻¹; **¹H NMR** (400MHz, CDCl₃): δ 5.08 (ddd, *J*=50.6, 10.8, 8.8 Hz, 1H, H₄), 4.77 (d, *J*=6.8 Hz, 1H, O-CHH-O), 4.59 (d, *J*=6.8 Hz, 1H, O-CHH-O), 3.70 (d, *J*=2.4 Hz, 1H, H₇), 3.67 (s, 3H, CO₂CH₃), 3.60 - 3.47 (m, 1H, H₃), 3.40 (s, 3H, OCH₃), 2.36 (ddd, *J*=15.5, 11.0, 5.0 Hz, 1H, H₂₃), 2.30-1.02 (m, 27H), 0.99 (s, 3H, H₁₉), 0.93 (d, *J*=6.4 Hz, 3H, H₂₁), 0.65 (s, 3H, H₁₈) ppm; **¹³C NMR** (100 MHz, CDCl₃): δ 174.7 (C₂₄), 98.0 (d, *J*=169.5 Hz, C₄), 95.0 (O-CH₂O), 74.3 (d, *J*=17.6 Hz, C₃), 73.6 (C₇), 56.3 (OCH₃), 55.6, 51.5 (CO₂CH₃), 49.7, 46.3 (d, *J*=15.4 Hz, C₅), 42.4, 39.2 (d, *J*=3.7 Hz, CH₂), 37.8, 35.4, 34.8, 34.2 (d, *J*=1.5 Hz, CH₂), 31.1 (C₂₃), 31.0 (CH₂), 28.1 (CH₂), 26.4 (d, *J*=8.4 Hz, CH₂), 24.2 (d, *J*=2.2 Hz, CH₂), 23.7 (CH₂), 22.6 (C₁₉), 20.6 (CH₂), 18.3 (C₂₁), 11.7 (C₁₈) ppm; **¹⁹F NMR** (CDCl₃, 376MHz): δ -193.84 (dtd, *J*=50.6, 11.9, 7.1 Hz) ppm; **[¹H]¹⁹F NMR** (CDCl₃, 376MHz): δ -193.85 (s) ppm; **MS (ESI+)** *m/z* : 486.2 [M+NH₄]⁺, 491.2 [M+Na]⁺; **HRMS** (HPLC-ESI) : (M+NH₄)⁺ Calcd. 486.3589; Found. 486.3591.

3.23: Formula: C₂₇H₄₃FO₅; **MW** 468.7; **m.p.** 86 - 88°C; **R_f** (PE/EtOAc : 75:25) 0.35; **I.R.** 3470 (br. w), 2937 (m), 1737 (m), 1442 (w), 1146 (m), 1031 (s) cm⁻¹; **¹H NMR** (400MHz, CDCl₃): δ 5.25 (ddd, *J*=45.2, 11.2, 3.2 Hz, 1H, H₄), 4.76 (d, *J*=6.8 Hz, 1H, O-CHH-O), 4.58 (d, *J*=6.8 Hz, 1H, O-CHH-O), 4.18 - 4.11 (m, 1H, H₃), 3.69 (d, *J*=2.4 Hz, 1H, H₇), 3.66 (s, 3H, CO₂CH₃), 3.39 (s, 3H, OCH₃), (ddd, *J*=15.5, 10.5, 5.5 Hz, 1H, H₂₃), 2.22 (ddd, *J*=15.6, 9.4, 6.0 Hz, 1H, H₂₃'), 2.17-1.04 (m, 25H), 1.00 (s, 3H, H₁₉), 0.92 (d, *J*=6.4 Hz, 3H, H₂₁), 0.65 (s, 3H, H₁₈) ppm; **¹³C NMR** (100 MHz, CDCl₃): δ 174.7 (C₂₄), 95.1 (O-CH₂O), 94.3 (d, *J*=169.2 Hz, C₄), 73.8 (C₇), 67.4 (d, *J*=17.6 Hz, C₃), 56.2 (d, *J*=1.5 Hz, (OCH₃), 55.6, 51.4 (CO₂CH₃), 49.8, 42.5, 40.9 (d, *J*=16.1 Hz, C₅), 39.3 (CH₂), 39.2, 37.5 (d, *J*=8.1 Hz), 35.4, 34.1, 31.0 (C₂₃), 31.0 (CH₂), 28.6 (CH₂), 28.1 (CH₂), 24.8 (d, *J*=6.6 Hz, CH₂), 23.8 (d, *J*=2.9 Hz, CH₂), 23.6 (CH₂), 22.7 (C₁₉), 20.9 (CH₂), 18.3 (C₂₁), 11.7 (C₁₈) ppm; **¹⁹F NMR** (CDCl₃, 376MHz): δ -193.71 (dq, *J*=45.1, 8.4 Hz) ppm; **[¹H]¹⁹F NMR** (CDCl₃, 376MHz): δ -193.73 (s) ppm; **MS (ESI+)** *m/z* : 486.2 [M+NH₄]⁺, 491.2 [M+Na]⁺; **HRMS** (HPLC-ESI) : (M+Na)⁺ Calcd. 491.3143; Found. 491.3137.

2β-fluorochenodeoxycholic acid (**1.37**)

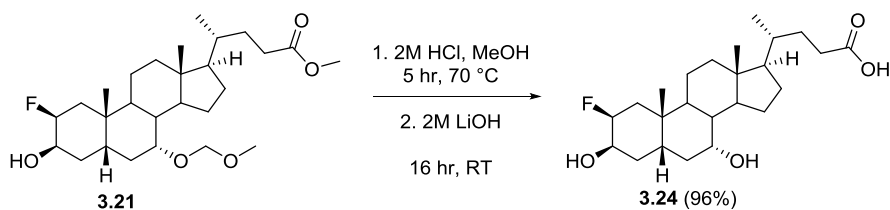


Using procedure D, followed by procedure B, **3.20** (118 mg, 0.25 mmol, 1 equiv) was deprotected to yield **1.37** as a pale yellow solid (72 mg, 0.18 mmol, 70%).

1.37: Formula: C₂₄H₃₉FO₄; **MW** 410.6; **[α]_D** +5.0 (c 1.0, MeOH, 22 °C); **m.p.** 186–188 °C; **R_f** (PE/acetone : 60:40) 0.24; **I.R.** 3377 (br. m), 2932 (s), 2868 (m), 1707 (s), 1082 (s), 1004 (m) cm⁻¹;

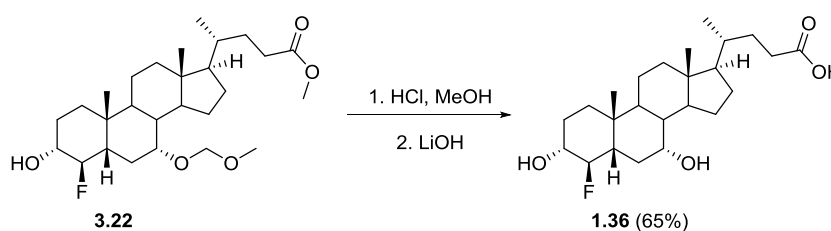
^1H NMR (400MHz, CD_3OD): δ 4.32 (dddd, $J=52.5, 12.5, 8.6, 4.0$ Hz, 1H, H_2), 3.78 (q, $J=2.3$ Hz, 1H, H_7), 3.44 (tdd, $J=12.0, 8.7, 5.0$ Hz, 1H, H_3), 2.43 (q, $J=13.2$ Hz, 1H, $\text{H}_{4\alpha}$), 2.33 (ddd, $J=15.5, 11.0, 5.0$ Hz, 1H, H_{23}), 2.25-2.11 (m, 2H, $\text{H}_{23}' + \text{H}_{1\alpha}$ or β), 2.04 (dt, $J=12.4, 2.9$ Hz, 1H), 1.99-1.04 (m, 22H), 1.00 (s, 3H, H_{19}), 0.97 (d, $J=6.5$ Hz, 3H, H_{21}), 0.70 (s, 3H, H_{18}) ppm; **^{13}C NMR** (100 MHz, CD_3OD): δ 178.2 (C_{24}), 94.2 (d, $J=173.9$ Hz, C_2), 75.5 (d, $J=16.9$ Hz, C_3), 68.8 (C_7), 57.4, 51.5, 43.7, 42.7 (d, $J=1.5$ Hz, C_5), 42.1 (d, $J=15.4$ Hz, C_1), 41.0 (CH_2), 40.8, 39.2 (d, $J=10.3$ Hz, C_{10}), 38.2 (d, $J=8.1$ Hz, C_4), 36.9, 35.5, 34.9 (CH_2), 32.4 (C_{23}), 32.1 (CH_2), 29.3 (CH_2), 24.7 (CH_2), 23.4 (C_{19}), 22.2 (CH_2), 19.0 (C_{21}), 12.3 (C_{18}) ppm; **^{19}F NMR** (376MHz, CD_3OD): δ -186.77 (ddq, $J=52.2, 11.9, 7.8$ Hz) ppm; **$[\text{H}]^{19}\text{F}$ NMR** (376MHz, CD_3OD): δ -186.76 (s) ppm; **MS (ESI+)** m/z : 393.1 $[\text{M}+\text{H}-\text{H}_2\text{O}]^+$, 821.2 $[2\text{M}+\text{H}]^+$, 843.3 $[2\text{M}+\text{Na}]^+$; **HRMS** (HPLC-ESI) : $[\text{M}+\text{Na}]^+$ Calcd: 433.2725; Found: 433.2719.

2 β -fluoro-3 β ,7 α -dihydroxy-5 β -cholanolic acid (**3.24**)



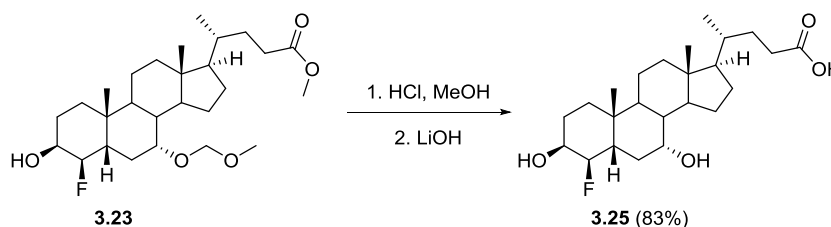
Using procedure D, followed by procedure B, **3.21** (25 mg, 0.053 mmol, 1 equiv) was deprotected to yield **3.24** as a gummy solid (21 mg, 0.05 mmol, 96%).

3.24: Formula: $\text{C}_{24}\text{H}_{39}\text{FO}_4$; **MW** 410.6; **$[\alpha]_D$** +0.6 (c 0.5, MeOH, 24 $^\circ\text{C}$); **m.p.** N/A; **R_f** (Petrol ether/acetone : 60/40) : 0.35; **I.R.** 3425 (br. w), 2931 (s), 2872 (m), 1710 (s), 1381 (w), 1050 (w), 983 (w) cm^{-1} ; **^1H NMR** (400MHz, Acetone- D_6): δ 10.42 (br. s., 1H, COOH), 4.58 (dddd, $J=47.7, 12.1, 4.4, 2.8$ Hz, 1H, H_2), 4.12-4.00 (m, 1H, H_3), 3.80 (q, $J=2.4$ Hz, 1H, H_7), 3.59 (br. s., 1H), 3.29 (br. s., 1H), 2.61 (ddd, $J=15.3, 12.8, 2.3$ Hz, 1H, $\text{H}_{4\alpha}$), 2.34 (ddd, $J=15.5, 11.0, 5.0$ Hz, 1H, H_{23}), 2.21 (ddd, $J=15.5, 9.6, 6.4$ Hz, 1H, H_{23}'), 2.03-1.03 (m, 31H), 1.01 (s, 3H, H_{19}), 0.97 (d, $J=6.5$ Hz, 3H, H_{21}), 0.70 (s, 3H, H_{18}) ppm; **^{13}C NMR** (100 MHz, Acetone- D_6): δ 175.1 (C_{24}), 91.2 (d, $J=173.1$ Hz, C_2), 68.3 (d, $J=16.1$ Hz, C_3), 68.1, 57.0, 51.2, 43.3, 40.7 (CH_2), 40.5, 38.5 (d, $J=11.0$ Hz, C_{10}), 36.4 (d, $J=8.0$ Hz, C_4), 36.3, 36.2, 35.8 (d, $J=16.1$ Hz, C_1), 34.4 (CH_2), 34.2, 31.9 (CH_2), 31.3 (C_{23}), 29.0 (CH_2), 24.3 (CH_2), 23.7 (C_{19}), 22.0 (CH_2), 18.8 (C_{21}), 12.3 (C_{18}) ppm; **^{19}F NMR** (376MHz, Acetone- D_6): δ -186.90 (dq, $J=47.6, 7.6$ Hz) ppm; **$[\text{H}]^{19}\text{F}$ NMR** (376MHz, Acetone- D_6): δ -186.90 (s) ppm; **MS (ESI+)** m/z : 393.4 $[\text{M}+\text{H}-\text{H}_2\text{O}]^+$, 373.4 $[\text{M}+\text{H}-\text{H}_2\text{O}-\text{HF}]^+$, 355.5 $[\text{M}+\text{H}-2\text{H}_2\text{O}-\text{HF}]^+$; **HRMS** (HPLC-ESI) : $[\text{M}+\text{H}-\text{H}_2\text{O}]^+$ Calcd. 393.2799; Found. 393.2794.

4 β -fluorochenodeoxycholic acid (1.36)

Using procedure D, followed by procedure B, **3.22** (125 mg, 0.27 mmol, 1 equiv) was deprotected to yield **1.36** as a pale orange solid (70 mg, 0.18 mmol, 65%).

1.36: Formula: C₂₄H₃₉FO₄; **MW** 410.6; [α]_D +21.9 (c 1.0, MeOH, 23 °C); **m.p.** 95–97 °C; **R_f** (PE/acetone : 60:40) 0.28; **I.R.** 3387 (br. m), 2935 (s), 2868 (m), 1708 (s), 1081 (m), 1007 (s) cm⁻¹; **¹H NMR** (400MHz, CD₃OD): δ 5.16 (ddd, $J=9.0, 10.5, 49.9$ Hz, 1H, H₄), 3.83 (q, $J=2.4$ Hz, 1H, H₇), 3.49 - 3.36 (m, 1H, H₃), 2.33 (ddd, $J=15.5, 11.0, 5.0$ Hz, 1H, H₂₃), 2.19 (ddd, $J=15.5, 9.2, 6.8$ Hz, 1H, H_{23'}), 2.11 (dt, $J=14.9, 2.2$ Hz, 1H, H_{6 β}), 2.03-1.04 (m, 24H), 0.99 (s, 3H, H₁₉), 0.96 (d, $J=6.4$ Hz, 3H, H₂₁), 0.70 (s, 3H, H₁₈) ppm; **¹³C NMR** (100 MHz, CD₃OD): δ 178.2 (C₂₄), 98.6 (d, $J=171.7$ Hz, C₄), 75.2 (d, $J=18.3$ Hz, C₃), 68.8 (C₇), 57.4, 51.6, 48.3 (d, $J=16.1$ Hz, C₅), 43.7, 41.0 (C_H₂), 40.5, 38.9 (d, $J=8.1$ Hz, C₁₀), 36.8, 35.9, 35.6 (d, $J=1.5$ Hz, C_H₂), 32.4 (C₂₃), 32.1 (C_H₂), 29.6 (d, $J=2.2$ Hz, C₆), 29.4 (C_H₂), 28.3 (d, $J=8.8$ Hz, C_H₂), 24.7 (C_H₂), 23.3 (C₁₉), 21.9 (C_H₂), 19.0 (C₂₁), 12.4 (C₁₈) ppm; **¹⁹F NMR** (376MHz, CD₃OD) δ : -192.3 (dtd, $J=49.9, 12.4, 6.2$ Hz) ppm; [**H**]**¹⁹F NMR** (376MHz, CD₃OD): δ -192.3 ppm (s) ppm; **MS (ESI+)** m/z : 393.1 [M+H-H₂O]⁺, 821.2 [2M+H]⁺, 843.3 [2M+Na]⁺, 1231.7 [3M+H]⁺; **HRMS (HPLC-ESI)** : [M+Na]⁺ Calcd: 433.2725; Found: 433.2712.

4 β -fluoro-3 β ,7 α -dihydroxy-5 β -cholanoic acid (3.25)

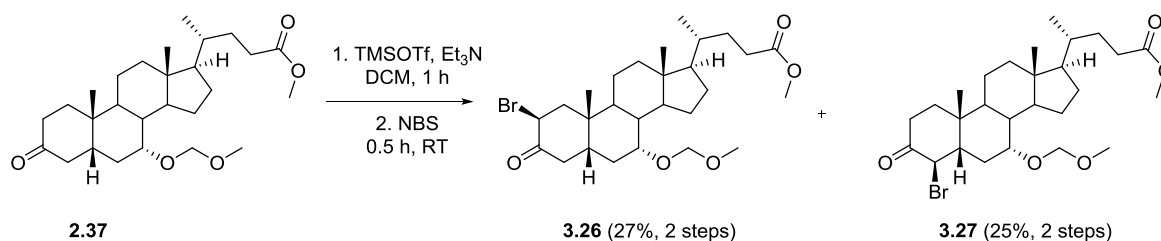
Using procedure D, followed by procedure B, **3.23** (118 mg, 0.25 mmol, 1 equiv) was deprotected to yield **3.25** as a pale pink solid (58 mg, 0.14 mmol, 83%).

3.25: Formula: C₂₄H₃₉FO₄; **MW** 410.6; [α]_D +6.6 (c 0.5, MeOH, 23 °C); **m.p.** 156–158 °C; **R_f** (PE/EtOAc : 60:40) 0.22; **I.R.** 3408 (br. w), 2935 (s), 2871 (m), 1709 (s), 1064 (m) cm⁻¹; **¹H NMR** (400MHz, CD₃OD): δ 5.28 (ddd, $J=45.2, 11.2, 3.2$ Hz, 1H, H₄), 4.08 (dtd, $J=7.2, 3.6, 3.2$ Hz, 1H, H₃),

3.83 (d, $J=2.4$ Hz, 1H, H7), 2.33 (ddd, $J=15.5, 11.0, 5.0$ Hz, 1H, H23), 2.20 (ddd, $J=15.7, 9.3, 6.8$ Hz, 1H, H23'), 2.12-1.05 (m, 24H), 1.01 (s, 3H, H19), 0.96 (d, $J=6.4$ Hz, 3H, H21), 0.70 (s, 3H, H18) ppm; ^{13}C NMR (100 MHz, CD_3OD): δ 178.2 (C24), 94.9 (d, $J=173.9$ Hz, C4), 69.1 (C7), 68.5 (d, $J=16.9$ Hz, C3), 57.5, 51.8, 43.8, 42.5 (d, $J=16.9$ Hz, C5), 41.1 (CH₂), 40.6, 38.8 (d, $J=8.8$ Hz, C10), 36.9, 35.3, 32.5 (C23), 32.1 (CH₂), 30.1 (CH₂), 29.4 (CH₂), 29.2 (d, $J=2.2$ Hz, CH₂), 26.7 (d, $J=7.3$ Hz, CH₂), 24.7 (CH₂), 23.5 (C19), 22.3 (CH₂), 19.0 (C21), 12.4 (C18) ppm; ^{19}F NMR (376MHz, CD_3OD): δ -194.25 ppm (dq, $J=44.9, 6.2$ Hz) ppm; [^1H] ^{19}F NMR (376MHz, CD_3OD): δ -194.27 (s) ppm; MS (ESI+) m/z : 393.1 (M+H- H_2O)⁺, 821.2 (2M+H)⁺; HRMS (HPLC-ESI) : [M+Na]⁺ Calcd: 433.2725; Found: 433.2723.

5.4.2 Synthesis of 2 α - and 4 α -fluorinated analogues

Methyl 2 β -bromo-7 α -methoxymethoxyl-3oxo-5 β -cholanoate (3.26) and methyl 4 β -bromo-7 α -methoxymethoxyl-3oxo-5 β -cholanoate (3.27)

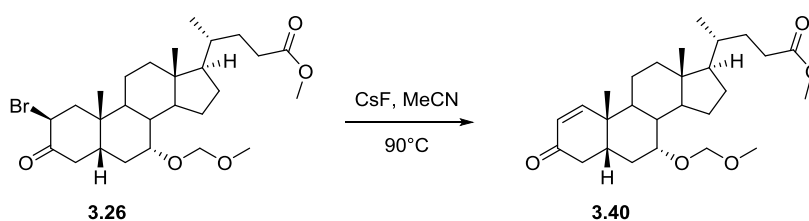


To a solution of isomeric enol ethers (synthesised through previously reported TMS-OTf method,^[100] from 50 mg, 0.11 mmol of ketone **3.27**) in DCM was added NBS (30 mg, 0.17 mmol, 1.5 equiv). The reaction was deemed complete after 0.5 h at RT and was quenched with water (5 mL) and DCM (5 mL). The layers were separated, and the aqueous washed with further DCM (5 mL). The combined organics were washed with brine (7.5 mL), dried over Na_2SO_4 and concentrated *in vacuo* to yield a pale orange solid. The crude material was purified using flash chromatography (PE/EtOAc : 80:20→75:25) to yield **3.26** (16 mg, 0.030 mmol, 27% over two steps) and **3.27** (13 mg, 0.025 mmol, 25% over two steps).

3.26: R_f (Petrol ether/EA : 85/15) : 0.25; ^1H NMR (400MHz, CDCl_3): δ 4.79 (dd, $J=14.3, 5.0$ Hz, 1H, H2), 4.67 (d, $J=6.8$ Hz, 1H, O-CHH-O), 4.54 (d, $J=6.8$ Hz, 1H, O-CHH-O), 3.73 - 3.62 (m, 4H, CO_2CH_3 + H7), 3.54 (t, $J=14.2$ Hz, 1H, H4 α), 3.37 (s, 3H, OCH_3), 2.67 (dd, $J=13.8, 5.3$ Hz, 1H, H1 α), 2.48 (dd, $J=14.7, 4.6$ Hz, 1H, H4 β), 2.42 - 1.10 (m, 28H), 1.05 (s, 3H, H19), 0.95 (d, $J=6.4$ Hz, 3H, H21), 0.69 (s, 3H, H18) ppm; ^{13}C NMR (100 MHz, CDCl_3): δ 202.0 (C2), 174.7 (C24), 96.1 (O-CH₂-O), 74.9 (C7), 56.4 (O-CH₃), 55.7, 53.0 (C2), 51.5 (CO_2CH_3), 49.7, 49.1 (C1), 44.5 (C4), 44.3, 42.5, 39.3, 39.2 (CH₂), 39.1, 35.4, 33.6, 31.0 (C23), 30.9 (CH₂), 30.2 (CH₂), 28.1 (CH₂), 23.7 (CH₂), 21.7 (C19), 21.2 (CH₂), 18.3 (C21), 11.8 (C18) ppm.

3.27: R_f (Petrol ether/EA : 85/15) : 0.38; $^1\text{H NMR}$ (400MHz, CDCl_3): δ 5.67 (d, $J=12.0$ Hz, 1H, H_4), 4.84 (d, $J=7.3$ Hz, 1H, O- CHH-O), 4.56 (d, $J=7.1$ Hz, 1H, O- CHH-O), 3.78 (q, $J=2.4$ Hz, 1H, H_7), 3.67 (s, 3H, CO_2CH_3), 3.39 (s, 3H, O- CH_3), 2.61 (td, $J=14.3, 4.9$ Hz, 1H, $\text{H}_{2\alpha}$), 2.52 - 1.12 (m, 28H), 1.09 (s, 3H, H_{19}), 0.94 (d, $J=6.4$ Hz, 3H, H_{21}), 0.70 (s, 3H, H_{18}) ppm; $^{13}\text{C NMR}$ (100 MHz, CDCl_3): δ 202.2 (C_3), 174.6 (C_{24}), 95.2 (O- CH_2O), 73.2 (C_7), 64.1 (C_4), 56.3 (O- CH_3), 55.7, 53.7, 51.5 (CO_2CH_3), 49.7, 42.5, 39.6, 39.2 (CH_2), 38.5, 36.6 (CH_2), 36.2 (C_2), 35.5, 34.0, 31.1 (C_{23}), 31.0 (CH_2), 28.1 (CH_2), 28.0 (CH_2), 23.4 (CH_2), 22.5 (C_{19}), 21.0 (CH_2), 18.3 (C_{21}), 11.8 (C_{18}) ppm.

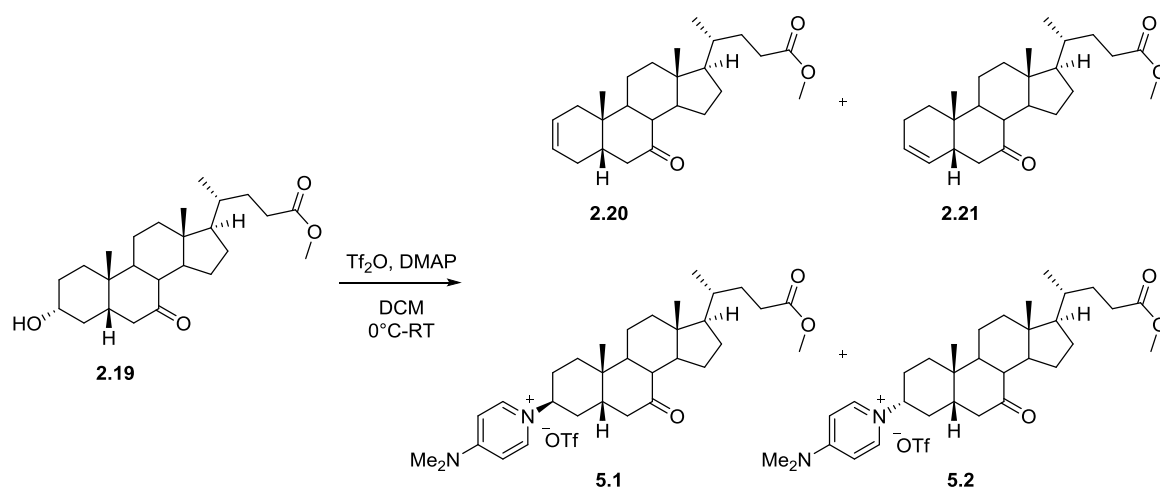
Methyl 3-keto-7 α -methoxymethoxy-5 β -chol-1-eneoate (3.40)



To a solution of α -bromo ketone **3.26** (30 mg, 0.06 mmol, 1 equiv) in dry MeCN (1 mL) was added CsF (15 mg, 0.09 mmol, 1.5 equiv) and allowed to stir at RT. No change was observed so the reaction was warmed to 60°C for 24 hr. Partial conversion (~20%) was observed after 24 hr, so the reaction was warmed to 90 °C and allowed to stir O/N. Complete consumption of starting material, solvent removed *in vacuo* and crude material taken up in DCM (2 mL) and brine (2 mL), layers separated and the organic phase dried (Na_2SO_4) and concentrated to yield 35 mg of a crude yellow gum. Analysis showed that elimination rather than the desired substitution had occurred, yielding enone **3.40**.

3.40: Formula: $\text{C}_{27}\text{H}_{42}\text{O}_5$; **MW** 446.6; **m.p.** N/A; R_f (PE/EtOAc : 80/20) : 0.24; **I.R** 2935 (m), 2870 (w), 1736 (s), 1165 (m), 1146 (m), 1092 (m), 1034 (s), 729 (w); $^1\text{H NMR}$ (400MHz, CDCl_3): 6.80 (d, $J=10.3$ Hz, 1H, H_1), 5.89 (d, $J=10.1$ Hz, 1H, H_2), 4.70 (d, $J=6.8$ Hz, 1H, O- CHH-O), 4.55 (d, $J=6.7$ Hz, 1H, O- CHH-O), 3.67 (s, 10H, CO_2CH_3), 2.45 - 2.28 (m, 5H), 2.28 - 2.15 (m, 6H), 1.99 - 1.23 (m, 47H), 1.19 (s, 7H), 1.15 - 0.99 (m, 10H), 0.93 (d, $J=6.4$ Hz, 9H), 0.70 (s, 4H) ppm; **MS (ESI+)** m/z : 447.2 $[\text{M}+\text{H}]^+$, 469.2 $[\text{M}+\text{Na}]^+$; **HRMS** (HPLC-ESI) : $[\text{M}+\text{Na}]^+$ Calcd: 469.2924; Found: 469.2938.

Methyl 7-oxo-5 β -chol-2-eneoate (2.20), methyl 7-oxo-5 β -chol-3-eneoate (2.21), methyl 3 β -(4-dimethylaminopyridinium-1-yl)-7-oxo-5 β -cholan-24-oate triflate (5.1) and methyl 3 α -(4-dimethylaminopyridinium-1-yl)-7-oxo-5 β -cholan-24-oate triflate (5.2)



A solution of alcohol **2.19** (5.5 g, 13.6 mmol, 1 equiv) and DMAP (5.0 g, 40.8 mmol, 3 equiv) in dry DCM (75 mL) was cooled to 0°C before the slow addition of Tf₂O (2.4 mL, 14.3 mmol, 1.05 equiv) over the course of 10 mins. The reaction was allowed to warm to room temperature and stir overnight, at which point the reaction was deemed complete. Crude mixture was extracted with 2M HCl and 10% CuSO₄ solution (50mL each), dried (Na₂SO₄) and concentrated to yield a pale yellow solid (5.05 g). Crude material separated *via* flash chromatography (PE/EtOAc : 95:5→0:100, then 100% acetone) to yield a mixture of alkenes **2.20** + **2.21** (840 mg, 2.2 mmol, 16%) and DMAP substitution mixture **5.1** + **5.2** (3.10 g, 4.7 mmol, 35%). Mixture of substitution products further purified *via* flash chromatography (DCM/MeOH : 95:5), which yielded a small amount (<10 mg) of the pure 3 β -isomer **5.1** for further analysis.

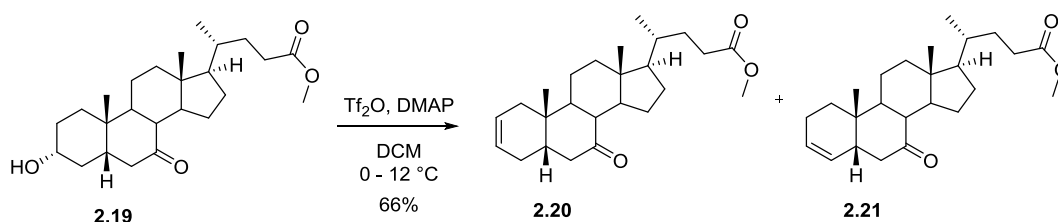
2.20 + 2.21: Formula: C₂₅H₃₈O₃; **MW** 386.58; **m.p.** N/A; **R_f** (PE/EtOAc : 70/30) : 0.70; **¹H NMR** (400MHz, CDCl₃): δ 5.67 - 5.30 (m, 2H, H_{alkene}), 3.65 (s, 3H, CO₂CH₃), 2.89 - 2.79 (m, 1H, H_{6 β}), 2.58 - 2.48 (m, 1H), 2.44 - 1.26 (m, 21H), 1.23 (s, 2H, H₁₉), 1.21 (s, 1H, H₁₉), 0.91 - 0.88 (m, 3H, H₂₁), 0.65 (m, 3H, H₁₈) ppm; **Selected ¹³C NMR** (100 MHz, CDCl₃): δ 212.6 (C₇), 212.2 (C₇), 174.6 (C₂₄), 129.4 (C=C), 127.4 (C=C), 125.3 (C=C), 124.1 (C=C), 18.3 (C₂₁), 12.0 (C₁₈), 11.9 (C₁₈) ppm; **MS (ESI+)** m/z : 387.2 [M+H]⁺, 404.2 [M+NH₄]⁺.

5.1 + 5.2: ¹H NMR (400MHz, CD₃OD): δ 8.39-8.15 (m, 2H, Ar-H_{ortho}), 7.10-6.88 (m, 2H, Ar-H_{meta}), 4.50 (quin, J=5.2 Hz, 0.65H, H₃ 3 β -isomer), 4.29 (tt, J=11.7, 4.0 Hz, 0.35H, H₃ 3 α -isomer), 3.65 (s, 3H, CO₂CH₃), 3.29 - 3.20 (m, 6H, N(CH₃)₂), 3.05 (dd, J=12.8, 6.1 Hz, 0.35H), 2.70 (dd, J=14.1, 4.1 Hz, 0.65H), 2.58 (t, J=11.3 Hz, 0.35H), 2.49 (t, J=11.0 Hz, 0.65H), 2.43 - 2.32 (m, 1H), 2.31-2.12 (m, 5H), 2.10 - 1.00 (m, 25H), 0.96 (d, J=6.5 Hz, 3H), 0.71 (s, 3H) ppm. **¹³C NMR** (101MHz, CD₃OD): δ 215.2

(C7), 214.1 (C7), 176.3 (C24), 158.0 (Ar-C_{3α}-isomer, *para*), 157.8 (Ar-C_{3β}-isomer, *para*), 141.7 (Ar-C_{3β}-isomer, *ortho*), 141.5 (Ar-C_{3α}-isomer, *ortho*), 121.8 (q, *J*=319.1 Hz, SO₂CF₃), 109.1 (Ar-C_{meta}), 68.5 (C_{3α}-isomer), 63.5 (C_{3β}-isomer), 56.2, 52.2, 50.8, 50.7, 49.3, 47.9, 46.0, 45.8, 44.5, 43.9, 43.8, 43.8, 41.5, 40.4, 40.3, 40.1, 39.9, 36.6, 36.3, 35.9, 35.8, 35.6, 32.9, 32.5, 32.3, 31.9, 29.4, 29.3, 27.8, 27.0, 26.4, 25.8, 23.4, 23.1, 23.0, 22.9, 19.0, 19.0, 14.6, 12.6, 12.6 ppm.

5.1: Formula: C₃₃H₄₉N₂O₃⁺ TfO⁻; **MW** (M⁺) 509.8; **I.R.** 2940 (m), 2873 (w), 1734 (m), 1708 (m), 1648 (s), 1570 (m), 1261 (s), 1160 (s) 1030 (s) cm⁻¹; **¹H NMR** (400MHz, CD₃OD): δ 8.27 (d, *J*=7.9 Hz, 2H, Ar-H_{ortho}), 6.98 (d, *J*=7.8 Hz, 2H, Ar-H_{meta}), 4.45 (quin, *J*=5.1 Hz, 1H, H₃), 3.65 (s, 3H, CO₂CH₃), 3.25 (s, 6H, N(CH₃)₂), 2.79 - 2.69 (m, 1H), 2.52 (t, *J*=11.2 Hz, 1H), 2.43 - 2.33 (m, 1H), 2.31 - 1.30 (m, 24H), 1.27 (s, 3H, H₁₉), 1.22 - 1.00 (m, 4H), 0.96 (d, *J*=6.5 Hz, 3H, H₂₁), 0.73 (s, 3H, H₁₈) ppm; **¹⁹F NMR** (376MHz, CD₃OD): δ -80.21 (s) ppm; **[H]¹⁹F NMR** (376MHz, CD₃OD): δ -80.21 (s) ppm; **MS (ESI+)** m/z : 509.3 [M]⁺; **HRMS (HPLC-ESI)** : [M]⁺ Calcd. 509.3738; Found. 509.3736.

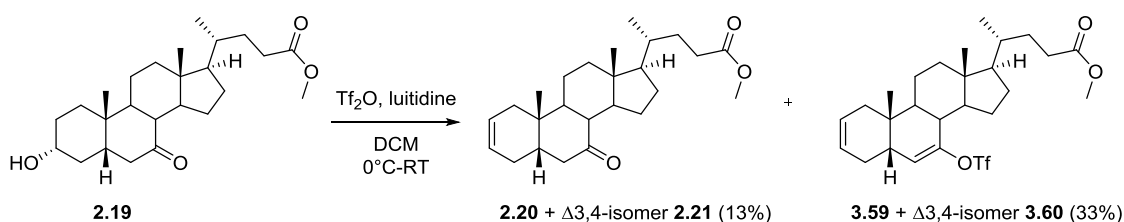
Methyl 7-oxo-5β-chol-2-eneoate (2.20) and methyl 7-oxo-5β-chol-3-eneoate (2.21)



Alcohol **2.19** (60 g, 148 mmol, 1.0 equiv) and DMAP (30 g, 122 mmol, 2.0 equiv) were dissolved in DCM (500 mL) and cooled to 0 °C on ice. Triflic anhydride (26.1 mL, 156 mmol, 1.05 equiv) was then added over the course of 15 mins. The reaction was stirred at 0 °C for 2 hours, although there was no reaction progress. Reaction was then slowly warmed to 10-12 °C and progress monitored *via* TLC. Deemed complete after 2 h, RM quenched with 2M HCl (500 mL) and stirred at RT for 10 mins. Layers separated and aqueous extracted with brine (500 mL), dried (Na₂SO₄) and concentrated to yield 78 g of a brown gummy solid. Crude purified *via* flash chromatography (Petrol ether/EtOAc : 95/5→90:10) to yield a mixture of alkenes **2.20** and **2.21** as a colourless gum (37.5 g, 97 mmol, 66%).

2.20 and **2.21: Formula:** C₂₅H₃₈O₃; **MW** 386.6; **m.p.** N/A; **R_f** (Petrol ether/EtOAc : 70/30) : 0.70; **¹H NMR** (400MHz, CDCl₃): δ 5.67 - 5.30 (m, 2H, H_{alkene}), 3.65 (s, 3H, CO₂CH₃), 2.89 - 2.79 (m, 1H, H_{6β}), 2.58 - 2.48 (m, 1H), 2.44 - 1.26 (m, 21H), 1.23 (s, 2H, H₁₉), 1.21 (s, 1H, H₁₉), 0.91 - 0.88 (m, 3H, H₂₁), 0.65 (m, 3H, H₁₈) ppm; **Selected ¹³C NMR** (100 MHz, CDCl₃): δ 212.6 (C7), 212.2 (C7), 174.6 (C24), 129.4 (C=C), 127.4 (C=C), 125.3 (C=C), 124.1 (C=C), 18.3 (C21), 12.0 (C18), 11.9 (C18) ppm; **MS (ESI+)** m/z : 387.2 [M+H]⁺, 404.2 [M+NH₄]⁺.

Methyl 7-oxo-5 β -chol-2-eneoate (2.20), methyl 7-oxo-5 β -chol-3-eneoate (2.21), methyl 7-trifluoromethylsulfonyloxy-5 β -chol-2,6-dieneoate (3.59) and methyl 7-trifluoromethylsulfonyloxy-5 β -chol-3,6-dieneoate (3.60)

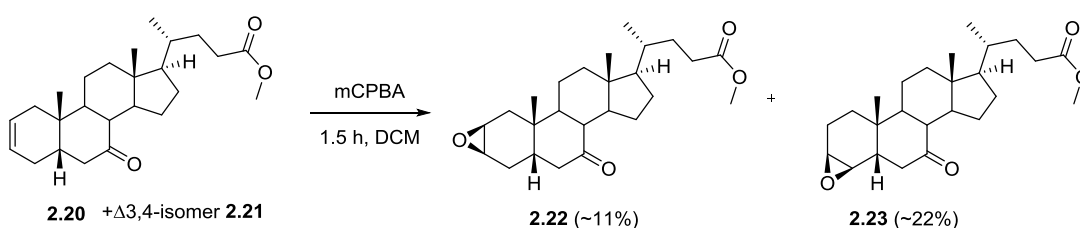


To a solution of alcohol **2.19** (500 mg, 1.24 mmol, 1equiv) in dry DCM (15 mL) was added lutidine (430 μL , 3.71 mmol, 3 equiv). The reaction mixture was cooled to 0°C before the slow addition of Tf_2O (230 μL , 1.36 mmol, 1.1 equiv) and allowed to warm to RT and stir O/N. Significant starting material remained, so further Tf_2O added (100 μL , 0.6 mmol, 0.5 equiv) and the reaction stirred for a further 4 h until completion. Organics washed with 2M HCl, 10% CuSO_4 , water and brine (10 mL each), dried (Na_2SO_4) and concentrated to yield 600 mg of a crude brown gum. Purified by flash chromatography (PE/EtOAc : 98:2 \rightarrow 88:12) to yield trifluoromethylsulfonyloxy derivatives **3.59** and **3.60** (211 mg, 0.41 mmol, 33 %) along with 7-keto alkene mixture **2.20** and **2.21** (60 mg, 13%).

2.20 and **2.21**: See above for characterisation.

3.59 and **3.60**: **Formula**: $\text{C}_{26}\text{H}_{37}\text{F}_3\text{O}_5\text{S}$; **MW** 518.6; **m.p.** N/A; **R_f** (PE/EtOAc : 75/25) : 0.86; **I.R.** 2951 (w), 2892 (w), 1740 (m), 1414 (m), 1244 (w), 1206 (s), 1142 (s), 898 (m) cm^{-1} ; **$^1\text{H NMR}$** (400MHz, CDCl_3): δ 5.96 - 5.26 (m, 3H, $3\times\text{C}=\text{CH}$), 3.67 (s, 3H, CO_2CH_3), 2.68 - 2.52 (m, 1H), 2.47 - 1.02 (m, 25H), 0.98 - 0.89 (m, 6H, H_{19} and H_{21}), 0.77 - 0.69 (m, 3H, H_{18}) ppm; **$^{13}\text{C NMR}$** (100 MHz, CDCl_3): δ 174.6 (C_{24}), 151.2 ($\text{C}=\text{C}-\text{OTf}$), 150.5 ($\text{C}=\text{C}-\text{OTf}$), 126.5, 125.7, 124.5, 124.1, 124.0, 120.8, 118.5 (q, $J=320.6$ Hz, CF_3), 54.7, 54.7, 53.4, 53.1, 51.5 (CO_2CH_3), 44.4, 44.4, 44.2, 42.7, 42.2, 41.3, 40.1, 39.91, 39.9, 39.6, 35.3, 35.2, 34.1, 32.5, 32.3, 31.4, 31.1, 31.0, 28.5, 28.5, 26.1, 26.0, 22.3 (C_{19}), 21.8, 21.6 (C_{19}), 21.4, 21.3, 18.4 (C_{21}), 12.3 (C_{18}), 12.2 (C_{18}) ppm; **$^{19}\text{F NMR}$** (376MHz, CDCl_3): δ -73.19 (s, 0.4F), -73.35 (s, 0.6F) ppm; **MS (ESI⁺)** m/z : 519.0 $[\text{M}+\text{H}]^+$, 554.1 $[\text{M}+\text{H}_2\text{O}+\text{NH}_4]^+$, 519.0 $[\text{M}+\text{H}_2\text{O}+\text{Na}]^+$; **HRMS (HPLC-ESI)** : $[\text{M}+\text{NH}_4]^+$ Calcd. 536.2652; Found. 536.2663.

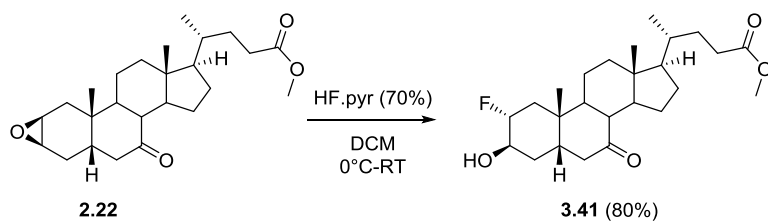
Methyl 2 β ,3 β -epoxy-7-oxo-5 β -cholanoate (2.22) and methyl 3 β ,4 β -epoxy-7-oxo-5 β -cholanoate (2.23)



The mixture of alkenes **2.20** and **2.21** (20 g, 51.8 mmol, 1 equiv) was dissolved in DCM (200 mL) at room temperature, before the addition of mCPBA (19.1 g, 77.7 mmol, 1.5 equiv). The reaction was deemed complete after 1.5 h, with the mixture changing from a solution to a suspension over the course of the reaction. The reaction was quenched with sat. aq. Na₂S₂O₃ (150 mL) and allowed to stir for 30 mins. Further DCM (200 mL) and H₂O (150 mL) added to aid solvation. Layers separated and aqueous extracted with further DCM (200 mL), then the combined organics were washed with sat. aq. NaHCO₃ (200 mL) and dried (Na₂SO₄) and concentrated to yield 20.5 g of a pale yellow, gummy solid. Crude purified *via* flash chromatography (Petrol ether/EtOAc : 92.5:7.5→92:8→80:10→88:12→80:20) to yield pure Δ3β,4β-epoxide **2.23** (2.00 g) along with 80% pure Δ2β,3β-epoxide **2.22** (1.85 g) and a significant amount of mixed fractions (8.5 g). The mixed fractions were re-purified (Petrol ether/EtOAc : 93:7→92:8→91:9→80:10→88:12→85:15→80:20) to yield pure Δ3β,4β-epoxide **2.23** (0.8 g) along with 80% pure Δ3β,4β-epoxide **2.23** (2.15 g) and 60% pure Δ2,3-epoxide **2.20** (1.30 g). Overall, Δ2β,3β-epoxide **2.22** was isolated as a white crystalline solid (~2.3 g, 5.8 mmol, 11%), along with Δ3β,4β-epoxide as a white solid **2.23** (~4.5 g, 11.3 mmol, 22%)

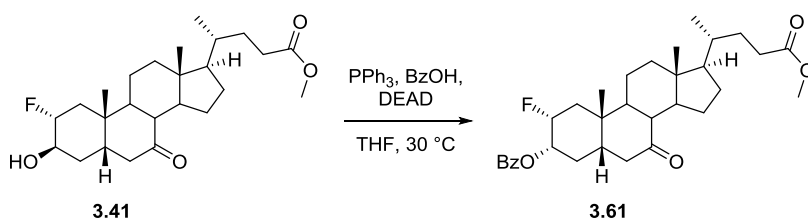
2.22: Formula: C₂₅H₃₈O₄; **MW** 402.6; **m.p.** 131 – 133°C; **R_f** (Petrol ether/EA : 75/25) : 0.39; **I.R** 2937 (m), 2874 (w), 1735 (s), 1707 (s), 1435 (m), 1166 (m), 813 (s) cm⁻¹; **¹H NMR** (400MHz, CDCl₃): δ 3.63 (s, 3H, CO₂CH₃), 3.13 - 3.09 (m, 1H, H₃), 2.98 (dd, *J*=5.3, 4.4 Hz, 1H, H₂), 2.78 (dd, *J*=12.3, 4.3 Hz, 1H, H_{6β}), 2.39 - 2.11 (m, 5H), 1.91 (m, 6H), 1.61 - 1.17 (m, 10H), 1.13 (s, 3H, H₁₉), 1.09 - 0.92 (m, 2H), 0.89 (d, *J*=6.5 Hz, 3H, H₂₁), 0.63 (s, 3H, H₁₈) ppm; **¹³C NMR** (100 MHz, CDCl₃): 212.0 (C₇), 174.5 (C₂₄), 54.6, 51.8 (C₃), 51.4 (CO₂CH₃), 50.2, 49.3 (C₂), 49.1, 44.3, 44.2 (C₆), 42.8, 39.0 (C₅), 38.9 (CH₂), 35.1, 34.1 (CH₂), 33.4, 30.9 (CH₂), 30.9 (CH₂), 28.2 (CH₂), 26.8 (CH₂), 24.8 (CH₂), 23.2 (C₁₉), 22.5 (CH₂), 18.3 (C₂₁), 12.1 (C₁₈) ppm; **MS (ESI+)** *m/z* : 403.1 [M+H]⁺, 425.2 [M+Na]⁺, 403.1 [M+H-MeCN]⁺; **HRMS** (HPLC-ESI) : [M+H]⁺ Calcd: 403.2843; Found: 403.2840.

2.23: Formula: C₂₅H₃₈O₄; **MW** 402.6; **m.p.** 114–115 °C; **R_f** (PE/EtOAc : 75/25) : 0.52; **I.R** 2935 (m), 2874 (w), 1736 (s), 1709 (s), 1439 (m), 1373 (m), 1238 (s), 1169 (m); **¹H NMR** (400MHz, CDCl₃): δ 3.64 (s, 3H, CO₂CH₃), 3.16 - 3.13 (m, 1H, H₃), 2.89 (dd, *J*=12.6, 7.0 Hz, 1H, H_{6β}), 2.82 (d, *J*=3.8 Hz, 1H, H₄), 2.42-1.17 (m, 24H), 1.13 (s, 3H, H₁₉), 0.89 (d, *J*=6.5 Hz, 3H, H₂₁), 0.64 (s, 3H, H₁₈) ppm; **¹³C NMR** (100 MHz, CDCl₃): δ 212.2 (C₇), 174.5 (C₂₄), 54.7, 54.5 (C₄), 53.1 (C₃), 51.4 (CO₂CH₃), 49.0, 48.6, 47.3 (C₅), 45.0, 44.0 (C₆), 42.3, 38.7 (CH₂), 35.1, 33.0, 30.9 (CH₂), 30.9 (CH₂), 28.1 (CH₂), 28.0 (CH₂), 24.6 (CH₂), 22.1 (C₁₉), 21.9 (CH₂), 20.1 (CH₂), 18.3 (C₂₁), 11.9 (C₁₈) ppm; **MS (ESI+)** *m/z* : 403.2 [M+H]⁺, 425.2 [M+Na]⁺; **HRMS** (HPLC-ESI) : [M+H]⁺ Calcd: 403.2843; Found: 403.2839.

Methyl 2 α -fluoro-3 β -hydroxy-7-oxo-5 β -cholanoate (3.41)

To a solution of epoxide **2.22** (830 mg, 2.06 mmol, 1 equiv) in dry DCM (25 mL) was cooled to 0 °C, before adding 70% HF.pyridine (830 μL) and allowing to warm to RT. Deemed complete after 2 d, reaction cooled to 0 °C again and carefully quenched with drop-wise addition of saturated NaHCO_3 (20 mL). Layers separated and aqueous extracted with further DCM (20 mL); combined organics washed with 2M HCl and brine (30 mL each), dried (Na_2SO_4) and concentrated to 840 mg of a white foamy solid. Crude purified *via* flash chromatography (PE/EtOAc : 70:30) to yield fluorohydrin **3.41** as a gummy solid (700 mg, 1.66 mmol, 80%).

3.41: Formula: $\text{C}_{25}\text{H}_{39}\text{FO}_4$; **MW** 422.6; **m.p.** N/A; **R_f** (PE/EtOAc : 60/40) : 0.30; **I.R.** 3459 (br. w), 2941 (m), 2875 (w), 1736 (m), 1707 (s), 1435 (m), 1201 (m), 1169 (m), 1051 (m); **¹H NMR** (400MHz, CDCl_3): δ .53 (dq, $J=47.0, 2.6$ Hz, 1H, H₂), 4.04 - 3.96 (m, 1H, H₃), 3.65 (s, 3H, CO_2CH_3), 2.87 (dd, $J=12.7, 6.1$ Hz, 1H, H_{6\beta}), 2.42 - 1.25 (m, 25H), 1.22 (s, 3H, H₁₉), 1.20-1.00 (m, 3H), 0.90 (d, $J=6.4$ Hz, 3H, H₂₁), 0.64 (s, 3H, H₁₈) ppm; **¹³C NMR** (100 MHz, CDCl_3): δ 212.8 (C₇), 174.7 (C₂₄), 91.3 (d, $J=171.7$ Hz, C₂), 67.0 (d, $J=29.3$ Hz, C₃), 54.6, 51.4, 49.8, 48.7, 45.0 (d, $J=4.4$ Hz), 44.8 (CH₂), 42.6, 40.5, 38.8 (CH₂), 35.6, 35.1, 34.3 (d, $J=18.3$ Hz, C₁), 31.0 (CH₂), 31.0 (CH₂), 30.6 (CH₂), 28.2 (CH₂), 24.8 (CH₂), 23.5 (C₁₉), 22.2 (CH₂), 18.3 (C₂₁), 12.0 (C₁₈) ppm; **¹⁹F NMR** (CDCl_3 , 376MHz): δ -184.60 (tt, $J=48.6, 8.7$ Hz) ppm; **[H]¹⁹F NMR** (CDCl_3 , 376MHz): δ -184.60 (s) ppm; **MS (ESI+)** m/z : 423.1 $[\text{M}+\text{H}]^+$, 445.1 $[\text{M}+\text{Na}]^+$, 845.5 $[\text{2M}+\text{H}]^+$; **HRMS** (HPLC-ESI) : $[\text{M}+\text{H}]^+$ Calcd. 423.2905; Found. 423.2907.

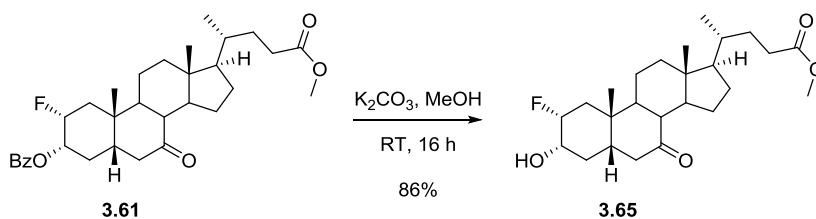
Methyl 2 α -fluoro-3 α -benzyloxy-7-oxo-5 β -cholanoate (3.61)

To a solution of alcohol **3.41** (1.05 g, 2.5 mmol, 1 equiv), PPh_3 (980 mg, 3.7 mmol, 1.5 equiv) and benzoic acid (450 mg, 3.7 mmol, 1.5 equiv) in dry THF (25 mL) was added DEAD (650 μL , 3.7 mmol, 1.5 equiv). The solution was allowed to stir at 30°C over the weekend, at which point crude ¹⁹F NMR indicated roughly 40% conversion to desired benzoate. Further PPh_3 , BzOH and DEAD (1.5

equiv each) was added and reaction allowed to stir O/N, at which point conversion was ≈60%. Further PPh₃, benzoic acid and DEAD (0.5 equiv each) added, stirred overnight and 80% conversion reached. More PPh₃, benzoic acid and DEAD (0.5 equiv each) added and stirred O/N once more, although no further progress noted. Solvent removed *in vacuo* and crude bright yellow material separated *via* flash chromatography (PE/EtOAc : 98:2→95:5→85:15→70:30→0:100) to yield 285 mg of the desired benzoate **3.61** (≈90% pure) along with 1.28 g of additional mixed fractions.

3.61: Formula: C₃₂H₄₃FO₅; **MW** 526.7; **m.p.** N/A; **R_f**(PE/EtOAc : 70/30) : 0.30; **I.R.** 2948 (m), 2874 (w), 1710 (s), 1270 (s), 1108 (m), 730 (m), 712 (s) cm⁻¹; **H NMR** (400MHz, CDCl₃): δ 8.04 (dd, *J*=7.8, 1.2 Hz, 2H, Ar-H_{ortho}), 7.56 (tt, *J*=7.6, 1.2 Hz, 1H, Ar-H_{para}), 7.44 (t, *J*=7.8 Hz, 2H, Ar-H_{meta}), 5.12 - 4.79 (m, 2H, H₂ + H₃), 3.67 (s, 3H, CO₂CH₃), 2.92 (dd, *J*=12.6, 5.9 Hz, 1H, H_{6β}), 2.53-1.29 (m, 21H), 1.26 (s, 3H, H₁₉), 1.24-1.04 (m, 4H), 0.93 (d, *J*=6.4 Hz, 3H, H₂₁), 0.67 (s, 3H, H₁₈) ppm; **¹³C NMR** (100 MHz, CDCl₃): δ 211.5 (C₃), 174.6 (C₂₄), 165.8 (C(O)Ph), 133.2 (Ar-C_{para}), 129.7 (2C, Ar-C_{ortho}), 128.3 (2C, Ar-C_{meta}), 128.1 (Ar-C_{ipso}), 89.2 (d, *J*=178.3 Hz, C₂), 72.8 (d, *J*=17.6 Hz, C₃), 54.7, 51.4 (CO₂CH₃), 49.9, 48.7, 46.2, 45.0 (C₆), 45.0 (d, *J*=5.9 Hz), 42.6, 38.7 (CH₂), 38.1 (d, *J*=18.3 Hz, C₁), 35.7, 35.2, 31.0 (CH₂), 31.0 (CH₂), 28.3 (CH₂), 28.2 (CH₂), 24.7 (CH₂), 23.1 (C₁₉), 22.5 (CH₂), 18.3 (C₂₁), 12.1 (C₁₈) ppm; **¹⁹F NMR** (CDCl₃, 376MHz): δ -199.45 (tdd, *J*=49.9, 28.6, 8.7 Hz) ppm; **[H]¹⁹F NMR** (CDCl₃, 376MHz): δ -199.45 (s) ppm; **MS (ESI+)** *m/z* : 527.2 [M+H]⁺, 544.1 [M+NH₄]⁺, 549.1 [M+Na]⁺; **HRMS (HPLC-ESI)** : [M+NH₄]⁺ Calcd. 544.3433; Found. 544.3444.

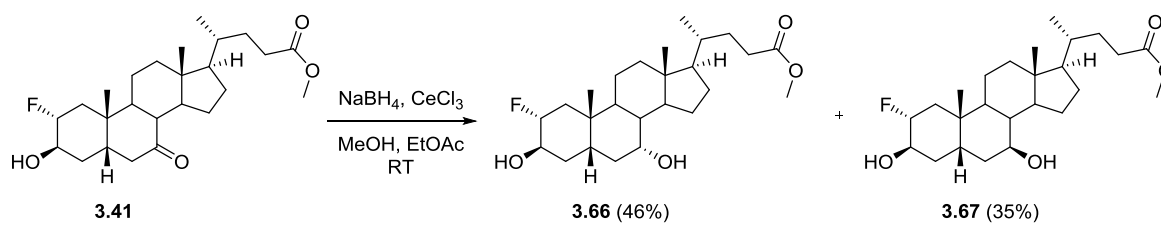
Methyl 2α-fluoro-3α-hydroxy-7-oxo-5β-cholanoate (3.65)



Using method of Zhao *et al.*^[127] A mixture of benzoate **3.61** (400 mg, 0.76 mmol, 1 equiv) and potassium carbonate (20 mg, 0.15 mmol, 0.2 equiv) were suspended in dry MeOH (20 mL) and allowed to stir for 16 h at RT. After 16 h reaction mixture had formed a colourless solution, and was deemed complete by TLC analysis. Solvent removed *in vacuo* and crude residue taken up between EtOAc/H₂O (5 mL each) and aqueous extracted with further EtOAc (2×5 mL). Combined organics dried (Na₂SO₄) and concentrated to yield 320 mg of a pale gum. Crude purified *via* flash chromatography (PE/acetone : 70:30) to yield the desired fluorohydrin **3.65** (275 mg, 0.65 mmol, 86%) as a gummy solid.

3.65: Formula: C₂₅H₃₉FO₅; **MW** 422.6; **m.p.** N/A; **R_f** (PE/EtOAc : 70/30) : 0.12; **I.R.** 3411 (br. w), 2924 (m), 2872 (w), 1732 (s), 1708 (s), 1075 (m), 911 (m), 728 (s) cm⁻¹; **¹H NMR** (400MHz, CDCl₃): δ 4.71 (d, *J*=52.0 Hz, 1H, H₂), 3.62 (s, 3H, CO₂CH₃), 3.59 - 3.45 (m, 1H, H₃), 2.84 (dd, *J*=12.5, 6.0 Hz, 1H, H_{6β}), 2.43 (d, *J*=8.3 Hz, 1H, C3-OH), 2.39 - 2.26 (m, 3H), 2.24 - 2.08 (m, 2H), 2.01 - 1.20 (m, 18H), 1.18 (s, 3H, H₁₉), 1.14 - 1.02 (m, 3H), 0.88 (d, *J*=6.5 Hz, 3H, H₂₁), 0.61 (s, 3H, H₁₈) ppm; **¹³C NMR** (100 MHz, CDCl₃): δ 211.8 (C₇), 174.6 (C₂₄), 92.0 (d, *J*=173.1 Hz, C₂), 70.6 (d, *J*=19.8 Hz, C₃), 54.6, 51.4 (CO₂CH₃), 49.7, 48.6, 46.1, 45.0 (C₆), 44.9 (d, *J*=5.9 Hz), 42.4, 38.7 (CH₂), 38.0 (d, *J*=19.1 Hz, C₁), 35.2 (d, *J*=1.5 Hz), 35.1, 31.9 (CH₂), 30.9 (CH₂), 30.9 (CH₂), 28.1 (CH₂), 24.6 (CH₂), 23.0 (C₁₉), 22.3 (CH₂), 18.2 (C₂₁), 11.9 (C₁₈) ppm; **¹⁹F NMR** (CDCl₃, 376MHz): δ -202.32 (tdd, *J*=51.2, 29.5, 8.7 Hz) ppm; **[H]¹⁹F NMR** (CDCl₃, 376MHz): δ -202.32 (s) ppm; **MS (ESI+)** *m/z* : 423.4 [M+H]⁺; **HRMS** (HPLC-ESI) : [M+Na]⁺ Calcd. 445.2725; Found. 445.2719.

Methyl 2α-fluoro-3β,7α-dihydroxy-5β-cholanoate (3.66) and methyl 2α-fluoro-3β,7β-dihydroxy-5β-cholanoate (3.67)

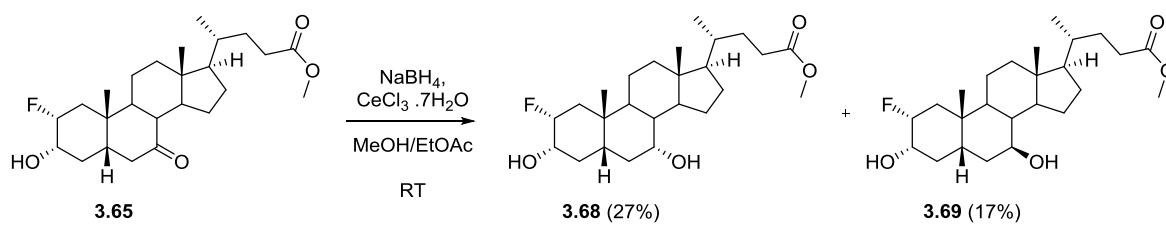


Using procedure G, ketone **3.41** (300 mg, 0.71 mmol, 1 equiv) was reduced. Crude material purified *via* flash chromatography (PE/EtOAc : 65:35→55:45) to yield 7α-OH **3.66** (140 mg, 0.33 mmol, 46%) and 7β-OH **3.67** (107 mg, 0.25 mmol, 35%).

3.66: Formula: C₂₅H₄₁FO₄; **MW** 424.6; **m.p.** 61 - 62 °C; **R_f** (PE/EtOAc : 55/45) : 0.32; **I.R.** 3446 (br. w), 2936 (s), 2871 (m), 1722 (s), 1436 (m), 1048 (s), 1009 (s), 735 (w) cm⁻¹; **¹H NMR** (400MHz, CDCl₃): δ 4.55 (dq, *J*=47.4, 2.8 Hz, 1H, H₂), 4.00 (dq, *J*=7.2, 3.4 Hz, 1H, H₃), 3.86 (q, *J*=2.6 Hz, 1H, H₇), 3.66 (s, 3H, CO₂CH₃), 2.72 (tt, *J*=14.3, 2.4 Hz, 1H, H_{4α}), 2.35 (ddd, *J*=15.5, 11.0, 5.0 Hz, 1H, H₂₃), 2.22 (ddd, *J*=15.7, 9.4, 6.5 Hz, 1H, H_{23'}), 2.11 - 1.06 (m, 27H), 0.97 (s, 3H, H₁₉), 0.92 (d, *J*=6.5 Hz, 3H, H₂₁), 0.66 (s, 3H, H₁₈) ppm; **¹³C NMR** (100 MHz, CDCl₃): δ 174.8 (C₂₄), 92.1 (d, *J*=171.7 Hz, C₂), 68.5 (C₇), 67.9 (d, *J*=27.9 Hz, C₃), 55.7, 51.5 (CO₂CH₃), 50.3, 42.7, 39.6, 39.5 (CH₂), 35.6, 35.4, 35.3, 35.3, 35.3 (d, *J*=18.3 Hz, seen in D135 NMR, C₁), 34.0 (CH₂), 32.9 (C₄), 31.0 (C₂₃), 31.0 (CH₂), 28.1 (CH₂), 23.7 (CH₂), 23.1 (C₁₉), 21.2 (CH₂), 18.2 (C₂₁), 11.8 (C₁₈) ppm; **¹⁹F NMR** (376MHz, CDCl₃): δ -184.70 (tt, *J*=48.6, 8.7 Hz) ppm; **[H]¹⁹F NMR** (376MHz, CDCl₃): δ -184.70 (s) ppm; **MS (ESI+)** *m/z* : 447.3 [M+Na]⁺; **HRMS** (HPLC-ESI) : [M+NH₄]⁺ Calcd. 442.3327; Found. 442.3316.

3.67: Formula: C₂₅H₄₁FO₄; **MW** 424.6; **m.p.** N/A; **R_f**(Petrol ether/EA : 55/45) : 0.18; **I.R.** 3414 (br. w), 2938 (m), 2874 (w), 1721 (m), 1437 (w), 1034 (m), 732 (s) cm⁻¹; **¹H NMR** (400MHz, CDCl₃): δ 4.50 (dq, *J*=47.3, 2.8 Hz, 1H, H₂), 3.95 (dq, *J*=7.2, 3.4 Hz, 1H, H₃), 3.63 (s, 3H, CO₂CH₃), 3.55 (td, *J*=9.7, 5.1 Hz, 1H, H₇), 2.32 (ddd, *J*=15.4, 10.2, 5.0 Hz, 1H, H₂₃), 2.19 (ddd, *J*=15.6, 9.4, 6.5 Hz, 1H, H_{23'}), 2.11 - 1.02 (m, 27H), 0.96 (s, 3H, H₁₉), 0.90 (d, *J*=6.4 Hz, 3H, H₂₁), 0.65 (s, 3H, H₁₈) ppm; **¹³C NMR** (100 MHz, CDCl₃): δ 174.8 (C₂₄), 92.1 (d, *J*=170.9 Hz, C₂), 71.6 (C₇), 67.4 (d, *J*=27.9 Hz, C₃), 55.6 (C₈), 54.7, 51.4 (CO₂CH₃), 43.6, 43.4, 41.6 (d, *J*=3.7 Hz), 39.8 (C_H₂), 36.3 (C₆), 36.2, 35.1, 35.1 (d, *J*=18.3 Hz, C₁), 34.9, 30.9 (C₂₃), 30.9 (C_H₂), 30.7 (C_H₂), 28.5 (C_H₂), 26.6 (C_H₂), 23.6 (C₁₉), 21.7 (C_H₂), 18.3 (C₂₁), 12.0 (C₁₈) ppm; **¹⁹F NMR** (376MHz, CDCl₃): δ -184.43 (tt, *J*=47.7, 8.7 Hz) ppm; **[H]¹⁹F NMR** (376MHz, CDCl₃): δ -184.43 (s) ppm; **MS (ESI+)** *m/z* : 447.2 [M+Na]⁺; **HRMS** (HPLC-ESI) : [M+NH₄]⁺ Calcd. 442.3327; Found. 442.3334.

Methyl 2α-fluoro-3α,7α-dihydroxy-5β-cholanoate (3.68) and methyl 2α-fluoro-3α,7β-dihydroxy-5β-cholanoate (3.69)



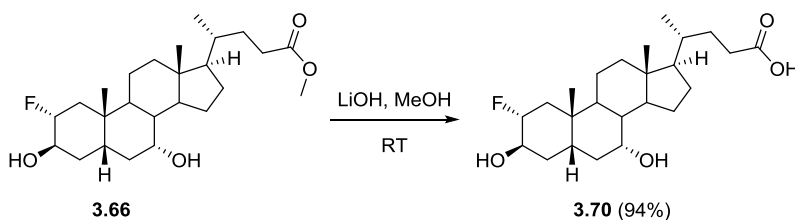
Using procedure D, ketone **3.65** (270 mg, 0.64 equiv, 1 equiv) was reduced. Crude purified *via* flash chromatography (PE/acetone : 75:25) to yield 33mg of pure 7α-OH analogue **3.68** along with 140 mg of a mixture of both 7α-OH **3.68** and 7β-OH **3.69** epimers. The mixture was re-purified *via* flash chromatography (PE/EtOAc : 60:40→50:50) to yield further pure 7α-OH analogue **3.68** (total - 74 mg, 0.17 mmol, 27%) and pure 7β-OH analogue **3.69** (45 mg, 0.11 mmol, 17%), both as gummy solids.

3.68: Formula: C₂₅H₄₁FO₄; **MW** 424.6; **m.p.** N/A; **R_f**(PE/Acetone : 70/30) : 0.33; **I.R.** 3404 (br. w), 2934 (s), 2867 (m), 1736 (s), 1435 (m), 1084 (s), 732 (s); **¹H NMR** (400MHz, CDCl₃): δ 4.67 (d, *J*=52.1 Hz, 1H, H₂), 3.78 (q, *J*=2.4 Hz, 1H, H₇), 3.59 (s, 3H, CO₂CH₃), 3.37 (dddd, *J*=28.5, 12.0, 4.4, 2.5 Hz, 1H, H₃), 2.46 (q, *J*=13.0 Hz, 1H, H_{4α}), 2.37 - 2.23 (m, 2H), 2.20 - 2.10 (m, 1H), 2.04 - 0.88 (m, 27H), 0.88 - 0.83 (m, 6H, H₁₉ with H₂₁), 0.59 (s, 3H, H₁₈) ppm; **¹³C NMR** (100 MHz, CDCl₃): δ 174.7 (C₂₄), 93.0 (d, *J*=172.4 Hz, C₂), 71.8 (d, *J*=19.8 Hz, C₃), 68.3 (C₇), 55.7, 51.4 (CO₂CH₃), 50.4, 42.7, 41.6, 39.7, 39.5 (C_H₂), 39.1 (d, *J*=19.1 Hz, C₁), 35.3, 35.3 (d, *J*=1.5 Hz), 35.2 (d, *J*=4.4 Hz), 34.3 (C_H₂), 34.1 (d, *J*=1.5 Hz, C₄), 31.0 (C_H₂), 31.0 (C_H₂), 28.1 (C_H₂), 23.6 (C_H₂), 22.9 (C₁₉), 21.3 (C_H₂), 18.2 (C₂₁), 11.8 (C₁₈) ppm; **¹⁹F NMR** (CDCl₃, 376MHz): δ -202.71 (tdd, *J*=52.0, 27.7, 8.7 Hz) ppm; **[H]¹⁹F**

NMR (CDCl₃, 376MHz): δ -202.60 (s) ppm; **MS (ESI+)** m/z : 407.4 [M+H-H₂O]⁺, 387.3 [M+H-H₂O-HF]⁺; **HRMS** (HPLC-ESI) : [M+NH₄]⁺ Calcd. 442.3327; Found. 442.3325.

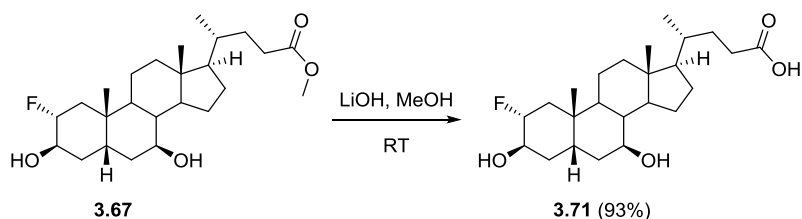
3.69: Formula: C₂₅H₄₁FO₄; **MW** 424.6; **m.p.** N/A; **R_f**(PE/Acetone : 70/30) : 0.24; **I.R.** 3380 (br. w), 2929 (s), 2867 (m), 1737 (s), 1436 (m), 1261 (m), 1080 (s), 1061 (s), 1038 (s), 731 (s); **¹H NMR** (400MHz, CDCl₃): δ 4.74 (d, *J*=52.1 Hz, 1H, H₂), 3.66 (s, 3H, CO₂CH₃), 3.63 - 3.35 (m, 2H, H₇ and H₃), 2.43 - 2.29 (m, 2H, H₁ α or H₁ β , and H₂₃), 2.28 - 2.14 (m, 1H, H₂₃'), 2.08 - 1.00 (m, 29H), 0.96 (s, 3H, H₁₉), 0.92 (d, *J*=6.2 Hz, 3H, H₂₁), 0.67 (s, 3H, H₁₈) ppm; **¹³C NMR** (100 MHz, CDCl₃): δ 174.7 (CO₂CH₃), 92.8 (d, *J*=172.4 Hz, 1C), 71.4 (C₇), 71.2 (d, *J*=19.1 Hz, C₂), 55.5, 54.8, 51.5 (CO₂CH₃), 43.9, 43.7, 42.5, 41.4 (d, *J*=5.1 Hz, 1C), 39.9 (CH₂), 38.8 (d, *J*=18.3 Hz, C₁), 36.7 (CH₂), 35.2, 34.5 (d, *J*=1.5 Hz, C₁₀), 32.1 (CH₂), 31.0 (C₂₃), 31.0 (CH₂), 28.6 (CH₂), 26.8 (CH₂), 23.5 (C₁₉), 21.9 (CH₂), 18.3 (C₂₁), 12.1 (C₁₈) ppm; **¹⁹F NMR** (CDCl₃, 376MHz): δ -202.49 (tdd, *J*=52.0, 29.5, 8.7 Hz) ppm; **[¹H]¹⁹F NMR** (CDCl₃, 376MHz): δ -202.49 (s) ppm; **MS (ESI+)** m/z 407.4 [M+H-H₂O]⁺, 387.3 [M+H-H₂O-HF]⁺; **HRMS** (HPLC-ESI) : [M+NH₄]⁺ Calcd. 442.3327; Found. 442.3328.

2 α -fluoro-3 β ,7 α -dihydroxy-5 β -cholanic acid (3.70)



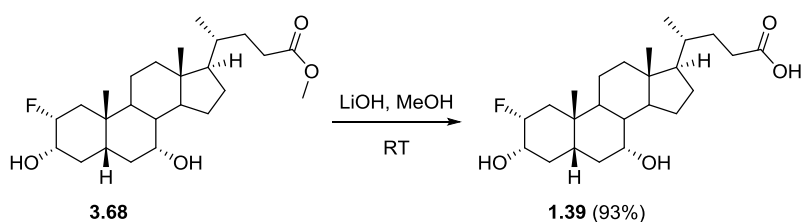
Using procedure B, methyl ester **3.66** (105 mg, 0.25 mmol, 1 equiv) was hydrolysed to yield **3.70** (96 mg, 0.23 mmol, 94%) as a pale solid.

3.70: Formula: C₂₄H₃₉FO₄; **MW** 410.6; **[α]_D** -2.6 (c 0.5, MeOH, 23 °C); **m.p.** 95–96 °C; **R_f** (Petrol ether/acetone : 60/40) : 0.28; **I.R.** 3424 (br. w), 2935 (s), 2871 (m), 1703 (s), 1437 (w), 1253 (m), 1074 (m), 1009 (m) cm⁻¹; **¹H NMR** (400MHz, acetone-D₆): δ 10.51 (br. s., 1H, COOH), 4.58 (dq, *J*=48.0, 2.7 Hz, 1H, H₂), 3.96 (dq, *J*=7.2, 3.4 Hz, 1H, H₃), 3.91 (q, *J*=2.8 Hz, 1H, H₇), 2.89 (tt, *J*=14.2, 2.6 Hz, 1H, H_{4 α}), 2.43 (ddd, *J*=15.5, 10.7, 5.3 Hz, 1H, H₂₃), 2.30 (ddd, *J*=15.0, 9.4, 6.7 Hz, 1H, H₂₃'), 2.20 - 2.06 (m, 4H), 2.01 - 1.13 (m, 21H), 1.11 - 0.97 (m, 6H, H₂₁ + H₁₉), 0.78 (s, 3H, H₁₈) ppm; **¹³C NMR** (100 MHz, acetone-D₆): δ 175.4 (C₂₄), 93.3 (d, *J*=170.9 Hz, C₂), 68.2 (C₇), 67.9 (d, *J*=27.1 Hz, C₃), 56.9, 51.2, 43.3, 40.8, 40.7 (CH₂), 36.5, 36.4, 36.3, 36.0 (d, *J*=3.7 Hz), 36.1 (d, *J*=19.1 Hz, C₁), 35.5 (CH₂), 33.7 (C₄), 31.9 (CH₂), 31.3 (C₂₃), 29.0 (CH₂), 24.3 (CH₂), 23.8 (C₁₉), 22.2 (CH₂), 18.8 (C₂₁), 12.3 (C₁₈) ppm; **¹⁹F NMR** (376MHz, acetone-D₆): δ -184.37 (tt, *J*=49.4, 8.7 Hz) ppm; **[¹H]¹⁹F NMR** (376MHz, acetone-D₆): δ -184.37 (s) ppm; **MS (ESI-)** m/z : 409.1 [M-H]⁻, 819.5 [M-H]⁻; **HRMS** (HPLC-ESI) : [M+NH₄]⁺ Calcd. 428.3171; Found. 428.3177.

2 α -fluoro-3 β ,7 β -dihydroxy-5 β -cholanic acid (3.71)

Using procedure B, methyl ester **3.67** (90 mg, 0.21 mmol, 1 equiv) was hydrolysed to yield **3.71** (80 mg, 0.19 mmol, 93%) as a colourless solid.

3.71: Formula: C₂₄H₃₉FO₄; **MW** 410.6; [α]_D +39.1 (c 0.5, MeOH, 23 °C); **m.p.** 105–107 °C; **R_f** (Petrol ether/acetone : 60/40) : 0.27; **I.R.** 3401 (br. w), 2936 (m), 2876 (w), 1697 (s), 1246 (s), 1044 (s), 1031 (m) cm⁻¹; **¹H NMR** (400MHz, acetone-D₆): δ 10.43 (br. s., 1H acetone-D₆), 4.58 (dq, $J=48.0, 3.1$ Hz, 1H, H₂), 3.99 (dq, $J=7.1, 3.3$ Hz, 1H, H₃), 3.57 (tdd, $J=10.2, 5.0, 1.0$ Hz, 1H, H₇), 2.42 (ddd, $J=15.5, 11.0, 5.0$ Hz, 1H, H₂₃), 2.29 (ddd, $J=15.8, 9.2, 6.8$ Hz, 1H, H_{23'}), 2.22 - 2.06 (m, 4H), 2.04 - 1.14 (m, 23H), 1.07 (s, 3H, H₁₉), 1.05 (d, $J=6.6$ Hz, 3H, H₂₁), 0.79 (s, 3H, H₁₈) ppm; **¹³C NMR** (100 MHz, acetone-D₆): δ 175.3 (C₂₄), 93.3 (d, $J=170.9$ Hz, C₂), 71.4 (C₇), 67.7 (d, $J=27.1$ Hz, C₃), 57.2, 56.1, 44.4, 44.4, 42.5, 41.1 (C_H₂), 38.3 (C_H₂), 37.4, 36.2, 35.8 (d, $J=18.3$ Hz, C₁), 35.7, 31.9 (C_H₂), 31.6 (C_H₂), 31.3 (C₂₃), ~29.3 (CH₂ – can see in D135 but not ¹³C), 27.7 (C_H₂), 24.4 (C₁₉), 22.8 (C_H₂), 18.9 (C₂₁), 12.7 (C₁₈) ppm; **¹⁹F NMR** (376MHz, acetone-D₆): δ -184.29 (tt, $J=49.4, 8.7$ Hz) ppm; **[¹H]¹⁹F NMR** (376MHz, acetone-D₆): δ -184.30 (s) ppm; **MS (ESI-)** m/z : 409.1 [M-H]⁻, 819.5 [2M-H]⁻; **HRMS (HPLC-ESI)** : [M+Na]⁺ Calcd. 433.2725; Found. 433.2719.

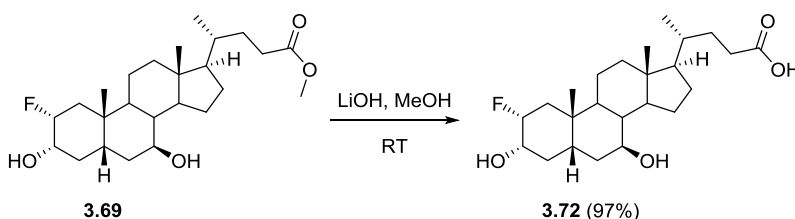
2 α -fluorocholeodeoxycholic acid (1.39)

Using procedure B, methyl ester **3.68** (74 mg, 0.17 mmol, 1 equiv) was hydrolysed to yield **1.39** (65 mg, 0.16 mmol, 93%) as a colourless solid.

1.39: Formula: C₂₄H₃₉FO₄; **MW** 410.6; [α]_D -9.0 (c 0.5, MeOH, 23 °C); **m.p.** 100–101 °C; **R_f** (Petrol ether/acetone : 60/40) : 0.22; **I.R.** 3307 (br. w), 2935 (s), 2869 (m), 1708 (s), 1376 (w), 1081 (m), 1051 (w) cm⁻¹; **¹H NMR** (400MHz, acetone-D₆): δ 4.65 (dq, $J=52.3, 1.7$ Hz, 1H, H₂), 3.81 (q, $J=2.8$ Hz, 1H, H₇), 3.40 (dddd, $J=29.7, 12.0, 3.9, 2.1$ Hz, 1H, H₃), 2.69 (q, $J=12.6$ Hz, 1H, H_{4 α}), 2.39 - 2.16 (m, 3H, H₂₃ and H_{23'} + H_{1 α} or H_{1 β}), 2.02 - 1.01 (m, 25H), 0.98 - 0.91 (m, 6H, H₁₉ with H₂₁), 0.69 (s, 3H,

$\underline{H18}$) ppm; ^{13}C NMR (100 MHz, acetone- D_6): δ 175.2 ($\underline{C24}$), 94.0 (d, $J=173.9$ Hz, $\underline{C2}$), 72.3 (d, $J=19.1$ Hz, $\underline{C3}$), 67.9 ($\underline{C7}$), 57.0, 51.3, 43.3, 43.0, 40.8, 40.7 ($\underline{CH_2}$), 40.0 (d, $J=18.3$ Hz, $\underline{C1}$), 36.3, 36.3 (d, $J=1.5$ Hz), 36.0 (d, $J=5.1$ Hz), 35.9 ($\underline{CH_2}$), 34.9 (d, $J=2.2$ Hz, $\underline{C4}$), 31.9 ($\underline{CH_2}$), 31.2 ($\underline{C23}$), 29.0 ($\underline{CH_2}$), 24.3 ($\underline{CH_2}$), 23.4 ($\underline{C19}$), 22.3 ($\underline{CH_2}$), 18.8 ($\underline{C21}$), 12.3 ($\underline{C18}$) ppm; ^{19}F NMR (376MHz, acetone- D_6): δ -200.79 (tdd, $J=51.2, 29.5, 8.7$ Hz) ppm; $[\text{}^1\text{H}]^{19}\text{F}$ NMR (376MHz, acetone- D_6): δ -200.79 (s) ppm; MS (ESI-) m/z : 841.4 $[\text{2M+H}]^+$, 393.4 $[\text{M+H-H}_2\text{O}]^+$, 375.4 $[\text{M+H-H}_2\text{O-HF}]^+$, 373.4 $[\text{M+H-2H}_2\text{O}]^+$; HRMS (HPLC-ESI) : $[\text{M-H}]^-$ Calcd. 409.2760; Found. 409.2752.

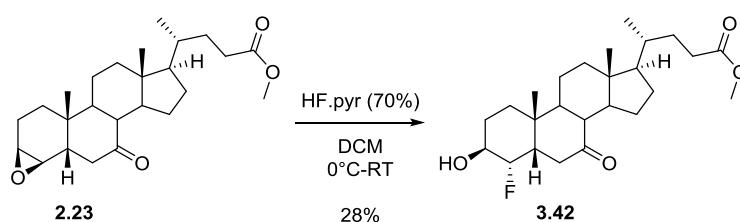
2 α -fluoroursodeoxycholic acid (**3.72**)



Using procedure B, **3.69** (44 mg, 0.10 mmol, 1 equiv) was hydrolysed to yield **3.72** (40 mg, 0.97 mmol, 97%) as a colourless solid.

3.72: Formula: $\text{C}_{24}\text{H}_{39}\text{FO}_4$; **MW** 410.6; $[\alpha]_{\text{D}}$ +28.8 (c 0.25, MeOH, 23 °C); **m.p.** 108–109 °C; **R_f** (Petrol ether/acetone : 60/40) : 0.22; **I.R.** 3371 (br. w), 2933 (s), 2869 (m), 1703 (s), 1377 (m), 1246 (m), 1057 (m), 1040 (m) cm^{-1} ; ^1H NMR (400MHz, acetone- D_6): δ 4.67 (dq, $J=52.1, 1.7$ Hz, 1H, $\underline{H2}$), 3.61 - 3.42 (m, 2H, $\underline{H3+H7}$), 2.39 - 2.15 (m, 3H, $\underline{H23}$ and $\underline{H23'}$ + $\underline{H1}_\alpha$ or $\underline{H1}_\beta$), 2.02 - 1.06 (m, 29H), 0.99 - 0.93 (m, 6H, $\underline{H19}$ with $\underline{H21}$), 0.70 (s, 3H, $\underline{H18}$) ppm; ^{13}C NMR (100 MHz, acetone- D_6): δ 175.2 ($\underline{C24}$), 93.9 (d, $J=174.6$ Hz, $\underline{C2}$), 71.6 (d, $J=18.3$ Hz, $\underline{C3}$), 71.3 ($\underline{C7}$), 57.2, 56.1, 44.6, 44.4, 43.8, 42.5 (d, $J=5.1$ Hz), 41.1 ($\underline{CH_2}$), 39.7 (d, $J=19.1$ Hz, $\underline{C1}$), 38.7 ($\underline{CH_2}$), 36.2, 35.4 (d, $J=1.5$ Hz), 32.7 ($\underline{CH_2}$), 32.0 ($\underline{CH_2}$), 31.3 ($\underline{CH_2}$), 29.4 ($\underline{CH_2}$, only visible in D135 NMR), 27.8 ($\underline{CH_2}$), 24.0 ($\underline{C19}$), 22.9 ($\underline{CH_2}$), 18.9 ($\underline{C21}$), 12.7 ($\underline{C18}$) ppm; ^{19}F NMR (376MHz, acetone- D_6): δ -200.58 (tdd, $J=50.7, 30.3, 6.9$ Hz) ppm; $[\text{}^1\text{H}]^{19}\text{F}$ NMR (376MHz, acetone- D_6): δ -200.58 (s) ppm; MS (ESI-) m/z : 393.4 $[\text{M+H-H}_2\text{O}]^+$, 375.4 $[\text{M+H-H}_2\text{O-HF}]^+$, 373.4 $[\text{M+H-2H}_2\text{O}]^+$; HRMS (HPLC-ESI) : $[\text{M-H}]^-$ Calcd. 409.2760; Found. 409.2770.

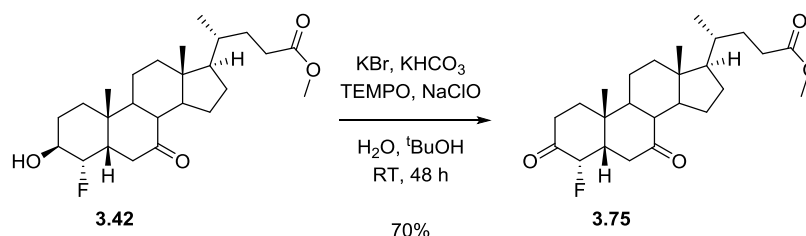
Methyl 4 α -fluoro-3 β -hydroxy-7-oxo-5 β -cholanoate (**3.42**)



A solution of epoxide **2.23** (1.3 g, 3.2 mmol, 1 equiv) in dry DCM (7 mL) was cooled to 0 °C before the careful, drop-wise addition of 70% HF.pyridine (3 mL) and allowed to warm to RT. Reaction deemed complete after 2 hr, reaction cooled to 0 °C before quenching slowly with sat. NaHCO₃ (25 mL). Aqueous extracted with DCM (2×30 mL), combined organics washed with 2M HCl and brine (40 mL) each, dried (Na₂SO₄) and concentrated to yield 1.25 g of a pale foam. Crude purified *via* flash chromatography (PE/EtOAc : 70:30) to yield desired fluorohydrin **3.42** as a gummy solid (385 mg, 0.91 mmol, 28%).

3.42: Formula: C₂₅H₃₉FO₄; **MW** 422.6; **m.p.** N/A; **R_f**(PE/EtOAc : 60/40) : 0.22; **I.R.** 3464 (br. w), 2942 (m), 2874 (w), 1735 (s), 1711 (s), 1436 (w), 1170 (m), 730 (s) cm⁻¹; **¹H NMR** (400MHz, CDCl₃): δ 4.50 (dt, *J*=46.9, 2.6 Hz, 1H, H₄), 4.06 (dqin, *J*=7.2, 3.4 Hz, 1H, H₃), 3.66 (s, 3H, CO₂CH₃), 2.79 (dd, *J*=14.5, 7.7 Hz, 1H, H_{6β}), 2.48 - 1.25 (m, 30H), 1.21 (s, 3H, H₁₉), 1.18 - 0.98 (m, 4H), 0.91 (d, *J*=6.4 Hz, 3H, H₂₁), 0.65 (s, 3H, H₁₈) ppm; **¹³C NMR** (100 MHz, CDCl₃): δ 211.3 (C₇), 174.7 (C₂₄), 95.3 (d, *J*=176.1 Hz, C₄), 67.1 (d, *J*=28.6 Hz, C₃), 54.5, 51.5 (CO₂C₃), 49.3, 49.0, 44.6 (d, *J*=17.6 Hz, C₅), 43.8 (d, *J*=5.1 Hz), 43.0, 41.8 (d, *J*=2.2 Hz, C₆), 38.8 (CH₂), 35.5, 35.2, 31.0 (CH₂), 31.0 (CH₂), 28.5 (CH₂), 28.3 (CH₂), 25.3 (CH₂), 23.4 (C₁₉), 23.4 (CH₂), 22.2 (CH₂), 18.4 (C₂₁), 12.1 (C₁₈) ppm; **¹⁹F NMR** (CDCl₃, 376MHz): δ -186.11 (t, *J*=43.3 Hz) ppm; **[¹H]¹⁹F NMR** (CDCl₃, 376MHz): δ -186.11 (s) ppm; **MS (ESI+)** *m/z* : 423.0 [M+H]⁺, 845.3 [2M+H]⁺, 867.3 [2M+Na]⁺; **HRMS** (HPLC-ESI) : [M+H]⁺ Calcd. 423.2905; Found. 423.2906.

Methyl 4α-fluoro-3,7-dioxo-5β-cholanoate (3.75)

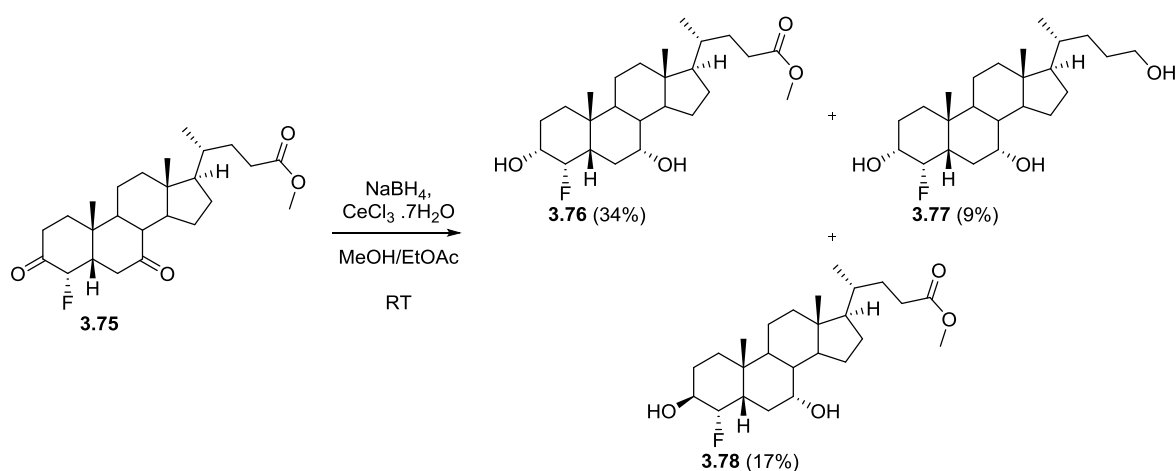


To a solution of Fluorohydrin **3.42** (95 mg, 0.22, 1 equiv), KBr (85 mg, 0.45 mmol, 2 equiv), KHCO₃ (225 mg, 2.2 equiv, 10 equiv) and TEMPO (55 mg, 0.34 mmol, 1.5 equiv) in ^tBuOH (5 mL) and H₂O (1.5 mL) was added 11% NaClO soln. (3.0 mL, 4.5 mmol, 20 equiv). Progress was monitored *via* TLC, and the reaction was deemed complete after stirring for 48 h at RT. The reaction mixture was quenched with Na₂S₂O₃ soln. (3.5g in 20 mL H₂O), the aqueous extracted with EtOAc (3×15 mL) and combined organics washed with brine, dried (Na₂SO₄) and concentrated to yield 105 mg of a thick red oil. Crude purified *via* flash chromatography (PE/EtOAc : 55/45) to yield di keto product **3.75** (65 mg, 0.15 mmol, 70%) as a gummy solid.

3.75: Formula: C₂₅H₃₇FO₄; **MW** 420.6; **m.p.** N/A; **R_f**(PE/EtOAc : 55/45) : 0.17; **I.R.** 2948 (m), 2873 (w), 1734 (s), 1716 (s), 1435 (w), 1262 (w), 1164 (m) cm⁻¹; **H NMR** (400MHz, CDCl₃): δ 44.66 (dd,

$J=2.8$, 50.4 Hz, 1H, H_4), 3.67 (s, 3H, CO_2CH_3), 2.86 - 2.69 (m, 2H, $H_{6\beta}$ and $H_{2\alpha}$), 2.49 - 1.29 (m, 22H), 1.27 (s, 3H, H_{19}), 1.25 - 1.04 (m, 4H), 0.94 (d, $J=6.5$ Hz, 3H, H_{21}), 0.69 (s, 3H, H_{18}) ppm; ^{13}C NMR (100 MHz, $CDCl_3$): δ 209.8 (C_7), 205.1 (d, $J=19.8$ Hz, C_3), 174.6 (C_{24}), 95.3 (d, $J=183.4$ Hz, C_4), 54.6, 51.5 (CO_2CH_3), 50.7 (d, $J=19.1$ Hz, C_5), 49.6, 48.8, 44.1 (d, $J=4.4$ Hz, 1C), 43.0, 41.0 (d, $J=3.7$ Hz, C_6), 38.8 (CH_2), 35.9, 35.5 (CH_2), 35.2, 33.9 (d, $J=2.2$ Hz, C_2), 31.1 (CH_2), 31.0 (CH_2), 28.3 (CH_2), 25.3 (CH_2), 22.9 (C_{19}), 22.4 (CH_2), 18.4 (C_{21}), 12.1 (C_{18}) ppm; ^{19}F NMR ($CDCl_3$, 376MHz): δ -189.68 (dd, $J=51.2$, 37.3 Hz) ppm; [H] ^{19}F NMR ($CDCl_3$, 376MHz): δ -189.68 (s) ppm; MS (ESI+) m/z : 421.3 [$M+H$] $^+$, 443.4 [$M+Na$] $^+$; HRMS (HPLC-ESI) : [$M+H$] $^+$ Calcd. 421.2749; Found. 421.2752.

Methyl 4 α -fluoro-3 α ,7 α -dihydroxy-5 β -cholanoate (3.76), 4 α -fluoro-3 α ,7 α -dihydroxy-5 β -cholanol-24-ol (3.77) and methyl 4 α -fluoro-3 β ,7 α -dihydroxy-5 β -cholanoate (3.78)



$CeCl_3 \cdot 7H_2O$ (65 mg, 0.17 mmol, 1.2 equiv) was dissolved in MeOH (2 mL) before ketone **3.75** (60 mg, 0.14 mmol, 1 equiv) was added dissolved in EtOAc (0.8 mL). $NaBH_4$ (50 mg, 1.4 mmol, 10 equiv) was then added portionwise - CARE gas evolution - and the reaction allowed to stir at RT. Further $NaBH_4$ (50 mg, 1.4 mmol, 10 equiv) added after 1 day, and the reaction was deemed complete after 2 d. The reaction quenched with ice cold 2M HCl (5 mL) and aqueous extracted with EtOAc (3 \times 5 mL), combined organics dried (Na_2SO_4) and concentrated to yield 80 mg of a white solid. Crude purified *via* flash chromatography (PE/EtOAc : 70:30 \rightarrow 60:40 \rightarrow PE/acetone : 70:30 \rightarrow 50:50) to yield, 7 α -OH cholanoate analogue **3.76** (20 mg, 0.05 mmol, 34%), 7 α -OH cholanol analogue **3.77** (5 mg, 0.01 mmol, 9%) and 7 β -OH cholanoate analogue **3.78** (10 mg, 0.02 mmol, 17%), as gummy solids.

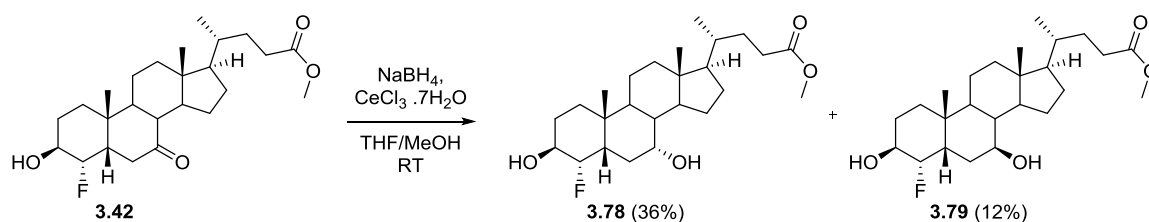
3.76: Formula: $C_{25}H_{41}FO_4$; **MW** 424.6; **m.p.** N/A; **R_f**(PE/Acetone : 70/30) : 0.25; **I.R.** 3587 (w), 3430 (br. w), 2930 (s), 2868 (m), 1739 (s), 1436 (m), 1378 (m), 1169 (m), 1019 (m); 1H NMR (400MHz, $CDCl_3$): δ 4.74 (d, $J=51.7$ Hz, 1H, H_4), 3.66 (s, 4H, H_7 and CO_2CH_3), 3.64 - 3.50 (m, 1H, H_3), 3.23 (dd, $J=38.6$, 11.4 Hz, 1H, C_{7OH}), 2.43 - 2.28 (m, 2H, H_{23} + unknown), 2.27 - 2.16 (m, 1H, $H_{23'}$), 2.07 -

1.00 (m, 38H), 0.97 (s, 3H, H19), 0.92 (d, $J=6.4$ Hz, 3H, H21), 0.65 (s, 3H, H18) ppm; ^{13}C NMR (100 MHz, CDCl_3): δ 174.7 (C24), 98.8 (d, $J=170.2$ Hz, C4), 71.9 (d, $J=21.3$ Hz, C3), 65.8 (C7), 55.6, 51.5 (CO_2CH_3), 50.8, 44.4 (d, $J=17.6$ Hz, C5), 42.4, 39.5 (CH2), 39.4, 35.4, 35.1 (d, $J=3.7$ Hz), 34.5 (CH2), 33.1 (d, $J=1.5$ Hz, CH2, C2 or C6), 31.0 (CH2), 31.0 (CH2), 29.7, 28.1 (CH2), 24.8 (d, $J=3.7$ Hz, CH2, C2 or C6), 23.8 (CH2), 23.2 (C19), 21.2 (CH2), 18.3 (C21), 11.9 (C18) ppm; ^{19}F NMR (CDCl_3 , 376MHz): δ -193.01 (tt, $J=52.2$, 34.5 Hz) ppm; [H] ^{19}F NMR (CDCl_3 , 376MHz): δ -193.02 (s) ppm; **MS (ESI+)** m/z 407.3 [$\text{M}+\text{H}-\text{H}_2\text{O}$] $^+$, 387.3 [$\text{M}+\text{H}-\text{H}_2\text{O}-\text{HF}$] $^+$; **HRMS (HPLC-ESI)** : [$\text{M}+\text{Na}$] $^+$ Calcd. 447.2881; Found. 447.2888.

3.77: Formula: $\text{C}_{24}\text{H}_{41}\text{FO}_3$; **MW** 396.6; **[α]_D** 14.6 (c 0.5, MeOH, 24 °C); **m.p.** N/A; **R_f** (PE/Acetone : 70/30) : 0.14; **I.R.** 3565 (w), 3375 (br. w), 2931 (s), 2867 (m), 1455 (w), 1378 (w), 1017 (w), 733 (w); ^1H NMR (400MHz, CDCl_3): δ 4.75 (d, $J=51.8$ Hz, 1H, H4), 3.77 - 3.50 (m, 4H, H3+H7+H24+H24'), 3.19 (dd, $J=38.3, 11.4$ Hz, 1H, C7OH), 2.35 (ddd, $J=5.6, 8.0, 14.8$ Hz, 1H), 2.05 - 1.01 (m, 34H), 0.98 (s, 3H), 0.94 (d, $J=6.4$ Hz, 3H), 0.66 (s, 3H) ppm; ^{13}C NMR (100 MHz, CDCl_3): δ 98.8 (d, $J=169.5$ Hz, C4), 71.9 (d, $J=22.0$ Hz, C3), 65.8 (C7 or C24), 63.6 (C7 or C24), 55.9, 50.8, 44.5 (d, $J=18.3$ Hz, C5), 42.3, 39.5, 39.5 (CH2), 35.6, 35.1, 35.1, 34.5 (CH2), 33.2 (d, $J=2.2$ Hz, CH2), 31.8 (CH2), 29.4 (CH2), 28.3 (CH2), 24.8 (d, $J=3.7$ Hz, CH2), 23.8 (CH2), 23.2 (C19), 21.2 (CH2), 18.7 (C21), 11.9 (C18) ppm; ^{19}F NMR (CDCl_3 , 376MHz): δ -193.24 (tt, $J=52.9$, 34.7 Hz) ppm; [H] ^{19}F NMR (CDCl_3 , 376MHz): δ -193.25 (s) ppm; **MS (ESI+)** m/z 359.4 [$\text{M}+\text{H}-\text{H}_2\text{O}$] $^+$, 379.4 [$\text{M}+\text{H}-\text{H}_2\text{O}-\text{HF}$] $^+$; **HRMS (HPLC-ESI)** : [$\text{M}+\text{Na}$] $^+$ Calcd. 419.2932; Found. 419.2929.

3.78: See below for characterisation.

Methyl 4 α -fluoro-3 β ,7 α -dihydroxy-5 β -cholanoate (3.78) and methyl 4 α -fluoro-3 β ,7 β -dihydroxy-5 β -cholanoate (3.79)



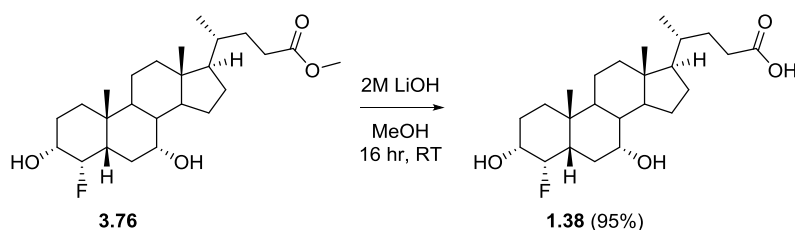
Ketone **3.42** (900 mg, 2.13 mmol, 1 equiv) was dissolved in THF before the addition of THF (20 mL) before the addition of NaBH_4 (160 mg, 4.26 mmol, 2.0 equiv) and allowed to stir O/N at RT. Just SM remained, so MeOH (5 mL), $\text{CeCl}_3 \cdot 7\text{H}_2\text{O}$ (950 mg, 2.55 mmol, 1.2 equiv) and further NaBH_4 (800 mg, 21.3 mmol, 10 equiv) added and progress monitored *via* TLC. Deemed complete after 16 hr at RT, RM quenched with 2M HCl (10 mL) and volatiles removed *in vacuo*. Crude residue taken up in EtOAc/ H_2O (15 mL) each, the layers were then separated and the aqueous extracted with further EtOAc (15 mL). Combined organics dried (Na_2SO_4) and concentrated to yield 950 mg of a

crude gum, purified *via* flash chromatography to yield pure 7 α -OH **3.78** as crystalline solid (330 mg, 0.78 mmol, 36%), and 90% pure 7 β -OH **3.79** as colourless gum (105 mg, 0.25 mmol, 12%).

3.78: Formula: C₂₅H₄₁FO₄; **MW** 424.6; **m.p.** 88–90 °C; **R_f** (Petrol ether/EtOAc : 60/40) : 0.27; **I.R.** 3569 (w), 3398 (br. w), 2930 (m), 2870 (w), 1731 (m), 1436 (w), 906.1 (s), 728 (s) cm⁻¹; **H NMR** (400MHz, CDCl₃): δ 4.55 (dt, *J*=46.7, 2.5 Hz, 1H, H₄), 4.08 (dd, *J*=10.2, 3.2 Hz, 1H, H₃), 3.74 - 3.60 (m, 4H, H₇ and CO₂CH₃), 3.06 (dd, *J*=35.7, 10.9 Hz, 1H, C7OH), 2.40 - 2.28 (m, 2H, H₂₃ + unknown), 2.21 (ddd, *J*=15.5, 9.4, 5.6 Hz, 1H, H_{23'}), 2.13 - 1.03 (m, 30H), 0.99 (s, 3H, H₁₉), 0.91 (d, *J*=6.5 Hz, 3H, H₂₁), 0.65 (s, 3H, H₁₈) ppm; **¹³C NMR** (100 MHz, CDCl₃): δ 174.8 (C₂₄), 97.6 (d, *J*=170.2 Hz, C₂), 67.6 (d, *J*=33.7 Hz, 1C, C₃), 66.1 (C₇), 55.6, 51.5 (CO₂CH₃), 50.7, 42.4, 39.4 (C₂H), 39.3, 39.2, 36.2 (d, *J*=2.9 Hz), 35.3, 35.3, 32.3 (C₂H), 31.0 (C₂₃), 31.0 (C₂H), 29.1 (C₂H), 28.1 (C₂H), 23.8 (C₂H), 23.6 (C₂H), 22.9 (C₁₉), 21.4 (C₂H), 18.3 (C₂₁), 11.9 (C₁₈) ppm; **¹⁹F NMR** (CDCl₃, 376MHz): δ -174.63 (br. s.) ppm; **[H]¹⁹F NMR** (CDCl₃, 376MHz): δ -174.61 (br. s.) ppm; **[¹H]¹⁹F NMR** (471MHz, DMSO-d₆, 100 °C): δ -179.71 ppm (br. s., narrower at high temperature); **MS (ESI+)** *m/z* : 442.0 [M+NH₄]⁺, 849.8 [2M+H]⁺; **HRMS** (HPLC-ESI) : [M+Na]⁺ Calcd. 447.2881; Found. 447.2884.

3.79: Formula: C₂₅H₄₁FO₄; **MW** 424.6; **m.p.** N/A; **R_f** (Petrol ether/EtOAc : 50/50) : 0.22; **I.R.** 3376 (br. w), 2934 (s), 2871 (m), 1736 (s), 1721 (s), 1438 (m), 1168 (s), 1026 (v. s), 971 (s) cm⁻¹; **H NMR** (400MHz, CDCl₃): δ 4.53 (dt, *J*=48.0, 3.0 Hz, 1H, H₄), 3.98 (dq, *J*=8.4, 3.7 Hz, 1H, H₃), 3.78 (tt, *J*=9.5, 4.9 Hz, 1H, H₇), 3.67 (s, 3H), 2.35 (ddd, *J*=15.5, 11.0, 5.0 Hz, 1H, H₂₃), 2.22 (ddd, *J*=15.5, 9.4, 6.6 Hz, 1H, H_{23'}), 2.04-1.04 (m, 30H), 0.99 (s, 3H, H₁₉), 0.92 (d, *J*=6.4 Hz, 3H, H₂₁), 0.68 (s, 3H, H₁₈) ppm; **¹³C NMR** (100 MHz, CDCl₃): δ 174.8 (C₂₄), 96.4 (d, *J*=175.3 Hz, C₄), 72.4 (d, *J*=5.9 Hz, C₇), 67.6 (d, *J*=29.3 Hz, C₃), 55.8, 54.9, 51.4, 43.5, 42.5, 41.6, 41.1 (d, *J*=17.6 Hz, C₅), 39.9 (C₂H), 35.2, 34.7, 33.8 (C₂H), 31.0 (C₂₃), 30.9 (C₂H), 29.1 (C₂H), 28.4, (C₂H) 26.5 (C₂H), 23.7 (C₂H), 23.2 (C₁₉), 21.8 (C₂H), 18.3 (C₂₁), 12.0 (C₁₈) ppm; **¹⁹F NMR** (CDCl₃, 376MHz): δ -181.35 (br. s.) ppm; **[H]¹⁹F NMR** (CDCl₃, 376MHz): δ -181.38 (br. s.) ppm; **MS (ESI+)** *m/z* : 407.4 [M+H-H₂O]⁺, 387.4 [M+H-H₂O-HF]⁺, 369.4 [M+H-2H₂O-HF]⁺; **HRMS** (HPLC-ESI) : [M+NH₄]⁺ Calcd. 442.3327; Found. 442.3324.

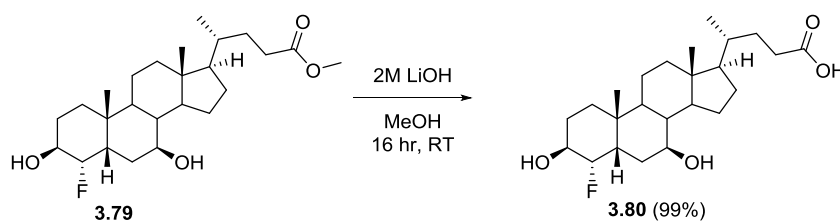
4 α -fluorochenodeoxycholic acid (**1.38**)



Using procedure B, ester **3.76** (75 mg, 0.18 mmol, 1 equiv) was hydrolysed to yield **1.38** as a white solid (70 mg, 0.17 mmol, 95%).

1.38: Formula: C₂₄H₃₉FO₄; **MW** 410.6; [α]_D +9.0 (c 0.5, MeOH, 24 °C); **m.p.** 125–126 °C; **R_f** (Petrol ether/Acetone : 50/50) : 0.42; **I.R.** 3561 (w), 3352 (br. w), 2932 (s), 2868 (m), 1708 (s), 732 (s) cm⁻¹; **¹H NMR** (400MHz, CDCl₃): δ 4.75 (d, *J*=52.0 Hz, 1H, H₄), 3.71 (br. s., 1H, H₇), 3.61 (ddd, *J*=32.0, 11.0, 5.0 Hz, 1H, H₃), 2.46-1.02 (m, 32H), 0.97 (s, 3H, H₁₉), 0.92 (d, *J*=6.4 Hz, 3H, H₂₁), 0.65 (s, 3H, H₁₈) ppm; **¹³C NMR** (100 MHz, CDCl₃): δ 179.4, 98.8 (d, *J*=170.2 Hz, C₄), 71.8 (d, *J*=21.3 Hz, C₃), 65.9 (C₇), 55.6, 50.8, 44.4 (d, *J*=17.6 Hz, C₅), 42.4, 39.4 (CH₂), 39.3, 35.4, 35.1, 35.0, 34.5 (CH₂), 33.0 (CH₂), 31.0 (CH₂), 30.8 (CH₂), 28.1 (CH₂), 24.7 (d, *J*=2.9 Hz, CH₂), 23.7 (CH₂), 23.2 (C₁₉), 21.2 (CH₂), 18.3 (C₂₁), 11.9 (C₁₈) ppm; **¹⁹F NMR** (376MHz, CDCl₃): δ -192.68 (td, *J*=52.0, 31.2 Hz, 1F) ppm; **[H]¹⁹F NMR** (376MHz, CDCl₃): δ -192.68 (s) ppm; **MS (ESI+)** *m/z* : 433.5 [M+Na]⁺, 393.4 [M+H-H₂O]⁺, 375.4 [M+H-2H₂O]⁺, 373.5 [M+H-HF-H₂O]⁺; **HRMS** (HPLC-ESI) : [M+NH₄]⁺ Calcd. 428.3171; Found. 428.3161.

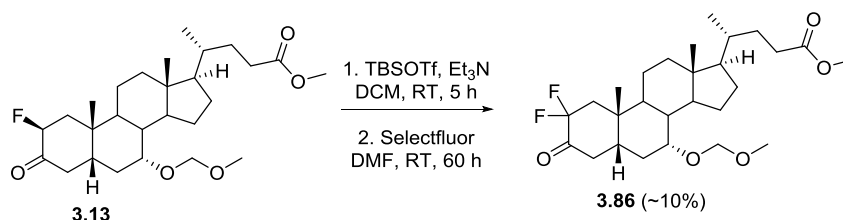
3 β ,7 β -dihydroxy-4 α -fluoro-5 β -cholanolic acid (3.80)



Using procedure B, ester **3.79** (65 mg, 0.15 mmol, 1 equiv) was hydrolysed to yield **3.80** as a white solid (61 mg, 0.15 mmol, 99%).

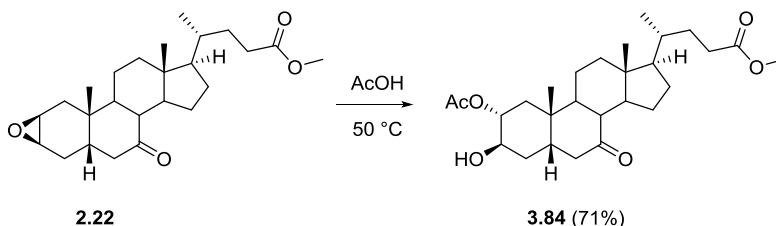
3.80: Formula: C₂₄H₃₉FO₄; **MW** 410.6; [α]_D +34.0 (c 0.5, MeOH, 24 °C); **m.p.** 109–111 °C; **R_f** (Petrol ether/EtOAc : 50/50) : 0.18; **I.R.** 3398 (br. w), 2930 (s), 2870 (m), 1736 (s), 1720 (s), 1089 (s), 1043 (s) cm⁻¹; **¹H NMR** (400MHz, Acetone-D₆): δ 4.48 (dt, *J*=48.3, 2.8 Hz, 1H, H₄), 3.89 (dq, *J*=9.3, 3.2 Hz, 1H, H₃), 3.65 (ddd, *J*=14.2, 10.3, 4.9 Hz, 1H, H₇), 2.34 (ddd, *J*=15.5, 11.0, 5.0 Hz, 1H, H₂₃), 2.20 (ddd, *J*=15.5, 9.6, 6.4 Hz, 1H, H_{23'}), 2.03-1.02 (m, 30H), 0.98 (s, 3H, H₁₉), 0.96 (d, *J*=6.6 Hz, 3H, H₂₁), 0.70 (s, 3H, H₁₈) ppm; **¹³C NMR** (100MHz, Acetone-D₆): δ 175.3 (C₂₄), 98.0 (d, *J*=174.6 Hz, C₄), 72.4 (d, *J*=7.3 Hz, C₇), 67.8 (d, *J*=28.6 Hz, C₃), 57.4, 56.2, 44.3, 43.4, 42.4 (d, *J*=4.4 Hz, 1C), 42.3 (d, *J*=17.6 Hz, C₅), 41.2 (CH₂), 36.2, 36.2 (CH₂), 35.5, 32.0 (CH₂), 31.3 (C₂₃), 29.9 (CH₂), 29.3 (CH₂), 27.5 (CH₂), 24.4 (CH₂), 24.0 (C₁₉), 22.7 (CH₂), 18.9 (C₂₁), 12.7 (C₁₈) ppm; **¹⁹F NMR** (376MHz, Acetone-D₆) δ -180.27 (br. s.) ppm; **[H]¹⁹F NMR** (376MHz, Acetone-D₆) δ -180.30 (br. s.) ppm; **MS (ESI+)** *m/z* : 393.3 [M+H-H₂O]⁺, 373.4 [M+H-H₂O-HF]⁺, 355.4 [M+H-2H₂O-HF]⁺; **HRMS** (HPLC-ESI) : [M+H-H₂O]⁺ Calcd. 373.2799; Found. 373.2798.

5.4.3 Synthesis of 2,2-difluorinated analogues

Methyl 2,2-difluoro-7 α -methoxymethoxyl-3oxo-5 β -cholanoate (**3.86**)

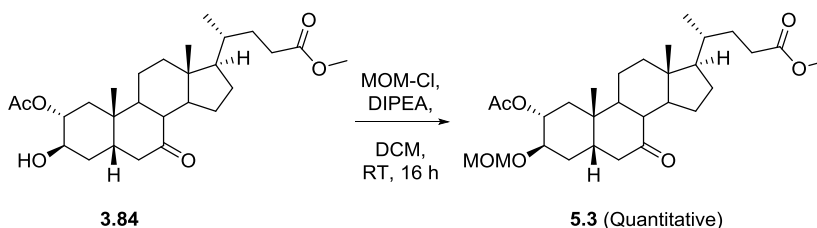
To a solution of fluoroketone **3.13** (310 mg, 0.66 mmol, 1 equiv) in dry DCM (10 mL) at 0 °C was added triethylamine (0.18 mL, 1.30 mmol, 2 equiv) and TBDMS triflate (0.17 mL, 0.74 mmol, 1.1 equiv). The reaction was warmed to RT and allowed to stir for 5 h, before removing the solvent *in vacuo* to yield a crude yellow oil (400mg). The crude was used in the subsequent fluorination reaction without further purification. The crude silyl enol ether mixture (~400 mg, assumed 0.66 mmol, 1 equiv) was dissolved in dry DMF (5 mL) before adding Selectfluor® (500 mg, 1.40 mmol, 2 equiv) and allowing to stir at RT for 60 h. The solvent was removed *in vacuo* before dissolving the residue in EtOAc (15 mL) and water (10 mL), the layers were separated and aqueous washed with further EA (2×10 mL). Combined organics washed with brine (2×25 mL), dried (Na₂SO₄) and concentrated to yield 350 mg a bright yellow/green solid. Crude was purified to yield 110 mg of difluorinated material, of which 30 mg of **3.86** was isolated as a pale green gummy solid (<10% yield).

3.86: Formula: C₂₇H₄₂F₂O₅; **MW** 484.6; **m.p.** N/A; **R_f** (PE/EtOAc : 70:30) 0.10; **I.R.** 3421 (br. w), 2940 (s), 1737 (s), 1441 (m), 1147 (m), 1092 (m), 1039 (s) cm⁻¹; **¹H NMR** (400MHz, CDCl₃): δ 4.69 (d, *J*=6.8 Hz, 1H, O-CHH-O), 4.55 (d, *J*=6.6 Hz, 1H, O-CHH-O), 3.79 (td, *J*=14.0, 3.4 Hz, 1H, H_{4 α}), 3.67 (s, 4H, CO₂CH₃ + H₇), 3.39 (s, 3H, OCH₃), 2.66 (ddd, *J*=16.0, 14.0, 7.6 Hz, 1H, H_{1 β}), 2.48 - 1.15 (m, 25H), 1.08 (s, 3H, H₁₉), 0.94 (d, *J*=6.4 Hz, 3H, H₂₁), 0.72 - 0.62 (m, 3H, H₁₈) ppm; **¹³C NMR** (100 MHz, CDCl₃): δ 199.3 (q, *J*=22.7 Hz, C₃), 174.7 (C₂₄), 116.8 (dd, *J*=255.3, 247.4 Hz, C₂), 87.83 (dd, *J*=219.0, 183.9 Hz, C₂), 96.1 (O-CH₂-O), 74.7 (C₇), 56.4 (OCH₃), 55.6, 51.5 (CO₂CH₃), 49.6, 44.3 (dd, *J*=22.0, 18.3 Hz, C₁), 43.5, 42.9 (C₄), 42.5, 39.5, 39.0 (CH₂), 37.2 (d, *J*=8.8 Hz), 35.3, 34.5 (d, *J*=3.7 Hz, C₅), 31.0 (CH₂), 31.0 (CH₂), 30.3 (CH₂), 28.1 (CH₂), 23.6 (CH₂), 22.6 (C₁₉), 21.3 (CH₂), 18.3 (C₂₁), 11.8 (C₁₈) ppm; **¹⁹F NMR** (CDCl₃, 376MHz): δ -104.68 (ddd, *J*=259.2, 38.1, 13.0 Hz, 1F, F_{2 α}), -110.69 (dq, *J*=258.4, 6.1 Hz, 1F, F_{2 β}) ppm; **[¹H]¹⁹F NMR** (CDCl₃, 376MHz): δ -104.69 (d, *J*=258.4 Hz, 1F, F_{2 α}), -110.69 (d, *J*=258.4 Hz, 1F, F_{2 β}) ppm; **MS (ESI+)** *m/z* : *Hydrate*: 521.1 [M+NH₄]⁺, 525.1 [M+Na]⁺, *ketone*: 534.1 [M+NH₄+MeCN]⁺, 539.0 [M+Na+MeCN]⁺; **HRMS** (HPLC-ESI) : *hydrate* [M+Na]⁺ Calcd: 525.2998; Found: 525.3002, *ketone* [M+Na]⁺ Calcd: 507.2893; Found: 507.2901.

Methyl 2 α -acetoxy-3 β -hydroxy-7-oxo-5 β -cholanoate (3.84)

Epoxide **2.22** (250 mg, 0.62 mmol, 1 equiv) was dissolved in AcOH (5 mL) and warmed to 50 °C. Reaction was deemed complete after 16 h, the solvent was then removed *in vacuo*, then azeotroped (EtOAc 2 × 5 mL, then DCM 2 × 5 mL) to complete dryness. The crude material was then purified *via* flash chromatography (pet ether/EtOAc : 70:30→50:50) to yield pure 2 α -acetate **3.84** as a gummy solid (205 mg, 0.44 mmol, 71%).

3.84: Formula: C₂₇H₄₂O₆ **MW** 462.6; **m.p.** N/A; **R_f** (Petrol ether/EtOAc : 50/50) : 0.30; **I.R.** 3465 (br. w), 2944 (m), 1736 (s), 1709 (s), 1436 (m), 1373 (m), 1242 (s) cm⁻¹; **¹H NMR** (400MHz, CDCl₃): δ 4.79 (qd, $J=3.2, 1.0$ Hz, 1H, H₂), 3.85 (q, $J=2.8$ Hz, 1H, H₃), 3.66 (s, 3H, CO₂C_H₃), 2.89 (dd, $J=12.6, 6.1$ Hz, 1H, H₆ β), 2.42-2.01 (m, 9H), 2.00 (s, 3H, C(O)C_H₃), 1.98-1.24 (m, 16H), 1.22 (s, 3H, H₁₉), 1.15-0.94 (m, 3H), 0.91 (d, $J=6.5$ Hz, 3H, H₂₁), 0.65 (s, 3H, H₁₈) ppm; **¹³C NMR** (100 MHz, CDCl₃): δ 212.9 (C₇), 174.6 (C₂₄), 170.1 (C(O)CH₃), 72.7 (C₂), 67.3 (C₃), 54.8, 51.5 (CO₂C_H₃), 49.8, 49.0, 45.2, 44.8 (C₆), 42.6, 40.6, 39.2 (C_H₂), 35.8, 35.2, 33.2 (C_H₂), 31.0 (C_H₂), 30.9 (C_H₂), 30.8 (C_H₂), 28.3 (C_H₂), 24.8 (C_H₂), 23.6 (C₁₉), 22.3 (C_H₂), 21.2 (C(O)C_H₃), 18.3 (C₂₁), 12.0 (C₁₈) ppm; **MS (ESI+)** m/z : 403.5 [M+H-HOAc]⁺, 463.6 [M+H]⁺, 485.5 [M+Na]⁺; **HRMS** (HPLC-ESI) : [M+H]⁺ Calcd. 463.3054; Found. 463.3045.

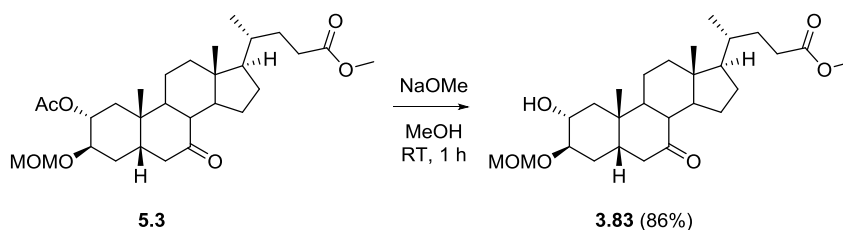
Methyl 2 α -acetoxy-3 β - methoxymethoxy-7-oxo-5 β -cholanoate (5.3)

Using procedure C, Alcohol **3.84** (2.9 g, 6.3 mmol, 1 equiv) was protected as a MOM functionality to yield **5.3** as a pale solid (3.2 g, 6.3 mmol, quantitative), used without further purification.

5.3: Formula: C₂₉H₄₆O₇; **MW** 506.7; **m.p.** 118–119 °C; **R_f** (Petrol ether/EtOAc : 65/35) : 0.25; **I.R.** 2941 (m), 2888 (m), 1736 (s), 1709 (s), 1240 (s), 1150 (m), 1049 (s), 1031 (s) cm⁻¹; **¹H NMR** (400MHz, CDCl₃): δ 4.88 (q, $J=2.3$ Hz, 1H, H₂), 4.66 (d, $J=6.8$ Hz, 1H, O-CHH'-O), 4.64 (d, $J=6.8$ Hz, 1H, O-CHH'-O), 3.69 (q, $J=2.7$ Hz, 1H, H₃), 3.67 (s, 3H, CO₂C_H₃), 3.36 (s, 3H, OCH₃), 2.92 (dd, $J=12.5,$

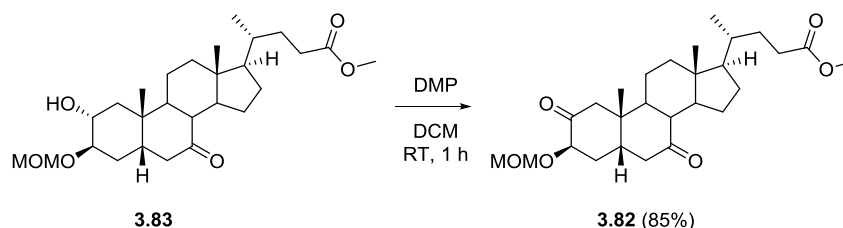
6.2 Hz, 1H, $\underline{H6\beta}$), 2.45-2.02 (m, 8H), 2.00 (s, 3H, C(O)CH_3), 1.99-1.24 (m, 15H), 1.23 (s, 3H, $\underline{H19}$), 1.18-0.94 (m, 3H), 0.92 (d, $J=6.4$ Hz, 3H, $\underline{H21}$), 0.66 (s, 3H, $\underline{H18}$) ppm; $^{13}\text{C NMR}$ (100 MHz, CDCl_3): δ 212.7 ($\underline{C7}$), 174.6 ($\underline{C24}$), 169.8 (C(O)CH_3), 95.3 ($\text{O-CH}_2\text{-O}$), 72.2 ($\underline{C3}$), 70.7 ($\underline{C2}$), 55.5 (OCH_3), 54.8, 51.4 (CO_2CH_3), 49.9, 48.9, 45.2, 45.0 ($\underline{C6}$), 42.6, 41.4, 39.2 (\underline{CH}_2), 35.6, 35.2, 33.4 (\underline{CH}_2), 31.0 (\underline{CH}_2), 30.9 (\underline{CH}_2), 28.8 (\underline{CH}_2), 28.3 (\underline{CH}_2), 24.7 (\underline{CH}_2), 23.7 ($\underline{C19}$), 22.3 (\underline{CH}_2), 21.2 (C(O)CH_3), 18.3 ($\underline{C21}$), 12.0 ($\underline{C18}$) ppm; **MS (ESI+)** m/z : 403.5 [$\text{M}+\text{H-HOAc}$, MOM cleavage] $^+$, 445.5 [$\text{M}+\text{H-HOCH}_2\text{OCH}_3$] $^+$, 463.5 [$\text{M}+\text{H}$, MOM cleavage] $^+$, 529.6 [$\text{M}+\text{Na}$] $^+$; **HRMS** HRMS (HPLC-ESI) : [$\text{M}+\text{NH}_4$] $^+$ Calcd. 524.3582; Found. 524.3578.

Methyl 2 α -hydroxy-3 β -methoxymethoxyl-7-oxo-5 β -cholanoate (3.87)



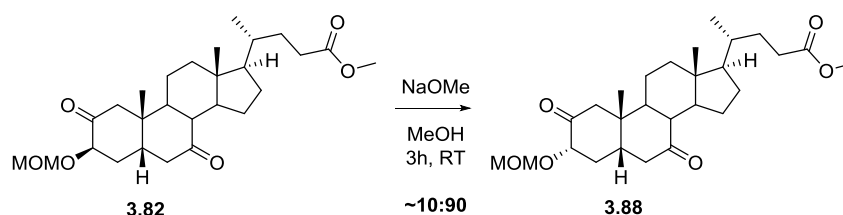
Acetate **5.3** (3.1 g, 6.12 mmol, 1 equiv) was dissolved in dry MeOH (30 mL) before the addition of 25% NaOMe in MeOH (20 mL) and the RM stirred at RT. Deemed complete after 1 hr, reaction acidified to pH 4-5 with 2M HCl (≈ 15 mL) and diluted with H_2O (15 mL). Aqueous extracted with DCM (2×75 mL), combined organics washed with NaHCO_3 (100 mL), dried (Na_2SO_4) and concentrated to yield alcohol **3.83** as a gummy solid (2.45 g, 5.27 mmol, 86%). Used without further purification. (**General procedure F**).

3.83: Formula: $\text{C}_{27}\text{H}_{44}\text{O}_6$; **MW** 464.6; **m.p.** N/A; **R_f** (Petrol ether/EtOAc : 50/50) : 0.58; **I.R.** 3471 (br. w), 2941 (s), 2882 (m), 1737 (s), 1708 (s), 1436 (m), 1099 (s), 1038 (s), 1019 (s) cm^{-1} ; $^1\text{H NMR}$ (400MHz, CDCl_3): δ 4.62 (d, $J=6.8$ Hz, 1H, $\text{O-CHH}'\text{-O}$), 4.59 (d, $J=6.8$ Hz, 1H, $\text{O-CHH}'\text{-O}$), 3.77 (q, $J=4.2$ Hz, 1H, $\underline{H3}$), 3.61 (s, 3H, CO_2CH_3), 3.52 (q, $J=3.9$ Hz, 1H, $\underline{H2}$), 3.32 (s, 3H, OCH_3), 2.70 (dd, $J=13.3, 5.7$ Hz, 1H, $\underline{H6\beta}$), 2.59 (br. s., 1H, \underline{OH}), 2.41-1.18 (m, 25H), 1.15 (s, 3H, $\underline{H19}$), 1.13-0.90 (m, 4H), 0.87 (d, $J=6.4$ Hz, 3H, $\underline{H21}$), 0.61 (s, 3H, $\underline{H18}$) ppm; $^{13}\text{C NMR}$ (100 MHz, CDCl_3): δ 213.3 ($\underline{C7}$), 174.6 ($\underline{C24}$), 95.6 ($\text{O-CH}_2\text{-O}$), 77.6 ($\underline{C2}$), 69.3 ($\underline{C3}$), 55.3 (OCH_3), 54.6, 51.3 (CO_2CH_3), 49.1, 48.9, 45.9, 44.5 ($\underline{C6}$), 42.5, 40.9, 38.8 (\underline{CH}_2), 37.3 (\underline{CH}_2), 35.6, 35.1, 30.9 (\underline{CH}_2), 30.9 (\underline{CH}_2), 29.2, (\underline{CH}_2) 28.2 (\underline{CH}_2), 24.9 (\underline{CH}_2), 23.3 ($\underline{C19}$), 22.3 (\underline{CH}_2), 18.3 ($\underline{C21}$), 11.9 ($\underline{C18}$) ppm; **MS (ESI+)** m/z : 403.5 [$\text{M}+\text{H-HOCH}_2\text{OCH}_3$] $^+$, 433.5 [$\text{M}+\text{H}$, partial MOM cleavage] $^+$, 487.6 [$\text{M}+\text{Na}$] $^+$; **HRMS** (HPLC-ESI) : [$\text{M}+\text{NH}_4$] $^+$ Calcd. 482.3476; Found. 482.3480.

Methyl 3 β -methoxymethoxyl-2,7-dioxo-5 β -cholanoate (3.82)

Using procedure E, alcohol **3.83** (2.5 g, 5.38 mmol, 1 equiv) was oxidised. Crude was purified *via* flash chromatography (pet ether/EtOAc : 70:30) to yield diketo **3.82** as a gummy solid (2.12 g, 4.58 mmol, 85%).

3.82: Formula: C₂₇H₄₂O₆ **MW** 462.6; **m.p.** N/A; **R_f** (Petrol ether/EtOAc : 60/40) : 0.56; **I.R.** 2942 (m), 2890 (m), 1735 (s), 1711 (s), 1436 (w), 1154 (m), 1024 (s) cm⁻¹; **¹H NMR** (400MHz, CDCl₃): δ 4.58 (s, 2H, O-CH₂-O), 3.72 (t, *J*=2.7 Hz, 1H, H₃), 3.63 (s, 3H, CO₂CH₃), 3.32 (s, 3H, OCH₃), 2.89 (dd, *J*=12.8, 5.9 Hz, 1H, H₆ β), 2.79 (d, *J*=13.0 Hz, 1H, H₁ β), 2.64-2.54 (m, 1H, H₅), 2.39-1.36 (m, 17H), 1.33 (s, 3H, H₁₉), 1.32-0.90 (m, 6H), 0.88 (d, *J*=6.4 Hz, 3H, H₂₁), 0.62 (s, 3H, H₁₈) ppm; **¹³C NMR** (100 MHz, CDCl₃): δ 211.1 (C₂ or C₇), 209.3 (C₂ or C₇), 174.5 (C₂₄), 95.9 (O-CH₂-O), 79.1 (C₃), 55.9 (OCH₃), 54.6, 51.4 (CO₂CH₃), 49.5, 48.6, 45.9 (C₁), 44.4, 43.7 (C₆), 42.5, 42.2, 41.3 (C₅), 38.5 (CH₂), 35.2 (CH₂), 35.1, 30.9 (CH₂), 30.9 (CH₂), 28.1 (CH₂), 24.7 (CH₂), 23.2 (C₁₉), 21.8 (CH₂), 18.2 (C₂₁), 12.0 (C₁₈) ppm; **MS (ESI⁺)** *m/z* : 431.5 [M+H, partial MOM cleavage]⁺, 485.6 [M+Na]⁺; **HRMS** (HPLC-ESI) : [M+NH₄]⁺ Calcd. 480.3320; Found. 480.3312.

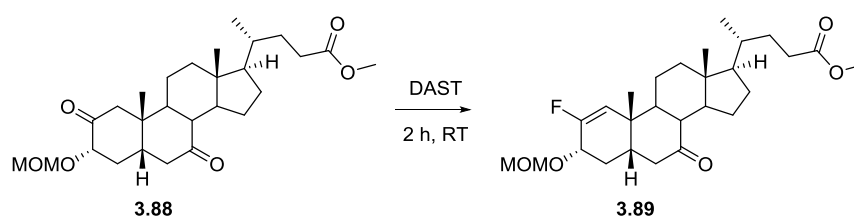
Methyl 3 α -methoxymethoxyl-2,7-dioxo-5 β -cholanoate (3.88)

3 β -MOM protected alcohol **3.82** (45 mg, 0.1 mmol, 1 equiv) was dissolved in MeOH (1 mL) before the addition of 25% NaOMe in MeOH (100 μ L) and allowed to stir at RT. Equilibrium deemed to be reached after 3 hr, RM diluted with DCM (5 mL) and acidified with 2M HCl (3 mL). Layers separated and aqueous with further DCM (4 mL), combined organics dried (Na₂SO₄) and concentrated to yield 30 mg of a colourless gum. ¹H NMR analysis indicated the equilibrium lay >90% towards 3 α -MOM derivative **3.88**. Used without further purification.

3.88: Formula: C₂₇H₄₂O₆; **MW** 462.6; **m.p.** N/A; **R_f** (Petrol ether/EtOAc : 60/40) : 0.25; **I.R.** 2943 (m), 2876 (w), 1731 (s), 1712 (s), 1437 (w), 1047 (m), 1027 (m) cm⁻¹; **¹H NMR** (400MHz, CDCl₃): δ 4.69

(d, $J=7.0$ Hz, 1H, O-CHH'-O), 4.67 (d, $J=7.0$ Hz, 1H, O-CHH'-O), 4.26 (dd, $J=12.0, 7.4$ Hz, 1H, H₃), 3.66 (s, 3H, CO₂CH₃), 3.36 (s, 3H, OCH₃), 2.89 (dd, $J=12.9, 5.7$ Hz, 1H, H_{6β}), 2.54 (d, $J=13.3$ Hz, 1H, H_{1β}), 2.45-2.38 (m, 1H, H₅), 2.37-2.14 (m, 7H), 2.10 (dd, $J=13.0, 2.2$ Hz, 1H, H_{6α}), 2.06-1.35 (m, 13H), 1.33 (s, 3H, H₁₉), 1.32-0.92 (m, 7H), 0.90 (d, $J=6.4$ Hz, 3H, H₂₁), 0.63 (s, 3H, H₁₈) ppm; ¹³C NMR (100 MHz, CDCl₃): δ 210.2 (C₇), 206.8 (C₂), 174.6 (C₂₄), 95.5 (O-CH₂-O), 77.7 (C₃), 55.7 (OCH₃), 54.6, 51.4 (CO₂CH₃), 49.5, 49.2 (C₁), 48.6, 45.2 (C₅), 44.2, 44.0, 42.6, 42.0 (C₆), 38.4 (CH₂), 36.4 (CH₂), 35.1, 31.0 (CH₂), 30.9 (CH₂), 28.2 (CH₂), 24.7 (CH₂), 22.7 (C₁₉), 21.8 (CH₂), 18.3 (C₂₁), 12.0 (C₁₈) ppm; MS (ESI+) m/z : 480.6 [M+ NH₄]⁺, 485.5 [M+Na]⁺; HRMS (HPLC-ESI) : [M+NH₄]⁺ Calcd. 480.3320; Found. 480.3319.

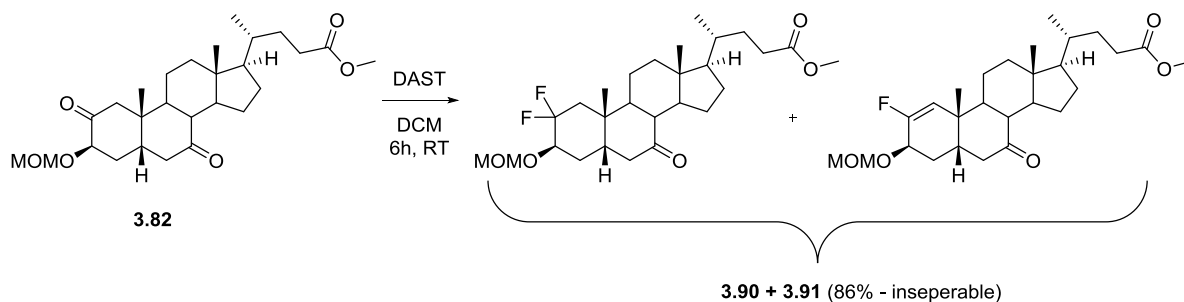
2-fluoro-3α-methoxymethoxy-7-oxo-5β-chol-1-enoate (3.89)



Ketone **3.88** (25 mg, 0.054 mmol, 1 equiv) was dissolved in DAST and allowed to stir at RT for 2 hr. Reaction diluted with DCM (10 mL) and then carefully quenched with sat. aq. NaHCO₃ (10 mL). Layers separated and aqueous extracted with DCM (5 mL). Combined organics dried (Na₂SO₄) and concentrated. Crude purified *via* flash chromatography (pet ether/EtOAc : 85:15) to yield fluoroalkene **3.89** as a colourless gum (30 mg, quantitative).

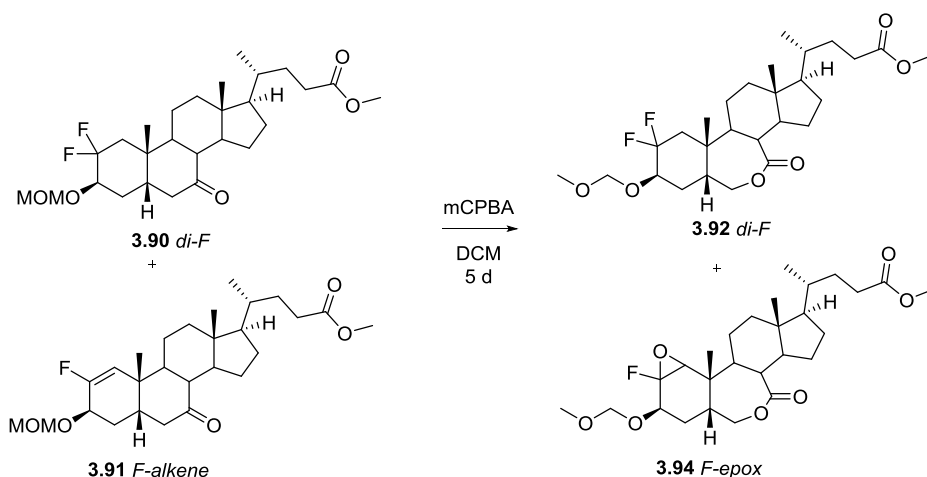
3.89: Formula: C₂₇H₄₁FO₅; **MW** 464.6; **m.p.** N/A; **R_f** (Petrol ether/EtOAc : 60/40) : 0.58; **I.R.** 2943 (m), 2876 (w), 1736 (s), 1711 (s), 1163 (s), 1152 (s), 1047 (s), 1024 (s) cm⁻¹; ¹H NMR (400MHz, CDCl₃): δ 5.29 (d, $J=17.9$ Hz, 1H, H₁), 4.74 (d, $J=6.9$ Hz, 1H, O-CHH'-O), 4.69 (d, $J=7.0$ Hz, 1H, O-CHH'-O), 4.35 (dd, $J=9.0, 8.0$ Hz, 1H, H₃), 3.67 (s, 4H, CO₂CH₃), 3.38 (s, 3H, OCH₃), 2.88 (dd, $J=12.4, 6.4$ Hz, 1H, H_{6β}), 2.47-1.35 (m, 26H), 1.32 (d, $J=0.6$ Hz, 3H, H₁₉), 1.31-0.95 (m, 10H), 0.92 (d, $J=6.5$ Hz, 4H, H₂₁), 0.67 (s, 3H, H₁₈) ppm; ¹⁹F NMR (376 MHz, CDCl₃): δ -120.99 (dd, $J=18.2, 6.1$ Hz) ppm; [¹H]¹⁹F NMR (376 MHz, CDCl₃): δ -120.99 (s) ppm; **MS (ESI+)** m/z : 403.4 [M+H-HOMOM]⁺.

Methyl 2,2-difluoro-3 β -methoxymethoxy-7-oxo-5 β -cholanoate (3.90) and 2-fluoro-3 β -methoxymethoxy-7-oxo-5 β -chol-1-enoate (3.91)



Ketone **3.82** (2.1 g, 4.54 mmol, 1 equiv) was dissolved in DCM (30 mL) before the careful addition of DAST (10 mL, 51 mmol, 11 equiv), then stirred at RT for 6hr until complete consumption of starting material. RM diluted with DCM (80 mL), before the organics were added dropwise to ice-cold sat. aq. NaHCO₃ (400 mL). Layers separated and aqueous extracted with DCM (2×150 mL), combined organics were washed with H₂O (200 mL), dried (Na₂SO₄) and concentrated to yield 2.85 g of a pale brown oil/gum. Crude purified *via* flash chromatography (pet ether/EtOAc : 85:15→80:20→70:30) to yield an inseparable mixture of difluoro analogue **3.90** and fluoroalkene **3.91** (1.8 g, ≈3.9 mmol, 86%) in a ratio of 1:0.6.

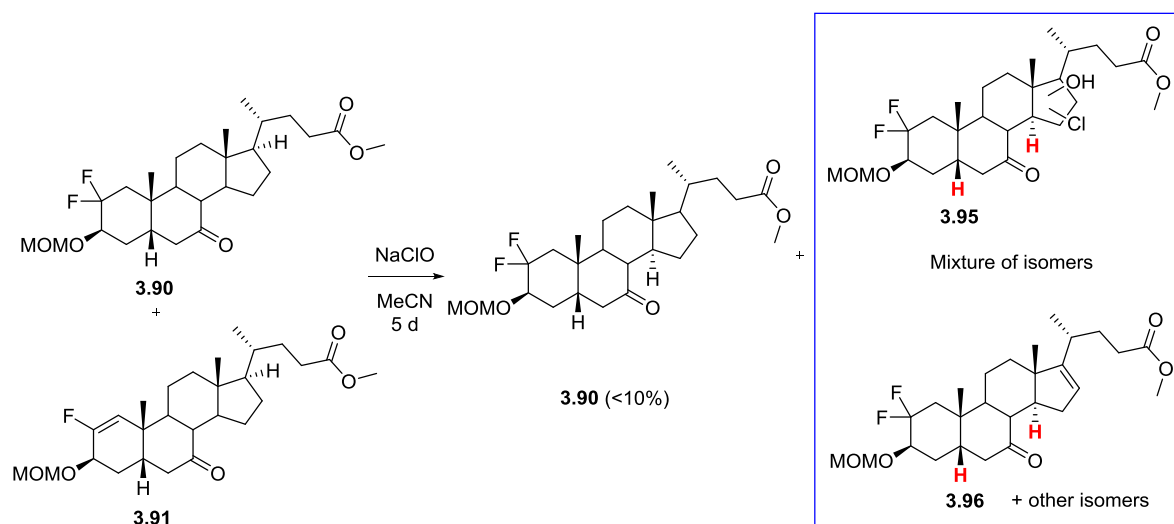
3.90 (C₂₇H₄₂F₂O₅, MW 484.6) and **3.91** (C₂₇H₄₁FO₅, MW 464.6) : **m.p.** N/A; **R_f** (Petrol ether/EtOAc : 60/40) : 0.65; **¹H NMR** (400MHz, CDCl₃): δ 5.38 (d, *J*=17.1 Hz, 0.4H, H₁, *F-alkene*), 4.71 (d, *J*=7.0 Hz, 1H, 0.6H, O-CHH'-O, *di-F*), 4.69 (s, 1H, 0.7H, O-CH₂-O, *F-alkene*), 4.65 (d, *J*=7.0 Hz, 1H, 0.6H, O-CHH'-O, *di-F*), 4.12-4.07 (m, 0.4H, H₃, *F-alkene*), 3.81 (br. s., 0.6H, H₃, *di-F*), 3.66 (s, 3H, CO₂CH₃), 3.39 (s, 1.3H, OCH₃, *F-alkene*), 3.37 (s, 1.7H, OCH₃, *di-F*), 2.95-2.87 (m, 1H, H_{6β}), 2.43-1.39 (m, 19H), 1.36 (s, 1.3H, H₁₉, *F-alkene*), 1.29 (s, 1.7H, H₁₉, *di-F*), 1.27-0.94 (m, 4H), 0.92 (d, *J*=6.4 Hz, H₂₁, 3H), 0.67 (s, 1.3H, H₁₈, *F-alkene*), 0.65 (s, 1.7H, H₁₈, *di-F*) ppm; **¹⁹F NMR** (376 MHz, CDCl₃): δ -100.62 (dquin, *J*=252.0, 5.0 Hz, 1F, F_{2β}, *di-F*), -102.94 (ddt, *J*=252.0, 41.0, 8.0 Hz, 1F, F_{2α}, *di-F*), -114.78 (ddd, *J*=17.0, 8.0, 5.0 Hz, 0.6F, F₂, *F-alkene*) ppm; **[¹H]¹⁹F NMR** (376 MHz, CDCl₃): δ -100.63 (d, *J*=253.2 Hz, 1F, F_{2β}, *di-F*), -103.41--102.50 (m, 1F, F_{2α}, *di-F*), -114.78 (s, 0.7F, F₂, *F-alkene*) ppm; **MS (ESI+)** *m/z* : *di-F*: 485.5 [M+H]⁺; *F-alkene*: 403.3 [M+H-HOCH₂OCH₃]⁺, 465.5 [M+H]⁺.

Baeyer-Villiger products: 2,2-difluoro (**3.92**) and fluoro-epoxide (**3.94**)

Inseparable mixture of 2,2-difluoro (**3.90**) and fluoroalkene (**3.91**) were dissolved in DCM (0.5 mL) before the addition of mCPBA (8 mg, ≈ 2 equiv), and stirred overnight at RT. TLC analysis/ ^1H NMR analysis showed Baeyer-Villiger reaction had occurred at the 7-keto, and a roughly 75:25 ratio of F-alkene:F-epoxide. Further mCPBA (36 mg) was added and the RM stirred at RT for 60hr, giving a 40:60 ratio of F-alkene:F-epoxide. The reaction was then heated to 50 °C for 16 hr, then 70 °C for 8 hr to give full conversion to from **3.91** to F-epoxide **3.94**. **3.92** was also formed, but could not be isolated from **3.94**.

3.91 ($\text{C}_{27}\text{H}_{42}\text{F}_2\text{O}_6$, MW 500.6) and **3.94** ($\text{C}_{27}\text{H}_{41}\text{FO}_7$, MW 496.6): **m.p.** N/A; **R_f** (Petrol ether/EtOAc : 70/30) : 0.18; ^{19}F NMR (376 MHz, CDCl_3): δ -100.14 (d, $J=254.9$ Hz, 1F, $\underline{\text{E}}2\beta$, *di-F*), -103.58 (ddt, $J=253.2, 39.9, 8.0$ Hz, 1F, $\underline{\text{E}}2\alpha$, *di-F*), -126.39--126.30 (m, 0.2F, *unknown*), -142.92 (d, $J=3.5$ Hz, 0.5F, $\underline{\text{E}}2$, *F-epox*) ppm; $[\text{H}]^{19}\text{F}$ NMR (376 MHz, CDCl_3): δ -100.14 (d, $J=254.9$ Hz, 1F, $\underline{\text{E}}2\beta$, *di-F*), -103.58 (d, $J=253.2$ Hz, 1F, $\underline{\text{E}}2\alpha$, *di-F*), -126.34 (s, 0.2F, *unknown*), -142.92 (s, 0.5F, $\underline{\text{E}}2$, *F-epox*) ppm; **MS (ESI+)** m/z : *di-F*: 501.4 $[\text{M}+\text{H}]^+$, 1001.6 $[\text{2M}+\text{H}]^+$, 1023.6 $[\text{2M}+\text{Na}]^+$; *F-epox*: 497.3 $[\text{M}+\text{H}]^+$, 560.3 $[\text{M}+\text{MeCN}+\text{Na}]^+$, 993.4 $[\text{2M}+\text{H}]^+$, 1015.7 $[\text{2M}+\text{Na}]^+$.

Methyl 2,2-difluoro-3 β -methoxymethoxy-7-oxo-5 β -cholanoate (3.90) + oxidation products (e.g. 3.95 and 3.96)



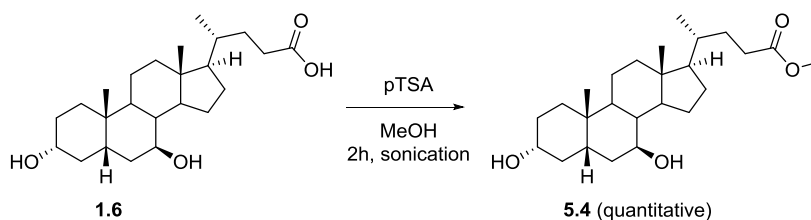
Mixture of **3.90/3.91** (1.8 g, ~3.71 mmol, 1equiv) was dissolved in MeCN (30 mL) before the addition of aq. NaClO (~11%, 7 mL, 11.1 mmol, 3 equiv). The reaction mixture was stirred overnight at RT, although reaction progress was slow so stirred for a further 24 h. Reaction still incomplete ($^1\text{H}/^{19}\text{F}$ NMR analysis) so further aq. NaClO (10 mL, ~4 equiv) and tetrabutyl ammonium bromide (60 mg, 0.18 mmol, 0.05 equiv) and stirred for an additional 24 h. Further NaClO (10 mL, ~4 equiv) added and stirred for a further 24 h. Some consumption of fluoroalkene observed, but significant degradation of **3.90** also. RM quenched with sat. aq. $\text{Na}_2\text{S}_2\text{O}_3$ (100 mL) and stirred for 15 min. Layers separated and aqueous extracted with EtOAc (3 \times 50 mL). Combined organics washed with brine (100 mL) and dried (Na_2SO_4) to yield 1.5 g of bright yellow gum. Crude purified *via* flash chromatography (pet ether/EtOAc : 90:10 \rightarrow 80:20 \rightarrow 70:30 \rightarrow 60:40 \rightarrow 50:50) to yield **3.90** (35 mg, <10% yield), along with \approx 700 mg of mixed fractions - deemed to contain oxidation products (e.g. **3.95** and **3.96**) by mass spectrometry analysis.

3.90: Formula: $\text{C}_{27}\text{H}_{42}\text{F}_2\text{O}_5$; MW : 484.6; **m.p.** N/A; **R_f** (Petrol ether/EtOAc : 70/30) : 0.60; ^1H NMR (400MHz, CDCl_3): δ 4.71 (d, $J=7.0$ Hz, 1H, O-CHH'-O), 4.64 (d, $J=7.0$ Hz, 1H, O-CHH'-O), 3.80 (br. s., 1H, H₃), 3.66 (s, 3H, CO_2CH_3), 3.36 (s, 3H, OCH_3), 2.90 (dd, $J=12.5, 6.4$ Hz, 1H, H_{6 β}), 2.43-1.31 (m, 31H), 1.29 (s, 3H, H₁₉), 1.27-0.93 (m, 7H), 0.91 (d, $J=6.4$ Hz, 3H, H₂₁), 0.65 (s, 3H, H₁₈) ppm; ^{19}F NMR (376 MHz, CDCl_3): δ -100.62 (dqin, $J=252.0, 5.0$ Hz, 1F, F_{2 β}), -102.94 (ddt, $J=252.0, 41.0, 8.0$ Hz, 1F, F_{2 α}) ppm; [H] ^{19}F NMR (376 MHz, CDCl_3): δ -100.62 (d, $J=252.0$ Hz, 1F, F_{2 β}), -102.94 (d, $J=251.4$ Hz, 1F, F_{2 α}) ppm; **MS (ESI+)** m/z : 485.6 [$\text{M}+\text{H}$] $^+$.

Chlorohydrin product (e.g. 3.95): Formula: $\text{C}_{27}\text{H}_{41}\text{ClF}_2\text{O}_6$; MW : 534.3; **MS (ESI+)** m/z : 535.6 [$\text{M}+\text{H}$] $^+$ (^{35}Cl), 537.6 [$\text{M}+\text{H}$] $^+$ (^{37}Cl), 557.4 [$\text{M}+\text{Na}$] $^+$ (^{35}Cl), 559.4 [$\text{M}+\text{H}$] $^+$ (^{37}Cl).

Alkene product (e.g. 3.96): Formula: $C_{27}H_{40}F_2O_5$; MW : 482.6; **MS (ESI+)** m/z : 483.6 $[M+H]^+$, 500.5 $[M+NH_4]^+$.

Methyl 3 α ,7 β -dihydroxy-5 β -cholanoate (5.4)

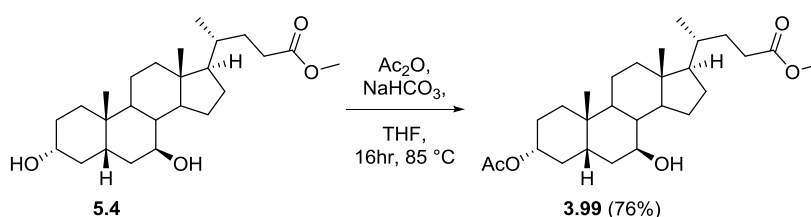


Using procedure A, UDCA **1.6** (100 g, 250 mmol, 1 equiv) was protected to yield methyl ester **5.4** as a white solid (103 g, 250 mmol, quantitative).

5.4: Formula: $C_{25}H_{42}O_4$; **MW** 406.6; **m.p.** 150-151 °C (lit 210-212 °C); **R_f** (Petrol ether/acetone : 50/50) : 0.66; **I.R.** 3350 (br. w), 2930 (s), 2864 (m), 1740 (s), 1452 (w), 1167 (w), 1051 (w) cm^{-1} ; **¹H NMR** (400MHz, CDCl_3): δ 3.66 (s, 3H, CO_2CH_3), 3.73-3.63 (m, 2H, H_3 and H_7), 3.58 (td, $J=10.4, 5.3$ Hz, 2H), 2.35 (ddd, $J=15.3, 10.1, 4.8$ Hz, 1H, H_{23}), 2.21 (ddd, $J=15.6, 9.6, 6.4$ Hz, 1H, H_{23}'), 1.99 (dt, $J=12.3, 2.8$ Hz, 1H), 1.95-0.97 (m, 26H), 0.94 (s, 3H, H_{19}), 0.92 (d, $J=6.4$ Hz, 3H, H_{21}), 0.67 (s, 3H, H_{18}) ppm; **¹³C NMR** (100 MHz, CDCl_3): δ 174.7 (C_{24}), 71.3 (C_3 or C_7), 71.3 (C_3 or C_7), 55.7, 54.9, 51.5 (CO_2CH_3), 43.7 (C_2), 42.4, 40.1 (CH_2), 39.2, 37.3 (CH_2), 36.8 (CH_2), 35.2, 34.9 (CH_2), 34.0, 31.0 (C_{23}), 31.0 (CH_2), 30.3 (CH_2), 28.6 (CH_2), 26.8 (CH_2), 23.3 (C_{19}), 21.1 (CH_2), 18.3 (C_{21}), 12.1 (C_{18}) ppm; **MS (ESI+)** m/z : 389.5 $[M+H-H_2O]^+$, 371.5 $[M+H-2H_2O]^+$; **HRMS (HPLC-ESI)** : $[M+NH_4]^+$ Calcd. 424.3421; Found. 424.3425.

Data consistent with literature (except m.p.)^[162]

Methyl 3 α -acetoxy-7 β -hydroxy-5 β -cholanoate (3.99)

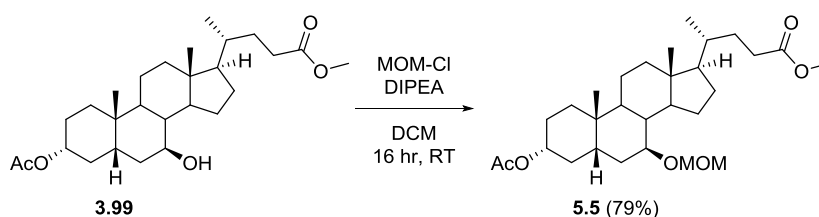


Diol **5.4** (30.0 g, 73.8 mmol, 1 equiv), acetic anhydride (35 mL, 369 mmol, 1 equiv) and NaHCO_3 (37.2 g, 443 mmol, 6 equiv) were taken up in THF (600 mL) and the reaction mixture was warmed to 85 °C overnight. Reaction mixture was cooled, filtered and the supernatant concentrated *in vacuo* to yield a crude residue. This was taken up in EtOAc and brine (300 mL each), the layers were then separated and the aqueous extracted with further EtOAc (2×200 mL). The combined organics were dried (Na_2SO_4) and concentrated to yield 37 g of clear gum/liquid. The crude was

purified *via* flash chromatography (pet ether/EtOAc : 85:15→80:20→70:30) to yield monoacetate **3.99** as a gummy solid (25.3 g, 56.4 mmol, 76%).

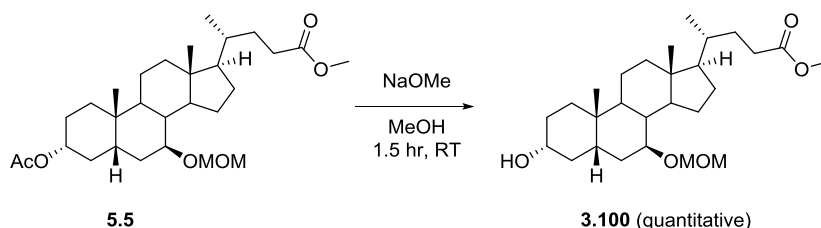
3.99: Formula: C₂₇H₄₄O₅; **MW** 448.6; **m.p.** N/A; **R_f** (Petrol ether/EtOAc : 60/40) : 0.52; **I.R.** 3518 (br. w), 2943 (m), 2868 (w), 1732 (s), 1238 (s), 1021 (s), 734 (s) cm⁻¹; **¹H NMR** (400MHz, CDCl₃): δ 4.64 (tt, *J*=10.5, 5.5 Hz, 1H, H3), 3.64 (s, 3H, CO₂CH₃), 3.55 (ddd, *J*=11.5, 8.7, 5.1 Hz, 1H, H7), 2.33 (ddd, *J*=15.5, 11.0, 5.0 Hz, 1H, H23), 2.20 (ddd, *J*=15.6, 9.6, 6.4 Hz, 1H, H23'), 2.00 (s, 3H, COCH₃), 1.97-0.98 (m, 24H), 0.93 (s, 3H, H19), 0.90 (d, *J*=6.4 Hz, 3H, H21), 0.65 (s, 3H, H18) ppm; **¹³C NMR** (100 MHz, CDCl₃): δ 174.6 (C24), 170.5 (COCH₃), 73.7 (C3), 71.1 (C7), 55.7, 54.9, 51.4 (CO₂CH₃), 43.6, 43.6, 42.2, 40.0 (CH₂), 39.1, 36.6 (CH₂), 35.2, 34.5 (CH₂), 34.0, 33.1 (C23), 31.0 (CH₂), 30.9 (CH₂), 28.5 (CH₂), 26.8 (CH₂), 26.4 (CH₂), 23.3 (C19), 21.3 (COCH₃), 21.1 (CH₂), 18.3 (C21), 12.0 (C18) ppm; **MS (ESI+)** *m/z* : 471.5 [M+Na]⁺, 371.4 [M+H-H₂O-HOAc]⁺; **HRMS** (HPLC-ESI) : [M+Na]⁺ Calcd. 471.3081; Found. 471.3091.

Methyl 3 α -acetoxo-7 β -methoxymethoxyl-5 β -cholanoate (**5.5**)



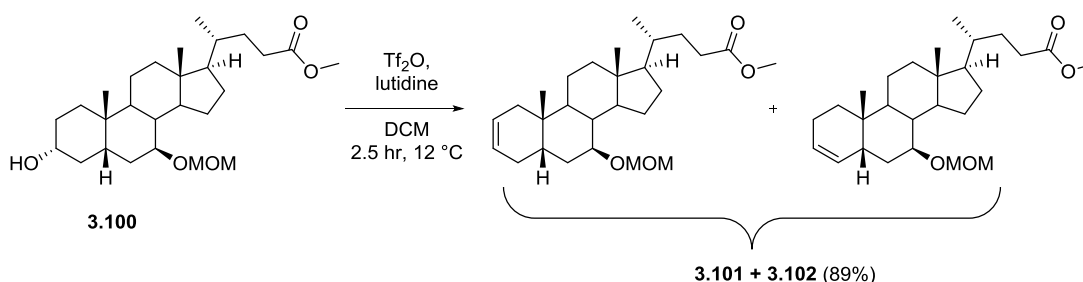
Using general procedure C, alcohol **3.99** (72 g, 160.5 mmol, 1 equiv) was protected as a MOM ether. Crude purified *via* flash chromatography (pet ether/EtOAc : 85:15→80:20→70:30→60:40) to yield **5.5** as a gummy solid (62 g, 126 mmol, 79%).

5.5: Formula: C₂₉H₄₈O₆; **MW** 492.7; **m.p.** 92-93 °C; **R_f** (Petrol ether/EtOAc : 80/20) : 0.37; **I.R.** 2942 (m), 2871 (w), 1734 (s), 1235 (s), 1104 (m), 1031 (s) cm⁻¹; **¹H NMR** (400MHz, CDCl₃): δ 4.70-4.61 (m, 1H, H3), 4.60 (s, 2H, O-CH₂-O), 3.64 (s, 3H, CO₂CH₃), 3.39-3.25 (m, 4H, OCH₃ and H7), 2.33 (ddd, *J*=15.5, 11.0, 5.0 Hz, 1H, H23), 2.19 (ddd, *J*=15.5, 9.6, 6.4 Hz, 1H, H23'), 2.00 (s, 3H, COCH₃), 1.90-0.98 (m, 25H), 0.94 (s, 3H, H19), 0.90 (d, *J*=6.4 Hz, 3H, H21), 0.65 (s, 3H, H18) ppm; **¹³C NMR** (100 MHz, CDCl₃): δ 174.6 (C24), 170.4 (COCH₃), 97.2 (O-CH₂-O), 79.8 (C7), 73.7 (C3), 55.8, 55.7 (OCH₃), 55.0, 51.4 (CO₂CH₃), 43.7, 42.1, 41.6, 40.0 (CH₂), 39.3, 35.2, 34.7 (CH₂), 34.5 (CH₂), 33.9, 33.0 (CH₂), 31.0 (C23), 31.0 (CH₂), 28.5 (CH₂), 26.4 (CH₂), 26.4 (CH₂), 23.3 (C19), 21.3 (COCH₃), 21.3 (CH₂), 18.4 (C21), 12.1 (C18) ppm; **MS (ESI+)** *m/z* : 515.5 [M+Na]⁺, 371.5 [M+H-HOCH₂OCH₃-HOAc]⁺; **HRMS** (HPLC-ESI) : [M+Na]⁺ Calcd. 515.3343; Found. 515.3356.

Methyl 3 α -hydroxy-7 β -methoxymethoxyl-5 β -cholanoate (3.100)

Using general procedure F, 3 α -acetate **5.5** (82 g, 166 mmol, 1 equiv) was hydrolysed to yield alcohol **3.100** as a pale yellow gum (75 g, 166 mmol, quantitative yield).

3.100: Formula: C₂₇H₄₆O₅; **MW** 450.7; **m.p.** N/A; **R_f** (Petrol ether/EtOAc : 60/40) : 0.30; **I.R.** 3429 (br. w), 2931 (m), 2868 (w), 1736 (m), 1102 (m), 1033 (s), 735 (s) cm⁻¹; **¹H NMR** (400MHz, CDCl₃): δ 4.61 (s, 2H, O-CH₂-O), 3.65 (s, 3H, CO₂CH₃), 3.56 (tt, *J*=10.5, 5.0 Hz, 1H, H₃), 3.41-3.25 (m, 4H, OCH₃ and H₇), 2.34 (ddd, *J*=15.5, 11.0, 5.0 Hz, 1H, H₂₃), 2.20 (ddd, *J*=15.5, 9.6, 6.4 Hz, 1H, H_{23'}), 2.02-1.90 (m, 1H), 1.89-1.72 (m, 6H), 1.70-0.97 (m, 19H), 0.94 (s, 3H, H₁₉), 0.90 (d, *J*=6.4 Hz, 3H, H₂₁), 0.66 (s, 3H, H₁₈) ppm; **¹³C NMR** (100 MHz, CDCl₃): δ 174.7 (C₂₄), 97.2 (O-CH₂-O), 80.0 (C₇), 71.3 (C₃), 55.8, 55.7 (OCH₃), 54.9, 51.4 (CO₂CH₃), 43.7, 42.3, 41.6, 40.0 (CH₂), 39.3, 37.2 (CH₂), 35.2, 34.9 (CH₂), 34.8 (CH₂), 33.9, 31.0 (C₂₃), 31.0 (CH₂), 30.2 (CH₂), 28.5 (CH₂), 26.4 (CH₂), 23.3 (C₁₉), 21.2 (CH₂), 18.4 (C₂₁), 12.1 (C₁₈) ppm; **MS (ESI+)** *m/z* : 371.5 [M+H-HOCH₂OCH₃-H₂O]⁺; **HRMS** (HPLC-ESI) : [M+Na]⁺ Calcd. 473.3237; Found. 473.3246.

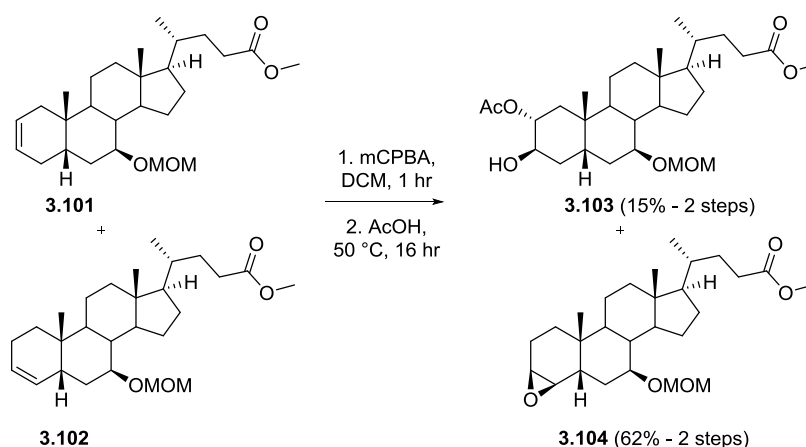
Methyl 7 β -methoxymethoxyl-5 β -chol-2-enoate (3.101) and methyl 7 β -methoxymethoxyl-5 β -chol-3-enoate (3.102)

3 α -OH derivative **3.100** (75 g, 166 mmol, 1 equiv) was dissolved in DCM (650 mL) and cooled to 5 °C on ic, before the addition of lutidine (58 mL < 500 mmol, 3 equiv) and Tf₂O (31 mL, 183 mmol, 1.1 equiv). Reaction mixture warmed to 8-10 °C for 1 h however reaction incomplete, further lutidine (25 mL) and Tf₂O (15 mL), and RM further warmed to 12-14 °C for a further 1.5 h. Reaction deemed complete by TLC analysis. Reaction mixture dry loaded onto silica, and purified *via* flash chromatography (pet ether/EtOAc : 98:2→97:3→95:5) to yield an inseparable mixture of alkenes **3.101** and **3.102** as a pale yellow gum (64.1 g, 148 mmol, 89%).

3.101/3.102: m.p. N/A; **R_f** (Petrol ether/EtOAc : 70/30) : 0.69; **¹H NMR** (400MHz, CDCl₃): δ 5.74-5.34 (m, 2H, C=CH), 4.68-4.62 (m, 2H, O-CH₂-O), 3.66 (s, 3H, CO₂CH₃), 3.37 (s, 3H, OCH₃), 3.13 (td, *J*=10.2, 5.0 Hz, 1H, H₇), 2.32 (ddd, *J*=15.5, 10.3, 5.0 Hz, 1H, H₂₃), 2.26-2.16 (m, 1H, H_{23'}), 2.15-1.00 (m, 27H), 0.98 (s, 2H, H₁₉), 0.92 (d, *J*=6.4 Hz, 2H, H₂₁), 0.86 (d, *J*=6.6 Hz, 2H, H₂₁), 0.68 (s, 3H, H₁₈) ppm.

Mixture of isomers used without full characterisation.

Methyl 2 α -acetoxy-3 β -hydroxy-7 β -methoxymethoxy-5 β -cholanoate (3.103) and methyl 3 β ,4 β -epoxy-7 β -methoxymethoxy-5 β -cholanoate (3.104)



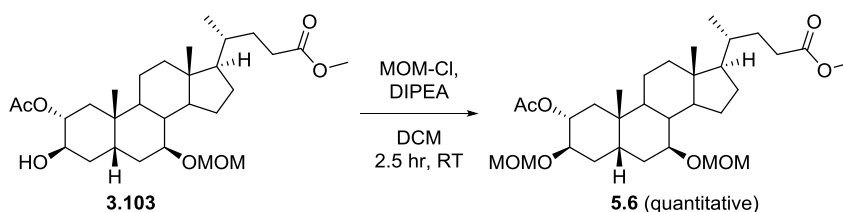
Mixture of **3.101** and **3.102** (63.0 g, 146 mmol, 1 equiv) alkenes, along with mCPBA (54.0 g, 1.5 equiv) was dissolved in DCM and stirred for 1 h at RT. RM quenched with sat. aq. Na₂S₂O₃ (250 mL) and stirred for 20 min at RT. Layers separated and aqueous extracted with DCM (300 mL). Combined organics washed with sat. aq. NaHCO₃ (300 mL), dried (Na₂SO₄) and concentrated, to yield 72 g of a pale yellow gum containing an inseparable mixture of Δ 2 β ,3 β - and Δ 3 β ,4 β -epoxides (assume quantitative yield). This mixture was then dissolved in AcOH (600 mL), and warmed to 50 °C for 16 hr. The reaction mixture was concentrated *in vacuo*, then azeotroped (EtOAc \times 3, DCM \times 1), before the crude was purified *via* flash chromatography (pet ether/EA : 85:15 \rightarrow 80:20 \rightarrow 70:30 \rightarrow 60:40 \rightarrow 50:50) to yield 2 α -acetate **3.103** as a gummy solid (11.1 g, 21.9 mmol, 15% - 2 steps) and Δ 3 β ,4 β -epoxide **3.104** as a gummy solid (40.5 g, 90 mmol, 62% - 2 steps).

3.103: Formula: C₂₉H₄₈O₇; **MW** 508.7; **m.p.** N/A; **R_f** (Petrol ether/EtOAc : 60/40) : 0.32; **I.R.** 3469 (br. w), 2938 (m), 2875 (w), 1731 (s), 1242 (s), 1046 (s), 1031 (s), 734 (s) cm⁻¹; **¹H NMR** (400MHz, CDCl₃): δ 4.74 (q, *J*=3.9 Hz, 1H, H₂), 4.62 (s, 2H, O-CH₂-O), 3.79 (q, *J*=3.7 Hz, 1H, H₃), 3.64 (s, 3H, CO₂CH₃), 3.36-3.31 (m, 4H, OCH₃ and H₇), 2.33 (ddd, *J*=15.5, 11.0, 5.0 Hz, 1H, H₂₃), 2.20 (ddd, *J*=15.5, 9.6, 6.4 Hz, 1H, H_{23'}), 2.03 (s, 3H, C(O)CH₃), 2.01-0.99 (m, 29H), 0.98 (s, 3H, H₁₉), 0.90 (d, *J*=6.4 Hz, 3H, H₂₁), 0.65 (s, 3H, H₁₈) ppm; **¹³C NMR** (100 MHz, CDCl₃): δ 174.7 (C₂₄), 170.4 (C(O)CH₃), 97.0 (O-CH₂-O), 80.5 (C₇), 73.8 (C₂), 68.0 (C₃), 56.1, 55.7 (OCH₃), 55.1, 51.4 (CO₂CH₃),

43.5, 42.4, 41.1, 40.1 ($\underline{\text{C}}_2$), 35.9, 35.2, 35.0, 34.7 ($\underline{\text{C}}_2$), 34.0 ($\underline{\text{C}}_2$), 31.6 ($\underline{\text{C}}_2$), 31.0 ($\underline{\text{C}}_{23}$), 30.9 ($\underline{\text{C}}_2$), 28.4 ($\underline{\text{C}}_2$), 26.1 ($\underline{\text{C}}_2$), 23.3 ($\underline{\text{C}}_{19}$), 21.9 ($\underline{\text{C}}_2$), 21.3 ($\text{C}(\text{O})\underline{\text{C}}_3$), 18.3 ($\underline{\text{C}}_{21}$), 12.0 ($\underline{\text{C}}_{18}$) ppm; **MS (ESI+)** m/z : 531.6 $[\text{M}+\text{Na}]^+$, 387.4 $[\text{M}+\text{H}-\text{HOCH}_2\text{OCH}_3-\text{HOCH}_2\text{OCH}_3]^+$; **HRMS (HPLC-ESI)** : $[\text{M}+\text{Na}]^+$ Calcd: 531.3292; Found: 531.3301.

3.104: Formula: $\text{C}_{27}\text{H}_{44}\text{O}_5$; **MW** 448.6; **m.p.** N/A; **R_f** (Petrol ether/EtOAc : 60/40) : 0.60; **I.R.** 2936 (m), 2874 (w), 1733 (s), 1105 (s), 1046 (s), 1033 (s), 734 (s) cm^{-1} ; **¹H NMR** (400MHz, CDCl_3): δ 4.64 (s, 2H, O- $\underline{\text{C}}_2$ -O), 3.64 (s, 3H, $\text{CO}_2\underline{\text{C}}_3$), 3.35 (s, 3H, OCH_3), 3.19 (br. s., 1H, $\underline{\text{H}}_3$), 3.10 (td, $J=10.8, 4.5$ Hz, 1H, $\underline{\text{H}}_7$), 2.88 (d, $J=3.7$ Hz, 1H, $\underline{\text{H}}_4$), 2.32 (ddd, $J=15.5, 11.0, 5.0$ Hz, 1H, $\underline{\text{H}}_{23}$), 2.19 (ddd, $J=15.5, 9.6, 6.4$ Hz, 1H, $\underline{\text{H}}_{23}'$), 2.12-2.04 (m, 1H), 2.03-0.95 (m, 25H), 0.90 (d, $J=6.4$ Hz, 3H, $\underline{\text{H}}_{21}$), 0.87 (s, 3H, $\underline{\text{H}}_{19}$), 0.65 (s, 3H, $\underline{\text{H}}_{18}$) ppm; **¹³C NMR** (100 MHz, CDCl_3): δ 174.6 ($\underline{\text{C}}_{24}$), 97.0 (O- $\underline{\text{C}}_2$ -O), 81.2 ($\underline{\text{C}}_7$), 55.8 ($\underline{\text{C}}_3$ or $\underline{\text{C}}_4$), 55.7 (OCH_3), 55.4, 54.8, 53.3 ($\underline{\text{C}}_3$ or $\underline{\text{C}}_4$), 51.4 ($\text{CO}_2\underline{\text{C}}_3$), 43.6, 43.0, 40.7, 40.6, 39.8 (CH_2), 35.1, 34.3 (CH_2), 31.6, 30.9 (CH_2), 30.9 ($\underline{\text{C}}_{23}$), 28.7 (CH_2), 28.4, (CH_2) 26.6 (CH_2), 22.2 ($\underline{\text{C}}_{19}$), 21.2 (CH_2), 20.3 (CH_2), 18.3 ($\underline{\text{C}}_{21}$), 12.0 ($\underline{\text{C}}_{18}$) ppm; **MS (ESI+)** m/z : 417.4 $[\text{M}, \text{partial -MOM cleavage}]^+$, 387.4 $[\text{M}+\text{H}-\text{HOCH}_2\text{OCH}_3]^+$; **HRMS (HPLC-ESI)** : $[\text{M}+\text{Na}]^+$ Calcd: 471.3081; Found: 471.3067.

Methyl 2 α -acetoxymethyl-3 β ,7 β -dimethoxymethoxymethyl-5 β -cholanoate (5.6)

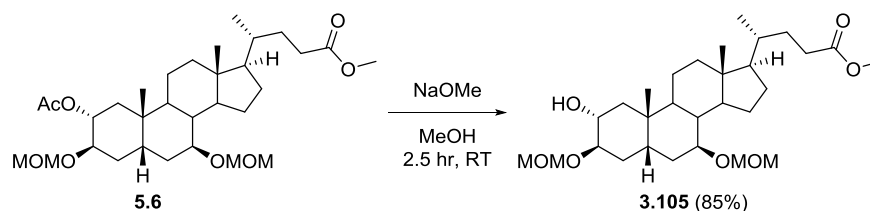


Using general procedure C, 3 β -OH derivative **3.103** (11.0 g, 21.6 mmol, 1 equiv) was protected as the MOM derivative to yield **5.6** as a pale yellow oil/gum (13.0 g, quantitative).

5.6: Formula: $\text{C}_{31}\text{H}_{52}\text{O}_8$; **MW** 552.8; **m.p.** N/A; **R_f** (Petrol ether/EtOAc : 60/40) : 0.73; **I.R.** 2939 (m), 2885 (m), 1737 (s), 1240 (s), 1102 (m), 1038 (s) cm^{-1} ; **¹H NMR** (400MHz, CDCl_3): δ 4.83 (q, $J=3.1$ Hz, 1H, $\underline{\text{H}}_2$), 4.62 (s, 2H, C3-O- $\underline{\text{C}}_2$ -O), 4.62 (s, 2H, C7-O- $\underline{\text{C}}_2$ -O), 3.67 (q, $J=2.9$ Hz, 1H, $\underline{\text{H}}_3$), 3.63 (s, 3H, $\text{CO}_2\underline{\text{C}}_3$), 3.33 (s, 3H, OCH_3), 3.33 (s, 3H, OCH_3), 3.32-3.30 (m, 1H, $\underline{\text{H}}_7$), 2.32 (ddd, $J=15.5, 11.0, 5.0$ Hz, 1H, $\underline{\text{H}}_{23}$), 2.19 (ddd, $J=15.6, 9.4, 6.5$ Hz, 1H, $\underline{\text{H}}_{23}'$), 2.01 (s, 3H, $\text{C}(\text{O})\underline{\text{C}}_3$), 1.99-1.25 (m, 25H), 0.95 (s, 3H, $\underline{\text{H}}_{19}$), 0.89 (d, $J=6.4$ Hz, 3H, $\underline{\text{H}}_{21}$), 0.65 (s, 3H, $\underline{\text{H}}_{18}$) ppm; **¹³C NMR** (100 MHz, CDCl_3): δ 174.6 ($\underline{\text{C}}_{24}$), 169.9 ($\text{C}(\text{O})\underline{\text{C}}_3$), 97.1 (C3-O- $\underline{\text{C}}_2$ -O), 95.1 (C7-O- $\underline{\text{C}}_2$ -O), 80.2 ($\underline{\text{C}}_7$), 72.5 ($\underline{\text{C}}_3$), 71.4 ($\underline{\text{C}}_2$), 55.9, 55.7 (OCH_3), 55.3 (OCH_3), 55.0, 51.4 ($\text{CO}_2\underline{\text{C}}_3$), 43.7, 41.6, 41.5, 40.3 ($\underline{\text{C}}_2$), 36.8, 35.2, 34.5 ($\underline{\text{C}}_2$), 34.4, 34.2 ($\underline{\text{C}}_2$), 31.0 ($\underline{\text{C}}_{23}$), 30.9 ($\underline{\text{C}}_2$), 28.8 ($\underline{\text{C}}_2$), 28.5 ($\underline{\text{C}}_2$), 26.3 ($\underline{\text{C}}_2$), 23.8 ($\underline{\text{C}}_{19}$), 21.9 ($\underline{\text{C}}_2$), 21.3 ($\text{C}(\text{O})\underline{\text{C}}_3$), 18.3 ($\underline{\text{C}}_{21}$), 12.1 ($\underline{\text{C}}_{18}$) ppm; **MS (ESI+)** m/z : 575.6 $[\text{M}+\text{Na}]^+$, 491.6 $[\text{M}$ -

$\text{HOCH}_2\text{OCH}_3]^+$, 429.5 $[\text{M}-2\text{HOCH}_2\text{OCH}_3]^+$; **HRMS** (HPLC-ESI) : $[\text{M}+\text{Na}]^+$ Calcd: 575.3554; Found: 575.3555.

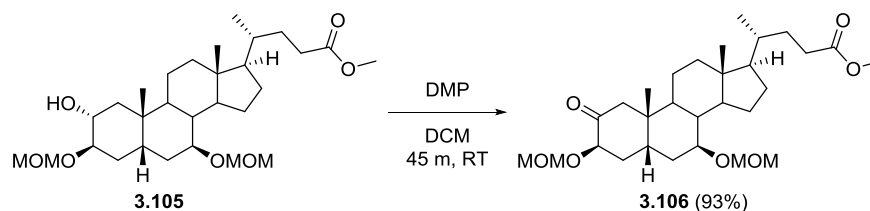
Methyl 2 α -hydroxy-3 β ,7 β -dimethoxymethoxyl-5 β -cholanoate (3.105)



Using general procedure F, 2 α -acetate derivative **5.6** (13.0 g, 21.6 mmol, 1 equiv) was methanolysed to yield **3.105** as a pale yellow gum (9.5 g, 18.3 mmol, 85%).

3.105: Formula: $\text{C}_{29}\text{H}_{50}\text{O}_7$; **MW** 510.7; **m.p.** N/A; **R_f** (Petrol ether/EtOAc : 60/40) : 0.41; **I.R.** 3472 (br. w), 2936 (m), 2883 (w), 1738 (m), 1146 (m), 1101 (m), 1041 (s) cm^{-1} ; **¹H NMR** (400MHz, CDCl_3): δ 4.65 (d, $J=6.8$ Hz, 1H, C3-O- CH_2 -O), 4.62 (d, $J=6.8$ Hz, 1H, C3-O- CH_2 -O), 4.60 (d, $J=6.8$ Hz, 1H, C7-O- CH_2 -O), 4.57 (d, $J=6.8$ Hz, 1H, C7-O- CH_2 -O), 3.65-3.59 (m, 4H, CO_2CH_3 + H_3), 3.43-3.36 (m, 1H, H_7), 3.34 (s, 3H, OCH_3), 3.33-3.31 (m, 1H, H_2), 3.31 (s, 3H, OCH_3), 2.96 (br. s., 1H, OH), 2.29 (ddd, $J=15.6, 10.5, 5.0$ Hz, 1H, H_{23}), 2.16 (ddd, $J=15.6, 9.4, 6.5$ Hz, 1H, H_{23}'), 1.97-1.23 (m, 21H), 1.16-0.96 (m, 4H), 0.92 (s, 3H, H_{19}), 0.86 (d, $J=6.4$ Hz, 3H, H_{21}), 0.61 (s, 3H, H_{18}) ppm; **¹³C NMR** (100 MHz, CDCl_3): δ 174.5 (C_{24}), 96.8 (C7-O- CH_2 -O), 96.0 (C3-O- CH_2 -O), 81.2 (C_3), 79.9 (C_7), 69.9 (C_2), 56.1, 55.7 (OCH_3), 55.3 (OCH_3), 55.0, 51.3 (CO_2CH_3), 44.5, 43.1, 40.1, 39.8 (CH_2), 39.6 (CH_2), 35.9, 35.2, 35.1, 33.3 (CH_2), 31.2 (CH_2), 30.9 (2C, C_{23} + CH_2), 28.2 (CH_2), 25.5 (CH_2), 22.4 (C_{19}), 22.0 (CH_2), 18.2 (C_{21}), 11.8 (C_{18}) ppm; **MS (ESI+)** m/z : 533.7 $[\text{M}+\text{Na}]^+$, 399.5 $[\text{M}-\text{HOCH}_2\text{OCH}_3-\text{H}_2\text{O}-\text{OMe}]^+$, 387.4 $[\text{M}+\text{H}-2\text{HOCH}_2\text{OCH}_3]^+$; **HRMS** (HPLC-ESI) : $[\text{M}+\text{Na}]^+$ Calcd: 533.3449; Found: 533.3448.

Methyl 2-oxo-3 β ,7 β -dimethoxymethoxyl-5 β -cholanoate (3.106)

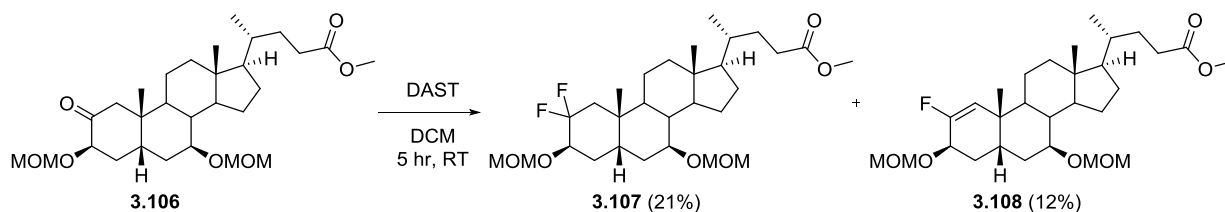


Using procedure E, 2 α -alcohol **3.105** (9.2 g, 18.0 mmol 1 equiv) was oxidised, then purified *via* flash chromatography (pet ether/EtOAc : 80:20 \rightarrow 70:30 \rightarrow 65:35) to yield **3.106** as a pale gummy solid (8.5 g, 16.7 mmol, 93%).

3.106: Formula: $\text{C}_{29}\text{H}_{48}\text{O}_7$; **MW** 508.7; **m.p.** N/A; **R_f** (Petrol ether/EtOAc : 60/40) : 0.54; **I.R.** 2940 (m), 1731 (s), 1099 (s), 1028 (s) cm^{-1} ; **¹H NMR** (400MHz, CDCl_3): δ 4.62 (d, $J=7.0$ Hz, 2H, C7-O- CH_2 -

O), 4.58 (d, $J=7.0$ Hz, 2H, C3-O-CH₂-O), 3.76 (t, $J=2.6$ Hz, 1H, H₃), 3.63 (s, 3H, CO₂CH₃), 3.34 (s, 3H, OCH₃), 3.32 (s, 3H, OCH₃), 3.31-3.23 (m, 1H, H₇), 2.64 (d, $J=12.8$ Hz, 1H, H_{1β}), 2.38-2.03 (m, 5H), 2.01-1.25 (m, 14H), 1.21-1.10 (m, 2H), 1.09 (s, 3H, H₁₉), 0.87 (d, $J=6.4$ Hz, 3H, H₂₁), 0.63 (s, 3H, H₁₈) ppm; ¹³C NMR (100 MHz, CDCl₃): δ 210.6 (C₂), 174.7 (C₂₄), 97.2 (C7-O-CH₂-O), 95.8 (C3-O-CH₂-O), 79.5 (C₇), 79.4 (C₃), 55.8 (OCH₃), 55.7 (OCH₃), 55.4, 54.8, 51.4 (CO₂CH₃), 46.8 (C₁), 43.6, 41.7, 41.6, 41.3, 39.6 (CH₂), 37.4, 35.1, 35.0 (CH₂), 33.1 (CH₂), 30.9 (CH₂), 30.9 (CH₂), 28.3 (CH₂), 26.1 (CH₂), 23.5 (C₁₉), 21.5 (CH₂), 18.3 (C₂₁), 12.1 (C₁₈) ppm; MS (ESI+) m/z : 531.6 [M+Na]⁺, 477.6 [M-OMe]⁺, 415.5 [M-HOCH₂OCH₃-OMe]⁺; HRMS (HPLC-ESI) : [M+Na]⁺ Calcd: 531.3292; Found: 531.3298.

Methyl 2,2-difluoro-3β,7β-dimethoxymethoxyl-5β-cholanoate (3.107) and methyl 2-fluoro-3β,7β-dimethoxymethoxyl-5β-chol-1-enoate (3.108)



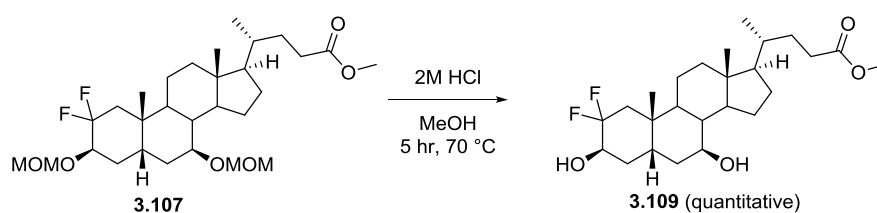
Ketone **3.106** (8.0 g, 15.7 mmol, 1 equiv) was dissolved in DCM (40 mL) before the addition of DAST (1004 mL, 78.6 mmol, 5 equiv) and the reaction mixture stirred at RT for 5 hr. Mixture was then diluted with DCM (100 mL) before adding dropwise to an ice-cold sat. aq. solution of NaHCO₃ (150 mL), then stirred for 20 mins. Layers were separated then aqueous was extracted with DCM (100 mL), combined organics were then dried (Na₂SO₄) and concentrated to yield 7.5 g of a pale brown gum/oil. Crude purified *via* flash chromatography (pet ether/EtOAc : 90:10→85:15→80:20) to yield 2,2-difluoro analogue **3.107** (1.75 g, 3.3 mmol, 21%) along with 2-fluoro alkene analogue **3.108** (970 mg, 1.9 mmol, 12%) both as gummy solids.

3.107: Formula: C₂₉H₄₈F₂O₆; **MW** 530.7; **m.p.** N/A; **R_f** (Petrol ether/EtOAc : 80/20) : 0.46; **I.R.** 2941 (m), 1737 (m), 1148 (m), 1103 (s), 1045 (s), 1032 (s) cm⁻¹; ¹H NMR (400MHz, CDCl₃): δ 4.72 (d, $J=6.6$ Hz, 1H, C3-O-CH₂-O), 4.66 (d, $J=6.6$ Hz, 1H, C3-O-CH₂-O), 4.63 (s, 2H, C7-O-CH₂-O), 3.81 (br. s., 1H, H₃), 3.66 (s, 3H, CO₂CH₃), 3.38 (s, 3H, C3-O-CH₂-O-CH₃), 3.36 (s, 3H, C7-O-CH₂-O-CH₃), 3.31-3.21 (m, 1H, H₇), 2.34 (ddd, $J=15.6, 10.5, 5.0$ Hz, 1H, H₂₃), 2.21 (ddd, $J=15.6, 9.4, 6.5$ Hz, 1H, H_{23'}), 2.12 (br. s., 1H, H₁), 2.05-1.08 (m, 25H), 1.04 (s, 3H, H₁₉), 0.92 (d, $J=6.4$ Hz, 3H, H₂₁), 0.67 (s, 3H, H₁₈) ppm; ¹³C NMR (100 MHz, CDCl₃): δ 174.7 (C₂₄), 122.7 (dd, $J=249.4, 241.4$ Hz, C₂), 97.4 (C7-O-CH₂-O), 95.8 (d, $J=2.2$ Hz, C3-O-CH₂-O), 79.9 (C₇), 72.5 (dd, $J=35.2, 20.5$ Hz, C₃), 55.8, 55.6, 55.5, 54.9, 51.4 (CO₂CH₃), 43.7, 41.7, 40.2 (d, $J=4.4$ Hz, C₉), 39.8 (CH₂), 37.7 (t, $J=20.5$ Hz, C₁), 36.3, 36.0 (d, $J=9.5$ Hz, C₁₀), 35.2, 33.8 (CH₂), 31.0 (C₂₃ + CH₂), 30.8 (d, $J=5.9$ Hz, C₄), 28.5 (CH₂), 26.4 (CH₂),

23.9 (C₁₉), 21.8 (CH₂), 18.4 (C₂₁), 12.2 (C₁₈) ppm; ¹⁹F NMR (376MHz, CDCl₃): δ -99.89 (d, J=259.0 Hz, F_{2β}), -102.89 (ddt, J=250.6, 40.7, 5.0 Hz, F_{2α}) ppm; [H]¹⁹F NMR (376MHz, CDCl₃): δ -99.89 (d, J=249.7 Hz, F_{2β}), -102.89 (d, J=249.7 Hz, F_{2α}) ppm; MS (ESI+) m/z : 553.5 [M+Na]⁺, 437.5 [M-HOCH₂OCH₃-OCH₃]⁺; HRMS (HPLC-ESI) : [M+Na]⁺ Calcd: 553.3311; Found: 553.3315.

3.108: Formula: C₂₉H₄₇FO₆; **MW** 510.7; **m.p.** N/A; **R_f** (Petrol ether/EtOAc : 80/20) : 0.34; **I.R.** 2939 (m), 2891 (w), 1737 (m), 1149 (s), 1098 (m), 1043 (s), 916 (m), 731 (m) cm⁻¹; ¹H NMR (400MHz, CDCl₃): δ 5.39 (d, J=17.7 Hz, 1H, H₁), 4.71 (d, J=6.8 Hz, 1H, C3-O-CH₂-O), 4.69 (d, J=6.8 Hz, 1H, C3-O-CH₂-O), 4.64 (s, 2H, C7-O-CH₂-O), 4.12-4.08 (m, 1H, H₃), 3.66 (s, 3H, CO₂CH₃), 3.40 (s, 3H, C3-O-CH₂-O-CH₃), 3.36 (s, 3H, C7-O-CH₂-O-CH₃), 3.27-3.17 (m, 1H, H₇), 2.34 (ddd, J=15.6, 10.5, 5.0 Hz, 1H, H₂₃), 2.21 (ddd, J=15.6, 9.4, 6.5 Hz, 1H, H_{23'}), 2.12-1.14 (m, 24H), 1.12 (s, 3H, H₁₉), 1.10-0.96 (m, 2H), 0.91 (d, J=6.4 Hz, 3H, H₂₁), 0.68 (s, 3H, H₁₈) ppm; ¹³C NMR (100 MHz, CDCl₃): δ 174.7 (C₂₄), 157.0 (d, J=259.0 Hz, C₂), 117.2 (d, J=11.0 Hz, C₁), 97.2 (C7-O-CH₂-O), 95.2 (C3-O-CH₂-O), 80.0 (C₇), 68.4 (d, J=24.9 Hz, C₃), 55.8 (C3-O-CH₂-O-CH₃), 55.3 (C7-O-CH₂-O-CH₃), 55.2, 54.9, 51.4 (CO₂CH₃), 45.2 (d, J=2.9 Hz, C₉), 43.8, 41.5, 39.8 (CH₂), 36.3 (d, J=5.9 Hz, C₁₀), 36.1 (d, J=1.5 Hz), 35.2, 34.4 (CH₂), 31.9 (d, J=8.8 Hz, C₄), 31.0 (C₂₃), 31.0 (CH₂), 28.4 (CH₂), 26.5 (CH₂), 22.5 (CH₂), 21.7 (d, 1.5 Hz, C₁₉), 18.4 (C₂₁), 12.2 (C₁₈) ppm; ¹⁹F NMR (376MHz, CDCl₃): δ -115.57 (dt, J=17.0, 8.5 Hz) ppm; [H]¹⁹F NMR (376MHz, CDCl₃): δ -115.57 (s) ppm; MS (ESI+) m/z : 448.6[M+H-HOCH₂-OCH₃]⁺, 387.4 [M+H-2HOCH₂OCH₃]⁺; HRMS (HPLC-ESI) : [M+Na]⁺ Calcd: 533.3249; Found: 533.3246.

Methyl 2,2-difluoro-3β,7β-dihydroxy-5β-cholanoate (3.109)

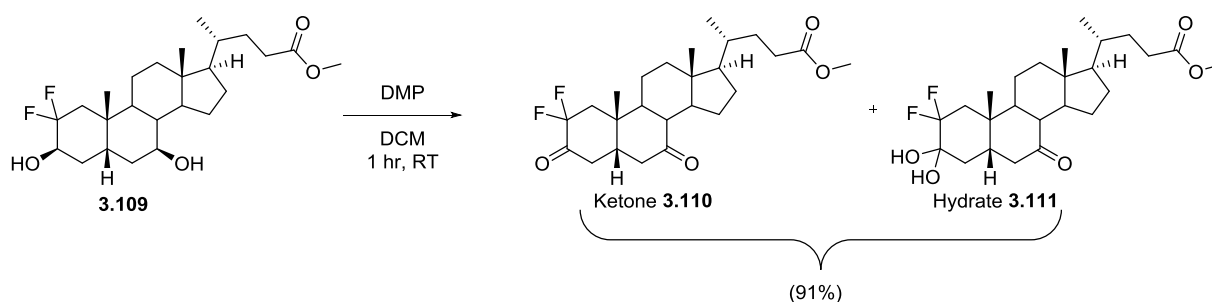


Di-MOM protected alcohol **3.107** (1.5 g, 1.76 mmol, 1 equiv) was dissolved in MeOH (50 mL) and 2M HCl (10 mL), then the mixture was warmed to 70 °C for 5 hr. Reaction mixture was cooled, and concentrated *in vacuo*, azeotroping to complete dryness (MeOH×3, CHCl₃×1) to yield **3.109** as a gummy solid (1.3 g, quantitative yield). (**General procedure D**).

3.109: Formula: C₂₅H₄₀F₂O₄; **MW** 442.6; **m.p.** N/A; **R_f** (Petrol ether/EtOAc : 50/50) : 0.35; **I.R.** 3432 (br. w), 2939 (m), 2870 (w), 1721 (m), 1071 (s), 1040 (s), 730 (s) cm⁻¹; ¹H NMR (400MHz, CDCl₃): δ 3.89 (t, J=5.7 Hz, 1H, H₃), 3.67 (s, 3H, CO₂CH₃), 3.54 (ddd, J=11.6, 9.2, 5.1 Hz, 1H, H₇), 2.36 (ddd, J=15.6, 10.5, 5.0 Hz, 1H, H₂₃), 2.22 (ddd, J=15.6, 9.4, 6.5 Hz, 1H, H_{23'}), 2.17-1.07 (m, 27H), 1.05 (s, 3H, H₁₉), 0.93 (d, J=6.4 Hz, 3H, H₂₁), 0.69 (s, 3H, H₁₈) ppm; ¹³C NMR (100 MHz, CDCl₃): δ 174.8

(C24), 123.2 (t, $J=243.0$ Hz, C2), 71.1 (C7), 68.5 (dd, $J=34.5, 22.7$ Hz, C3), 55.5, 54.8, 51.5 (CO₂CH₃), 43.8, 43.7, 39.9 (d, $J=4.4$ Hz), 39.8 (CH₂), 37.0 (t, $J=20.5$ Hz, C1), 36.3 (dd, $J=10.3, 1.5$ Hz, C10), 35.8, 35.5 (CH₂), 35.2, 31.5 (d, $J=5.1$ Hz, CH₂), 31.1 (C23), 31.0 (CH₂), 28.6 (CH₂), 26.8 (CH₂), 23.9 (C19), 21.7 (CH₂), 18.4 (C21), 12.2 (C18) ppm; ¹⁹F NMR (376MHz, CDCl₃): δ -100.05 (d, $J=251.4$ Hz, F2β), -105.16 (ddt, $J=252.1, 40.5, 7.2$ Hz, F2α) ppm; [¹H]¹⁹F NMR (376MHz, CDCl₃): δ -100.05 (d, $J=253.2$ Hz, F2β), -105.16 (d, $J=253.2$ Hz, F2α) ppm; MS (ESI+) m/z : 425.5 [M+H-H₂O]⁺, 405.5 [M+H-H₂O-HF]⁺; HRMS (HPLC-ESI) : [2M+H]⁺ Calcd. 885.5862; Found. 885.5862.

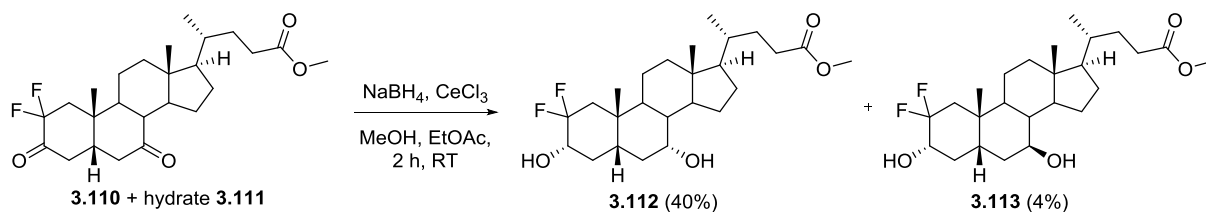
Methyl 2,2-difluoro-3,7-dioxo-5β-cholanoate (3.110) + hydrate (3.111)



Using general procedure E, diol **3.109** (1.0 g, 2.26 mmol, 1 equiv) was oxidised to yield a mixture of di-keto **3.110** and hydrate **3.111** (900 mg, 2.05 mmol, 91% - combined yield).

3.110 (Formula: C₂₅H₃₆F₂O₄, MW 438.6)/**3.111** (Formula: C₂₅H₃₈F₂O₅, MW 456.6): m.p. N/A; R_f (Petrol ether/EtOAc : 50/50) : 0.20; I.R. 3428 (br. w), 2948 (m), 2874 (w), 1731 (m), 1708 (s), 1172 (m), 1100 (m), 730 (s) cm⁻¹; ¹H NMR (400MHz, CDCl₃): δ 3.67 (s, 3H, CO₂CH₃), 2.93 (ddd, $J=13.2, 5.5, 0.8$ Hz, 1H, H₆β), 2.77-2.63 (m, 2H, H₁α or H₁β + unknown), 2.52-1.38 (m, 23H), 1.37 (s, 3H, H₁₉), 1.35-0.96 (m, 6H), 0.94 (d, $J=6.5$ Hz, 3H, H₂₁), 0.70 (s, 3H, H₁₈) ppm; ¹³C NMR (100 MHz, CDCl₃): δ 211.6 (C7), 210.1 (C6), 196.8 (dd, $J=27.1, 23.5$ Hz, C3), 174.7 (C24), 174.6 (C24), 116.2 (q, $J=256.0$ Hz, C2), 54.6, 51.5 (CO₂CH₃), 49.6, 49.5, 48.6, 48.6, 47.9, 44.3 (C6), 43.9 (d, $J=5.1$ Hz), 43.1 (dd, $J=22.0, 19.1$ Hz, C1), 42.6, 40.7, 38.6, 38.5, 38.0 (d, $J=2.2$ Hz, CH₂), 37.2 (d, $J=9.5$ Hz, C10), 35.2, 35.1, 31.0 (CH₂), 31.0 (CH₂), 30.9 (CH₂), 30.9 (CH₂), 28.2 (CH₂), 28.2 (CH₂), 24.7 (CH₂), 24.6 (CH₂), 23.0 (C19), 22.9 (C19), 22.4 (CH₂), 22.2 (CH₂), 18.3 (C21), 12.1 (C18), 12.0 (C18) ppm; ¹⁹F NMR (376MHz, CDCl₃): δ -104.37 (ddd, $J=263.6, 39.9, 12.1$ Hz, F2α), -111.15 (dq, $J=263.6, 5.0$ Hz, F2β) ppm; [¹H]¹⁹F NMR (376MHz, CDCl₃): δ -104.37 (d, $J=263.6$ Hz, F2α), -111.15 (d, $J=263.6$ Hz, F2β) ppm; MS (ESI+) m/z : Ketone : 439.5 [M+ H]⁺; Hydrate : 457.5 [M+ H]⁺; HRMS (HPLC-ESI) : Ketone [M+H]⁺ Calcd. 439.2654; Found. 439.2647; Hydrate HRMS (ESI) : [M+H]⁺ Calcd. 457.2754; Found. 457.2760.

Methyl 2,2-difluoro-3 α ,7 α -dihydroxy-5 β -cholanoate (3.112) + methyl 2,2-difluoro-3 α ,7 β -dihydroxy-5 β -cholanoate (3.113)



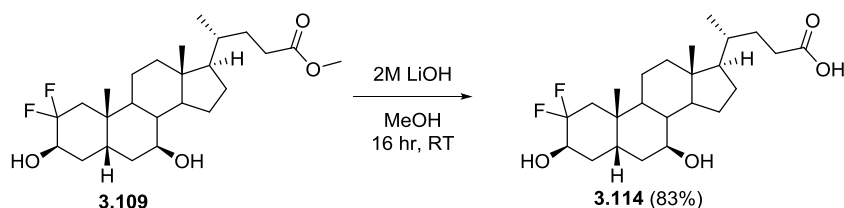
Using general procedure G, ketone **3.110**/hydrate **3.111** (750 mg, 1.71 mmol, 1 equiv) were reduced. Crude was purified *via* flash chromatography (petrol ether/EtOAc : 70:30→60:40→50:50) to yield CDCA analogue **3.112** (300 mg, 0.68 mmol, 40%) and UDCA analogue **3.113** (26 mg, 0.06 mmol, 4%).

3.112: Formula: C₂₅H₄₀F₂O₄; **MW** 442.6; **m.p.** N/A; **R_f** (Petrol ether/EtOAc : 70/30) : 0.32; **I.R.** 3435 (br. w), 2937 (m), 2868 (w), 1728 (m), 1164 (m), 1097 (m), 729 (s) cm⁻¹; **¹H NMR** (400MHz, CDCl₃): δ 3.86 (q, *J*=2.7 Hz, 1H, H7), 3.67 (s, 3H, CO₂CH₃), 3.65-3.56 (m, 1H, H3), 2.54 (q, *J*=13.2 Hz, 1H, H4 α), 2.47-2.31 (m, 2H, H23 + unknown), 2.28-2.17 (m, 1H, H23'), 2.05-1.04 (m, 19H), 1.00 (s, 3H, H19), 0.94 (d, *J*=6.5 Hz, 3H, H21), 0.67 (s, 3H, H18) ppm; **¹³C NMR** (100 MHz, CDCl₃): δ 174.7 (C24), 122.4 (t, *J*=244.2 Hz, C2), 72.2 (t, *J*=20.9 Hz, C3), 68.1 (C7), 55.7, 51.5 (CO₂CH₃), 50.2, 42.6, 41.7 (dd, *J*=22.4, 18.7 Hz, C1), 41.0, 39.4, 39.3 (CH₂), 37.6 (d, *J*=8.8 Hz, C10), 35.8 (d, *J*=6.6 Hz, C4), 35.3, 33.9 (d, *J*=4.4 Hz), 33.4 (CH₂), 30.9 (C23), 30.9 (CH₂), 28.1 (CH₂), 23.6 (CH₂), 22.9 (C19), 21.2 (CH₂), 18.2 (C21), 11.8 (C18) ppm; **¹⁹F NMR** (376MHz, CDCl₃): δ -101.58 (dq, *J*=235.8, 5.2 Hz, F2 β), -119.95 (dddd, *J*=235.8, 39.9, 20.8, 10.4 Hz, F2 α) ppm; **[H]¹⁹F NMR** (376MHz, CDCl₃): δ -101.58 (d, *J*=235.8 Hz, F2 β), -119.96 (d, *J*=235.8 Hz, F2 α) ppm; **MS (ESI+)** *m/z* : 425.5 [M+H-H₂O]⁺; **HRMS** (HPLC-ESI) : [M+Na]⁺ Calcd. 465.2787; Found. 465.2790.

3.113: Formula: C₂₅H₄₀F₂O₄; **MW** 442.6; **m.p.** N/A; **R_f** (Petrol ether/EtOAc : 70/30) : 0.23; **I.R.** 3394 (br. w), 2938 (s), 2869 (m), 1728 (s), 1439 (m), 1175 (s), 1097 (s), 732 (s) cm⁻¹; **¹H NMR** (400MHz, CDCl₃): δ 3.73 (ddt, *J*=19.7, 10.9, 5.4 Hz, 1H, H3), 3.67 (s, 3H, CO₂CH₃), 3.57 (ddd, *J*=11.3, 9.5, 5.1 Hz, 1H, H7), 2.43-2.30 (m, 2H), 2.22 (ddd, *J*=15.7, 9.4, 6.6 Hz, 2H), 2.04-1.05 (m, 31H), 1.02 (s, 3H, H19), 0.93 (d, *J*=6.4 Hz, 3H, H21), 0.68 (s, 3H, H18) ppm; **¹³C NMR** (100 MHz, CDCl₃): δ 174.7 (C24), 122.3 (dd, *J*=243.2, 245.4 Hz, C2), 71.7 (t, *J*=21.3 Hz, C3), 70.9 (C7), 55.4, 54.7, 51.5 (CO₂CH₃), 43.7 (2C), 42.0 (d, *J*=1.5 Hz), 41.5 (dd, *J*=22.0, 19.1 Hz, C1), 40.1 (d, *J*=5.1 Hz), 39.7 (CH₂), 36.7 (dd, *J*=9.5, 1.5 Hz, C10), 35.8 (CH₂), 35.2, 33.5 (d, *J*=7.3 Hz, C4), 31.0 (CH₂), 31.0 (CH₂), 28.6 (CH₂), 26.8 (CH₂), 23.5 (C19), 21.8 (CH₂), 18.3 (C21), 12.1 (C18) ppm; **¹⁹F NMR** (376MHz, CDCl₃): δ -101.31 (dq, *J*=237.6, 5.2 Hz, F2 β), -119.06 (dddd, *J*=237.6, 38.2, 19.0, 10.2 Hz, F2 α) ppm; **[H]¹⁹F NMR** (376MHz,

CDCl₃): δ -101.31 (d, $J=237.6$ Hz, $F_{2\beta}$), -119.06 (d, $J=237.6$ Hz, $F_{2\alpha}$) ppm; **MS (ESI+)** m/z : 425.5 [M+H-H₂O]⁺; **HRMS** (HPLC-ESI) : [M+H]⁺ Calcd. 443.2967; Found. 443.2962.

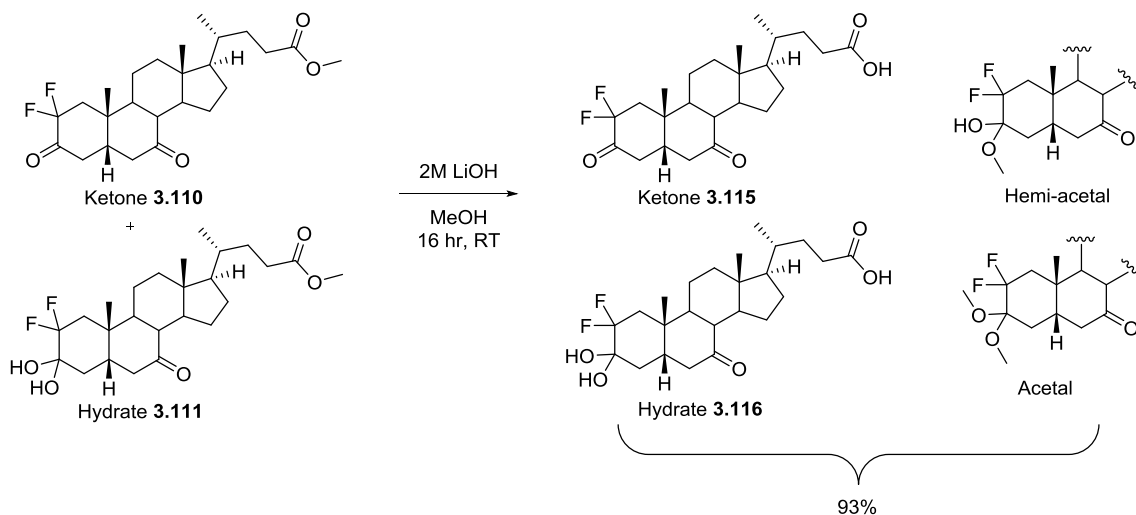
2,2-difluoro-3 β ,7 β -dihydroxy-5 β -cholanic acid (3.114)



Using general procedure B, **3.109** (60 mg, 0.14 mmol, 1 equiv) was hydrolysed to yield **3.114** as a pale solid (50 mg, 0.12 mmol, 83%).

3.114: Formula: C₂₄H₃₈F₂O₄; **MW** 428.6; [α]_D +25.6 (c 0.5, MeOH, 24 °C); **m.p.** 94-95 °C; **R_f** (Petrol ether/EtOAc : 50/50) : 0.16; **I.R.** 3377 (br. w), 2937 (m), 2870 (w), 1705 (m), 1070 (m), 1040 (m), 907 (s), 728 (s) cm⁻¹; **¹H NMR** (400MHz, CDCl₃): δ 3.89 (br. s., 1H, H_3), 3.55 (ddd, $J=11.4, 9.2, 5.2$ Hz, 1H, H_7), 2.39 (ddd, $J=15.6, 10.5, 5.0$ Hz, 1H, H_{23}), 2.26 (ddd, $J=15.8, 9.4, 6.5$ Hz, 1H, $H_{23'}$), 2.18-1.07 (m, 26H), 1.05 (s, 3H, H_{19}), 0.94 (d, $J=6.5$ Hz, 3H, H_{21}), 0.69 (s, 3H, H_{18}) ppm; **¹³C NMR** (100 MHz, CDCl₃): δ 179.7 (C_{24}), 123.1 (t, $J=244.3$ Hz, C_2), 71.1 (C_7), 68.5 (dd, $J=23.5, 35.2$ Hz, C_3), 55.5, 54.7, 43.7, 43.7, 39.9 (d, $J=4.4$ Hz), 39.8 (CH_2), 36.9 (t, $J=20.9$ Hz, C_1), 36.2 (d, $J=9.5$ Hz, C_{10}), 35.7, 35.4 (CH_2), 35.2, 31.4 (d, $J=5.1$ Hz, CH_2), 30.9 (C_{23}), 30.8 (CH_2), 28.6 (CH_2), 26.8 (CH_2), 23.9 (C_{19}), 21.7 (CH_2), 18.3 (C_{21}), 12.1 (C_{18}) ppm; **¹⁹F NMR** (376MHz, CDCl₃): δ -100.00 (d, $J=253.2$ Hz), -105.12 (ddt, $J=251.4, 41.6, 8.0$ Hz) ppm; [**H**]**¹⁹F NMR** (376MHz, CDCl₃): δ -100.01 (d, $J=251.4$ Hz), -105.12 (d, $J=251.4$ Hz) ppm; **MS (ESI+)** m/z : 411.5 [M+H-H₂O]⁺, 391.5 [M+H-H₂O-HF]⁺; **HRMS** (HPLC-ESI) : [2M+H]⁺ Calcd. 857.5549; Found. 857.5539.

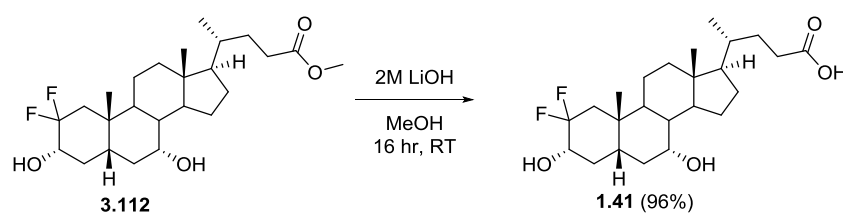
2,2-difluoro-3,7-dioxo-5 β -cholanic acid (3.115) + hydrate (3.116)



Using general procedure B, **3.110** and **3.111** (60 mg, 0.14 mmol, 1 equiv) were hydrolysed to yield **3.115/3.116** as a white solid, as a mixture of ketone/hydrate/acetal adducts (55 mg, 0.13mmol, 93%).

3.115 (Formula: C₂₄H₃₄F₂O₄, MW 424.5)/3.116 (Formula: C₂₄H₃₆F₂O₅, MW 442.5): m.p. 128-129 °C; **R_f** (Petrol ether/EtOAc : 50/50) : 0.11; **I.R.** 3391 (s), 2944 (m), 2874 (w), 1704 (s), 1099 (s), 1082 (s), 1043 (s) cm⁻¹; **¹H NMR** (400MHz, CD₃CN): δ 2.93 (dd, *J*=13.1, 5.9 Hz, 1H, H6β), 2.90-2.84 (m, 1H), 2.70-1.97 (m, 9H), 1.93-0.93 (m, 19H), 0.91 (d, *J*=6.4 Hz, 2H, H21), 0.89 (d, *J*=6.4 Hz, 1H, H21), 0.67 (s, 2H, H18), 0.64 (s, 1H, H18) ppm; **¹³C NMR** (100 MHz, CD₃CN): δ 211.5 (C7), 198.1 (dd, *J*=23.5, 27.1 Hz, C3), 176.0, 131.6 (t, *J*=244.3 Hz, C2), 55.6, 50.2, 50.1, 50.0 (d, *J*=2.2 Hz), 49.9, 47.8, 44.9 (CH₂), 43.5, 43.2 (dd, *J*=19.4, 21.9 Hz, C1), 41.5 (d, *J*=1.5 Hz, CH₂), 39.7 (CH₂), 38.1 (d, *J*=9.5 Hz), 36.1, 31.8 (CH₂), 31.2 (CH₂), 29.0 (CH₂), 25.5 (CH₂), 23.2 (CH₂), 22.9 (C19), 18.8 (C21), 12.5 (C18) ppm; **¹⁹F NMR** (376MHz, CD₃CN): δ -103.96 (ddd, *J*=261.6, 38.1, 15.0 Hz, 1F), -108.59 (ddd, *J*=246.2, 39.0, 11.3 Hz, 0.2F), -110.91 (dq, *J*=263.6, 5.2 Hz, 1F), -113.71--112.69 (dq, *J*=246.2, 5.2 Hz, 0.11F), -116.15 (dq, *J*=246.2, 5.2 Hz, 0.1F), -117.09 (dq, *J*=246.2, 5.2 Hz, 0.2F) ppm; **[H]¹⁹F NMR** (376MHz, CD₃CN): -103.96 (d, *J*=261.8 Hz, 1F), -108.59 (d, *J*=246.2 Hz, 0.2F), -110.91 (d, *J*=261.8 Hz, 1F), -113.11 (d, *J*=246.2 Hz, 0.1F), -116.16 (d, *J*=246.2 Hz, 0.1F), -117.09 (d, *J*=246.2 Hz, 0.2F) ppm; **MS (ESI+)** *m/z* : **Ketone** : 425.5 [M+H]⁺; **Hydrate** : 443.5 [M+H]⁺; **Hemi-acetal** : 457.7 [M+H]⁺, 439.5 [M+H-H₂O]⁺; **Acetal** : 443.5 [M+H]⁺, 439.5 [M+H-MeOH]⁺; **HRMS (HPLC-ESI)** : **Hydrate** [M+H]⁺ 443.2604; Found. 443.2599; **Hemi-acetal** HRMS (ESI) : [M+H]⁺ 457.2760; Found. 457.2749.

2,2-difluorochenodeoxycholic acid (**1.41**)

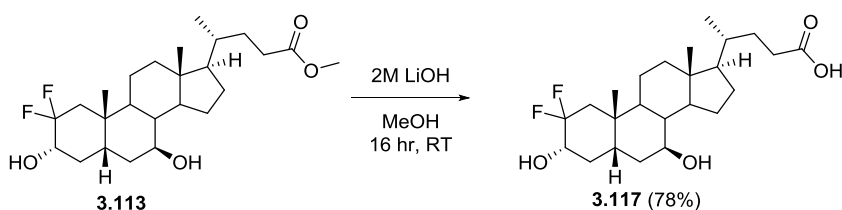


Using general procedure B, **3.112** (75 mg, 0.17 mmol, 1 equiv) was hydrolysed to yield **1.41** as a white solid (70 mg, 0.16 mmol, 96%).

1.41: Formula: C₂₄H₃₈F₂O₄; **MW** 428.6; **[α]_D** +1.0 (c 0.5, MeOH, 24 °C); **m.p.** 108-109 °C; **R_f** (Petrol ether/EtOAc : 50/50) : 0.08; **I.R.** 3409 (br. w), 2937 (s), 2869 (m), 1707 (s), 1095 (s), 909 (m), 732 (s) cm⁻¹; **¹H NMR** (400MHz, CDCl₃): δ 33.86 (q, *J*=2.0 Hz, 1H, H7), 3.62 (ddt, *J*=19.7, 10.9, 5.4 Hz, 1H, H3), 2.54 (q, *J*=13.0 Hz, 1H, H4α), 2.44-2.35 (m, 2H, H23 + H1α or H1β), 2.25 (ddd, *J*=15.9, 9.6, 6.5 Hz, 1H, H23'), 2.02-1.02 (m, 25H), 0.99 (s, 3H, H19), 0.94 (d, *J*=6.4 Hz, 3H, H21), 0.67 (s, 3H, H18) ppm; **¹³C NMR** (100 MHz, CDCl₃): δ 179.6 (C24), 122.4 (t, *J*=244.7 Hz, C2), 72.1 (t, *J*=20.7 Hz, C3), 68.2, 55.7, 50.1, 42.7, 41.7 (dd, *J*=18.7, 21.6 Hz, C1), 41.0, 39.4, 39.4 (CH₂), 37.6 (d, *J*=9.5 Hz, C10),

35.8 (d, $J=6.6$ Hz, C₄), 35.3, 33.9 (d, $J=4.4$ Hz), 33.4 (CH₂), 30.9 (CH₂), 30.7 (CH₂), 28.1 (CH₂), 23.5 (CH₂), 23.0, (C₁₉) 21.2 (CH₂), 18.2 (C₂₁), 11.8 (C₁₈) ppm; ¹⁹F NMR (376MHz, CDCl₃): δ -119.67 (d, $J=235.8$ Hz, F_{2β}), -119.67 (dddd, $J=235.8$, 38.2, 19.1, 10.4 Hz, F_{2α}) ppm; [¹H]¹⁹F NMR (376MHz, CDCl₃): δ -101.41 (d, $J=237.6$ Hz, F_{2β}), -119.67 (d, $J=237.6$ Hz, F_{2α}) ppm; **MS (ESI+)** m/z : 411.5 [M+H-H₂O]⁺, 393.4 [M+H-2H₂O]⁺; **HRMS (HPLC-ESI)** : [M+NH₄]⁺ Calcd. 446.3076; Found. 446.3076.

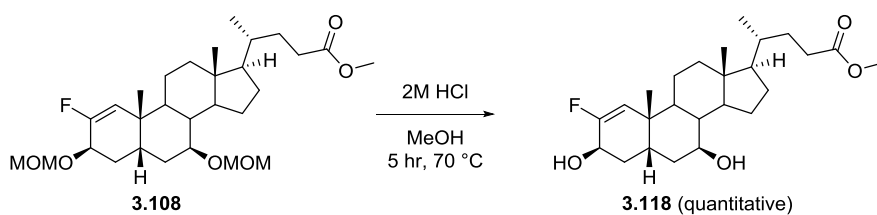
2,2-difluoroursodeoxycholic acid (3.117)



Using general procedure B, **3.113** (25 mg, 0.06 mmol, 1 equiv) was hydrolysed to yield **3.117** as a gummy solid (20 mg, 0.05 mmol, 78%).

3.117: Formula: C₂₄H₃₈F₂O₄; **MW** 428.6; [α]_D +5.0 (c 0.5, MeOH, 24 °C); **m.p.** 125-126 °C; **R_f** (Petrol ether/acetone : 60/40) : 0.22; **I.R.** 3354 (br. w), 2936 (m), 2870 (w), 1705 (m), 1181 (m), 1096 (s), 1008 (m), 971 (s) cm⁻¹; ¹H NMR (400MHz, CD₃OD): δ 3.69 (ddt, $J=21.0$, 11.0, 5.0 Hz, 1H, H₃), 3.44 (ddd, $J=11.5$, 9.8, 5.0 Hz, 1H), 2.38-2.26 (m, 2H), 2.25-2.14 (m, 2H), 2.08-1.06 (m, 32H), 1.03 (s, 3H), 0.96 (d, $J=6.5$ Hz, 3H), 0.72 (s, 3H) ppm; ¹³C NMR (100 MHz, CD₃OD): δ 178.5 (C₂₄), 123.8 (dd, $J=242.8$, 244.2 Hz, C₂), 72.3 (t, $J=21.3$ Hz, C₃), 71.8 (C₇), 57.6, 56.7, 44.9, 44.6, 43.6, 42.7 (t, $J=22.7$ Hz, C₁), 41.9 (d, $J=5.1$ Hz), 41.4 (CH₂), 41.0 (d, $J=9.5$ Hz, C₁₀), 37.8 (CH₂), 36.8, 34.8 (d, $J=7.3$ Hz, C₄), 32.5 (CH₂), 32.3 (CH₂), 29.8 (CH₂), 28.0, (CH₂) 24.0 (C₁₉), 23.2 (CH₂), 19.1 (C₂₁), 12.8 (C₁₈) ppm; ¹⁹F NMR (376MHz, CD₃OD): δ -101.64 (dq, $J=239.3$, 5.0 Hz, F_{2β}), -120.18 (dddd, $J=239.3$, 38.2, 20.8, 10.4 Hz, F_{2α}), ppm; [¹H]¹⁹F NMR (376MHz, CD₃OD): δ -101.64 (d, $J=239.3$ Hz, 1F), -120.18 (d, $J=239.3$ Hz, 1F) ppm; **MS (ESI+)** m/z : 411.4 [M+H-H₂O]⁺, 393.3 [M+H-2H₂O]⁺; **HRMS (HPLC-ESI)** : [M+NH₄]⁺ Calcd. 446.3076; Found. 446.3074.

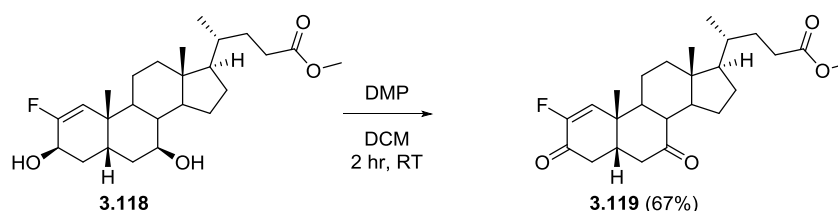
Methyl 2-fluoro-3β,7β-dihydroxy-5β-chole-1-enoate (3.118)



Using general procedure D, di-MOM protected alcohol **3.108** (900 mg, 1.76 mmol, 1 equiv) was deprotected to yield **3.118** as a white gummy solid (750 mg, quantitative yield).

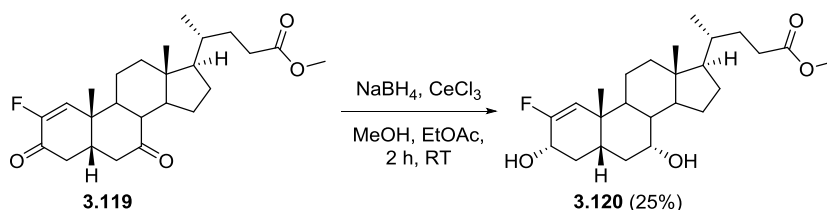
3.118: Formula: C₂₅H₃₉FO₄; **MW** 422.6; **m.p.** N/A; **R_f** (Petrol ether/EtOAc : 50/50) : 0.21; **I.R.** 3388 (br. w), 2935 (m), 2868 (w), 1724 (m), 908 (m), 729 (s) cm⁻¹; **¹H NMR** (400MHz, CDCl₃): δ 5.34 (d, *J*=17.6 Hz, 1H, H₁), 4.20 (ddd, *J*=7.7, 4.7, 1.3 Hz, 1H, H₃), 3.67 (s, 3H, CO₂C₃), 3.50 (ddd, *J*=11.2, 9.6, 4.8 Hz, 1H, H₇), 2.35 (ddd, *J*=15.6, 10.5, 5.0 Hz, 1H, H₂₃), 2.22 (ddd, *J*=15.6, 9.4, 6.5 Hz, 1H, H_{23'}), 2.12 (td, *J*=14.0, 5.3 Hz, 1H, H_{4α}), 2.04-1.21 (m, 23H), 1.12 (d, *J*=0.7 Hz, 3H, H₁₉), 0.92 (d, *J*=6.5 Hz, 3H, H₂₁), 0.70 (s, 3H, H₁₈) ppm; **¹³C NMR** (100 MHz, CDCl₃): δ 174.7 (C₂₄), 158.1 (d, *J*=257.5 Hz, C₂), 116.2 (d, *J*=11.0 Hz, C₁), 71.3 (C₇), 64.1 (d, *J*=26.4 Hz, C₃), 55.1, 54.8, 51.5 (CO₂C₃), 45.0 (d, *J*=2.9 Hz), 43.7, 43.4, 39.8 (C_H₂), 36.6 (d, *J*=6.6 Hz, C₁₀), 36.3 (C_H₂), 35.8 (d, *J*=1.5 Hz, C₅), 35.2, 34.1 (d, *J*=8.1 Hz, C₄), 31.0 (C₂₃), 30.9 (C_H₂), 28.5 (C_H₂), 26.8 (C_H₂), 22.3 (C_H₂), 21.8 (d, *J*=1.5 Hz, C₁₉), 18.3 (C₂₁), 12.1 (C₁₈) ppm; **¹⁹F NMR** (376MHz, CDCl₃): δ -117.65 (dt, *J*=17.0, 8.5 Hz) ppm; **[H]¹⁹F NMR** (376MHz, CDCl₃): δ -117.65 (s) ppm; **MS (ESI+)** *m/z* : 405.5 [M+H-H₂O]⁺, 387.5 [M+H-2H₂O]⁺; **HRMS** (HPLC-ESI) : [M+NH₄]⁺ Calcd: 440.3171; Found: 440.3176.

Methyl 2-fluoro-3β,7β-dihydroxy-5β-chol-1-enoate (3.119)



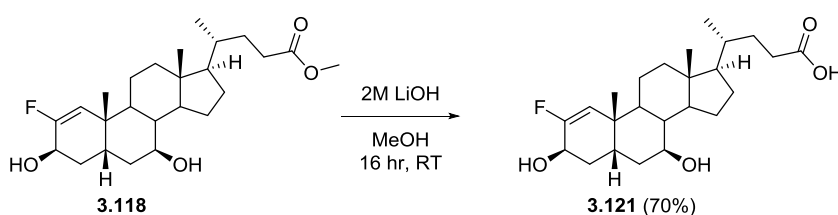
Using general procedure E, diol **3.119** (600 mg, 1.42 mmol, 1 equiv) was oxidised, then purified *via* flash chromatography (Petrol ether/EtOAc : 80:20→70:30→60/40) to yield diketone **3.119** as a gummy solid (400 mg, 0.96 mmol, 67%).

3.119: Formula: C₂₅H₃₅FO₄; **MW** 418.6; **m.p.** N/A; **R_f** (Petrol ether/EA : 70/30) : 0.38; **I.R.** 2948 (m), 2873 (w), 1731 (m), 1698 (s), 1167 (m), 914 (m), 730 (s) cm⁻¹; **¹H NMR** (400MHz, CDCl₃): δ 6.34 (d, *J*=14.7 Hz, 1H, H₁), 3.66 (s, 3H, CO₂C₃), 2.89 (dd, *J*=12.8, 5.9 Hz, 1H, H_{6β}), 2.61 (dtd, *J*=13.5, 5.8, 2.0 Hz, 1H, H₅), 2.55-2.11 (m, 7H), 2.07 (dd, *J*=13.2, 2.0 Hz, 1H, H_{6α}), 2.04-1.71 (m, 5H), 1.51 (s, 3H, H₁₉), 1.49-0.94 (m, 8H), 0.92 (d, *J*=6.4 Hz, 3H, H₂₁), 0.70 (s, 3H, H₁₈) ppm; **¹³C NMR** (100 MHz, CDCl₃): δ 209.9, 189.6 (d, *J*=20.5 Hz, C₃), 174.5 (C₂₄), 152.1 (d, *J*=264.1 Hz, C₂), 133.1 (d, *J*=11.0 Hz, C₁), 54.7, 51.5 (CO₂C₃), 49.0, 48.2, 48.1 (d, *J*=2.9 Hz), 44.7 (C₅), 43.7 (C₆), 42.5, 39.9 (d, *J*=3.7 Hz, C_H₂), 38.8 (d, *J*=4.4 Hz, C₁₀), 38.5 (C_H₂), 35.1, 31.0 (C_H₂), 30.9 (C_H₂), 28.0 (C_H₂), 24.7 (C_H₂), 23.2 (C_H₂), 21.2 (C₁₉), 18.3 (C₂₁), 12.1 (C₁₈) ppm; **¹⁹F NMR** (376MHz, CDCl₃): δ -131.67 (dd, *J*=15.6, 3.5 Hz), ppm; **[H]¹⁹F NMR** (376MHz, CDCl₃): δ -131.67 (s) ppm; **MS (ESI+)** *m/z* : 419.5 [M+ H]⁺, 460.5 [M+H+MeCN]⁺; **HRMS** (HPLC-ESI) : [M+H]⁺ Calcd: 419.2592; Found: 419.2590.

Methyl 2-fluoro-3 α ,7 α -dihydroxy-5 β -chol-1-enoate (3.120)

Using general procedure G, diketo **3.119** (400 mg, 0.96 mmol, 1 equiv) was reduced, then purified *via* flash chromatography (Petrol ether/EtOAc : 70:30→60:40→50:50) to yield CDCA analogue **3.120** as a gummy solid (99 mg, 0.22 mmol, 25%).

3.120: Formula: C₂₅H₃₉FO₄; **MW** 422.6; **m.p.** N/A; **R_f** (Petrol ether/EtOAc : 50/50) : 0.27; **I.R.** 3380 (br. w), 2932 (m), 2868 (w), 1732 (m), 1079 (m), 731 (s) cm⁻¹; **¹H NMR** (400MHz, CDCl₃): δ 5.25 (d, *J*=18.2 Hz, 1H, H₁), 4.35 (t, *J*=7.9 Hz, 1H, H₃), 3.85 (q, *J*=1.7 Hz, 1H, H₇), 3.67 (s, 3H, CO₂CH₃), 3.65 (d, *J*=1.8 Hz, 1H), 2.53-2.32 (m, 2H), 2.29-2.17 (m, 1H), 2.04-1.07 (m, 29H), 1.04 (d, *J*=0.9 Hz, 3H), 0.93 (d, *J*=6.4 Hz, 3H, H₁₈), 0.68 (s, 3H, H₁₈) ppm; **¹³C NMR** (100 MHz, CDCl₃): δ 174.7 (C₂₄), 158.2 (d, *J*=259.0 Hz, C₂₄), 114.9 (d, *J*=11.7 Hz, C₁), 68.0 (C₇), 66.4 (d, *J*=22.0 Hz, C₃), 55.7, 51.5 (C_O₂Me), 49.9, 42.6, 39.5, 39.4 (C_H₂), 39.3 (d, *J*=2.2 Hz), 38.8 (d, *J*=2.2 Hz, C₅), 37.7 (d, *J*=7.3 Hz, C₁₀), 37.1 (d, *J*=4.4 Hz, C₄), 35.3, 34.1 (C_H₂), 30.9 (C₂₃), 30.9 (C_H₂), 28.0 (C_H₂), 23.6 (C_H₂), 21.7 (C_H₂), 21.5 (d, *J*=1.5 Hz, C₁₉), 18.3 (C₂₁), 11.8 (C₁₈) ppm; **¹⁹F NMR** (376MHz, CDCl₃): δ -125.36 (dd, *J*=19.1, 6.9 Hz) ppm; **[H]¹⁹F NMR** (376MHz, CDCl₃): δ -125.36 (s) ppm; **MS (ESI+)** *m/z* : 405.5 [M+H-H₂O]⁺, 387.5 [M+H-2H₂O]⁺; **HRMS (HPLC-ESI)** : [M+NH₄]⁺ Calcd: 440.3171; Found: 440.3166.

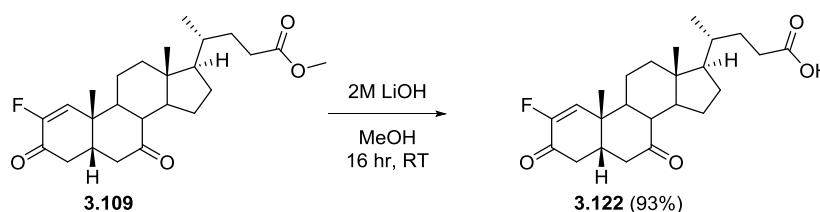
2-fluoro-3 β ,7 β -dihydroxy-5 β -chol-1-enic acid (3.121)

Using general procedure B, **3.118** (60 mg, 0.14 mmol, 1 equiv) was hydrolysed to yield **3.121** as a white solid (40 mg, 0.10 mmol, 70%).

3.121: Formula: C₂₄H₃₇FO₄; **MW** 408.6; **[α]_D** +99.2 (c 0.5, MeOH, 24 °C); **m.p.** 110-112 °C; **R_f** (Petrol ether/EtOAc : 50/50) : 0.09; **I.R.** 3350 (br. m), 2930 (s), 1694 (s), 1381 (s), 1048 (s) cm⁻¹; **¹H NMR** (400MHz, CD₃OD): δ 5.32 (d, *J*=17.7 Hz, 1H, H₁), 4.10 (ddd, *J*=8.0, 4.5, 1.0 Hz, 1H, H₃), 3.38 (td, *J*=10.5, 4.8 Hz, 1H, H₇), 2.40-1.15 (m, 29H), 1.13 (s, 3H, H₁₉), 0.95 (d, *J*=6.5 Hz, 3H, H₂₁), 0.73 (s, 3H, H₁₈) ppm; **¹³C NMR** (100MHz, CD₃OD): δ 179.7 (C₂₄), 160.0 (d, *J*=257.5 Hz, C₂), 117.1 (d, *J*=12.5 Hz, C₁), 72.1 (C₇), 64.9 (d, *J*=25.7 Hz, C₃), 57.0, 56.7, 46.8 (d, *J*=2.2 Hz), 44.9, 44.5, 41.5

(CH₂), 38.3 (CH₂), 37.8 (d, *J*=6.6 Hz, C₁₀), 37.5, 36.9, 36.0 (d, *J*=8.1 Hz, CH₂), 33.3 (CH₂), 33.0 (CH₂), 29.7 (CH₂), 28.1 (CH₂), 23.8 (CH₂), 22.4 (C₁₉), 19.1 (C₂₁), 12.8 (C₁₈) ppm; ¹⁹F NMR (376MHz, CD₃OD): δ -117.71 (dt, *J*=15.6, 7.6 Hz) ppm; [**H**]¹⁹F NMR (376MHz, CD₃OD): δ -117.71 (s) ppm; **MS (ESI+)** *m/z* : 391.5 [M+H-H₂O]⁺, 373.5 [M+H-2H₂O]⁺; **HRMS (HPLC-ESI)** : [M+H-H₂O]⁺ Calcd: 391.2643; Found: 391.2645.

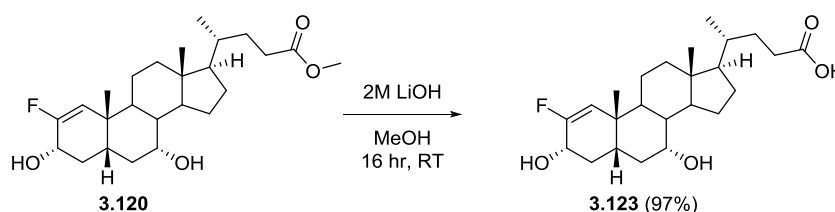
2-fluoro-3,7-dioxo-5β-chol-1-enic acid (3.122)



Using general procedure B, **3.119** (50 mg, 0.12 mmol, 1 equiv) was hydrolysed to yield **3.122** as a white solid (45 mg, 0.11 mmol, 93%).

3.122: Formula: C₂₄H₃₃FO₄; **MW** 404.5; [**α**]_D +13.1 (c 0.5, MeOH₃, 24 °C); **m.p.** 178-180 °C; **R_f** (Petrol ether/EtOAc : 50/50) : 0.32; **I.R.** 2945 (m), 2875 (w), 1699 (s), 912 (m), 731 (s) cm⁻¹; **¹H NMR** (400MHz, CDCl₃): δ 6.34 (d, *J*=14.7 Hz, 1H, H₁), 2.89 (dd, *J*=13.0, 6.1 Hz, 1H, H_{6β}), 2.62 (dtd, *J*=13.5, 5.8, 2.0 Hz, 1H, H₅), 2.55-1.73 (m, 13H), 1.51 (s, 3H, H₁₉), 1.49-0.95 (m, 9H), 0.93 (d, *J*=6.4 Hz, 3H, H₂₁), 0.70 (s, 3H, H₁₈) ppm; **¹³C NMR** (100 MHz, CDCl₃): δ 210.1 (C₃), 189.7 (d, *J*=19.8 Hz, C₃), 180.0 (C₂₄), 152.1 (d, *J*=264.1 Hz, C₂), 133.2 (d, *J*=11.0 Hz, C₁), 54.7, 49.0, 48.2, 48.1 (d, *J*=2.9 Hz), 44.7 (C₅), 43.7 (C₆), 42.5, 39.9 (d, *J*=3.7 Hz, C₄), 38.8 (d, *J*=5.1 Hz, C₁₀), 38.5 (CH₂), 35.1, 30.9 (CH₂), 30.6 (CH₂), 28.0 (CH₂), 24.7 (CH₂), 23.2 (CH₂), 21.2 (C₁₉), 18.3 (C₂₁), 12.1 (C₁₈) ppm; **¹⁹F NMR** (376MHz, CDCl₃): δ -131.63 (dd, *J*=13.9, 3.5 Hz) ppm; [**H**]¹⁹F NMR (376MHz, CDCl₃): δ -131.63 (s) ppm; **MS (ESI+)** *m/z* : 405.4 [M+H]⁺, 446.5 [M+H+MeCN]⁺; **HRMS (HPLC-ESI)** : [M+H]⁺ Calcd: 405.2436; Found: 405.2441.

2-fluoro-3α,7α-dihydroxy-5β-chol-1-enic acid (3.123)

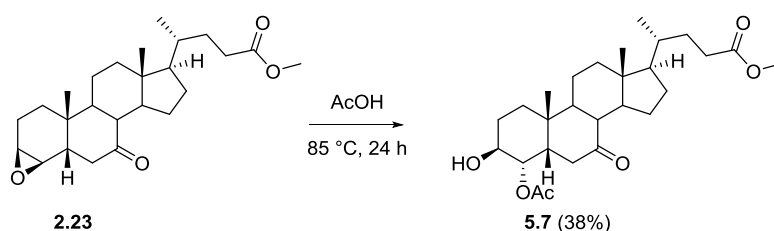


Using general procedure B, **3.120** (50 mg, 0.11 mmol, 1 equiv) was hydrolysed to yield **3.123** as a pale solid (45 mg, 0.11 mmol, 97%).

3.123: Formula: C₂₄H₃₇FO₄; **MW** 408.6; **[α]_D** +18.5 (c 0.5, MeOH, 24 °C); **m.p.** 209-210 °C; **R_f** (Petrol ether/EtOAc : 50/50) : 0.06; **I.R.** 3393 (br. w), 2932 (m), 2868 (m), 1698 (s), 1247 (m), 1079 (m) cm⁻¹; **¹H NMR** (400MHz, Acetone-D₆): δ 5.16 (d, *J*=18.6 Hz, 1H, H1), 4.23 (ddd, *J*=9.0, 7.0, 2.5 Hz, 1H, H3), 4.07 (br. s., 1H, OH), 3.82 (q, *J*=2.7 Hz, 1H, H7), 3.32 (br. s., 1H, OH), 2.54 (td, *J*=13.7, 10.0 Hz, 1H, H4α), 2.34 (ddd, *J*=15.5, 11.0, 5.0 Hz, 1H, H23), 2.21 (ddd, *J*=15.6, 9.4, 6.5 Hz, 1H, H23'), 2.02-1.06 (m, 25H), 1.05 (d, *J*=1.0 Hz, 3H, H19), 0.96 (d, *J*=6.6 Hz, 3H, H21), 0.71 (s, 3H, H18) ppm; **¹³C NMR** (100 MHz, Acetone-D₆): δ 175.2 (C24), 160.5 (d, *J*=259.7 Hz, C2), 115.0 (d, *J*=12.5 Hz, C1), 67.9 (C7), 66.7 (d, *J*=21.3 Hz, C3), 57.0, 50.9, 43.3, 40.7 (CH₂), 40.6, 40.5 (d, *J*=2.2 Hz), 40.4 (d, *J*=2.2 Hz), 38.8 (d, *J*=5.9 Hz, C4), 38.5 (d, *J*=6.6 Hz, C10), 36.3, 35.5 (CH₂), 31.9 (CH₂), 31.3 (C23), 28.9 (CH₂), 24.3 (CH₂), 22.6 (CH₂), 22.1 (d, *J*=1.5 Hz, C19), 18.8 (C21), 12.3 (C18) ppm; **¹⁹F NMR** (376MHz, Acetone-D₆): δ -123.32 (dd, *J*=19.1, 6.9 Hz) ppm; **[H]¹⁹F NMR** (376MHz, Acetone-D₆): δ -123.32 (s) ppm; **MS (ESI+)** *m/z* : 373.5 [M+H-2H₂O]⁺; **HRMS (HPLC-ESI)** : [M+NH₄]⁺ Calcd: 426.3014; Found: 426.3020.

5.4.4 Towards the synthesis of 4,4-difluorinated analogues

Methyl 3β-hydroxy-4α-acetoxy-7-oxo-5β-cholanoate (5.7)

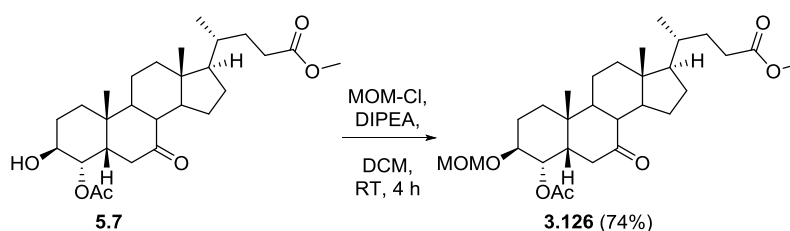


Epoxide **2.23** (250 mg, 0.62 mmol, 1 equiv) was dissolved in AcOH (5 mL) before warming to 85 °C and stirred for 24 hr. Reaction mixture concentrated *in vacuo*, then azeotroped (EtOAc 2 × 5 mL, then DCM 2 × 5 mL) to complete dryness. Crude material purified *via* flash chromatography (pet ether/EtOAc : 70:30→60:40) to yield pure 4α-acetate **5.7** as a gummy solid (110 mg, 0.24 mmol, 38%).

5.7: Formula: C₂₇H₄₂O₆; **MW** 462.6; **m.p.** N/A; **R_f** (Petrol ether/EA : 60/40) : 0.27; **I.R.** 3462 (br. w), 2943 (m), 2873 (w), 1736 (s), 1708 (s), 1374 (m), 1230 (s), 1042 (s), 1027 (s) cm⁻¹; **¹H NMR** (400MHz, CDCl₃): δ 4.81 (t, *J*=3.1 Hz, 1H, H4), 3.76 (q, *J*=2.4 Hz, 1H, H3), 3.63 (s, 3H, CO₂CH₃), 2.69 (dd, *J*=14.5, 7.4 Hz, 1H, H6β), 2.48-1.94 (m, 11H), 1.92 (s, 3H, C(O)CH₃), 1.90-1.20 (m, 18H), 1.17 (s, 3H, H19), 1.15-0.93 (m, 3H), 0.89 (d, *J*=6.5 Hz, 3H, H21), 0.62 (s, 3H, H18) ppm; **¹³C NMR** (100 MHz, CDCl₃): δ 211.2 (C7), 174.6 (C24), 170.3 (C(O)CH₃), 75.7 (C4), 66.9 (C3), 54.5, 51.4 (CO₂CH₃), 50.0, 49.0, 43.4, 43.3, 43.0, 41.6 (C6), 39.0 (CH₂), 35.3, 35.1, 30.9 (2×CH₂), 28.4 (CH₂), 28.2 (CH₂), 25.3 (CH₂), 23.6 (C19), 23.2 (CH₂), 22.1 (CH₂), 20.9 (C(O)CH₃), 18.3 (C21), 12.0 (C18) ppm; **MS (ESI+)**

m/z : 463.5 $[M+H]^+$, 480.5 $[M+NH_4]^+$, 485.5 $[M+Na]^+$; **HRMS** HRMS (HPLC-ESI) : $[M+NH_4]^+$ Calcd. 480.3320; Found. 480.3316.

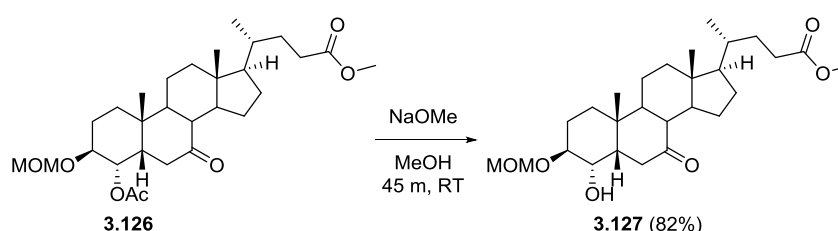
Methyl 3 β -methoxymethoxyl-4 α -acetoxy-7-oxo-5 β -cholanoate (3.126)



Using general procedure C, alcohol **5.7** (110 mg, 0.24 mmol, 1 equiv) was protected as a MOM ether. Crude purified *via* flash chromatography (pet ether/EtOAc : 75:25) to yield MOM-protected alcohol **3.126** as gummy solid (90 mg, 0.18 mmol, 74%).

3.126: Formula: $C_{29}H_{46}O_7$; **MW** 506.7; **m.p.** N/A; **R_f** (Petrol ether/EtOAc : 60/40) : 0.53; **I.R.** 2943 (m), 2876 (w), 1737 (s), 1709 (s), 1230 (s), 1030 (s) cm^{-1} ; **¹H NMR** (400MHz, $CDCl_3$): δ 4.92 (t, $J=3.1$ Hz, 1H, H₄), 4.67 (d, $J=6.9$ Hz, 1H, O-CHH'-O), 4.63 (d, $J=6.9$ Hz, 1H, 1H, O-CHH'-O), 3.64 (s, 4H, $CO_2CH_3 + H_3$), 3.35 (s, 3H), 2.71 (dd, $J=14.3, 7.5$ Hz, 1H, H_{6 β}), 2.39-1.94 (m, 10H), 1.92 (s, 3H, C(O)CH₃), 1.91-1.22 (m, 16H), 1.19 (s, 3H, H₁₉), 1.17-0.97 (m, 4H), 0.91 (d, $J=6.4$ Hz, 3H, H₂₁), 0.64 (s, 3H, H₁₈) ppm; **¹³C NMR** (100 MHz, $CDCl_3$): δ 210.7 (C₇), 174.5 (C₂₄), 169.9 (C(O)CH₃), 95.1 (O-CH₂-O), 73.6 (C₄), 72.1 (C₃), 55.4 (OCH₃), 54.6, 51.4 (CO_2CH_3), 50.0, 49.1, 44.1, 43.3, 43.1, 41.8 (C₆), 39.1 (CH₂), 35.1, 35.1, 30.9 (2 \times CH₂), 28.9 (CH₂), 28.3 (CH₂), 25.3 (CH₂), 23.7 (C₁₉), 22.2 (CH₂), 21.2 (CH₂), 20.9 (C(O)CH₃), 18.4 (C₂₁), 12.1 (C₁₈) ppm; **MS (ESI+)** m/z : 524.5 $[M+NH_4]^+$, 529.5 $[M+Na]^+$; **HRMS** HRMS (HPLC-ESI) : $[M+NH_4]^+$ Calcd. 524.3582; Found. 524.3583.

Methyl 3 β -methoxymethoxyl-4 α -hydroxy-7-oxo-5 β -cholanoate (3.127)

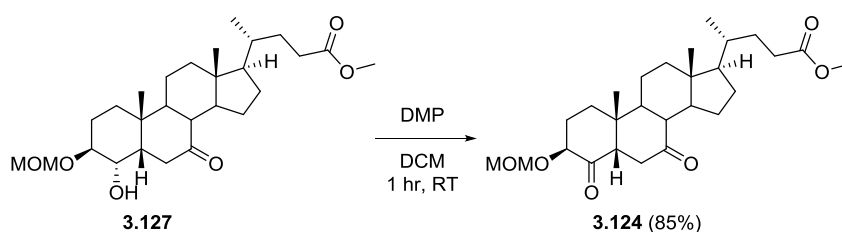


Using general procedure F, 4 α -acetate **3.126** (85 mg, 0.17 mmol, 1 equiv) was methanolysed to yield 4 α -OH **3.127** (65 mg, 0.14 mmol, 82%) as a colourless gum.

3.127: Formula: $C_{27}H_{44}O_6$; **MW** 464.6; **m.p.** N/A; **R_f** (Petrol ether/EtOAc : 60/40) : 0.37; **I.R.** 3451 (br. w), 2940 (m), 2876 (w), 1737 (m), 1708 (m), 1100 (m), 1036 (s) cm^{-1} ; **¹H NMR** (400MHz, $CDCl_3$): δ 4.66 (d, $J=7.0$ Hz, 1H, O-CHH'-O), 4.63 (d, $J=7.0$ Hz, 1H, O-CHH'-O), 3.82 (t, $J=3.4$ Hz, 1H, H₄), 3.65 (s, 4H, H₃ + CO_2CH_3), 3.35 (s, 3H, OCH₃), 2.78 (dd, $J=14.3, 6.8$ Hz, 1H, H_{6 β}), 2.49-2.15 (m, 7H), 2.10

(dd, $J=14.4, 2.9$ Hz, 1H, $H_{6\alpha}$), 2.07-1.20 (m, 19H), 1.15 (s, 3H, H_{19}), 1.14-0.94 (m, 2H), 0.90 (d, $J=6.2$ Hz, 3H, H_{21}), 0.64 (s, 3H, H_{18}) ppm; ^{13}C NMR (100 MHz, CDCl_3): δ 214.9 (C_7), 174.6 (C_{24}), 95.3 (O- CH_2 -O), 76.3 (C_3), 73.4 (C_4), 55.4 (O CH_3), 54.5, 51.4 (CO_2CH_3), 49.4, 49.2, 45.7, 44.4, 43.0, 42.5 (C_6), 38.9 (CH_2), 35.5, 35.2, 31.0 (CH_2), 31.0 (CH_2), 29.5 (CH_2), 28.3 (CH_2), 25.4 (CH_2), 23.7 (C_{19}), 22.2 (CH_2), 21.1 (CH_2), 18.3 (C_{21}), 12.0 (C_{18}) ppm; **MS (ESI+)** m/z : 403.4 [$\text{M}+\text{H}-\text{HOCH}_2\text{OCH}_3$] $^+$, 487.5 [$\text{M}+\text{Na}$] $^+$; **HRMS** HRMS (HPLC-ESI) : [$\text{M}+\text{NH}_4$] $^+$ Calcd. 465.3211; Found. 465.3206.

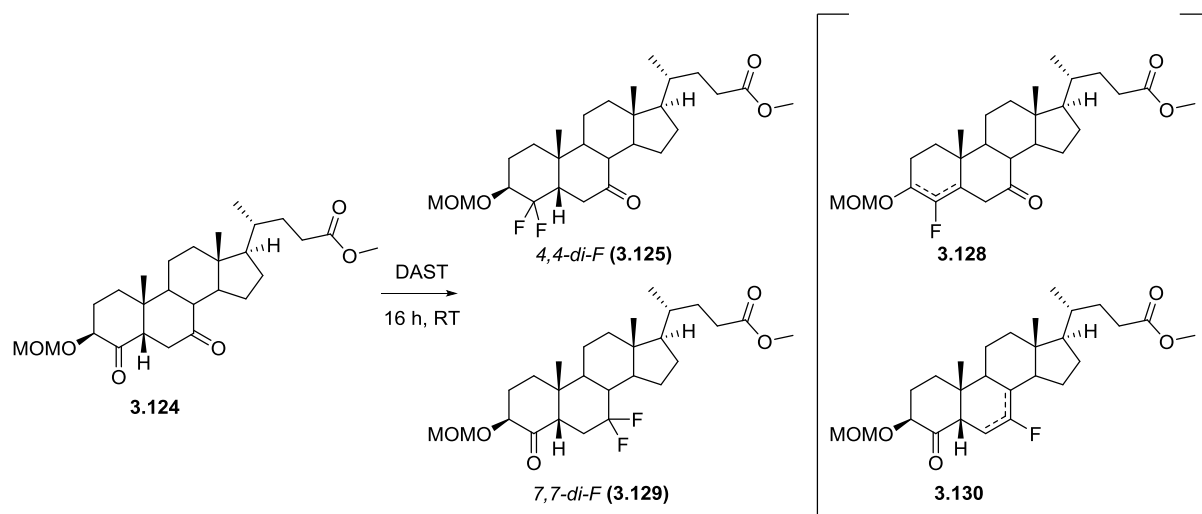
Methyl 3 β -methoxymethoxyl-4,7-dioxo-5 β -cholanoate (3.124)



Using general procedure E, 4 α -OH **3.127** (65 mg, 0.14 mmol, 1 equiv) was oxidised. Purified *vis* flash chromatography (pet ether/EA : 75:25) to yield diketo **3.124** as a gummy solid (55 mg, 0.12 mmol, 85%).

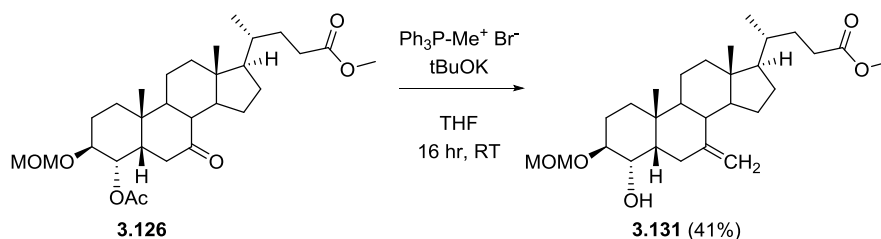
3.124: Formula: $\text{C}_{27}\text{H}_{42}\text{O}_6$; **MW** 462.6; **m.p.** N/A; **R_f** (Petrol ether/EtOAc : 60/40) : 0.41; **I.R.** 2944 (m), 2883 (w), 1723 (s), 1438 (s), 1159 (w), 1029 (s) cm^{-1} ; ^1H NMR (400MHz, CDCl_3): δ 4.62 (d, $J=7.0$ Hz, 1H, O- CHH' -O), 4.59 (d, $J=7.0$ Hz, 1H, O- CHH' -O), 3.83 (t, $J=3.0$ Hz, 1H, H_3), 3.65 (s, 3H, CO_2CH_3), 3.31 (s, 3H, OCH_3), 3.28 (dd, $J=6.1, 2.0$ Hz, 1H, H_5), 2.59 (dd, $J=14.4, 2.0$ Hz, 1H, $H_{6\alpha}$), 2.48-1.37 (m, 20H), 1.35 (s, 3H, H_{19}), 1.34-0.91 (m, 10H), 0.89 (d, $J=6.4$ Hz, 3H, H_{21}), 0.62 (s, 3H, H_{18}) ppm; ^{13}C NMR (100 MHz, CDCl_3): δ 210.0 (C_4 or C_7), 208.7 (C_4 or C_7), 174.6 (C_{24}), 96.0 (O- CH_2 -O), 79.3 (C_3), 55.9 (O CH_3), 54.5, 54.5 (C_5), 51.4 (CO_2CH_3), 49.1, 49.1, 42.8, 42.4, 42.1, 38.5 (CH_2), 37.4 (C_6), 35.1, 31.0 (CH_2), 30.9 (CH_2), 29.6 (CH_2), 28.2 (CH_2), 27.3 (CH_2), 25.4 (CH_2), 22.7 (C_{19}), 21.8 (CH_2), 18.3 (C_{21}), 11.9 (C_{18}) ppm; **MS (ESI+)** m/z : 463.5 [$\text{M}+\text{H}$] $^+$, 480.5 [$\text{M}+\text{NH}_4$] $^+$, 485.5 [$\text{M}+\text{Na}$] $^+$, 947.8 [$2\text{M}+\text{Na}$] $^+$; **HRMS** HRMS (HPLC-ESI) : [$\text{M}+\text{H}$] $^+$ Calcd. 463.3054; Found. 463.3058.

Methyl 3 β -methoxymethoxyl-4,4-difluoro-7-oxo-5 β -cholanoate (3.125) and methyl 3 β -methoxymethoxyl-7,7-difluoro-4-oxo-5 β -cholanoate (3.129) + fluoroalkenes (e.g. 3.128 and 3.130)



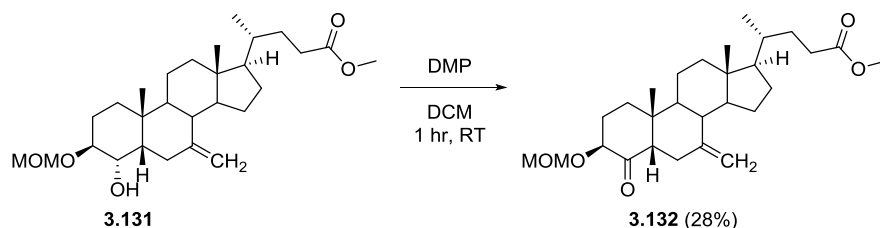
Di-keto **3.124** (55 mg, 0.12, 1 equiv) was dissolved in DAST (1 mL) and allowed to stir at RT for 16 hr. Reaction diluted with DCM (15 mL) and then carefully quenched with sat. aq. NaHCO₃ (15 mL). Layers separated and aqueous extracted with DCM (10 mL). Combined organics dried (Na₂SO₄) and concentrated. Crude purified *via* flash chromatography (pet ether/EA : 90:10→85:15→80:20) to yield 4,4-difluoroanalogue **3.125** and 7,7-difluoroanalogue **3.129**, along with unknown fluoroalkenes, as an inseparable mixture.

Formula: C₂₇H₄₂O₅F₂ (**3.125/3.129**); **MW** 484.6 (**3.125/3.129**); **m.p.** N/A; **R_f** (Petrol ether/EtOAc : 75/25) : 0.45; **¹⁹F NMR** (376 MHz, CDCl₃): δ -100.48 (d, $J=237.5$ Hz, 0.3F, **3.129** F7 β), -104.70 (ddd, $J=260.0, 33.0, 6.0$ Hz, 1F, **3.125** F4 α), -105.90 (dt, $J=260.0, 6.0$ Hz, 1F, **3.125** F4 β), -118.12 (dddd, $J=240.0, 38.0, 25.0, 12.0$ Hz, 0.3F, **3.129** F7 α), -125.45 (br. s., 0.7F, *unknown fluoro-alkene*), -132.92 (br. s., 0.2F, *unknown fluoro-alkene*) ppm; **[H]¹⁹F NMR** (376 MHz, CDCl₃): δ -100.48 (d, $J=239.3$ Hz, 0.3F, **3.129** F7 β), -104.70 (d, $J=260.0$ Hz, 1F, **3.125** F4 α), -105.90 (d, $J=260.0$ Hz, 1F, **3.125** F4 β), -118.12 (d, $J=239.3$ Hz, 0.3F, **3.129** F7 α), -125.45 (s, 0.7F, *unknown fluoro-alkene*), -132.92 (s, 0.2F, *unknown fluoro-alkene*) ppm; **MS (ESI+)** m/z : 485.3 [M+H]⁺, 502.4 [M+NH₄]⁺, 507.3 [M+Na]⁺.

Methyl 3 β -methoxymethoxyl-4 α -hydroxy-7-oxo-5 β -cholanoate (3.131)

Methyltriphenylphosphonium bromide (1.48 g, 4.43 mmol, 3.5 equiv) and potassium *tert*-butoxide (330 mg, 2.95 mmol, 2.5 equiv) were taken up in THF (15 mL) and stirred for 30 min at RT, before the dropwise addition of 7-keto derivative **3.126** (600 mg, 1.18 mmol, 1 equiv) in THF (10 mL). RM was deemed complete after 16 h, concentrated *in vacuo* and dry loaded onto silica gel (MeOH/DCM). Crude material was purified *via* flash chromatography (pet ether/EtOAc : 95:5→90:10→80:20) to yield 7-methylene **3.131** as a gummy solid (225 mg, 0.49 mmol, 41%). Note hydrolysis of 4 α -acetate.

3.131: Formula: C₂₈H₄₆O₅; **MW** 462.7; **m.p.** N/A; **R_f** (Petrol ether/EtOAc : 80/20) : 0.46; **I.R.** 3541 (w), 2942 (m), 2879 (m), 1739 (s), 1041 (s) cm⁻¹; **¹H NMR** (400MHz, CDCl₃): δ 5.01 (s, 1H, C7=CH₂), 4.77 (s, 1H, C7=CH₂), 4.66 (d, *J*=6.9 Hz, 1H, O-CHH'-O), 4.63 (d, *J*=6.9 Hz, 1H, O-CHH'-O), 3.99 (t, *J*=3.0 Hz, 1H, H₄), 3.66 (s, 3H, CO₂CH₃), 3.62 (q, *J*=2.6 Hz, 1H, H₃), 3.35 (s, 3H, OCH₃), 3.23 (s, 1H, OH), 2.76 (dd, *J*=14.0, 6.4 Hz, 1H, H₆ β), 2.35 (ddd, *J*=15.5, 10.5, 5.0 Hz, 1H, H₂₃), 2.29-1.09 (m, 29H), 1.07 (s, 3H, H₁₉), 0.94 (d, *J*=6.5 Hz, 3H, H₂₁), 0.69 (s, 3H, H₁₈) ppm; **¹³C NMR** (100 MHz, CDCl₃): δ 174.6 (C₂₄), 156.8 (C₇), 106.8 (C=CH₂), 95.2 (O-CH₂-O), 76.5 (C₄), 75.4 (C₃), 55.3 (OCH₃), 54.6, 51.4 (CO₂CH₃), 50.6, 44.9, 43.6, 43.2, 42.3, 38.8 (CH₂), 38.2 (C₆), 36.2, 35.1, 31.0 (C₂₃), 30.9 (CH₂), 29.6 (CH₂), 28.1 (CH₂), 25.7 (CH₂), 23.9 (C₁₉), 21.7 (CH₂), 20.7 (CH₂), 18.4 (C₂₁), 12.3 (C₁₈) ppm; **MS (ESI+)** *m/z* : 401.5 [M+H-HOCH₂OCH₃]⁺, 413.5 [M+H-H₂O, partial MOM cleavage]⁺, 485.5 [M+Na]⁺; **HRMS** HRMS (HPLC-ESI) : [M+H]⁺ Calcd. 463.3418; Found. 463.3406.

Methyl 3 β -methoxymethoxyl-4 α -hydroxy-7-oxo-5 β -cholanoate (3.132)

Using general procedure E, 4 α -OH **3.131** (200 mg, 0.43 mmol, 1 equiv) was oxidised. Crude was purified *via* flash chromatography (pet ether/EtOAc : 90:10→80:20) to yield 4-keto **3.132** as a gummy solid (55 mg, 0.12 mmol, 28%).

3.132: Formula: $C_{28}H_{44}O_5$; **MW** 460.7; **m.p.** N/A; **R_f** (Petrol ether/EtOAc : 80/20) : 0.46; **I.R.** 2944 (m), 2883 (w), 1737 (s), 1716 (m), 1161 (m), 1027 (s) cm^{-1} ; **¹H NMR** (400MHz, $CDCl_3$): δ 4.93 (d, $J=1.0$ Hz, 1H, C7=CH₂), 4.75 (s, 1H, C7=CH₂), 4.61 (d, $J=6.9$ Hz, 1H, O-CHH'-O), 4.59 (d, $J=6.9$ Hz, 1H, O-CHH'-O), 3.75 (t, $J=2.8$ Hz, 1H, H₃), 3.66 (s, 3H, CO₂CH₃), 3.34 (s, 3H, OCH₃), 2.73 (dd, $J=13.3, 1.9$ Hz, 1H, H₆ α), 2.68 (dd, $J=5.5, 2.0$ Hz, 1H, H₅), 2.35 (ddd, $J=15.5, 10.6, 5.0$ Hz, 1H, H₂₃), 2.31-1.28 (m, 22H), 1.25 (s, 3H, H₁₉), 1.21-0.95 (m, 6H), 0.92 (d, $J=6.5$ Hz, 3H, H₂₁), 0.67 (s, 3H, H₁₈) ppm; **¹³C NMR** (100 MHz, $CDCl_3$): δ 208.8 (C₄), 174.6 (C₂₄), 147.7 (C₇), 108.9 (C=CH₂), 95.4 (O-CH₂-O), 78.0 (C₃), 55.7, 54.7 (OCH₃), 54.7 (C₅), 51.4 (CO₂CH₃), 50.2, 45.2, 42.7, 41.6, 41.3, 38.6 (CH₂), 35.1, 31.7 (C₆), 31.0 (C₂₃), 30.9 (CH₂), 29.8 (CH₂), 28.0 (CH₂), 26.1 (CH₂), 25.5 (CH₂), 23.3 (C₁₉), 21.3 (CH₂), 18.4 (C₂₁), 12.1 (C₁₈) ppm; **MS (ESI+)** m/z : 461.5 [M+H]⁺, 483.5 [M+Na]⁺; **HRMS HRMS** (HPLC-ESI) : [M+H]⁺ Calcd. 461.3262; Found. 461.3272.

Bibliography

- [1] G. P. Moss, *Eur. J. Biochem.* **1989**, *186*, 429-458.
- [2] a. A. P. Davis, M. G. Orchard, *J. Chem. Soc. Perkin Trans 1* **1993**, 919; b. R. P. Bonarlaw, A. P. Davis, *Tetrahedron* **1993**, *49*, 9829-9844.
- [3] A. F. Hofmann, L. R. Hagey, M. D. Krasowski, *J. Lipid Res.* **2010**, *51*, 226-246.
- [4] a. M. Baptissart, A. Vega, E. Martinot, S. Baron, J. M. Lobaccaro, D. H. Volle, *Cell. Mol. Life. Sci.* **2013**, *70*, 4511-4526; b. T. Li, J. Y. Chiang, *Pharmacol. Rev.* **2014**, *66*, 948-983.
- [5] P. B. Hylemon, H. Zhou, W. M. Pandak, S. Ren, G. Gil, P. Dent, *J. Lipid Res.* **2009**, *50*, 1509-1520.
- [6] T. Maruyama, Y. Miyamoto, T. Nakamura, Y. Tamai, H. Okada, E. Sugiyama, T. Nakamura, H. Itadani, K. Tanaka, *Biochem. Biophys. Res. Commun.* **2002**, *298*, 714-719.
- [7] H. Wang, J. Chen, K. Hollister, L. C. Sowers, B. M. Forman, *Mol. Cell* **1999**, *3*, 543-553.
- [8] A. F. Hofman, D. M. Small, *Annu. Rev. Med.* **1967**, *18*, 333-376.
- [9] A. F. Hofmann, *News Physiol. Sci.* **1999**, *14*, 24-29.
- [10] L. R. Hagey, D. L. Crombie, E. Espinosa, M. C. Carey, H. Igimi, A. F. Hofmann, *J. Lipid Res.* **1993**, *34*, 1911-1917.
- [11] F. G. Schaap, M. Trauner, P. L. Jansen, *Nat. Rev. Gastroenterol. Hepatol.* **2014**, *11*, 55-67.
- [12] a. P. N. Maton, G. M. Murphy, R. H. Dowling, *Lancet* **1977**, *310*, 1297-1301; b. R. Poupon, R. Poupon, Y. Calmus, Y. Chrétien, F. Ballet, F. Darnis, *The Lancet* **1987**, *329*, 834-836.
- [13] J. S. Rudic, G. Poropat, M. N. Krstic, G. Bjelakovic, C. Gluud, *Cochrane Database Syst. Rev.* **2012**, *12*, CD000551.
- [14] N. M. Delzenne, P. B. Calderon, H. S. Taper, M. B. Roberfroid, *Toxicol. Lett.* **1992**, *61*, 291-304.
- [15] H. Jackson, M. Solaymani-Dodaran, T. R. Card, G. P. Aithal, R. Logan, J. West, *Hepatology* **2007**, *46*, 1131-1137.
- [16] M. Hansen, D. P. Sonne, F. K. Knop, *Curr. Diab. Rep.* **2014**, *14*, 482.
- [17] D. B. DB00930, *Vol. 2014*, The metabolomics innovation centre, **2005**.
- [18] B. M. Forman, E. Goode, J. Chen, A. E. Oro, D. J. Bradley, T. Perlmann, D. J. Noonan, L. T. Burka, T. Mcmorris, W. W. Lamph, R. M. Evans, C. Weinberger, *Cell* **1995**, *81*, 687-693.
- [19] a. M. Makishima, A. Y. Okamoto, J. J. Repa, H. Tu, R. M. Learned, A. Luk, M. V. Hull, K. D. Lustig, D. J. Mangelsdorf, B. Shan, *Science* **1999**, *284*, 1362-1365; b. D. J. Parks, S. G. Blanchard, R. K. Bledsoe, G. Chandra, T. G. Consler, S. A. Kliewer, J. B. Stimmel, T. M. Willson, A. M. Zavacki, D. D. Moore, J. M. Lehmann, *Science* **1999**, *284*, 1365-1368.
- [20] K. E. Swales, M. Korbonits, R. Carpenter, D. T. Walsh, T. D. Warner, D. Bishop-Bailey, *Cancer Res.* **2006**, *66*, 10120-10126.

Bibliography

- [21] N. Alasmael, R. Mohan, L. B. Meira, K. E. Swales, N. J. Plant, *Cancer Lett.* **2016**, *370*, 250-259.
- [22] R. M. Gadaleta, M. Cariello, C. Sabba, A. Moschetta, *Biochim. Biophys. Acta.* **2015**, *1851*, 30-39.
- [23] Y. Kawamata, R. Fujii, M. Hosoya, M. Harada, H. Yoshida, M. Miwa, S. Fukusumi, Y. Habata, T. Itoh, Y. Shintani, S. Hinuma, Y. Fujisawa, M. Fujino, *J. Biol. Chem.* **2003**, *278*, 9435-9440.
- [24] H. Sato, A. Macchiarulo, C. Thomas, A. Gioiello, M. Une, A. F. Hofmann, R. Saladin, K. Schoonjans, R. Pellicciari, J. Auwerx, *J. Med. Chem.* **2008**, *51*, 1831-1841.
- [25] Y. Calmus, J. Guechot, P. Podevin, M. T. Bonnefis, J. Giboudeau, R. Poupon, *Hepatology* **1992**, *16*, 719-723.
- [26] T. W. Pols, *Biochem. Soc. Trans.* **2014**, *42*, 244-249.
- [27] H. Duboc, Y. Tache, A. F. Hofmann, *Dig. Liver. Dis.* **2014**, *46*, 302-312.
- [28] T. Kida, Y. Tsubosaka, M. Hori, H. Ozaki, T. Murata, *Arterioscler. Thromb. Vasc. Biol.* **2013**, *33*, 1663-1669.
- [29] M. Watanabe, S. M. Houten, C. Matak, M. A. Christoffolete, B. W. Kim, H. Sato, N. Messaddeq, J. W. Harney, O. Ezaki, T. Kodama, K. Schoonjans, A. C. Bianco, J. Auwerx, *Nature* **2006**, *439*, 484-489.
- [30] D. P. Kumar, S. Rajagopal, S. Mahavadi, F. Mirshahi, J. R. Grider, K. S. Murthy, A. J. Sanyal, *Biochem. Biophys. Res. Commun.* **2012**, *427*, 600-605.
- [31] H. Mortiboys, J. Aasly, O. Bandmann, *Brain* **2013**, *136*, 3038-3050.
- [32] K. F. Winkhofer, C. Haass, *Biochim. Biophys. Acta.* **2010**, *1802*, 29-44.
- [33] H. Mortiboys, R. Furmston, G. Bronstad, J. Aasly, C. Elliott, O. Bandmann, *Neurology* **2015**, *85*, 846-852.
- [34] L. Z. Mi, S. Devarakonda, J. M. Harp, Q. Han, R. Pellicciari, T. M. Willson, S. Khorasanizadeh, F. Rastinejad, *Mol. Cell* **2003**, *11*, 1093-1100.
- [35] a. R. Pellicciari, S. Fiorucci, E. Camaioni, C. Clerici, G. Costantino, P. R. Maloney, A. Morelli, D. J. Parks, T. M. Willson, *J. Med. Chem.* **2002**, *45*, 3569-3572; b. R. Pellicciari, A. Gioiello, A. Macchiarulo, C. Thomas, E. Rosatelli, B. Natalini, R. Sardella, M. Pruzanski, A. Roda, E. Pastorini, K. Schoonjans, J. Auwerx, *J. Med. Chem.* **2009**, *52*, 7958-7961.
- [36] C. D'Amore, F. S. Di Leva, V. Sepe, B. Renga, C. Del Gaudio, M. V. D'Auria, A. Zampella, S. Fiorucci, V. Limongelli, *J. Med. Chem.* **2014**, *57*, 937-954.
- [37] G. M. Hirschfield, A. Mason, V. Luketic, K. Lindor, S. C. Gordon, M. Mayo, K. V. Kowdley, C. Vincent, H. C. Bodhenheimer, Jr., A. Pares, M. Trauner, H. U. Marschall, L. Adorini, C. Sciacca, T. Beecher-Jones, E. Castelloe, O. Bohm, D. Shapiro, *Gastroenterol.* **2015**, *148*, 751-761 e758.
- [38] B. A. Neuschwander-Tetri, R. Loomba, A. J. Sanyal, J. E. Lavine, M. L. Van Natta, M. F. Abdelmalek, N. Chalasani, S. Dasarthy, A. M. Diehl, B. Hameed, K. V. Kowdley, A. McCullough, N. Terrault, J. M. Clark, J. Tonascia, E. M. Brunt, D. E. Kleiner, E. Doo, N. C. R. Network, *Lancet* **2015**, *385*, 956-965.

- [39] <http://www.fiercebiotech.com/biotech/top-10-possible-blockbusters-might-launch-year>, Accessed on 03/08/2016.
- [40] a. R. E. Martin, C. Bissantz, O. Gavelle, C. Kuratli, H. Dehmlow, H. G. Richter, U. Obst Sander, S. D. Erickson, K. Kim, S. L. Pietranico-Cole, R. Alvarez-Sanchez, C. Ullmer, *ChemMedChem* **2013**, *8*, 569-576; b. H. Dehmlow, R. A. Sanchez, S. Bachmann, C. Bissantz, F. Bliss, K. Conde-Knape, M. Graf, R. E. Martin, U. O. Sander, S. Raab, H. G. F. Richter, S. Sewing, U. Sprecher, C. Ullmer, P. Mattei, *Bioorg. Med. Chem.* **2013**, *23*, 4627-4632.
- [41] A. T. Londregan, D. W. Piotrowski, K. Futatsugi, J. S. Warmus, M. Boehm, P. A. Carpino, J. E. Chin, A. M. Janssen, N. S. Roush, J. Buxton, T. Hinchey, *Bioorg. Med. Chem. Lett.* **2013**, *23*, 1407-1411.
- [42] D. P. Phillips, W. Gao, Y. Yang, G. Zhang, I. K. Lerario, T. L. Lau, J. Jiang, X. Wang, D. G. Nguyen, B. G. Bhat, C. Trotter, H. Sullivan, G. Welzel, J. Landry, Y. Chen, S. B. Joseph, C. Li, W. P. Gordon, W. Richmond, K. Johnson, A. Bretz, B. Bursulaya, S. Pan, P. McNamara, H. M. Seidel, *J. Med. Chem.* **2014**.
- [43] a. P. R. Maloney, D. J. Parks, C. D. Haffner, A. M. Fivush, G. Chandra, K. D. Plunket, K. L. Creech, L. B. Moore, J. G. Wilson, M. C. Lewis, S. A. Jones, T. M. Willson, *J. Med. Chem.* **2000**, *43*, 2971-2974; b. M. Downes, M. A. Verdecia, A. J. Roecker, R. Hughes, J. B. Hogenesch, H. R. Kast-Woelbern, M. E. Bowman, J. L. Ferrer, A. M. Anisfeld, P. A. Edwards, J. M. Rosenfeld, J. G. Alvarez, J. P. Noel, K. C. Nicolaou, R. M. Evans, *Mol. Cell* **2003**, *11*, 1079-1092; c. D. P. Phillips, W. Gao, Y. Yang, G. Zhang, I. K. Lerario, T. L. Lau, J. Jiang, X. Wang, D. G. Nguyen, B. G. Bhat, C. Trotter, H. Sullivan, G. Welzel, J. Landry, Y. Chen, S. B. Joseph, C. Li, W. P. Gordon, W. Richmond, K. Johnson, A. Bretz, B. Bursulaya, S. Pan, P. McNamara, H. M. Seidel, *J. Med. Chem.* **2014**, *57*, 3263-3282.
- [44] A. Macchiarulo, A. Gioiello, C. Thomas, T. W. H. Pols, R. Nuti, C. Ferrari, N. Giacche, F. De Franco, M. Pruzanski, J. Auwerx, K. Schoonjans, R. Pellicciari, *ACS Med. Chem. Lett.* **2013**, *4*, 1158-1162.
- [45] a. D. O'Hagan, *Chem. Soc. Rev.* **2008**, *37*, 308-319; b. L. Hunter, *Beilstein J. Org. Chem.* **2010**, *6*, 38.
- [46] J. D. Dunitz, *ChemBioChem* **2004**, *5*, 614-621.
- [47] H. J. Bohm, D. Banner, S. Bendels, M. Kansy, B. Kuhn, K. Muller, U. Obst-Sander, M. Stahl, *Chembiochem* **2004**, *5*, 637-643.
- [48] a. O. Šifner, *Int. J. Thermophys.* **1999**, *20*, 1653-1666; b. D. A. D. Eric V. Anslyn, *Modern Physical Organic Chemistry*, University Science Books, **2006**.
- [49] M. B. van Niel, I. Collins, M. S. Beer, H. B. Broughton, S. K. Cheng, S. C. Goodacre, A. Heald, K. L. Locker, A. M. MacLeod, D. Morrison, C. R. Moyes, D. O'Connor, A. Pike, M. Rowley, M. G. Russell, B. Sohal, J. A. Stanton, S. Thomas, H. Verrier, A. P. Watt, J. L. Castro, *J. Med. Chem.* **1999**, *42*, 2087-2104.
- [50] B. E. Smart, *J. Fluorine Chem.* **2001**, *109*, 3-11.
- [51] J. Graton, Z. Wang, A. M. Brossard, D. Goncalves Monteiro, J. Y. Le Questel, B. Linclau, *Angew. Chem. Int. Ed. Engl.* **2012**, *51*, 6176-6180.
- [52] P. W. Kenny, *J. Chem. Inf. Model.* **2009**, *49*, 1234-1244.
- [53] R. I. Bayliss, *Proc. R. Soc. Med.* **1959**, *52*, 929-932.

Bibliography

- [54] R. Pellicciari, G. Costantino, E. Camaioni, B. M. Sadeghpour, A. Entrena, T. M. Willson, S. Fiorucci, C. Clerici, A. Gioiello, *J. Med. Chem.* **2004**, *47*, 4559-4569.
- [55] S. Purser, P. R. Moore, S. Swallow, V. Gouverneur, *Chem. Soc. Rev.* **2008**, *37*, 320-330.
- [56] B. Linclau, F. Peron, E. Bogdan, N. Wells, Z. Wang, G. Compain, C. Q. Fontenelle, N. Galland, J. Y. Le Questel, J. Graton, *Chem. Eur. J.* **2015**, *21*, 17808-17816.
- [57] a. E. Rutkowska, K. Pajak, K. Jozwiak, *Acta. Pol. Pharm.* **2013**, *70*, 3-18; b. H. van de Waterbeemd, R. E. Carter, G. Grassy, H. Kubinyi, Y. C. Martin, M. S. Tute, P. Willett, in *Pure Appl. Chem.*, Vol. 69, **1997**, p. 1137.
- [58] J. A. Arnott, S. L. Planey, *Expert. Opin. Drug. Discov.* **2012**, *7*, 863-875.
- [59] M. J. Waring, *Expert. Opin. Drug. Discov.* **2010**, *5*, 235-248.
- [60] B. Linclau, Z. Wang, G. Compain, V. Paumelle, C. Q. Fontenelle, N. Wells, A. Weymouth-Wilson, *Angew. Chem. Int. Ed. Engl.* **2015**, *55*, 674-678.
- [61] N. S. Keddie, A. M. Z. Slawin, T. Lebl, D. Philp, D. O'Hagan, *Nat. Chem.* **2015**, *7*, 483-488.
- [62] M. Jaccaud, R. Faron, D. Devilliers, R. Romano, in *Ullmann's Encyclopedia of Industrial Chemistry*, Wiley-VCH Verlag GmbH & Co. KGaA, **2000**.
- [63] T. Liang, C. N. Neumann, T. Ritter, *Angew. Chem. Int. Ed. Engl.* **2013**, *52*, 8214-8264.
- [64] T. Furuya, C. A. Kuttruff, T. Ritter, *Curr. Opin. Drug. Discov. Devel.* **2008**, *11*, 803-819.
- [65] W. R. Hasek, W. C. Smith, V. A. Engelhardt, *J. Am. Chem. Soc.* **1960**, *82*, 543-551.
- [66] W. J. Middleton, *J. Org. Chem.* **1975**, *40*, 574-578.
- [67] G. S. Lal, G. P. Pez, R. J. Pesaresi, F. M. Prozonc, H. S. Cheng, *J. Org. Chem.* **1999**, *64*, 7048-7054.
- [68] F. Dolle, C. Hetru, B. Rousseau, F. Sobrio, C. Blais, R. Lafont, M. Descamp, B. Luu, *Tetrahedron* **1993**, *49*, 2485-2498.
- [69] Q. J. Li, G. P. Tochtrop, *Tetrahedron Lett.* **2011**, *52*, 4137-4139.
- [70] J. Rohacova, M. Luisa Marin, A. Martinez-Romero, J.-E. O'Connor, M. Jose Gomez-Lechon, M. Teresa Donato, J. V. Castell, M. A. Miranda, *Org. Biomol. Chem.* **2009**, *7*, 4973-4980.
- [71] R. Pellicciari, A. Gioiello, P. Sabbatini, F. Venturoni, R. Nuti, C. Colliva, G. Rizzo, L. Adorini, M. Pruzanski, A. Roda, A. Macchiarulo, *ACS Med. Chem. Lett.* **2012**, *3*, 273-277.
- [72] C. Festa, B. Renga, C. D'Amore, V. Sepe, C. Finamore, S. De Marino, A. Carino, S. Cipriani, M. C. Monti, A. Zampella, S. Fiorucci, *J. Med. Chem.* **2014**, *57*, 8477-8495.
- [73] P. S. Dangate, C. L. Salunke, K. G. Akamanchi, *Steroids* **2011**, *76*, 1397-1399.
- [74] J. L. Luche, *J. Am. Chem. Soc.* **1978**, *100*, 2226-2227.
- [75] I. Černý, M. Buděšínský, V. Pouzar, V. Vyklický, B. Krausová, L. Vyklický Jr, *Steroids* **2012**, *77*, 1233-1241.
- [76] a. T. Hiyama, *Organofluorine Compounds: Chemistry and Applications*, Vol. 1, Springer-Verlag, Germany, **2000**; b. W. R. Dolbier, Jr., *Guide to Fluorine NMR for Organic Chemists*, John Wiley & Sons inc., Hoboken, New Jersey, **2009**.

- [77] Q. Li, G. P. Tochtrop, *Tetrahedron Lett.* **2011**, *52*, 4137-4139.
- [78] I. Takashi, K. Ichiro, Y. Sciichiro, G. Junichi, N. Toshio, F. C. Chang, *Steroids* **1990**, *55*, 530-539.
- [79] B. Dayal, G. Salen, B. Toome, G. S. Tint, S. Shefer, J. Padia, *Steroids* **1990**, *55*, 233-237.
- [80] O. Mitsunobu, M. Yamada, *Bull. Chem. Soc. Jpn.* **1967**, *40*, 2380-2382.
- [81] O. Mitsunobu, *Synthesis-Stuttgart* **1981**, *1981*, 1-28.
- [82] P. Geoffroy, B. Ressault, E. Marchioni, M. Miesch, *Steroids* **2011**, *76*, 1166-1175.
- [83] M. K. Nielsen, C. R. Ugaz, W. Li, A. G. Doyle, *J. Am. Chem. Soc.* **2015**, *137*, 9571-9574.
- [84] A. C. Burns, P. W. Sorensen, T. R. Hoye, *Steroids* **2011**, *76*, 291-300.
- [85] a. M. Angelin, M. Hermansson, H. Dong, O. Ramstrom, *Eur. J. Org. Chem.* **2006**, 4323-4326; b. A. E. J. d. Nooy, A. C. Besemer, H. v. Bekkum, *Synthesis* **1996**, *1996*, 1153-1176.
- [86] T. Oishi, K. Ootou, H. Shibata, M. Murata, *Tetrahedron Lett.* **2010**, *51*, 2600-2602.
- [87] H. D. Soule, J. Vazquez, A. Long, S. Albert, M. Brennan, *J. Natl. Cancer Inst.* **1973**, *51*, 1409-1416.
- [88] R. Cailleau, R. Young, M. Olive, W. J. Reeves, Jr., *J. Natl. Cancer Inst.* **1974**, *53*, 661-674.
- [89] C. A. Hudis, *N. Engl. J. Med.* **2007**, *357*, 39-51.
- [90] T. Mosmann, *J. Immunol. Methods* **1983**, *65*, 55-63.
- [91] K. Uhr, W. J. Prager-van der Smissen, A. A. Heine, B. Ozturk, M. Smid, H. W. Gohlmann, A. Jager, J. A. Foekens, J. W. Martens, *Springerplus* **2015**, *4*, 611.
- [92] S. L. Fink, B. T. Cookson, *Infect. Immun.* **2005**, *73*, 1907-1916.
- [93] a. M. E. Wall, M. C. Wani, C. E. Cook, K. H. Palmer, A. T. McPhail, G. A. Sim, *J. Am. Chem. Soc.* **1966**, *88*, 3888-3890; b. C. W. Zeng, X. J. Zhang, K. Y. Lin, H. Ye, S. Y. Feng, H. Zhang, Y. Q. Chen, *Mol. Pharmacol.* **2012**, *81*, 578-586.
- [94] J. Baudoux, D. Cahard, in *Org. React.*, John Wiley & Sons, Inc., **2004**.
- [95] J. Liu, J. Chan, C. M. Bryant, P. A. Duspara, E. E. Lee, D. Powell, H. Yang, Z. P. Liu, C. Walpole, E. Roberts, R. A. Batey, *Tetrahedron Lett.* **2012**, *53*, 2971-2975.
- [96] S. Stavber, M. Zupan, *Tetrahedron Lett.* **1996**, *37*, 3591-3594.
- [97] T. Fujimoto, Y. Tomata, J. Kunitomo, M. Hirozane, S. Marui, *Bioorg. Med. Chem. Lett.* **2011**, *21*, 6409-6413.
- [98] P. Allevi, M. Anastasia, P. Ciuffreda, A. Fiecchi, A. M. Sanvito, *Steroids* **1990**, *55*, 303-307.
- [99] S. Karimi, K. G. Grohmann, L. Todaro, *J. Org. Chem.* **1995**, *60*, 554-559.
- [100] J. W. Barlow, A. P. McHugh, O. Woods, J. J. Walsh, *Eur. J. Med. Chem.* **2011**, *46*, 1545-1554.
- [101] C. Wolfrum, Carreira, E., Meissburger, B., A61K 31/575 A61P 3/10 ed. (Ed.: W. I. P. Organisation), **2013**, p. 81.

Bibliography

- [102] J. K. Busse, E. J. Stoner, C. L. Ladd, in *Encyclopedia of Reagents for Organic Synthesis*, John Wiley & Sons, Ltd, **2001**.
- [103] K. S. Bhandari, R. E. Pincock, *Synthesis-Stuttgart* **1974**, 1974, 655-656.
- [104] H.-Y. Li, H. Sun, S. G. DiMugno, in *Encyclopedia of Reagents for Organic Synthesis*, John Wiley & Sons, Ltd, **2001**.
- [105] D. W. Kim, H. J. Jeong, S. T. Lim, M. H. Sohn, *Tetrahedron Lett.* **2010**, 51, 432-434.
- [106] A. S. Pilcher, H. L. Ammon, P. DeShong, *J. Am. Chem. Soc.* **1995**, 117, 5166-5167.
- [107] a. R. Raju, B. F. Castillo, S. K. Richardson, M. Thakur, R. Severins, M. Kronenberg, A. R. Howell, *Bioorg. Med. Chem. Lett.* **2009**, 19, 4122-4125; b. W. Meyer, *Angew. Chem.* **1967**, 79, 151-152; c. J. O. Karlsson, T. Frejd, *J. Org. Chem.* **1983**, 48, 1921-1923; d. J. B. Milbank, R. J. Stevenson, D. C. Ware, J. Y. Chang, M. Tercel, G. O. Ahn, W. R. Wilson, W. A. Denny, *J. Med. Chem.* **2009**, 52, 6822-6834; e. A. J. Liston, *J. Org. Chem.* **1966**, 31, 2105-2109; f. P. PEVARELLO, M. VILLA, M. VARASI, A. ISACCHI, in *Espace.net*, Vol. WO/2000/069846 (Ed.: US Patent 6, 845 B1), **2004**; g. E. Boyd, S. Buksha, G. S. Coumbarides, M. Dingjan, J. Eames, R. V. H. Jones, M. Motevalli, R. A. Stenson, M. J. Suggate, *J. Chem. Crystallogr.* **2007**, 37, 233-241.
- [108] A. J. Liston, M. Howarth, *J. Org. Chem.* **1967**, 32, 1034-1041.
- [109] Popadyuk, II, A. V. Markov, O. V. Salomatina, E. B. Logashenko, A. V. Shernyukov, M. A. Zenkova, N. F. Salakhutdinov, *Bioorg. Med. Chem.* **2015**, 23, 5022-5034.
- [110] E. J. Tavares da Silva, F. M. F. Roleira, M. L. Sá e Melo, A. S. Campos Neves, J. A. Paixão, M. J. de Almeida, M. R. Silva, L. C. R. Andrade, *Steroids* **2002**, 67, 311-319.
- [111] K. G. Davenport, in *Encyclopedia of Reagents for Organic Synthesis*, John Wiley & Sons, Ltd, **2001**.
- [112] H.-Y. Li, in *Encyclopedia of Reagents for Organic Synthesis*, John Wiley & Sons, Ltd, **2001**.
- [113] S. Hara, in *Encyclopedia of Reagents for Organic Synthesis*, John Wiley & Sons, Ltd, **2001**.
- [114] S. P. Kotun, G. K. S. Prakash, J. Hu, in *Encyclopedia of Reagents for Organic Synthesis*, John Wiley & Sons, Ltd, **2001**.
- [115] G. A. Molander, D. J. Cooper, S. W. Wright, in *Encyclopedia of Reagents for Organic Synthesis*, John Wiley & Sons, Ltd, **2001**.
- [116] M. A. McClinton, *Aldrichimica Acta* **1992**, 28, 31-35.
- [117] G. A. Olah, J. T. Welch, Y. D. Vankar, M. Nojima, I. Kerekes, J. A. Olah, *J. Org. Chem.* **1979**, 44, 3872-3881.
- [118] R. Franz, *J. Fluorine Chem.* **1980**, 15, 423-434.
- [119] O. E. Okoromoba, J. Han, G. B. Hammond, B. Xu, *J. Am. Chem. Soc.* **2014**, 136, 14381-14384.
- [120] A. Sattler, G. Haufe, *J. Fluorine Chem.* **1994**, 69, 185-190.
- [121] G. Haufe, S. Bruns, M. Runge, *J. Fluorine Chem.* **2001**, 112, 55-61.
- [122] O. E. Okoromoba, J. Han, G. B. Hammond, B. Xu, *J. Am. Chem. Soc.* **2014**, 136, 14381-14384.

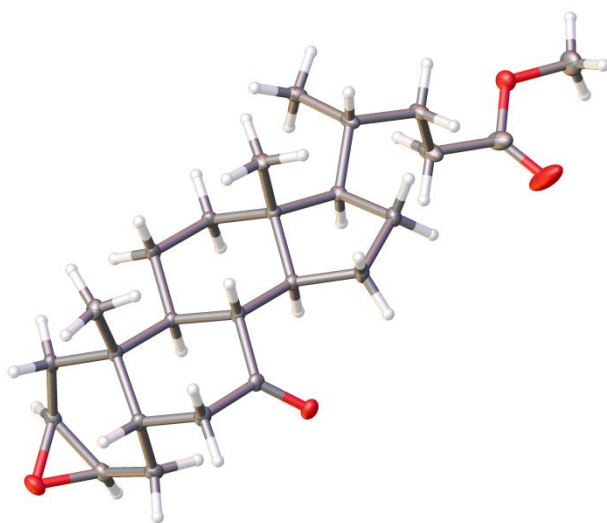
- [123] G. K. S. Prakash, F. Pertusati, in *Encyclopedia of Reagents for Organic Synthesis*, John Wiley & Sons, Ltd, **2001**.
- [124] R. R. Kumar, S. D. Haveli, H. B. Kagan, *Synlett* **2011**, 2011, 1709-1712.
- [125] M. Saïah, M. Bessodes, K. Antonakis, *Tetrahedron Lett.* **1992**, 33, 4317-4320.
- [126] E. Lee, D. V. Yandulov, *J. Fluorine Chem.* **2009**, 130, 474-483.
- [127] Y.-R. Zhao, B. Guang, R. Bouillon, A. Verstuyf, P. De Clercq, M. Vandewalle, *Eur. J. Org. Chem.* **2005**, 2005, 4414-4427.
- [128] T. F. Al-Azemi, A. A. Mohamod, *Polymer* **2011**, 52, 5431-5438.
- [129] P. Barbier, P. Mohr, M. Muller, R. Masciadri, *J. Org. Chem.* **1998**, 63, 6984-6989.
- [130] S. E. Denmark, Z. Wu, C. M. Crudden, H. Matsushashi, *J. Org. Chem.* **1997**, 62, 8288-8289.
- [131] D. B. Dess, J. C. Martin, *J. Org. Chem.* **1983**, 48, 4155-4156.
- [132] P. L. Coe, A. W. Mott, J. C. Tatlow, *J. Fluorine Chem.* **1982**, 20, 243-254.
- [133] T. Iida, T. Yamaguchi, R. Nakamori, M. Hikosaka, N. Mano, J. Goto, T. Nambara, *J. Chem. Soc., Perkin Trans. 1* **2001**, 2229-2236.
- [134] S. H. Hilal, L. L. Bornander, L. A. Carreira, *QSAR & Combinatorial Science* **2005**, 24, 631-638.
- [135] P. A. Champagne, J. Desroches, J. F. Paquin, *Synthesis-Stuttgart* **2015**, 47, 306-322.
- [136] J. A. K. Howard, V. J. Hoy, D. O'Hagan, G. T. Smith, *Tetrahedron* **1996**, 52, 12613-12622.
- [137] G. T. Giuffredi, V. Gouverneur, B. Bernet, *Angew. Chem. Int. Ed. Engl.* **2013**, 52, 10524-10528.
- [138] E. Arunan, R. Desiraju Gautam, A. Klein Roger, J. Sadlej, S. Scheiner, I. Alkorta, C. Clary David, H. Crabtree Robert, J. Dannenberg Joseph, P. Hobza, G. Kjaergaard Henrik, C. Legon Anthony, B. Mennucci, J. Nesbitt David, in *Pure Appl. Chem., Vol. 83*, **2011**, p. 1637.
- [139] H. J. Schneider, *Chem. Sci.* **2012**, 3, 1381-1394.
- [140] E. D'Oria, J. J. Novoa, *CrystEngComm* **2008**, 10, 423.
- [141] J. D. Dunitz, R. Taylor, *Chem. Eur. J.* **1997**, 3, 89-98.
- [142] R. W. Taft, D. Gurka, L. Joris, P. v. R. Schleyer, J. W. Rakshys, *J. Am. Chem. Soc.* **1969**, 91, 4801-4808.
- [143] E. M. Arnett, L. Joris, E. Mitchell, T. S. S. R. Murty, T. M. Gorrie, P. v. R. Schleyer, *J. Am. Chem. Soc.* **1970**, 92, 2365-2377.
- [144] C. Ouvrard, M. Berthelot, C. Laurence, *J. Chem. Soc., Perkin Trans. 2* **1999**, 1357-1362.
- [145] C. Dalvit, C. Invernizzi, A. Vulpetti, *Chem. Eur. J.* **2014**, 20, 11058-11068.
- [146] M. H. Abraham, D. V. Prior, R. A. Schulz, J. J. Morris, P. J. Taylor, *J. Chem. Soc., Faraday Trans.* **1998**, 94, 879-885.
- [147] M. D. Struble, C. Kelly, M. A. Siegler, T. Lectka, *Angew. Chem. Int. Ed. Engl.* **2014**, 53, 8924-8928.

Bibliography

- [148] A. Allerhand, P. Von Rague Schleyer, *J. Am. Chem. Soc.* **1963**, *85*, 1715-1723.
- [149] P. Dauber, A. T. Hagler, *Acc. Chem. Res.* **1980**, *13*, 105-112.
- [150] B. Bernet, A. Vasella, *Helv. Chim. Acta* **2000**, *83*, 995-1021.
- [151] H. Takemura, M. Kotoku, M. Yasutake, T. Shinmyozu, *Eur. J. Org. Chem.* **2004**, *2004*, 2019-2024.
- [152] I. Rozas, I. Alkorta, J. Elguero, *J. Phys. Chem. A* **2001**, *105*, 10462-10467.
- [153] H. Takemura, R. Ueda, T. Iwanaga, *J. Fluorine Chem.* **2009**, *130*, 684-688.
- [154] a. Y. Takagi, H. Sohtome, T. Tsuchiya, S. Umezawa, T. Takeuchi, *J. Antibiot.* **1992**, *45*, 355-362; b. K. Nakai, Y. Takagi, T. Tsuchiya, *Carbohydr. Res.* **1999**, *316*, 47-57; c. B. Bernet, A. Vasella, *Helv. Chim. Acta* **2007**, *90*, 1874-1888.
- [155] A. E. Reed, L. A. Curtiss, F. Weinhold, *Chem. Rev.* **1988**, *88*, 899-926.
- [156] J. R. Lane, J. Contreras-Garcia, J. P. Piquemal, B. J. Miller, H. G. Kjaergaard, *J. Chem. Theory. Comput.* **2013**, *9*, 3263-3266.
- [157] R. F. W. Bader, H. Essen, *J. Chem. Phys.* **1984**, *80*, 1943-1960.
- [158] R. A. Cormanich, R. Rittner, M. P. Freitas, M. Buhl, *Phys. Chem. Chem. Phys.* **2014**, *16*, 19212-19217.
- [159] J. Graton, F. Besseau, A. M. Brossard, E. Charpentier, A. Deroche, J. Y. Le Questel, *J. Phys. Chem. A* **2013**, *117*, 13184-13193.
- [160] R. P. Gil, C. S. P. Martinez, F. C. Machado, *Synthetic Commun.* **1998**, *28*, 3387-3396.
- [161] a. J. Takerhara, Yokohama-shi, K., in *Espacenet.com*, Vol. WO 2007/080951 (Ed.: E. p. office), Japan, **2008**; b. O. Bortolini, G. Fantin, M. Fogagnolo, R. Forlani, S. Maietti, P. Pedrini, *J. Org. Chem.* **2002**, *67*, 5802-5806.
- [162] J. Ren, Y. Wang, J. Wang, J. Lin, K. Wei, R. Huang, *Steroids* **2013**, *78*, 53-58.

Appendices - Crystal structure data

A.1 X-ray structure analysis data for compound 2.22



Thermal ellipsoids drawn at the 50% percent probability level.

Experimental. Single clear colourless Fragment-shaped crystals of (2014sot0035) were recrystallised from a mixture of EA and hexane by slow evaporation. A suitable crystal ($0.220 \times 0.180 \times 0.080 \text{ mm}^3$) was selected and mounted on a MITIGEN holder in perfluoroether oil on a Rigaku AFC12 FRE-HF diffractometer. The crystal was kept at $T = 100(2) \text{ K}$ during data collection. Using **Olex2** (Dolomanov et al., 2009), the structure was solved with the ShelXT (Sheldrick, 2008) structure solution program, using the Direct Methods solution method. The model was refined with version of **ShelXL** (Sheldrick, 2008) using Least Squares minimisation.

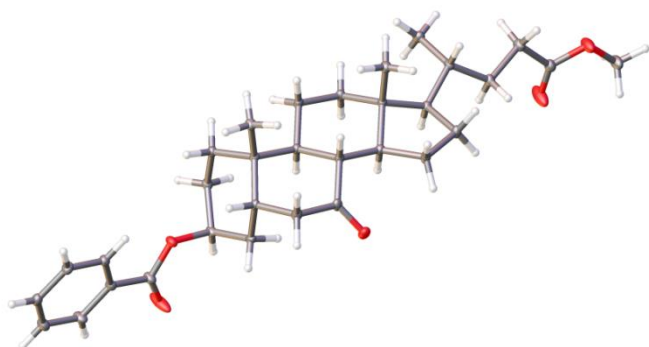
Crystal Data. $\text{C}_{25}\text{H}_{38}\text{O}_4$, $M_r = 402.55$, orthorhombic, $P2_12_12_1$ (No. 19), $a = 7.5668(2) \text{ \AA}$, $b = 9.4755(3) \text{ \AA}$, $c = 31.6332(7) \text{ \AA}$, $\alpha = \beta = \gamma = 90^\circ$, $V = 2268.08(11) \text{ \AA}^3$, $T = 100(2) \text{ K}$, $Z = 4$, $Z' = 1$, $\mu (\text{MoK}\alpha) = 0.078$,

15050 reflections measured, 7102 unique ($R_{int} = 0.0271$) which were used in all calculations. The final wR_2 was 0.1098 (all data) and R_1 was 0.0447 ($I > 2(I)$).

Compound	2014sot0035
Formula	$\text{C}_{25}\text{H}_{38}\text{O}_4$
$D_{calc.}/\text{g cm}^{-3}$	1.179
μ/mm^{-1}	0.078
Formula Weight	402.55
Colour	clear colourless
Shape	Fragment
Max Size/mm	0.220
Mid Size/mm	0.180
Min Size/mm	0.080
T/K	100(2)
Crystal System	orthorhombic
Space Group	$P2_12_12_1$
$a/\text{\AA}$	7.5668(2)
$b/\text{\AA}$	9.4755(3)
$c/\text{\AA}$	31.6332(7)
$\alpha/^\circ$	90
$\beta/^\circ$	90
$\gamma/^\circ$	90
$V/\text{\AA}^3$	2268.08(11)
Z	4
Z'	1
$\Theta_{min}/^\circ$	2.244
$\Theta_{max}/^\circ$	31.962
Measured Refl.	15050
Independent Refl.	7102
Reflections Used	6199
R_{int}	0.0271
Parameters	266
Restraints	0
Largest Peak	0.287
Deepest Hole	-0.187
GooF	1.032
wR_2 (all data)	0.1098
wR_2	0.1049
R_1 (all data)	0.0540
R_1	0.0447

Absolute structure*Not reliably determined*

A.2 X-ray structure analysis data for compound 2.30



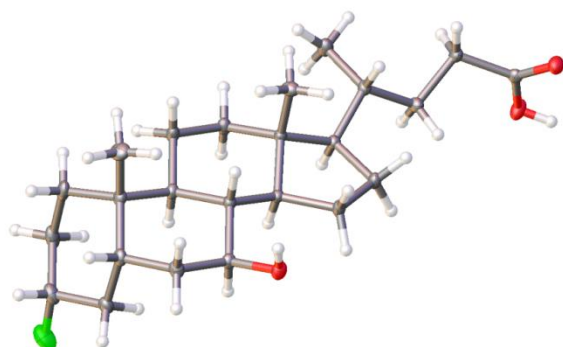
Thermal ellipsoids drawn at the 50% probability level.

Experimental. Single clear colourless slab-shaped crystals of (**2014sot0026**) were recrystallised from by. A suitable crystal ($0.08 \times 0.06 \times 0.01 \text{ mm}^3$) was selected and mounted on a MITIGEN holder in perfluoroether oil on a Rigaku AFC12 FRE-HF diffractometer. The crystal was kept at $T = 100(2) \text{ K}$ during data collection. Using **Olex2** (Dolomanov et al., 2009), the structure was solved with the **olex2.solve** (Bourhis et al., 2013) structure solution program, using the Charge Flipping solution method. The model was refined with version 2014-3 of **ShelXL** (Sheldrick, 2008) using Least Squares minimisation.

Crystal Data. $\text{C}_{32}\text{H}_{44}\text{O}_5$, $M_r = 508.67$, orthorhombic, $P2_12_12_1$ (No. 19), $a = 7.4504(3) \text{ \AA}$, $b = 13.2293(4) \text{ \AA}$, $c = 26.8545(12) \text{ \AA}$, $\alpha = \beta = \gamma = 90^\circ$, $V = 2646.87(18) \text{ \AA}^3$, $T = 100(2) \text{ K}$, $Z = 4$, $Z' = 1.000$, $\mu (\text{MoK}\alpha) = 0.084$, 15489 reflections measured, 6691 unique ($R_{int} = 0.0315$) which were used in all calculations. The final wR_2 was 0.1178 (all data) and R_1 was 0.0476 ($I > 2(I)$).

Compound	2014sot0026
Formula	$\text{C}_{32}\text{H}_{44}\text{O}_5$
$D_{calc.}/ \text{g cm}^{-3}$	1.276
μ/mm^{-1}	0.084
Formula Weight	508.67
Colour	clear colourless
Shape	slab
Max Size/mm	0.08
Mid Size/mm	0.06
Min Size/mm	0.01
T/K	100(2)
Crystal System	orthorhombic
Space Group	$P2_12_12_1$
$a/\text{\AA}$	7.4504(3)
$b/\text{\AA}$	13.2293(4)
$c/\text{\AA}$	26.8545(12)
$\alpha/^\circ$	90
$\beta/^\circ$	90
$\gamma/^\circ$	90
$V/\text{\AA}^3$	2646.87(18)
Z	4
Z'	1.000
$\Theta_{min}/^\circ$	3.034
$\Theta_{max}/^\circ$	28.698
Measured Refl.	15489
Independent Refl.	6691
Reflections Used	5797
R_{int}	0.0315
Parameters	338
Restraints	0
Largest Peak	0.567
Deepest Hole	-0.398
GooF	1.022
wR_2 (all data)	0.1178
wR_2	0.1118
R_1 (all data)	0.0580
R_1	0.0476

A.3 X-ray structure analysis data for compound 2.1



Thermal ellipsoids drawn at the 50% probability level.

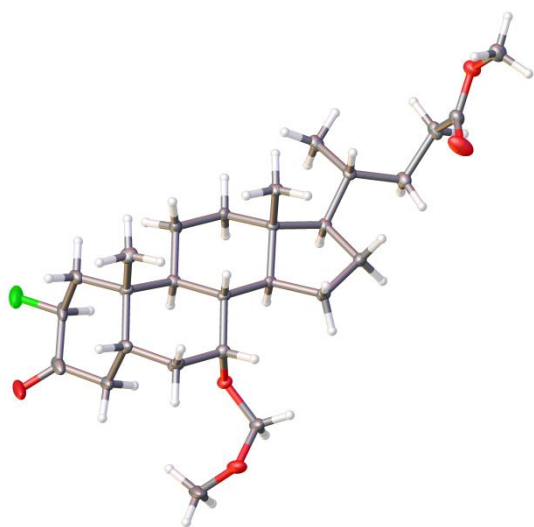
Experimental. Single clear colourless block-shaped crystals of (**2015sot0069-R-100K**) were obtained by recrystallisation from EtOAc. A suitable crystal (0.13×0.08×0.03) was selected and mounted on a MITIGEN holder in perfluoroether a Rigaku AFC12 FRE-VHF diffractometer. The crystal was kept at $T = 100(2)$ K during data collection. Using **Olex2** (Dolomanov et al., 2009), structure was solved with the **ShelXT** (Sheldrick, structure solution program, using the Direct Methods solution method. The model was refined **ShelXL** (Sheldrick, 2008) using Least Squares minimisation.

Crystal Data. $C_{24}H_{39}FO_3$, $M_r = 394.55$, monoclinic, (No. 4), $a = 11.5897(3)$ Å, $b = 6.41940(16)$ Å, $c = 28.8064(7)$ Å, $\beta = 97.295(2)^\circ$, $\alpha = \gamma = 90^\circ$, $V = 2125.81(9)$ Å³, $T = 100(2)$ K, $Z = 4$, $Z' = 2$,

$\mu(\text{MoK}\alpha) = 0.085$, 30602 reflections measured, 10935 unique ($R_{int} = 0.0249$) which were used in all calculations. The final wR_2 was 0.0989 (all data) and R_I was 0.0389 ($I > 2(I)$)

Compound	2015sot0069-R-100K	
Formula	$C_{24}H_{39}FO_3$	
$D_{calc./g\ cm^{-3}}$	1.233	
μ/mm^{-1}	0.085	
Formula Weight	394.55	
Colour	clear colourless	
Shape	block	
Max Size/mm	0.13	
Mid Size/mm	0.08	
Min Size/mm	0.03	
T/K	100(2)	
Crystal System	monoclinic	
Flack Parameter	-0.03(19)	
Hooft Parameter	-0.04(15)	
Space Group	$P2_1$	
$a/\text{Å}$	11.5897(3)	
$b/\text{Å}$	6.41940(16)	
$c/\text{Å}$	28.8064(7)	
$\alpha/^\circ$	90	
$\beta/^\circ$	97.295(2)	
$\gamma/^\circ$	90	
$V/\text{Å}^3$	2125.81(9)	
Z	4	
Z'	2	oil on
$\theta_{min}/^\circ$	2.946	
$\theta_{max}/^\circ$	28.699	
Measured Refl.	30602	the
Independent Refl.	10935	2015)
Reflections Used	10099	
R_{int}	0.0249	
Parameters	527	with
Restraints	1	
Largest Peak	0.669	
Deepest Hole	-0.203	
GooF	1.013	$P2_1$
wR_2 (all data)	0.0989	
wR_2	0.0962	
R_I (all data)	0.0436	
R_I	0.0389	

A.4 X-ray structure analysis data for compound 3.13



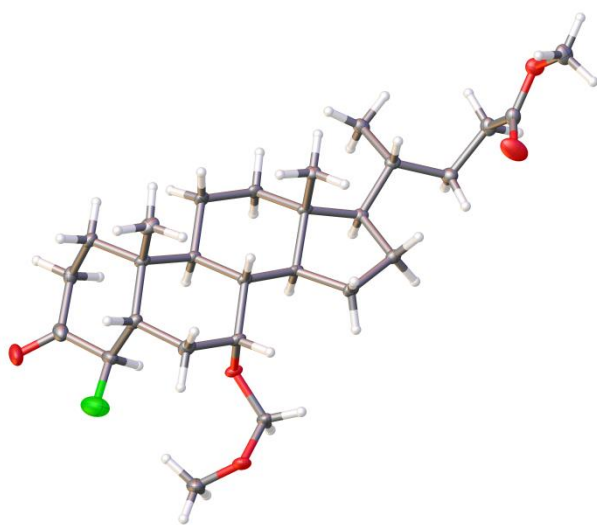
Thermal ellipsoids drawn at the 50 percent probability level.

Experimental. Single clear colourless Prism-shaped crystals of (2014sot0032) were obtained by recrystallisation from A suitable crystal ($0.200 \times 0.080 \times 0.010 \text{ mm}^3$) was selected and mounted on a MITIGEN holder in perfluoroether oil on a Rigaku AFC12 FRE-VHF diffractometer. The crystal was kept at $T = 100(2) \text{ K}$ during data collection. Using **Olex2** (Dolomanov et al., 2009), the structure was solved with the **Superflip** (L. Palatinus & G. Chapuis, 2007) structure solution program, using the Charge Flipping solution method. The model was refined with version 2014-3 of **ShelXL** (Sheldrick, 2008) using Least Squares minimisation.

Crystal Data. $\text{C}_{27}\text{H}_{43}\text{FO}_5$, $M_r = 466.61$, monoclinic, C2 (No. 5), $a = 20.8658(18) \text{ \AA}$, $b = 7.6706(6) \text{ \AA}$, $c = 15.7970(11) \text{ \AA}$, $\beta = 102.125(7)^\circ$, $\alpha = \gamma = 90^\circ$, $V = 2472.0(3) \text{ \AA}^3$, $T = 100(2) \text{ K}$, $Z = 4$, $Z' = 1$, $\mu (\text{MoK}\alpha) = 0.089$, 9922 reflections measured, 5897 unique ($R_{int} = 0.0352$) which were used in all calculations. The final wR_2 was 0.1628 (all data) and R_1 was 0.0726 ($I > 2(I)$).

Compound	2014sot0032
Formula	$\text{C}_{27}\text{H}_{43}\text{FO}_5$
$D_{calc.} / \text{g cm}^{-3}$	1.254
μ / mm^{-1}	0.089
Formula Weight	466.61
Colour	clear colourless
Shape	Prism
Max Size/mm	0.200
Mid Size/mm	0.080
Min Size/mm	0.010
T / K	100(2)
Crystal System	monoclinic
Space Group	C2
$a / \text{Å}$	20.8658(18)
$b / \text{Å}$	7.6706(6)
$c / \text{Å}$	15.7970(11)
$\alpha / ^\circ$	90
$\beta / ^\circ$	102.125(7)
$\gamma / ^\circ$	90
$V / \text{Å}^3$	2472.0(3)
Z	4
Z'	1
$\Theta_{min} / ^\circ$	2.955
$\Theta_{max} / ^\circ$	28.488
Measured Refl.	9922
Independent Refl.	5897
Reflections Used	4995
R_{int}	0.0352
Parameters	303
Restraints	1
Largest Peak	0.415
Deepest Hole	-0.291
GooF	1.043
wR_2 (all data)	0.1628
wR_2	0.1552
R_1 (all data)	0.0866
R_1	0.0726

A.5 X-ray structure analysis data for compound 3.15



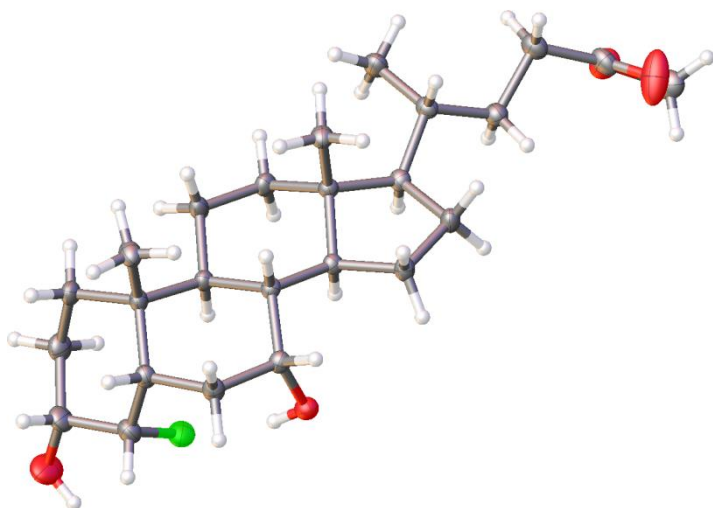
Thermal ellipsoids drawn at the 50 percent probability level.

Experimental. Single clear colourless Fragment-shaped crystals of (2014sot0033) were ?. A suitable crystal ($0.140 \times 0.050 \times 0.030$ mm³) was selected and mounted on a MITIGEN holder in perfluoroether oil on a Rigaku AFC12 FRE-VHF diffractometer. The crystal was kept at $T = 100(2)$ K during data collection. Using **Olex2** (Dolomanov et al., 2009), the structure was solved with the ?structure solution program, using the ?methods solution method. The model was refined with version 2014-3 of **ShelXL** (Sheldrick, 2008) using Least Squares minimisation.

Crystal Data. C₂₇H₄₃FO₅, $M_r = 466.61$, monoclinic, C2 (No. 5), $a = 20.955(14)$ Å, $b = 7.651(4)$ Å, $c = 15.768(9)$ Å, $\beta = 103.061(11)^\circ$, $\alpha = \gamma = 90^\circ$, $V = 2463(3)$ Å³, $T = 100(2)$ K, $Z = 4$, $Z' = 1$, μ (MoK α) = 0.090, 9393 reflections measured, 4399 unique ($R_{int} = 0.0764$) which were used in all calculations. The final wR_2 was 0.1228 (all data) and R_1 was 0.0517 ($I > 2(I)$).

Compound	2014sot0033
Formula	C ₂₇ H ₄₃ FO ₅
$D_{calc.}/\text{g cm}^{-3}$	1.258
μ/mm^{-1}	0.090
Formula Weight	466.61
Colour	clear colourless
Shape	Fragment
Max Size/mm	0.140
Mid Size/mm	0.050
Min Size/mm	0.030
T/K	100(2)
Crystal System	monoclinic
Space Group	C2
$a/\text{Å}$	20.955(14)
$b/\text{Å}$	7.651(4)
$c/\text{Å}$	15.768(9)
$\alpha/^\circ$	90
$\beta/^\circ$	103.061(11)
$\gamma/^\circ$	90
$V/\text{Å}^3$	2463(3)
Z	4
Z'	1
$\theta_{min}/^\circ$	2.634
$\theta_{max}/^\circ$	27.510
Measured Refl.	9393
Independent Refl.	4399
Reflections Used	3563
R_{int}	0.0764
Parameters	303
Restraints	1
Largest Peak	0.284
Deepest Hole	-0.398
GooF	0.939
wR_2 (all data)	0.1228
wR_2	0.1196
R_1 (all data)	0.0596
R_1	0.0517

A.6 X-ray structure analysis data for compound 3.76



Thermal ellipsoids drawn at the 50% probability level.

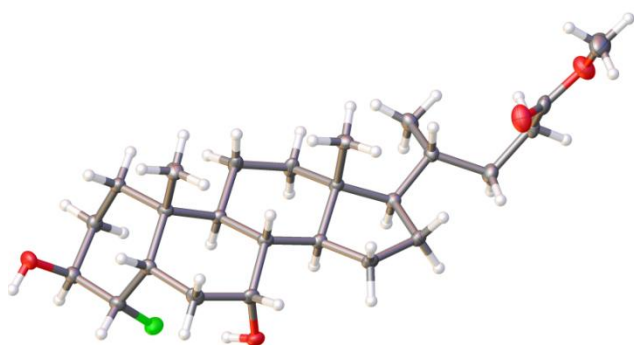
Experimental. Single clear colourless slab-shaped crystals of (2015sot0072-K-100K) were obtained by recrystallisation from EtOAc. A suitable crystal (0.29×0.11×0.05) was selected and mounted on a MITIGEN holder in perfluoroether oil on a Rigaku AFC12 FRE-HF diffractometer. The crystal was kept at $T = 100(2)$ K during data collection. Using **Olex2** (Dolomanov et al., 2009), the structure was solved with the **ShelXT** (Sheldrick, 2015) structure solution program, using the Direct Methods solution method. The model was refined with **ShelXL** (Sheldrick, 2008) using Least Squares minimisation.

Crystal Data. $C_{25}H_{41}FO_4$, $M_r = 424.58$, monoclinic, $P2_1$ (No. 4), $a = 7.5055(2)$ Å, $b = 31.0676(9)$ Å, $c = 9.8213(3)$ Å, $\beta = 91.812(3)^\circ$, $\alpha = \gamma = 90^\circ$, $V = 2288.97(12)$ Å³, $T = 100(2)$ K, $Z = 4$, $Z' = 2$, $\mu(\text{MoK}\alpha) =$

0.086, 22493 reflections measured, 10763 unique ($R_{int} = 0.0335$) which were used in all calculations. The final wR_2 was 0.1648 (all data) and R_I was 0.0619 ($I > 2(I)$).

Compound	2015sot0072-K-100K
Formula	$C_{25}H_{41}FO_4$
$D_{calc.}/\text{g cm}^{-3}$	1.232
μ/mm^{-1}	0.086
Formula Weight	424.58
Colour	clear colourless
Shape	slab
Max Size/mm	0.29
Mid Size/mm	0.11
Min Size/mm	0.05
T/K	100(2)
Crystal System	monoclinic
Flack Parameter	0.0(3)
Hooft Parameter	0.2(3)
Space Group	$P2_1$
$a/\text{Å}$	7.5055(2)
$b/\text{Å}$	31.0676(9)
$c/\text{Å}$	9.8213(3)
$\alpha/^\circ$	90
$\beta/^\circ$	91.812(3)
$\gamma/^\circ$	90
$V/\text{Å}^3$	2288.97(12)
Z	4
Z'	2
$\Theta_{min}/^\circ$	3.015
$\Theta_{max}/^\circ$	28.699
Measured Refl.	22493
Independent Refl.	10763
Reflections Used	9273
R_{int}	0.0335
Parameters	553
Restraints	511
Largest Peak	0.496
Deepest Hole	-0.242
Goof	1.014
wR_2 (all data)	0.1648
wR_2	0.1572
R_I (all data)	0.0722
R_I	0.0619

A.7 X-ray structure analysis data for compound 3.78



Thermal ellipsoids drawn at the 50% probability level.

Experimental. Single clear colourless rod-shaped crystals of (**2015sot0022**) were recrystallised from a mixture of EA and hexane by slow evaporation. A suitable crystal (0.26×0.05×0.03) was selected and mounted on a MITIGEN holder in perfluoroether oil on a Rigaku AFC12 FRE-HF diffractometer. The crystal was kept at $T = 100(2)$ K during data collection. Using **Olex2** (Dolomanov et al., 2009), the structure was solved with the **ShelXT** (Sheldrick, 2015) structure solution program, using the Direct Methods solution method. The model was refined with version of **ShelXL** (Sheldrick, 2008) using Least Squares minimisation.

Crystal Data. $C_{25}H_{41}FO_4$, $M_r = 424.58$, orthorhombic, $P2_12_12_1$ (No. 19), $a = 7.70623(18)$ Å, $b = 13.6497(3)$ Å, $c = 21.6829(5)$ Å, $\alpha = \beta = \gamma = 90^\circ$, $V = 2280.78(9)$ Å³, $T = 100(2)$ K, $Z = 4$, $Z' = 1$, $\mu(\text{MoK}\alpha) = 0.087$, 22737 reflections measured, 7300 unique ($R_{int} = 0.0363$) which were used in all calculations. The final wR_2 was 0.1091 (all data) and R_1 was 0.0467 ($I > 2(I)$).

Compound	2015sot0022
Formula	$C_{25}H_{41}FO_4$
$D_{calc.}/g\text{ cm}^{-3}$	1.236
μ/mm^{-1}	0.087
Formula Weight	424.58
Colour	clear colourless
Shape	rod
Max Size/mm	0.26
Mid Size/mm	0.05
Min Size/mm	0.03
T/K	100(2)
Crystal System	orthorhombic
Flack Parameter	-0.7(4)
Hooft Parameter	-0.4(3)
Space Group	$P2_12_12_1$
$a/\text{\AA}$	7.70623(18)
$b/\text{\AA}$	13.6497(3)
$c/\text{\AA}$	21.6829(5)
α°	90
β°	90
γ°	90
$V/\text{\AA}^3$	2280.78(9)
Z	4
Z'	1
$\theta_{min}/^\circ$	2.805
$\theta_{max}/^\circ$	32.020
Measured Refl.	22737
Independent Refl.	7300
Reflections Used	6263
R_{int}	0.0363
Parameters	283
Restraints	0
Largest Peak	0.337
Deepest Hole	-0.225
GooF	1.025
wR_2 (all data)	0.1091
wR_2	0.1038
R_1 (all data)	0.0582
R_1	0.0467